SAN-1569-2

OCEAN THERMAL ENERGY CONVERSION POWER SYSTEM DEVELOPMENT

Phase 1
Final Report

December 4, 1978

Work Performed Under Contract No. EG-77-C-03-1569

Westinghouse Electric Corporation
Power Generation Divisions
Lester, Pennsylvania

U.S. Department of Energy

Solar Energy

DISCLAIMER

NOTICE

SAN-1569-2
Distribution Category UC-64

OCEAN THERMAL ENERGY CONVERSION POWER SYSTEM DEVELOPMENT

Phase 1
Final Report

December 4, 1978

Contract No. EG-77-C-03-1569

Department of Energy
Division of Solar Technology

Westinghouse Electric Corporation
Power Generation Divisions
Lester, Pennsylvania

Abstract

This report covers the conceptual and preliminary design of closed-cycle, ammonia, ocean thermal energy conversion power plants by Westinghouse Electric Corporation. Preliminary designs for evaporator and condenser test articles (0.13 MWe size) and a 10 MWe modular experiment power system are described. Conceptual designs for 50 MWe power systems, and 100 MWe power plants are also described.

Design and cost algorithms were developed, and an optimized power system design at the 50 MWe size was completed. This design was modeled very closely in the test articles and in the 10 MWe Modular Application.

Major component and auxiliary system design, materials, biofouling, control response, availability, safety and cost aspects are developed with the greatest emphasis on the 10 MWe Modular Application Power System.

It is concluded that all power plant subsystems are state-of-practice and require design verification only, rather than continued research. A complete test program, which verifies the mechanical reliability as well as thermal performance, is recommended and described.

THIS PAGE

WAS INTENTIONALLY

LEFT BLANK

Foreword

U.S. Department of Energy efforts toward exploring means of decreasing the dependence of the United States on imported oil is comprised in part by research directed at renewable energy resources. One of the renewable energy resources is the temperature gradient which is known to exist in the oceans. For the study described in this report, the warm (80°F) surface water and cold (40°F) deep water are used as heat source and heat sink for a closed Rankine cycle power system. The working fluid in this cycle is ammonia.

More specifically, this document reports the results of power system conceptual design of 50 MWe, 100 MWe and 400 MWe plants and preliminary design of a 10 MWe plant and heat exchanger test articles. These studies concentrate on the major components of the power system, i.e. the heat exchangers, warm and cold seawater pumps, turbine, generator and in-cycle ammonia pumps. A full power system was considered, including all starting, storing and transferring systems as well as valves, piping, control and instruments.

Study results indicate that major equipment design goals for a 10 MWe system can be met: 90% power system availability, 30-year major equipment design life, effective biofouling control, compact power system arrangement, and a safe working environment. In addition, the power system is suitable for connection to a power grid to provide base load power without the need for costly storage systems and can be built with already existing technology and facilities.

The study also indicates that the power system capital costs are approximately $1350 per kilowatt for 50 MWe. Including hull, cold water pipe, and the power system, the OTEC closed-cycle system with titanium tubes is considerably more capital-intensive than large conventional power plants in terms of dollars per kilowatt. However, an OTEC plant has lower operating costs which are independent of the fluctuations of the oil, coal, and uranium markets. Further, there is reason to believe that developments in the future could substantially lower OTEC plant costs through innovative design and the qualification of less costly materials than are currently specified in OTEC system designs. By comparison, conventional power system costs, which are highly refined, are likely to increase by approximately \$100/kW/yr.

TABLE OF CONTENTS

Page No.

Abstract i
Foreword iii
Table of Contents v
List of Figures xi
List of Tables xix

1 SUMMARY AND CONCLUSIONS 1-1
1.1 Test Articles 1-1
1.1.1 Test Article Selection 1-1
1.1.2 Aluminum Qualification 1-1
1.1.3 Performance Verification 1-3
1.2 10 MWe Modular Application 1-8
1.2.1 Arrangement 1-8
1.2.2 System Operation 1-13
1.2.3 Modeling of Larger Plants 1-14
1.3 Optimum Power System (50 MWe) 1-14
1.3.1 Economic Optimization 1-14
1.3.2 Forecast Power System Cost 1-18
1.3.3 Technology Assessment 1-18
1.3.4 Heat Exchanger Design and System Arrangement 1-20
1.4 Commercial Plants (100 MWe and 400 MWe) 1-22
1.5 Conclusion 1-27
2 INTRODUCTION 2-1
3 PROGRAM OBJECTIVES 3-1
4 STUDY APPROACH 4-1
4.1 Constraints 4-1
4.1.1 Design Requirements 4-1
4.1.2 Functional Requirements 4-3
4.2 Study Logic 4-3
4.3 Approach to Commercialization 4-4

5	TEST ARTICLES	5-1
5.1	Approach to Design	5-1
5.1.1	Objectives	5-1
5.1.2	Trade-off Analysis	5-7
5.2	Design Description	5-16
5.2.1	System Schematic	5-16
5.2.2	Heat Exchangers	5-16
5.2.3	Thermal and Hydraulic Design	5-17
5.2.4	Mechanical Design	5-24
5.3	Manufacturing	5-32
5.4	Installation/Interfaces	5-37
5.5	Testing Considerations	5-39
5.5.1	Objectives	5-39
5.5.2	Test Plans	5-39
5.5.3	Reliability, Availability, Maintainability, and Safety Performance	5-47
5.5.4	Test Setup	5-48
5.6	Costs	5-48
6	MODULAR APPLICATION (10 MWe)	6-1
6.1	Approach to Design	6-1
6.2	Component Design	6-2
6.2.1	Heat Exchangers	6-2
6.2.2	Seawater Pumps	6-41
6.2.3	Turbine	6-50
6.2.4	Generator	6-66
6.2.5	Fouling Control Systems	6-71
6.2.6	Instrumentation and Controls	6-94
6.2.7	Valves	6-102
6.2.8	Ammonia Pumps	6-112
6.2.9	Auxiliaries	6-116

6.3 System Design.................................. 6-129
6.3.1 Material Compatibility............. 6-129
6.3.2 Arrangement........................ 6-143
6.3.3 System Control..................... 6-169
6.3.4 Availability....................... 6-176
6.3.5 Safety............................. 6-181
6.3.6 Plant Statistics Summary........... 6-182
6.4 Manufacturing and Installation............... 6-182
6.4.1 Heat Exchangers.................... 6-182
6.4.2 Turbine............................ 6-192
6.4.3 Generator.......................... 6-196
6.4.4 Cold and Warm Water Pumps.......... 6-198
6.4.5 Assembly and Checkout.............. 6-199
6.5 System Operation............................. 6-203
6.5.1 Normal Operation................... 6-203
6.5.2 Off-Design Performance............. 6-210
6.5.3 Dynamic Response................... 6-213
6.5.4 Maintainability.................... 6-220
6.6 Testing Considerations....................... 6-221
6.6.1 Test Objectives.................... 6-222
6.6.2 Program Development................ 6-222
6.6.3 Research Plans..................... 6-223
6.6.4 Test Setup......................... 6-231
6.6.5 Conclusions and Recommendations.... 6-243
6.7 Costs.. 6-244
6.7.1 Capital Costs...................... 6-244
6.7.2 Operating Costs.................... 6-246
6.7.3 Economics of Multiple Plants....... 6-252

7 DEMONSTRATION PLANT (50 MWe)...................... 7-1
7.1 Approach to Design Optimization............. 7-1
7.1.1 Computer Model..................... 7-2
7.1.2 Results........................... 7-3
7.1.3 Heat Transfer Enhancements......... 7-8
7.1.4 Single Heat Exchangers............ 7-12
7.2 Component Design............................ 7-13
7.2.1 Heat Exchangers................... 7-13
7.2.2 Seawater Pumps.................... 7-39
7.2.3 Turbine........................... 7-41
7.2.4 Generator......................... 7-52
7.2.5 Fouling Control Systems........... 7-57
7.2.6 Instrumentation and Controls....... 7-58
7.2.7 Valves............................ 7-58
7.2.8 Ammonia Pumps..................... 7-65
7.2.9 Auxiliaries....................... 7-65
7.3 System Design............................... 7-68
7.3.1 Materials Compatibility........... 7-68
7.3.2 Arrangement....................... 7-68
7.3.3 System Control.................... 7-73
7.3.4 Availability...................... 7-73
7.3.5 Safety............................ 7-75
7.3.6 Plant Statistics Summary.......... 7-76
7.4 Manufacturing and Installation.............. 7-77
7.4.1 Heat Exchangers................... 7-77
7.4.2 Turbine........................... 7-79
7.4.3 Generator......................... 7-79
7.4.4 Seawater Pumps.................... 7-80
7.4.5 Assembly and Checkout............. 7-80
7.5 System Operation............................ 7-82
7.5.1 Normal Operation.................. 7-82
7.5.2 Off-Design Performance............ 7-84
7.5.3 Dynamic Response.................. 7-84
7.5.4 Maintainability................... 7-84

7.6 Net Energy Balance.......................... 7-85
7.6.1 Concept.......................... 7-85
7.6.2 Methodology.......................... 7-86
7.6.3 Energy Input.......................... 7-87
7.6.4 Energy Output.......................... 7-90
7.6.5 Results.......................... 7-90
7.7 Costs.......................... 7-91
7.7.1 Capital Costs.......................... 7-91
7.7.2 Operating Costs.......................... 7-102
7.7.3 Economics of Multiple Plants....... 7-102
7.7.4 Cost Improvements.......................... 7-104
8 COMMERCIAL PLANTS (100 MWe and 400 MWe).......... 8-1
8.1 Approach to Design.......................... 8-1
8.2 System Design.......................... 8-1
8.2.1 Arrangements.......................... 8-1
8.2.2 Availability.......................... 8-3
8.3 Manufacturing.......................... 8-4
8.4 Cost.......................... 8-7
8.4.1 The Aluminum Scenario.............. 8-7
8.4.2 Zoning of Heat Exchangers.......... 8-13

BIBLIOGRAPHY REFERENCES

OTHER BIBLIOGRAPHY

THIS PAGE

WAS INTENTIONALLY

LEFT BLANK

LIST OF FIGURES

Figure	Title	Page No.
1-1	Test Article Arrangement	1-2
1-2	Test Article Evaporator	1-4
1-3	Test Article Condenser	1-5
1-4	Test Article Flow Diagram	1-6
1-5	Biofouling Measurement Loop	1-7
1-6	10 MWe Power System	1-9
1-7	10 MWe Condenser	1-11
1-8	10 MWe Evaporator	1-12
1-9	Control System, 50 MWe	1-13
1-10	Design Logic	1-15
1-11	Module and Hull Cost	1-16
1-12	Tube Enhancement Selection	1-17
1-13	Ultimate Power Module Cost	1-19
1-14	Modular Heat Exchanger Design	1-21
1-15	Tube Bundle Installation	1-21
1-16	50 MWe Evaporator	1-23
1-17	Typical Compact 50 MWe OTEC Module Arrangements	1-24
1-18	400 MWe Ship-type Platform	1-25
1-19	400 MWe Spar-type Platform	1-26
1-20	Ship-shape 100 MWe Arrangement	1-27
2-1	OTEC Power Cycle Schematic	2-2
4-1	Study Logic	4-5
4-2	Project Approach	4-7
5-1	Evaporator Heat Exchanger Model	5-9
5-2	Heat Exchanger Test Loop Schematic	5-13
5-3	Heat Exchanger Model Confidence Level Ratio Vs. Cost Ratio	5-15

5-4	Evaporator Test Article Heat Exchanger	5-18
5-5	Condenser Test Article Heat Exchanger	5-18
5-6	Evaporator Pure Water Loop	5-25
5-7	Condenser Pure Water Loop	5-25
5-8	Evaporator Test Article	5-27
5-9	Formed Vane Separator	5-30
5-10	Condenser Test Article	5-33
5-11	Manufacturing Flow diagram	5-35
5-12	Test Article Piping Arrangement	5-38
5-13	Test Articles - Test Data Requirements	5-49
6-1	Droplet Hit/Miss Curve	6-9
6-2	Evaporator Bundle Arrangement	6-15
6-3	Condenser Bundle Arrangement	6-15
6-4	Modular Exchanger Design	6-18
6-5	Evaporator (10 MWe)	6-19
6-6	OTEC Modular Heat Exchanger, Tube Bundle Installation	6-20
6-7	OTEC Modular Heat Exchanger, 50 MWe Condenser Bundle Assembly	6-21
6-8	Evaporator and Condenser Supports and Internal Bracing	6-23
6-9	Condenser (10 MWe)	6-25
6-10	Westinghouse Formed Vane Separator	6-27
6-11	Westinghouse OTEC Heat Exchanger Design Unit Design Welded Tubeplate Junction	6-31
6-12	Westinghouse OTEC Heat Exchanger Design Unit Design Flanged Tubeplate Junction	6-33
6-13	Tube Wall Thickness Titanium Tube SB 338 GD 2	6-38
6-14	Tube Wall Thickness Aluminum Tube SB 234 Alloy 5052	6-38

6-15	Seawater Pump Configuration Considered for OTEC Application	6-43
6-16	OTEC Seawater Pump	6-44
6-17	Warm Water Pump and Diffuser Performance	6-47
6-18	Overall Efficiency of Seawater Pumps	6-48
6-19	OTEC Seawater Pump Layout	6-49
6-20	OTEC 10 MWe Ammonia Turbine Part Load Internal Total-Static Efficiency	6-56
6-21	OTEC 10 MWe Ammonia Turbine Part Load Mass Flow	6-57
6-22	OTEC 10 MWe Ammonia Turbines Part Load Inlet Pressure	6-58
6-23	10 MWe Turbine Side Elevation Partial Section	6-59
6-24	OTEC 10 MWe Ammonia Turbines Rotor Hub Section Inlet Angle and Turning Vs. Mean Diameter Gauging	6-62
6-25	OTEC Rotation Blade Preliminary Inlet Angle Distribution	6-63
6-26	Turbine Bearing and Seal Assembly Thrust Bearing End	6-65
6-27	10 MWe Turbine-Generator Outline and Weights	6-68
6-28	Projected Contribution by Different Types of Fouling	6-72
6-29	Microfouling Rates in Ocean Water	6-73
6-30	Fouling Resistance Vs. Time	6-74
6-31	Comparative Costs of Uncontrolled Vs. Controlled Fouling	6-75
6-32	Fouling Control Assessment	6-78
6-33	Sanilec Seawater Call Power Consumption	6-81
6-34	Relationship of Ammonia Nitrogen and Organic Nitrogen and Chlorine	6-82
6-35	Relationship Between Chlorine Consumed and Contact Time	6-82

6-36	Biofouling System Flow Diagram	6-85
6-37	Amertap Concept	6-87
6-38	Amertap Effectiveness Against Fouling	6-88
6-39	Residual Tin in Immersed No Foul 0.080"	6-89
6-40	Weight/Loss/Time Curves for 90/10 Cu-Ni in Seawater	6-89
6-41	Ammonia Liquid Cleanup System	6-90
6-42	On-Load Cleaning System for Condensers and Tubular Heat Exchangers	6-92
6-43	MAN Brush Effectiveness	6-93
6-44	10 MWe Power Cycle Control System, Schematic Diagram	6-97
6-45	Ammonia Power Cycle Flow Diagram	6-99
6-46	Turbine Bypass Valves, Ammonia Vapor	6-105
6-47	Liquid Ammonia Control Valves	6-107
6-48	Control Valves and Electrical/Hydraulic Schematic Flow Diagram	6-113
6-49	Ammonia Storage, Handling and Purification System	6-117
6-50	Nitrogen System Flow Diagram	6-121
6-51	Circulating Seawater and Component Cooling Water System Flow Diagram	6-123
6-52	Compressed Air System Flow Diagram	6-125
6-53	Diesel Generator System Flow Diagram	6-127
6-54	Preliminary Electrical One-Line	6-131
6-55	Conceptual Design 50 MWe Module	6-145
6-56	Conceptual Design 100 MWe Power Plant	6-146
6-57	General Arrangement Plant - Elevation 71	6-147
6-58	General Arrangement - Elevation 45	6-149
6-59	General Arrangement - Elevation 21	6-151
6-60	General Arrangement - Sections 1-1 and 2-2	6-153

6-61	Piping Arrangement-Profile	6-157
6-62	Piping Arrangement-Elevation 71	6-159
6-63	Piping Arrangement-Elevation 45	6-161
6-64	Piping Arrangement-Elevation 21	6-163
6-65	Piping Arrangement-Section 1-1 and 2-2	6-165
6-66	Candidate Control Configurations	6-173
6-67	Valve Configuration Evaluation	6-175
6-68	Primary Power System	6-177
6-69	Five-Year Scheduled Outage Cycle	6-179
6-70	Condenser-Evaporator Assembly	6-187
6-71	OTEC Tube Bundle Assembly	6-188
6-72	Heat Exchanger Manufacturing Flow Diagram for Modular Design	6-190
6-73	OTEC Turbine 10 MW Scale Model Lead Time Diagram	6-194
6-74	OTEC Pilot Plant Manufacturing Events	6-197
6-75	OTEC Equipment Installation Slipway	6-201
6-76	Heat Exchanger Manufacturing and Assembly Network	6-204
6-77	System Manufacturing and Assembly Sequence (2 Sheets)	6-205
6-78	Detailed OTEC Power Cycle Schematic	6-208
6-79	Temperature Effect on Performance	6-212
6-80	Biofouling Effect on Performance	6-212
6-81	10 MWe Turbine Speed Characteristics	6-215
6-82	10 MWe Turbine Overspeed Protection	6-217
6-83	10 MWe Transient System Response to Opening Step Function of Bypass Valves Flow Area from 0 to 88.9 Square Inches	6-219
6-84	Test Program Development	6-224
6-85	Test Objectives vs. System Element Data Requirements Matrix	6-225
6-86	Modular Experiment - Test Data Requirements	6-232
6-87	Data Acquisition System Functional Block Diagram	6-240
6-88	Processing Center Block Diagram	6-242

7-1	Module and Hull Cost	7-5
7-2	Module Cost vs Module Size	7-6
7-3	Modular Cost vs System Variables	7-9
7-4	Tube Diameter Selection	7-11
7-5	Multiple Heat Exchanger Per Power Module	7-12
7-6	Tube Surface Enhancements	7-14
7-7	Condenser Outside Heat Flux	7-17
7-8	Heat Transfer Surface Area Ratio vs Number of Tubes Ratio	7-26
7-9	Relative Cost vs Power for the Condenser and Evaporator	7-28
7-10	Modular Heat Exchanger Design	7-31
7-11	Evaporator, 50 MWe	7-33
7-12	Condenser, 50 MWe	7-35
7-13	Evaporator and Condenser Structural Supports and Internal Bracing, 50 MWe	7-37
7-14	Longitudinal Section OTEC Turbine 50 MWe Net	7-43
7-15	Mean Diameter, Blade Width and Aspect Ratio at Various Loads vs RPM	7-46
7-16	50 MWe Rating, OTEC Turbine, Efficiency vs. Turbine RPM	7-47
7-17	50 MWe OTEC Turbine, Efficiency and Blade Height vs. Gauging	7-48
7-18	50 MWe OTEC Turbine, Efficiency vs. Wheel Speed at Variable Gauging	7-49
7-19	50 MWe OTEC Turbine, Efficiency vs. Mean Diameter at Constant Speed (1800 RPM)	7-50
7-20	50 MWe OTEC Turbine, Change in Efficiency vs. Aspect Ratio	7-51
7-21	50 MWe OTEC Turbine, Load vs. Speed	7-53
7-22	Cross Section of Conceptual Design of 50 MWe, 1800 RPM Generator	7-54

7-23	OTEC Initial Generator Estimates, Block Dimensions, and Weight	7-54
7-24	Protective Relay Diagram	7-57
7-25	50 MWe OTEC Module "Back To Back" Configuration	7-69
7-26	50 MWe OTEC Module "Side By Side" Configuration	7-71
7-27	50 MWe OTEC Module "Stacked" Configuration	7-72
7-28	Tube Life Probability	7-101
7-29	Distributed Life-Cycle Costs	7-101
8-1	400 MWe OTEC Plant Surface Platform "Square" Configuration	8-2
8-2	400 MWe OTEC Plant Surface Platform "Long" Configuration	8-5
8-3	400 MWe OTEC Plant "Star" Configuration	8-6
8-4	Ultimate Power Module Cost	8-9
8-5	Aluminum Module Costs	8-11
8-6	Temperature/Area Diagram	8-13

THIS PAGE

WAS INTENTIONALLY

LEFT BLANK

LIST OF TABLES

Table	Title	Page No.
1-1	Performance Summary, 10 MWe Power Module	1-8
2-1	Facets of OTEC Power Plant Development	2-1
5-1	Aluminum Tube-To-Tubesheet Joint Selection	5-8
5-2	Heat Exchanger Model-Parameter Rating	5-14
5-3	Heat Exchanger Model - Comparison Study	5-14
6-1	Power Module Comparison	6-3
6-2	Heat Exchanger Comparison	6-4
6-3	Scaling Parameter Comparison	6-5
6-4	Heat Exchanger Thermal Design Data	6-7
6-5	Distribution Tray Hole Data	6-11
6-6	Cost Comparison Unit vs. Modular Design	6-28
6-7	OTEC Heat Exchanger Unit Design Feasibility Study	6-36
6-8	Heat Exchanger Mechanical Design Data Modular Design - 10 MWe	6-42
6-9	OTEC Seawater Pump/Diffuser Design Configuration	6-46
6-10	Potential Control Methods	6-77
6-11	Costs of Fouling Control Methods	6-79
6-12	Valve Type Comparison	6-103
6-13	Steels Susceptible to Stress Corrosion Cracking in Liquid Ammonia	6-135
6-14	Titanium Tube-To-Tubesheet Joint Selection	6-139
6-15	10 MWe Modular Application Power System Weight Summaries	6-167
6-16	Packing Factor and Cost Data	6-168

6-17	Shutdown/Start-Up Time Estimate Summary	6-178
6-18	RAM Summary for Major Components 10 MWe Power Module	6-179
6-19	RAM Characteristics of 10 MWe Modular Application Power Module	6-180
6-20	Heat Exchanger Design Data (10 MWe)	6-183
6-21	Rotating Machinery	6-184
6-22	10 MWe Modular Application Power System Weight Summary	6-185
6-23	Warm and Cold Water Pump System, Manufacturing Plan Fabrication and Assembly Schedule	6-200
6-24	10 MWe Thermodynamic Cycle Data	6-207
6-25	Heat Exchanger Data	6-207
6-26	Power Summary Data	6-208
6-27	10 MWe Modular Application Ammonia Flow Distribution	6-209
6-28	Heat Exchanger Cost Algorithms	6-247
6-29	10 MWe Power System Costs	6-248
6-30	Maintenance Activity Categories	6-249
6-31	Skills Levels for Maintenance	6-249
6-32	Maintenance Personnel Requirements Summary	6-250
6-33	Annual Maintenance Manhour Requirement by Skill Category	6-252
6-34	List of Machinery, Tools and Parts for Maintenance (3 sheets)	6-253
6-35	Detail List of Machinery, Tools and Parts for Maintenance (2 Sheets)	6-256
6-36	10 MWe Power System Costs	6-258

7-1	OTEC System Variables	7-1
7-2	50 MWe Preliminary Design	7-7
7-3	Module Cost of Enhancement Combinations	7-10
7-4	Operands	7-21
7-5	Enhancement Arrangements Considered	7-24
7-6	Ratio of Heat Transfer Improvement to Friction Factor Impairment	7-24
7-7	Thermal and Hydraulic Design Parameters (50 MWe)	7-29
7-8	Heat Exchanger Mechanical Design Data, Modular Design - 50 MWe	7-38
7-9	Pump/Diffuser Design Configuration for 100 m^3/s Flow Capacity at 3.5 m Head	7-40
7-10	Preliminary Instrument List (6 Sheets)	7-59
7-11	Power Summary Data	7-66
7-12	50 MWe Demonstration Plant Ammonia Flow Distribution	7-66
7-13	Outage Summary for Major Components of 50 MWe Power Module	7-74
7-14	Power Industry Data	7-75
7-15	Heat Exchanger Design Data (50 MWe)	7-76
7-16	50 MWe Thermodynamic Cycle Data	7-82
7-17	Heat Exchanger Data	7-83
7-18	50 MWe OTEC Power Plant - Mass of Materials, Short Tons	7-88
7-19	Westinghouse OTEC Power System Energy Analysis	7-89
7-20	Power Summary	7-90
7-21	Subsystem Cost Analysis Types	7-92
7-22	50 MWe Power Module Cost Summary	7-93
7-23	Heat Exchanger Related Costs	7-94
7-24	50 MWe Modular Bundle Costs	7-97
7-25	Titanium Discounted Cash Flow Summary	7-98
7-26	Aluminum Discounted Cash Flow Summary	7-99
7-27	Estimated Tube Life (Years)	7-100
7-28	Break-Even Life	7-102
7-29	50 MWe Power System Prototype and Production Costs, Titanium Tubing	7-103
7-30	Cost of Aluminum Tubes vs. Titanium Tubes	7-105

8-1	Shipbuilding Capabilities	8-8
8-2	Enhancement Codes	8-12

1 SUMMARY AND CONCLUSIONS

This report documents the major accomplishments of the conceptual and preliminary design phases of a study dealing with closed-cycle systems for extracting energy from ocean thermal gradients. The current plan for developing these new power systems calls for the construction of small evaporators and condensers (test articles), followed by deployment of a 10 MWe power system which will, in turn, be followed by 50 MWe and larger plants. The results obtained by Westinghouse in the design studies of the above systems are presented here in the same order. Also, these studies revealed that the OTEC plant specifications (e.g. 80°F warm water, 40°F cold water, power output, connection to shore-based AC grid, ammonia working fluid, closed-cycle, etc.) determine an optimized power system design. This optimized power system was evaluated for its response to off-design conditions, such as variations in warm seawater temperatures and variations in biofouling levels.

A change in OTEC plant specifications would result in a new optimized power system and a new dollar per kilowatt capital cost figure. Also, if off-design specifications were added, the power system design would be affected.

The design procedures and computer programs developed would facilitate rapid response to a change in OTEC plant specifications.

1.1 Test Articles

1.1.1 Test Article Selection

The proposed test article arrangement is shown in Figure 1-1. It is designed to provide heat exchanger data to allow scale up to any size heat exchanger. The test article heat exchangers, using aluminum tubes, are designed to have the same construction aspects as the 10 MWe modular experiment and the 50 MWe size power module. The evaporator shown in Figure 1-2 and the condenser shown in Figure 1-3 are both constructed using modular bundles, explosively clad tube sheets, an integral

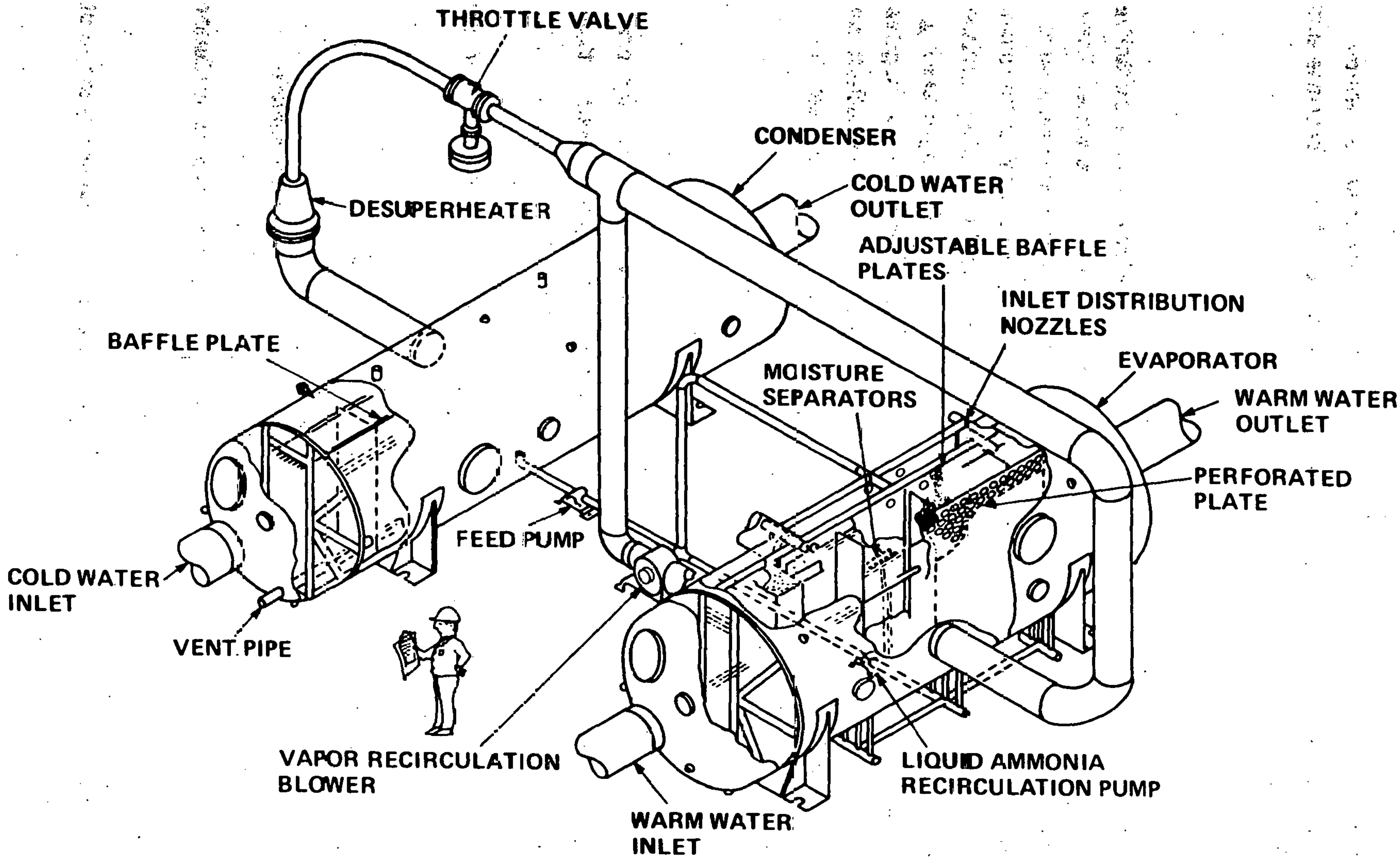

Figure 1-1
TEST ARTICLE ARRANGEMENT

separator and hotwells. In addition, provisions are made to allow simulation of the full-size bundle flow patterns to verify performance and mechanical characteristics.

1.1.2 Aluminum Qualification

An important goal of the test article is to qualify aluminum as a suitable material for commerical OTEC plants in seawater and ammonia service. This is important because of the potential savings that aluminum offers over titanium, the only other material presently considered suitable for such service. Therefore, a number of aluminum alloy and coating configurations will be included to evaluate corrosion, erosion and biofouling cleaning impacts. All of these tube variations will include teflon-coated samples (on inside diameter) and both seamless and welded tubing. The selection represents the best opportunities to qualify aluminum for use in commercial size plants.

1.1.3 Performance Verification

The test article system has been designed with provisions to vary the fluid and vapor flows to simulate the performance of any foreseeable tube module size. The variable features in the evaporator include:

- Variable vapor flow through use of a vapor recycling blower in the evaporator
- Variable liquid recycle to simulate tube loadings
- Adjustable lane baffle to simulate vapor flow past a bundle
- Compartmentalized distribution and collection trays to evaluate liquid distribution
- Fast-acting feed shut-off valves to evaluate inventory dry-out rates under varying conditions of operation.

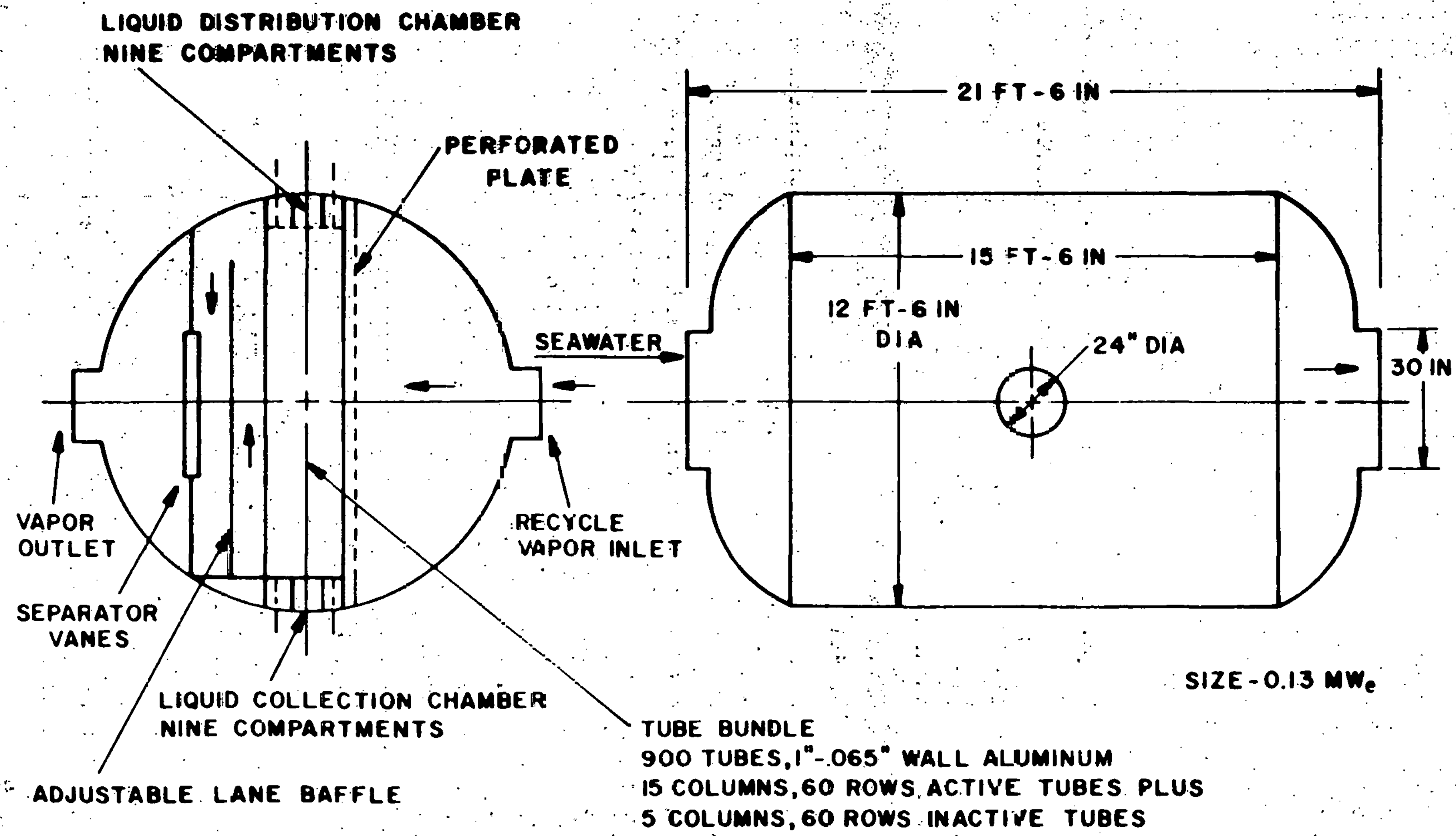

Figure 1-2
TEST ARTICLE EVAPORATOR

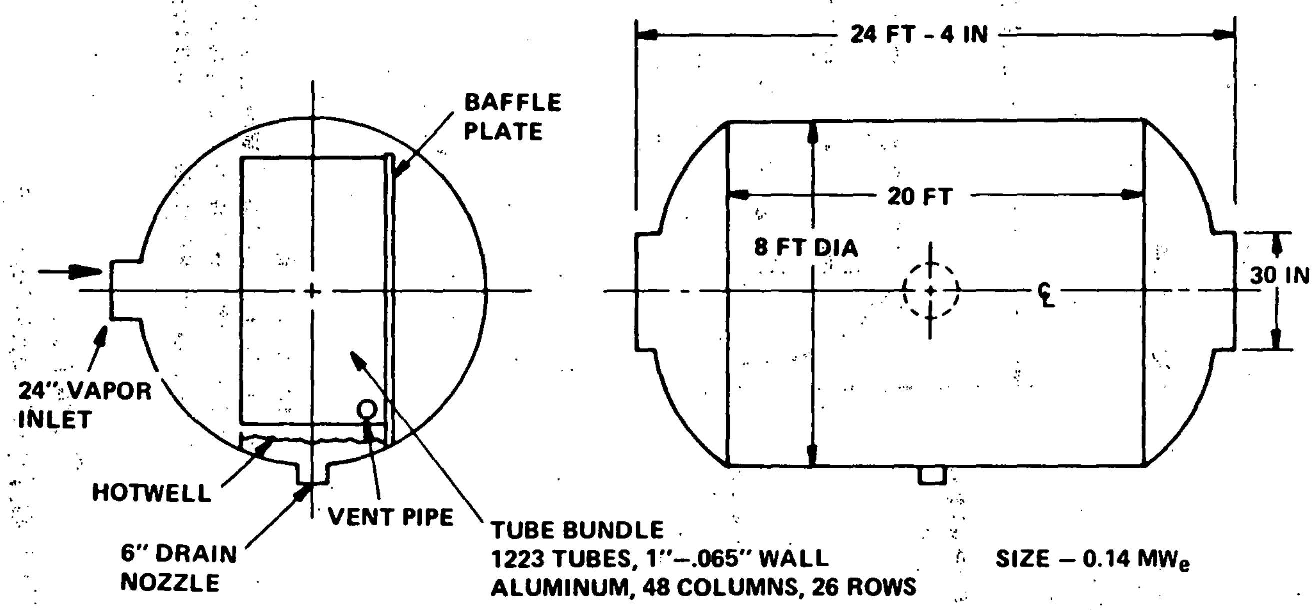

Figure 1-3
TEST ARTICLE CONDENSER

The condenser model has a scaled flow path to an orificed non-condensible core pipe to simulate the venting and condensing phenomena. A flow diagram of the test article system is shown in Figure 1-4.

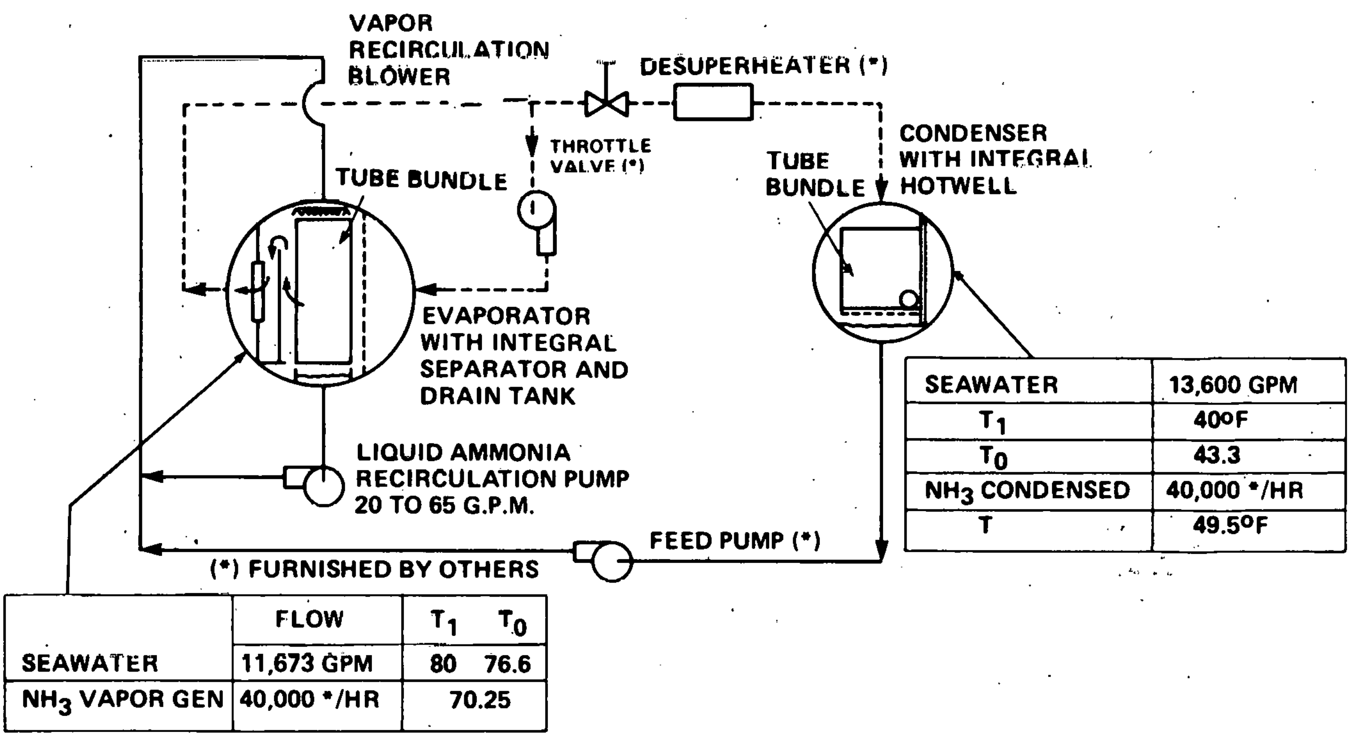

	FLOW	T_1	T_0
SEAWATER	11,673 GPM	80	76.6
NH_3 VAPOR GEN	40,000 */HR	70.25	

SEAWATER	13,600 GPM
T_1	40°F
T_0	43.3
NH_3 CONDENSED	40,000 */HR
T	49.5°F

Figure 1-4
TEST ARTICLE FLOW DIAGRAM

The normal ASME power test code for separating tube fouling effects is not practical because continuous monitoring is necessary. A clean water circulating loop (Figure 1-5) is provided for both evaporator and condenser to provide biofouling measurements.

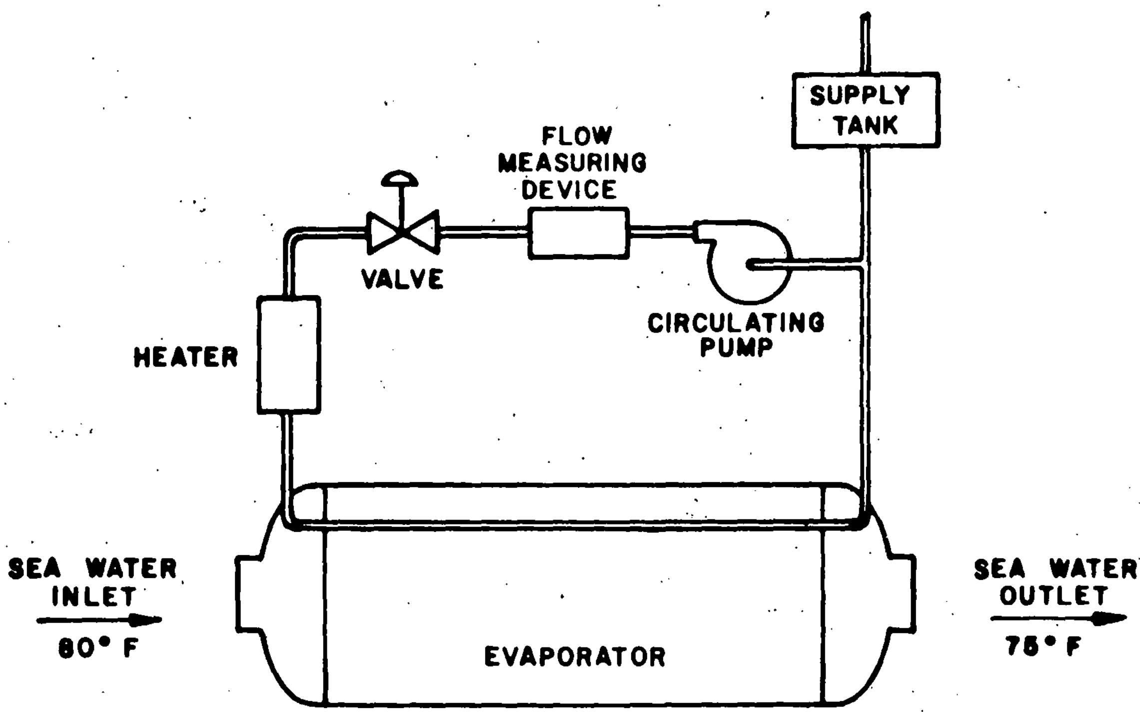

Figure 1-5
BIOFOULING MEASUREMENT LOOP

1.2 10 MWe Modular Application

A performance summary of the 10 MWe modular experiment design is shown in Table 1-1.

Table 1-1
PERFORMANCE SUMMARY 10 MWe POWER MODULE

EVAPORATOR		CONDENSER	
Inlet NH_3 Temperature, °F	59.7	Inlet NH_3 Temperature, °F	49.1
Exit NH_3 Temperature, °F	70.5	Exit NH_3 Temperature, °F	49.0
Tube Velocity, ft/sec	6.5	Tube Velocity, ft/sec	5.6
Water Flow, 10^6 lb/hr	305.4	Water Flow, 10^6 lb/hr	263.0
Seawater Δ P of Heat Exchanger, PSI	2.90	Seawater Δ P of Heat Exchanger, PSI	3.7
TURBINE		**AUXILIARY POWER (MW)**	
Inlet Temperature, °F	70.2	Cold Water Pump	2.30
Exit Temperature, °F	49.1	Warm Water Pump	1.52
RPM	3600.	NH_3 Pump	0.28
NH_3 Flow, 10^6 lb/hr	3.0	Recycle Pump	0.05
Power	14.4	Hypochlorite Generator	0.17

1.2.1 Arrangement

Arrangement of the 10 MWe OTEC power module achieves maximum practical packing density in a surface platform/ship, minimizes heating and cooling water management problems and ammonia working fluid piping runs, offers innovative space utilization to facilitate construction and maintenance, and is readily adaptable to all alternative platform configurations. A profile view in Figure 1-6 shows the consolidation of components, the submerged heat exchangers, and the downsteam location of seawater pumps to allow for long, efficient diffusers in the discharge pipes below the hull.

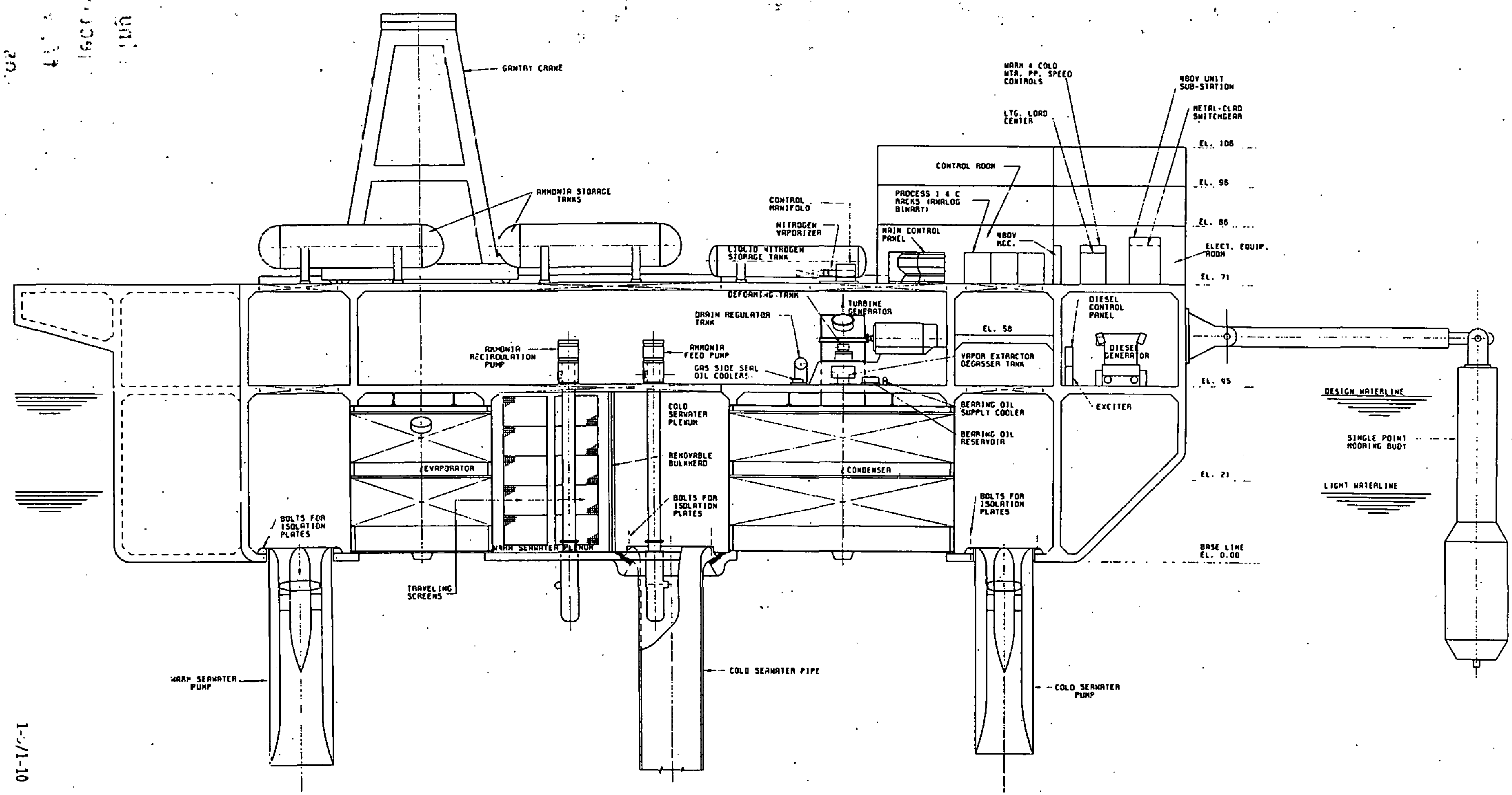

Figure 1-6
10 MWe POWER SYSTEM

The equipment can be mounted in a variety of hulls in addition to the reference hull selected. The 50 MWe modules have equal flexibility for accommodation in a variety of hull configurations.

The end views of the condenser and evaporator in Figures 1-7 and 1-8 show that the modular square tube bundles permit the moisture separator and the evaporator drain tank and condenser hotwell to be placed within the shell to reduce cost and piping runs.

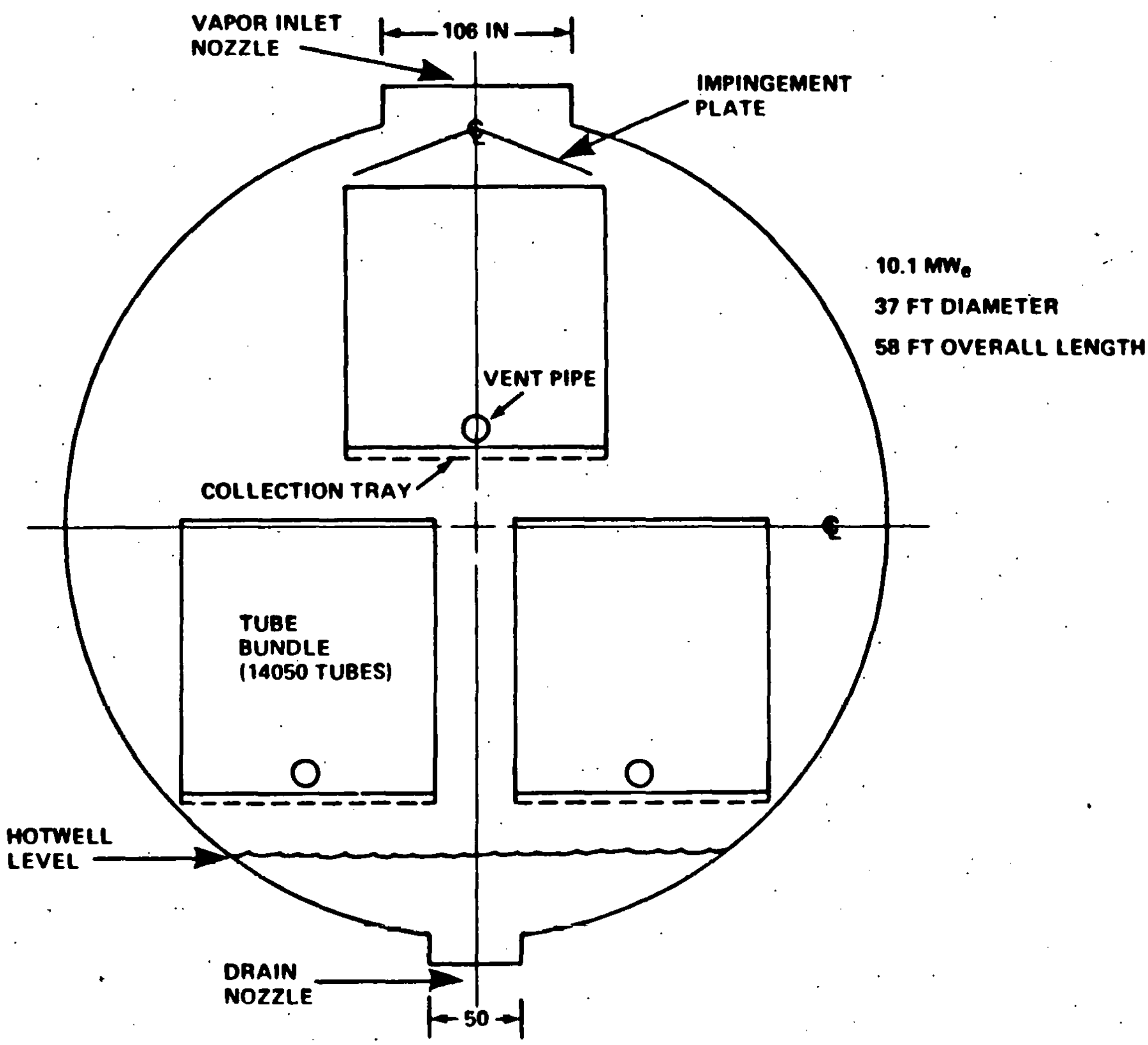

Figure 1-7
10 MWe CONDENSER

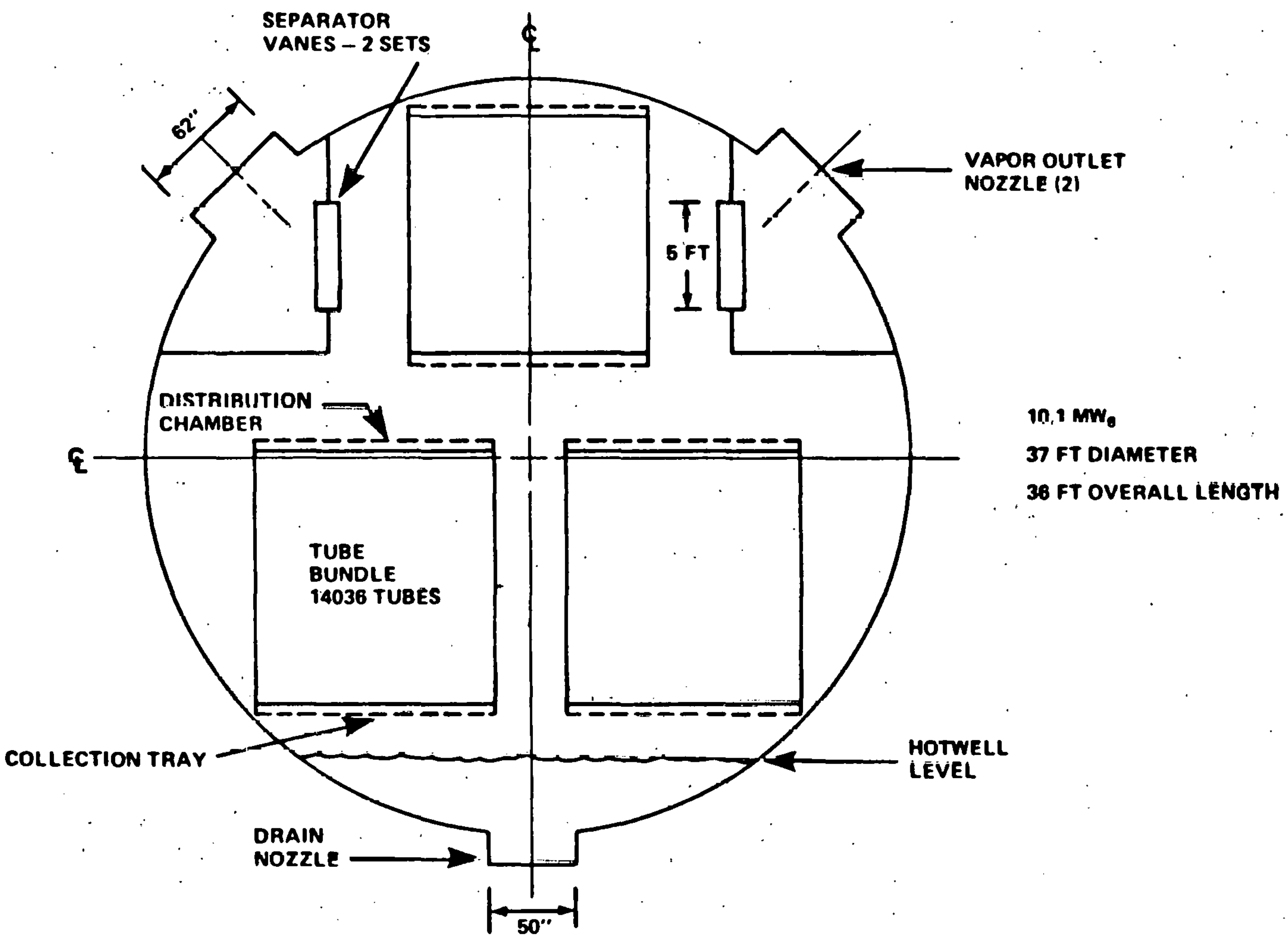

Figure 1-8
10 MWe EVAPORATOR

1.2.2 System Operation

A performance summary of the 10 MWe Modular Application design is shown in Table 1-1.

The control system diagramed in Figure 1-9 was selected to provide redundant turbine overspeed protection as well as RAM provision for on-line exercising of all control valves, without the losses associated with conventional turbine control and stop valves. It makes use of multiple large bypass valves and feedvalves. Redundancy of function in the selected arrangement will ensure that an unacceptable turbine overspeed is extremely remote.

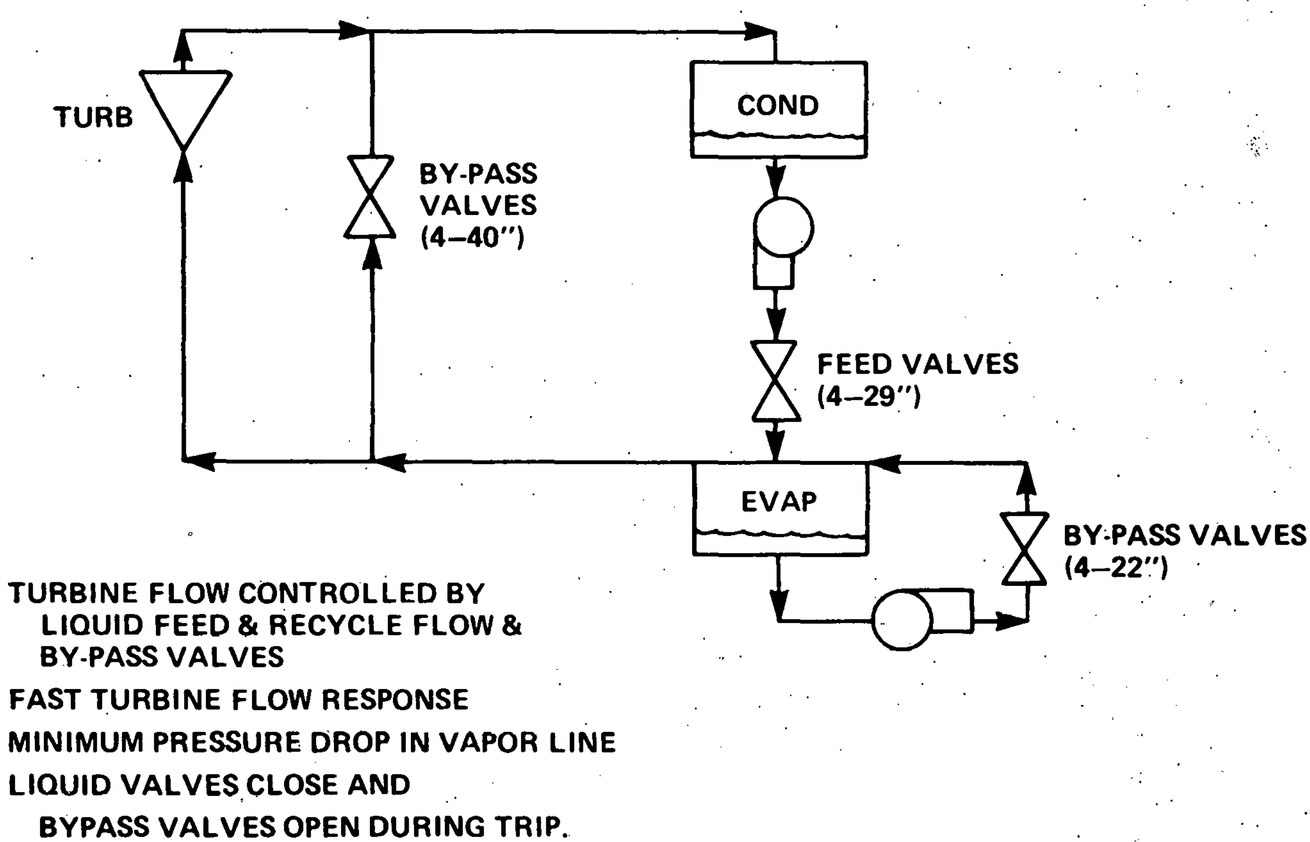

Figure 1-9
CONTROL SYSTEM, 50 MWe

1.2.3 Modeling of Larger Plants

The heat exchangers in the 10 MWe plant exactly model the heat exchangers of larger commercial plants in all respects (40 MWe and larger) because the tube modules are thermodynamically and structurally equivalent to the larger plant. The turbine is a one-half size, double speed exact scale model of a 40 MWe turbine, and models the thermodynamic, structural and vibration characteristics of the larger turbine. Only a modest extrapolation of the data from this size is required to predict the operating characteristics of the 50 MWe turbine design.

1.3 Optimum Power System (50 MWe)

1.3.1 Economic Optimization

The 50 MWe system design is based on an economic optimization supported by technology assessments and producibility analyses. The design procedure is shown in Figure 1-10. The central optimization computer model is composed of heat balance, mechanical design and cost models. This computer program uses pattern search techniques to find the optimum cost design using the models of the entire power system. The specific optimum designs are further qualified by a dynamic response analysis and technology and producibility assessments. Off-design data is provided by a steady-state analysis program.

The results of the cost studies showed that power system cost is affected by module size. Figure 1-11 plots the conceptual cost of the heat exchangers, power module and hull, and indicates that the optimum cost is at the 50 MWe level. It is for this reason primarily that the 50MWe size is the power system whose characteristics are sought in the test articles and the Modular Application.

Seventeen types of tube enhancement for the heat exchangers were studied along with the entire range of tube diameters. Only those enhancements that had manufacturing experience and available correlation data were considered. Typical results are shown in Figure 1-12. The optimum

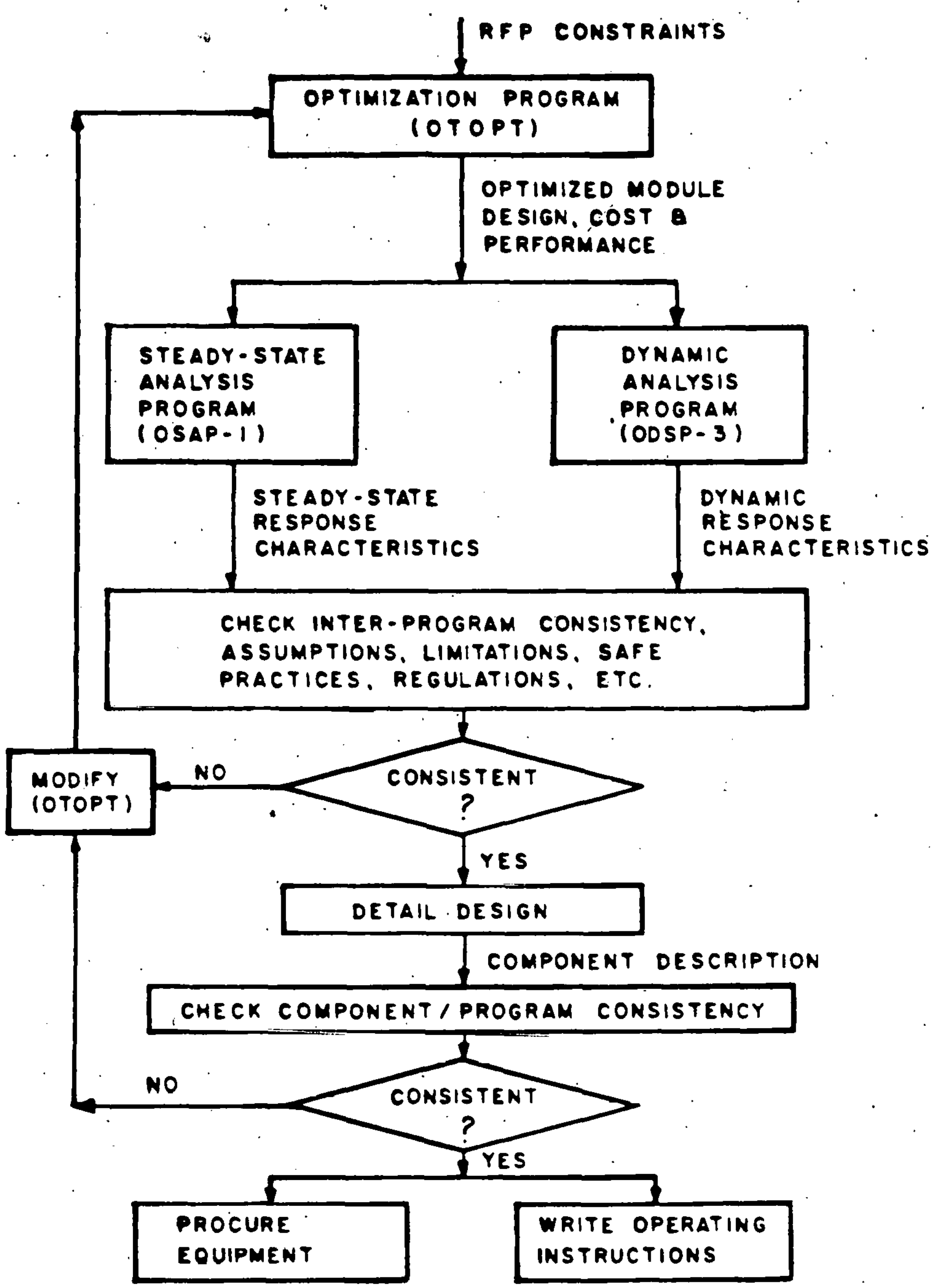

Figure 1-10
DESIGN LOGIC

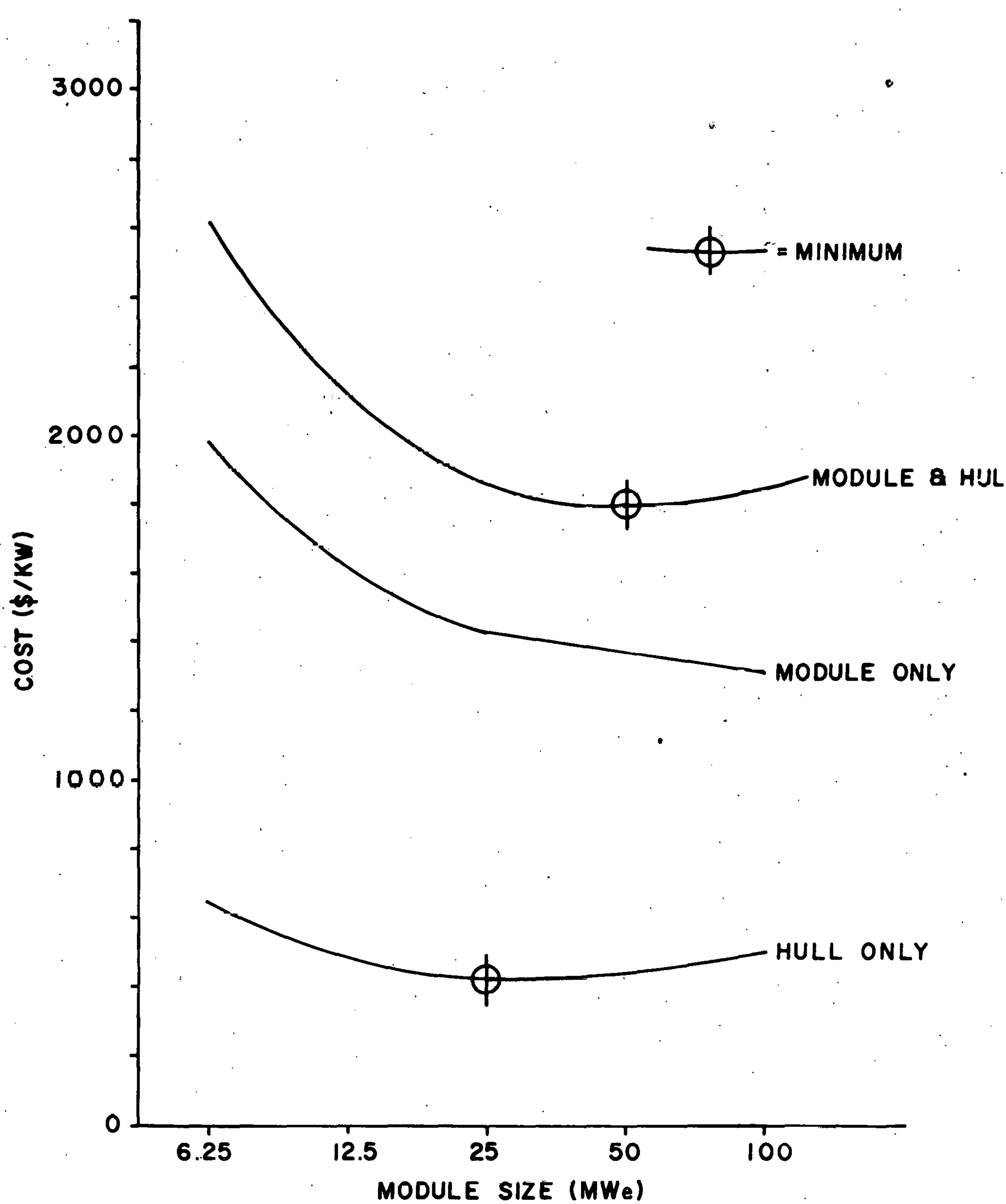

Figure 1-11
MODULE AND HULL COST

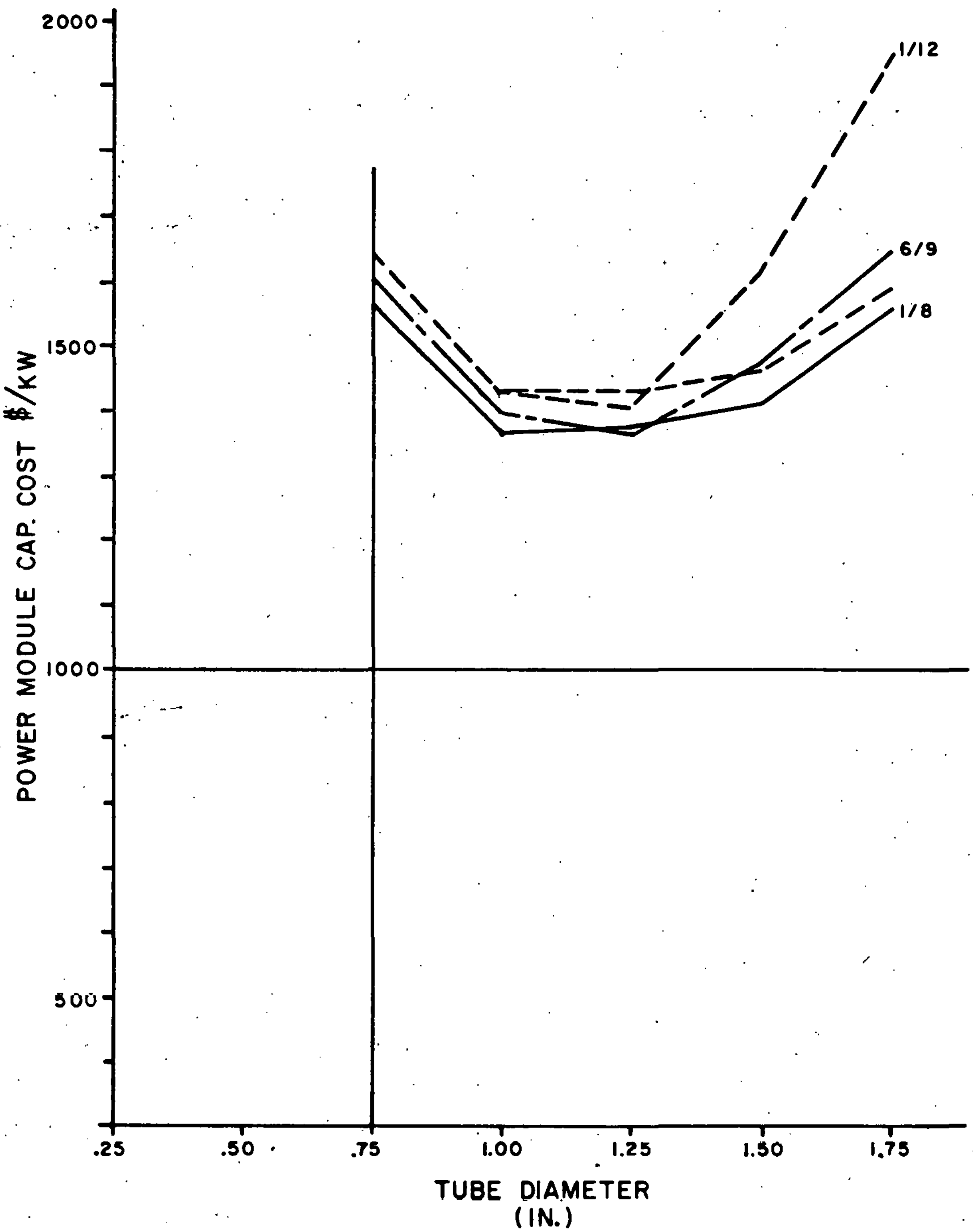

Figure 1-12
TUBE ENHANCEMENT SELECTION

enhancement selection is currently the Linde High Flux coating on the evaporator, with plain inside surfaces and plain tubes in the condenser. Although many of the enhancement options had higher heat transfer coefficients, they did not provide the lowest system cost when initial cost and operating losses were considered.

1.3.2 Forecast Power System Cost

The estimate of power system module cost is shown in Figure 1-13. The cost has an upper limit given by aluminum tubed units with expected replacement consistent with current technology. A lower bound is an aluminum unit assuming tubing costs to be equal to the simple aluminum strip cost (this is tantamount to assuming negligible manufacturing cost for producing welded tubing) without corrosion allowance. It is expected that potential cost improvements associated with aluminum tubing will be balanced by other factors such as higher prices for long-lasting tubing, which are difficult to predict and are not included.

1.3.3 Technology Assessment

The major technical issues addressed in the demonstration plant conceptual design were the tube material selection, biofouling control and power system availability. All have critical impacts on the ultimate competitiveness of the OTEC concept.

Although titanium has a significantly higher initial cost than aluminum or copper nickel tubing, it is the only material that has been qualified for both seawater and ammonia service and was selected as the material for the 10 MWe Modular Application and 50 MWe commercial power module. The requirement of high reliability for the power system reinforces this selection, unless testing of aluminum developes a viable alloy.

Biofouling has a significant impact on OTEC viability. It is expected that chlorination will maintain tube cleanliness with a fouling resistance from .0001 to .00025 hr-°F-ft^2/BTU. The required amount of chlorination is within current allowable EPA limits for chlorine discharges.

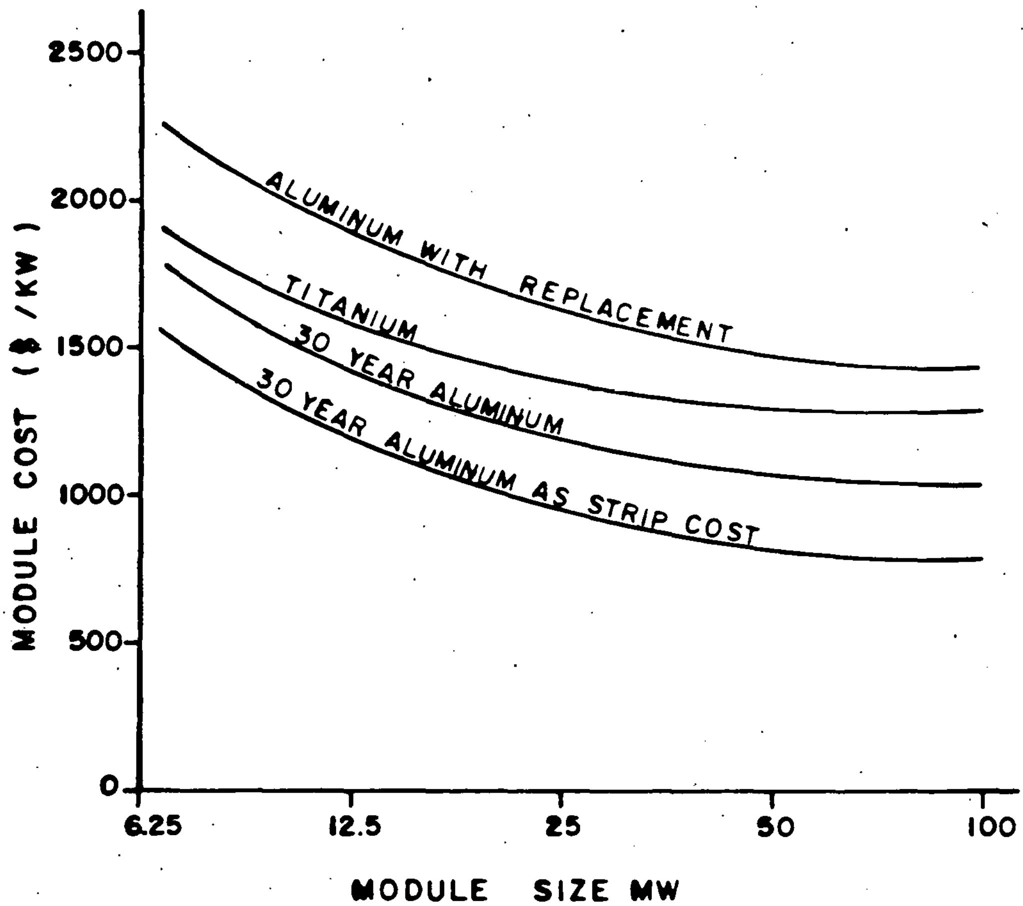

Figure 1-13
ULTIMATE POWER MODULE COST

Chlorination is also essential for controlling biofouling situations in other areas. However, without actual OTEC plant ocean experience, a back-up cleaning system will be required. Amertap is selected as the back-up mechanical system. Toxic coatings, foamed solvents, ozone, MAN brushes and manual cleaning methods were considered, but are not as effective as the chosen methods.

An additional concern is material corrosion with liquid and gaseous ammonia. However, a minimum water content of 0.2% in the ammonia has been demonstrated to be an effective corrosion inhibitor with liquid ammonia, while lower percentages are sufficient with ammonia vapor. Further study may identify other effective inhibitors. Also the detail effect of water or other inhibitors on the heat exchanger performance must be determined and verified in the test article program.

The condenser vent pipe is carefully sized and located to create a low pressure sink in the center of the tube bundle bottom, where a small amount of ammonia together with the non-condensibles are scavenged and removed by the purification system. The ammonia is returned to the system while the non-condensibles are discarded. The removal of the non-condensibles is imperative because their build-up within the heat exchanger would blanket the tube surface and degrade the ammonia condenser performance.

Analysis of the operating environment, design strategies, and field histories of similar equipment indicates that an availability of over 90% is obtainable.

1.3.4 Heat Exchanger Design and System Arrangement

Very large heat exchangers are required for the most economical power modules. To produce such large heat exchangers with automated drilling and tube welding equipment currently available in the heat exchanger industry, a modular heat exchanger design was developed. The concept is illustrated in Figure 1-14 showing rail-shippable bundles and the arrangement of multiple tube bundles in the shell. The detailed tube plate assembly is shown in Figure 1-15.

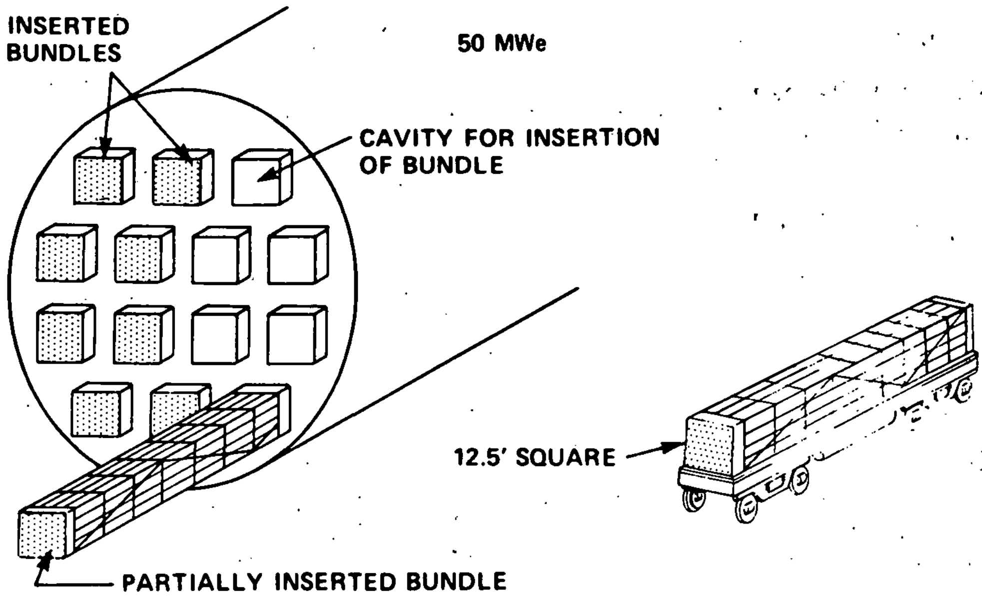

Figure 1-14
MODULAR HEAT EXCHANGER DESIGN

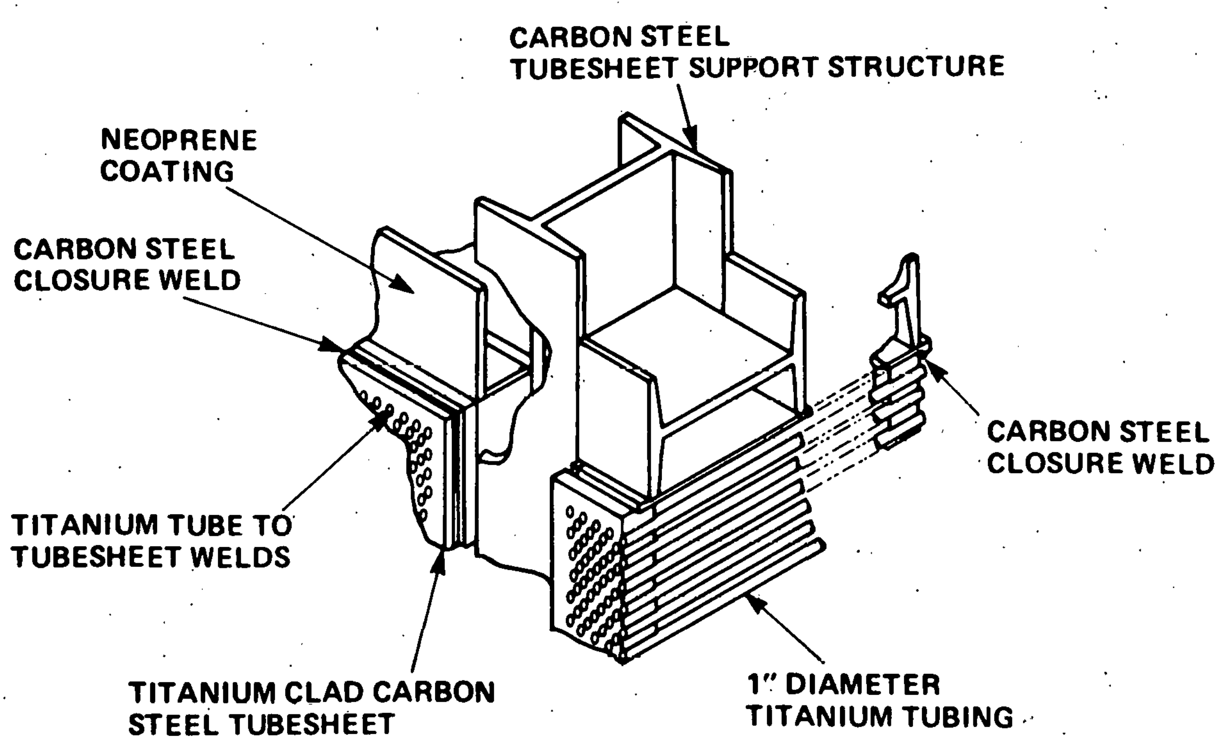

Figure 1-15
TUBE BUNDLE INSTALLATION

The evaporator design selected for the 50 MWe system is shown in Figure 1-16. Note that moisture separators are integral to the heat exchanger shell and that there is ample volume in the bottom of the shell for holding excess feed for the recirculation pump. The condenser arrangement is very similar, with volume for the condensate hotwell included within its shell.

A typical compact arrangement for the power system is shown in Figure 1-17. It compares favorably with other OTEC plant designs in terms of power density (tons displacement per MWe).

1.4 Commercial Plants (100 MWe and 400 MWe)

The 50 MWe power module has adaptability as one of its principal advantages. These modules may be arranged in various ways to accommodate to a large variety of plant sizes and configurations. The incorporation of these power modules into a 400 MWe barge in Figure 1-18 and a spar-type platform in Figure 1-19 indicates their arrangement flexibility.

A 100 MWe power plant platform has been designed to allow construction in a number of existing U.S. facilities. Heat exchanger water boxes were made an integral part of the hull to minimize seawater pressure drops. A diagram of the conceptual 100 MWe hull is shown in Figure 1-20. A similar plant with the preliminary design 50 MWe modules would be significantly smaller.

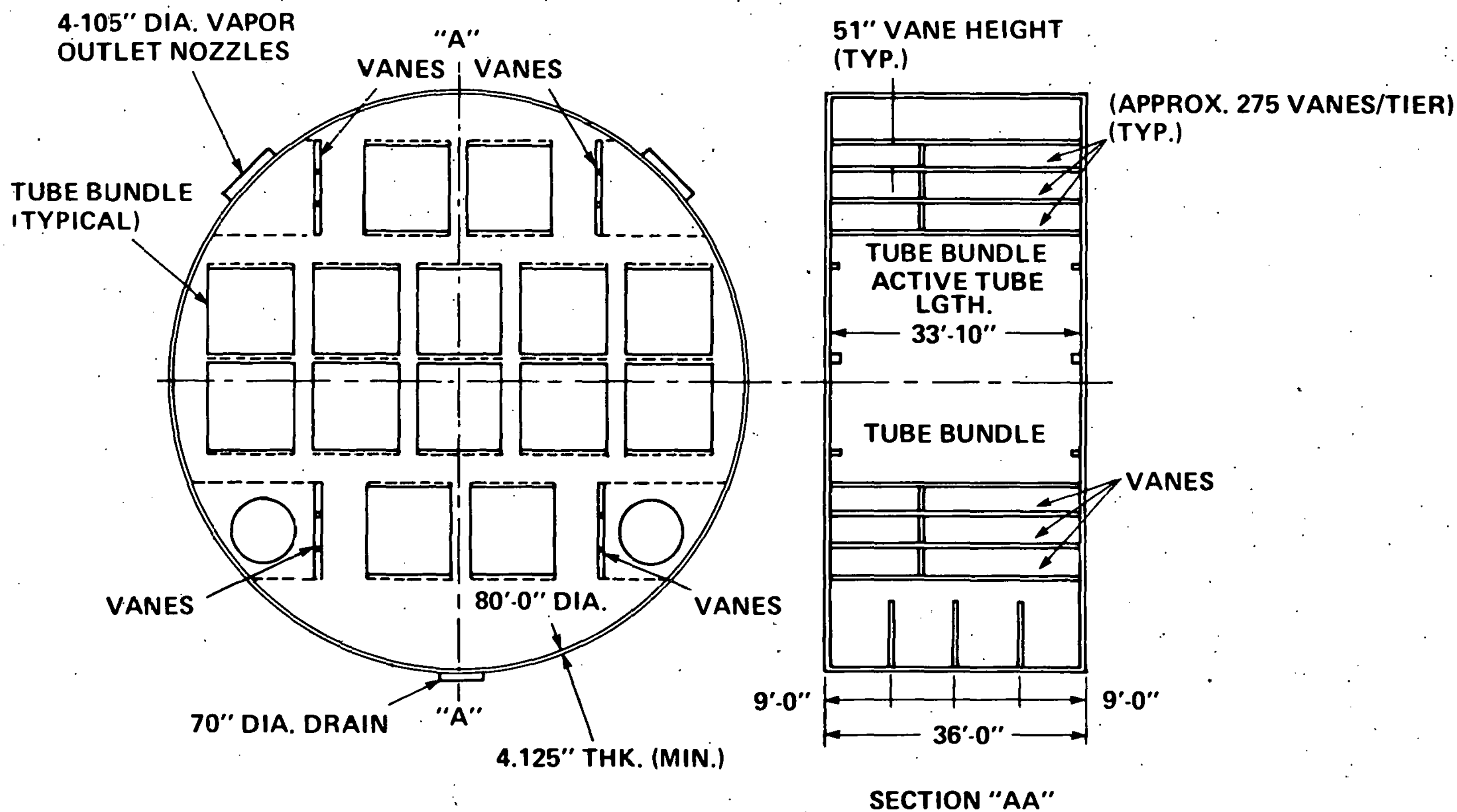

Figure 1-16
50 MWe EVAPORATOR

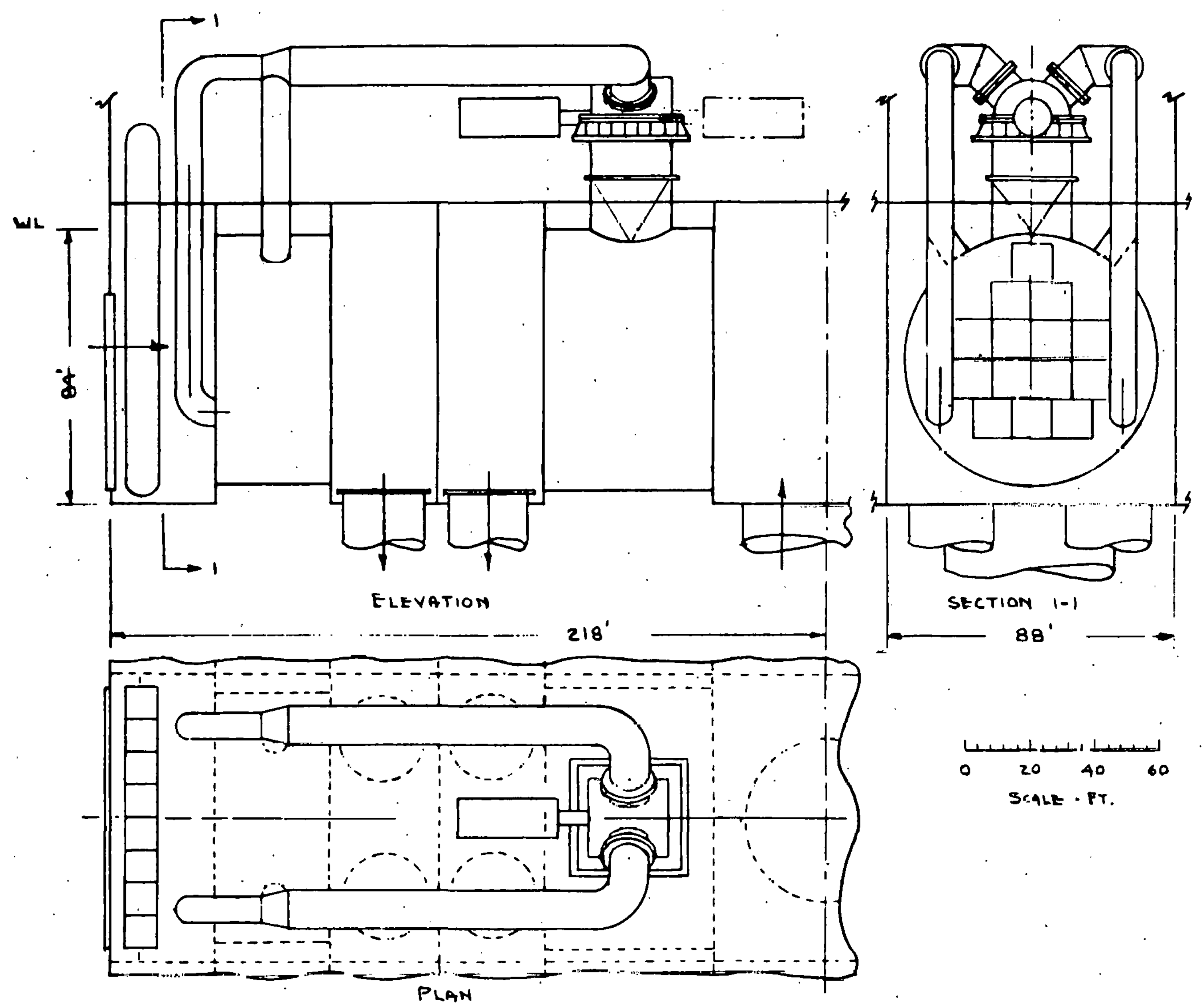

Figure 1-17
TYPICAL COMPACT 50 MWe OTEC MODULE ARRANGEMENTS

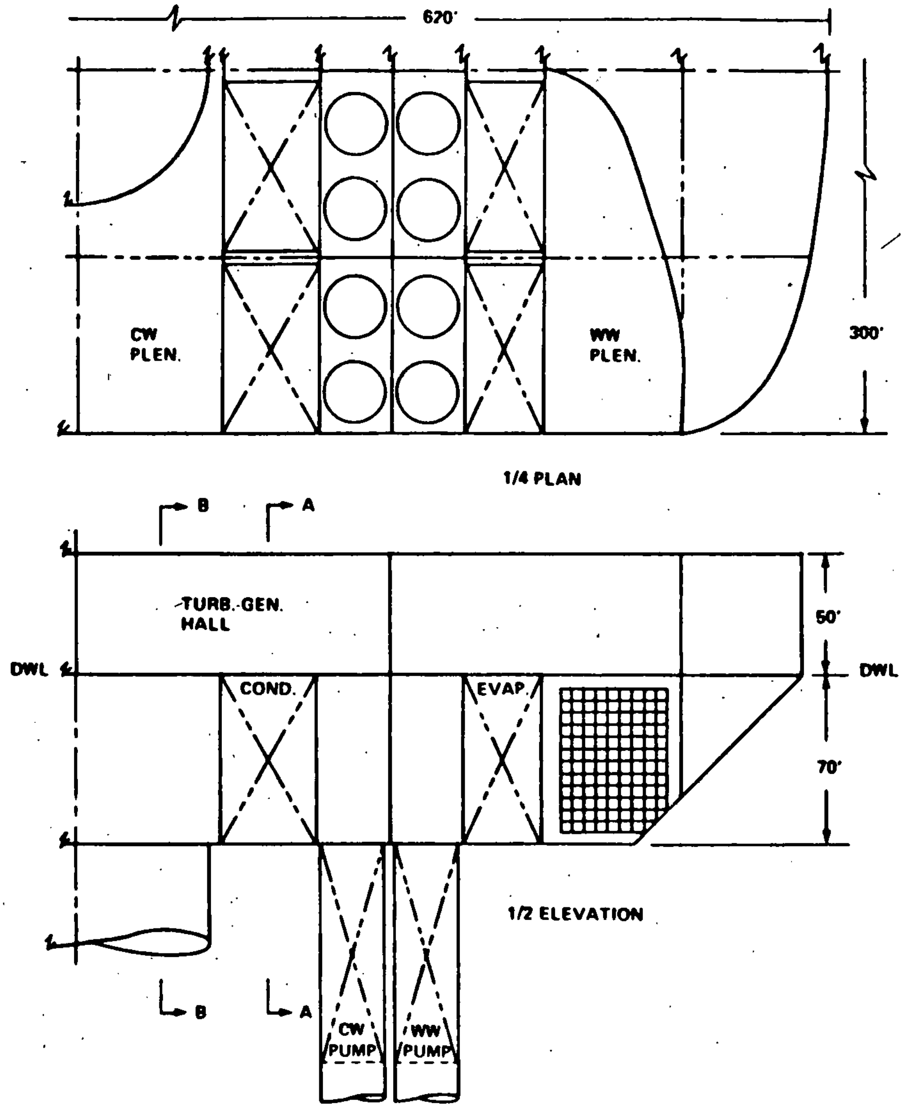

Figure 1-18
400 MWe SHIP-TYPE PLATFORM

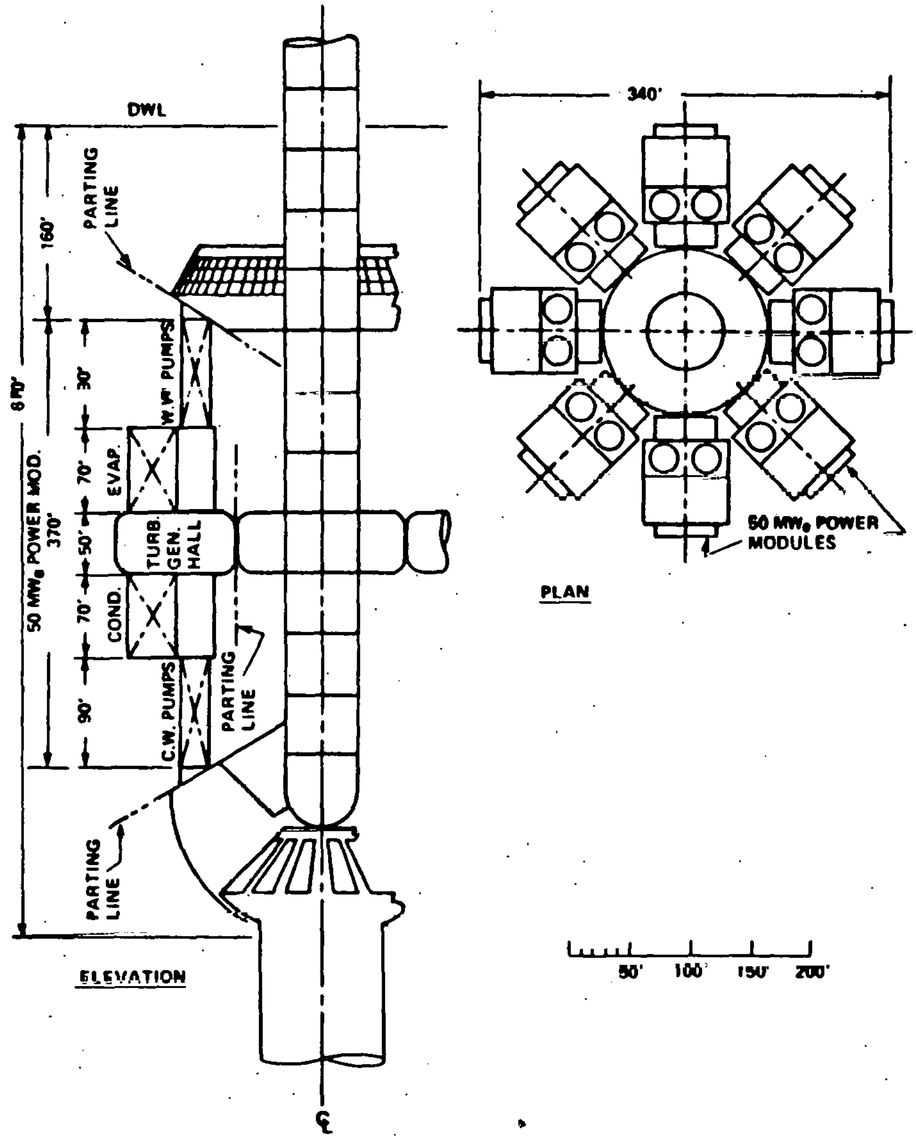

Figure 1-19
400 MWe SPAR PLATFORM

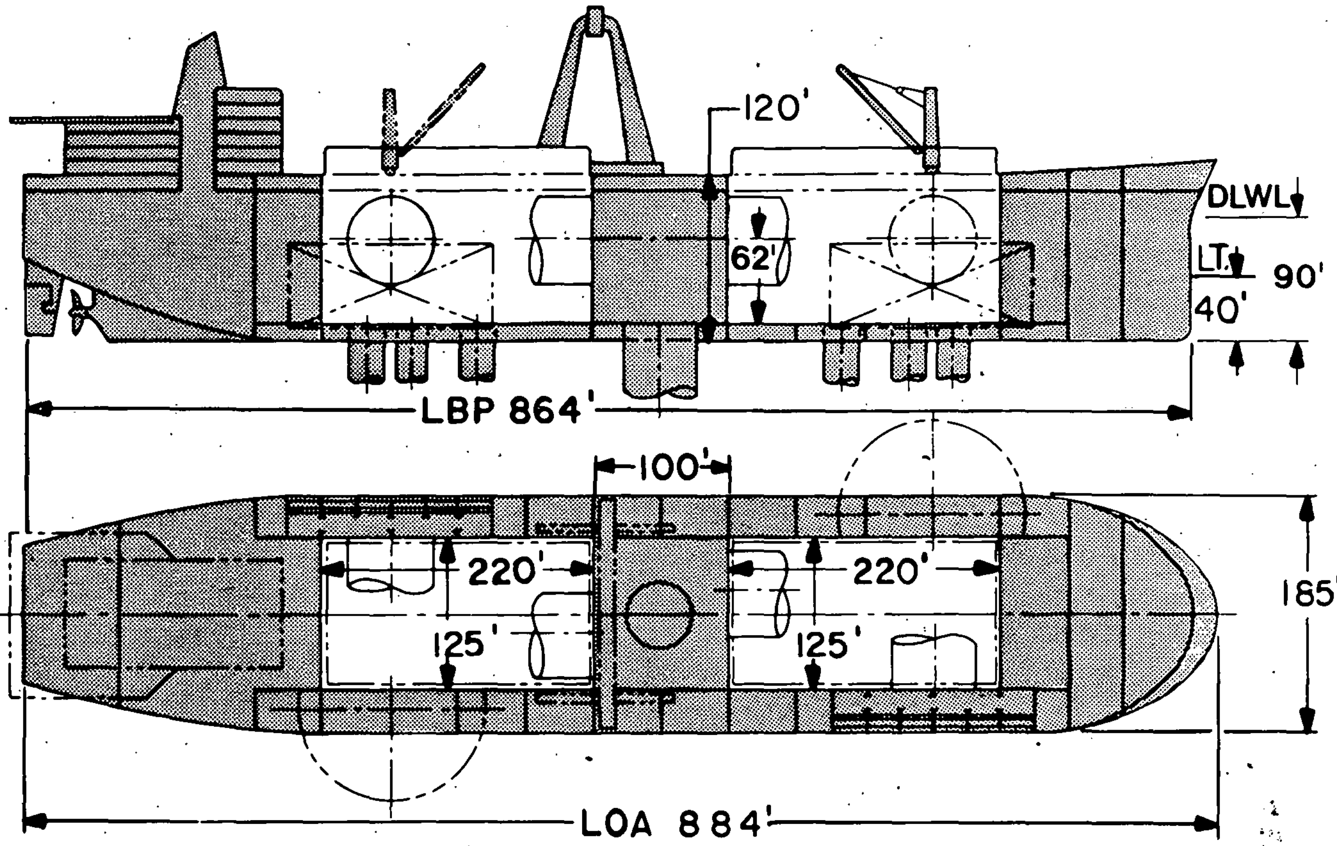

Figure 1-20
SHIP-SHAPE 100 MWe ARRANGEMENT

1.5 Conclusion

The OTEC power module concept is technically feasible. The designs and concepts are consistent with state-of-art technical knowledge; the manufacturing requirements can be handled by existing facilities in a manner which permits timely completion of the plans for OTEC power system deployment. In addition, a net energy analysis (which compares the life-cycle plant output energy with that required for its manufacture and operation) compares favorably with other energy-source options. (Refer to bibliography Reference 145).

The power system is designed to permit the use of high productivity, proven manufacturing techniques to provide a predictable, low cost OTEC power module through the use of relatively small tube-bundle modules in very large heat exchangers.

2 INTRODUCTION

The current directives from the Department of Energy for developing OTEC power systems call for the construction of small evaporators and condensers (test articles), followed by deployment of a 10 MWe power system which will, in turn, be followed by 50 MWe and larger plants. The results obtained by Westinghouse in the design studies of the above systems are presented.

OTEC power plant development has many facets as shown in Table 2-1. This report deals exclusively with the power system aspects. The OTEC power system cycle schematic arrangement shown in Figure 2-1 has been basic to the system configuration studied. The evaporator tube bundles, the moisture separator, and the liquid storage are all integrally contained in the evaporator shell; and the condenser tube bundles and hotwell storage are integrally contained in the condenser shell.

Table 2-1
FACETS OF OTEC POWER PLANT DEVELOPMENT

Technical	Non-Technical
Hull	Legal
Cold Water Pipe	Political
Mooring	Financial
Power Delivery	
Working Fluid	
Power System	
- Evaporator	
- Condenser	
- Turbine	
- Pumps	
- Piping and Valves	
- Controls	
- Other	
Environmental Impact	

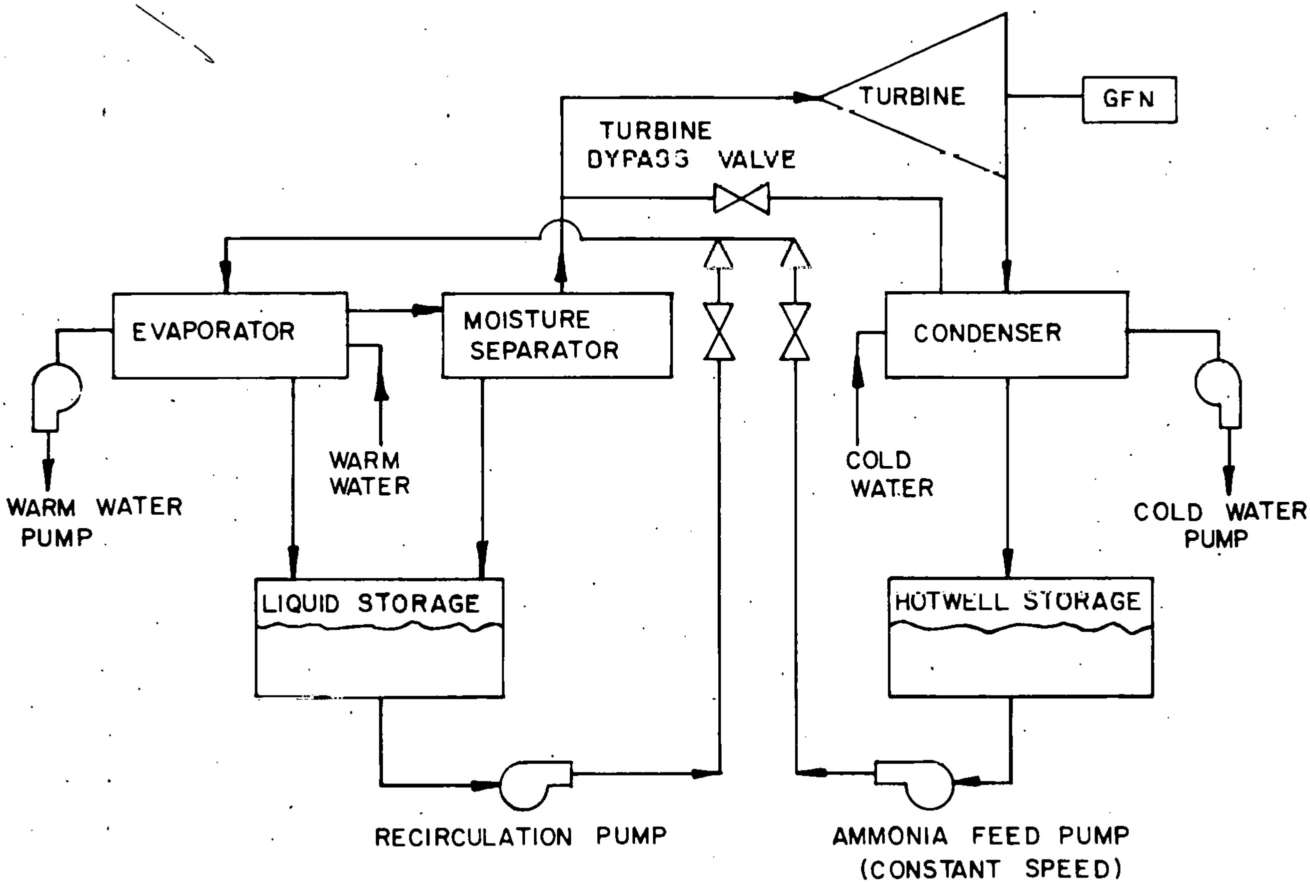

Figure 2-1
OTEC POWER CYCLE SCHEMATIC

Referring to Figure 2-1,liquid ammonia is supplied to the evaporator as a mix of condensate from the condenser hotwell and recirculated liquid from the evaporator liquid storage. The ammonia vapor, which may contain up to 10% liquid as it comes from the evaporator tube banks, flows through moisture separators from which it passes to the turbine with less than 0.1% moisture. The vapor is expanded in the turbine, after which it exhausts directly to the condenser. To minimize pressure losses, there are no control valves in the turbine inlet piping. Vapor flow to the turbine is controlled by liquid feed and recycle flow valves, and by turbine bypass valves. For very low loads and for startup operations, liquid flow to the evaporator is reduced by the feed and recycle control valves to partially dry out the evaporator, thereby reducing the quantity of vapor produced. This control is supplemented by the fine flow adjustment provided by turbine bypass valves.

Westinghouse, the prime contractor, was supported in this study by Carnegie-Mellon University, Union Carbide Corp. (Linde Division), Gibbs and Hill Inc., Middle South Services, Inc., and Dr. A.E. Bergles (Iowa State University). Westinghouse was responsible for major component design, systems engineering and economic analyses. Carnegie-Mellon University provided advanced technology heat exchanger experience and a control system dynamic model which was subsequently modified by Westinghouse. Union Carbide Corporation also provided advance technology heat exchanger experience along with tube enhancement techniques. Middle South Services, Inc. contributed knowledge of electric utility practices and operating procedures. Dr. A.E. Bergles provided tube enhancement experience. Gibbs and Hill Inc. contributed the skills and knowledge of integration of major equipment for a total power plant.

The work described in this report was performed under contract number EG-77-C-1569 for the U.S. Department of Energy. This contract covered the conceptual and preliminary design of power systems and related equipment for closed-cycle ocean thermal energy conversion (OTEC). More detailed reports written under this contract are recommended to the reader seeking greater depth of knowledge of the work performed. The titles of the pertinent reports are: <u>Phase 1 Conceptual Design Final Report</u> and <u>Phase 1 Preliminary Design Final Report</u>.

3 PROGRAM OBJECTIVES

The objectives of the work described in this report are to develop:

- Conceptual designs for 50 MWe, 100 MWe and 400 MWe power systems

- The preliminary design for a complete 10 MWe Modular Application power system

- The preliminary design for heat exchanger test articles.

The 10 MWe and test article heat exchangers are to be designed such that operating data and experience may be used for the design of larger systems, made up of 40 MWe to 50 MWe power modules. All equipment manufacturing is to be state-of-the-art; no development is required except for the aluminum alloy tubes in the test articles.

The power system design uses a closed Rankine cycle, employing ammonia as the working fluid.

The design life of the power systems is to be 30 years. The test article heat exchangers are designed for 5 years of testing.

The power system availability goal is 90%.

All auxiliaries necessary for power system installation, maintenance and operation are included in the designs. Specifically excluded from the engineering study are power system containment (hull), cold water pipe, power delivery system, and station-keeping system designs.

All of the designs generated have costs delineated for major components. The power systems cost analysis also addresses the issue of sensitivity to various parameters.

4 STUDY APPROACH

4.1 Constraints

The OTEC power modules were designed to conform to the design and functional requirements contained originally in the ERDA Request for Proposal EG-77-R-03-1400 and finally in D.O.E. Contract No. EG-77-C 03-1569, January 1978, and subsequent modifications. These constraints are summarized below.

4.1.1 Design Requirements

4.1.1.1 Energy (Ocean) Resource

Surveys of potential OTEC sites near U.S. territorial waters indicate that average available seawater temperature difference is about 36-40°F. The OTEC design point temperature difference is 40°F, operating between a warm surface water temperature of 80°F and a subsurface (3000 ft) temperature of 40°F.

4.1.1.2 Power System Containment

A surface platform/ship was used as the basic reference hull during Conceptual Design. The power system is capable of normal operation in a surface vessel under sea-state six conditions and must survive, i.e., maintain structural integrity under sea-state nine conditions.

Containment studies are currently in progress or planned for evaluating existing candidate platforms for the Early Ocean Test Platforms and the Demonstration Plant. Although available containment vessels were investigated, optimum power system design was the prime consideration.

4.1.1.3 Design Life Goals

Design life goals of the major components of the 100 MWe power system are:

- 30-year major component life
- 1000 start/stop cycles
- 6000 hrs/yr operation.

4.1.1.4 Sizing/Configuration

The design for approximate total pressure drops for the heat source and sink is as follows:

- Warm water system, 10 ft of H_2O
- Cold water system, 15 ft of H_2O

4.1.1.5 Working Fluid

The properties of anhydrous ammonia (NH_3) were used for all thermodynamic calculations.

4.1.1.6 Materials

The 100 MWe power system components have an operational life in an ocean environment (salt water corrosion, biofouling, etc.) consistent with the design life goals noted above.

4.1.1.7 Biofouling

Biofouling of heat exchangers must be controlled not to exceed a fouling factor of .0005 hr-ft^2-°F/BTU, to ensure that at least minimum economic levels of plant performance are maintained.

4.1.2 Functional Requirements

4.1.2.1 Handling and Installation

Consideration was given to transportation, to general shipyard constraints for material handling, and to installation.

4.1.2.2 Startup/Shutdown

The auxiliary starting power and operational auxiliary power were quantified.

4.1.2.3 Control and Instrumentation

Design of the OTEC power system includes transient characteristics and component response.

4.1.2.4 Safety

Human factors (heat, light, ventilation, adequate exits, etc.), are consistent with recognized standards (ABS, U.S. Coast Guard). Other factors such as fire-hazard, explosion hazard, development of toxic compounds, electrical hazards, etc., were considered. All designs are fail-safe.

4.1.2.5 Maintenance

Redundancy is provided to ensure continuity of operation of critical functions (e.g., controls, lubrication, cooling). Provisions were made for efficient maintenance during downtime of critical equipment.

4.2 Study Logic

Many design parameters affect the performance and cost of an OTEC power module. How they are treated depends on their characteristics.

The selection of tube material and the method of biofouling control can be made independently of the other system variables, since these choices are primarily dependent on the present or projected state of technology as related to the environment and objectives of the OTEC power system.

The remaining parameters are strongly interdependent and must be optimized together. These are module size, temperature drop allocations between heat exchangers and turbine, water velocities in the heat exchanger tubes, shell length and diameter, and type of enhancement on the tubes (which affect heat transfer, pressure drop and cost). A computerized system optimization program has been developed to determine the optimum combination of these interacting parameters.

Candidate designs generated by the design optimization program were evaluated with respect to technology constraints, hull constraints, operability, producibility and cost. The optimization program was periodically refined, based on the evaluations. Module sizes up to 100 MWe were considered. The study logic is illustrated in Figure 4-1.

4.3 Approach to Commercialization

The scope of the study included:

- Conceptual design of a commercial size power system between 40-50 MWe (net).
- Preliminary design of a 10 MWe net modular application power module with titanium tubes, analogous to the commercial size power module.
- Preliminary design of a heat exchanger test article.

The 40-50 MWe power system module, conceptually designed in accordance with the logic in paragraph 4.2, proved to be the most economical building block for larger commercial plants of 100-400 MWe net power output.

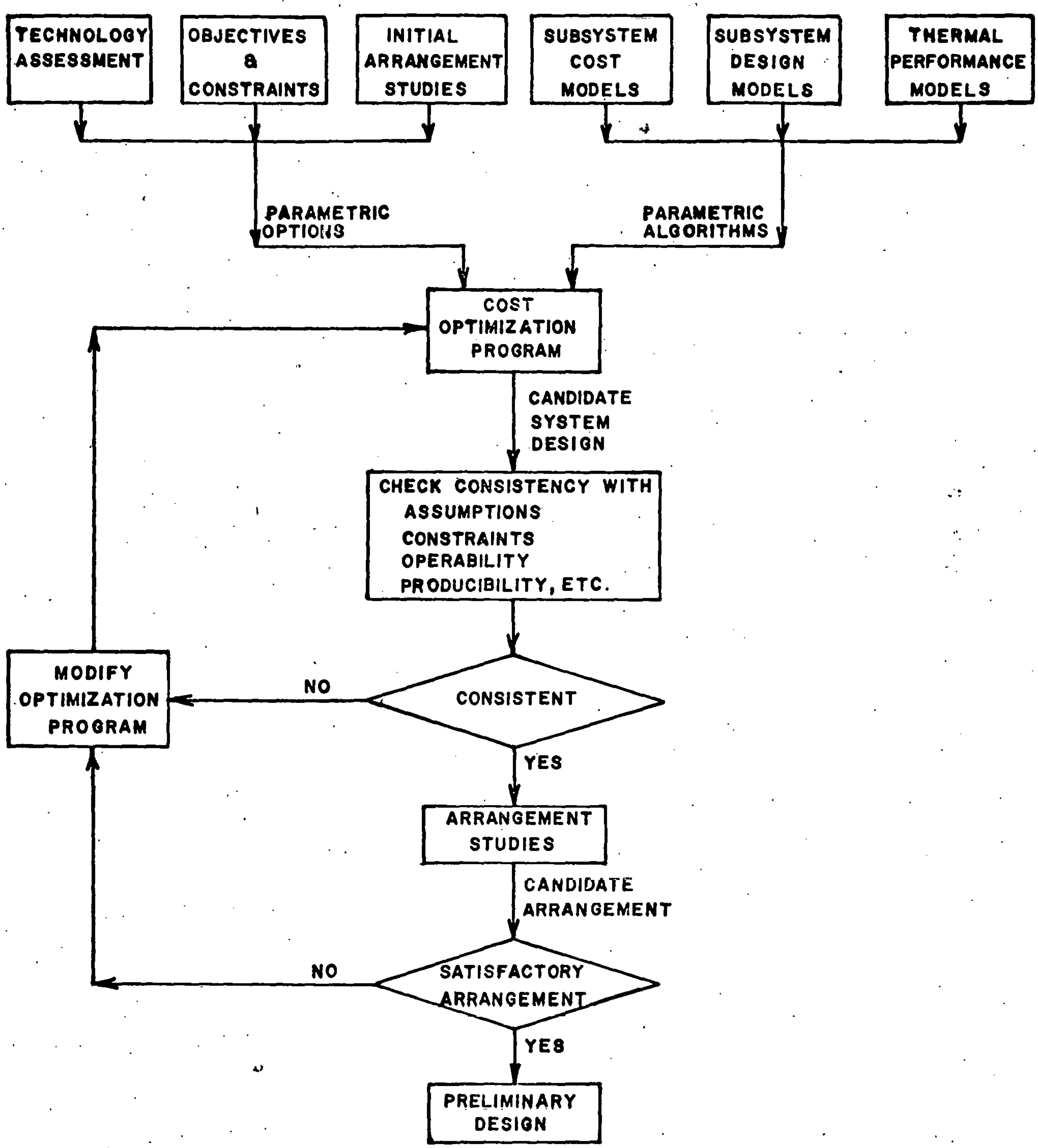

Figure 4-1
STUDY LOGIC

The Modular Application power system configuration was designed to model the commercial plant module, and its component and subsystem details were developed accordingly. Its 10 MWe size will be manageable with respect to cost, fabrication, and test operations. Yet, it will provide credible verification of thermodynamic and mechanical design and performance through its provisions of operating data and experience. Design verification will provide the confidence required to scale-up the design to demonstration plant size.

Because the tube bundles for the 10 MWe plant are thermodynamically and structurally equivalent to those of larger or commercial-sized plants, the 10 MWe heat exchangers model the larger heat exchangers. The 10 MWe turbine models the 40 MWe turbine in terms of thermodynamic, structural, and vibration characteristics because it is a one-half size, double-speed version of the larger machine. The 10 MWe turbine characteristics may be related to 50 MWe characteristics by a small extrapolation from the directly scaled 40 MWe turbine design.

The major components for both a 10 MWe Modular Application power module and a 50 MWe module suitable for use in commercial plants of 100 MWe to 400 MWe size have been designed so that they can be fabricated in manufacturing facilities with currently available machine tools. Also, with the exception of concrete platforms in the 400 MWe size, platforms can be constructed, and most of the power plant components and auxiliary systems can be installed and given preliminary operational checks in existing shipbuilding facilities.

The recommended test article configuration was determined using a different logic process. Initial hull constraints and test objectives focused on an approximate size. A heat exchanger model trade-off, which considered modeling characteristics confidence level versus cost, was used to determine the recommended configuration.

The project approach is diagrammed in Figure 4-2.

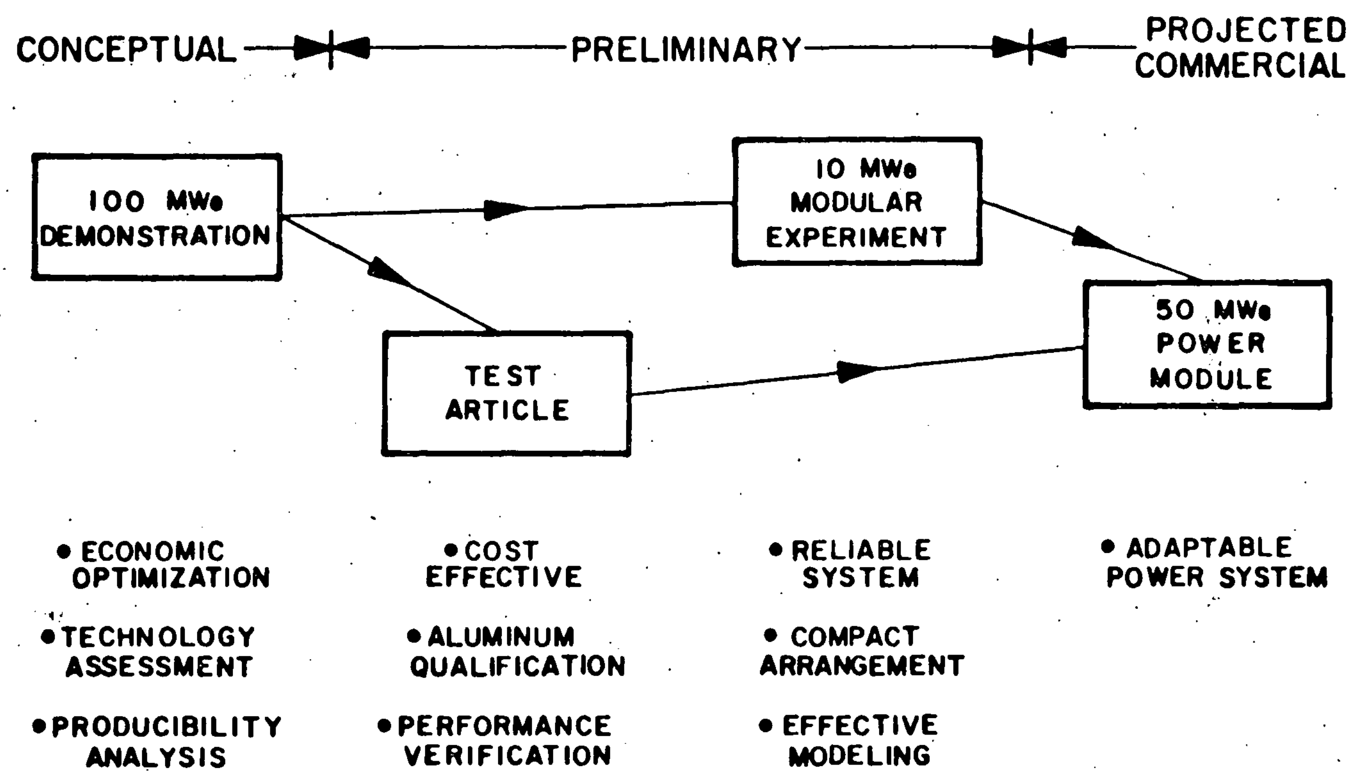

Figure 4-2
PROJECT APPROACH

5 TEST ARTICLES

5.1 Approach to Design

5.1.1 Objectives

A primary concern in the OTEC Program is scale-up to large heat exchangers and the magnitude of installation needed to demonstrate economic feasibility on a commercial scale (50 MWe modules in a 400 MWe plant). It is imperative, therefore, to devise test articles to verify thermodynamic and mechanical performance of the design concept envisioned, developing operating data and experience to:

- Provide solutions to critical issues
- Confirm design decisions
- Verify design algorithms to permit scaling to larger sizes
- Define a cost effective tube material
- Establish operating procedures

In choosing a model concept and size, platform constraints and cost must be balanced against benefits expected, for a reasonable solution. Westinghouse has developed a cost-effective test article system that addresses the basic needs delineated above. The design also incorporates modular structural features of the prototype commercial plant to demonstrate that required manufacturing operations are indeed within current capabilities. A perspective view of the test article system is shown in Figure 1-1.

The evaporator test article includes:

- Full size tubes and tube pitch
- Near full height bundle (90% of demonstration size plant)
- Twenty columns of tubes to eliminate end effects for establishing full vapor distribution around tubes
- Exact tube side seawater velocity
- Variable full range liquid and vapor recycle capability (above and below design) permitting:
  - Optimization of vapor velocity in lanes
  - Study of liquid deflection
  - Optimization of tube loading.
- Adjustable baffle to further control lane velocity
- Compartmentalized liquid chambers above and below the bundle to study ammonia migration through the bundle
- Integral separator with full width and height vanes (demonstration plant size)
- Variable approach velocity to separator lanes
- Integral drain tank
- Tube support spacing scaled exactly and off-design vapor velocity capability for tube vibration study
- Fast-acting feed control valves to verify dry-out rates of NH_3 inventory under all conditions of operation

- Numerous manways and sight ports for maximum accessibility
- Unit shippable by rail or truck.

The condenser test article includes:

- Full size tubes and tube pitch
- Forty-eight columns of tubes to eliminate end effects and to establish full vapor distribution around tubes
- Exact tube side seawater velocity
- Scaled vapor path to vent pipe to study removal of non-condensibles
- Off-design condensing capability
- Tube support spacing scaled exactly and off design velocity capability for tube vibration study
- Integral hotwell
- Numerous manways and sight ports for maximum accessibility
- Unit shippable by rail or truck.

The overall performance will be determined by monitoring the inlet and outlet fluid properties (temperature, pressure, flow) on each side of the heat exchangers. Of further interest, temperature traverses, both of the fixed and variable types as required, will be made near the tube entrance and exit to ascertain any variation of individual tube loading from the assumed uniform tube flow. This approach has been used by Westinghouse and others with success[1,2]. Variation of tube loading is of particular interest in the evaporator to assure that complete wetting of the tube surface is occurring at all modes of operation. Particular attention will be given to verifying constants in heat transfer correlations to perhaps reduce surface requirements and costs for the eventual demonstration design.

The hydraulic performance will be studied in detail. The ammonia recycle pump flow will be varied to optimize the recirculation ratio and reduce the pumping losses. The ammonia recycle blower flow will be varied to study tube loading and liquid deflection. This flow variation will determine optimum vapor velocities in the unit, including: (1) bundle velocities for maximum heat transfer; (2) upper velocity limits to preclude tube vibration; (3) lane velocities; and (4) approach velocities to the separator.

The lane baffle will be adjusted to study the effect of lane velocities on the bundle performance along with liquid deflection and approach velocities to the separator.

The pressure drop on both sides of the heat exchangers will be verified to accurately predict pumping losses for the demonstration plant.

The impact of biofouling on the cost of the heat exchangers can be significant. Hence, it is imperative that rates of fouling, methods of control, and subsequent cleaning of tube surfaces be adequately defined to minimize plant cost. These tests will be a unique opportunity to observe the phenomenon under plant operating conditions at a representative ocean site. The 3-year anticipated test time will be sufficient to develop meaningful conclusions. The major areas of interest are:

- Effectiveness of continuous low level chlorination in controlling fouling resistance

- Fouling resistance from cold deep water

- Effect of fouling caused by mixing deep water with warm surface water

- Study of long-term uncontrolled fouling rates

- Parametric study of chlorination (up to double design capacity) to define minimum flows needed for adequate protection

- Effect of repeated chemical and mechanical cleaning

- Effect of smoothness and type of tube material

- Study of Amertap and MAN cleaning systems

- Environmental impact from biofouling control methods

- Study of alternative chemical methods.

Use of aluminum tubing for the test article is considered essential to evaluate the low cost aluminum alloys in relation to the much higher cost titanium and AL6X alloy types. If aluminum tubing is proved acceptable, enormous cost reductions are possible in the condenser and evaporator. The most likely alloys and materials have been identified for use in the aluminum-tube test model.

a. Tubing - Al 3003 Alclad, Al 5052 Alclad, or Al 5052, all with Linde-enhanced outside surface

b. Tubesheets - Al 5000 series explosively clad on carbon steel with Charpy "V" notch toughness of 20 ft-lbs at +10°F to ASTM A370 to essentially eliminate the possibility of brittle fracture in the carbon steel at the low OTEC temperatures

c. Tube supports - aluminum alloy

d. Tube welds - Analysis of aluminum tube-to-tubesheet welds. Table 5-1 indicates that the recessed/chambered tube weld is the recommended choice for good reliability at reasonable cost.

The materials for the remainder of the module components are the same as those used in the 10 MWe power module (Section 6).

The proper choice of tube material is paramount in heat exchanger cost. Initial cost is only one consideration; life of the tube material and subsequent retubing will significantly impact overall plant cost. Hence, careful observation of corrision, erosion, pitting, and other modes of wastage is required during testing at an ocean site under the hostile conditions anticipated. The 3-year anticipated test time will show meaningful results in aluminum and other materials being investigated.

The test articles will be fabricated with several alloys of aluminum tubing with and without teflon inside surface coating, explosively clad tube sheets, aluminum tube support plates, and a carbon steel shell. The tubes will be rolled and automatically welded to the tubesheets. In addition to the variety of component materials, "coupons" of numerous other materials will be placed in representative areas for observation.

During testing, significant parameters of the demonstration plant to be duplicated are:

- Hot and cold water regimes
- Heat transfer gradients
- Fluid velocities at all locations, in particular, in tubes and at tube inlets

- Fouling, both mineral and organic
- Erosion effects from operating velocities and cleaning methods.

Areas of particular interest in the heat exchangers are:

- Erosion
- Corrosion
- Fouling
- Susceptibility to pitting
- Evaluation of teflon coating
- Evaluation of Linde enhancement in ammonia environment
- Adequate water level in ammonia to prevent stress corrosion in carbon and low alloy steel parts throughout the system.

At various stages of testing, visual observations of parts and coupons will be conducted and recorded. For installed tubes, borescopic examination will be used. After completion of tests, samples will be removed for destructive testing and metalographic examination.

5.1.2 Trade-Off Analysis

The proposed model arrangement was chosen from seven study models of varying shapes, lengths and concepts. They were evaluated by establishing a cumulative confidence level and cost ratio for each, based on performance against numerous parameters. The seven models considered are shown diagramatically in Figure 5-1. The direction of flow of seawater, liquid ammonia, generated vapor and recycle vapor, if applicable, are indicated.

Table 5-1
ALUMINUM TUBE-TO-TUBESHEET JOINT SELECTION

Joint Type	Leak Tightness Reliability*	Inspection Reliability*	Repair Reliability*	Erosion/ Corrosion Resistance Reliability*	Total Reliability	Relative Cost	Reliability Divided By Cost
Rolled	1	1	2	1	5	0.5	10.0
Double Tubesheet	2	1	2	1	6	5.0	1.2
Integrally Grooved Tubesheet	2	1	2	1	6	1.0	6.0
Explosive Bonded	2	1	2	2	7	4.0	1.8
Fillet Weld	3	3	3	1	10	1.2	8.3
Fillet Weld With Trepan	3	3	3	1	10	1.5	6.7
Added Ring	2	2	3	1	8	2.0	4.0
Recessed	2	2	3	3	10	0.9	11.1
Recessed and Chamfered	3	3	3	3	12	1.0	12.0
Flush Weld	2	2	3	2	9	0.8	11.3

* 1 = Poor, 2 = Fair, 3 = Good

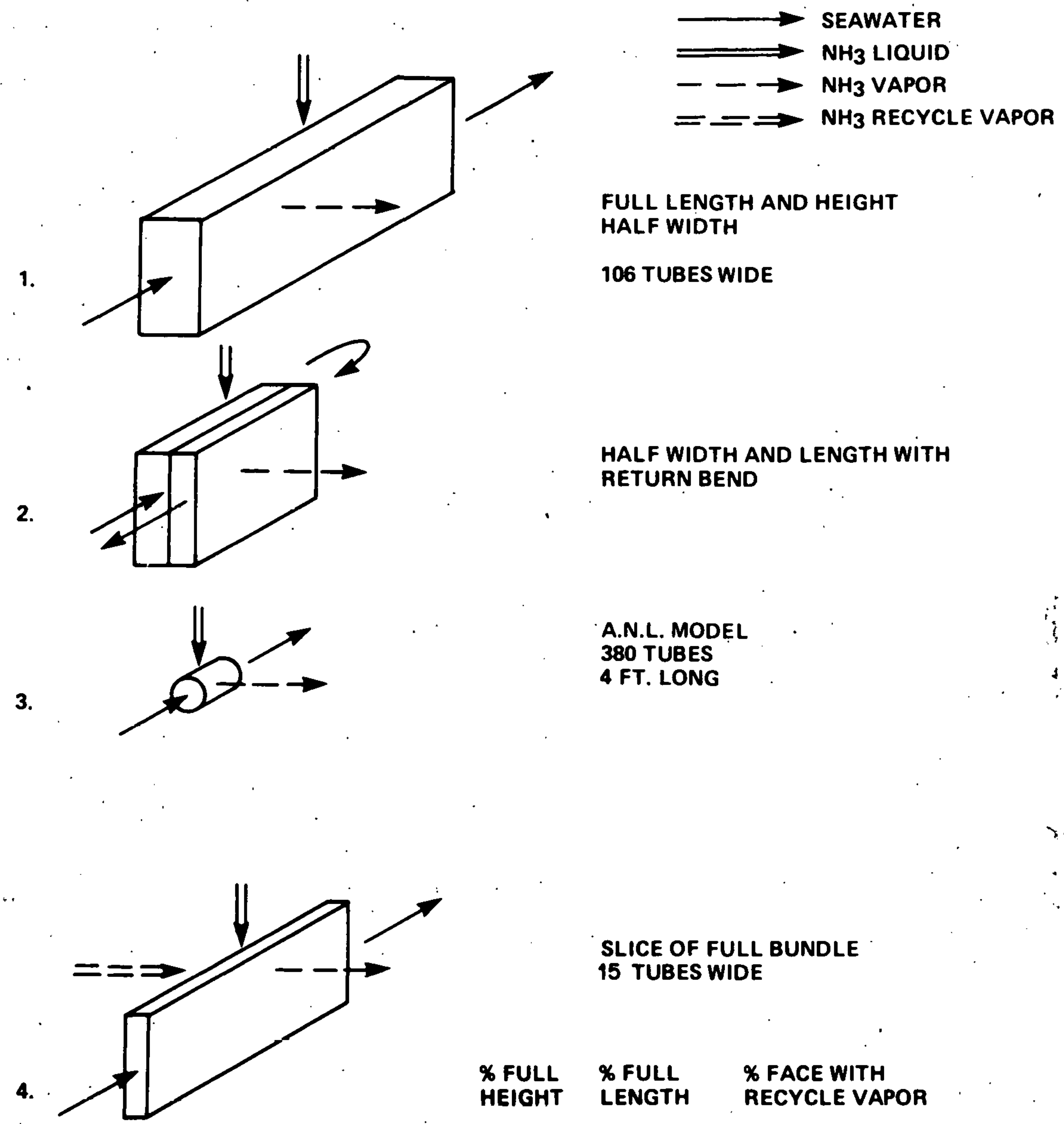

	% FULL HEIGHT	% FULL LENGTH	% FACE WITH RECYCLE VAPOR
4A.	90	100	100
4B.	90	50	100
4C.	50	50	100
4D.	90	50	30

Figure 5-1
EVAPORATOR HEAT EXCHANGER MODEL

The first model is a full-size ideal situation with a full-height and half-width bundle. Since the bundle in a prototype plant would generate vapor symetrically about its vertical centerline, a half width bundle is sufficient. The cost, fluid capacities and power requirements of this concept are high and were used as a baseline to evaluate other concepts.

The second model is a square bundle of half width and length with full height and a return bend. On the tube side, the seawater flow enters on one side, flows through half the tubes provided, reverses in a channel head on the other end, and returns through the other half of the tubes. Liquid ammonia is distributed through a tray above the bundle and is discharged from the side of the bundle. With this arrangement, a full-size model of the vapor flow path and a full length tube flow path at design velocities is provided. This model was discarded as a viable model due to excessive cost, fluid capacities and power requirements for the benefits available.

The third model is currently located at Argonne National Laboratories (A.N.L.) and is included in this analysis to evaluate whether or not existing equipment could be used to acquire the necessary data for design. This small model was discarded as a viable candidate because of concerns about vapor distribution and the ability to sense differences in seawater outlet temperature with changing conditions.

The above three models have been shown here for reference and are an indication of the upper and lower bounds of selection of a test article size. Models 4A through 4D are variations using a slice of the full-size prototype bundle. Several combinations of heights and lengths were considered to arrive at the best model size. The maximum bundle height was limited to 90% of the prototype height so that the encompassing shell diameter would be within the 12.5-foot limit required for rail shipment.

A slice of the bundle will generate far less vapor than that of a prototype bundle. With full-size tube diameters and pitch design, high enough vapor velocities could not be achieved. Consequently, a blower (with appropriate valving) was added to the heat exchanger test loop to recycle the vapor generated (see Figure 5-2). Using this concept, the design flow capacity can be achieved yielding design velocities. By opening the throttle valve leading to the condenser in the loop, the system can continue to operate with design conditions prevailing throughout.

In model 4D (Figure 5-1), the blower recycle vapor would be directed by appropriate ducting to flow only over 30% of the side face of the bundle to decrease the blower size.

Significant parameters and factors that affect test article performance, availability, and cost are delineated as follows:

- Heat transfer coefficient
  - Fluid temperatures
  - Temperature gradient along tube length
- Pressure drop
  - Tubeside velocity, length
  - Shellside velocity
- Vent design and location (for condenser)
- Liquid ammonia deflection
  - Vapor velocity and direction
  - Liquid quantity
  - Skimming velocity and direction
- Tube dryout and recycle liquid quantity
- Materials erosion/corrosion
  - Tubeside velocity
  - Temperature

        Fluid properties
- Shellside velocity
        Temperature
        Fluid properties
- Mechanical failure of Linde surface

- Biofouling
    - Tubeside velocity
        Temperature
        Fluid properties
    - Cleaning

- Tube vibration
    - Vapor velocity, direction

- Test availability

- Test equipment risk

A numerical rating system was developed to define the significance of each parameter and the confidence level that the modeling characteristics would match those of the prototype. Those ratings were applied to each test parameter and model. The tabulated results are given in Table 5-2.

By multiplying each parameter rating by each model rating number and summing, a total confidence rating for each model was obtained. Also, an approximate cost was developed for each model configuration for comparative reasons only.

As discussed previously, model 1 would provide the ideal test. Hence, each cost and confidence rating was divided by that of model 1, and a confidence level ratio and cost ratio were obtained for each model and each factor considered. The final tabulated results are shown in Table 5-3. A comparative plot for each model is shown in Figure 5-3.

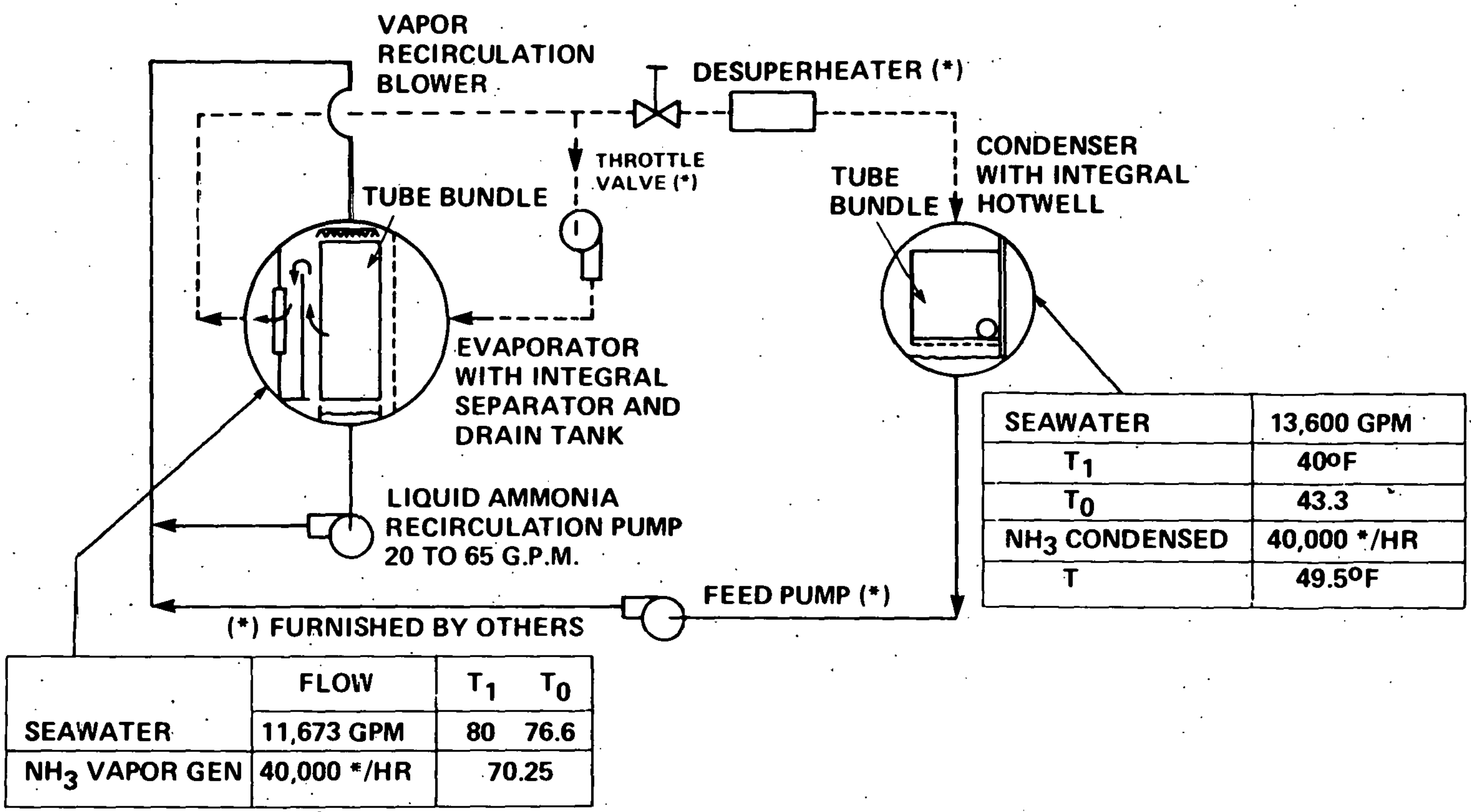

SEAWATER	13,600 GPM
T_1	40°F
T_0	43.3
NH_3 CONDENSED	40,000 */HR
T	49.5°F

	FLOW	T_1 T_0
SEAWATER	11,673 GPM	80 76.6
NH_3 VAPOR GEN	40,000 */HR	70.25

Figure 5-2
HEAT EXCHANGER TEST LOOP SCHEMATIC

Table 5-2
HEAT EXCHANGER MODEL - PARAMETER RATING

PARAMETER \ DESIGN	PARAMETER RATING	1	2	3	4A	4B	4C	4D
HEAT TRANSFER COEFF.								
FLUID TEMP.	3	4	2	1	3	3	1	2
LONG. GRADIENT	1	4	2	0	4	2	2	2
PRESSURE DROP, TUBE SIDE	1	4	3	1	4	4	4	4
SHELL SIDE	3	3	2	1	3	3	2	1
VENT	2	4	2	1	1	1	1	1
LIQUID AMMONIA DEFLECTION								
VAPOR VELOCITY, DIRECTION	3	4	2	1	3	3	2	1
QUANTITY	2	4	4	0	4	4	1	4
SKIMMING VELOCITY	2	3	3	1	3	3	2	1
TUBE DRYOUT, RECYCLE	2	4	3	0	3	3	1	3
MATERIALS, TUBESIDE VELOCITY	3	4	4	4	4	4	4	4
TEMP.	1	4	2	1	3	3	1	2
PROP.	2	4	4	4	4	4	4	4
SHELLSIDE VELOCITY	1	4	2	1	3	3	2	1
TEMP.	1	4	3	1	3	3	2	2
PROP.	1	4	4	4	4	4	4	4
MECH. FAILURE/LINDE	3	4	3	1	3	3	2	1
BIOFOULING TUBE SIDE VELOCITY	2	4	4	4	4	4	4	4
TEMP.	1	4	2	1	3	3	1	2
PROP.	3	4	4	4	4	4	4	4
CLEANING	2	3	2	1	2	2	2	2
TUBE VIBRATION								
VAPOR VELOCITY, DIRECTION	3	4	3	1	3	3	2	1
TEST AVAILABILITY	3	3	3	3	1	3	3	1
TEST EQUIPMENT RISK	3	3	3	3	1	3	3	3

Table 5-3
HEAT EXCHANGER MODEL - COMPARISON STUDY

DESIGN	1	2	3	4A	4B	4C	4D
CONFIDENCE RATING	179	140	88	141	151	115	109
CONFIDENCE LEVEL RATIO	1.0	.78	.49	.79	.84	.64	.61
COST RATIO	1.0	.65	.02	.27	.15	.08	.15

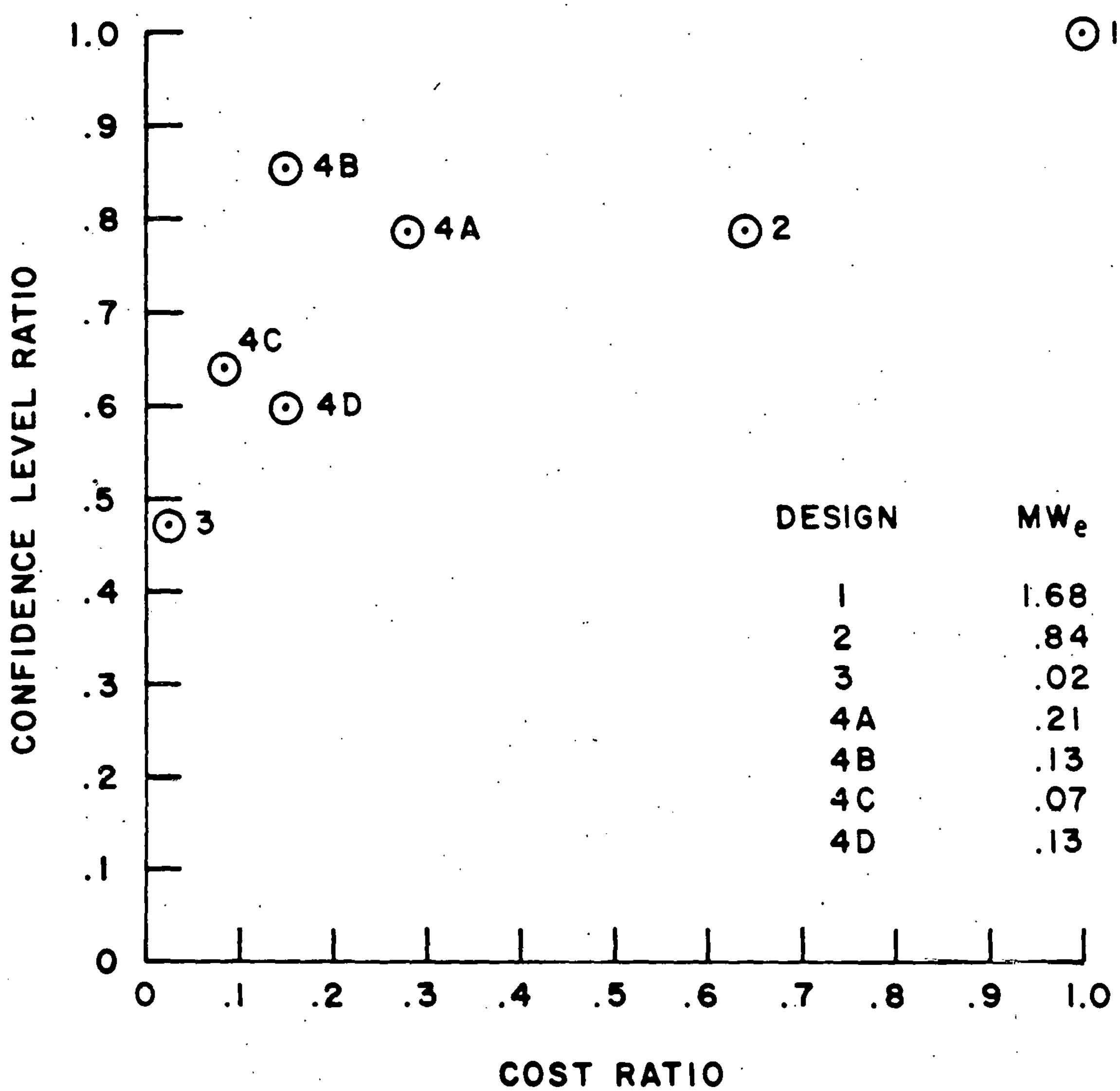

Figure 5-3
HEAT EXCHANGER MODEL CONFIDENCE LEVEL RATIO VS. COST RATIO

A review of Figure 5-3 indicates that model 4B is the prudent choice. Its confidence level is second only to the high cost ideal --model 1. Although model 4C is somewhat lower in cost, its confidence level is significantly lower than the recommended model 4B.

5.2 Design Description

5.2.1 System Schematic

A system schematic is illustrated in Figure 5-2. Liquid ammonia supplied to the evaporator is a mix consisting of the condensate from the condenser hotwell and recirculated liquid ammonia from the evaporator integral drain tank. Within the evaporator shell, ammonia vapor is generated, mixes with recycled vapor, and flows over a lane baffle to the vapor separator. The vapor may contain up to 10% moisture at this point. It exits from the separator and enters the vapor recirculation blower at a pressure of 129 PSIA with about 0.1% moisture. The throttle valve will remain closed until the desired quantity of vapor is generated to achieve vapor design flow through the evaporator bundle. At this time, the valve is opened sufficiently to discharge only model design flow--about 40,000 lb/hr--to the condenser.

5.2.2 Heat Exchangers

The evaporator test article recommended is illustrated in Figure 5-4. The evaporator has a 12.5-foot carbon steel shell with 900 one-inch diameter x 0.065-inch wall aluminum tubes. The overall length is 21.5 feet. An integral separator and a drain tank are included within the shell.

Seawater enters a 30-inch diameter inlet nozzle in a neoprene coated carbon steel channel head and flows through the tubes at 7 ft/sec., exiting through an identical channel head on the other end.

Recycle vapor enters a 24-inch diameter nozzle in the shell, passes through a flow distributor plate and over five columns (60 tubes per column) of flow distribution inactive aluminum tubes (300 total) which assure proper distribution of the recycled vapor, then through 15 columns of active aluminum tubes. After leaving the bundle, the total vapor flow passes over the lane baffle through the separator vanes and exits through a 24-inch diameter nozzle.

The lane baffle provided between the bundle and separator can be adjusted to vary lane velocities from 6 to 17 ft/sec.

Ammonia liquid enters the top through nine nozzles feeding the nine compartments in the flow distribution chamber. Nine collection chambers and outlet nozzles are similarly placed at the bottom.

A unit support (not shown) will be designed to conform to the site conditions when details are supplied.

The condenser test article proposed is illustrated in Figure 5-5. The condenser has an 8-foot carbon steel shell with 1223, 1-inch diameter by 0.65-inch wall aluminum tubes. The overall length is 24 feet. An integral hotwell is included within the shell. Seawater enters a 30-inch diameter inlet nozzle in a neoprene-coated carbon steel channel head and flows through the tubes at 6.5 ft/sec, exiting through an identical channel head on the other end.

Ammonia vapor enters a 24-inch nozzle, passes over the tube bundle, and condensate exits through a 6-inch diameter drain nozzle. By placing a baffle on one side and appropriately choosing the bundle dimensions, a scaled vapor path to the 2-inch vent pipe has been achieved.

5.2.3 Thermal and Hydraulic Design

Thermal and hydraulic features of the heat exchangers were identified and are duplicated or simulated in the test articles to be installed in the

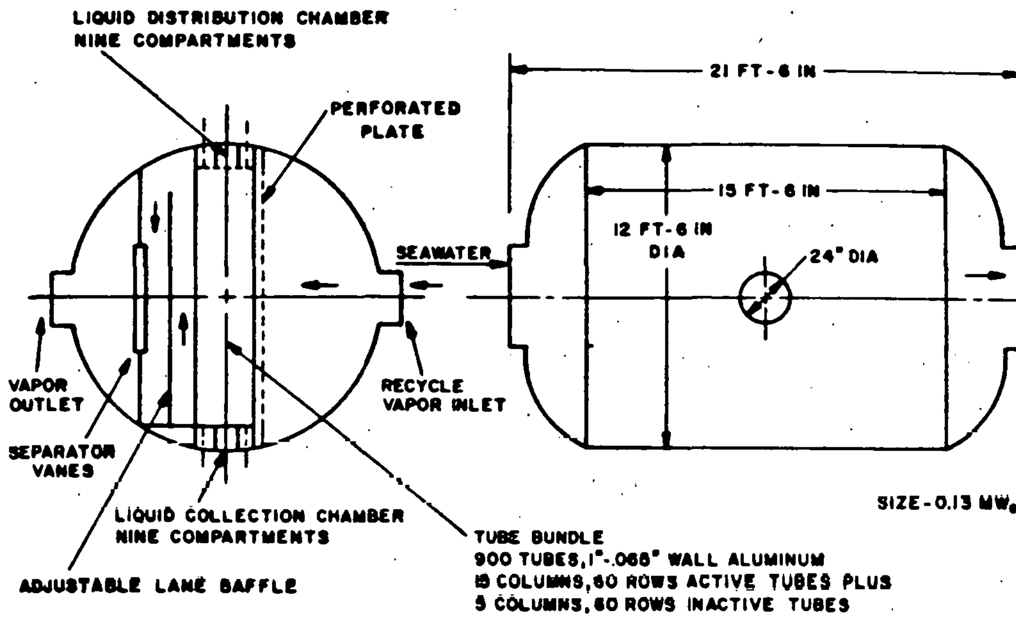

Figure 5-4
EVAPORATOR TEST ARTICLE HEAT EXCHANGER

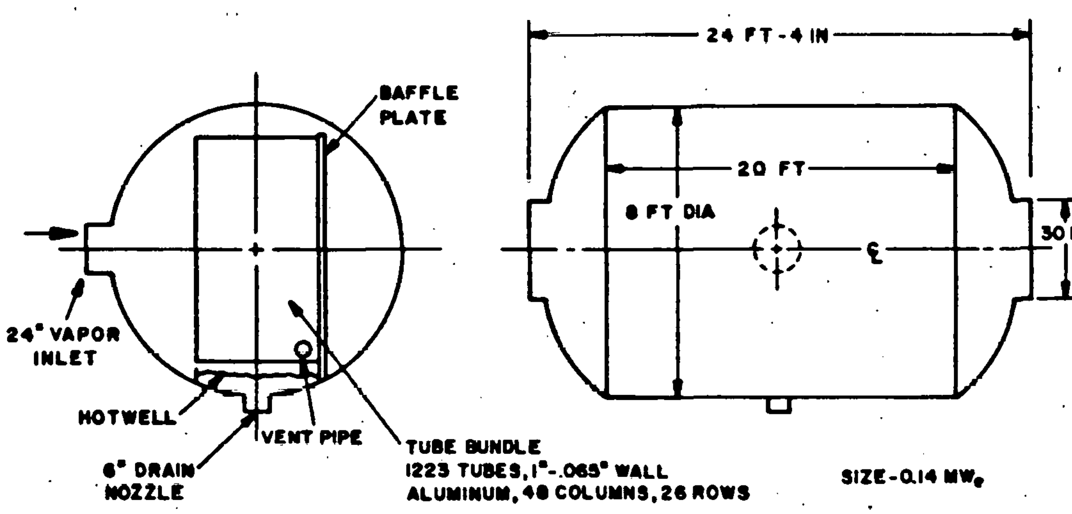

Figure 5-5
CONDENSER TEST ARTICLE HEAT EXCHANGER

OTEC-1 platform. Definitions and brief explanations of the areas in which investigations will be pursued follow:

5.2.3.1 Tubeside (Seawater) Heat Transfer and Pressure Drop

This is to provide a verification of the more or less conventional correlations used.

5.2.3.2 Shellside (Ammonia) Heat Transfer and Pressure Drop

The test articles, mounted on the OTEC-1 platform, will have the capability of duplicating the actual ocean environmental temperatures anticipated for the demonstration plant. The verification of the design algorithms will be obtainable under actual conditions.

5.2.3.3 Shellside Vapor Lanes

The size and location of the shellside (NH_3) vapor flow lanes for the best vapor distribution, minimum power loss, and avoidance of high vapor velocity areas will be determined. In both the evaporator and condenser, high vapor velocities can cause flow-induced vibration. The limits of these velocities will be investigated so that structural integrity will be maintained. Variable velocities are obtained through a moveable plate adjacent to the evaporator bundle and by the excess vapor flow capability. In the evaporator, excessive velocities can result in moisture entrainment and carryover to and from the separator elements. Sufficient excess vapor capability is available in the test articles to create velocities well above those realized in the demonstration system. It is anticipated that a realistic safe operating range will be obtained for the components.

5.2.3.4 Moisture Separators

Separator effectiveness as a function of vapor velocity and moisture content will be determined to establish maximum and minimum thresholds for satisfactory operation.

5.2.3.5 Liquid Drain Trays

The operation of the liquid NH_3 drain trays in the evaporator and condenser will be confirmed, since the test articles will be subjected to real sea-site conditions. Extrapolation to the limiting sea states can then be made with more certainty.

5.2.3.6 Vent System

The condenser scavenging vent operation was simulated, and the design of a suitable system will be obtained. The scavenging system will ensure that all areas of the bundle operate to maximum potential.

5.2.3.7 Liquid Distribution Trays

The evaporator distribution system will have sufficient liquid NH_3 capacity to verify the required liquid head, hole size, and location in the distributing trays. This investigation will ensure that all tubes receive sufficient liquid NH_3 to avoid "dry out", but not be subjected to excessive flooding. In addition, the trays will compensate for the axial temperature differential effects where the boiling heat flux of the warm end may be two to five times that of the cool end. As a result of this area of investigation, a minimum recycle rate will be obtained. This rate will lead to minimum NH_3 pumping cost and minimum liquid holdup in the bundle which is available for flashing under pressure fluctuations. Holdup will be minimized to assist in the normal control system operation and, more critically, overspeed control system operation.

5.2.3.8 Liquid Distribution Mode

The determination of NH_3 droplet type and size distribution in the evaporator shell and also within the bundle confines will probably be made by visual observation, since quantitative data will be extremely difficult to obtain. Verification of the column mode of distribution is expected.

5.2.3.9 Effect of Included Water

The effect of included water on the enhanced evaporator surface will be determined. A small (0.2%) percentage by weight of water is added to the ammonia to aid in the prevention of stress corrosion in the turbine and pump systems.

The quantity of water is greatly increased on the evaporator enhanced surface because of NH_3 evaporation and the concentration of included water. The effect of this water on heat transfer performance will be investigated. It is possible that water remaining in or on the surface after a short down period may require some time to be diluted and displaced by NH_3 before full evaporating potential is reached.

5.2.3.10 Deflection of Liquid in Bundle

The deflection of the liquid NH_3 falling from tube to tube in the evaporator will be investigated. The vapor generated in the bundle flows in a direction generally normal to the falling liquid sheets, columns, and drops. The result is that the deflections of the liquid could, at certain vapor velocities, be sufficient to prevent it from hitting the next lower tube. Should this occur, a potential for "dry out" could exist. To determine the deflection effect, the test article distribution and drain tray is compartmented width and lengthwise such that a pattern may be obtained. This, along with the excess vapor flow capability, will substantiate the data used in the design.

5.2.3.11 Liquid Film Stripping

The velocity limits which will avoid the actual stripping of the liquid film from the tubes in the evaporator bundle is to be investigated. This problem is related to the liquid deflection problem but has an additional effect in that the liquid stripped away could be in the form of droplets small enough for entrainment and "carry over" from the bundle.

5.2.3.12 Operation Procedures

Procedures and operating limits, if any, will be established for startup, shutdown and nominal operational modes.

5.2.3.13 Off-design Capability

The test articles and the fluid flow rates and temperatures are sufficiently variable to verify off-design operation.

5.2.3.14 Test Article Capacity

The test article heat exchangers as proposed will have the capability of varying the ammonia vapor flows by recycling from a minimum to well beyond design rates. The liquid ammonia recycle rate is also available. The vapor lane velocity effects are varied by changing the position of a moveable plate. Velocities ranging from approximately 6 to 17 ft/sec are available. The test articles are thermally and hydraulically identical or similar to both the 10 MWe Modular Application Plant and the Demonstration Plant. These points are covered in more detail in the 10 MWe Modular Application section on thermal and hydraulic design (Section 6.2.1.1).

Approximate design points about which the test article capabilities were established are presented in a typical sample evaporator and condenser design.

5.2.3.15 Fouling Determination Control Loop

The performance of the evaporator and the condenser is affected to a large extent by the resistance to heat transfer caused by the deposit of scaling products and bio-slime on the tube surfaces exposed to seawater.

Since it is impractical to remove and replace tubes in the test articles, a modified ASME - Power Test Code - 12.2 test is proposed.

To evaluate the rate of increase of the fouling effect, the heat transfer of control tubes will be measured and compared with the bulk test article tubes. The control tubes in both test articles will be isolated from the seawater flow by substituting a separate closed pure water loop.

The pure water loops will consist of a supply tank, circulating pump, flow measuring device, control valve and a means of balancing the heat transferred. See Figures 5-6 and 5-7. For a direct comparison, the water velocity and inlet temperatures must match the corresponding seawater conditions very closely.

The degree of tube fouling will be determined by evaluating the cleanliness factor (defined as the ratio of the thermal transmittance of the test article tubes to that of the control tubes) while operating under identical conditions of seawater temperature and velocity, and the same external vapor temperature and flow.

An in-line heater is required for the evaporator loop to replace the heat lost in the evaporation process. The condenser loop will require an in-line cooler to remove the heat gained in the condensing process.

By continuous comparison of the heat transfer of the pure water with the seawater loops, the rate of performance degradation of the test articles due to the increase of fouling resistance will be determined.

The following equipment is required for the test loop:

a. Platinum resistance bulbs, wells, and temperature indicators to measure tube inlet and outlet temperature of control tubes - quantity of eight
b. Bourdon pressure gages - to measure inlet and outlet deaerated water pressure to control tubes - quantity of eight
c. Flow nozzles, flow transmitters and flow indicating controllers to measure deaerated water flow rate through control tubes - quantity of two

d. Circulating water pumps - each 35 GPM, 35 ft. TDH--quantity of two
e. 100-gallon carbon steel supply tanks - quantity of two
f. 1-inch flow control valves with air diaphragm operators - quantity of two
g. 1.5-inch hand control shutoff valves - quantity of eight
h. 15-square foot heater for evaporator loop - quantity of one
i. 5-ton air cooled chiller for condenser loop - quantity of one

5.2.4 Mechanical Design

Early work by other OTEC developers has resulted in very large shell and tube units which pose costly manufacturing, inspection, shipping, and installation problems. The innovative design being offered in this report virtually eliminates size as a constraint while providing maximum shop-tested reliability. Individual tube bundles of shippable size will be inserted through the tube sheet at final assembly aboard the platform or at dockside as desired. A detail description is given in Section 6.2.1.2.

The test article design incorporates the modular structural features of the prototype. Sizes, shapes, thicknesses and materials - except for tubes - have been selected to duplicate those of the prototype design within a shell size that is shippable. Hence, the detail design and fabrication of the heat exchanger described below will verify the practicality, reliability, low cost of manufacture, assembly, and shipment of the modular design.

The evaporator test article is shown in detail in Figure 5-8. It is a simple all-welded shell and tube design. A carbon steel shell for minimum wall thickness and cost is used. At each end of the shell, an I-beam structure array is perpendicular to the shell centerline. In the approximately 15 inch x 134 inch rectangular opening on each end, a carbon steel box slightly longer than the I-beam height is inserted and welded all around to the adjacent beams. Longitudinal rails, I-beams at the bottom corners and angles at the top corners, are between the corners of

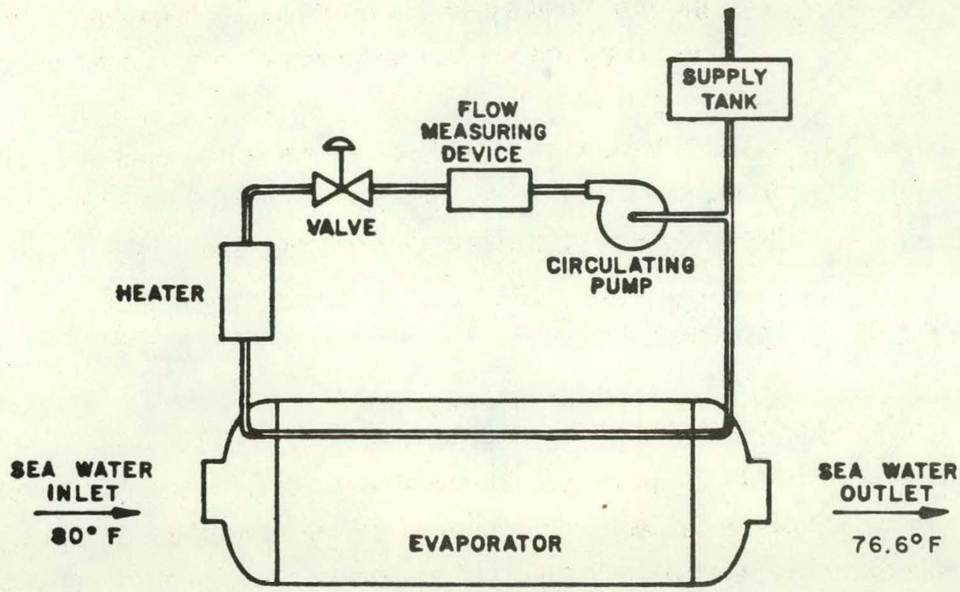

Figure 5-6
EVAPORATOR PURE WATER LOOP

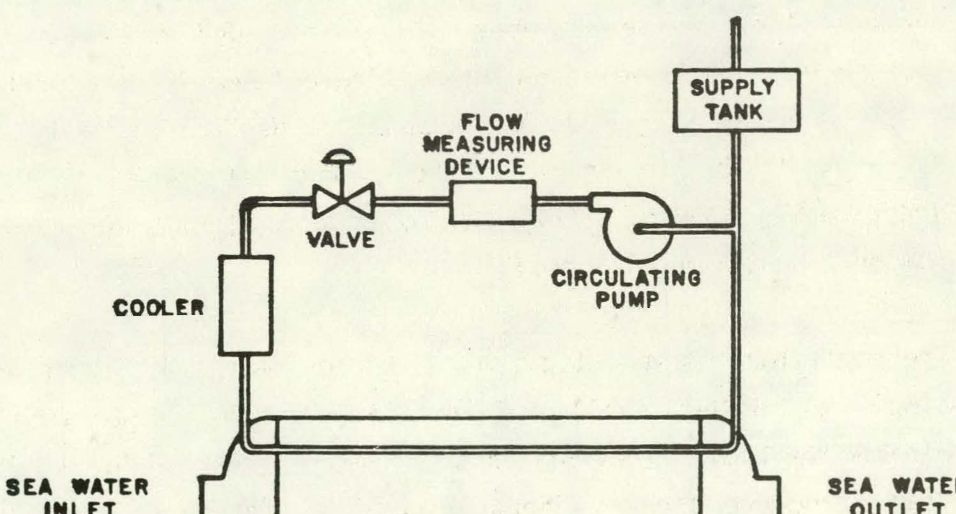

Figure 5-7
CONDENSER PURE WATER LOOP

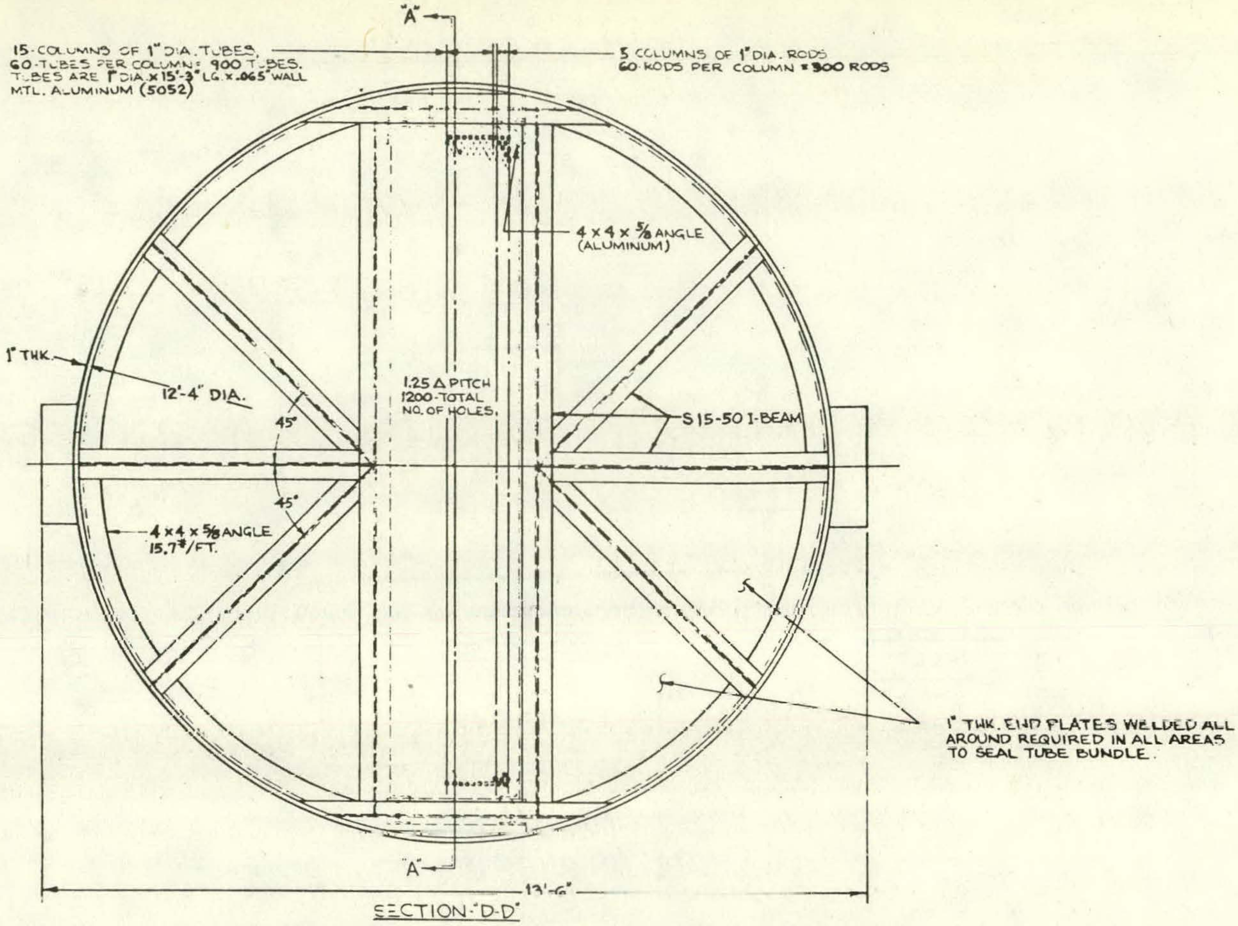

SECTION-"D-D"

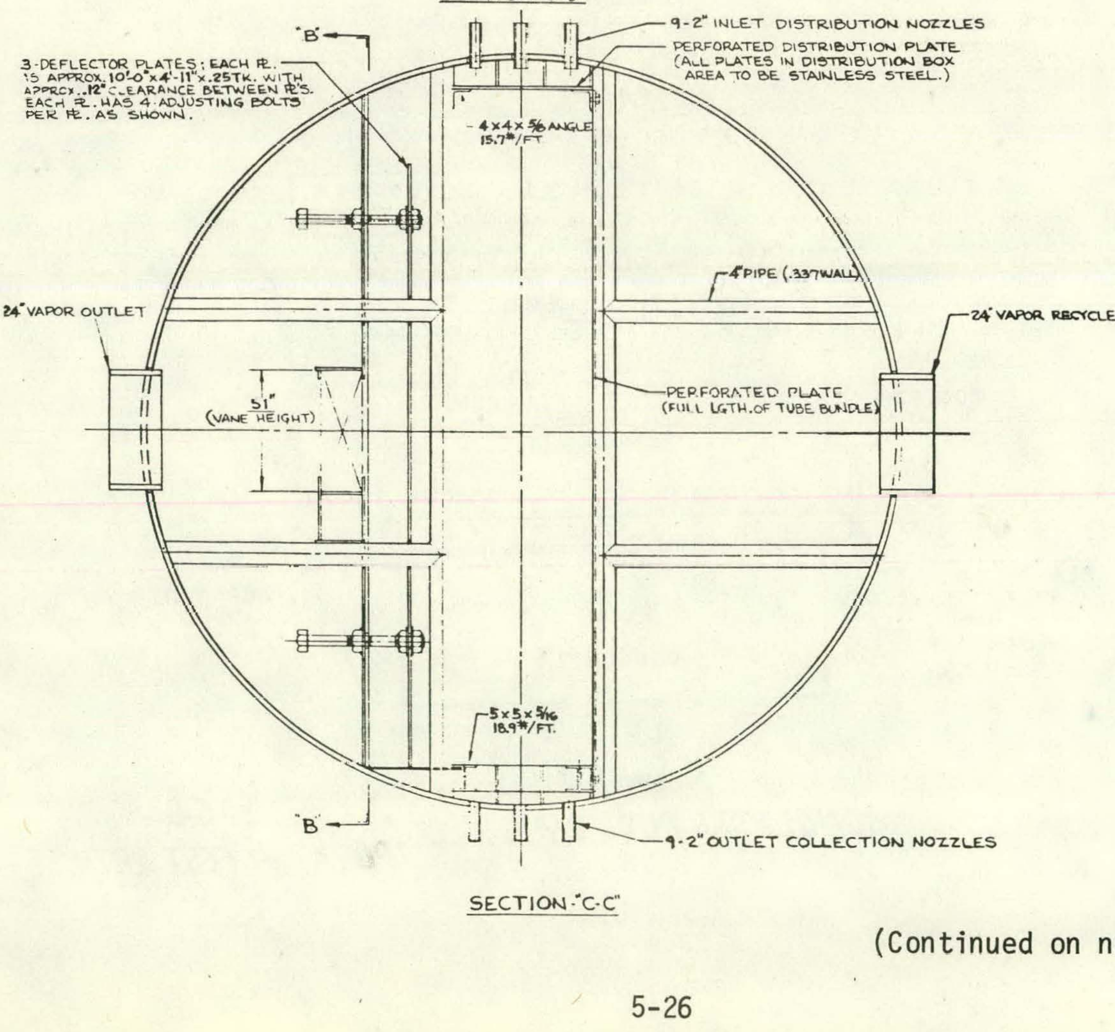

SECTION-"C-C"

(Continued on next page)

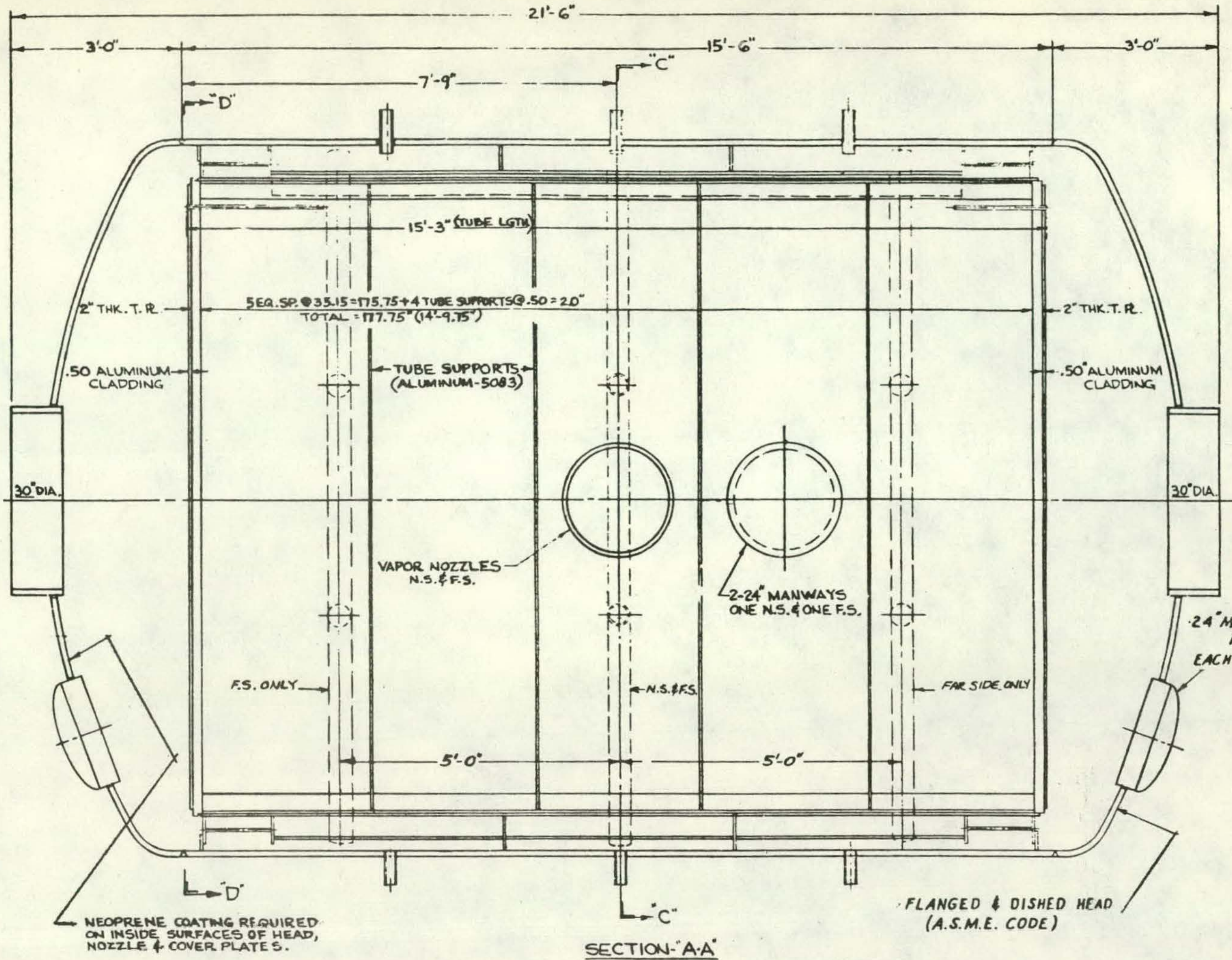

SECTION-"A-A"

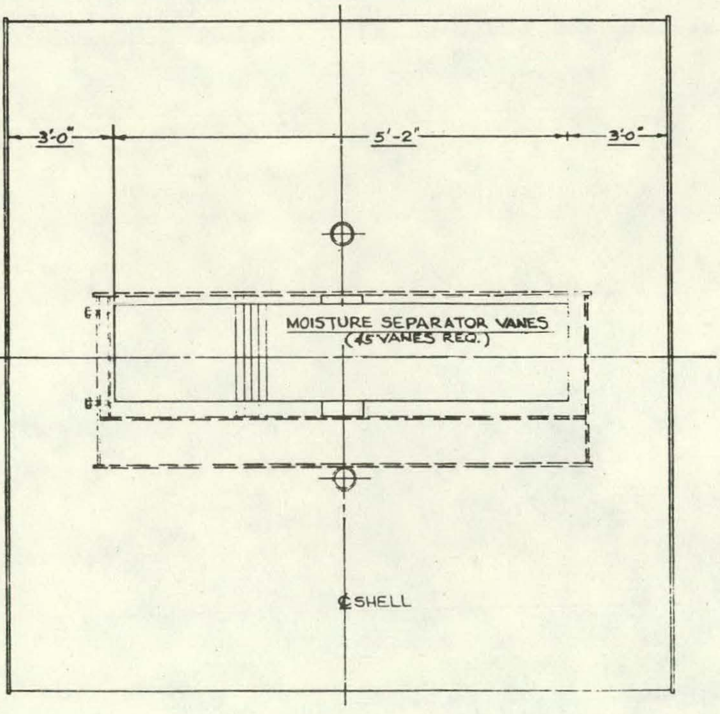

SECTION-"B-B"

(NOT TO SCALE)

Figure 5-8
EVAPORATOR TEST ARTICLE

THIS PAGE

WAS INTENTIONALLY

LEFT BLANK

each box and run the length of the shell. End plates are welded to the I-beams in the tubesheet plane to close the shell chamber in all but the rectangular opening where the assembled tube bundle is subsequently inserted. In the center of the shell, a lattice work of pipes, shown in Section C-C, supports the tube bundle at its center.

The tube bundle is constructed outside the shell. It consists of an explosively clad aluminum-to-carbon steel tubesheet at each end, nine hundred 1 inch x .065 inch wall aluminum tubes on a 1.25-inch triangular pitch, rolled and welded and rolled at each end; three hundred 1-inch diameter aluminum rods welded at each end; four intermediate aluminum tube support plates spaced 35.2 inches apart to avoid tube vibration failures; and a number of diagonal stiffeners and corner angles to form a rigid box-like bundle assembly.

Also shown in Section C-C is an enclosed ammonia distribution box. It will be constructed with nine compartments, each containing a 2-inch diameter inlet nozzle. The shell wall serves as the top of the box. The bottom will be a stainless steel plate with perforations to assure proper ammonia flow over the tubes. Below the bundle, the I-beam rails and shell wall serve as an ammonia collection tray which is also compartmentalized with nine 2-inch diameter outlet nozzles.

Shown in Sections B-B and C-C is the integral ammonia liquid-vapor separator. The 45 vanes provided are the full height required for a demonstration size plant (400 MWe). The Westinghouse patented formed vane separator shown in Figure 5-9 will be employed.

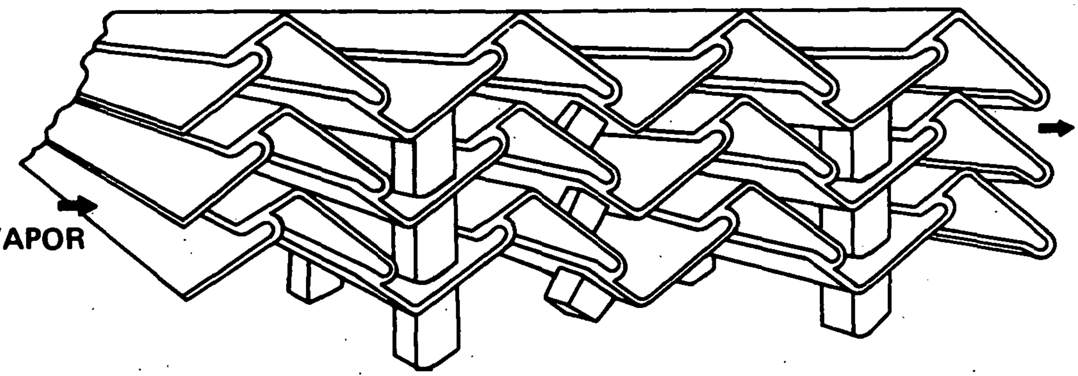

Figure 5-9
FORMED VANE SEPARATOR

A perforated plate is provided to distribute incoming ammonia vapor over the entire bundle. To the left of the tube bundle is an adjustable solid deflector plate to vary lane velocity leaving the bundle and entering the moisture separator. The deflector plate consists of three sections for ease of handling. Each section is supported on two horizontal pipes and held in position by four adjusting bolts.

At final shell assembly, the tube bundle is placed into the rectangular opening of the tubesheet on one end and pulled into the shell from the other end. Final carbon steel closure welds are made at each end box wall. With completion of these welds, a complete seal is formed between the ammonia and water sides of the unit.

After the shell is completed and inspected, the elliptical carbon steel channel heads are welded at each end and neoprene-coated on the inside surfaces up to the tubesheet edge.

Appropriate inlet and outlet seawater and ammonia vapor nozzles are provided. Also, manways, handholes, viewports, and instrumentation openings are provided in all chambers. Support designs, unit sizes, and nozzle locations will be reviewed and changed if necessary to accommodate interface compatability as defined by the System Integration Contractor.

The condenser test article is shown in Figure 5-10. It is essentially identical to the evaporator, except no separator or distribution box is required and the side baffle plate is not perforated.

One major difference is the tube bundle. The condenser tube bundle consists of an explosively clad aluminum-to-carbon steel tubesheet at each end, 1223 one-inch x .065-inch wall aluminum tubes on a 1.25-inch triangular pitch, rolled and welded at each end; five intermediate aluminum tube support plates 35.8 inches apart to avoid tube vibration failures; a 2-inch diameter vent pipe; and a number of diagonal stiffeners and corner angles to form a rigid box-like bundle assembly.

Both units have been preliminarily sized in accordance with the requirements of the ASME Code[3]. The tube support spacing is primarily dependent on shellside fluid velocity. Tube vibration due to tubeside flow effects, and acoustic and external excitation, are negligible. With low density vapor on the shell side, fluid elasticity is the primary excitation mechanism, and effects of vortex shedding and turbulent axial and cross-flow are of little importance. Hence, the critical span was calculated using Connors' criteria [4].

$$L_{CRIT} = 0.365\ \beta^{1/2} \left[\frac{E\ I\ g\delta_o}{\rho\ \mu^2_{CRIT}} \right]^{1/4}$$

Where

L_{CRIT} = Critical tube span, inches

μ_{CRIT} = Critical fluid velocity at which large scale whirling motions initiate, ft/section.

β = Dimensionless proportionality constant

δ_o = Dimensionless logarithmic decrement

ρ = Fluid density, lb-m/ft^3

E = Modulus of Elasticity, PSI

I = Tube cross-sectional moment of inertia, $(\text{inches})^4$

g = Acceleration of gravity, 386 $\frac{lb_m - in}{lb_f - sec^2}$

The OTEC heat exchangers share many mechanical and fluid flow parameters with condensing sections of existing Westinghouse heat exchangers. From experience on similar designs, with tubes clamped at each end and simply supported at each tube support plate, a critical velocity of 40 feet/second, log decrement of .036 and a β of 4.0 were used to determine the required tube support plate spacing. Actual maximum velocity is 5 ft/sec.

5.3 Manufacturing

The most critical manufacturing operations for the heat exchanger design are the welding of the tube-to-tubesheet joints and the assembly and welding of the tube bundle into the shell. In most cases, the test articles have identical structural features and sizes to the full size prototype design. Consequently, the industrial practicality of manufacturing and installing highly reliable tube bundles and heat exchangers of the modular design will be demonstrated.

Preliminary studies have been made of the manufacturing processes and sequence required to fabricate the test articles shown in Figures 5-8 and 5-10 to the requirements of The American Society of Mechanical Engineering Boiler and Pressure Vessel Code, Section VIII, Division I. These were used to establish construction feasibility and as a basis for preparing cost estimates.

A manufacturing flow diagram is shown in Figure 5-11. Key manufacturing operations are shown for major component manufacture, for subassembly, final assembly, test, and shipment of the test articles.

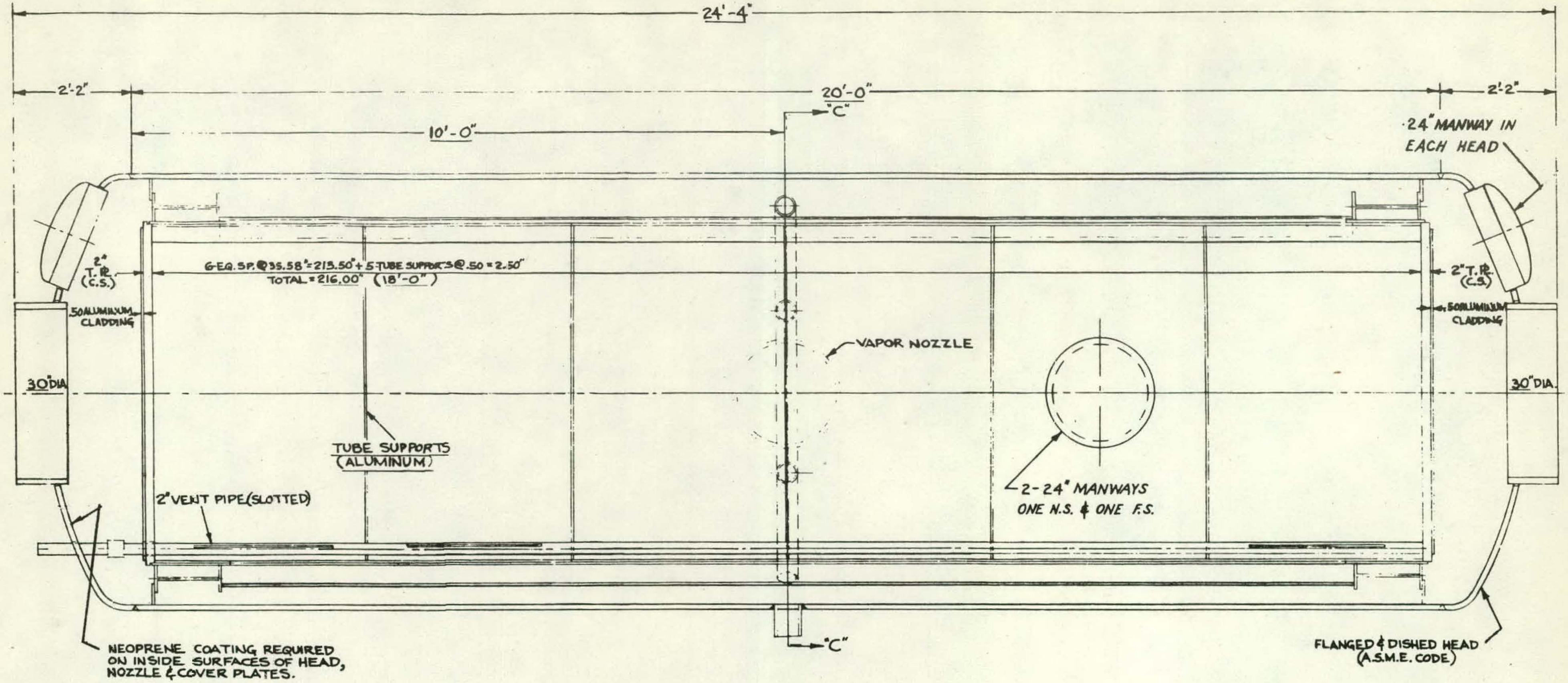

SECTION-"A-A"

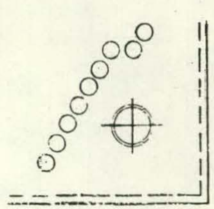

AIR VENT PIPE

Figure 5-10
CONDENSER TEST ARTICLE

(Continued on next page)

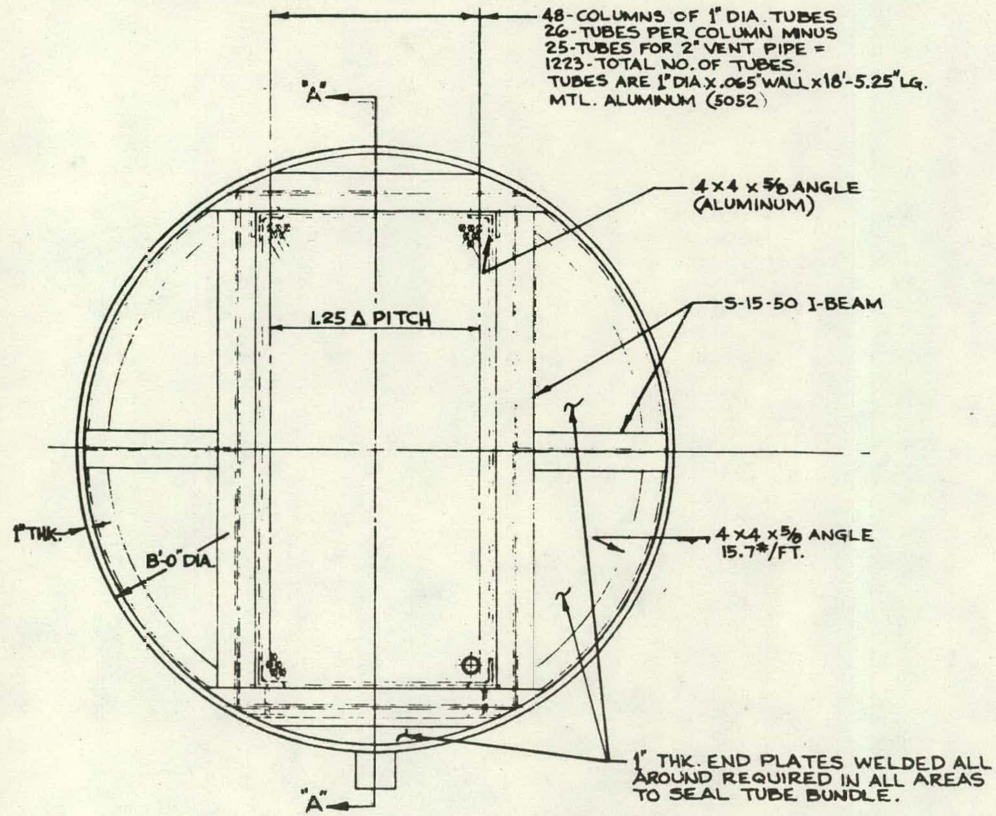

SECTION-"B-B"

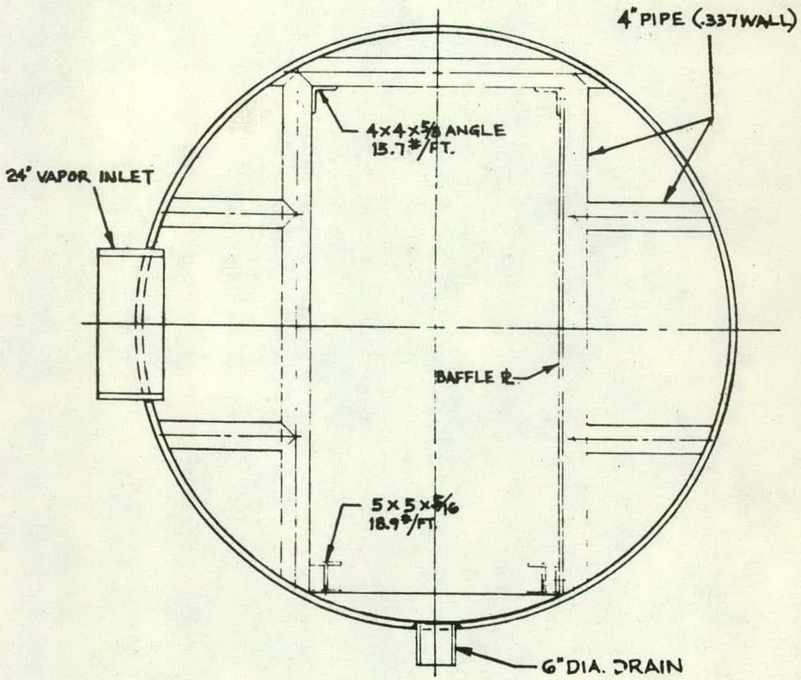

SECTION-"C-C"

THIS PAGE

WAS INTENTIONALLY

LEFT BLANK

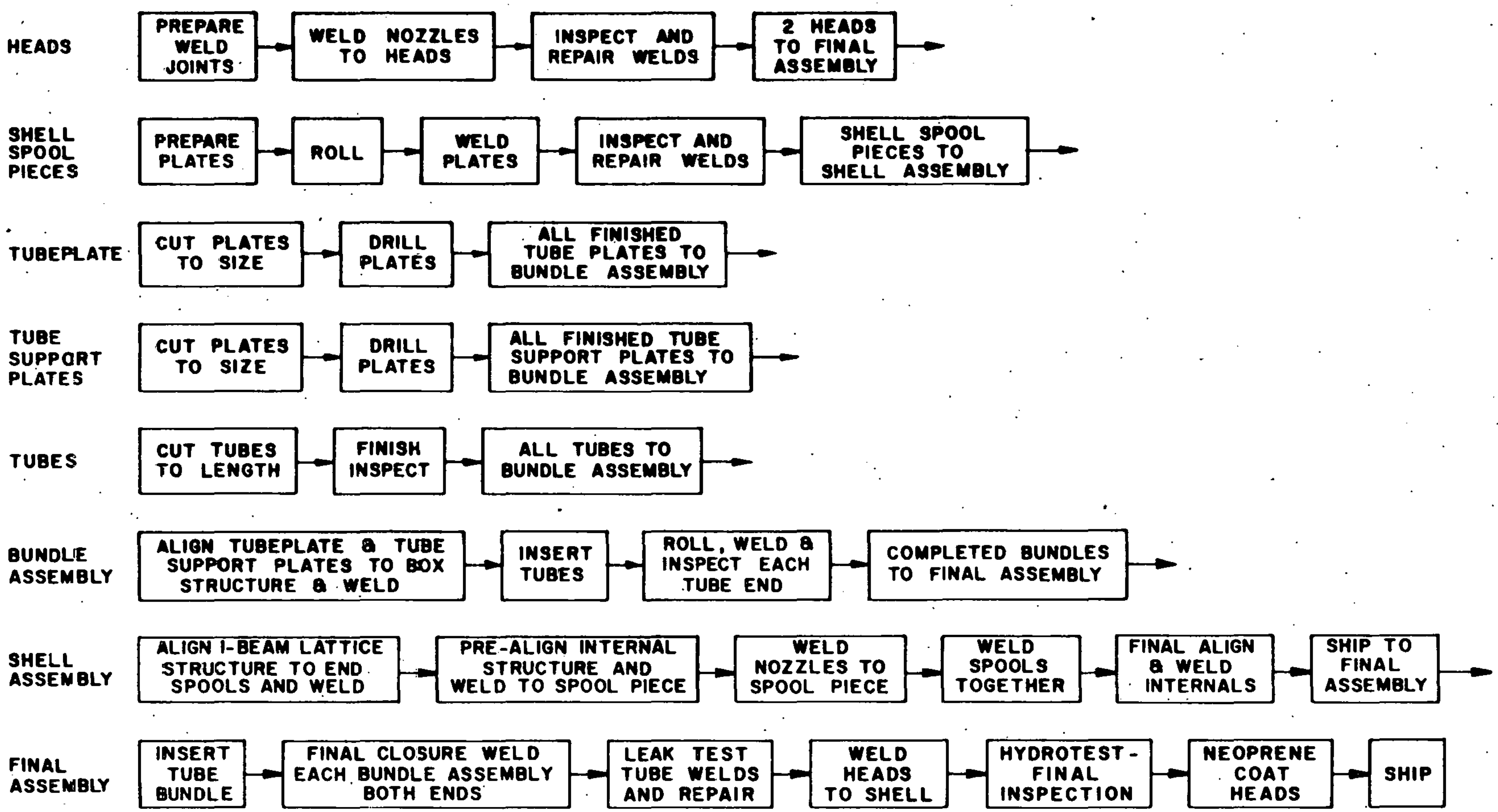

Figure 5-11
MANUFACTURING FLOW DIAGRAM

The manufacturing plan uses existing tooling, fixtures, facilities, and manufacturing processes. It includes automatic tube-to-tubesheet welding, explosively clad tubesheets, and commercial techniques for inspection to ASME Code, Section VIII, Division I, and/or U.S. Coast Guard requirements.

Beyond ASME Code requirements, the following tests and inspections will be performed during fabrication.

For the Linde surface applied to the outer surface of tubes, one sample per manufacturing lot will be subjected to:

- Flatten and flare tests of bare tube
- Hydrostatic burst test
- Heat transfer performance test

Tube-to-tubesheet welds will be subjected to:

- Visual inspection at 5 to 10x magnification
- Leak test with gas pressure on shell side
- 100% dye-penetrant inspection

Tubesheet cladding bond will be subjected to:

- 100% ultrasonic testing with maximum of 3/8-inch diameter unbond criteria
- 100% X-ray testing

All shell welds not radiographed will be magnetic-particle or dye-penetrant inspected.

A "holiday" detector test of neoprene coating will locate voids.

5.4 Installation/Interfaces

The heat exchanger test articles are to be installed within a test loop aboard the OTEC-1 platform. The function of the test loop is to determine the heat transfer characteristics of selected tubes and tube arrangements under actual OTEC operating conditions. The test loop will have a closed NH_3 circuit, a warm seawater circuit and a cold seawater circuit. The NH_3 circuit is illustrated in Figure 5-2. The warm and cold seawater circuits (furnished by others) will each consist of the appropriate heat exchanger, circulating pump and a head tank.

The evaporator and condenser flows and temperatures for both seawater and ammonia are detailed in Figure 5-2.

Controls for the water flow and temperature to the evaporator and condenser, ammonia gas and liquid flows, and the evaporator pressure will be provided by others.

The heat exchangers have been preliminarily designed in accordance with the ASME Boiler and Pressure Vessel Code, Section VIII, Division I.

Appropriate ammonia storage, make-up systems and waste disposal systems will be provided by others.

All the OTEC-1 constraints have not been defined. An example of the test article equipment and piping arrangement is illustrated in Figures 1-1 and 5-12. For this assumed arrangement, a space 20 feet high x 36 feet wide x 25 feet long is required. However, the test article heat exchangers are very compact, and no difficulty is anticipated in arranging them aboard the platform when more detailed requirements are furnished.

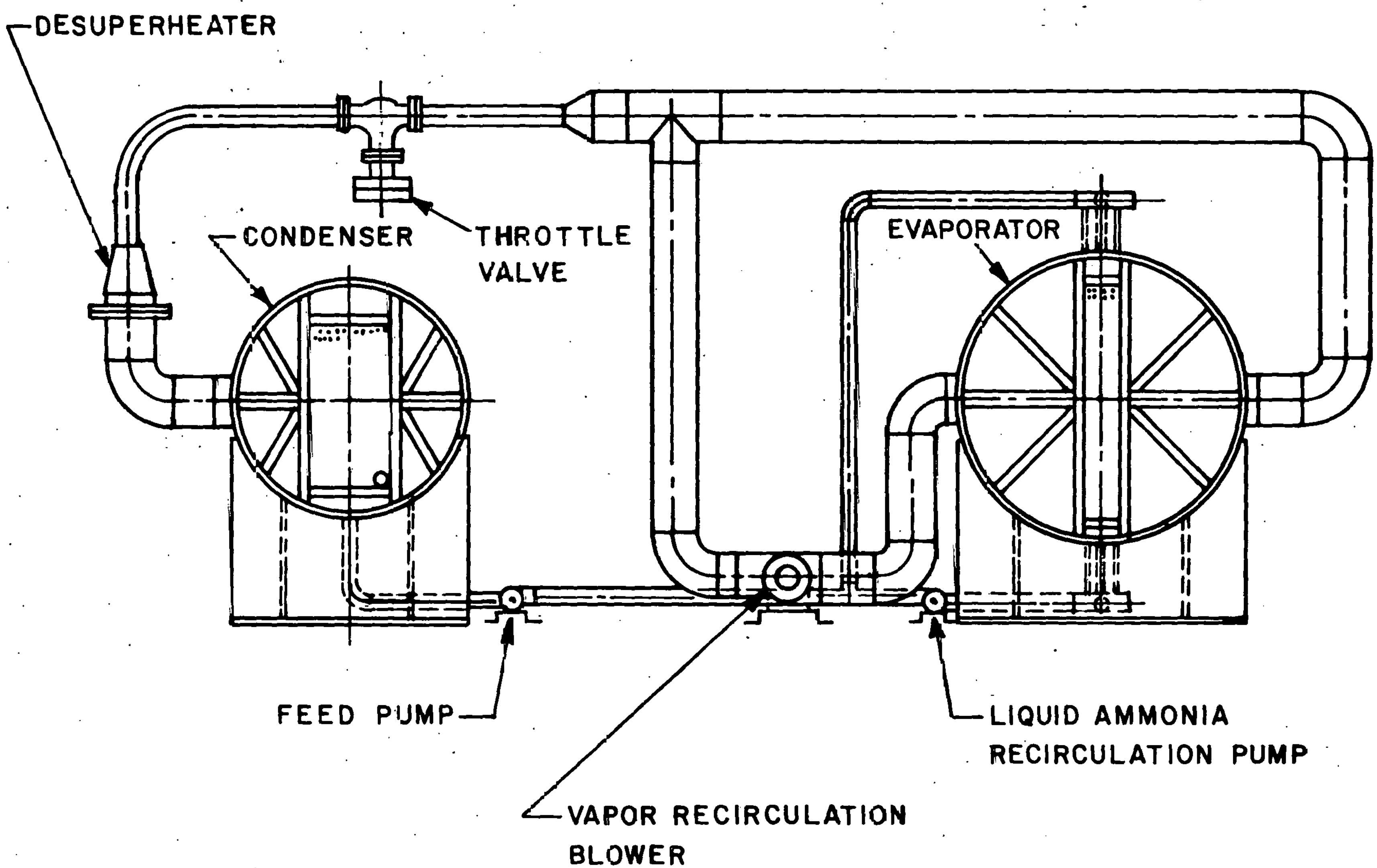

Figure 5-12
TEST ARTICLE PIPING ARRANGEMENT

5.5 Testing Considerations

5.5.1 Objectives

The purpose of the test program is to demonstrate heat exchanger operational performance in situ and to obtain data for future OTEC designs. This will be achieved by development of overall system and individual element research plans for operational data measurement, recording, playback and analysis.

The hardware includes an evaporator, condenser and an ammonia recycle pump. Specific objectives achievable from testing include verification of:

- Thermodynamic performance
- Heat exchanger dynamic stability and operational controls
- Mechanical design
- Reliability/availability/maintainability and safety

5.5.2 Test Plans

The test articles research plans answer questions about overall heat exchanger performance. Specifically, the heat transfer algorithms will be verified. Pressure drops of both seawater and ammonia across the heat exchangers will be measured. Seawater distribution from the plenum through the waterbox and to the tube bundle will be recorded. The distribution of ammonia liquid and vapor in the heat exchangers will be verified. In addition, fouling, materials and reliability issues will be addressed.

The design of the test articles and their proposed test loop facilitates testing specific heat exchanger characteristics. Tests will verify the relationship between evaporator vapor output and the magnitude of ammonia feed and recirculation.

Within the evaporator, the tube bundle ammonia exit velocity distribution will be determined. Vapor-liquid entrainment as a function of skimming velocity will be noted, as well as separator exit quality.

Other areas of concern regarding specific evaporator phenomena include:

- Liquid distribution
- Tube wetting
- Film stripping and deflection
- Minimum film thickness
- Dynamic dry-out characteristics

Tube vibration characteristics will be measured over the entire design range and at overload values.

Heat exchanger performance under off-design conditions will include:

- Changes in ΔT
- Various feed/recirculation conditions
- Load changes and loss of load
- Changes in vapor velocity
- Changes in seawater velocity

To calculate the performance characteristics, pressure, temperature, and flow measurements will be taken at the inlet and outlet of the seawater side of each heat exchanger. On the ammonia side, pressure drops in the evaporator, separator, and condenser will be measured. Elsewhere in the ammonia system, temperatures and pressures will be measured for both liquid and vapor phases. Techniques for obtaining reliable data, for the heat exchangers, tube bundles, and individual tubes, are developed and presented in this section.

Both operation and performance analysis require vapor flow measurements through the vapor recirculation loop. Measurements will be made at the evaporator outlet, throttle inlet, and evaporator vapor recirculation inlet. Vapor flow rate and velocity will be recorded and also presented in "real time"* to facilitate test operation.

All ammonia liquid flows will be measured directly including: (1) feed, (2) recirculation, (3) evaporator liquid drain, and (4) separator liquid drain. Liquid distribution in the evaporator will be observed by taking individual flow measurements at nine distribution chamber inlets and at nine collection chamber outlets.

Individual tube vibration measurements will be taken in six tubes on the seawater side of the evaporator and condenser. Instrumentation will consist of two inductive displacement sensors per tube (horizontal and vertical).

Seawater temperature traverses will be made near individual tube entrances and exits to ascertain any variation in tube loadings. This measurement will be made on clusters of six tubes each, in six locations in the evaporator and condenser. These measurements are especially important in the evaporator to verify complete wetting of tube surface during all modes of operation.

Sight ports will be located on the shell of both the evaporator and condenser. These ports will be of particular help on the evaporator where

---

*Instantaneous on-line display of measured and/or calculated test parameters they will be used for visual and photographic observation of evaporator phenomena.

The calculated outside heat transfer coefficient is the key design parameter used to verify the heat transfer algorithms. The outside heat transfer coefficient calculated using test data will be compared with that obtained using design equations. Concurrence of these two values validate the heat transfer algorithms.

In the event of non-concurrence, design equations may be revised to a form that is in better agreement with the heat exchanger configuration by using a technique such as the Wilson Plot to derive better values for constants and exponents. Off-design values of overall and outside resistance are obtained by performing this test and varying the seawater volume rate of flow.

The heat exchangers will be tested by running the test loop at normal steady-state design conditions. During this operation, measurements will provide data for tabulations, plots, and input for the performance calculations. It is planned to employ "real time" data reduction to facilitate graphic presentation of intermediate results during testing. In addition to steady-state operation testing, other tests will require specific procedures as follows:

The test article evaporator design includes a perforated plate located at the vapor recirculation loop outlet to the tube bundle. The perforated plate simulates design vapor distribution in the tube bundle. Verification of the evaporator perforated plate design should be performed early in the test series. To accomplish this test, the test loop will be run with the vapor recirculation line blanked and the vapor recirculation blower stopped. The ammonia vapor exit velocity distribution will be measured as it leaves the evaporator tube bundle. This data will be used to modify the perforated plate as necessary, before it is replaced in the evaporator. After the blank is removed from the vapor recirculation line, the loop will be ready for subsequent testing.

During testing, vapor recirculation flow and velocity will be determined by the throttle valve and blower controls. It is expected that flow will be split approximately nine-to-one between recirculation and throttle control, respectively. The vapor velocity will be varied through the normal expected range and also into overload regions, and the following characteristics will be recorded and/or observed:

- Film stripping and deflection

- Vapor-liquid entrainment resulting from exit velocity skimming

- Tube vibration

- Dynamic tube dry-out characteristics

The evaporator design includes an adjustable lane baffle which is used to vary the size of the passage between the tube bundle exit and separator inlet. This baffle provides another means, independent of the ammonia vapor recirculation loop, of varying the skimming velocity and separator inlet velocity. Tests will be run at various baffle settings to verify designed tube bundle separation in larger evaporator applications.

Flow distribution of ammonia in the heat exchanger will be measured by temperature traverses of individual tubes on the seawater side. In addition to this measurement, liquid distribution in the evaporator will be checked using the flow instrumentation in the distribution/ collection chambers. Liquid ammonia will be recirculated through the evaporator with the warm seawater pump stopped to verify balance of flows between respective distribution/collection chambers. These flows will again be monitored during normal test loop steady-state operation to verify balanced distribution.

Reflux rate testing will establish the relationship between evaporator vapor flow out, total liquid flow in, and the ratio of recirculated ammonia to total ammonia flow into the evaporator. The reflux rate test will be performed by a process of varying evaporator feed and recording all flows. First, ammonia feed flow will be slowly increased until the ammonia level begins to rise in the evaporator drain tank.

Finally, the ammonia feed flow will be slowly increased again until the ammonia vapor flow out of the evaporator no longer is increasing. The actual ammonia vapor flow out of the evaporator will be equal to evaporator vapor outlet flow less vapor recirculation flow. Several runs of the reflux rate test will be required to document the ammonia reflux ratio.

Off-design performance tests will include varying warm and cold seawater temperatures and/or flow rates and observing heat exchanger performance, and changing throttle valve settings to simulate changes in test loop loads. A sudden full opening of the throttle valve will simulate the turbine by-pass valve during a loss of load situation. As the throttle valve is opened, the liquid ammonia flow to the evaporator will be shut off to further simulate the loss of load situation. The flashing and increase in ammonia vapor flow effects will be observed and recorded.

The OTEC heat exchanger feasibility and cost are significantly dependent upon fouling characteristics. A test period of 6 six months to one year in situ should provide answers to the following key issues (test program research plans will take into account any new information obtained from current DOE testing programs):

- What are the rates of fouling on heat transfer surfaces? (Seawater and ammonia side).

- Can fouling be controlled?

- Can heat transfer surfaces be cleaned to provide economic plant operation? What is the best method of cleaning?

- Is the rate of fouling dependent upon external conditions, e.g., seasonal, weather, etc?

- Does fouling reach an asymptote, or is periodic cleaning required?

Fouling data measurements will be taken over the duration of the test program. Fouling characteristics will be determined directly by measurement and observation, and indirectly by calculation.

The effect of fouling will be measured by a direct comparison between tubes on the seawater side, allowed to foul at their normal rate, and one or two control tubes where no fouling will be permitted. This measurement will be made on both the evaporator and condenser. The effect of fouling will be a function of individual tube inlet/outlet ΔT's for the controlled versus the uncontrolled tubes.

The control will be achieved by a closed distilled water circuit. This loop will supply distilled water to the control tube inlets. This supply will be monitored and controlled to assure that the distilled water parameters at the control tube inlet, temperature, pressure and flow, duplicate those of the seawater. The ammonia side will be exactly the same for both controlled and uncontrolled tubes.

The result of this measurement will be the effect of fouling, in terms of a ΔT measurement. It may be presented with respect to time, system performance, etc. This technique will achieve the same comparative results as ASME Test Procedure PTC-12.2.

During periods of shutdown for cleaning, the condition of the heat exchanger tubes will be observed directly from the waterbox before and after cleaning. Periodically, fouling coupons will be removed from various coupon racks throughout the system. Coupon samples will consist of various tube and system element materials provided with fouling prevention coatings and a corresponding unprotected control group.

Instrumentation in the vicinity of these racks will measure local temperatures, pressures, and flows.

Testing will include an uncontrolled fouling buildup situation. After establishing a condition of clean heat transfer surfaces (either when plant is first started or after shutdown for tube cleaning), the plant will be run with no fouling control, and fouling buildup will be monitored with respect to time. Then fouling control, will be introduced and heat transfer performance will be observed.

Materials data will be collected both during testing and after testing has been completed.

During periods of maintenance shutdowns, all system materials will be examined for corrosion and galvanic effects. The following effects are of special interest:

- Tube inlet-end erosion
- Tube ID pitting
- Other tube corrosion problems
- Pump erosion and corrosion problems.

Some tubes will be partially blocked during operation to evaluate this effect on the tubing. The condition of tubes with teflon coatings, especially coatings at the inlets, are of special interest during periodic examination.

Intermediate test data will be obtained by examination of specimens located on coupon racks throughout the system. Sufficient specimens will be provided for removal and examination for different periods of operation. Specimens for the coupon racks will include:

- Several types of aluminum, including the Linde enhancement surface

- Carbon steel and coated carbon steel

- 316SS pump alloys

- Ni-Cr-Mo-V other turbine alloys in ammonia

- Titanium

- Stressed specimens of many alloys including carbon steel.

Whenever possible, the material racks will be located in the vicinity of fouling racks, thus sharing local measurements of temperature, pressure and flow.

An additional source of materials data will be performing destructive testing consisting of metallographic tests upon test conclusions. Of special interest is the condition of the Linde thermally enhanced OD surface of evaporator tubes.

5.5.3 Reliability, Availability, Maintainability, and Safety Performance

Reliability, availability, maintainability, and safety considerations will be determined for the test articles by a technique of record keeping and post-test evaluation. Detail maintenance and safety logs will be recorded during all on-site tests. They will contain reports of the causes and effects of all failures, times to repair, and logged hours of plant operation.

Post-test analyses will use these records to determine heat exchanger data such as:

- Availability

- Mean time between failures

- Mean time to repair

- Verification of failure modes and effects analysis

- Safety record

5.5.4 Test Setup

The test data requirements and instrumentation locations for the test articles are shown in Figure 5-13. This schematic represents a summary of all the various data requirements identified by individual research plans. Individual sensors are numbered for purposes of identification.

The support hardware developed for the test program includes instrumentation and a data acquisition system. The instrumentation effort is a survey of hardware and technologies applicable to the OTEC program. A complete data acquisition system, including signal conditioning, central processor, and peripheral displays was developed for the Modular Application. Both efforts are discussed in modular application testing considerations, Section 6.6.

5.6 Costs

Test article design engineering costs and engineering expense associated with production and field support were developed for the heat exchanger test articles described in Section 5.2.2.

The tube material and enhancement, explosively bonded tubesheets and purchased equipment (recycle pump, blower, etc.) costs were obtained from current supplier quotations on the specific needs of this design. All other costs are based on current price lists.

The manufacturing cost for the evaporator and condenser is based on a current quotation from a subcontractor, for the units described in Figures 5-8 and 5-10.

The total system costs for items tabulated below were presented to D.O.E. in the Business/Cost proposal, dated October 2, 1978.

1. Detailed engineering and analysis for components and loop design
2. Fabrication of test articles and procurement of materials and auxiliary equipment
3. Engineering of instrumentation selection and design, calibration techniques, vendor selection, specification, test requirements, test and evaluation plan, etc.
4. Engineering required for support of field installation of equipment supplied on government-furnished platform
5. Engineering required for test operation support on the platform

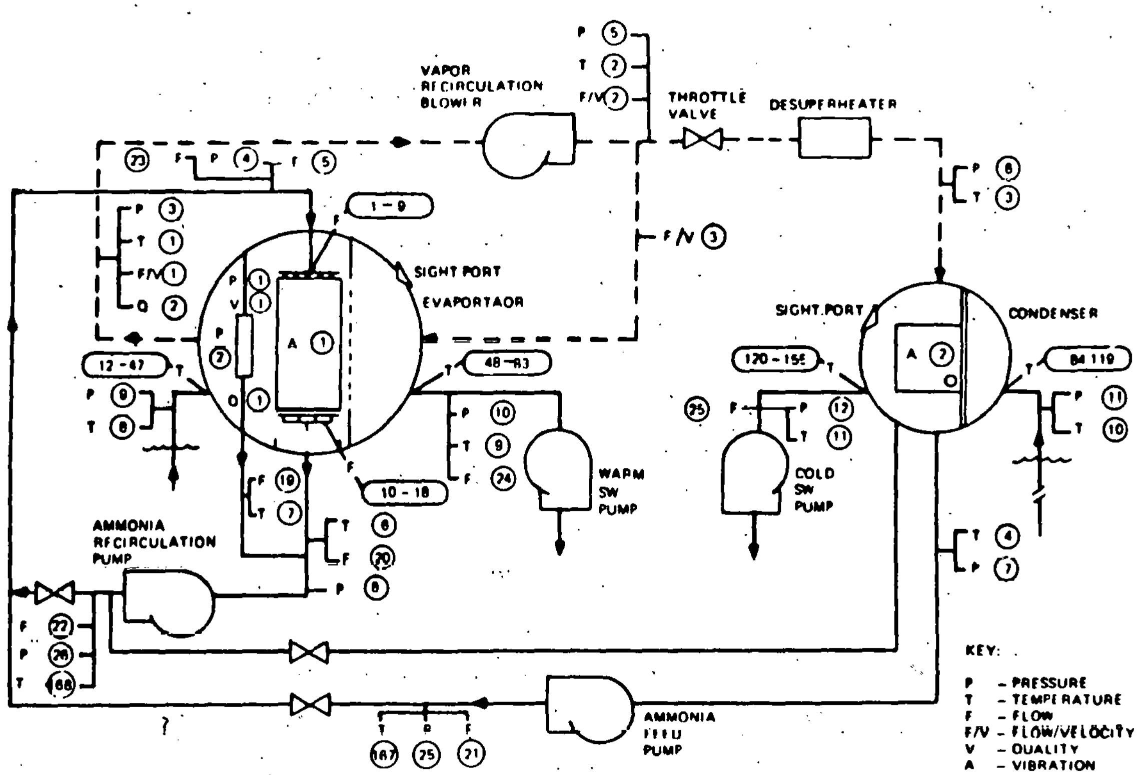

Figure 5-13
TEST ARTICLES-TEST DATA REQUIREMENTS

6 MODULAR APPLICATION (10 MWe)

6.1 Approach to Design

The design criterion for the 10 MWe power module is accurate modeling of a 40-50 MWe power module, not cost optimization.

The principal issue involved in the design of the 10 MWe module was the modeling accuracy as applied to the heat exchangers and turbine. The preferred design would use one or more full-sized modular tube bundles and a half-sized, 1/4 power, double speed turbine. This preferred design would accurately model the ammonia and seawater flow distribution in the thermodynamically independent tube bundles as well as the specific speed and mechanical stress characteristics of the turbine.

With respect to seawater pumps, they (one each for the evaporator and condenser) are rated at one-half the flow of the pumps for the 40-50 MWe power module. The reason for this is that two pumps are used for each heat exchanger in the larger system. The large scale factor, one-half for the pumps as compared with that for the heat exchangers and turbine, represents a favorable step toward testing of full-scale seawater pumps.

The application of these modeling constraints to the optimized 50 MWe power module results in a 12.5 MWe turbine and two 10.7 MWe heat exchangers (using three of the 14 modular bundles in the 50 MWe design) -- clearly an unworkable solution.

The approach taken was to model a cost-optimized 40 MWe power module which has 12 tube bundles per heat exchanger. In this model, the 1/4 power turbine generates enough power for 10 MWe, and three of the 12 tube bundles result in a matching 10 MWe. Unscaled differences in the power cycle necessitated a slight (less than 3%) lengthening of the tube bundles, but the critical bundle cross section was retained.

Westinghouse believes that the 10 MWe module accurately represents the 40 MWe optimized module, and that the 40 MWe module design and performance can be confidently extended to the recommended 50 MWe size.

Tables 6-1 and 6-2 numerically compare the power module and heat exchangers of the 10, 40 and 50 MWe designs. Table 6-3 shows the scale of selected modeling parameters, referenced to the 40 MWe optimized power module.

6.2 Component Design

6.2.1 Heat Exchangers

6.2.1.1 Thermal Design

The thermal design aspects to which particular attention has been given in the preliminary design of the 10 MWe evaporator and condenser are:

- Evaporator recycle flow
- Evaporator liquid distribution system
- Evaporator vapor distribution
- Evaporator drainage
- Condenser vapor distribution
- Condenser drainage

Tube material selection, heat transfer coefficient calculation procedures, and pressure drop correlations are contained in Sections 6.3.1 and 7.2.1.1.

Table 6-1
POWER MODULE COMPARISON

	10 MW	40 MW	50 MW
Flows (10^6 lbm/hr)			
Ammonia	2.99	11.8	14.8
Cold Seawater	263	921	1300
Warm Seawater	305	1190	1500
Temperatures (°F)			
Warm Seawater Inlet	80.00	80.00	80.00
Warm Seawater Outlet	74.57	74.54	74.51
Evaporator Saturation	70.50	70.35	70.25
Turbine Inlet	70.20	70.05	69.95
Turbine Outlet	49.09	50.15	49.59
Condenser Saturation	49.00	50.06	49.50
Cold Seawater Outlet	46.13	46.89	46.17
Cold Seawater Inlet	40.00	40.00	40.00
Performance			
Turbine Efficiency	.790	.799	.800
Seawater Pump Efficiencies	.670	.680	.680
Ammonia Pump Efficiencies	.750	.750	.750
Condenser Effectiveness	.681	.685	.647
Evaporator Effectiveness	.572	.566	.564
Power (MWe)			
Turbine/Generator Gross	14.42	54.09	70.01
Cold Seawater Pump	2.30	6.74	10.05
Warm Seawater Pump	1.52	5.31	6.65
Ammonia Feed Pump	0.28	1.14	1.49
Ammonia Recycle Pump	0.05	0.27	0.11
Chlorination	0.17	0.63	1.21
Estimated Hotel Load	0.10	0.0	0.50
Net Power Output	10.00	40.00	50.00

Table 6-2
HEAT EXCHANGER COMPARISON

	Condenser			Evaporator		
	10 MW	40 MW	50 MW	10 MW	40 MW	50 MW
Tube Velocity, ft/s	5.6	5.1	5.6	5.5	6.5	6.5
h(water), BTU/hr-ft^2-°F	854	804	862	1160	1160	1160
h(foul), BTU/hr-ft^2-°F	3780	3780	3780	3780	3780	3780
h(metal), BTU/hr-ft^2-°F	4820	4820	4820	4770	4770	4770
h(ammonia), BTU/hr-ft^2-°F	1870	1830	1920	4930	4980	5010
H.T. Coeff., BTU/hr-ft^2-°F	459.3	441.6	464.2	648.2	649.0	649.5
L.M.T.D., °F	5.37	5.97	5.90	6.40	6.54	6.63
Surface Area, ft^2	623007	2294117	2787795	382786	1468647	1831138
Tube O.D. inches	1.0	1.0	1.0	1.0	1.0	1.0
Tubes	42150	159692	206453	42107	164613	206649
Bundles	3	12	14	3	12	14
Bundle Length, ft	55.5	54.9	51.6	34.7	34.1	33.8
Tubeside Press Drop, PSI	3.72	3.14	3.47	2.90	2.82	2.81
Amertap Press Drop, PSI	0.29	0	0	0.29	0	0

Table 6-3
SCALING PARAMETER COMPARISON (Normalized to 40 MW Module)

	10 MW	40 MW	50 MW
Turbine			
Flow	0.253	1.000	1.254
Speed	2.000	1.000	1.000
Gross Power	0.267	1.000	1.294
Condenser			
Tubeside Velocity	1.098	1.000	1.098
Seawater Flow	0.286	1.000	1.412
Seawater Flow/Ammonia Flow	1.127	1.000	1.125
Tubes per Bundle	1.023	1.000	1.108
Bundle Length	1.029	1.000	0.940
H.T. Coefficient	1.040	1.000	1.051
Evaporator			
Tubeside Velocity	1.000	1.000	1.000
Seawater Flow	0.256	1.000	1.260
Seawater Flow/Ammonia Flow	1.011	1.000	1.005
Tubes per Bundle	1.056	1.000	1.076
Bundle Length	1.018	1.000	0.991
H.T. Coefficient	0.999	1.000	1.001
Power Allocations			
Turbine Generator	0.266	1.000	1.294
Cold Sea Pump	0.341	1.000	1.491
Warm Sea Pump	0.286	1.000	1.252
Ammonia Feed Pump	0.246	1.000	1.307
Ammonia Recycle Pump	0.185	1.000	0.407
Chlorination	0.270	1.000	1.921
Net Power Output	0.250	1.000	1.250

6.2.1.1.1 Design Criteria

The 10 MWe power system is a model for larger units. Therefore, the thermal design of the 10 MWe heat exchangers is analogous to the design of the heat exchangers in a 40 MWe plant, which can be easily extended to a 50 MWe size, as discussed in Section 6.1. The 10 MWe Modular Application thermal design data is itemized in Table 6-4.

6.2.1.1.2 Tubing Selection

The heat exchangers used in the 10 MWe power module are analogous to their larger counterparts. Consequently, the tube material and enhancement type in the 10 MWe heat exchangers are identical to the selections made for the 50 MWe power modules, as discussed in Section 7.2.1.1.

The tube material is titanium. Linde high heat flux coating is bonded to the otherwise plain evaporator tubes, and the condenser tubes are completely unenhanced. All tubing is 1-inch diameter with a wall thickness of 0.028 inch.

Heat transfer and pressure drop relationships for the selected tubing are described in Section 7.2.1.1.

6.2.1.1.3 Thermal Design Data

The evaporator consists of three modular bundles. Each bundle has 14,307 tubes arranged in a triangular pattern. The bundles are each 12.5 feet high by 12.5 feet wide by 36 feet long. The tubes are arranged in 210 columns of 67 tubes each, with a full length vertical plate at the bundle center to assure symmetrical flow.

The condenser consists of three modular bundles. Each bundle has 14,050 tubes arranged in a triangular pattern. Each bundle is 12.5 feet high by 12.5 feet wide by 56 feet long. The tubes are arranged in 213 columns of 67 tubes each.

Table 6-4
HEAT EXCHANGER THERMAL DESIGN DATA

	Condenser	Evaporator
Ammonia Flow, lbs/hr	2987375	5974750
Temp. In, °F	49.09	59.74
Temp. Out, °F	49.00	70.50
Seawater Flow, lbs/hr	262958443.	305384916.
Temp. In, °F	40.0	80.0
Temp. Out, °F	46.13	74.57
Tube Metal	Titanium	Titanium
Tube O.D., inches	1	1
Wall Thickness, inches	.028	.028
LMTD, °F	5.364	6.406
Tube Velocity, ft/sec.	5.57	6.50
HT Coeff., BTU/hr ft^2F	459.3	648.2
h (water)	854	1160.
h (fouling)	3780.	3780.
h (metal)	4820	4770
h (ammonia)	1870	4930
HT Surface, ft^2	623007	382786
No. Bundles	3	3
Total Tubes	42150	42107
Eff. Length, inches	677	416
Seawater Pressure Drop, PSI	3.7	2.9

The evaporator and the condenser shells are 444 inches in diameter. Pertinent thermal design data for the heat exchangers is listed in Table 6-4.

6.2.1.1.4 Evaporator Recycle Flow

The proper operation of each evaporator bundle depends, to a large extent, on keeping the tubes wet with liquid ammonia. Tube "dry out", or the absence of sufficient excess liquid ammonia on a tube, is caused by longitudinal liquid maldistribution and by lateral liquid deflection. Longitudinal maldistribution is precluded by an effectively designed liquid distribustion system, discussed in Section 6.2.1.1.5. Lateral deflection occurs when the ammonia vapor velocity within the bundle is high enough to cause the liquid falling from one tube to miss the tube directly beneath it. This velocity is plotted in Figure 6-1.

Liquid ammonia falling from one tube to the next may be in the form of droplets or columns, depending on the volume of flow (continuous falling sheets are not possible because of the Taylor instability criteria for falling films). The amount of excess ammonia liquid required to flood all the tubes results in column flow, so stable column flow was selected as the design mode.

The minimum liquid excess required for proper operation of the Linde surface is a function of the flowing vapor velocity. This liquid excess may be considered to be the liquid draining from the lowest tube in each column of tubes. For the vapor flow conditions in the tube bundle (refer to Section 6.2.1.1.6), the theoretical critical flow rate above which stable column flow[5] is formed is approximately 27 lbs/hr/ft of tube. The empirical values, based on Linde test data, are 38 lbs/hr/ft at the warm end and 22 lbs/hr/ft at the cool end.

The stable column flow rate, calculated over the entire length of a single bundle, results in a liquid mass flow of 1,241,400 lb/hr. Since each bundle only generates 1,044,400 lb/hr of vapor, excess ammonia liquid must be recycled through the evaporator. The minimum recycle ratio is:

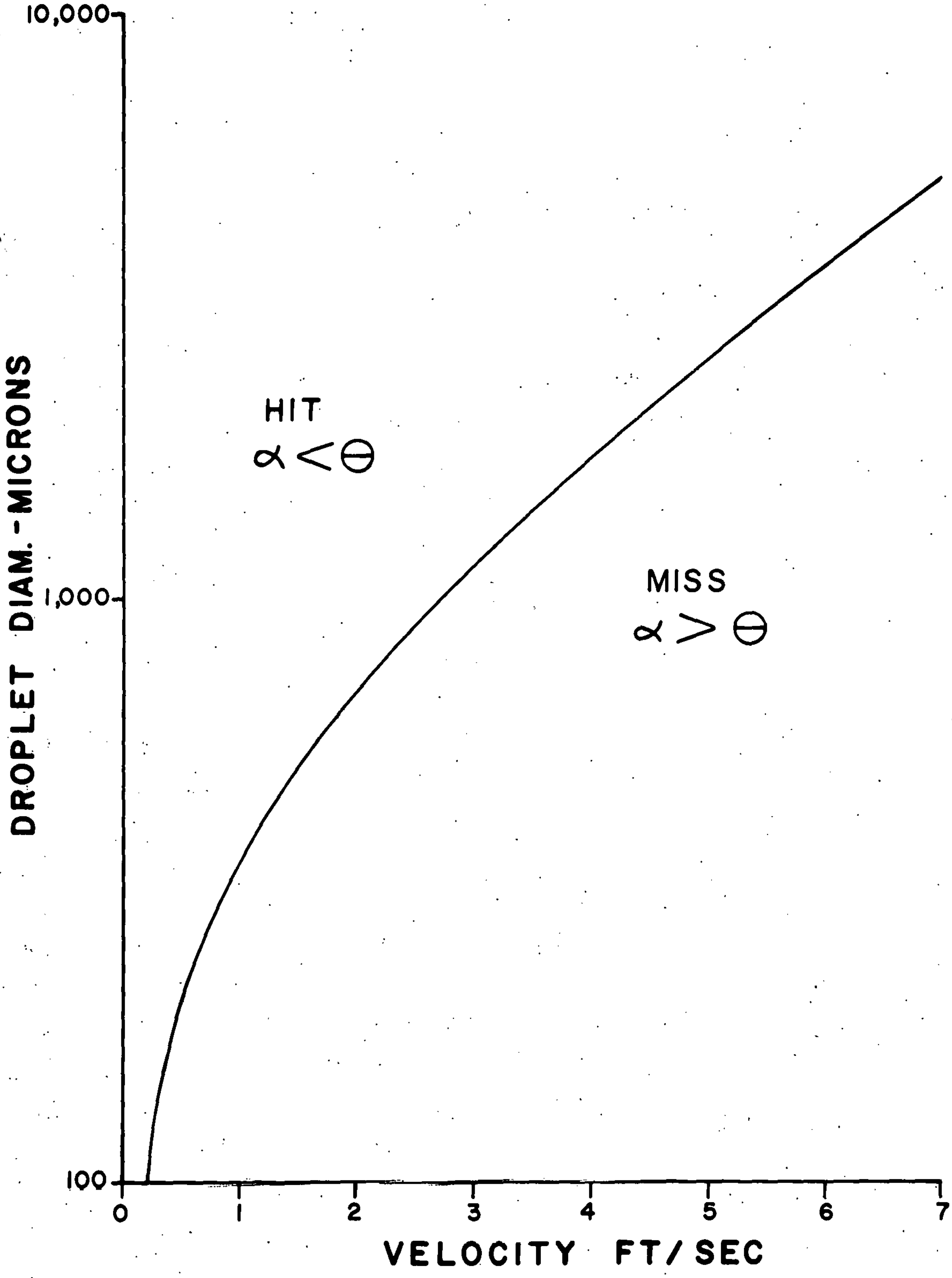

Figure 6-1
DROPLET HIT/MISS CURVE

$$\text{Minimum recycle} = \frac{1241400}{1044400} = 1.189$$

This minimum flow is well below the design recycle flow.

6.2.1.1.5 Evaporator Liquid Distribution System

Because the evaporation rate for any tube section varies with the ammonia-seawater temperature difference which changes from the inlet end of a tube to the exit end, particular attention must be given to incoming liquid ammonia flow distribution. At the warm end of the evaporator, an overall temperature difference of 9.5°F exists which results in a 6319 BTU/hr-ft^2 heat flux for boiling and an overall heat transfer coefficient of 665 BTU/hr-ft^2°F. The cool end has a temperature difference of 4.1°F, a heat flux of 2560 BTU/hr-ft^2, and an overall coefficient of 629 BTU/hr-ft^2°F. The warm end generates 2.5 times as much vapor as the cool end. This unbalance requires that the liquid feed trays be designed to supply only the required amount to each increment of bundle length for maximum output of vapor, with the minimum recycle liquid excess being returned to the drain trays.

For design purposes, the evaporator was divided into four equal heat load zones. Integrating the axial heat transfer effect and, consequently, the vapor generation rate along the length of the bundle in each of the four zones, results in zone lengths of 6.0, 7.5, 9.5, and 12.0 feet. Each of these zones requires approximately the same amount of ammonia liquid.

A full-width, full-length, pressurized liquid distribution tray is located above each bundle. Each distribution tray has a series of 1/8-inch diameter holes in rows above each column of tubes. Considered as sharp-edged orifice openings operating under a minimum head, each hole is capable of passing approximately 44 lbs/hr of liquid. The lengthwise spacing of the holes is dependent on the liquid ammonia flow rate to be supplied to each zone and on the length of each zone. Table 6-5 summarizes the hole-spacing calculation results.

Table 6-5
DISTRIBUTION TRAY HOLE DATA

Bundle Zone	1	2	3	4
Vapor Flow, lbs/hr	261100	261100	261100	261100
Length, ft.	6.0	7.5	9.5	12.0
Max. Vapor Velocity, ft/sec	5.04	4.03	3.18	2.52
Min. Liquid Drain, lbs/hr	47900	45700	47900	55500
Liquid Supply, lbs/hr	309000	306800	309000	316600
Holes	7023	6973	7023	7195
Spacing, inches	2.15	2.71	3.41	4.20

6.2.1.1.6 Evaporator Vapor Distribution

In each bundle, the tube support plates prevent axial vapor flow, so that the vapor velocities leaving the bundle are proportional to the vapor production in that section of bundle. In each section, the velocity of the vapor at the center plate is essentially zero, increasing linearly toward the outermost tubes to a maximum of 5 ft/sec at the warm end (6 feet long) and 2.5 ft/sec at the cool end (12 feet long). The reason for the longitudinal variation is given in Section 6.2.1.1.5.

Columns of liquid ammonia and some large droplets fall from tube to tube within the bundle. Most of the ammonia liquid droplets falling from the tubes will be in the size range of 1000 to 5000 microns. The corresponding vapor velocities required to break up or atomize droplets of this size are 19.8 ft/sec to 8.8 ft/sec. The prevailing low vapor velocities prevent these droplets from being shattered or atomized, so they can fall onto the next level of tubes.

In addition to the large droplets and columns formed by the falling liquid, there are very small droplets caused by bursting of the evaporation bubbles. These very small droplets are carried by the flowing vapor until they coalesce or impact a target surface. As the flowing vapor passes over the tubes, it continuously changes direction so that its flow path may be considered as a type of sine wave. A simplified analysis of the centrifugal effect and droplet trajectory indicated that droplets greater than 100 microns hit tubes and will not escape the confines of the bundle.

Any escaping droplets will be carried by the shellside vapor streams to the separator section, where the majority will be removed.

The shell diameter and bundle position are such that the vapor streams outside the bundle have velocities in the range of 1 to 2 ft/sec except in a few areas where the local velocity may reach 6 to 7 ft/sec. These high velocity areas are kept remote from the approach zone of the separators to avoid excessive liquid loading in the vanes.

The formed vane separators selected were tested in a steam-water environment and have negligible carryover. Dynamic head modeling permits the extension of the vane separator use to other fluids such as ammonia. Because of the unusually high concentration of small droplets, the maximum separator carryover expected is less than 0.1% moisture.

6.2.1.1.7 Evaporator Drainage

A full-length, full-width drain tray is located under each bundle. Each tray has sides to channel the flow, but the ends are open to permit the return of the liquid ammonia through internal channeling to the bottom of the shell.

The height of the tray sides is a function of the critical flow depth and the roll/pitch requirement. The critical flow depth, which is the depth required to transport all the design liquid drain flow out of one end of the tray, is 1.61 inches. The fluid depth caused by a 4° pitch/ roll is 4.12 inches. The sides of the drain trays are specified as 6 inches high. A full-length, 6-inch high strip, dividing the 12-foot width, prevents side spill and possible reentainment of the liquid.

The bundles, as shown in Figure 6-2 are arranged in the shell such that a maximum hotwell capacity of 2.5 minutes holding time is available, and the shell can be rolled and/or pitched 4° without flooding the tubes. This volume at 4° requires a clear height of 78 inches. Stilling baffles may be required to avoid the "sloshing" effect if the period of oscillation is short.

6.2.1.1.8 Condenser Vapor Distribution

Because the ammonia entering the condenser contains a small amount of moisture, the condenser tubes must be shielded from the erosive effect of the high velocity liquid droplets. An inlet vapor impingement plate above the upper bundle protects the tubes from direct impact.

The bundles are separated by vapor lanes which are large enough to permit easy access of the vapor to each bundle and reduce the incoming vapor velocity to an acceptable level.

A full-length controlled flow vent system, located at the bottom center of each bundle, scavenges the non-condensible gases and promotes balanced vapor flow throughout the bundle. This vent manifold is a perforated pipe with the spacing between the holes determined by the local condensing mass flow rate.

6.2.1.1.9 Condenser Drainage

A full-length, full-width drain tray is located under each bundle. Each tray has sides to channel the flow, but the ends are open to permit the return of liquid ammonia through internal channeling to the bottom of the shell.

The height of the tray sides is a function of the critical flow depth and the roll/pitch requirement. The critical flow depth, which is the depth required to transport all the design liquid drain flow out of one end of the tray, is 4.65 inches. The fluid depth caused by a 4° pitch/ roll is

5.20 inches. The sides of the drain trays are designed to be 6 inches high. A full-length, 6-inch high strip, dividing the 12-foot width prevents side spill and possible reentrainment of the liquid.

The bundles, as shown in Figure 6-3, are arranged in the shell such that a hotwell with 6 minutes maximum holding time is available. The nominal depth of liquid is 83 inches. At 4° pitch/roll, this volume requires 106 inches of bottom free space. At 2.5 minutes normal holding time, the free space required for 4° roll/pitch is 68 inches. Since the 6- minute maximum is an emergency situation in which the condenser is not expected to operate to full potential, the actual bottom free space is set at the untilted emergency depth of 83 inches.

6.2.1.2 Mechanical Design Features

Early designs by other OTEC plant developers borrowed heavily from conventional power plant heat exchanger state-of-the-art practice. A similar initial approach was taken by the Westinghouse team. The resulting very large shell and tube units, as described in following sections, either would pose difficult transportation problems between the manufacturing site and the OTEC plant assembly site, or would require field assembly of large, unwieldy parts. Such field assembly would be more costly and significantly increase the problem of achieving adequate quality control. Consequently, Westinghouse devised a unique modular design which virtually eliminates size as a constraint in producing very large heat exchangers.

The heat exchanger is composed of structurally independent modular tube bundles which are designed to be rail shippable. The tube bundles are easily adaptable to any tube material and can be built by many heat exchanger manufacturers. The size allows the use of automated drilling and welding machines, standard testing procedures, and currently existing high productivity methods in commercially mature, competitive, manufacturing facilities.

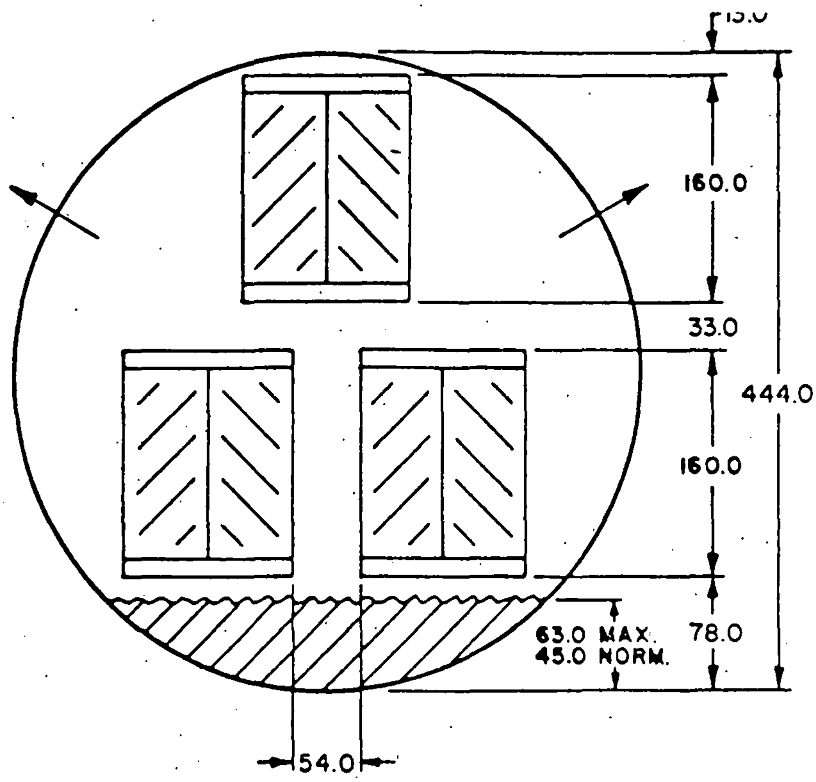

Figure 6-2
EVAPORATOR BUNDLE ARRANGEMENT

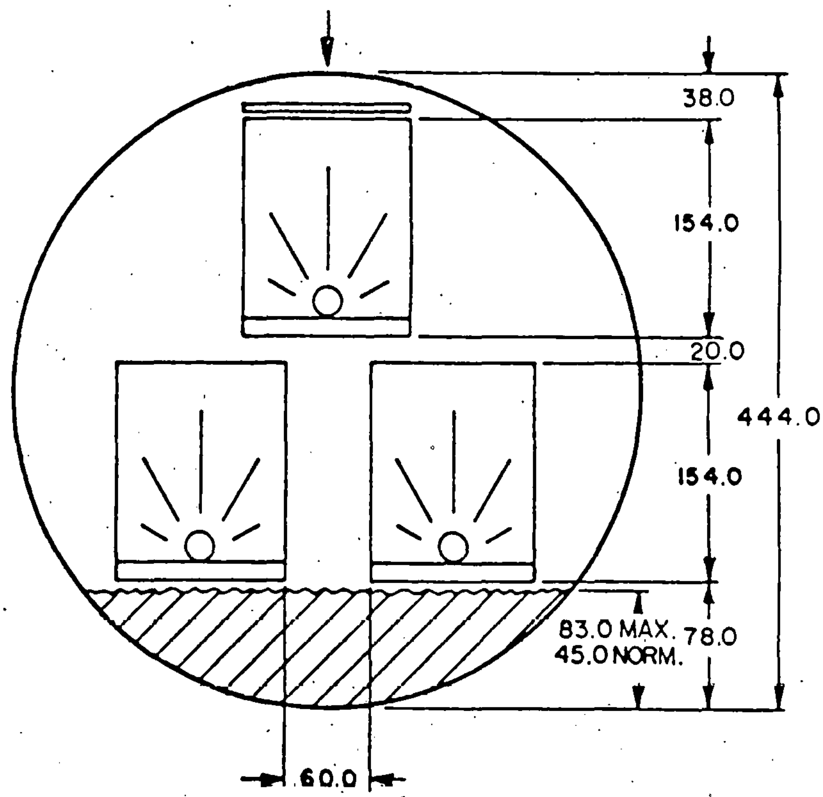

Figure 6-3
CONDENSER BUNDLE ARRANGEMENT

The 10 MWe Modular Application design which follows incorporates the identical features of a full-size commercial 400 MWe size plant (with 50 MWe modules).

6.2.1.2.1 Modular Design

The modular design was developed to simplify construction of very large OTEC heat exchangers. The standardized bundle assembly can be utilized in any size heat exchanger, only the number of bundles and shell diameter varies.

In addition to substantial savings in field labor costs for the evaporator, the modular approach permits the elimination of a separator vessel and drain tank since their functions are included within the evaporator shell. The separator vanes are preassembled in modular groups for later insertion in the shell.

The 37-foot diameter by 36-foot long modular evaporator is shown in perspective in Figure 6-4. Figures 6-5 through 6-8 show other facets of the design in greater detail. The design offers the following primary features:

- Three individual compact, shippable bundles
- Independent operation of each bundle for improved performance
- Integral separator assembly
- Integral drain tank

As with the evaporator design, the condenser has tubes arranged in modular bundles, permitting incorporation of the hotwell into the heat exchanger shell. The 37-foot diameter by 58-foot long modular condenser is shown in Figure 6-9. The details in Figures 6-6 through 6-8 also apply to the condenser design. The primary features of the condenser are:

- Three individual compact, shippable bundles
- Independent venting and ammonia collection for each bundle for improved performance.
- Integral hotwell

The diameters and lengths of the heat exchangers in this arrangement are established by the cost-optimization program. However, small variations of length and diameter from their optimum values have a minor effect on power module cost as long as the required tube surface area is maintained. This allows some flexibility in plant arrangement on the hull.

The vapor outlet nozzles are shown in the center on the top of the shell. However, they may be placed anywhere: along the shell on the top, or on either or both ends to suit any platform arrangement subsequently defined. The following structural details apply to both the evaporator and the condenser.

A cylindrical shell is employed for minimum wall thickness and cost. The tube array encompassed by the shell is divided into three identically shaped bundles (Figures 6-4 through 6-7). They are inserted as units on rails within the shell assembly. Although three square bundles are shown (and described below) any number and shape can be used. The criteria for bundle design is to choose a shape that achieves maximum shell cross-sectional area and uniformity of design within a limiting width of 12.5 feet to facilitate rail shipment of a completed bundle. This approach maximizes the amount of heat transfer area per bundle, thereby reducing the number of bundles.

On each end of the shell, a lattice of I-beams is constructed perpendicular to the shell centerline to form three square openings (see Figures 6-5 and 6-6). In each square opening, a box slightly longer than the I-beam height is inserted and welded all around to the adjacent beams (Figure 6-6). Longitudinal rails are placed between the corners of each

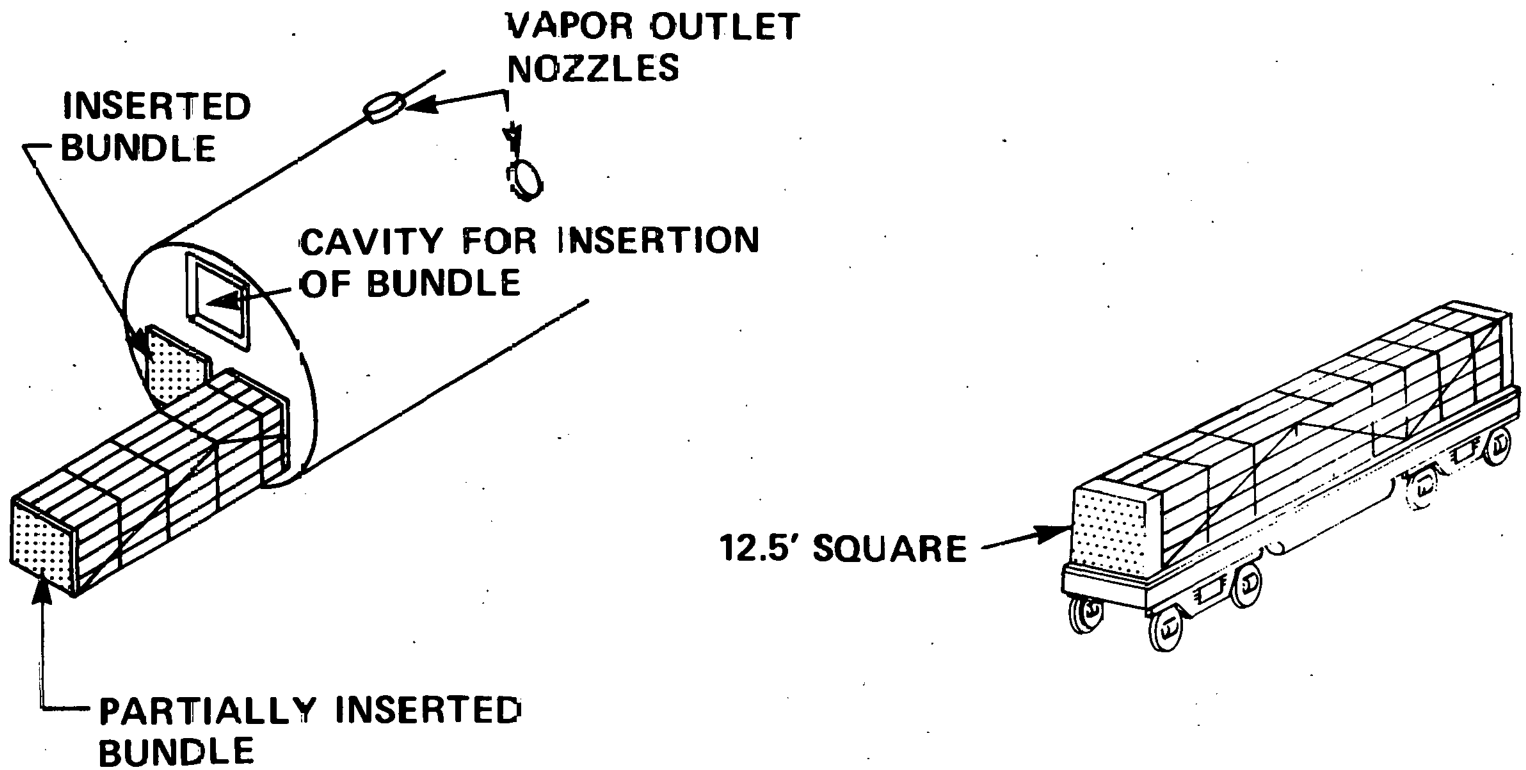

Figure 6-4
MODULAR HEAT EXCHANGER DESIGN

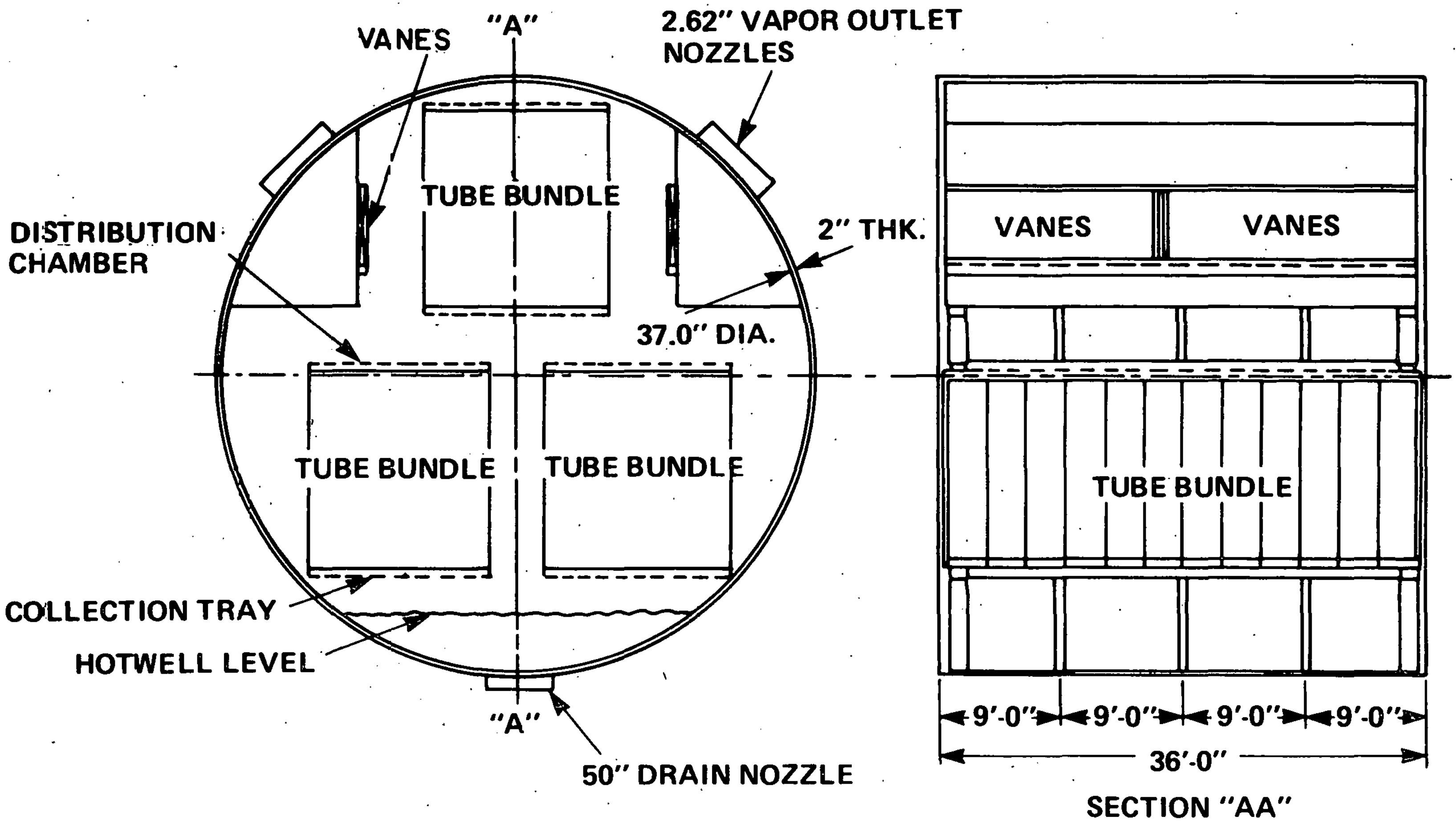

Figure 6-5
EVAPORATOR (10 MWe)

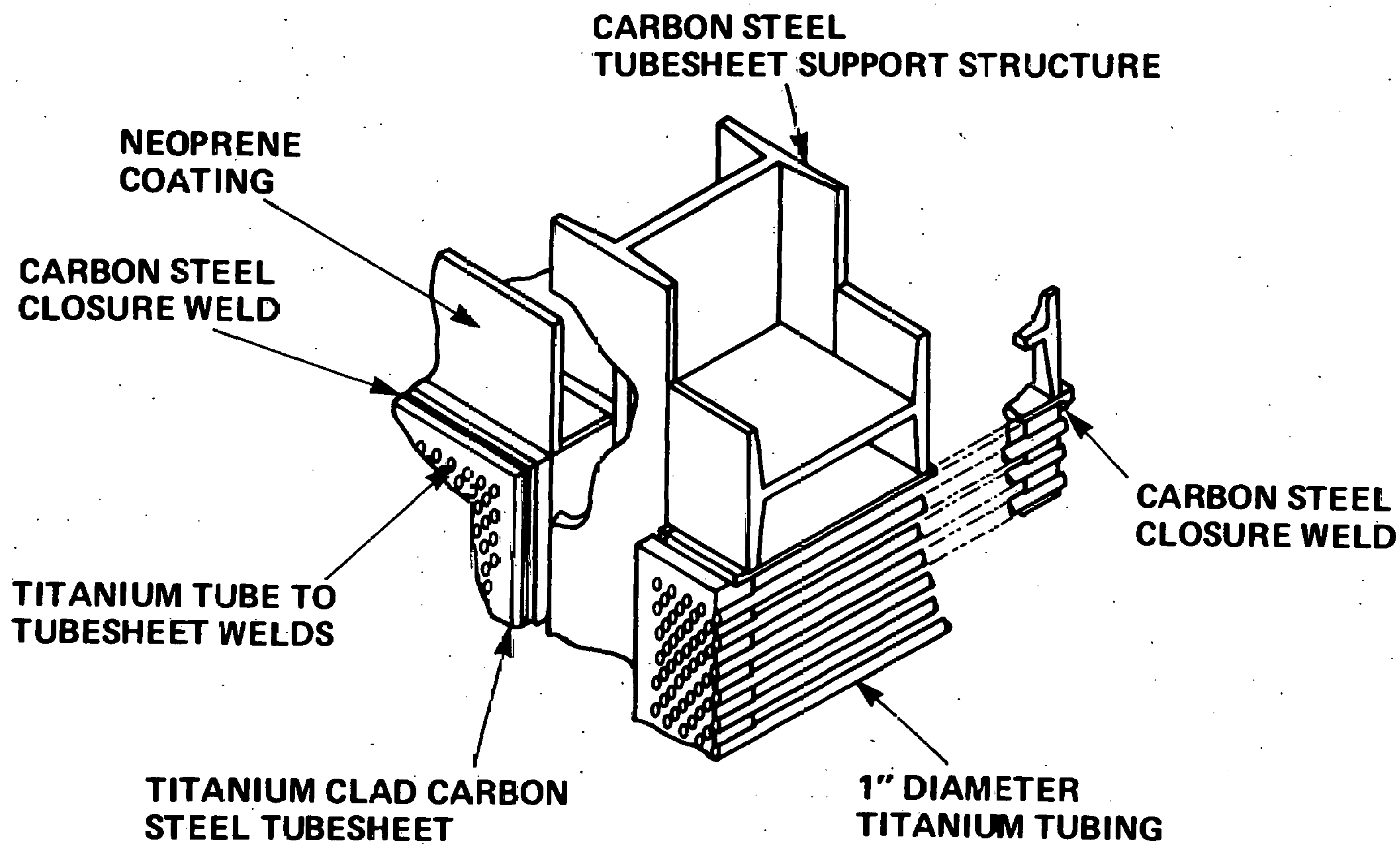

Figure 6-6
OTEC MODULAR HEAT EXCHANGER, TUBE BUNDLE INSTALLATION

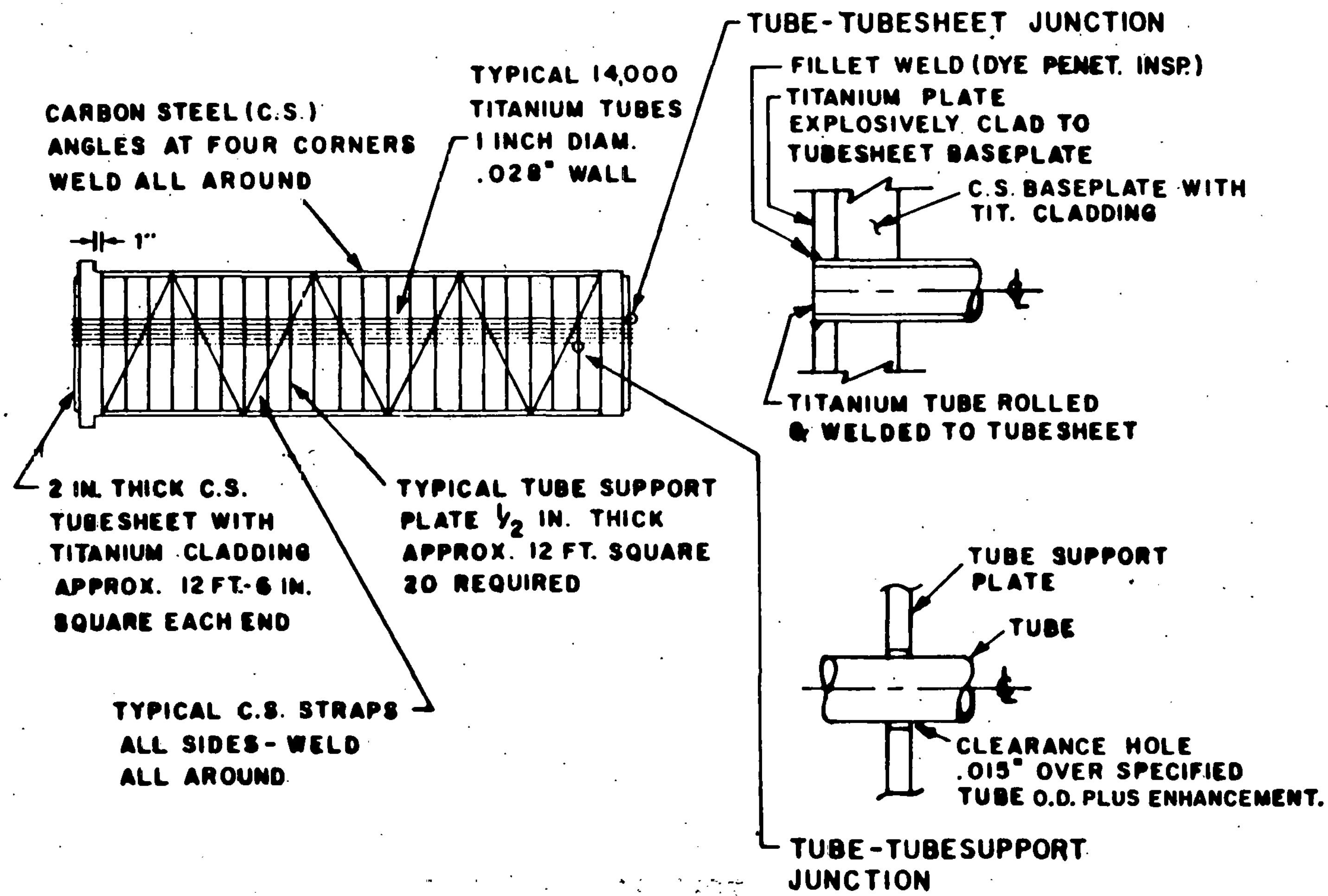

Figure 6-7

OTEC MODULAR HEAT EXCHANGER, 50 MWe CONDENSER BUNDLE ASSEMBLY

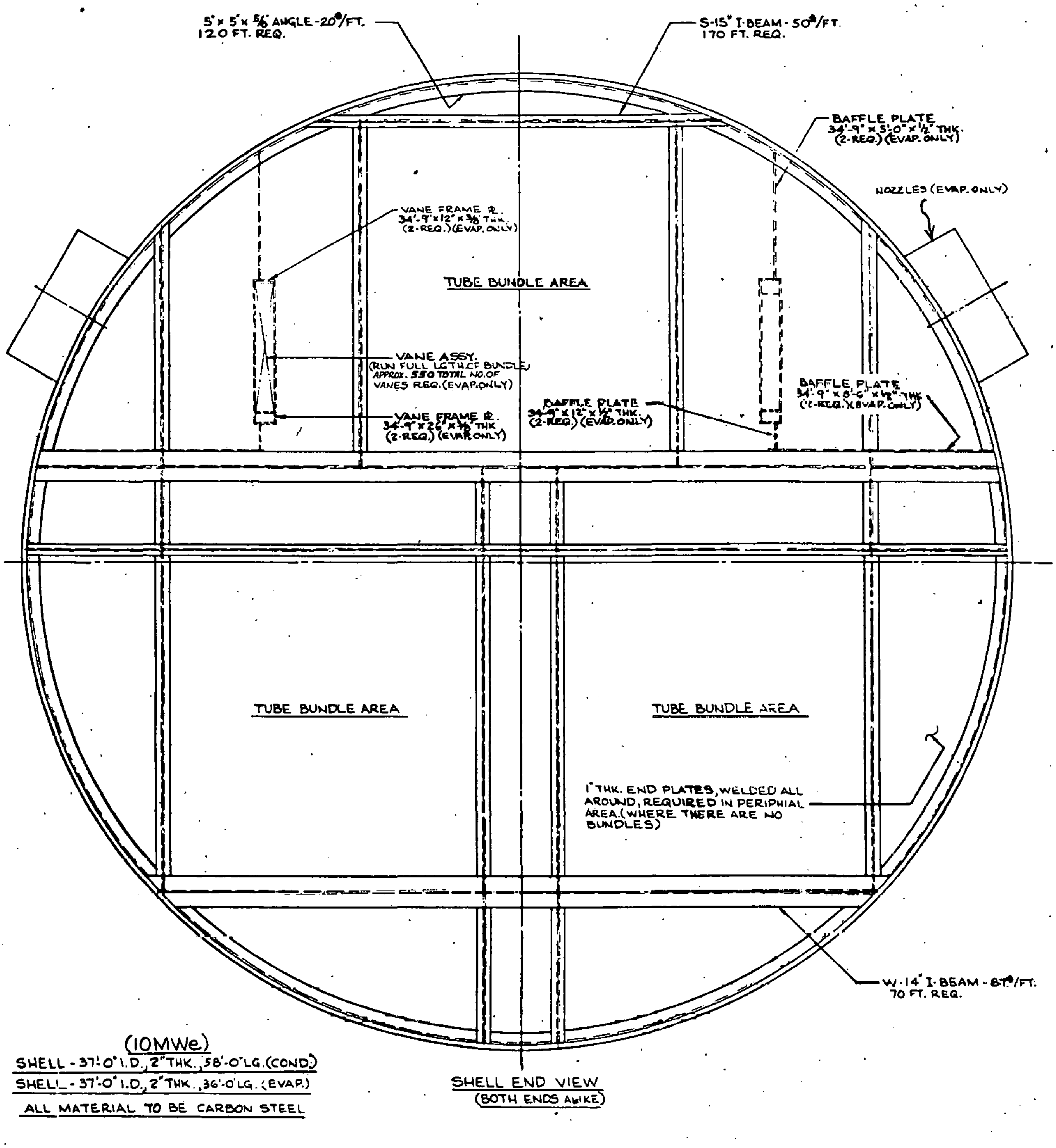

Figure 6-8
EVAPORATOR AND CONDENSER SUPPORTS AND INTERNAL BRACING

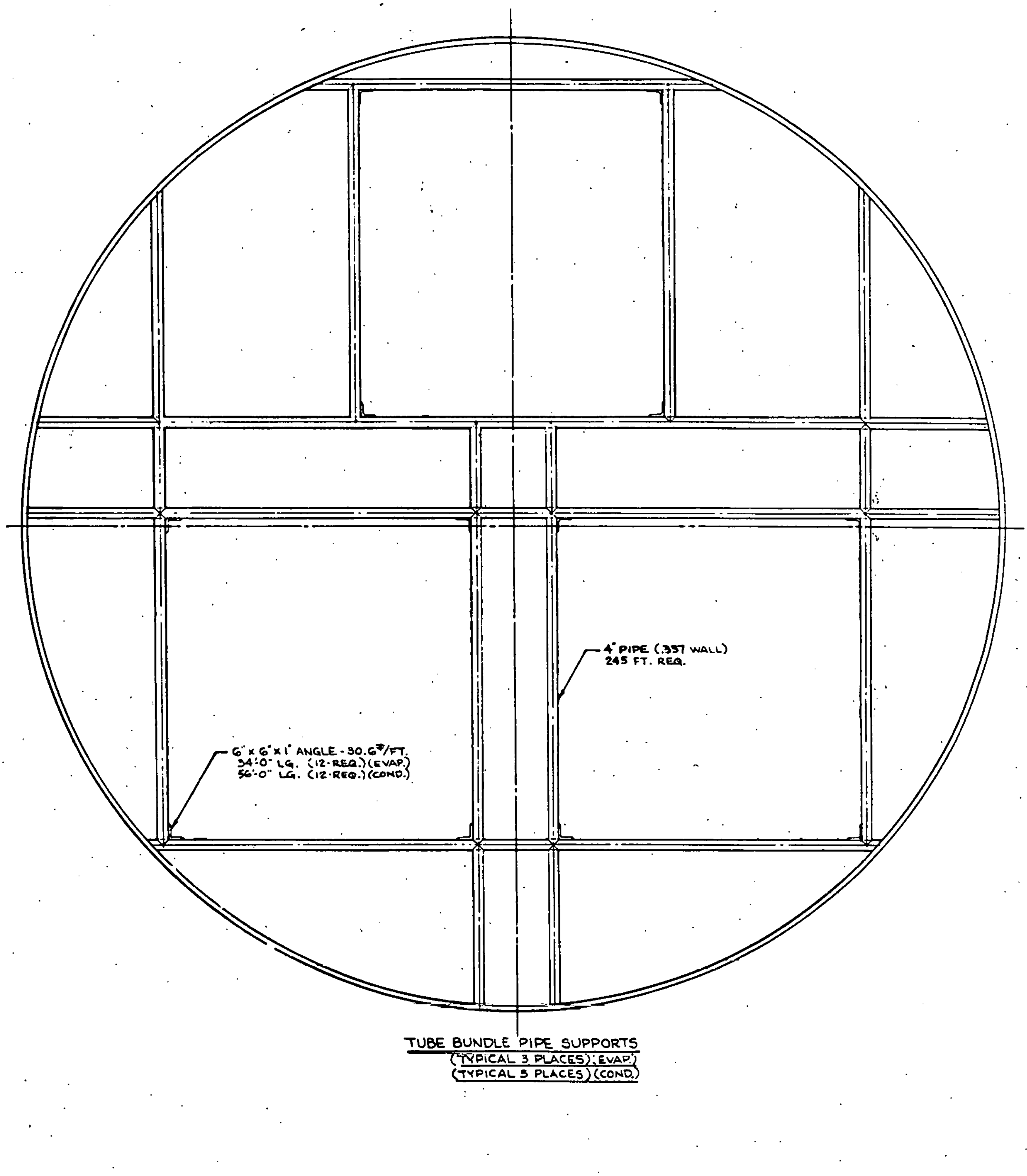

Figure 6-8 Continued

LAYOUT NO.
746J477

THIS PAGE

WAS INTENTIONALLY

LEFT BLANK

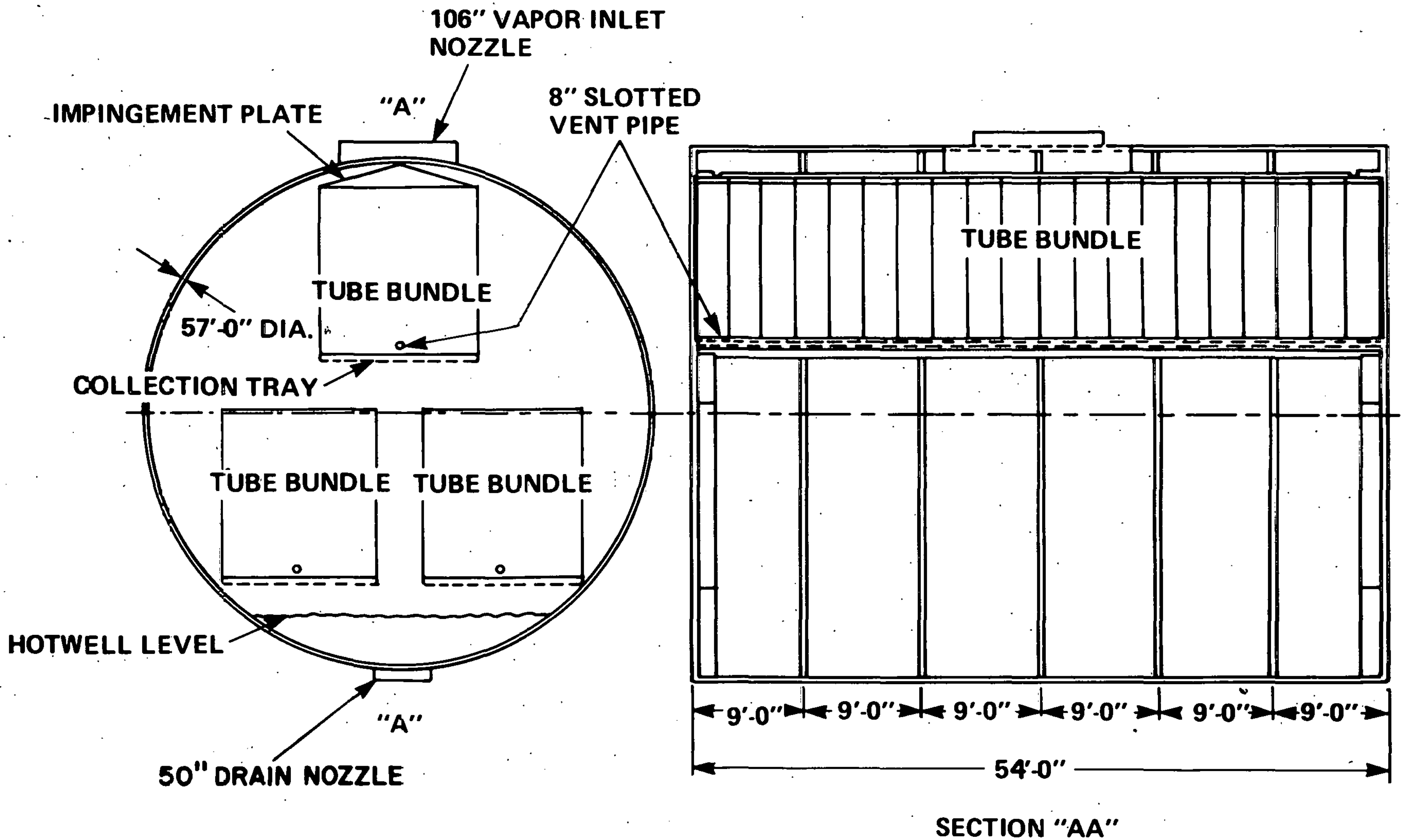

Figure 6-9
CONDENSER (10 MWe)

box from one end of the shell to the other. At intermediate locations (three in the evaporator and five in the condenser), a lattice work of pipes (Figure 6-8) perpendicular to the shell supports the rails and maintains their level. End plates are welded to the faces of the I-beams in the tubesheet plane on both ends to close the shell chamber in all but the square opening where the assembled bundle is subsequently inserted.

Three tube bundles for each unit are constructed independently (Figure 6-7). Each bundle consists of two end tubesheets, about 11 (19 in the condenser) intermediate tube support plates (to avoid possibility of tube vibration failures); 14,000 1-inch diameter titanium tubes rolled and welded at each end for increased reliability; and a number of diagonal stiffener and corner angles to form a rigid box-like bundle assembly.

The welded joint selected for connecting the tubes to tubesheets reflects many years of successful experience in high pressure feedwater heaters, nuclear steam generators, and condensers. It is expected to provide the most reliable approach to a leak-proof joint, using automated manufacturing methods. (A more detailed discussion is given in Section 6.3.1.4, "Titanium").

The proposed design is all welded and is shown in the figures with titanium tubes and a titanium-clad carbon steel tubesheet. However, the design is also suitable for aluminum or other tube materials, should the acquisition of future test data suggest this change. For an aluminum tube, the tubesheet will be clad with aluminum. In addition, for this alternate design, the tube support plates and the boxes at each end of the shell will be aluminum. The I-beam flange faces will be explosively clad aluminum to facilitate welding of the boxes. The remainder of the internals and shell can be made of carbon steel.

The ammonia liquid-vapor separator assembly is placed in the evaporator shell, thereby saving a large external separator vessel and achieving a significant cost reduction. Figures 6-5 and 6-8 show the vertical arrangement running the entire length of the shell. Approximately 464 vanes (see Figure 6-10 for vane shape) will be provided. These patented Westinghouse vanes have been used successfully in hundreds of similar applications, including nuclear moisture-separator reheaters, combined cycle heat recovery steam generators, and nuclear steam generators. The hotwell for both the evaporator and condenser is also placed within the main shells, eliminating two additional large external vessels and resulting in a considerable savings.

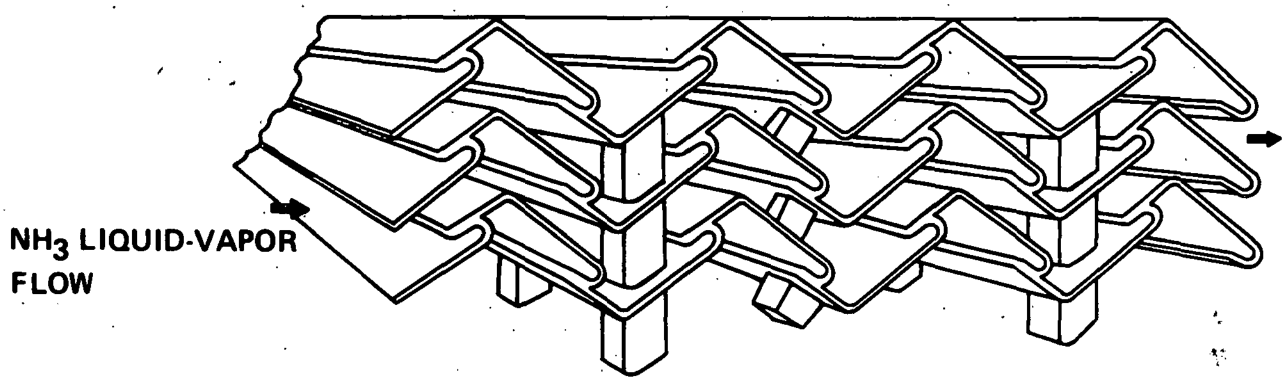

Figure 6-10
WESTINGHOUSE FORMED VANE SEPARATOR

The modular bundle approach also yields improvement of the evaporator shell side liquid distribution. For large single bundle units, a number of feed tubes, either extensively manifolded or fed through a double tubesheet arrangement is required (at great cost). With the modular approach, each bundle is an independent unit. The liquid to be evaporated is distributed equally by internal piping to a perforated tray above each tube bundle. The perforation size and location for each tray is designed to ensure uniform liquid distribution to avoid drying areas on the tubes. To avoid sloshing and spilling from ship movement, each tray will be internally baffled, covered, and pressurized to promote equal flow through all holes. A tray at the bottom of each bundle collects the unevaporated liquid and channels it to the bottom of the evaporator or hotwell. Tube spacing and location, tube support plate spacing, plus distance between bundles are sized for structural adequacy while permitting free flow of the escaping vapor at velocities that minimize pressure drop and preclude damage to the internals.

The condenser design is treated similarly. Collection trays are provided at the bottom of each bundle, but feed trays are not necessary. Bundles are vented individually for improved performance. Internal manifolding of the collection trays and vents requires only one shell penetration for the condensate and another for the vent.

Table 6-6 lists the results of a study made during the conceptual phase of this contract. The major heat exchanger components are listed as per cent of total cost for the conventional shell and tube heat exchanger design; the new modular design concept is compared with it using the conventional design costs as the basis for the percentages.

Table 6-6
COST COMPARISON UNIT VS. MODULAR DESIGN

	Unit Design	Modular Design
Total Heat Exchanger Costs		
Labor	30%	21%
Tube Material	63%	63%
Other Material	7%	7%
	100%	91%
Heat Exchanger Cost Breakdown		
Tube Material	63%	63%
Tube Labor	5%	3%
Tube Sheet (Labor and Material)	11%	6%
Shell (Labor and Material)	7%	7%
Internals (Labor and Material)	14%	12%
	100%	91%

It is apparent that the modular design with lower tube labor, tubesheet (labor and material) and internals is the prudent choice. An overall reduction of 9% is expected.

The major advantages of modular design are as follows:

- Modular bundles can be built simultaneously to shorten manufacturing cycle time.
- Modular bundles are compact and can be constructed at many existing shops.
- Modular bundles are rail shippable.
- Modular bundles allow for standardization of many parts.
- Tubesheets are smaller, thinner and less costly.
- Automated tube hole drilling/tube welding will be utilized.
- Tube-to-tubesheet connection can be shop tested.
- No high cost tube assembly is required on board ship.
- Shell internals can be aligned in shop.
- Modular bundle can be removed at any time for inspection and/or repair.
- Customer may stock spare bundle(s).
- Shellside evaporator ammonia distribution is improved.

- Each bundle can be operationally independent.

- Simple model testing is possible with high degree of confidence.

- Very minimal field labor is required on board ship.

- Size constraint for OTEC heat exchangers is removed.

- Higher reliability is achieved at lower cost.

6.2.1.2.2 Unit (Single Bundle) Design Investigations

Prior to the selection of the modular heat exchanger design, variations of conventional single bundle configurations were investigated. The effects of tube diameter, surface enhancement, tube-to-tubesheet connection techniques, etc., on heat exchanger effectiveness, size and cost were evaluated. The two major variations in mechanical design were all-welded and flanged tubeplate junctions.

a. Single Bundle Design, All Welded

The initial design is shown in Figure 6-11. The unit is cylindrically shaped, for minimum wall thickness and cost, surrounding a number of tubes in a horizontal position with tube plates at each end. The seawater enters the tubes from the left and exits at the right. Ammonia is on the shellside of the unit. An annular space is provided around the tubes to accommodate the vapor distribution.

The design is all welded and suitable for both titanium and aluminum tubes. When titanium tubes are used, all other parts are made of lower cost carbon steel; however, the tubeplate must be clad with titanium to facilitate tube-to-tubeplate welding.

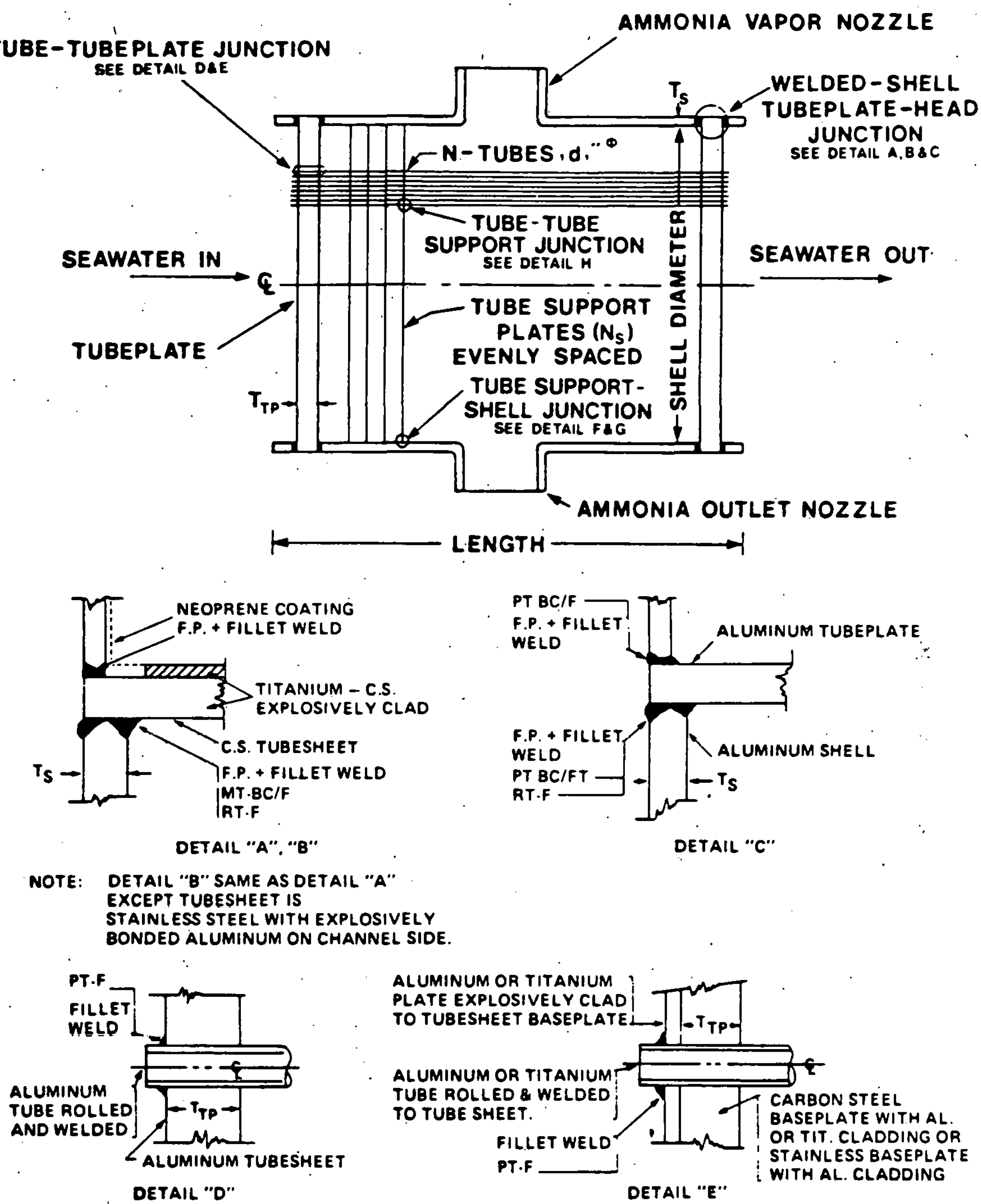

Figure 6-11
WESTINGHOUSE OTEC HEAT EXCHANGER DESIGN UNIT DESIGN WELDED TUBEPLATE JUNCTION

Two important areas of consideration are the tube-to-tubeplate junction and the shell-to-tubeplate junction. For the latter, a full penetration weld on either side of the tubeplate is envisioned; for the former, a rolled and welded tube connection is recommended for increased reliability.

This design would have to be fabricated and assembled either at a special shore-side facility to permit barge shipment to the platform assembly facility, or it would have to be assembled at the platform assembly facility. Neither alternative appears particularly attractive from a cost or quality control standpoint.

b. Single Bundle Design, Flanged Tubeplate Junction

Another approach to the unit design for the aluminum tubes is shown in Figure 6-12. Rather than the all-welded construction previously described, an alternate flanged tubeplate junction is employed. This variation uses all-aluminum tubesheets along with aluminum tubes and tube support plates. The shell is carbon steel.

The major difference in the design is the flanged junction. The primary feature is the electrical separation of the aluminum and carbon steel parts, accomplished with an insulating gasket and insulating bolt sleeves. This electrical separation precludes galvanic corrosion when aluminum and steel are in contact in the presence of an electrolyte. The flanges are forged into arc sections and welded together to form the cylindrical shape. Because of the high hydro-static loading, a 30-inch thick flange with 326, 3-inch diameter high strength bolts is required. Also, for attachment of each aluminum tube support plate to the shell, a number of electrically insulated bolted supports must be provided about the circumference.

This design has the same fabrication and assembly limitations as the all-welded design.

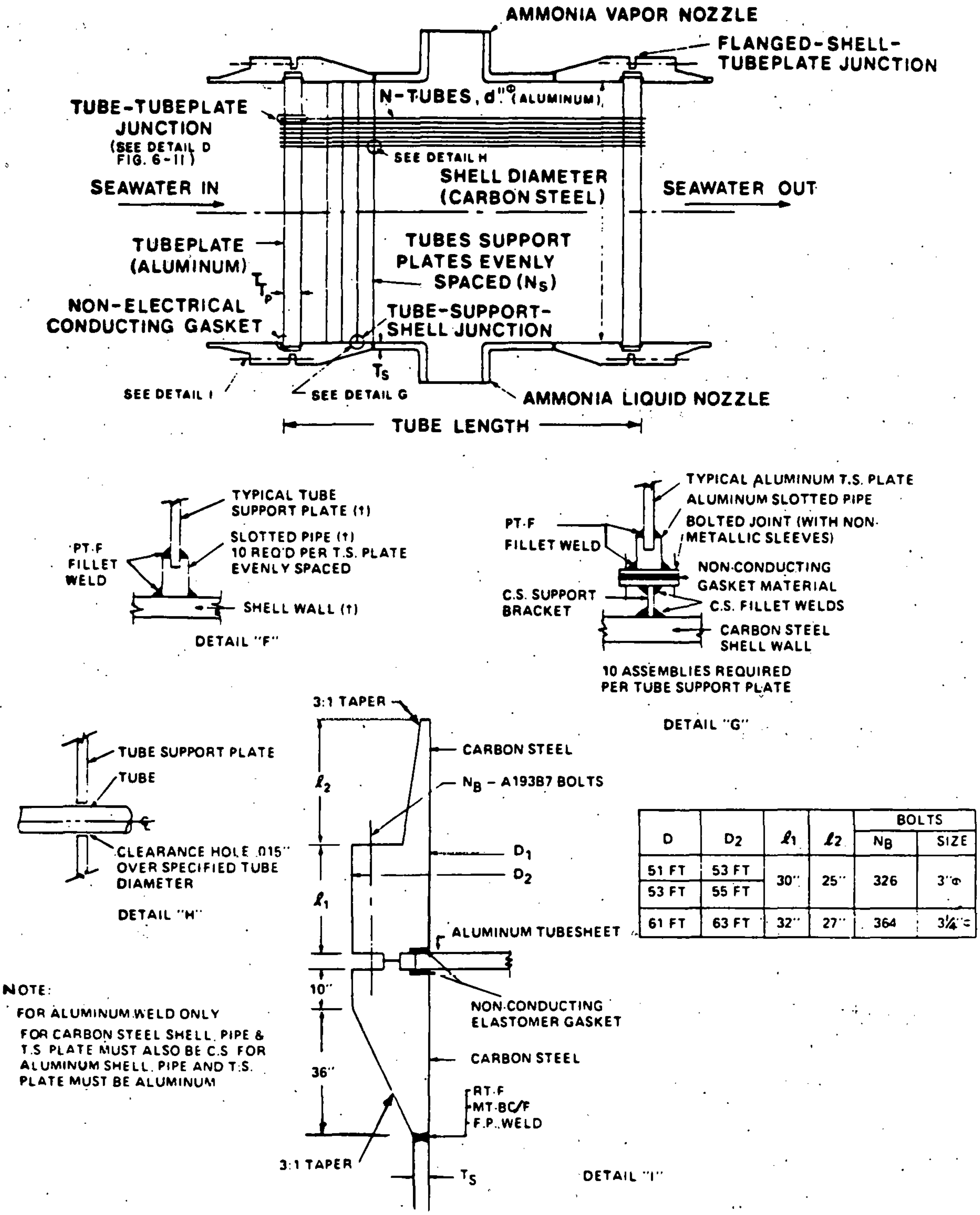

D	D2	ℓ_1	ℓ_2	BOLTS N_B	BOLTS SIZE
51 FT	53 FT	30"	25"	326	3"φ
53 FT	55 FT				
61 FT	63 FT	32"	27"	364	3¼"φ

Figure 6-12
WESTINGHOUSE OTEC HEAT EXCHANGER DESIGN UNIT DESIGN FLANGED TUBEPLATE JUNCTION

c. Single Bundle Design

Design feasibility studies of unit designs covering a variety of tube diameters, heat exchanger materials and detail manufacturing concepts were made to uncover problem areas, formulate desirable design details, and develop cost algorithms for large OTEC-type heat exchangers.

In these studies, plain tubes were assumed and heat exchanger sizes were developed using shell diameters from 48 to 61 feet, tube diameters from 1 to 2 inches, and lengths from 38 to 150 feet.

In Table 6-7, pertinent details of the eight cases studied are outlined. Cases A through C are all-welded designs with three titanium tube diameter sizes; cases D through F are flanged designs with a carbon steel shell with three aluminum tube diameter sizes. Case G is similar to Case E, except that a stainless steel tube plate clad with aluminum to facilitate tube welding is used. This feature permits use of aluminum tubes without the costly flange design, since the stainless steel tubeplate can be welded to a carbon steel shell and the aluminum tubes should not experience galvanic corrosion in contact with the tubeplate. Case H is an all-aluminum design.

From Table 6-4, it is apparent that:

- For an all-welded plain titanium tube design, a 1-inch diameter tube has the lowest cost.

- For a flanged plain aluminum tube design, a 1.5-inch diameter tube has the lowest cost, and is lower than the titanium tube design for initial manufacturing cost.

- A stainless steel tubeplate with an aluminum tube (Case G) has a higher cost than a flanged design with aluminum tube (Case E).

- The all-aluminum design (Case H) has a higher cost than the flanged design (Case E).

The unit design obviously has many disadvantages. With the large diameters and thousands of tubes necessary, fabrication and assembly is very difficult. The designs permit shipment of few subassemblies but a great deal of fabrication and assembly is necessary at a coastal fabricator's shop (with heavy lift equipment) or aboard the OTEC hull.

Maintaining flatness is a formidable problem in welding millsize plates together to form tubeplates and tube support plates with subsequent tube hole drilling in the weld area. Also, aligning and fastening these large plates within the shell while maintaining perpendicularity to the shell to facilitate tube assembly is costly and difficult. Developing a scheme of feed tubes to provide uniform shellside ammonia distribution within a minimum of nozzles and piping is troublesome.

For the above reasons, the Westinghouse modular heat exchanger design concept was developed to:

- Maximize lower cost shop fabrication where skilled tradesmen and specialized machinery and automatic welding equipment exist

- Make parts and subassemblies shippable by conventional means

- Permit the development of less costly shellside liquid distribution and collection systems.

6.2.1.2.3 Mechanical Design Procedures

Both the modular and single bundle heat exchanger designs were developed in accordance with the requirements of the ASME code rules[3].

Table 6-7
OTEC HEAT EXCHANGER UNIT DESIGN FEASIBILITY STUDY

Case	A	B	C	D	E	F	G	H
Materials (see Material Designation below)								
Shell	1	1	1	1	1	1	1	2
Tubesheet	6	6	6	2	2	2	7	2
Tube Support Plates	1	1	1	2	2	2	2	2
Tube	4	4	4	3	3	3	3	3
Shell Flanges	-	-	-	5	5	5	-	-
Tube								
Diameter (in.)	1.0	1.5	2.0	1.0	1.5	2.0	1.5	1.5
Thickness (in.)	.028	.036	.048	.065	.084	.102	.084	.084
Length (feet)	59	107	150	38	84	120	84	84
Number (n)	120,000	47,170	25,930	168,600	56,375	30,170	56,375	56,375
Shell								
Diameter (feet)	51	48	48	61	53	51	53	53
Thickness (T_s) (in.)	2.75	2.5	2.5	3.25	2.75	2.75	2.75	5.0
Other Sizes								
Number of supports (N_s)	20	25	26	12	18	20	18	18
Tubesheet Thk (Ttp)(in.)	2.25	2.5	2.75	4	3.75	3.88	2.5	4.5
Manufacturing Detail								
Design Type	Welded	Welded	Welded	Flanged	Flanged	Flanged	Welded	Welded
Tube-Tubesheet Detail*	E	E	E	D	D	D	D	E
Shell-Tubesheet Detail*	A	A	A	K	K	K	B	C
Tube Support-Shell Detail*	F	F	F	G	G	G	G	F
Cost Ratio $\frac{\text{(Total Cost)}}{\text{(Total Cost of Case A)}}$	1.0	1.25	1.43	.91	.77	.87	.84	.9

Material Designation

1. C.S. Plate A516 Gr. 70
2. Al. Plate SB209 Alloy 5083
3. Al. Tube SB234 Alloy 5052
4. Tit. Tube SB338 Gr. 2
5. C.S. Forging A266 Gr. II
6. C.S. Clad with Titanium
7. S.S. Clad with Aluminum
   (S.S. Plate - A240 TP304)

*See Figures 6-11 and 6-12

a. Pressure Boundary Wall

The shell wall was calculated for both internal and external pressure. An internal design pressure of 150 PSI was selected by the system designers for both the evaporator and condenser. During startup of the system while purging of the vessels is occurring, a vacuum exists in the vessels. Also, since the heat exchangers are submerged in the sea, a hydrostatic force proportional to the depth exists. Conservatively, the external design pressure assumed was full vacuum plus a hydrostatic head of the vessel diameter plus 10 feet. The pressure boundary thickness and additional stiffening where required, were calculated using rules of Paragraphs UG-27, UG-28 and UG-29 of the ASME Code[(3)].

b. Tube Wall Thickness

The minimum wall thickness for the heat exchanger tube is calculated in accordance with the ASME Code[(3)] and is plotted as a function of tube diameter in Figures 6-13 and 6-14. Since the shell pressure is much higher than the tubeside pressure, the limiting design condition is failure by buckling from external pressure. The method for determining the tube wall is as described in Paragraph UG-28 of the ASME Code [(3)] (using an external design pressure of 150 PSI for both the evaporator and condenser). This method is based on experimental data and theory, continually reviewed by an industry committee, considering quality, manufacturing tolerances and normal material property variations of commercial tubing with many years of successful experience. Thicknesses were calculated by use of Figure UNF 28.28 for unalloyed SB338 GR 2 titanium tubing and Figure UNF 28.18 for SB234-5052 aluminum tubing.

With titanium tubing, a lower limit of 28 mils was used for tube thickness, based on experience with handling during manufacture and assembly.

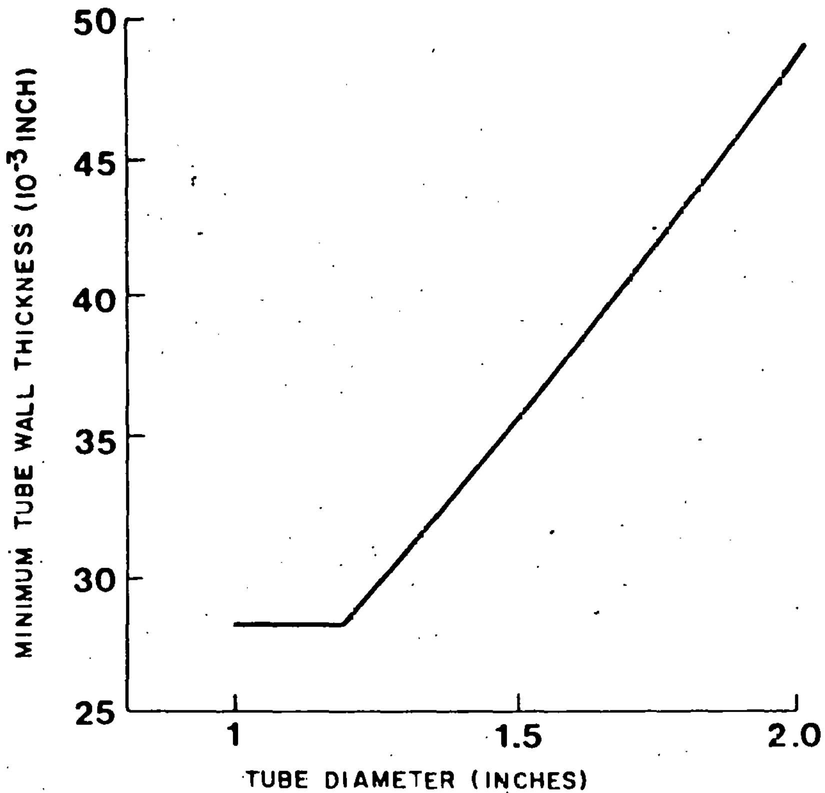

Figure 6-13
TUBE WALL THICKNESS
TITANIUM TUBE SB 338 GD 2

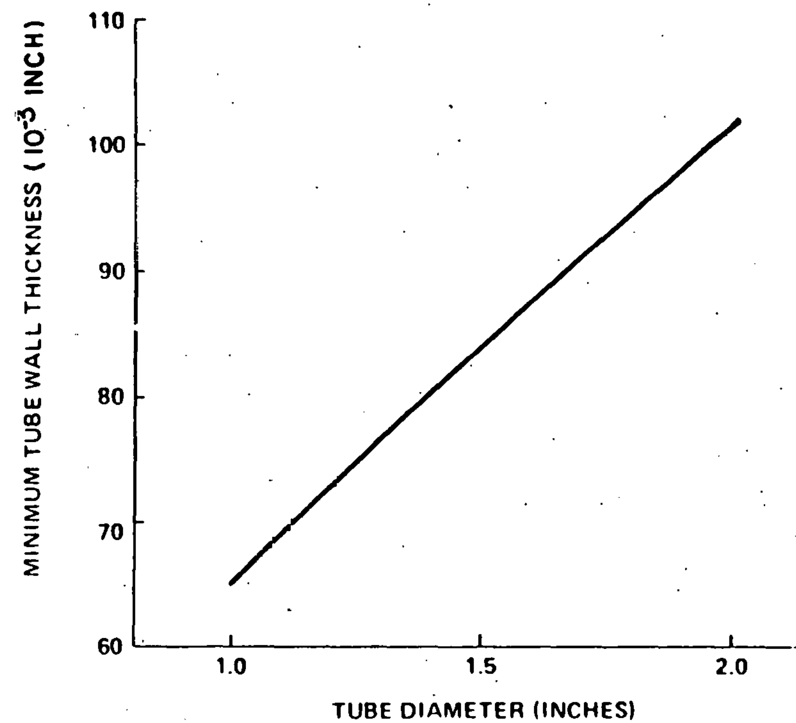

Figure 6-14
TUBE WALL THICKNESS
ALUMNNUM TUBE SB 234 ALLOY 5052

With aluminum tubing, a corrosion and erosion allowance of 27 mils is included in Figure 6-14, resulting in a thickness of .065 for a 1-inch diameter tube.

c. Tubesheet Thickness

The tubesheet thickness was calculated by use of an available computer program[6] for fixed tubesheets on both ends of a heat exchanger. The program is based fundamentally on papers by K.A. Gardner[7] and Yi Yuan Yu[8]. An additional feature of the program not considered by Yu is allowance for the added stiffness of an unperforated rim between the outer tubes and the tubeplate connection.

The perforated region is considered to be an "equivalent solid plate" through transformation described by W.J. O'Donnell and B.F. Langer[9] and accepted by Appendix Four of the ASME Code[10].

The tube bundle is considered to create an elastic foundation for the tube sheet, carrying a significant portion of the load and resulting in a relatively thin tubesheet. It also creates a loading force with relation to the shell due to axial thermal expansion differences in the unit (for this application the difference is rather small) which is taken up by bending and rotation of the tubesheet and the shell end.

The heat exchanger assembly is divided into free body elements (shell, unperforated rim, perforated disc, and tubes) and equations of compatibility are established and solved at their common junction to determine internal moments and forces and resulting stresses. These stresses are compared to allowable stresses defined in Appendix Four of the ASME Code Rules[10].

For the single-bundle design, the shell diameters defined in Table 6-7 were used. For the preliminary design of the Modular Application, a diameter through the corners of square tubeplate was assumed. Of course, during the detail design phase, a new program must be developed including the deflection and rotation of the I-beam lattice.

d. Internal Structure

The internal structure was sized using static loads along the beams and pipes based on internal pressure and flooded bundle weights. With the interlocking of the structure in a number of planes within the shell by the longitudinal rails, a very rigid structure is achieved.

e. Dynamic Analysis

A preliminary dynamic analysis for the tube support arrangement determined the maximum tube support spacing. With proper spacing of the tube support plates, tube vibration failures caused by shellside flow velocity can be avoided. Tube vibration due to tubeside flow effects, acoustic and external excitation, have been shown through testing of units similar to the OTEC design to be negligible. Almost all damaging tube vibration in heat exchangers with a low density shell side vapor is due to fluid elasticity. The effects of vortex shedding and turbulent axial flow and crossflow are of negligible importance. Hence, the critical tube span was calculated using an expression based on H.J. Connor's[11] criteria.

The OTEC heat exchangers share many mechanical and fluid flow parameters with condensing sections of existing Westinghouse heat exchangers. Thus, experience on similar designs, with tubes clamped at each end and simply supported at each tube support plate, facilitated the calculation of the required tube support plate spacing. The 1-inch diameter, 0.028-inch wall titanium tubes need to be supported every 35.5 inches or less, and the corresponding length for the 1-inch diameter, 0.065-inch wall aluminum tube is 37.9 inches.

A summary of pertinent data outlined above for the 10 MWe modular heat exchangers is given in Table 6-8.

6.2.2 Seawater Pumps

6.2.2.1 Background

Seawater flow rates of 3 to 4 m^3/sec per MWe of plant output are required for both evaporator and condenser flow paths. Typical flow path head losses range from 2 to 4 meters. The total pumping power for ideal (100% efficient) seawater pumps ranges from 12 to 32% of plant net output for this range of flow and head loss. Seawater pumping will constitute a major parasitic loss in OTEC plants, and overall pump efficiency is a primary concern in pump design.

The general configuration of a high efficiency pump is a function of operating point flow and head. The OTEC seawater pump operating conditions lead directly to the choice of an axial flow, propeller-type pump. Several configurations of this pump type are feasible for OTEC application. Figure 6-15 illustrates the configurations considered. The self-contained immersed bulb or pod configuration was chosen based upon considerations of efficiency, flexibility and ease of maintenance.

Preliminary pump analysis showed that diffuser design is critical to achieve the high efficiency required of OTEC pumps. Kinetic losses associated with poor diffuser design could reduce overall pump/diffuser efficiency to below 50%, doubling the parasitic loss for an ideal pump. The pump configuration chosen permits the most efficient diffuser design possible. Design data developed in this analysis provides an upper limit for pump performance which could be easily modified to compensate for reduced diffuser efficiency of the alternate configurations.

Table 6-8
HEAT EXCHANGER MECHANICAL DESIGN DATA MODULAR DESIGN - 10 MWe

Heat Exchanger Type		Evaporator	Condenser
Number of Bundles		3	3
Tubes			
Material		SB338GD2	SB338GD2
O.D.	inches	1	1
Wall Thickness	inches	.028	.028
Pitch	inches	1.25	1.25
Layout	-	60° Tri.	60° Tri.
Active Length	feet	34.7	56.5
Total Length	feet	34.9	56.7
Number per Bundle	-	14036	14050
Total Number	-	42108	42150
Tube Sheet			
Size (Rectangular)	feet	12.33 x 11.46	12.33 x 11.46
Baseplate Material	-	SA516GD70	SA516GD70
Baseplate Thickness	inches	2	2
Cladding Type	-	Explosive	Explosive
Cladding Material	-	SB265GD1	SB265GD1
Cladding Thickness	inches	.25	.25
Tube Support Plate			
Size (Rectangular)	feet	12.08 x 11.17	12.08 x 11.17
Material	-	SA283GD.C	SA283GD.C
Thickness	inches	0.5	0.5
Number per Bundle	-	11	19
Spacing	inches	34.7	33.9
Shell			
Material	-	SA516GD.70	SA516GD.70
I.D.	feet	37	37
Thickness	inches	2	2
Length (Overall)	feet	36	58
Total Surface Area	sq. feet.	382786	623007
Bundle Weight	tons	53	84
Total H.X. Weight	tons	365	571

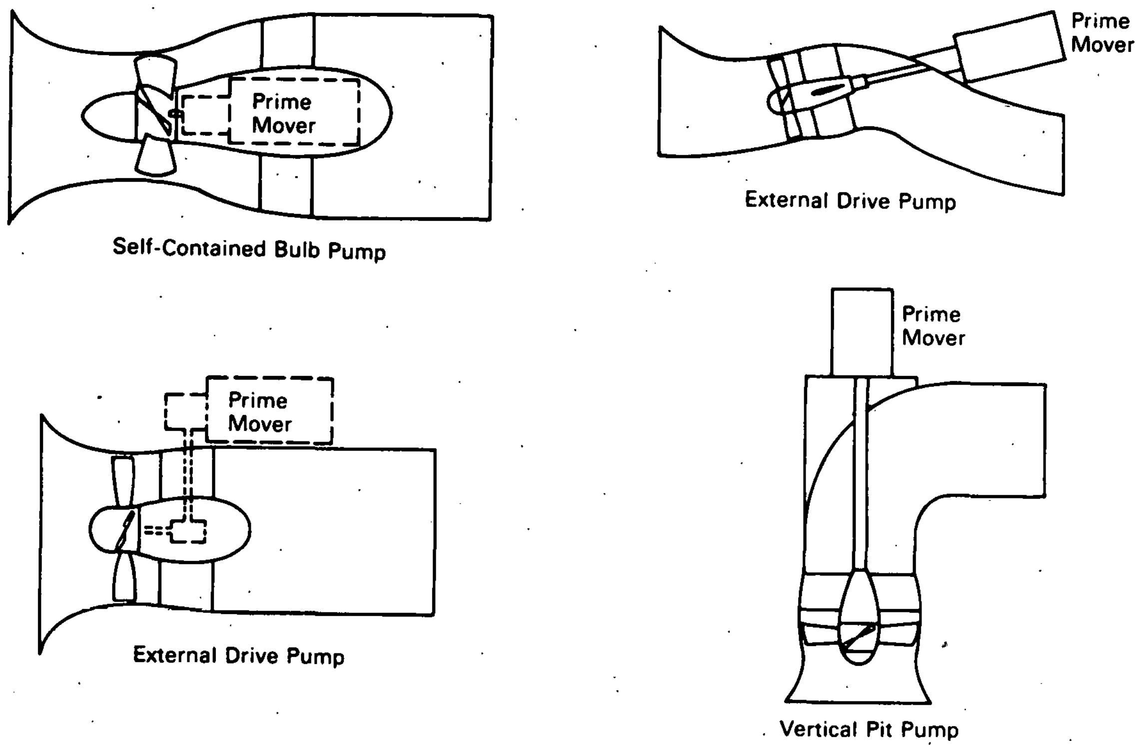

Figure 6-15
SEAWATER PUMP CONFIGURATIONS CONSIDERED FOR OTEC APPLICATION

6.2.2.2 Pump Design and Performance

Since the 10 MWe Modular Application power system was designed to model, to the extent possible, an optimized 50 MWe power system, optimized point designs for the two 10 MWe plant pumps were developed during the preliminary design phase. The flow rate and pumping head requirements for the 10 MWe Modular Application are 37.6 m^3/sec at a 2.7-meter head for the warm water loop, and 32.3 m^3/sec at a 4.7-meter head for the cold loop. The resultant pump configuration is illustrated in Figure 6-16. One warm and one cold seawater pump was selected. Note that the diffuser is an integral part of the pump design. This configuration yields a combined pump/diffuser efficiency of 80.6% at design flow and head. Inlet and outlet velocities were selected to minimize kinetic losses and to assure flexibility of interface in any portion of an OTEC seawater transport system.

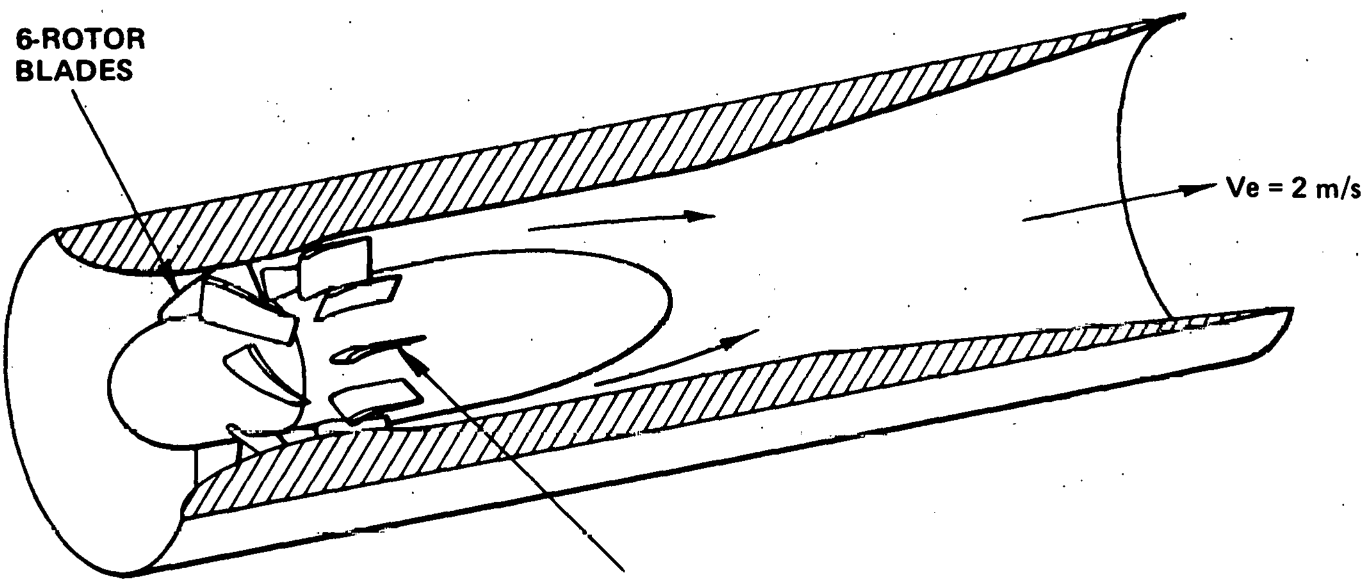

Figure 6-16
OTEC SEAWATER PUMP

Table 6-9 summarizes pump operational characteristics and major dimensions.

The 10 MWe designs are constrained to provide performance margins for pump surge, cavitation sensitivity, and startup and shutdown. Figure 6-17 summarizes performance of the 10 MWe warm water pump, and demonstrates the design operating point and resultant surge margin.

Pump start-up and shut-down analyses were conducted to establish design and operational criteria for the pump control hardware. Cold water loop startup is the controlling case due to the high inertia of the water in the cold water pipe. Analysis of the 10 MWe cold water loop leads to a 1-hour pump start-up time which includes a step speed increase to 10 percent of design speed, followed by a linear increase to full speed and flow. Continuous control of pump speed is required and would be accomplished using a variable frequency controller for a synchronous drive motor.

Preliminary designs of pump motors and controls were developed to assess overall pump system efficiency. Figure 6-18 includes a breakdown of efficiencies for major pump system elements. The overall system efficiency is 70%. This efficiency is based upon the ratio of delivered hydraulic power to the pump system busbar power.

The pump design layout shown in Figure 6-19 illustrates that the seawater pump configurations developed are feasible and that sufficient volume and structural margins exist to accommodate modifications that may arise during more detailed design phases.

The design consists of a pump pod supported within an outer shell by the stator vanes. The pump rotor is direct coupled to the motor rotor and is supported by two sets of roller bearings. The pod includes rotor and blades, shaft and bearings, motor rotor and stator, and tail cone. Corrosion-resistant stainless steels are used for surfaces in contact with seawater.

Table 6-9
OTEC SEAWATER PUMP/DIFFUSER DESIGN CONFIGURATION

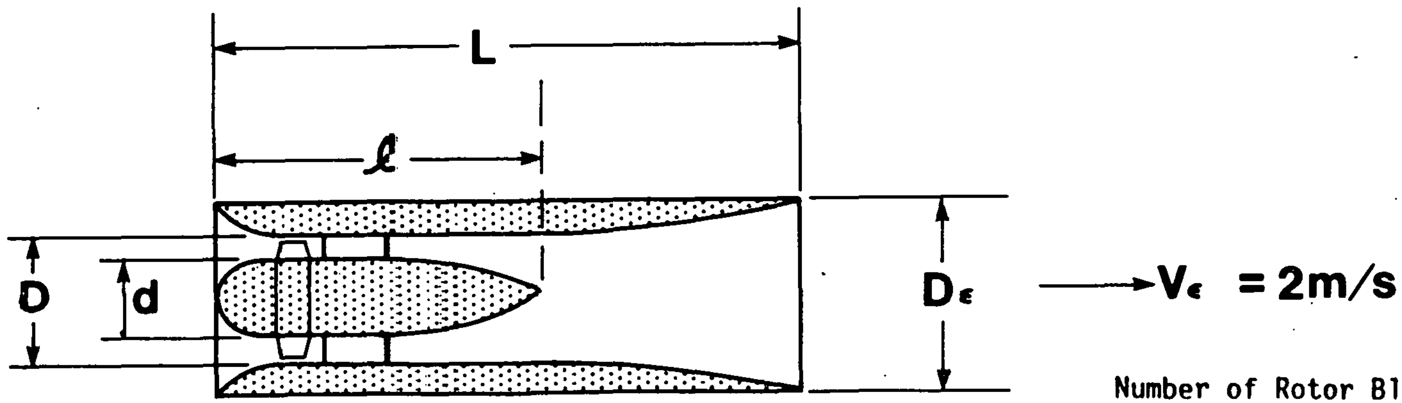

Number of Rotor Blades = 6
Number of Stator Blades = 11

Application	Capacity Q (m^3/s)	Head H (m)	Speed N (rpm)	Power P (KW)	Efficiency η' (5)	Casing Dia. D (m)	Pod Dia. d (m)	Length Overall L (m)	Pod Length P (m)	Exit Dia. D_ε (m)
10 MWe Module Warm Water	37.6	2.7	60	1267	80.6	3.43	2.30	19.6	17.1	4.89
10 MWe Module	32.3	4.7	98	1911	80.6	2.76	1.85	18.9	14.6	4.52

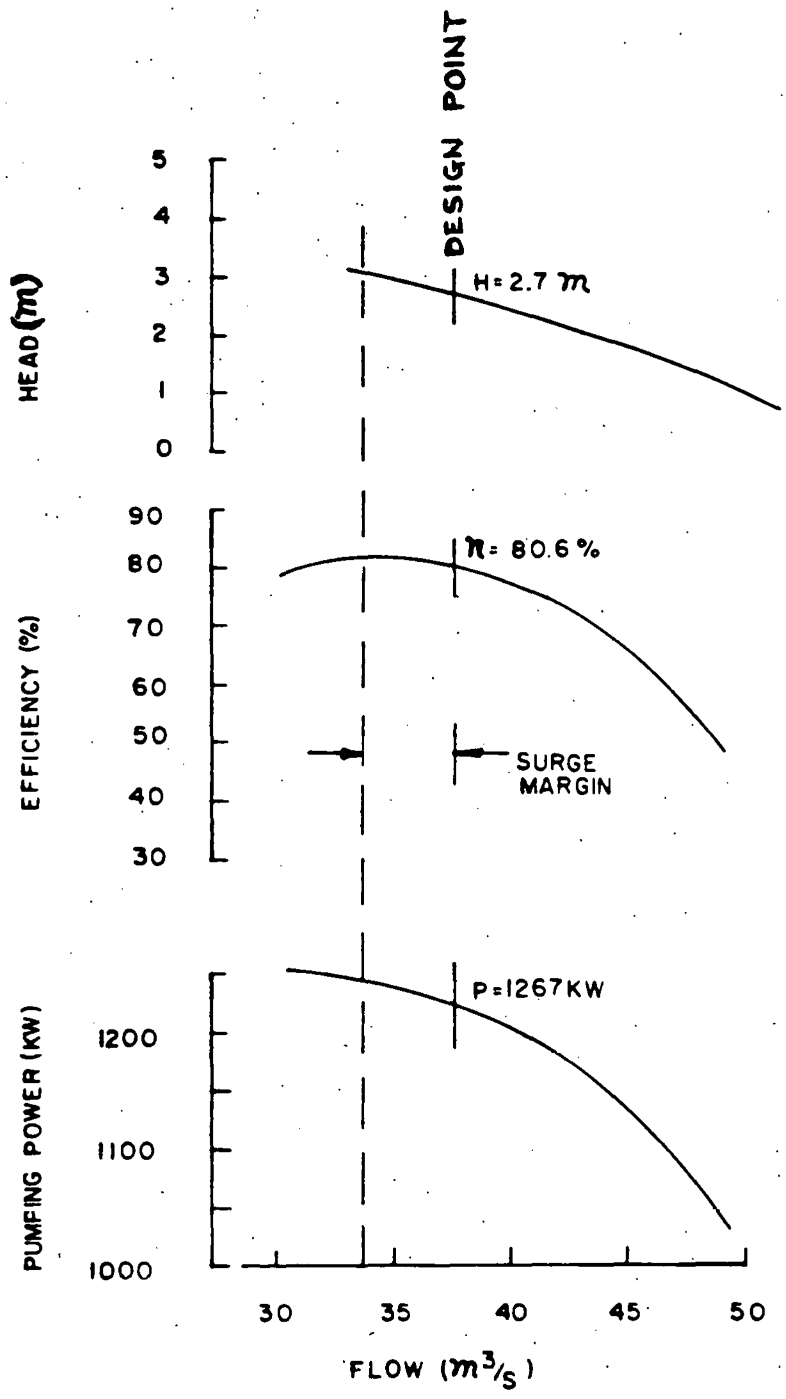

Figure 6-17
WARM WATER PUMP AND DIFFUSER PERFORMANCE

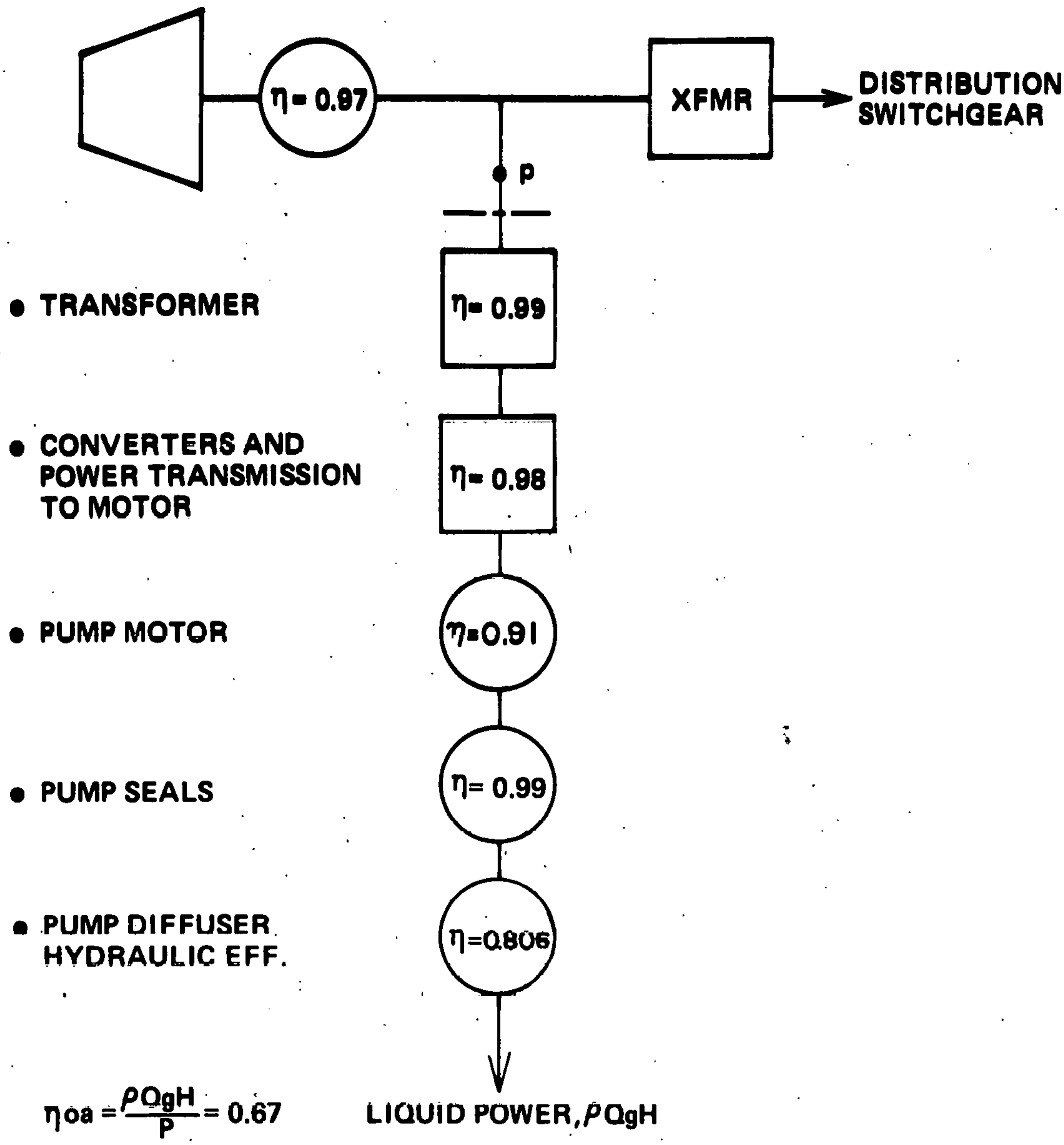

Figure 6-18
OVERALL EFFICIENCY OF SEAWATER PUMPS

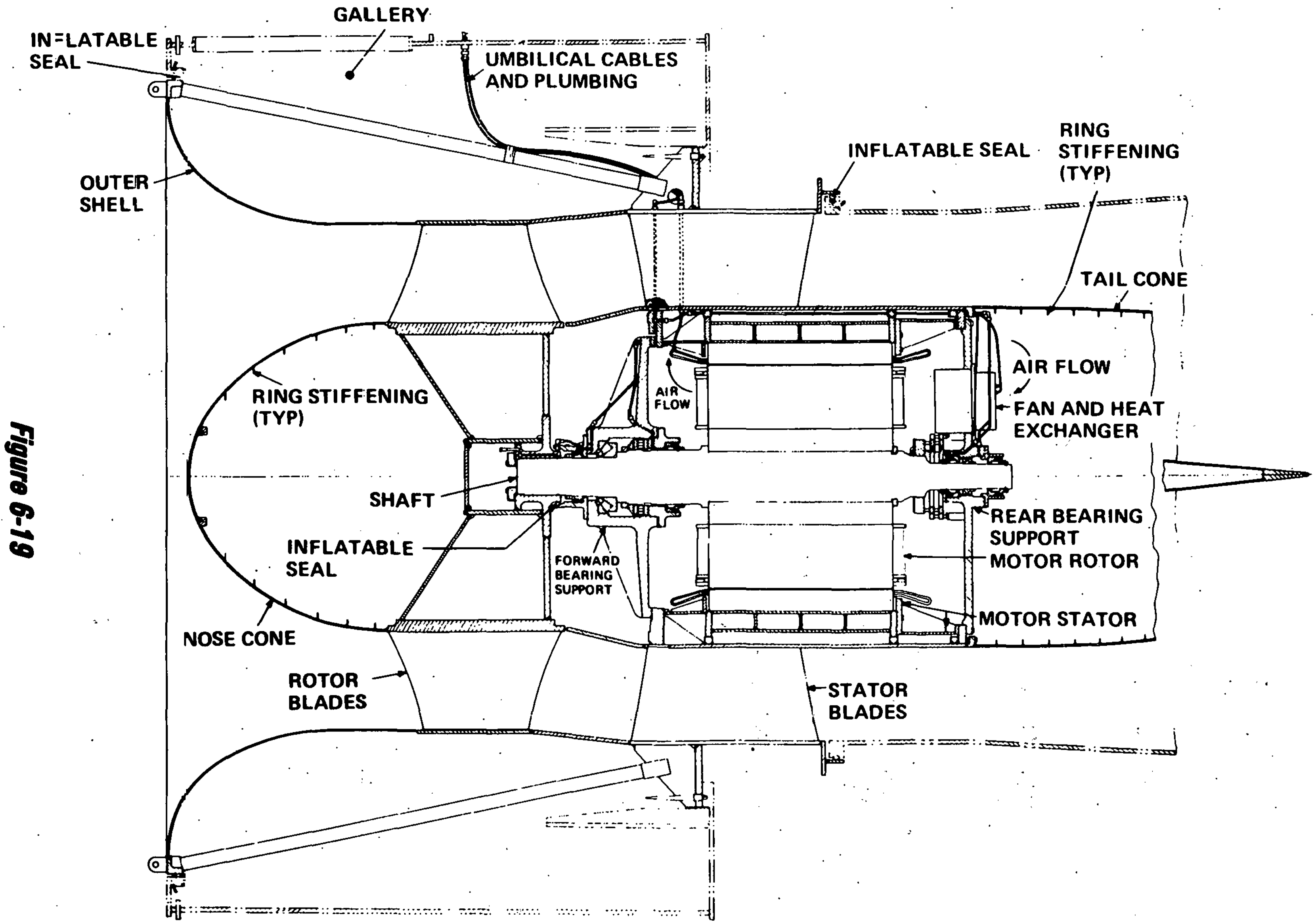

Figure 6-19
OTEC SEAWATER PUMP LAYOUT

The pod external structure is constructed of stainless steel plates, such as 316, formed to the shapes desired and ring-stiffened to provide the required strength with a minimum weight penalty. The nose and tail cone shapes were determined by hydrodynamic considerations. This structure is sized to provide a pressure boundary, with margin, for the motor cavity when submerged to 10 meters and also to provide a foundation for the motor stator, shaft bearing and seal supports. Access for assembly and maintenance is provided through closure plates in the nose and tail cones.

Several schemes of pump/platform interface were considered, with the configuration shown in Figure 6-19 chosen for ease of pump hookup with minimum umbilical exposure to the seawater environment.

6.2.3 Turbine

The primary objective in the development of the 10.0 MWe scale model turbine included: optimization of performance characteristics over the expected range of operating conditions; minimum complexity to achieve low initial cost and good maintainability; adequate strength in the rotating and stationary parts without unnecessary weight penalty; and provision of maximum sealing capability in view of the ammonia working fluid.

Major considerations in the development of the design were:

- Optimum efficiency within certain economic constraints
- Blading configurations to have passage control and aspect ration (blade height divided by blade width) with maximum reliability at high centrifugal, tangential and axial stress levels
- Capability to withstand a 50% overspeed after loss of load
- Zero or at most minimal gland seal leakage under all modes of operation, including stopped

- Material selections to provide the necessary strength with appropriate erosion and corrosion characteristics to operate in the ammonia atmosphere.

6.2.3.1 Materials

The final selection of materials for the turbine is dictated by the required high yield stress in conjunction with operation in an ammonia atmosphere with minimum corrosion effects.

It was initially believed that a similarity existed between the ammonia environment and a nuclear steam-type environment. Consequently, the original material evaluated for the rotor was CL 403 (as specified by the U.S. Navy) with a yield strength of 95,000 PSI and a tensile strength of 115,000 PSI. A subsequent investigation indicated this material to be questionable in the relatively low temperature ammonia environment, so the rotor material was changed to a nickel, chromium, molybdenum, vanadium material with approximately 2 to 3% chromium and with a yield strength of 90,000 PSI. The proposed cylinder material is carbon steel A-516.

These material selections may be modified or changed as the material test program develops.

6.2.3.2 Performance

The performance, or efficiency, of a turbine-generator set is a function of a large number of variables which include:

a. Ratio of blade throat width to pitch (gauging)
b. Ratio of blade height to width (aspect ratio)
c. Variation of inlet angle from base section to tip section (stagger angle)
d. Clearance between rotating blade and stationary parts

(leakage area ratio)

e. Magnitude of inlet and exit gas velocities which have an effect on the inlet and exhaust losses

f. Blade surface finish and trailing edge thickness

g. Mechanical and electrical losses

In addition to operating at optimum efficiency, the unit must operate reliability and safely under all possible off-design modes. The requirement that the turbine-generator set be capable of operation at approximately 50% overspeed resulted in high tangential and axial blade forces which forced a compromise with optimum efficiency to ensure maximum reliability. However, the resulting design in terms of efficiency, reliability, and required ammonia flow was acceptable in all respects. The calculated wheel efficiency and flow required to develop 14.5 MWe at the generator terminals (approximately 10 MWe) are 82.9% and 3.0 x 10^6 lbs/hr, respectively.

6.2.3.2.1 Efficiency Definition

The turbine internal or wheel efficiency is the total-to-static efficiency as calculated from the ammonia state point immediately upstream of the inlet plenum to the state point at the condenser. This includes the blade path efficiency as well as the efficiency drops caused by the inlet plenum losses and losses of kinetic energy at the discharge diffuser exit.

The efficiency at the generator terminals, or overall efficiency, is the turbine internal efficiency multiplied by the generator mechanical and electrical efficiency times the turbine mechanical efficiency. The generator losses are composed of the I^2R and eddy current losses, core losses, windage losses and journal bearing losses. The turbine losses are due to journal bearing and thrust bearing losses and the windage loss of the turbine-generator coupling.

The blade path total efficiency depends on the blading profile and secondary losses. The profile losses depend on the geometry of the section in conjunction with the gas angles together with the area contraction ratio between inlet and throat, and Reynolds and Mach numbers.

The approach used to establish the OTEC blading secondary flow losses is based on a proprietary Westinghouse empirical correlation which is the result of many field traverse tests of low pressure turbines over the years. However, because the OTEC blading has a much lower aspect ratio (height-to-chord ratio) than typical low pressure turbines, estimates of the secondary flow losses must be increased. This increase in loss due to an aspect ratio of approximately 2 for OTEC, compared with 4.5 or higher for typical low pressure turbines, was calculated by Craig and Cox.[12]

6.2.3.2.2 Internal Loss Definition

As a result of analysis, a rotor total mass averaged loss coefficient of 0.10

$$1 - \frac{(\text{exit velocity})^2}{\text{isentropic exit velocity}}$$

and a stator loss coefficient of 0.0725 are specified.

The inlet loss represents the total pressure loss between the inlet flange on the radial inlet and the station immediately upstream of the stator blade. Proprietary Westinghouse testing of inlets similar to the 10 MWe power system turbine design indicates a loss coefficient

$$K = \frac{\text{change in total pressure}}{\text{dynamic head at inlet of stator blade}}$$

of 1.5. This is equivalent to a 1.4 percent drop in total pressure, or a loss of 0.79 BTU/lbm.

The exhaust diffuser is predicted to have a pressure recovery coefficient

$$C_p = \frac{\text{increase in static pressure}}{\text{dynamic head at inlet of diffuser}}$$

of 0.3. Values just slightly below this have been measured on low pressure turbine diffusers which have a much lower diffuser length to blade height ratio; thus, 0.3 is a conservative estimate of the recovery. The energy recovered is given by:

$$h_{recovered} = \frac{a^2}{778\ (32.17)(k-1)} \left\{ \frac{\left[1 + C_p\ 1 + \left(\frac{k-1}{2}\right) M^2 \left(\frac{k}{k-1}\ -1\right)\right] \left(\frac{k-1}{k}\ - 1\right)}{1 + \frac{k-1}{2}\ M^2} \right\}$$

where: M is the absolute Mach number at the rotor exit
a is the acoustic velocity
k is the ratio of specific heats

This amounts to a recovery of 0.249 BTU/lbm of the potential 0.828 BTU/lbm energy equivalent of the turbine exhaust gas.

6.2.3.2.3 Resulting Efficiency

The turbine internal efficiency is then:

$$TS = \frac{h_{\text{BTU to Work}}}{\underset{\text{isentropic}}{h_{\text{tot-static}}} + \underset{\text{loss}}{h_{\text{inlet}}} - h_{\text{recovered}}} = 0.8285$$

The generator mechanical and electrical efficiency is 0.966.

The turbine mechanical efficiency is 0.998.

The resulting overall efficiency is equal to

$$0.8285 \times 0.966 \times 0.998 = 79.87\%$$

6.2.3.2.4 Off-Design Performance

The efficiency given in the previous section pertains to operation at the turbine design point. The turbine efficiency degradation at part load is needed as input principally for control system design as well as for economic analysis of the plant during its operating life and for transient analyses, such as overspeeds, etc. As can be seen in Figure 6-20, the turbine internal efficiency is nearly constant over the range of full load down to 60% of full load. Beyond this point, a noticeable decrease in efficiency occurs.

A plot of mass flow versus power results in the curve shown in Figure 6-21. This curve is essentially linear from full load down to 25% load. The classic approximation of this curve, called the Willans Line, is linear all the way down to the no-load point. The predicted mass flow at the no-load point is approximately 43% of the full load flow. Thus, the single-stage 10 MWe turbine value for zero load flow is much higher than typical multi-stage values of around 5%.

The corresponding turbine inlet pressure versus power curve is shown in Figure 6-22.

6.2.3.3 Technical Details

6.2.3.3.1 General Configuration and Support

As noted from the longitudinal section drawing, Figure 6-23, the overall turbine configuration is relatively simple and consists essentially of a double flow type rotor with a single reaction stage at each end together with an inner blade ring and outer cylinder.

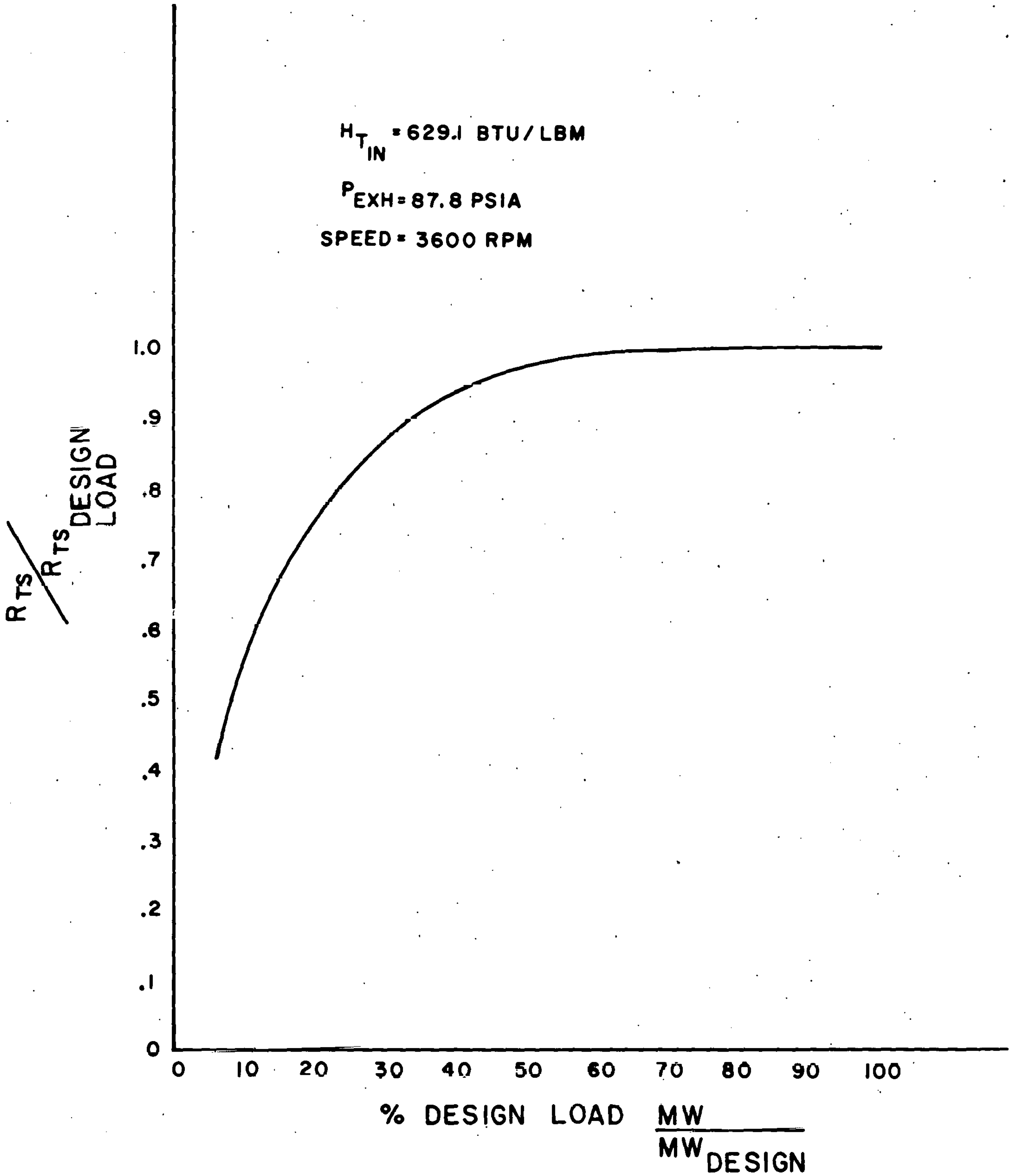

Figure 6-20
OTEC 10 MWe AMMONIA TURBINE PART LOAD INTERNAL TOTAL-STATIC EFFICIENCY

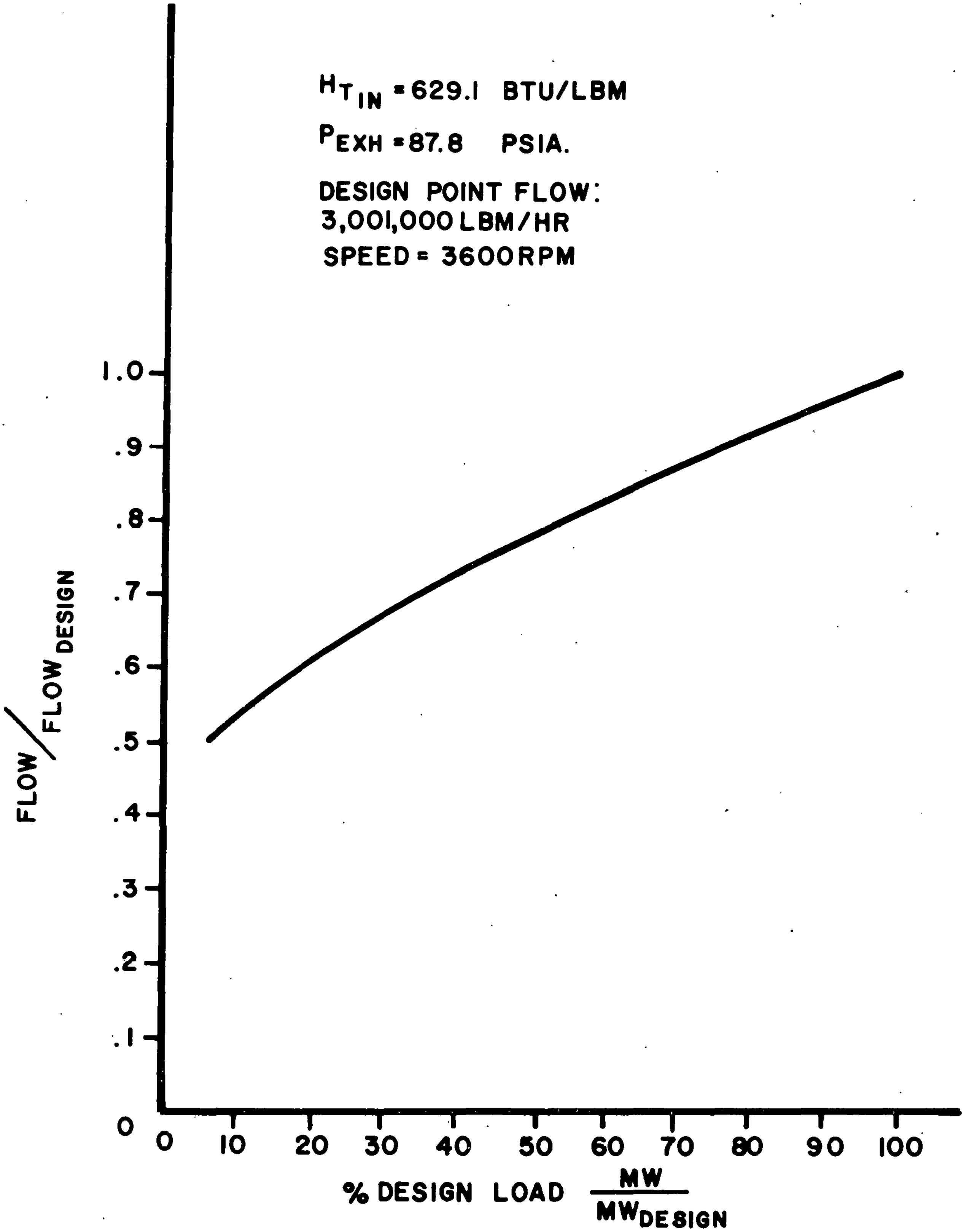

Figure 6-21
OTEC 10 MWe AMMONIA TURBINES PART LOAD MASS FLOW

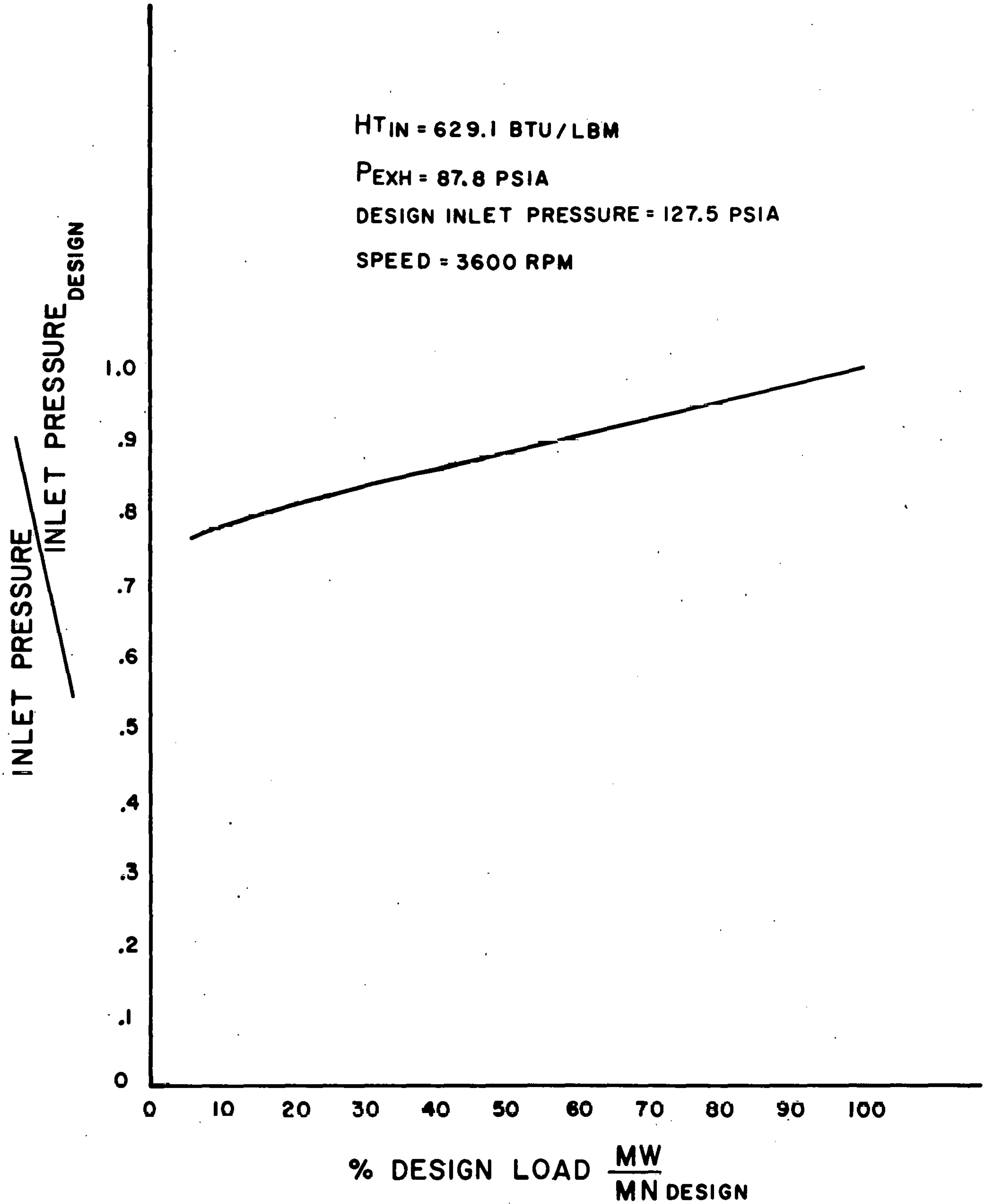

Figure 6-22
OTEC 10 MWe AMMONIA TURBINES PART LOAD INLET PRESSURE

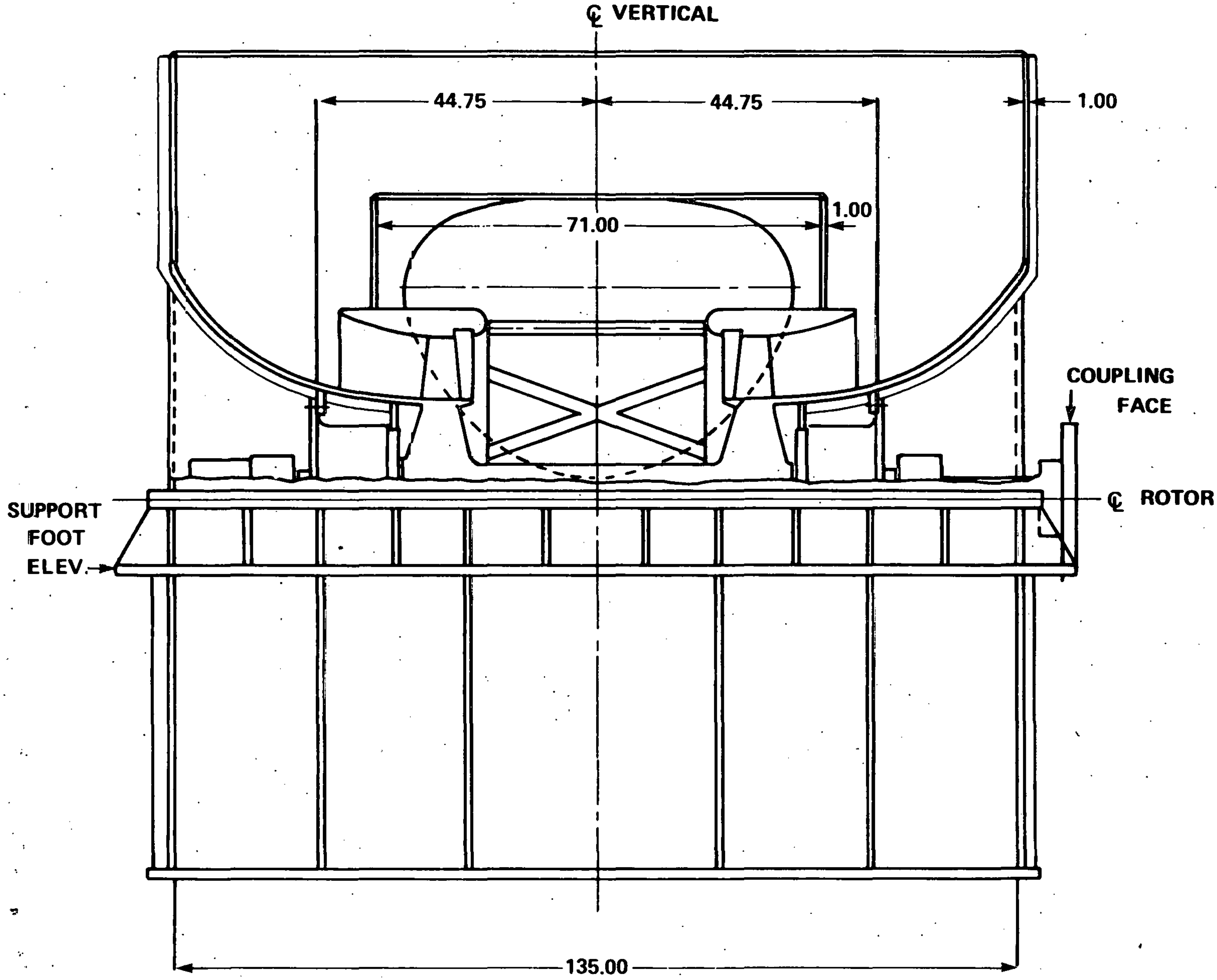

Figure 6-23
10 MWe TURBINE SIDE ELEVATION PARTIAL SECTION

The inlet arrangement consists of two 62-inch diameter pipes located in the turbine cylinder cover. The exhaust opening is rectangular (135 x 140 inches) and is located in the cylinder base.

The support for the turbine is a relatively heavy subbase located just below the turbine horizontal centerline, as shown in Figure 6-23.

The overall cylinder and support configuration is similar to the type used for years on Westinghouse large low pressure turbine designs, where extensive experience has been accumulated in the aerodynamic and structural design concepts of these units.

6.2.3.3.2 Rotor Design and Dynamics

The 3600-RPM rotor is designed as a flexible shaft, wherein the first critical speed is within the running range and contains two integral blade discs. The lateral critical speed calculated was performed with a Westinghouse proprietary computer program and is based on the transfer-matrix approach of Myklestad[13] and Prohl[14] with extensions found necessary to correlate data from hundreds of field units. In addition, the rotor is modeled as a beam, wherein both shear deflection and rotary inertia are included. The calculated first and second critical speeds for the turbine rotor only (single span system), based on oil damping and bearing pedestal stiffness, are 2330 RPM and 4050 RPM, respectively. The calculated first and second critical speeds for the multi-span system (turbine and direct-connected generator) are 1916 RPM and 4680 RPM, respectively.

6.2.3.3.3 Blading Design

Initial optimization studies reveal that a significant gain in efficiency is attainable with reduced blade gauging (blade throat width divided by blade pitch) which is attributable to the decreased leaving loss, i.e., kinetic energy of the exit gas. At the same time, however, the reduced gauging results in a longer blade for a given volumetric flow which in turn requires a wider blade to provide the necessary stress capability.

After a series of analyses of various gaugings, it was agreed that in view of the efficiency and stress parameters, a 30% gauging blade is the optimum design. The analysis indicates that although the lower gauging blades result in reduced leaving loss, they also require a reduced inlet angle which increases the turning at the blade hub (Figure 6-24). This required increase in turning results in a lower blade energy coefficient which affects the efficiency gain for reduced leaving loss. In the final blade design, the inlet angle is 35° and the exit angle is 20.50°, which results in an efficient hub section. Figure 6-25 illustrates the variation in inlet flow angle between 25% and 30% gauge blading.

The three most important stresses normally associated with the rotating blades are due to the tangential, axial and vibratory forces acting on the blading. However, because of the possibility of a slow trip with loss of load, calculations show that the turbine could reach a 50% overspeed (5400 RPM). Consequently the stress due to centrifugal force becomes a major factor in the blade design.

Calculation of the blade root and disc stresses disclosed that the initial blade selected had insufficient blade area for the tangential and axial force loads. To alleviate this situation, various blade modifications were evaluated:

a. Addition of a shroud to increase the blade stiffness and reduce the vibratory buildup. The added weight at the blade tip aggravated the unacceptably high direct blade and root stresses at the overspeed condition.
b. Addition of a lashing wire which welds blades together in groups at the port section resulted in additional weight and increased centrigufal force at overspeed. In addition, it causes flow irregularities in the blade passage which has an adverse effect on efficiency.
c. In view of the above, a free-standing blade was selected.
d. For the final selection, the pitch and width of the blade were established at 1.692 inches and 6.0 inches, respectively, which

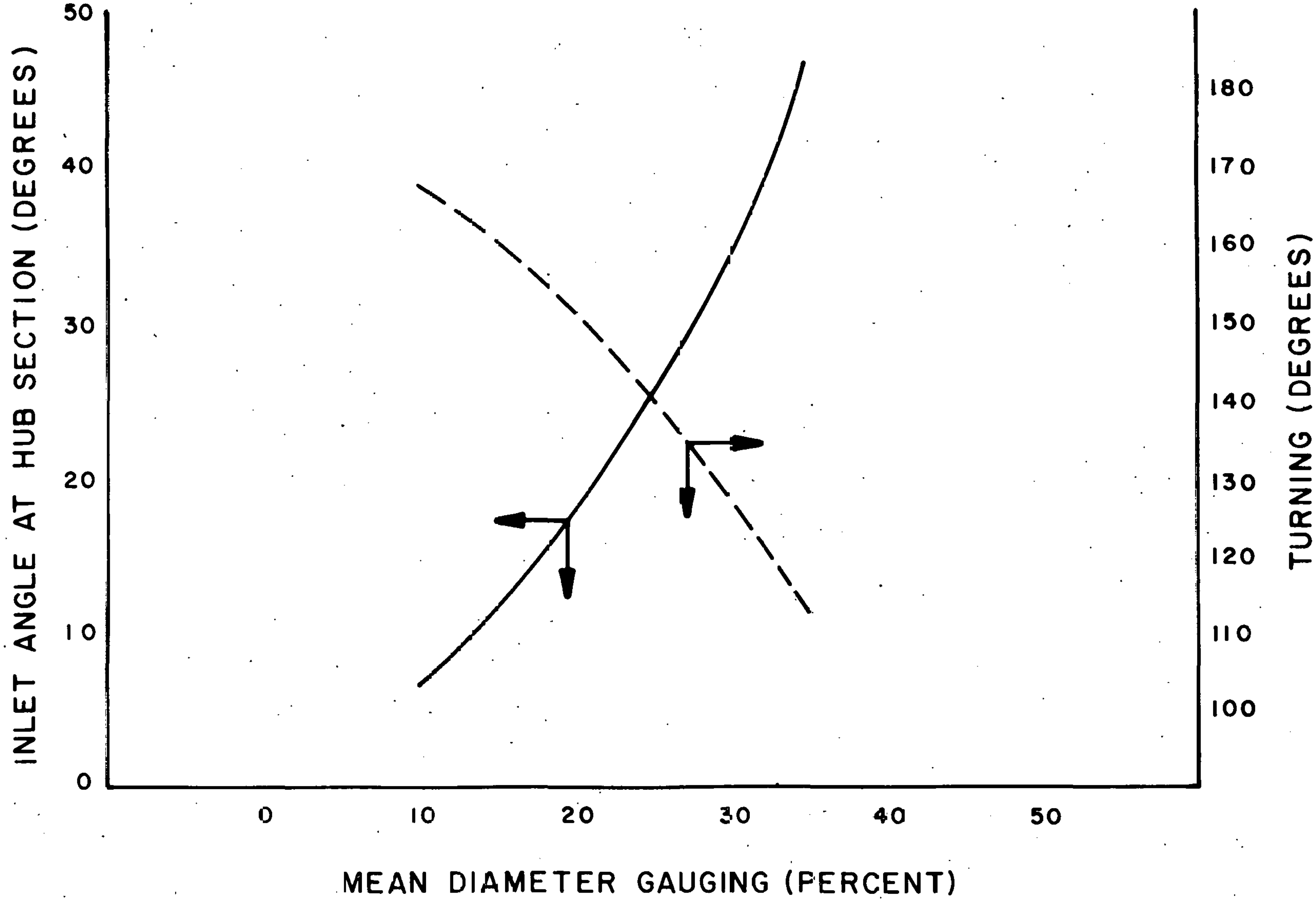

Figure 6-24
OTEC 10 MWe AMMONIA TURBINES
ROTOR HUB SECTION INLET ANGLE AND TURNING VS. MEAN DIAMETER GAUGING

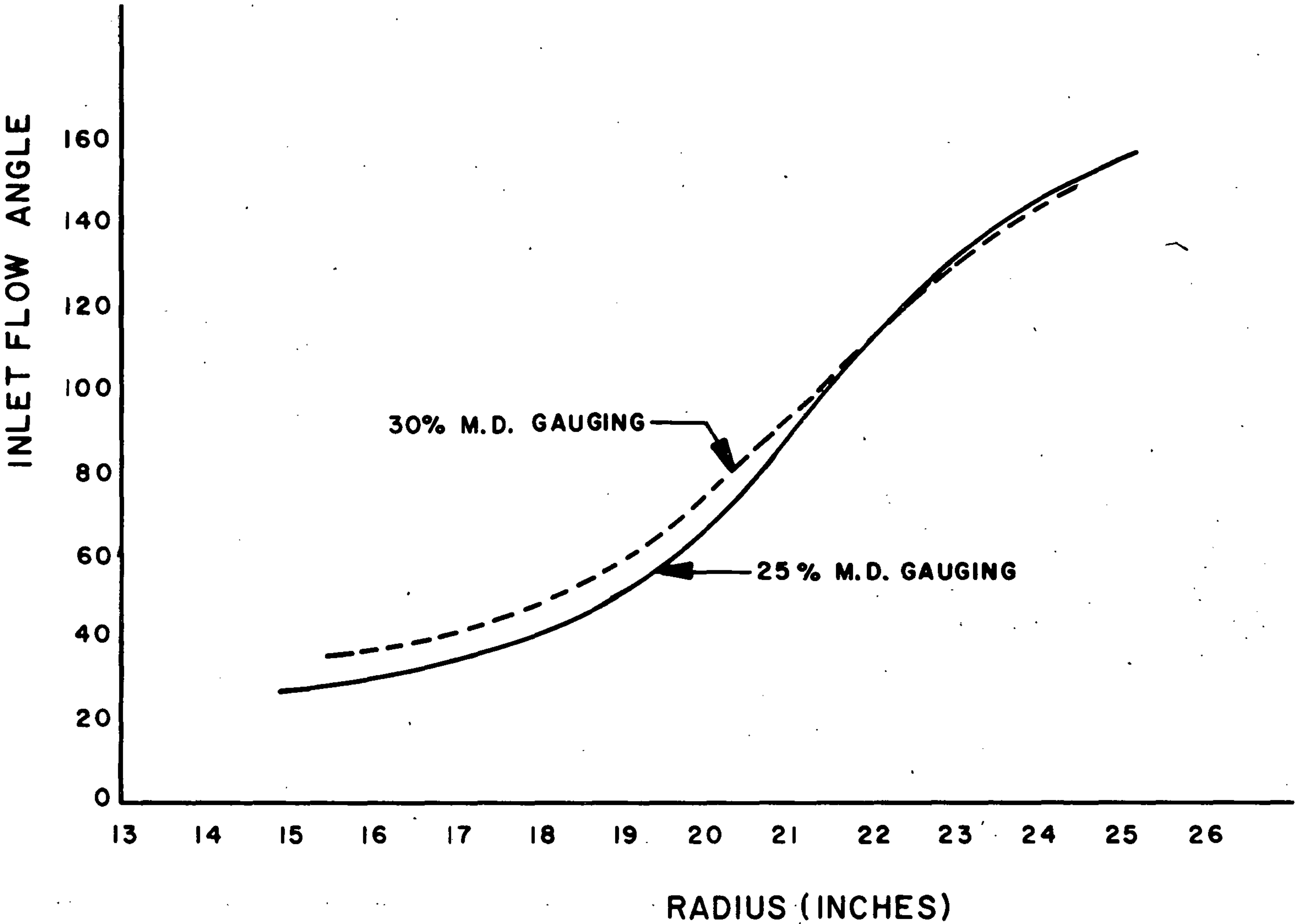

Figure 6-25
OTEC ROTATING BLADE PRELIMINARY INLET ANGLE DISTRIBUTION

result in a pitch-to-width ratio of 0.282. Based on 30% gauging, the blade height is 9.025 inches on a base diameter of 31 inches and a resulting 58 blades per row.

Calculations show that the stresses and resonances with this configuration are within allowable limits as follows:

At 3600 RPM:

a.	Blade is resonant with 15th harmonic	
b.	Blade vibratory stress at point of root fixity	2500 PSI
c.	Blade vibratory stress at blade base	1450 PSI
d.	Direct centrifugal stress at point of root fixity	9250 PSI
e.	Direct centrifugal stress at blade base	13300 PSI
f.	Average tangential rotor stress	8600 PSI

At the overspeed condition, the root stress is approximately 50,000 PSI due to centrifugal force and 2000 PSI vibratory stress. The blade has a natural frequency of 945 cps and is resonant with the 10th harmonic. The average tangential rotor stress at this condition is 30,000 PSI.

6.2.3.3.4 Gland Seal Design

To ensure zero or absolute minimal leakage of air into the turbine, or ammonia into air, the hydraulic-type gland seal (Figure 6-26) was developed. The gland seal ring contains two oil-lubricated babbitted steel rings, designated as air side and gas side seals, which are each supplied by a hydraulic loop. The air side loop is vented to the atmosphere, and the gas side loop is a closed pressurized loop. The seal rings are designed to seal under all dynamic operating conditions and, if necessary, can seal under a static or standstill condition if the hydraulic pumps are kept running.

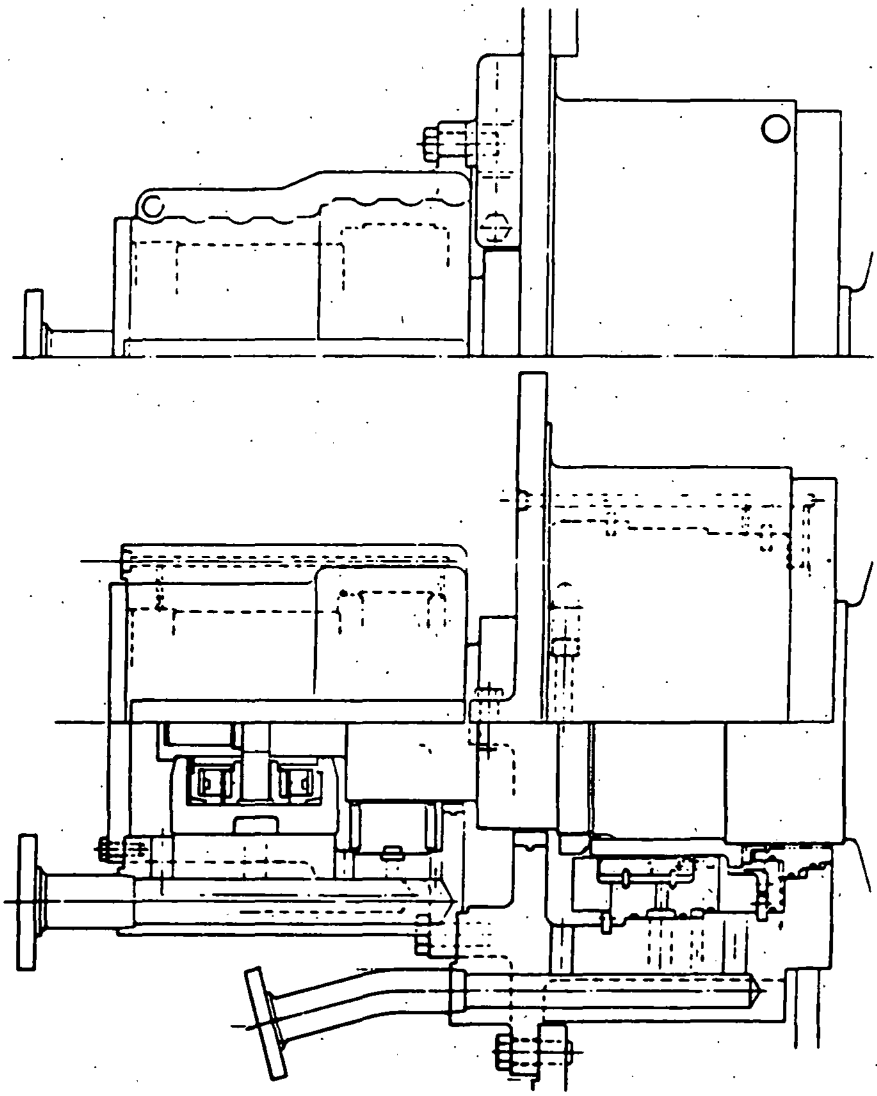

Figure 6-26
TURBINE BEARING AND SEAL ASSEMBLY THRUST BEARING END

However, a static seal and static seal piston were added to the gland seal design, which, when activated by changing a valve sequence, provides a positive seal which confines the ammonia within the turbine and allows the pumps to be shut down. Drains for oil exposed to ammonia are kept separated and drained to a defoaming and degassing tank for purification.

Except for certain refinements and small modifications, this type of design concept for sealing rotating shafts has been used for years on large hydrogen-cooled generators and for various sizes and types of compressors for different types of gases. Consequently, the concept is considered a state-of-the-art design.

6.2.4 Generator

6.2.4.1 Design Goals

The purpose of the preliminary design work performed for the 10 MWe Modular Application generator was to determine the design options consistent with minimum complexity and minimum cost, along with the required output and performance characteristics imposed by the turbine, the electrical load, and the shipboard application. The options thus identified were analyzed within the overall power system optimization program to determine a preferred configuration.

6.2.4.2 Approach

The general approach to the design problem included the following steps:

- Review interface characteristics of the turbine, the shipboard electrical system, and the motion of the ship.
- Select the optimum design for the cooling system.
- Perform conceptual design work (approximate size, weight, and performance) to assure the feasibility of the proposed design.

- Justify or modify the choices made by comparing other possible designs.

- Identify areas which will require further design work during subsequent, more detailed design.

6.2.4.3 Generator Design

The generator must be designed to meet the following external constraints:

- Generate 3-phase, 60-Hertz power to permit the use of motors of normal design aboard ship.

- Produce power at 6900 volts and 0.80 power factor to suit the power system planned for the pilot plant.

- Provide a two-pole generator for operation at 3600 RPM directly connected to the turbine to eliminate the bulk, weight, and cost of a reduction gear.

- Use a special generator rotor capable of withstanding 50% overspeed to suit the response of the turbine speed control system during the dumping of full load.

- Provide a 14.5 MWe generator to supply the specified net electrical output of 10 MWe and also the power used aboard ship by pump motors, lighting, and other ship-service loads.

- Provide a generator with two bearings to suit the configuration planned for the turbine generator set.

With the exception of a requirement for increased overspeed capability, the generator will be a state-of-the-art design similar to generators manufactured for industrial application and small electric utilities. Figure 6-27 shows the dimensions including lifting requirements and weights for the combined turbine-generator set.

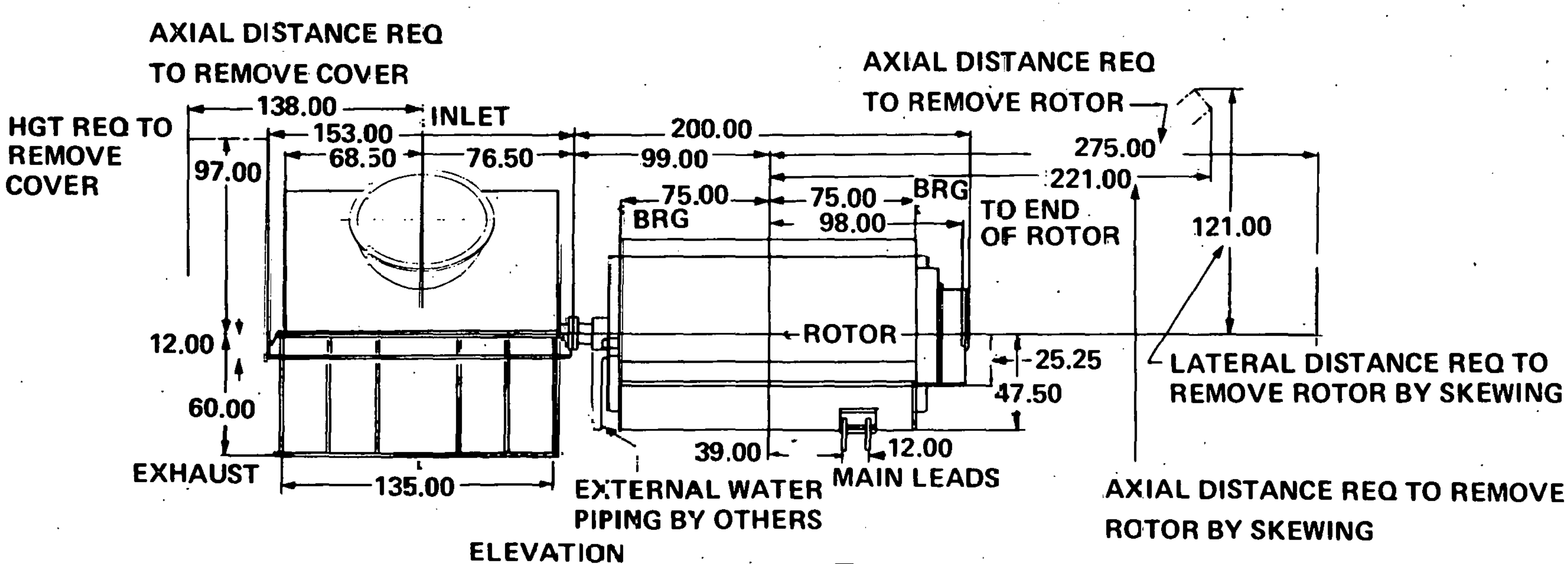

GENERATOR	GENERATOR SHIPPED ASSEMBLED (INCLUDING ROTOR & AIR COOLERS)	107500
	COLLECTOR HOUSING	233
	COLLECTOR HOUSING ADAPTER	290
	FLOOR PLATES (TURBINE END)	80
	FLOOR PLATES (COLLECTOR END)	80
	TOTAL	108183 LBS
	ROTOR	22300
	EACH OF TWO AIR COOLERS (EMPTY)	1700
TURBINE	ROTOR	5200
	CYLINDER COVER	19000
	CYLINDER BASE	22500
	GLAND & BRG ASSY	3300
	TOTAL	50000

Figure 6-27
10 MWe TURBINE-GENERATOR OUTLINE AND WEIGHTS

6.2.4.3.1 Overspeed Capability

With the present type of system load control, wherein the flow is bypassed to the condenser, the turbine-generator set could attain an overspeed of 50% with loss of load for a period of approximately 5 minutes. To attain this overspeed capability, the following approach will be used:

- The material for the rotor forging will meet all physical and chemical property requirements.

- The number of field coil slots will be decreased, which will increase the size of the teeth that retain the field coil wedges.

- The material and thickness of the coil end retaining rings will be analyzed to ensure that no distortion occurs in the event of an overspeed.

- Other components of the generator which will be investigated and analyzed include: rotor slot wedges, radial field lead studs, axial field leads and cleats, collector ring assembly, and blowers.

6.2.4.3.2 Excitation System

To enhance the overall flexibility of the turbine-generator set in terms of reduced length and elimination of rotating components, a static exciter containing the voltage regulator -- all within a separate cabinet -- will be used. The following benefits will result:

- Elimination of a rotating exciter to meet the 50% overspeed capability

- Reduced overall length of the turbine-generator set
- Improved critical speed characteristics resulting from the elimination of a rotating component
- Improved system stability as a result of improved response speed with a static exciter.

6.2.5 Fouling Control Systems

This section summarizes the investigation into fouling and its control for OTEC Power Systems.

6.2.5.1 Background for Fouling Control Selection

The primary impact of fouling is on efficiency because of reduced heat exchanger capacity. This reduction is caused by an increase in heat transfer resistance from microbifouling of the heat exchanger tubes. (See Figure 6-28). The rate of formation in warm oceanic seawater produces an increase of 0.0005 hr-°F-ft^2/BTU in the fouling resistance within 8 weeks (Reference 1 in Figure 6-29).

Secondarily, reduced capacity is due to increased fluid frictional resistance from slime and macrofouling (e.g. shell fish). In general, fouling will build asymptotic alloy to a maximum thickness. (See Figure 6-30). The rate of formation and ultimate thickness are functions of film temperature, fluid shear forces, and nutrients.

The conclusion that fouling must be controlled can be reached by studying Figure 6-31. If the asymptotic slime thickness is greater than 0.002 inch (equivalent to approximately 0.0005 hr-°F-ft^2/BTU fouling resistance) fouling control methods are necessary. Data from seawater heat exchangers indicates that unchecked asymptotic fouling resistance will greatly exceed 0.0005.

If fouling does not occur in the condenser because of the colder water, the above conclusion is still valid, since the costs of fouling control will roughly be halved (though the plant design would change).

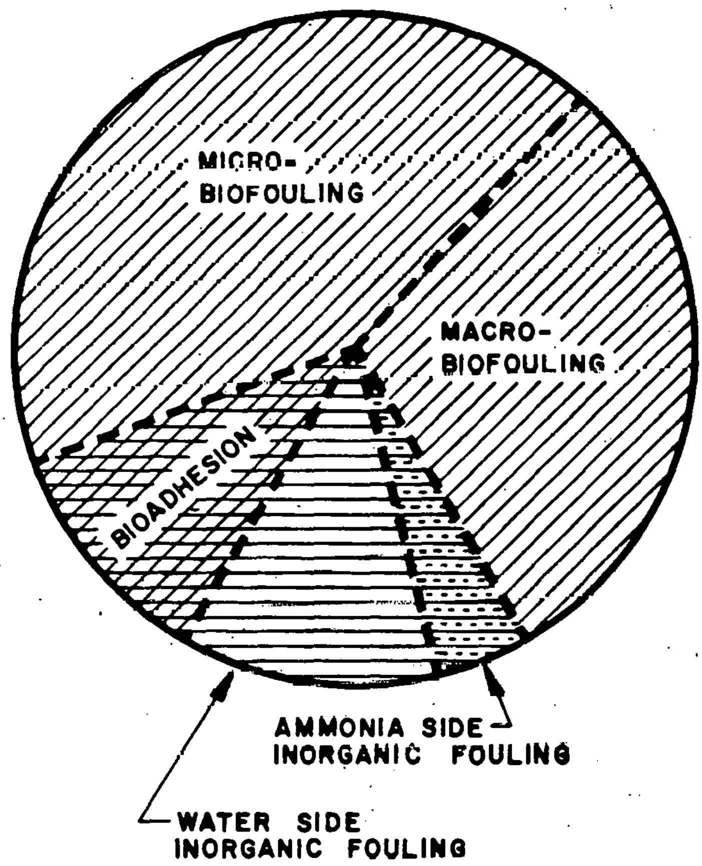

Figure 6-28
PROJECTED CONTRIBUTION BY DIFFERENT TYPES OF FOULING

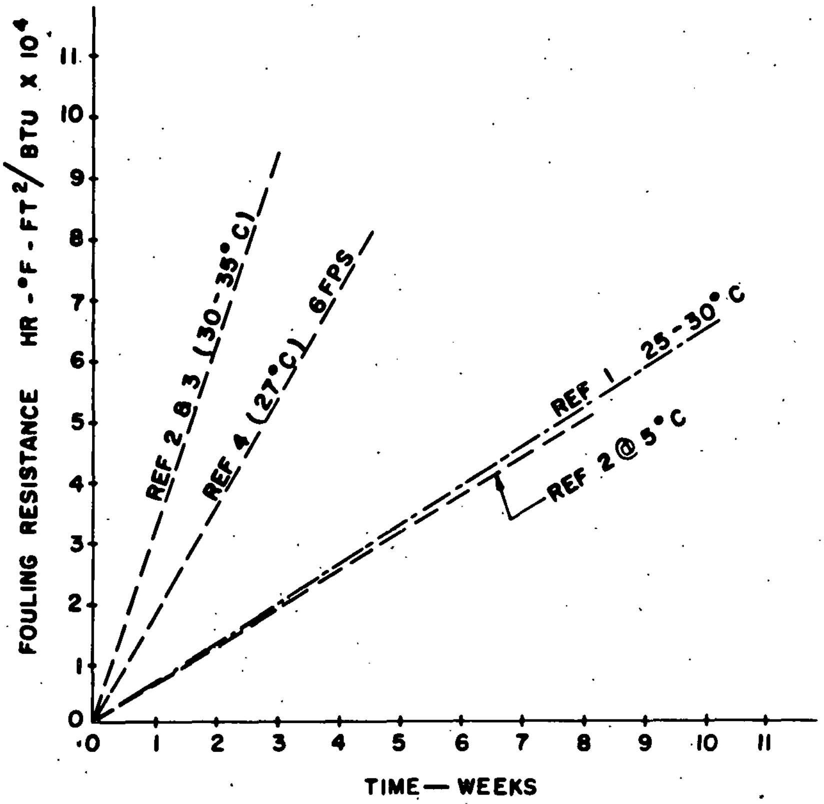

SITE	WATER SOURCE	RATE OF FOULING RESISTANCE INCREASE $HR \cdot °F \cdot FT^2/HR \times 10^5$	AVERAGE SEA WATER TEMPERATURE	FLUID VELOCITY FPS	HEAT TRANSFER MODE/FLOW MODE	HEAT TRANSFER SURFACE	REFERENCE
PANAMA CITY, FLORIDA	COASTAL SEA WATER	33	30	6	ELECTRIC HEATERS/ TUBULAR	TI AND AL 5052 & 6061	2
P.S.E.&G. BERGEN STATION	ESTUARY	33	30-35	7	STEAM CONDENSER/ TUBULAR	304 S.S.	3
L.A.P.&W. HAYNES STEAM STATION	COSTAL SEA WATER	18.5 6.7	27 (SURFACE TEMPERATURE)	6 8	ELECTRIC HEATERS/ ANNULAR	TI TI	4
KEAHOLE PT. HAWAII & ST. CROIX	OPEN OCEAN	6.4	25-30	3, 6 & 7	ELECTRIC HEATERS/ TUBULAR	TI AL 6061	1

Figure 6-29
MICROFOULING RATES IN OCEAN WATER

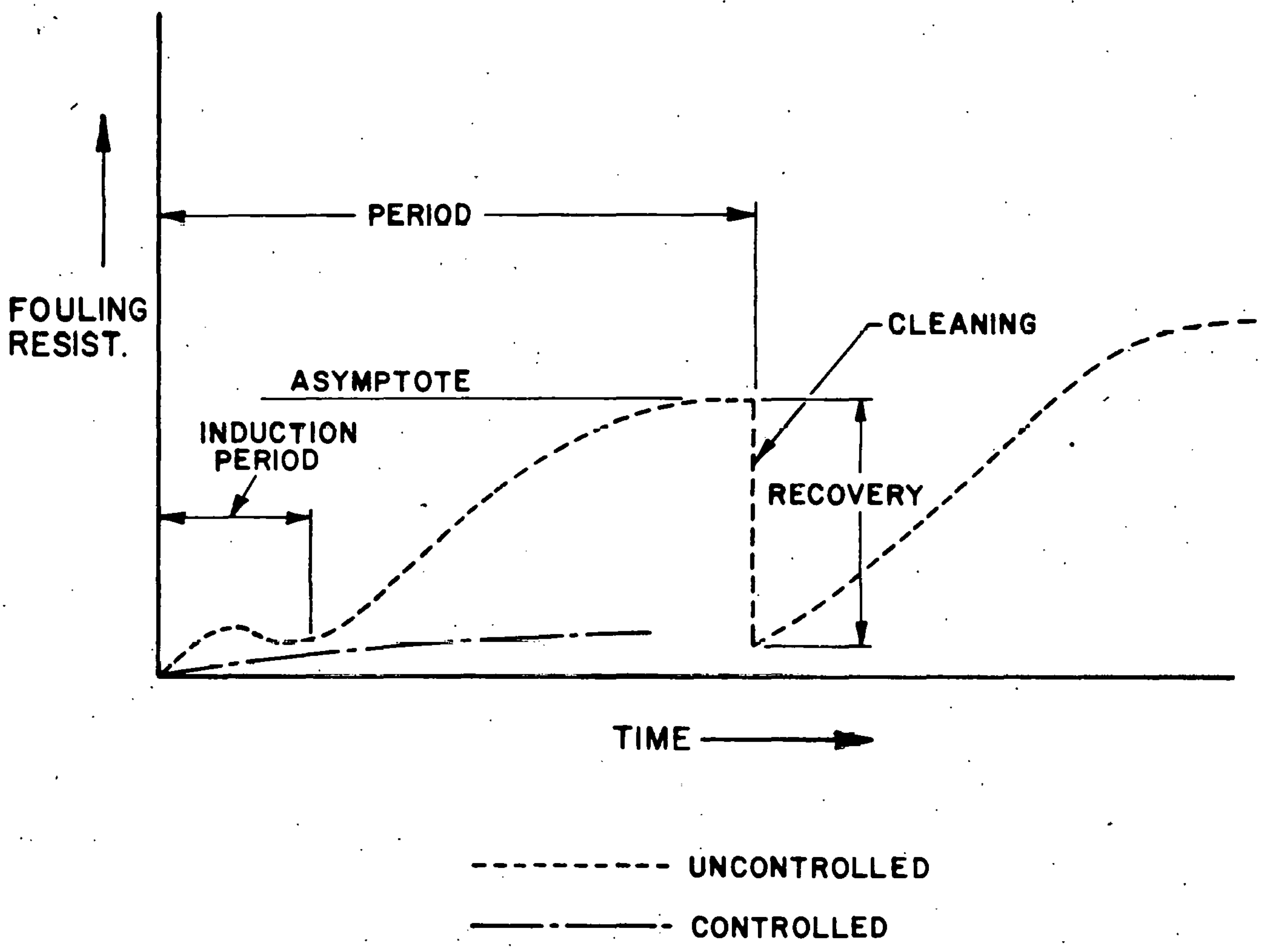

Figure 6-30
FOULING RESISTANCE VS. TIME

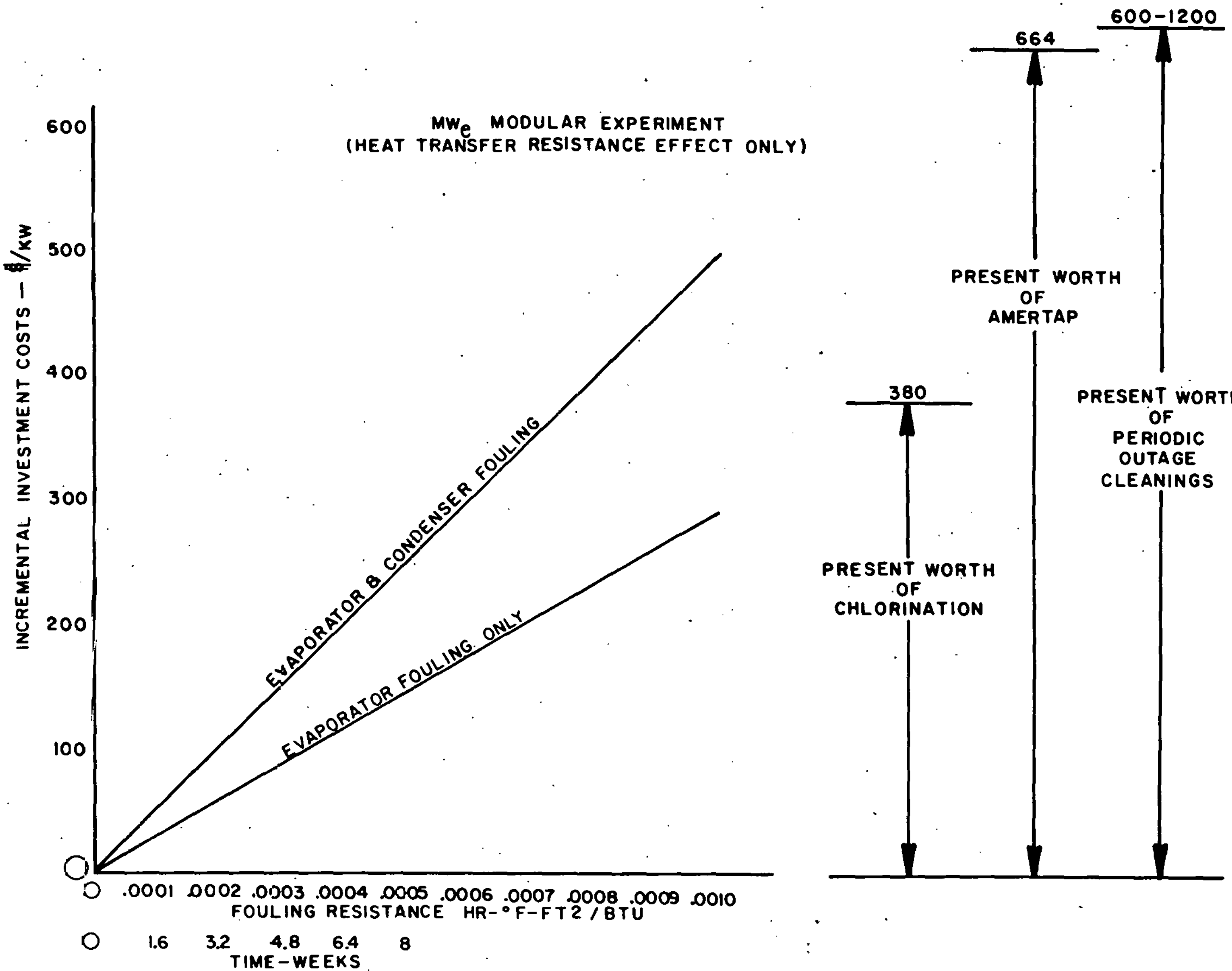

Figure 6-31
COMPARATIVE COSTS OF UNCONTROLLED VS. CONTROLLED FOULING

6.2.5.2 Control Method

Table 6-10 lists the major types of available control methods. Most can be eliminated because of high costs, hazards, or lack of reliable information. The remaining candidate methods were assessed against the criteria for OTEC plants. (See Figure 6-32.) Table 6-11 summarizes the major cost factors in the selection.

Chlorination was selected as the primary control method. It is expected that chlorination will maintain tube cleanliness with a fouling resistance from .0001 to .00025 hr-°F-ft^2/BTU. The required amount of chlorination is within current allowable EPA limits for chlorine discharges. Chlorination is also essential for controlling biofouling in other areas.

Supplementary control methods for the seawater side and ammonia side are recommended for the test articles and initial 10 MWe Modular Application, since no OTEC plant ocean experience exists. These additional measures are recommended to cover unknowns such as actual long-term fouling rates, refractory fouling, inorganic fouling, and environmental questions. These supplementary systems are Amertap, toxic coatings, and ammonia-side cleanup. In addition, other promising methods -- such as MAN and periodic foamed chemical cleaning -- should be investigated further as contingency methods.

Amertap is currently considered the most effective back-up system with the most experience for seawater side fouling control. The actual decision on fouling control systems in the 10 MWe Modular Application depends upon the specific knowledge at the time of installation. If the data at the time of installation indicates that chlorination is sufficient for complete biofouling control, no Amertap provision will be necessary. If chlorination data is inconclusive, but appears to be a good risk, a provision for Amertap inclusion will be provided. At this time, the conservative approach is to include both Amertap and chlorination systems.

Table 6-10
POTENTIAL CONTROL METHODS

Physical Methods
Amertap
MAN
Heat Treatment
Fluid Velocity
Slurry Cleaning (on line & off line)
Periodic Manual Cleaning by Driven Brushes and Plugs
Ultrasonic
Ultraviolet Radiation
Twisted Tape Inserts
Physical Deaeration
Water Jets
Magnetic Treatment
Chemical Methods
Halogens Including Chlorine (and dechlorination), Bromine
Chloride, Chlorine Dioxide
Ozone
Peroxide
Permanganate
Antifouling Coatings
Periodic Outage Chemical Cleanings
Antiprecipitants
Chemical Deaeration
Organic Biocides

CATEGORY	CHEMICAL					MECHANICAL		
	CONTINUOUS CHLORINATION	"SHOCK" CHLORINATION	TOXIC COATING	FOAMED SOLVENT	OZONE	AMERTAP	M.A.N. BRUSH	MANUAL
MICRO-BIOFOULING PROTECTION	EXCELLENT	EXCELLENT	EXCELLENT	EXCELLENT	EXCELLENT	EXCELLENT	EXCELLENT	EXCELLENT
MACRO-BIOFOULING PROTECTION	EXCELLENT	FAIR	EXCELLENT	EXCELLENT	EXCELLENT	POOR	POOR	EXCELLENT
INORGANIC FOULING PROTECTION	POOR	POOR	POOR	EXCELLENT	POOR	GOOD	GOOD	EXCELLENT
OUTAGE FOULING PROTECTION	YES	YES	YES	NO	YES	NO	NO	NO
ON-LINE METHOD	YES	YES	YES	NO	YES	YES	NO	NO
COST	GOOD	EXCELLENT	EXCELLENT	POOR	POOR	FAIR	FAIR	POOR
RELIABILITY	EXCELLENT	EXCELLENT	EXCELLENT	EXCELLENT	EXCELLENT	EXCELLENT	EXCELLENT	EXCELLENT
ENVIRONMENT	FAIR	GOOD	GOOD	FAIR	EXCELLENT	EXCELLENT	EXCELLENT	EXCELLENT
PARASITIC POWER REQ.	GOOD	EXCELLENT	EXCELLENT	EXCELLENT	POOR	GOOD	FAIR	EXCELLENT

EXCELLENT GOOD FAIR POOR

Figure 6-32
FOULING CONTROL ASSESSMENT

Table 6-11
COSTS OF FOULING CONTROL METHODS
10 MWe MODULAR EXPERIMENT
(EVAPORATOR AND CONDENSER)

	Chlorination	Amertap	MAN	Toxic Coatings	Liquid Ammonia Cleanup
Capital and Installation	600,000	2,200,000	700,000*	200,000	75,000
Annual Power (@$.041/kw) Costs	118,900	10,660	180,000	-	16,400
Present Worth**	3,810,000	6,640,000	3,880,000	590,000	503,000

* Includes 10% estimated increase in seawater pumps cost for reversibility function and pumping head increase of 10%

** Interest rate of 10%, escalation rate of 6%, 30-year time period, and 17% fixed costs to cover replacements repairs, labor etc.

In the test articles, both chlorination and Amertap should be supplied to evaluate cleaning effectiveness and material compatibility. Although no documented experience exists utilizing an Amertap system with an aluminum tube heat exchanger, there is experience in a brass heat exchanger system which has similar hardness. It is possible that pitting effects will be reduced as the Amertap system tends to remove the pitting corrodants. Erosion resistance is a critical item to be considered in this system. It is expected that the erosion effects can be minimized by proper selection of ball softness and by extending the time between cleanings to as long a period as necessary. This consideration, as well as the selection of an alloy compatible with Amertap system, can be evaluated in the test articles.

6.2.5.3 Chlorination

Chlorination is a proven and most frequently used method of biofouling control for condensers. It can be generated on-site, in the form of hypochlorite, by passing a direct current through seawater:

$$NaCl + H_2O + \text{Electric Current} \rightarrow NaOCl + H_2$$

Power requirements for this reaction are shown in Figure 6-33.

Chlorine dosage is expected to be 0.25 ppm into the evaporator seawater and 0.1 ppm into the condenser seawater.

Chlorine residual is a measure of the biocidal potency of the treatment. (See Figure 6-34). Residuals are effective down to 0.05 ppm. Quantitatively, it is the difference between the demand and the dosage. Since the demand is a function of time (Figure 6-35), the residual is highest at the heat exchanger inlet. For the evaporator, this is probably the area of most severe biofouling, because that is where the warmest water is located.

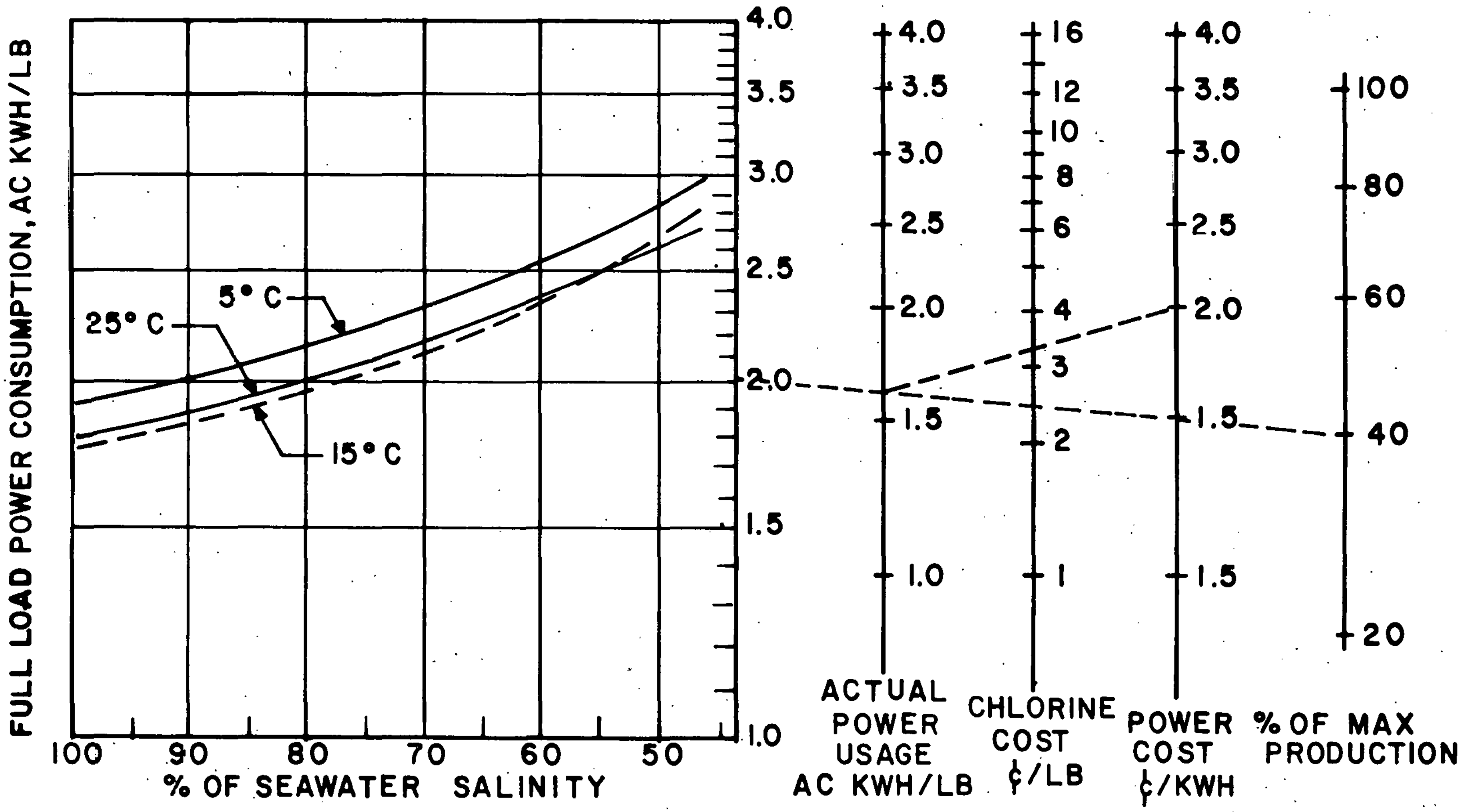

EXAMPLE:

ELECTROLYSIS OF 80% SEAWATER AT 25°C PRODUCES CHLORINE AT 2.0 KWH/LB AT FULL LOAD. AT 40% OF MAXIMUM PRODUCTION, CHLORINE IS PRODUCED AT 1.6 KWH/LB IF LOCAL POWER IS 2c / KWH, CHLORINE COST IS 3.2c / LB.

Figure 6-33
SANILEC SEAWATER CELL POWER CONSUMPTION

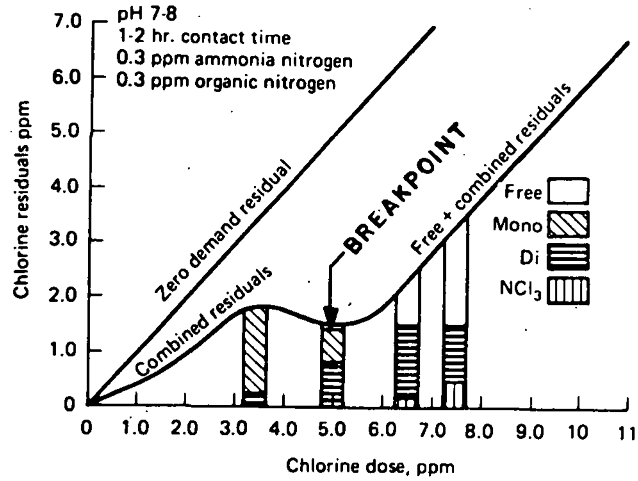

Figure 6-34
RELATIONSHIP OF AMMONIA NITROGEN AND ORGANIC NITROGEN AND CHLORINE

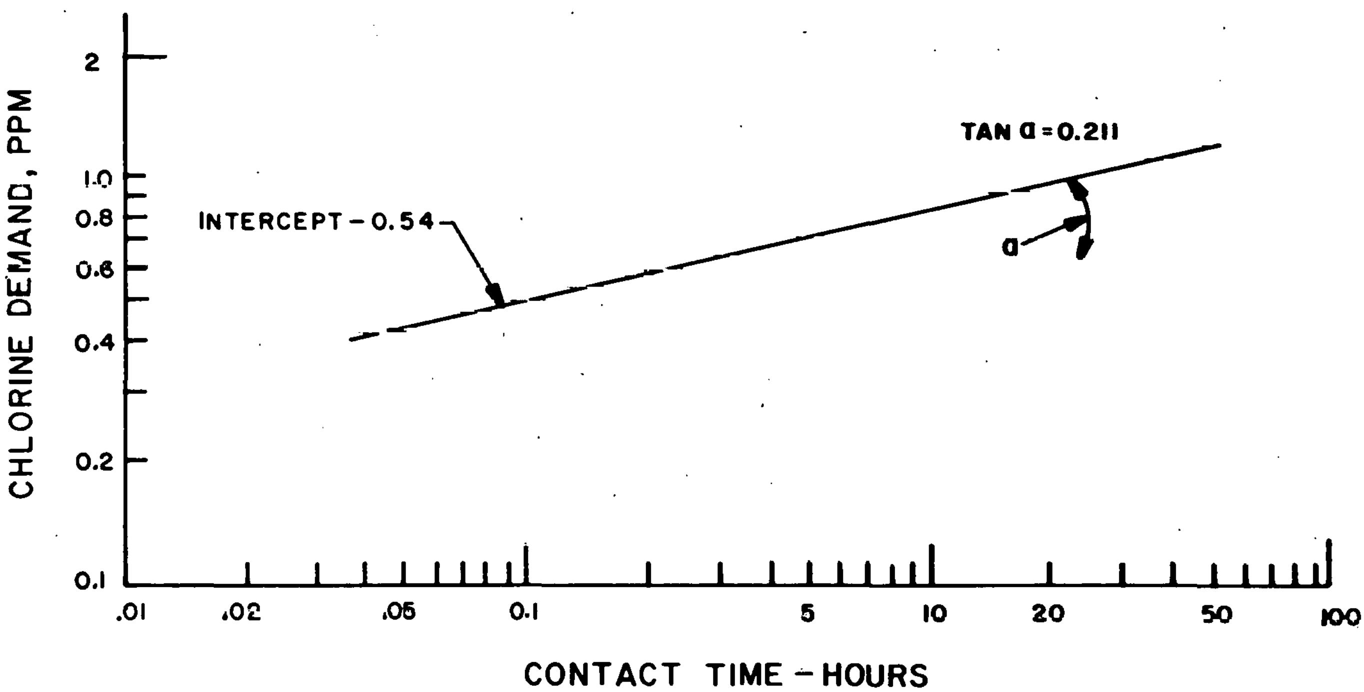

Figure 6-35
RELATIONSHIP BETWEEN CHLORINE CONSUMED AND CONTACT TIME

Figure 6-36 shows the chlorination system composed of seawater booster pumps, strainers, hypochlorite generators, hydrogen release tanks and feedback control system.

6.2.5.4 Supplementary Methods

Amertap is the only method of continuous mechanical cleaning with proven ability. Sponge rubber balls are circulated through the heat exchanger tubes. In passing through the tubes, the balls scrub off the fouling material. The balls are then caught by a screen in the heat exchanger outlet piping and recirculated to the heat exchanger inlet (See Figures 6-36 and 6-37).

The performance of a successful Amertap installation is shown in Figure 6-38.

Toxic coatings such as Goodrich "No-Foul" -- a tin-containing, organic, neoprene sheet, and copper nickel sheet -- are cost effective, long-lived materials. They should be utilized sparingly in the warm seawater piping and outlet coldwater piping to prevent macrofouling. Figure 6-39 shows potential antifouling lifetimes of "No-Foul" as extrapolated by the manufacturer.

Toxic release is very low for these coatings. Figure 6-40 shows release rate data for copper-nickel in seawater. Most of the copper release occurs in the first year of immersion until a stable oxide film is established. Tin release from "No Foul" is sub-detectable.

Both of these coatings display the potential for ease of cleaning residual fouling and in-situ repair.

Ammonia side fouling is expected to be minor, but should be anticipated in initial designs. A system to remove fouling material such as corrosive products or seawater particulates by distillation/filtration is recommended. (See Figure 6-41)

THIS PAGE

WAS INTENTIONALLY

LEFT BLANK

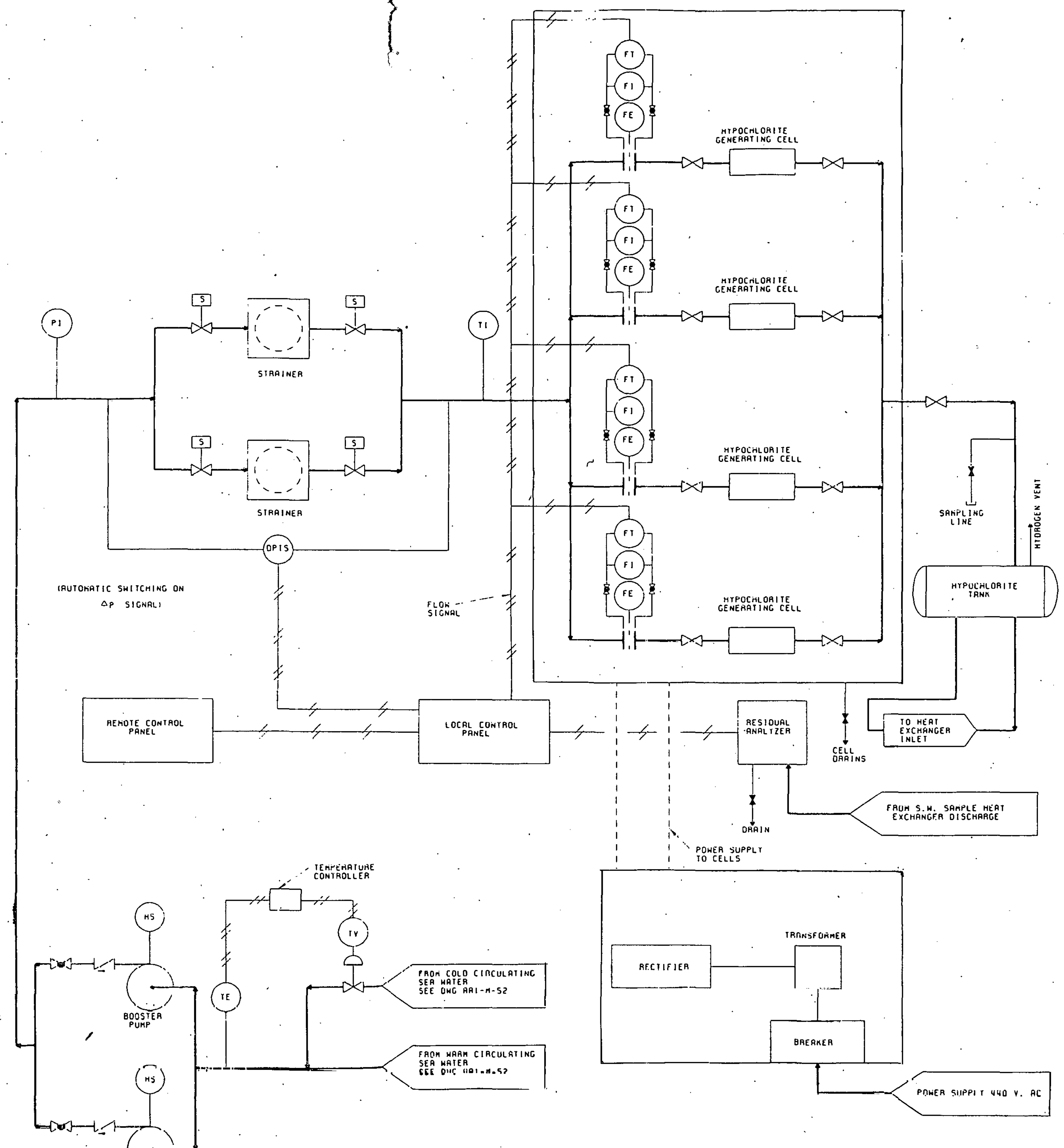

CHLORINATION SYSTEM

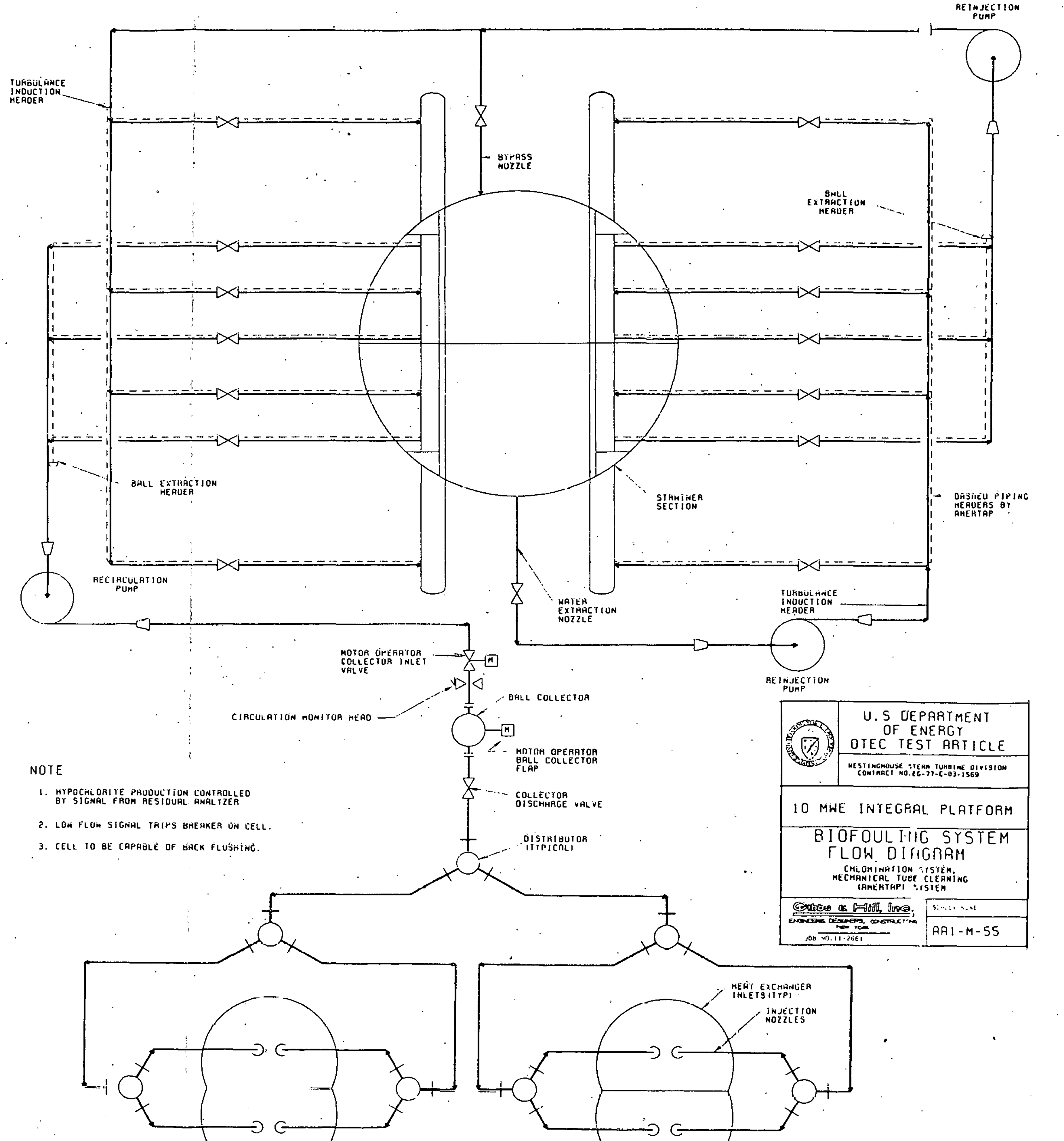

MECHANICAL TUBE
CLEANING SYSTEM
(CONVENTIONAL AMERTAP SYSTEM)

NOTE

1. HYPOCHLORITE PRODUCTION CONTROLLED BY SIGNAL FROM RESIDUAL ANALYZER
2. LOW FLOW SIGNAL TRIPS BREAKER ON CELL.
3. CELL TO BE CAPABLE OF BACK FLUSHING.

	U.S DEPARTMENT OF ENERGY OTEC TEST ARTICLE
	WESTINGHOUSE STEAM TURBINE DIVISION CONTRACT NO.EG-77-C-03-1569
10 MWE INTEGRAL PLATFORM	
BIOFOULING SYSTEM FLOW DIAGRAM CHLORINATION SYSTEM, MECHANICAL TUBE CLEANING (AMERTAP) SYSTEM	
Gibbs & Hill, Inc. ENGINEERS, DESIGNERS, CONSTRUCTORS NEW YORK JOB NO. 11-2661	AA1-M-55

THIS PAGE

WAS INTENTIONALLY

LEFT BLANK

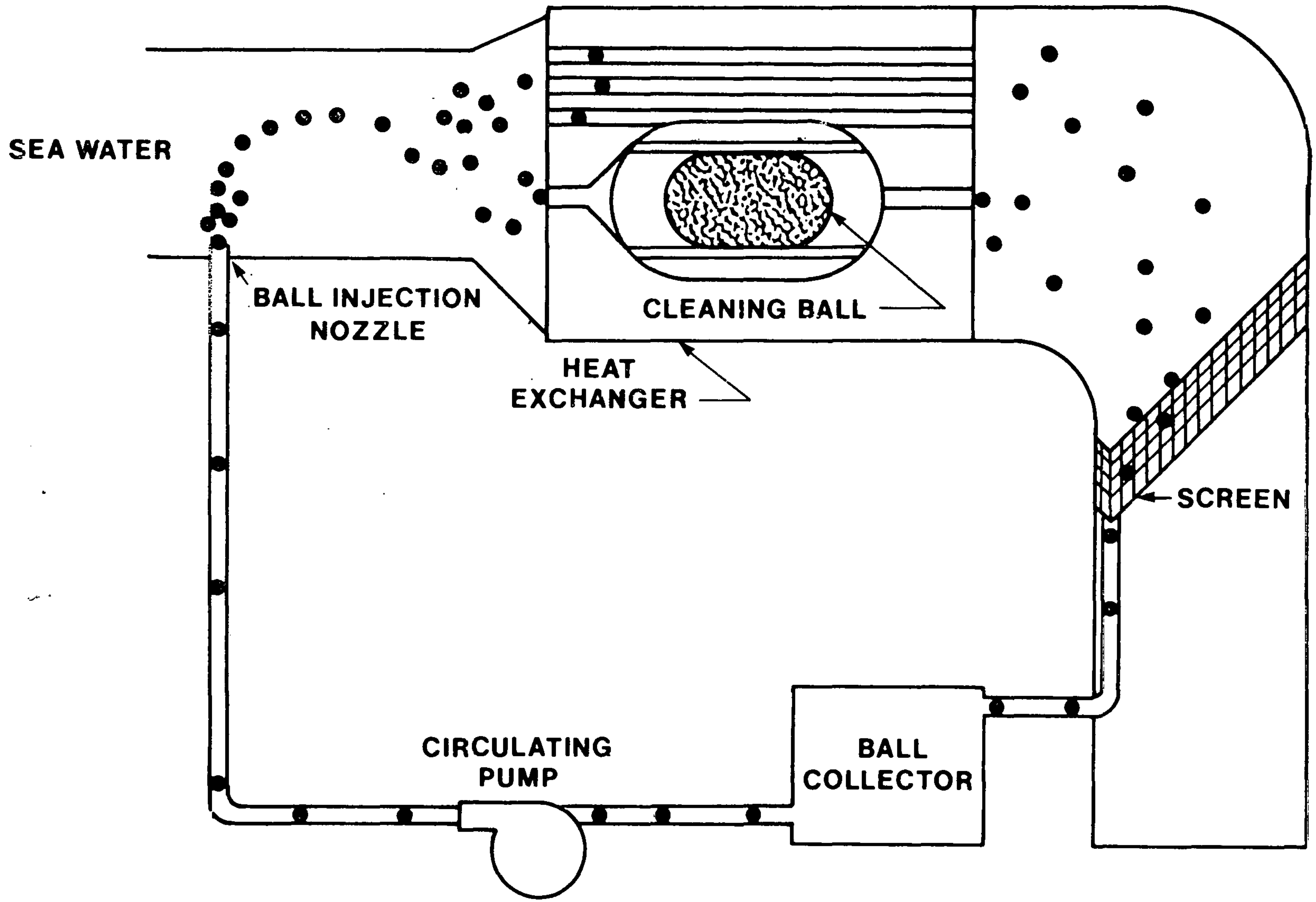

Figure 6-37
AMERTAP CONCEPT

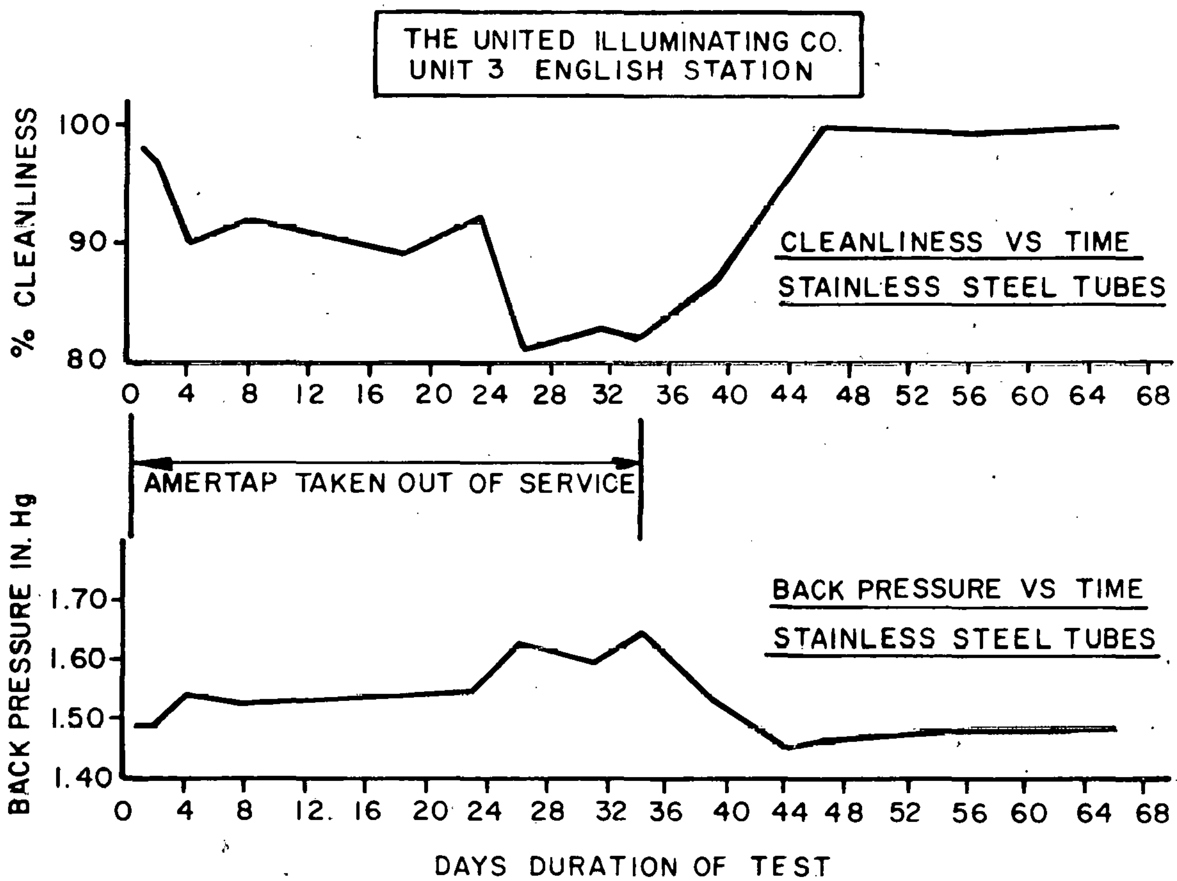

Figure 6-38
AMERTAP EFFECTIVENESS AGAINST FOULING

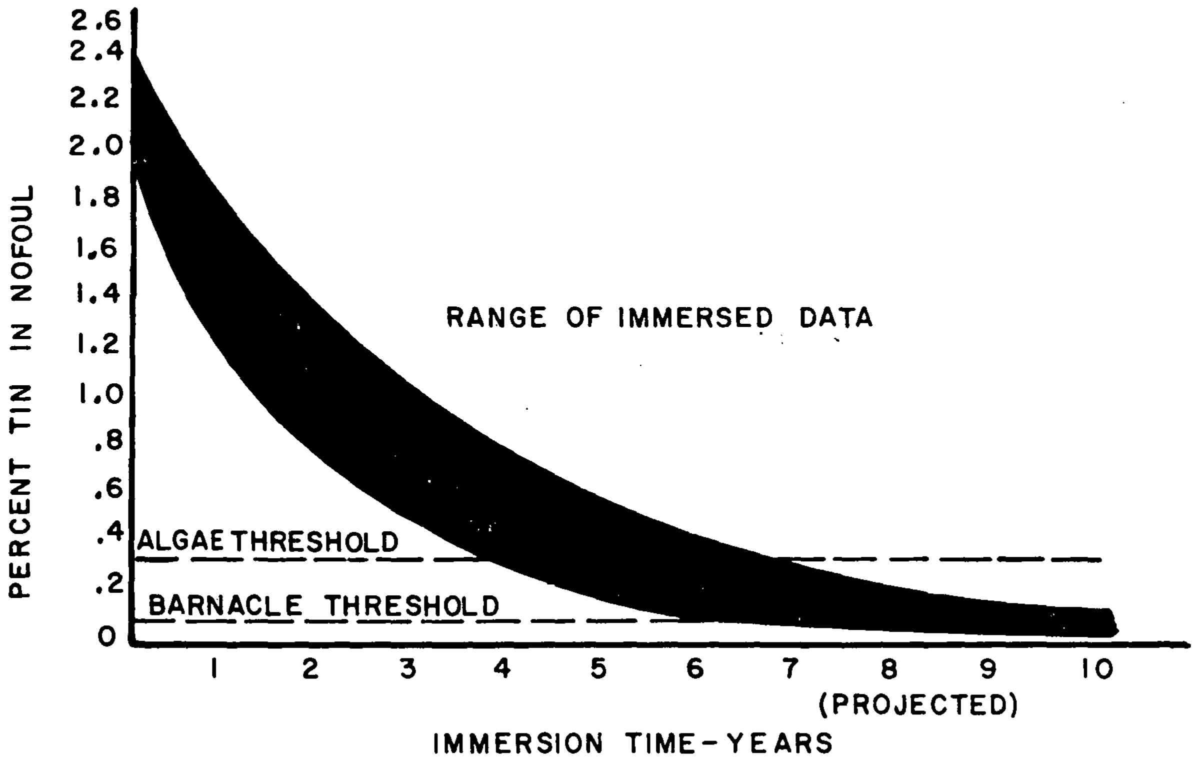

Figure 6-39
RESIDUAL TIN IN IMMERSED NO FOUL 0.080"

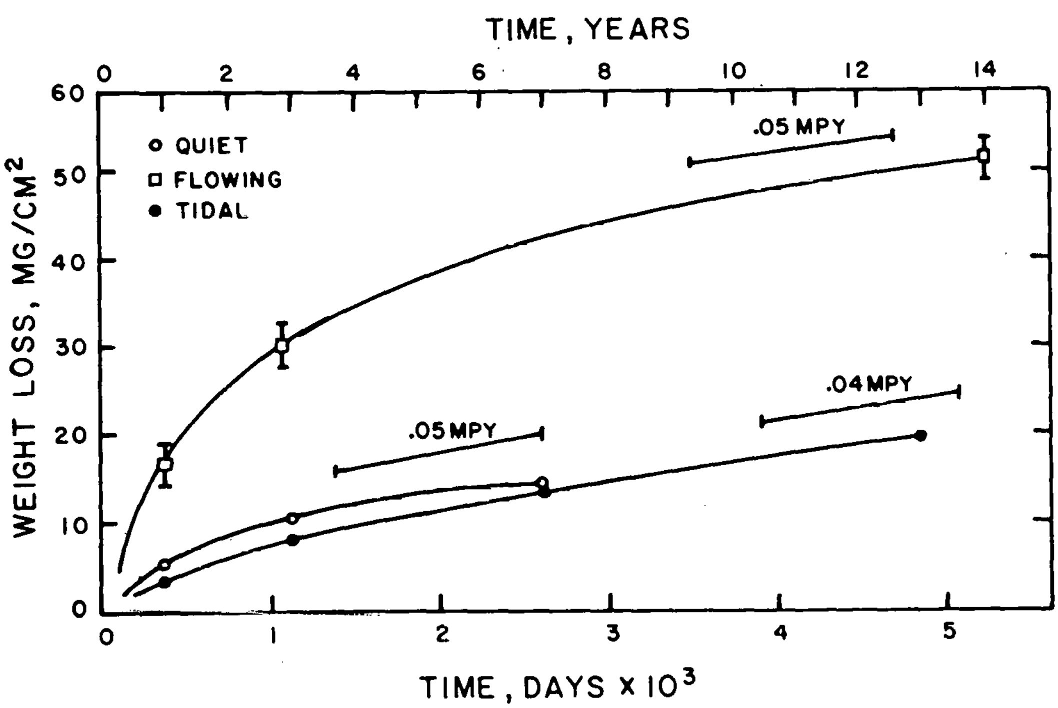

Figure 6-40
WEIGHT/LOSS/TIME CURVES FOR 90/10 CU-NI IN SEAWATER

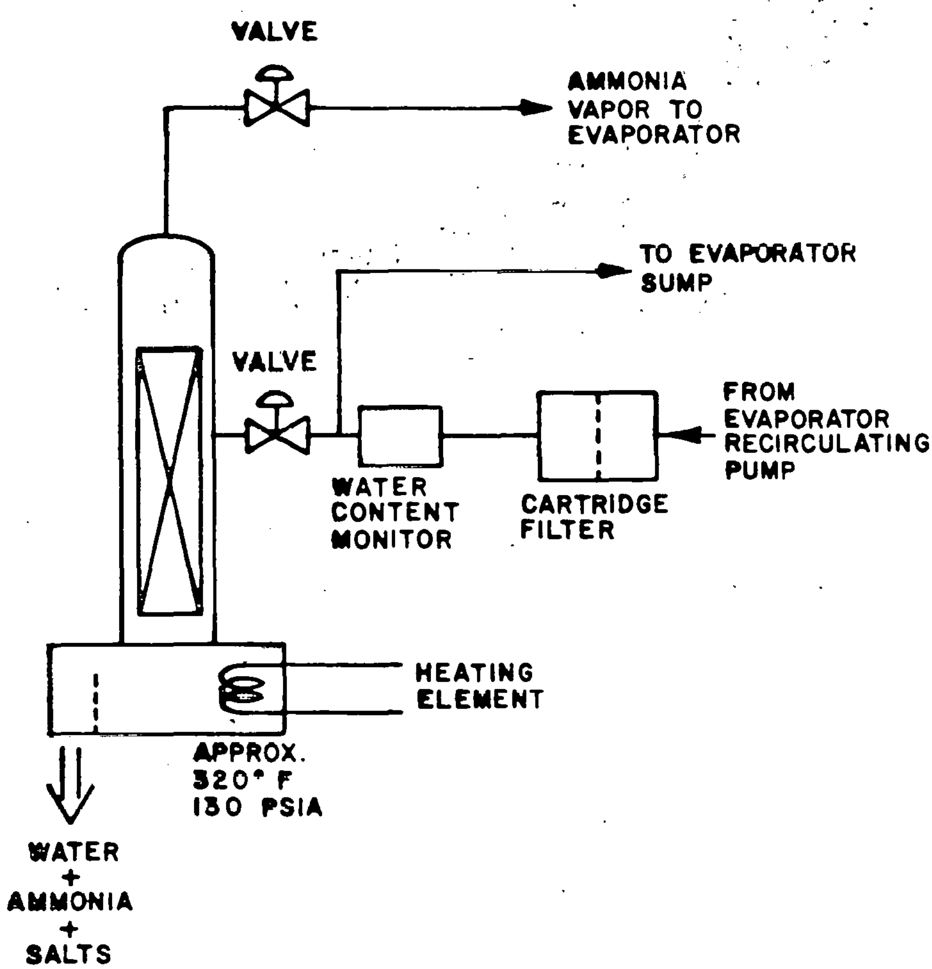

Figure 6-41
AMMONIA LIQUID CLEANUP SYSTEM

6.2.5.5 Contingency Methods

Methods which require further development, but show potential attractiveness, are MAN and foamed chemical cleaning. The MAN brush system utilizes brushes to clean the tubes. (See Figure 6-42). Flow reversal propels the brushes through the tubes. Restraining brush cages are located at each tube end to keep the brushes from being carried away by the flow.

These brushes maintained a 0.0001 hr-°F-ft^2/BTU fouling resistance in coastal seawater testing at Panama City, Florida. Figure 6-43 is the supplier's information on performance of MAN. The major problem with MAN is the requirement for flow reversibility which has a major impact on seawater pumps and piping.

Foamed chemical cleaning, during periodic outages, could be excellent because of the low capital investment. Development is required on economics, time for cleaning, and environmental aspects. Flexibility is inherent since the solvent used can be varied from concentrated hypochlorite for organic deposits to strong acid for inorganic deposits.

6.2.5.6 Environmental Considerations

Discharge from the power system is expected to meet current U.S. EPA limitations on emissions. Chlorine residual should be sub-detectable in the outlet piping, even without dechlorination procedures.

It is believed that even if new, more stringent EPA guidelines are issued in the future that "best available demonstrated technology" will be sufficient to meet the guidelines without imparing the fouling control function.

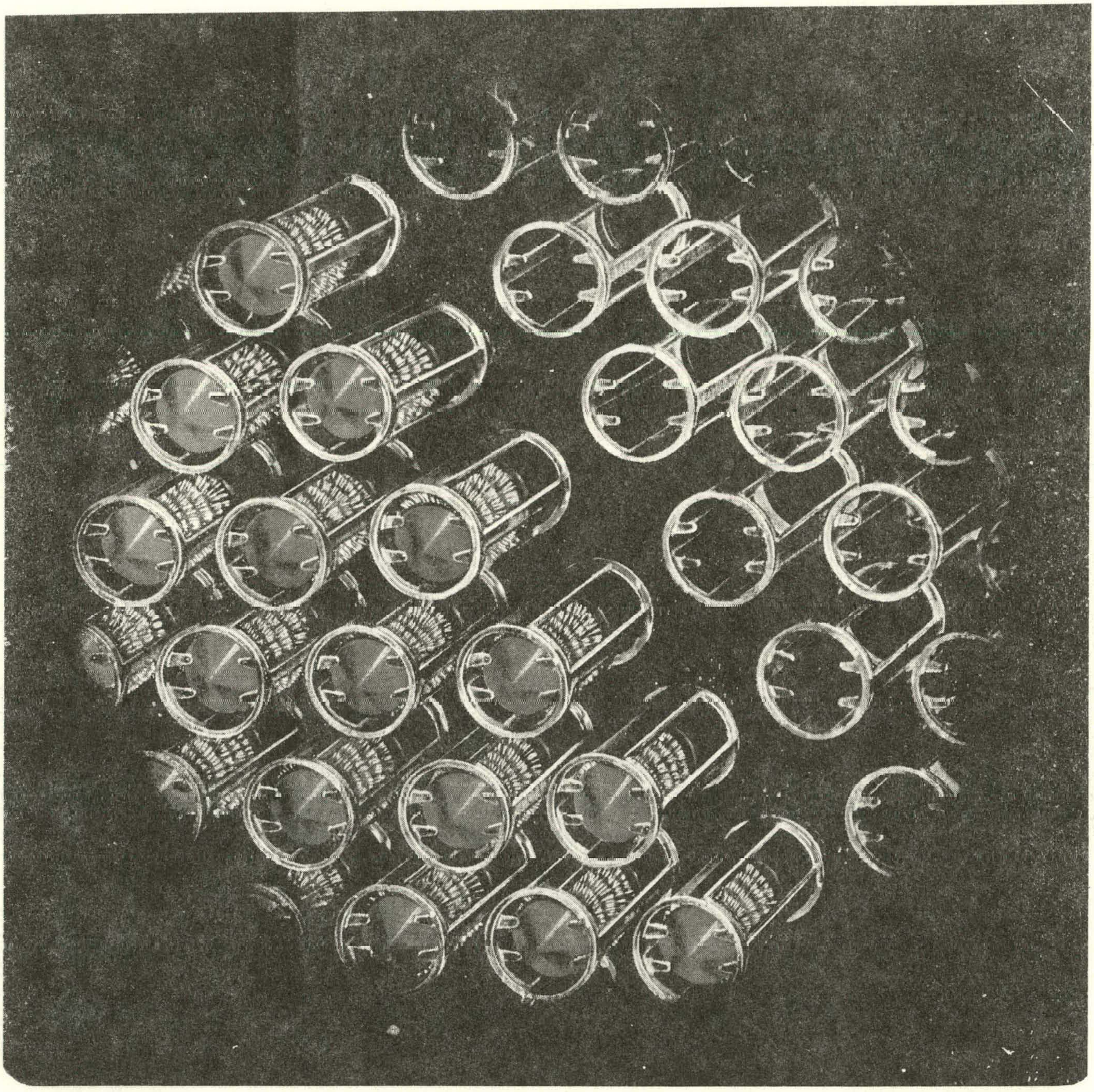

Figure 6-42
ON-LOAD CLEANING SYSTEM FOR CONDENSERS AND TABULAR HEAT EXCHANGERS

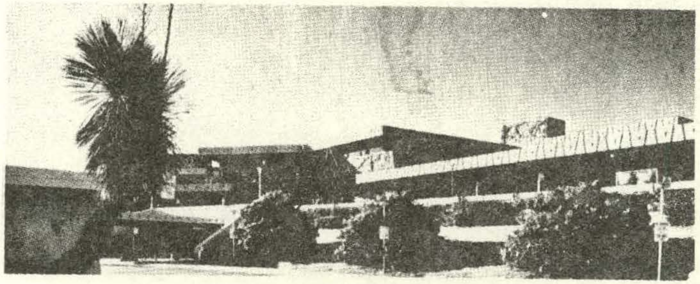

WSA ON-LOAD BRUSH CLEANING SYSTEM

CASE HISTORY

TUCSON INTERNATIONAL AIRPORT
TUCSON, ARIZONA

HARD WORKING CHILLERS COOL THIS ENTIRE AIRPORT COMPLEX IN A DESERT ENVIRONMENT WHERE TEMPERATURES ARE MORE THAN 100°F DURING THE SUMMER. EVEN NIGHT TEMPERATURES STAY IN THE HIGH 80's! DEPENDABLE PERFORMANCE IS ABSOLUTELY NECESSARY AND PEAK LOAD CONDITIONS ARE ALMOST CONSTANT.

water services of america inc.
BOX 23421/MILWAUKEE, WISCONSIN 53223

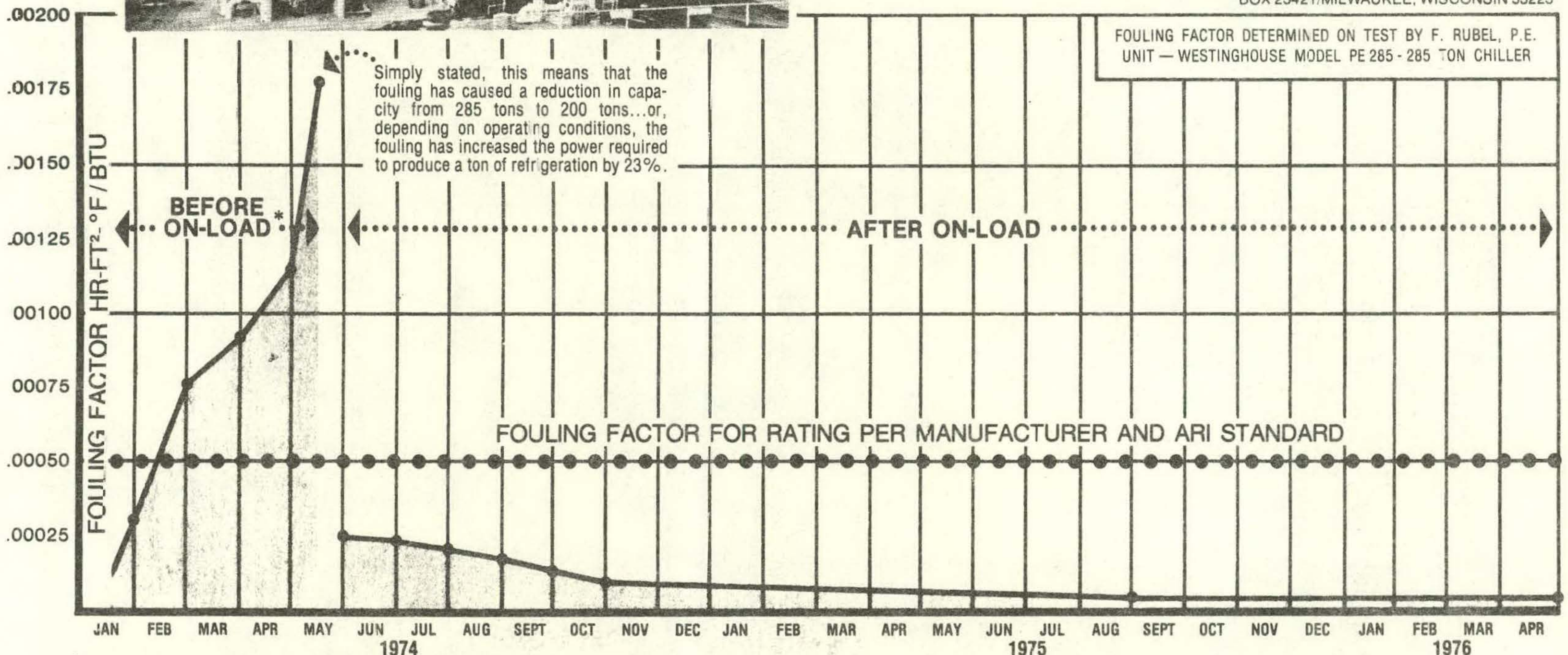

*Conventional cooling tower water treatment under supervision of control specialists.

Figure 6-43
MAN BRUSH EFFECTIVENESS

6.2.6 Instrumentation and Controls

6.2.6.1 Design Considerations

The following design requirements and objectives were established for the preliminary design of the 10 Mwe power cycle control and instrumentation system.

a. The system was designed to provide for total automatic control of the power module from plant shutdown to full power operation. The system automatically controls the following plant operations:

   - Initial air and nitrogen purge
   - Plant startup
   - Generator synchronization and load control
   - Normal plant shutdown
   - Emergency plant shutdown and NH_3 purge
   - Control valve on-line testing

b. The system provides a manual backup for all automatic control functions. The transfer of control between the automatic and the manual modes is without surges or interruptions. The system automatically rejects to the manual mode whenever an automatic control failure occurs.

c. The plant control system provides the operator with the information, controls and alarms needed to:

   - Quickly determine the status of plant systems and equipment
   - Take any planned or emergency action
   - Be alerted to process or equipment malfunctions that are, or could become, a hazard to equipment, personnel, or sustained power generation

- Examine current and historical parameter trend information for use in fault diagnostics, normal operation and performance evaluation

d. The automatic and the manual modes are, to the maximum extent possible, isolated physically and electrically. Elements are employed which service both systems, such as transmitters, actuators and subcontrol loops. The decision to employ such common elements was based on engineering judgement and trade-offs of cost, reliability, failure effects, and time to isolate and repair failures.

e. The system is sufficiently flexible to easily accommodate changes in control philosophy.

f. The system was designed using existing hardware. No portion of the control system depends on the development of new technology.

The control requirements for the OTEC 10 Mwe power module were reviewed. These requirements are discussed in Section 6.3.3, System Control, and Section 6.5.3, Dynamic Response. The results of this review lead to the definition of a plant control system configuration that has the capability of meeting all the functional requirements, while providing a high degree of system reliability and maintainability.

6.2.6.2 Control System Configuration

The configuration chosen was a hybrid system, combining both digital and analog hardware. This configuration was chosen because of its excellent "track record" in the control of large steam turbine-generators. Systems of this type are in widespread usage in commercial power plants, and hardware and software support is readily available.

Refer to Figure 6-44. The major system components are as follows:

- Digital subsystems
- Analog subsystems
- Plant protection systems
- Annunciator system
- Main control panel
- Process mounted transmitters and switches
- High pressure hydraulic system

The digital subsystem consists of a 16-bit mini-computer with floating point hardware and 16K words of random access memory. The system input/output structure is capable of accepting binary, analog, and pulse inputs, and transmitting binary and analog outputs. System peripherals include a disk drive, a magnetic tape drive, two typewriters, and multipoint strip chart recorders. Operator interface with both systems is through pushbutton stations and a cathode-ray tube (CRT) display and keyboard, all located on the main control panel.

System software is modular and provides for the following:

- Automatic start-up and shut-down sequence control
- Turbine-generator speed and load control
- Normal and emergency NH_3 purge sequence control
- Binary input scan
- Analog input scan, limit monitoring, and transmitter failure detection
- Analog input trend display
- Past trip diagnostic review

The analog system consists of printed circuit cards using integrated circuit logic elements and operational amplifiers. These components are completely separated (including power supplies) from the digital subsystem. This method ensures a smooth transfer to the analog subsystem if a failure occurs in the digital subsystem.

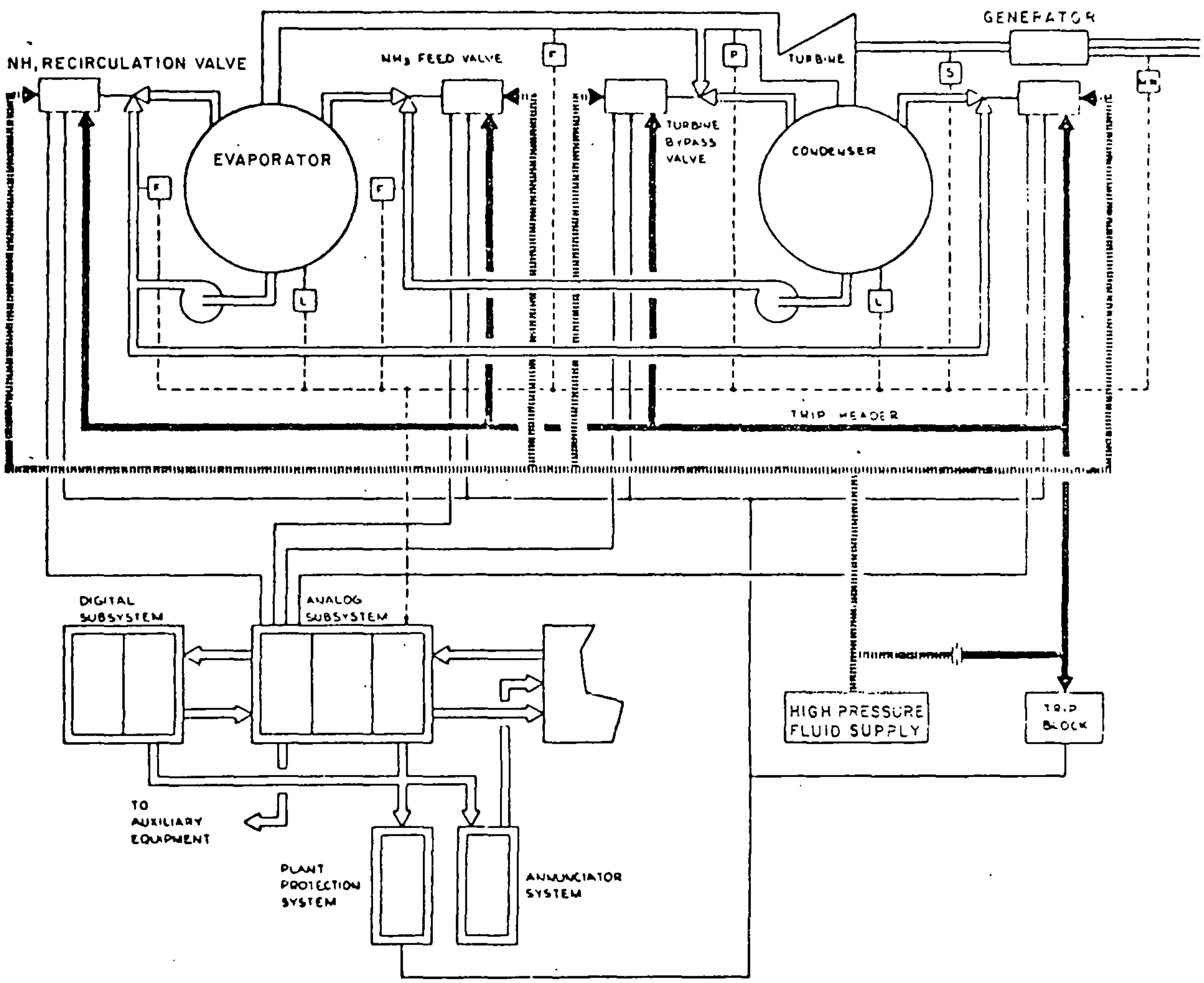

Figure 6-44
10 MWe POWER CYCLE CONTROL SYSTEM, SCHEMATIC DIAGRAM

The analog subsystem acts as the manual control portion of the system. It interfaces the plant process systems and equipment with the digital subsystem and the manual controls and displays located on the main control panel.

A transmitter and gauge list was developed for the ammonia power loop. (Refer to Table 7-10). This list is based on preliminary parametric data developed during the design of the fluid system and on the results of the computer simulation. The list includes a description of the measured parameter, the range, span, primary element, and output signal of the transmitter, any known alarm setpoints, and the operational or diagnostic functions of the measurements. These instruments are shown in Figure 6-45.

All signals from plant-mounted transmitters, process switches, and equipment enter the control system through the analog portion. The signals are then conditioned and retransmitted to the computer and to indicators on the main control panel. These provide the feedback for closed loop control. In the automatic mode, the computer software generates control outputs based on the speed or load reference established by the operator, and the feedback received. In the manual mode, the operator observes the indicators and manually controls plant equipment using panel mounted pushbuttons. All control signals, whether initiated by the operator or the computer, pass through the analog system. The plant operator selects which control signal is finally transmitted to the plant equipment. Manual control may be selected at any time. Automatic control, however, requires that all conditions for automatic control be satisfied. If all conditions are not met, and the operator selects automatic control, the system rejects to manual. The transfer to manual control may also occur automatically as a result of a self-detected control malfunction. If an automatic transfer occurs during a plant transient, the transfer is annunciated and the transient does not continue. It is the operator's responsibility to re-initiate the transient.

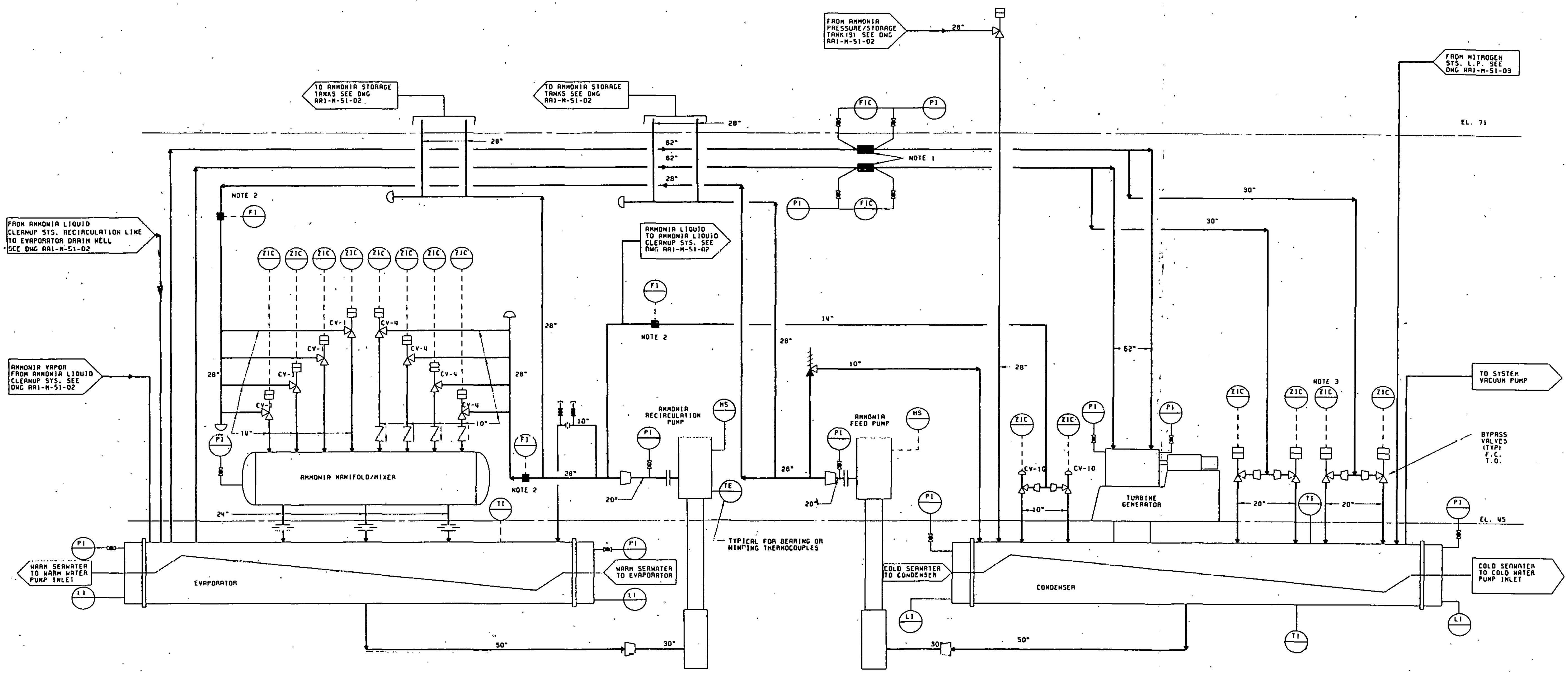

NOTES

1. MULTI AXIS ANNUBAR
2. ULTRASONIC L.E. FLOW ELEMENT 4-PATH
3. FOR VALVE HYDRAULICS SEE DWG. AA1-M-56

Figure 6-46
AMMONIA POWER CYCLE FLOW DIAGRAM

As stated previously, the main control panel is the interface between the plant equipment and controls and the operator. All interface equipment required by the operator to control the plant in either the automatic or manual mode is provided on the main control panel. This equipment includes:

- Pushbuttons for computer interface
- CRT and keyboard for computer information display
- Analog and digital indicators for parameter display
- Multipoint trend recorders
- A/M stations for analog subloop control
- Pushbutton stations for control of contactors, circuit breakers and binary control valves
- Hardwired alarm annunciators

The plant annunciator system provides alarm information for use by the operator when controlling in the manual mode. The system is a backup to computer-generated alarm displays, and consequently provides a lower level of information detail. The annunciator alarms on a system or component basis, rather than on a specific parameter basis. The plant operator determines the exact cause of the alarm from panel-mounted displays. The alarm displays are located directly over the area of the panel where the controls required for correction action are located.

The plant protection system is an independent logic system that monitors critical plant parameters and equipment and automatically shuts down the plant when an equipment or personnel hazard exists. This system overrides all other automatic and manual controls. The protection system employs redundant solid-state logic and is fully testable during power operation. A single failure of an active component will not cause or prevent a plant trip.

Major features of the control system configuration:

- The analog control system is completely separate from the digital computer. This separation maximizes the ability to perform on-line maintenance and testing on the digital computer.

- Modular solid-state hardware is used throughout. Solid-state reliability, plus plug-in modules, maximizes system availability.

- The system is designed with flexibility as a major requirement; it can be easily changed to accommodate the various control methods outlined in Section 6.5.

- All hardware and software used are field-proven and in wide usage for power plant control.

- Redundant power supplies are provided for each system. This redundancy eliminates power supply failure as a common-mode failure, thus increasing plant availability.

6.2.7 Valves

6.2.7.1 Valve/Control Configuration Selection

Four possible configurations were considered for control of the ammonia power cycle as discussed in detail in Section 6.3.3. The configuration using turbine bypass valves along with liquid ammonia feed and recirculation valves was selected because it offers the minimum pressure drop in the vapor lines and, consequently, highest cycle efficiency while providing required control response and overspeed protection. The control valves are shown in Figure 6-45.

6.2.7.2 Valve Type Selection

Conventional valve types in current use are shown in Table 6-12. Each valve type is rated for its relative capability to meet the requirements listed.

Table 6-12
VALVE TYPE COMPARISON

Valve Type	Low Press Drop Applicat'n	Control Applicat'n	Fast Action Applicat'n	Vibration Resistant	Weight Req'mt	Space Req'mt	Seals To Atmos.
Ball	Good	Poor	Poor	Good	Good	Poor	
Butterfly	Fair	Fair	Good	Poor	Good	Poor	
Gate	Good	Poor	Poor	Poor	Poor	Good	
Plug	Poor	Good	Good	Good	Poor	Good	
Swing-Check	Good	Poor	Poor	Good	Fair	Poor	

As can be seen, the plug valve is the only one that meets the requirements of good control response and fast action. It also has good vibration resistance and can provide positive sealing of the working medium to atmosphere. Therefore, the plug valve was selected for both the turbine bypass and the liquid ammonia flow control valves in the power loop.

Figure 6-46 shows the configuration for the turbine bypass valves. It also shows the basic configuration outline, the scaled dimensionless ratios for sizing of the internal flow geometry, and tabulated sizing data for the 10 MWe. Figure 6-47 provides the same information for the liquid ammonia valves.

THIS PAGE
WAS INTENTIONALLY
LEFT BLANK

AREA/RATIO PRESSURE
DROP-VOLUTE VALVE

AREA	RATIO
A1/A6	1.45
A2/A6	1.60
A3/A6	4.10
A4/A6	1.90
A5/A6	1.00
A6/A5	1.00
A7/A1	.56
A8/A1	.44
A9/A1	.33
A10/A1	.21
A11/A1	.14
A12/A1	.0

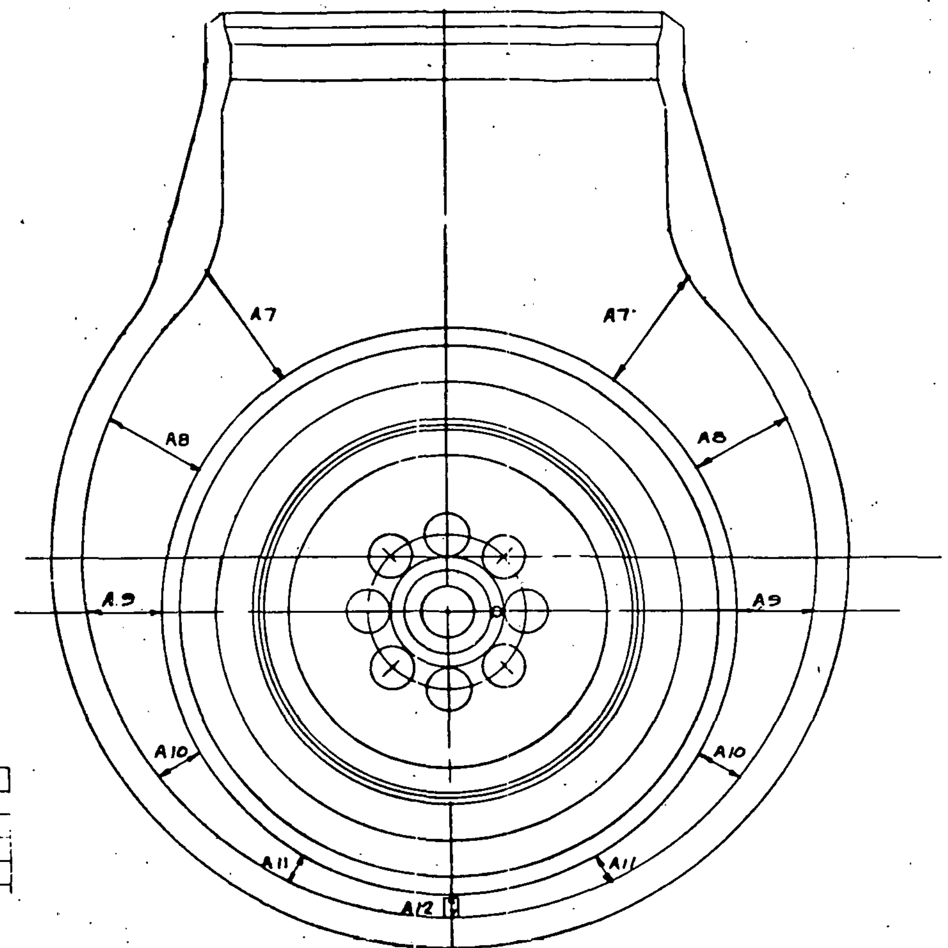

SECTION A-A

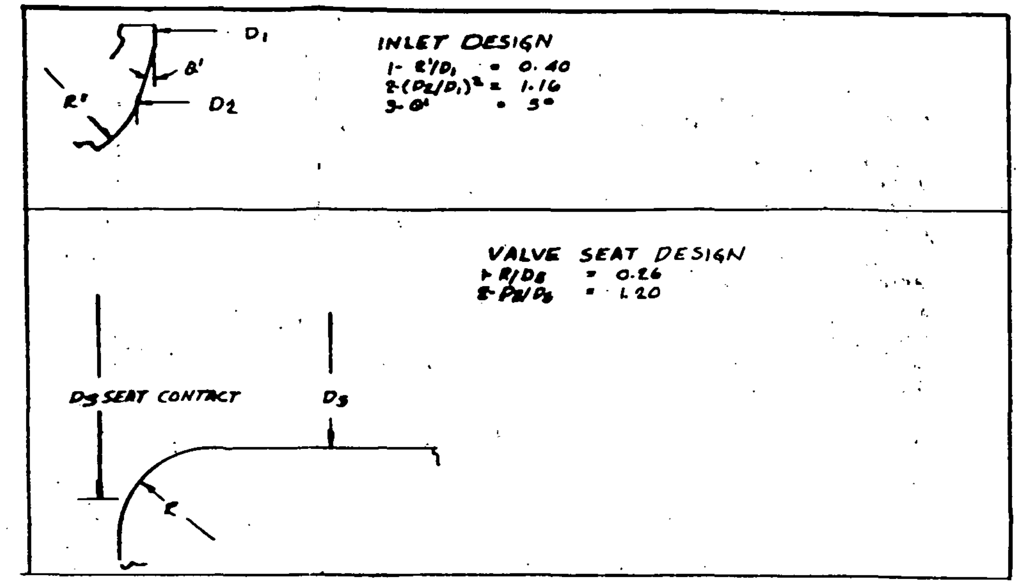

TURBINE BYPASS VALVE SIZE		
CONFIGURATION	10.0MWe	50MWe
Ds, THROAT DIAMETER	20.00"	45.00"
MAX LIFT/THROAT DIA	0.4	0.4
NO. OF VALVES	4	4

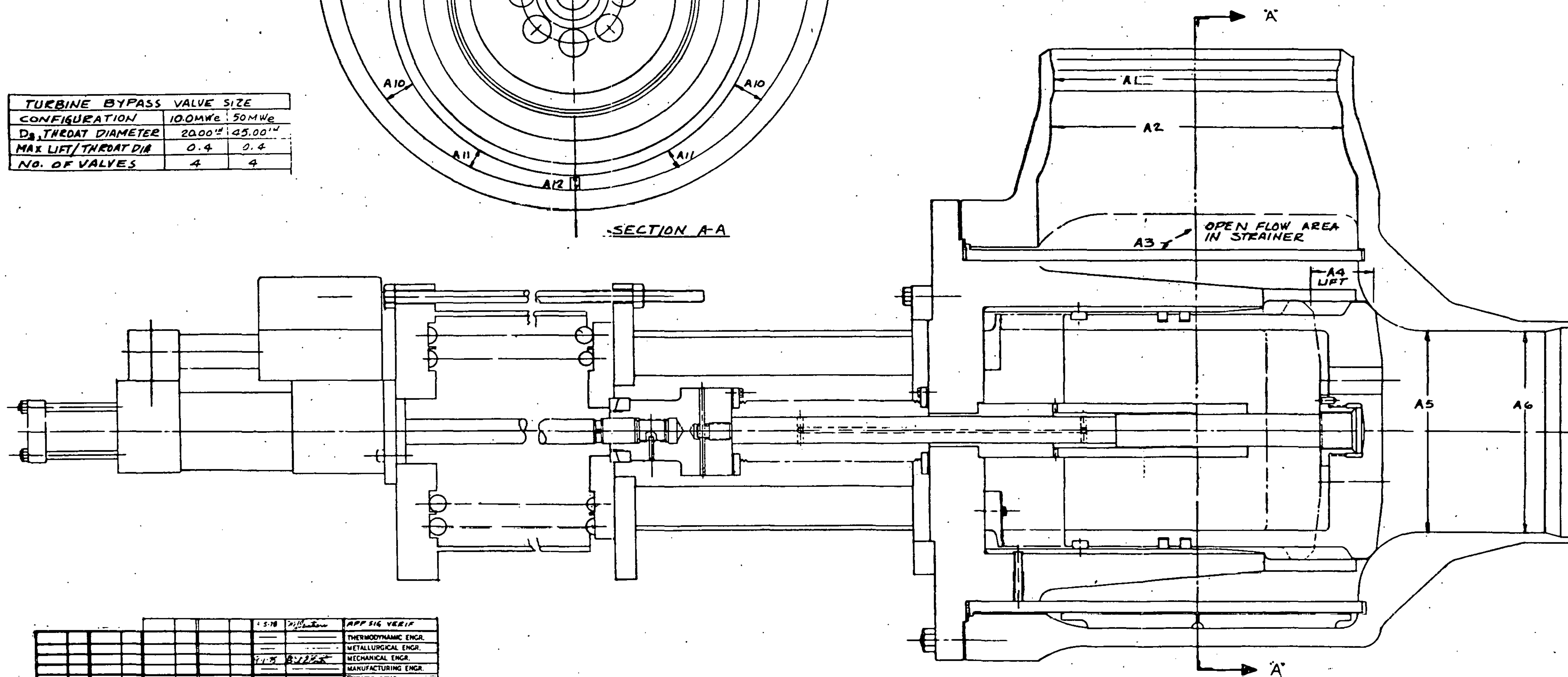

SUB 5 DATE	INIT.	SUB 4 DATE	INIT.	SUB 3 DATE	INIT	SUB 2 DATE	INIT	SUB 1 DATE	SIGNATURE	APPROVED BY:
								4-5-78	[illegible]	APP SIG VERIF
										THERMODYNAMIC ENGR.
										METALLURGICAL ENGR.
								[illegible]	[illegible]	MECHANICAL ENGR.
										MANUFACTURING ENGR.
										CONTROL ENGR.
								[illegible]	[illegible]	PROJECT ENGR.
								[illegible]	[illegible]	DRAFTING MGR.
								[illegible]	[illegible]	LAYOUT DRAFTSMAN

Westinghouse Electric Corporation
STEAM TURBINE DIVISION, LESTER, PA., U.S.A.

ISSUE DATE 7/ /75

APPLICATION: OTEC-1

TITLE: TURBINE BYPASS VALVES AMMONIA VAPOR

LAYOUT NO. 746J480

S.O. AA123100 | ORIG. LO. SCALE =1:1.00 | CODE NO. | DISTR. CODE [illegible] | SHEET 1 OF

AREA/RATIO PRESSURE DROP - VOLUTE VALVE

AREA	RATIO
A1/A6	1.45
A2/A6	1.60
A3/A6	4.10
A4/A6	1.90
A5/A6	1.00
A6/A5	1.00
A7/A1	.56
A8/A1	.44
A9/A1	.33
A10/A1	.21
A11/A1	.14
A12/A1	.00

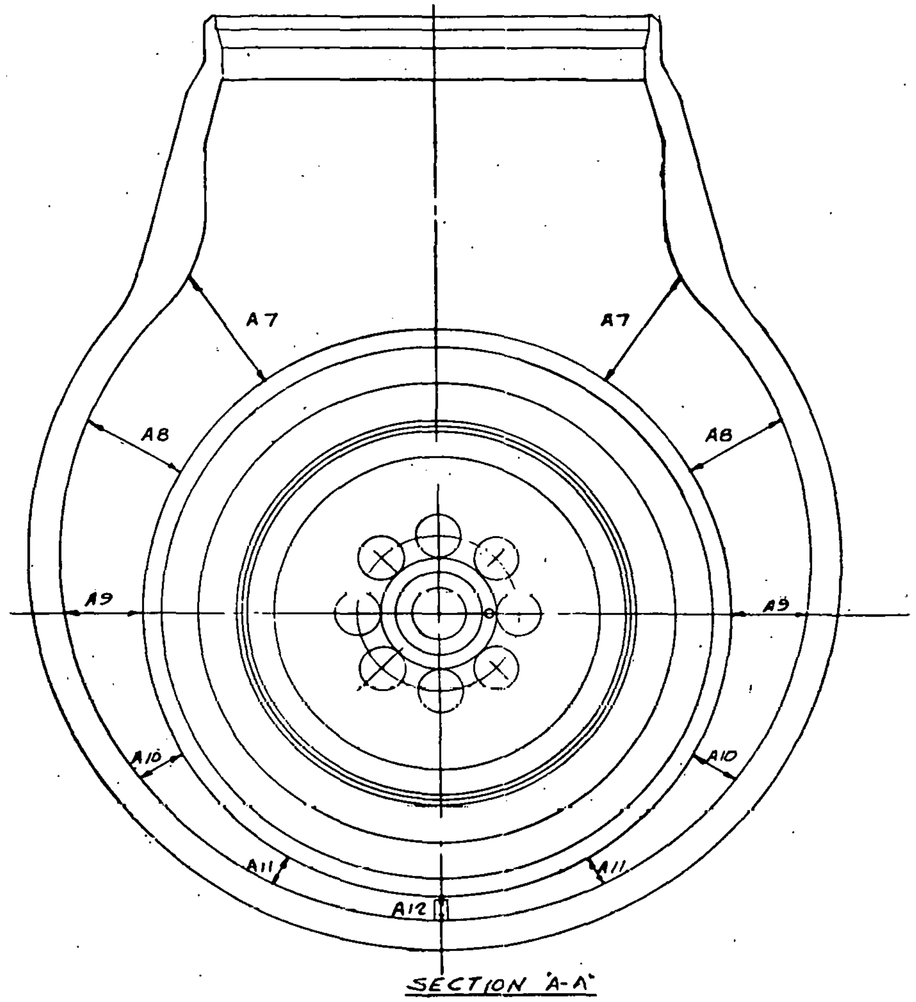

SECTION "A-A"

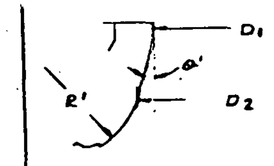

INLET DESIGN

1- R'/D_1 = 0.40

2 $(D_2/D_1)^2$ = 1.16

3 θ' = 5°

VALVE SEAT DESIGN

1- R/D_s = 0.26

2 D_B/D_s = 1.20

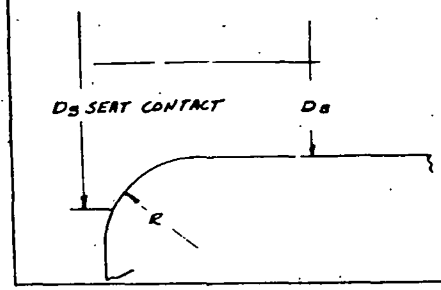

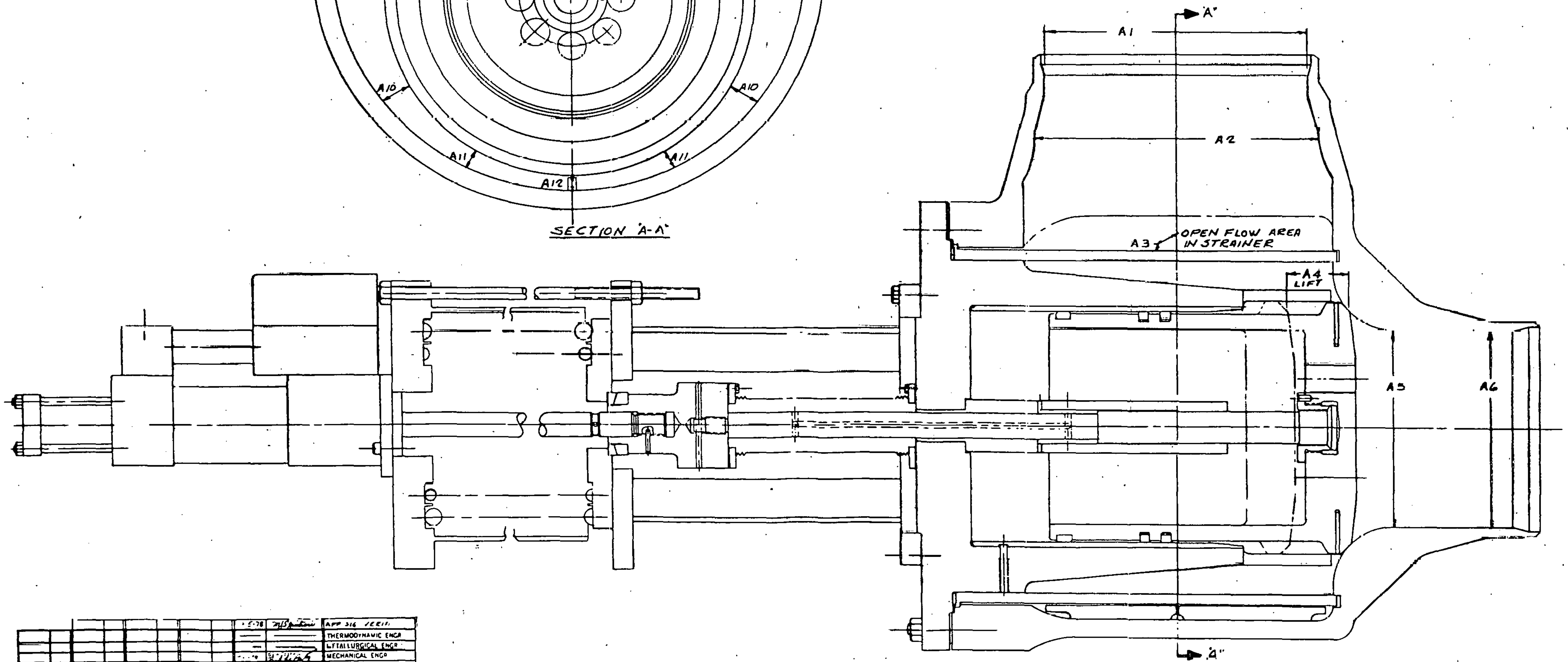

VALVE SIZE 10.0 MWe CONFIGURATION						
VALVE LOCATIONS	CV#1	CV#4	CV#10	CV#9	CV#2	CV#3
Ds, THROAT DIAMETER	14.00"	10.00"	[illegible]	20.00"	20.00"	20.00"
MAX LIFT/THROAT DIA.	0.4	0.4	0.4	0.4	0.4	0.4
NO OF VALVES	4	4	2	2	2	1

VALVE SIZE 50MWe CONFIGURATION						
VALVE LOCATIONS	CV#1	CV#4	CV#10	CV#9	CV#2	CV#3
Ds, THROAT DIAMETER	32.00"	22.00"	22.00"	32.00"	32.00"	32.00"
MAX LIFT/THROAT DIA.	0.4	0.4	0.4	0.4	0.4	0.4
NO OF VALVES	4	4	2	4	4	2

SUB 5 DATE	INIT.	SUB 4 DATE	INIT	SUB 3 DATE	INIT	SUB 2 DATE	INIT.	SUB 1 DATE	SIGNATURE	APPROVED BY
								5-78		APP 316 VERIF.
										THERMODYNAMIC ENGR
										METALLURGICAL ENGR
										MECHANICAL ENGR
										MANUFACTURING ENGR
										CONTROL ENGR
										PROJECT ENGR
								78		DRAFTING MGR
										LAYOUT DRAFTSMAN

Westinghouse Electric Corporation
STEAM TURBINE DIVISION, LESTER, PA. U.S.A.

ISSUE DATE

APPLICATION: OTEC #1

TITLE: LIQUID AMMONIA CONTROL VALVES

LAYOUT NO. 746J479

S.O. AA 123100 | ORIG. L.O. SCALE = 12.00 | CODE NO. | DISTR. CODE 399 LAB 000 | SHEET OF.

6.2.7.3 Valve Design Requirements

Requirements of size, flow capacity and response time for the ammonia control valves were determined from system steady-state and dynamic analysis as discussed in Section 6.5, System Operation. The following criteria were established for the design of the ammonia control valves:

6.2.7.3.1 Turbine Bypass Valves

- Valves are sized to bypass 70-75% of maximum rated vapor flow (110% x rated flow) from the evaporator, around the turbine, to the condenser, when wide open.
- Pressure balanced plug-type configuration (90° turn) is closed by spring force, opened by hydraulic pressure. The liquid ammonia valves have the same general configuration.
- Valves have both modulating (control operation) and rapid opening (emergency trip operation) capabilities.
- For controlling mode, the servo control loop has a frequency response of 2-5 Hertz at 90° full stroking capability of 2 to 4.0 seconds and synchronous speed regulation of 2-5% of rated speed. A three-way electro-hydraulic "Moog" servo valve for positioning bypass valves, has a flow capability of meeting the above servo loop response characteristics.
- During fast-opening trip operation, valves traverse full-opening stroke in less then 250 milliseconds. Auxiliary hydraulic accumulator is provided to suddenly apply hydraulic pressure to actuator piston when dump valve is suddenly opened. Two 4-inch diameter fast-opening WECO dump valves are provided with opening response time of less than 5 milliseconds. One dump valve hydraulic actuated, the other dump valve electrical solenoid actuated. Both dump valves open fully in event of loss of electrical power or hydraulic pressure service.

- Turbine By-Pass Valve Size:

Throat Diameter	20 inch
Number of Valves (Parallel Flow Path)	4
Active Stroke	6 inch

6.2.7.3.2 Liquid NH_3 Feed Valves (CV-1)

- Each valve is sized to pass 110% of rated evaporator vapor flow, with a liquid flow velocity past valve throat diameter of approximately 6 ft/sec.
- The valves are of the pressure balanced plug-type configuration (90° turn); closed by spring force; opened by hydraulic pressure.
- Valves have both modulating and rapid closing capabilities.
- In controlling mode, the servo control loop has a frequency response of 2-5 Hertz at 90° and a full stroking capability of 2 to 4 seconds. A three-way electro-hydraulic "Moog" servo valve, with a flow capability which meets the above control responses, is used for valve positioning.
- During fast-closing trip operation, valves traverse the full closing stroke in less than 250 milliseconds. Two 4-inch diameter fast-opening dump valves evacuate hydraulic oil from within the actuator piston cavity. Both dump valves have an opening response time of less then 5 milliseconds. One dump valve is hydraulically activated, the other dump valve is electrical solenoid actuated. Both dump valves open fully in event of loss of electrical power or hydraulic pressure.

- Valve size for liquid NH_3 feed valves (CV-1):

Throat Diameter	14 inch
Number of Valves	4
Active Stroke	4.2 inch

6.2.7.3.3 Evaporator Liquid Recirculating Valves (CV-4)

- Each valve is sized to pass 40% of rated evaporator vapor flow with a liquid flow velocity past valve throat diameter of approximately 6 ft/sec.
- The valves are of the pressure balanced plug-type configuration (90° turn); closed by spring force; opened by hydraulic pressure.
- Valves have both modulating and rapid closing capabilities.
- In controlling mode, the servo control loop has a frequency response to 2-5 Hertz at 90° and a full stroking capability of 2 to 4 seconds. A three-way electro-hydraulic "Moog" servo valve, with a flow capability which meets the above control responses, is used for valve positioning.
- During fast-closing trip operation, valves traverse the full closing stroke in less then 250 milliseconds. Two 4-inch diameter fast-opening dump valves evacuate hydraulic oil from within the actuator piston cavity. Both dump valves have an opening response time of 5 milliseconds. One dump valve is hydraulic activated, the other dump valve is electrical solenoid activated. Both dump valves open fully in event of loss of electrical power or hydraulic pressure.

- Valve sizes for evaporator liquid recirculating valves (CV-4):

Throat Diameter	10 inch
Number of Valves	4
Active Stroke	3 inch

6.2.7.4 Control Valve Hydraulic Supply System

The size of the main control valves and the speed with which they must respond requires the use of hydraulic operators. A preliminary design for the hydraulic supply system and the control valve actuators was prepared.

The system is shown in (Figure 6-48). The significant features of this system are listed as follows:

- The hydraulic pumping system is redundant. Dual pumps and motors, dual high pressure filters, unloading valves for the control of fluid pressure, dual return filters and heat exchangers are provided. Any of the devices can be replaced with the unit in service by shutting down one system and operating on the other.

- The accumulators are connected to a manifold control block which permits the base charge to be checked in each accumulator with the unit in operation.

- Each valve actuator and associated control trim is independent. Maintenance can be performed on the valve hydraulics with the unit in operation.

6.2.8 Ammonia Pumps

6.2.8.1 Ammonia Feed Pump

During startup and normal power operation, liquid ammonia collects in the hotwell of the condenser and is pumped into the evaporator using the ammonia feed pump. This pump is also utilized when ammonia is transferred from the power cycle into storage during system shutdown and ammonia evacuation.

A vertical turbine pump appears to be the only suitable pump for the OTEC application. A conventional horizontal centrifugal would require an increase in the platform vessel's depth in order to accomodate another deck to house this type of pump. Instead, the vertical turbine pump allows only the barrel section and suction line to extend beyond the bottom of the OTEC hull.

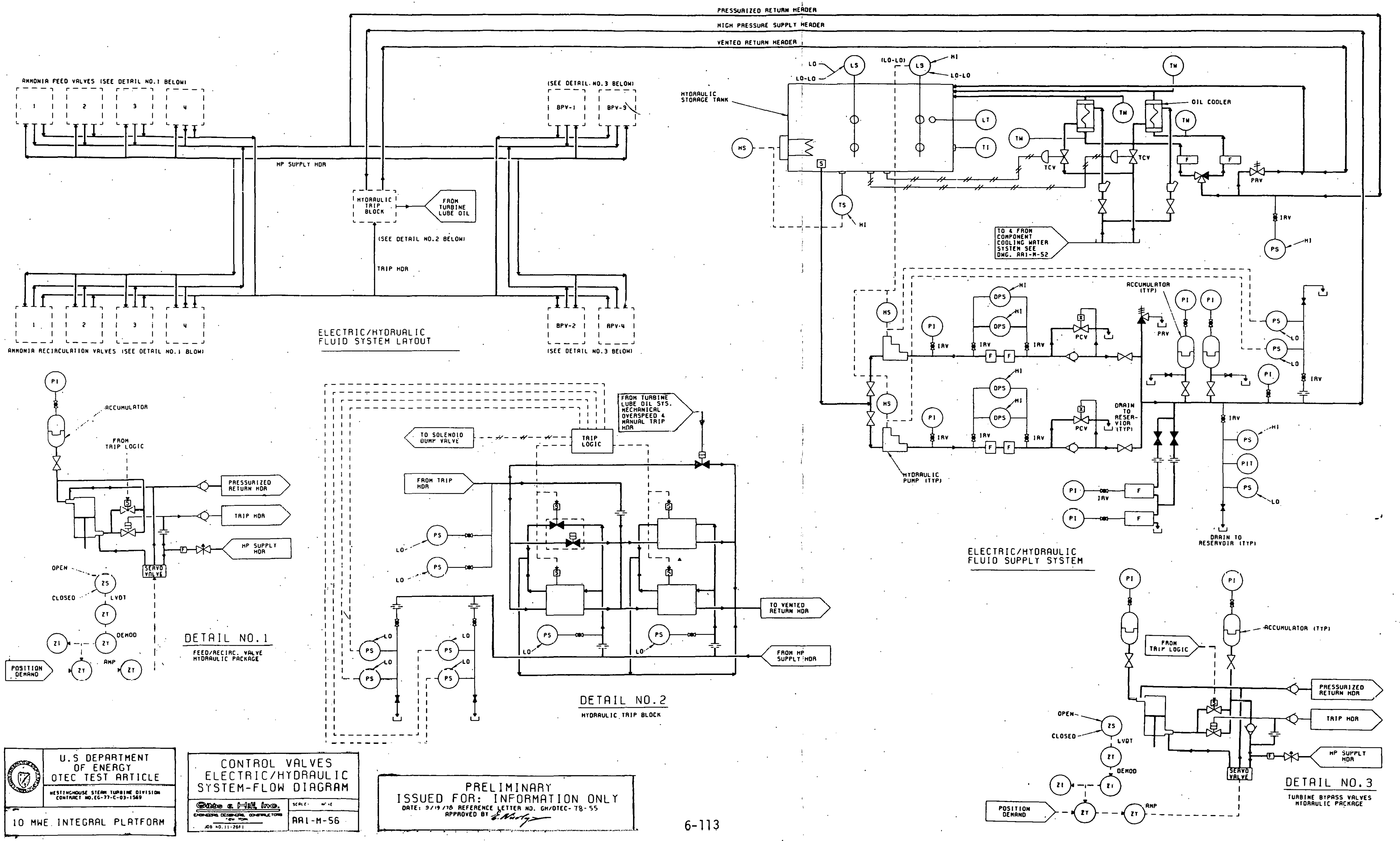

U.S DEPARTMENT OF ENERGY
OTEC TEST ARTICLE
WESTINGHOUSE STEAM TURBINE DIVISION CONTRACT NO. EG-77-C-03-1569
10 MWE INTEGRAL PLATFORM

CONTROL VALVES
ELECTRIC/HYDRAULIC
SYSTEM-FLOW DIAGRAM
Gibbs & Hill, Inc.
AA1-M-56

PRELIMINARY
ISSUED FOR: INFORMATION ONLY
DATE: 9/19/78 REFERENCE LETTER NO. GH/OTEC-78-55
APPROVED BY

THIS PAGE

WAS INTENTIONALLY

LEFT BLANK

The selected ammonia feed pump is a standard industrial vertical turbine type. The motor for this pump is located on elevation 45.0 of the platform vessel. The motor is a vertically oriented drive, mounted on a fabricated steel discharge head/base plate which is fastened to the hull structure. The ammonia feed pump requires a 600-hp motor supplied by a 3-phase, 60-cycle, 6900-volt power source. Large access openings are furnished in the upper portion of the head for ease of mechanical seal adjustment. The motor is coupled to a vertical shaft which extends down to the impeller/bowl assembly of the pump.

The pump drive shaft is located within sections of flanged steel pipe which serves as the pump discharge line and shaft housing. The pipe assembly consists of discharge line sections, bearings and bearing retainers, carbon steel shaft sections and couplings. The bearing retainers and pipe flanges form a close tolerance fit to ensure positive alignment. The outside surface of the flanged steel pipe is coated with a material suitable for marine exposure. Cast iron or carbon steel is employed for the bearing retainers, and graphalloy is used for the shaft bearings. The pipe is connected to a barrel section. The barrel extends from the bottom of the platform vessel to satisfy the net positive suction head requirements of the pump. The barrel section is carbon steel with a fabricated suction nozzle. The outside surface of the barrel section is also exposed to a seawater environment and is suitably coated. The pump suction line also extends beyond the bottom of the platform vessel from the condenser and is connected to the barrel suction nozzle. The location of the pump impeller is below the liquid level of the condenser, which allows the pump to be started without priming.

The pump bowl assembly is housed in the barrel and consists of cast iron bowls, impellers, and stainless steel wear rings and bowl shaft. Ammonia lubricates the shaft bearings. The pump is furnished with a mechanical shaft seal to prevent leakage.

The ammonia feed pump is designed to maintain a constant flow. During power cycle steady-state and transient conditions, the capacity of the feed pump remains constant while the associated control valves are exercised or positioned.

Additional information pertaining to the ammonia feed pump is contained in Tables 6-21, 6-26 and 6-27.

6.2.8.2 Ammonia Recirculation Pump

During startup and normal power operation, feed ammonia which is not evaporated collects in the evaporator drain well and is pumped/recirculated back into the evaporator via the ammonia manifold, using the ammonia recirculation pump. This pump is also utilized when ammonia is transferred from the power cycle into storage during system shutdown and ammonia evacuation.

The ammonia recirculation pump to be furnished for the 10 MWe power system is, like the ammonia feed pump, a standard industrial vertical turbine type. The motor for this pump is also located on elevation 45.0 of the platform vessel. The recirculation pump requires a 70-hp motor supplied by a 3-phase, 60-cycle, 480-volt power source. This pump is similar in design concept to the ammonia feed pump; its capacity, head and horsepower requirements differ substantially, however.

Additional information pertaining to the ammonia recirculation pump is contained in Tables 6-21, 6-26 and 6-27.

6.2.9 Auxiliaries

6.2.9.1 Ammonia Storage, Handling and Purification System

An ammonia storage system is required, having sufficient capacity to store the ammonia power cycle charge and to maintain a reserve quantity of ammonia for make-up. (Figure 6-49.) During a maintenance cycle, large quantities of ammonia must be transferred into storage in a reasonably short time. This is accomplished by using both the ammonia feed pump and

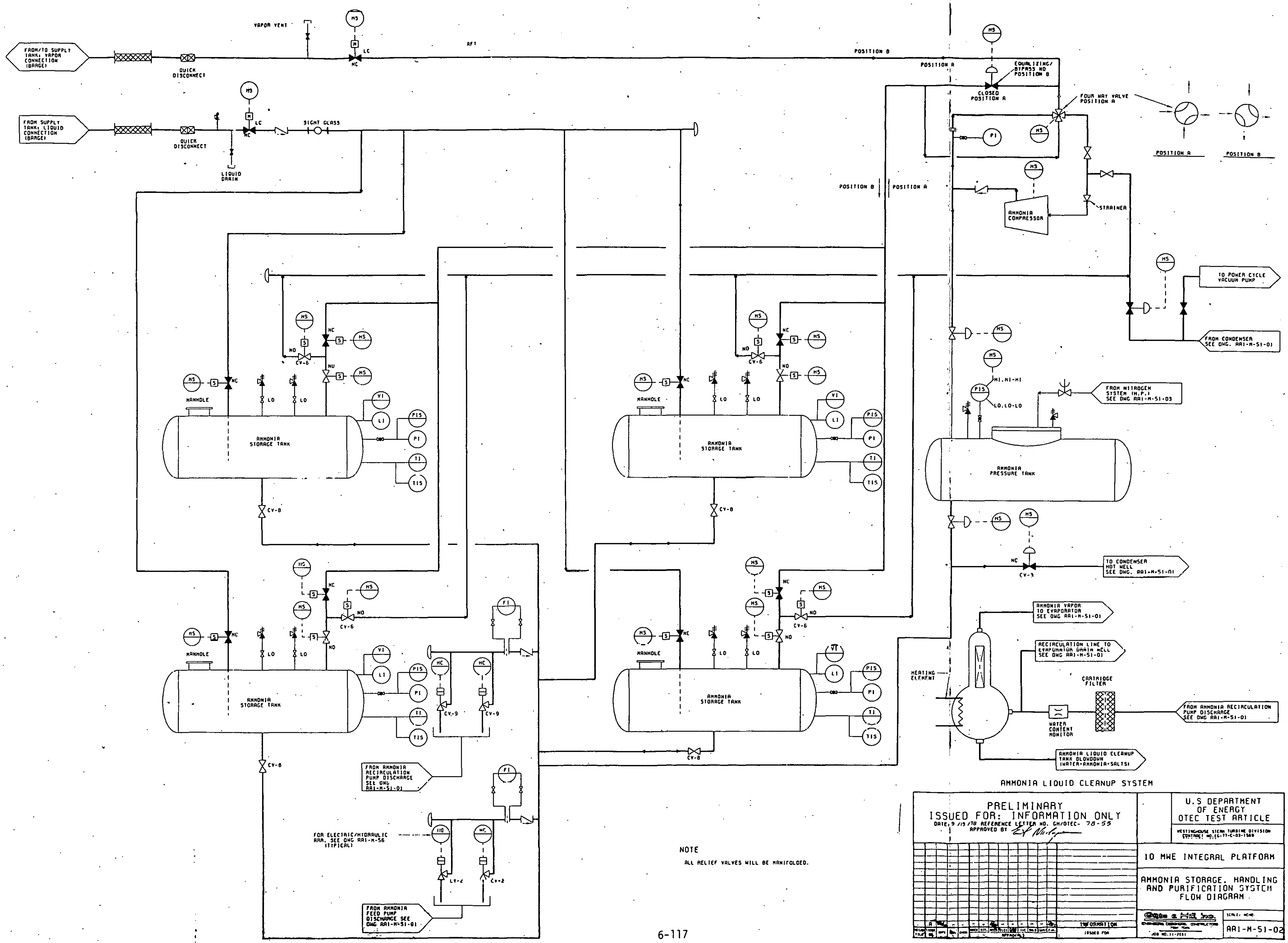
FROM/TO SUPPLY TANK: VAPOR CONNECTION (BARGE)
QUICK DISCONNECT
VAPOR VENT
FROM SUPPLY TANK: LIQUID CONNECTION (BARGE)
LIQUID DRAIN
SIGHT GLASS
POSITION B
POSITION A
EQUALIZING/ BYPASS NO POSITION B
CLOSED POSITION A
FOUR WAY VALVE POSITION A
AMMONIA COMPRESSOR
STRAINER
TO POWER CYCLE VACUUM PUMP
FROM CONDENSER SEE DWG. AR1-M-51-01
FROM NITROGEN SYSTEM (H.P.) SEE DWG AR1-M-51-03
AMMONIA PRESSURE TANK
TO CONDENSER HOT WELL SEE DWG. AR1-M-51-01
MANHOLE
AMMONIA STORAGE TANK
AMMONIA VAPOR TO EVAPORATOR SEE DWG AR1-M-51-01
RECIRCULATION LINE TO EVAPORATOR DRAIN WELL SEE DWG AR1-M-51-01
HEATING ELEMENT
CARTRIDGE FILTER
WATER CONTENT MONITOR
FROM AMMONIA RECIRCULATION PUMP DISCHARGE SEE DWG AR1-M-51-01
AMMONIA LIQUID CLEANUP TANK BLOWDOWN (WATER-AMMONIA-SALTS)
AMMONIA LIQUID CLEANUP SYSTEM
FROM AMMONIA RECIRCULATION PUMP DISCHARGE SEE DWG AR1-M-51-01
FOR ELECTRIC/HYDRAULIC ARR. SEE DWG AR1-M-56 (TYPICAL)
FROM AMMONIA FEED PUMP DISCHARGE SEE DWG AR1-M-51-01
NOTE
ALL RELIEF VALVES WILL BE MANIFOLDED.
PRELIMINARY
ISSUED FOR: INFORMATION ONLY
U.S DEPARTMENT OF ENERGY
OTEC TEST ARTICLE
10 MWE INTEGRAL PLATFORM
AMMONIA STORAGE, HANDLING AND PURIFICATION SYSTEM FLOW DIAGRAM
AR1-M-51-02

THIS PAGE

WAS INTENTIONALLY

LEFT BLANK

the recirculation pump in conjunction with a compressor to transfer liquid and vapor. Pressurized and one-atmosphere refrigerated storage systems were studied. The pressurized system was selected because it offers lower parasitic losses than the refrigerated system. Multiple standard size storage tanks mounted on saddle supports are utilized. They are readily adaptable to other platform configurations. Because of manufacturing considerations, the multiple tank arrangement was selected instead of one large storage vessel. A single storage tank of this size would have to be field-fabricated at greater cost than "off-the-shelf" shop-fabricated tanks. Further, a single large tank is less easily fitted into alternative arrangement configurations. Incorporation of the condenser hotwell, the evaporator drain well, and the moisture separator into the OTEC heat exchangers, as well as short pipe runs, minimized the ammonia power system volume requirements. Temperatures in the storage tanks will be controlled by a batch cooling system served by the component cooling water system. Impurities in the ammonia will be removed by a system consisting of a pressure tank with a separator diaphragm, a compressor, and a distillate column.

6.2.9.2 Nitrogen Storage and Supply System

Nitrogen is used in the power system to purge it of air prior to the introduction of ammonia. Two potential methods of storing nitrogen were considered during the OTEC preliminary design phase. The first method utilizes a cryogenic storage vessel containing low temperature liquid nitrogen.

The second method consists of multiple compressed gas cylinders. Because the cryogenic nitrogen storage system was less expensive than the more conventional compressed gas cylinder arrangement, it was selected. (Figure 6-50). Another possible method of nitrogen storage could be in the form of a supply service contract with a nitrogen supplier. If the availability of this type arrangement can be ascertained, a cryogenic liquid nitrogen storage tank could be transported to the OTEC station during or just prior to scheduled maintenance outages. The disadvantage of this arrangement is the delay in service during an unscheduled outage when access or maintenance on the power cycle is required in a short period of time to minimize down-time. Also, a limited supply of high pressure compressed gas cylinders would have to be maintained on-board to service the ammonia pressure tank.

6.2.9.3 Circulating Seawater and Component Cooling Water (CCW) System

An efficient utilization of available energy in the form of heat sinks and sources is the basis for design of the circulating seawater and component cooling water system, Figure 6-51. A warm seawater system/warm CCW loop and a cold seawater system/cold component cooling water loop are provided with pumps, heat exchangers and connecting piping to furnish the power cycle components and the hull support equipment with cooling water at appropriate temperature levels. Further refinement of this system would occur during the detailed design phase when it is integrated with the hull contractor's "hotel" water system(s). The closed loop system is utilized to minimize system maintenance.

6.2.9.4 Compressed Air System

The primary purpose of the compressed air system is to furnish the power cycle diesel-generator with a reliable supply of starting air. (Figure 6-52). As with the component cooling water system, future design efforts would integrate the compressed air requirements of the power cycle with the hull contractor's compressed air requirements. The resulting system would furnish ship's service, instrument and seawater pump pod pressurization air, as well as diesel-generator start-up air.

6.2.9.5 Auxiliary Power Supply System

A 4500-kW, 6900-volt diesel-generator would supply a reliable source of power for startup and safe shutdown of the power cycle. Figure 6-53 illustrates the auxiliary systems required for its support. With the exception of diesel fuel storage and day tanks, all of the diesel-

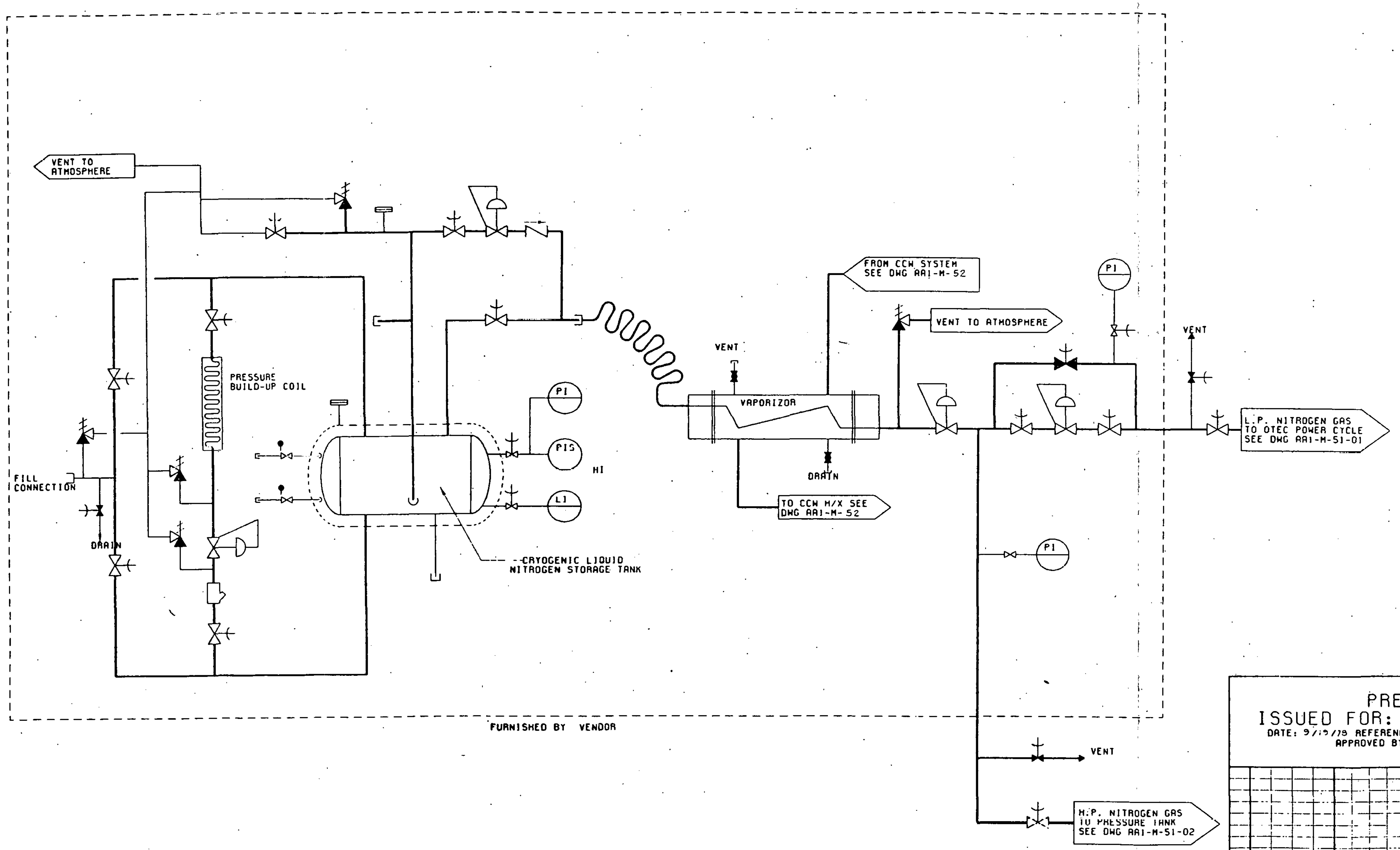

PRELIMINARY
ISSUED FOR: INFORMATION ONLY
DATE: 9/19/78 REFERENCE LETTER NO. GH/OTEC-78-55
APPROVED BY

U.S. DEPARTMENT OF ENERGY
OTEC TEST ARTICLE

WESTINGHOUSE STEAM TURBINE DIVISION
CONTRACT NO. EG-77-C-03-1589

10 MWE INTEGRAL PLATFORM

NITROGEN SYSTEM FLOW DIAGRAM

MICRO FILM	ISSUE NO.	DATE	DWN.	CHKD.	APPROVALS: ARCH	STR.	MECH	ELEC	I&C	SHLD	CONST	P.M.	ISSUED FOR
✓	A	9/19/78											INFORMATION

Gibbs & Hill, Inc.
ENGINEERS, DESIGNERS, CONSTRUCTORS
NEW YORK
JOB NO. 11-2661

SCALE: NONE

AA1-M-51-03

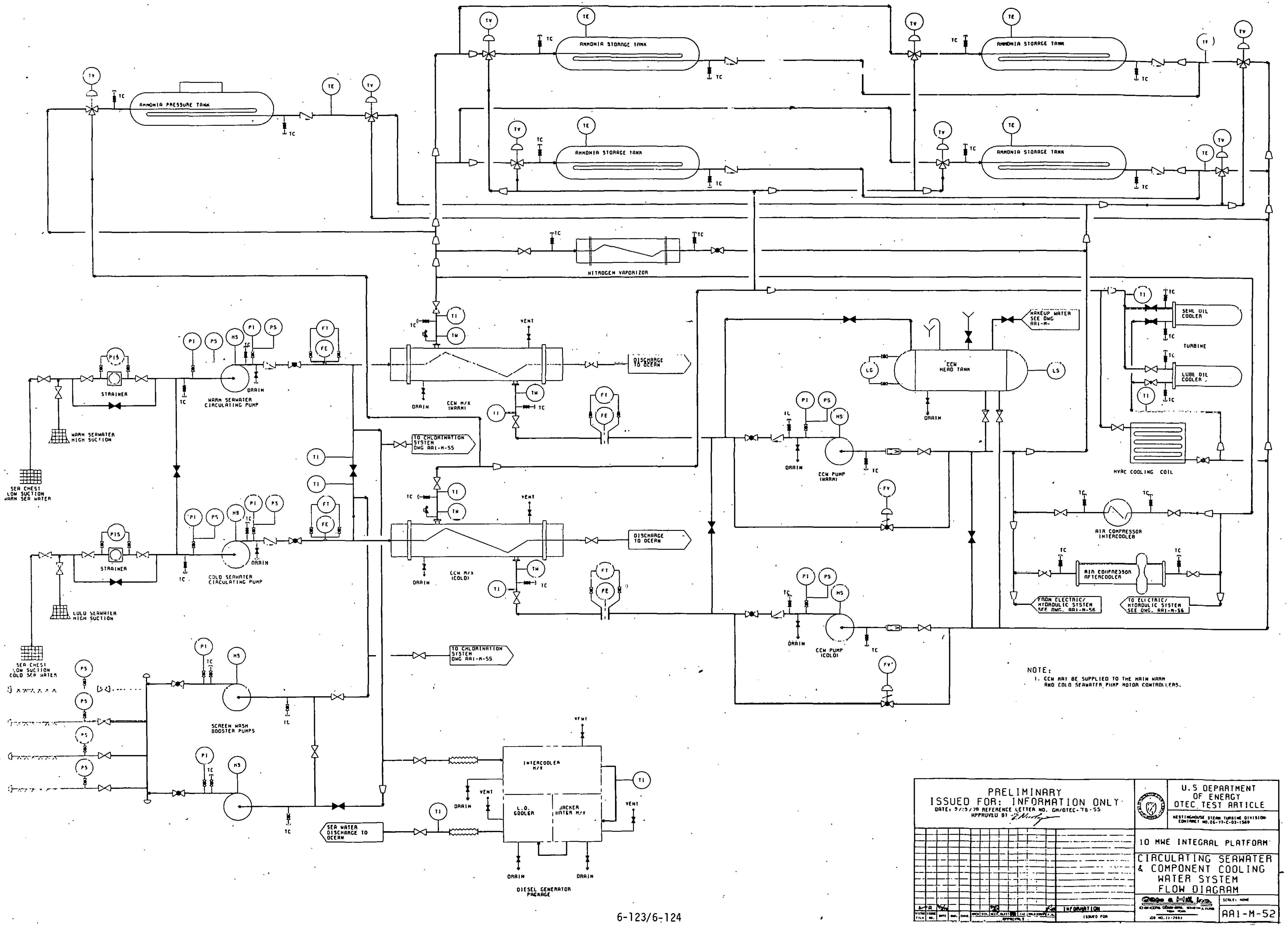
AMMONIA PRESSURE TANK
AMMONIA STORAGE TANK
AMMONIA STORAGE TANK
AMMONIA STORAGE TANK
AMMONIA STORAGE TANK
NITROGEN VAPORIZER
STRAINER
WARM SEAWATER HIGH SUCTION
SEA CHEST LOW SUCTION WARM SEA WATER
WARM SEAWATER CIRCULATING PUMP
DRAIN
VENT
CCW H/X (WARM)
DISCHARGE TO OCEAN
TO CHLORINATION SYSTEM DWG AA1-M-55
STRAINER
COLD SEAWATER HIGH SUCTION
SEA CHEST LOW SUCTION COLD SEA WATER
COLD SEAWATER CIRCULATING PUMP
CCW H/X (COLD)
DISCHARGE TO OCEAN
TO CHLORINATION SYSTEM DWG AA1-M-55
SCREEN WASH BOOSTER PUMPS
INTERCOOLER H/X
L.O. COOLER
JACKET WATER H/X
SEA WATER DISCHARGE TO OCEAN
DIESEL GENERATOR PACKAGE
MAKEUP WATER SEE DWG AA1-M-
CCW HEAD TANK
CCW PUMP (WARM)
CCW PUMP (COLD)
SEAL OIL COOLER
TURBINE
LUBE OIL COOLER
HVAC COOLING COIL
AIR COMPRESSOR INTERCOOLER
AIR COMPRESSOR AFTERCOOLER
FROM ELECTRIC/ HYDRAULIC SYSTEM SEE DWG. AA1-M-56
TO ELECTRIC/ HYDRAULIC SYSTEM SEE DWG. AA1-M-56
NOTE:
1. CCW HAT BE SUPPLIED TO THE MAIN WARM AND COLD SEAWATER PUMP MOTOR CONTROLLERS.
PRELIMINARY
ISSUED FOR: INFORMATION ONLY
DATE: 9/5/78 REFERENCE LETTER NO. GH/OTEC-78-55
APPROVED BY
U.S DEPARTMENT OF ENERGY
OTEC TEST ARTICLE
WESTINGHOUSE STEAM TURBINE DIVISION
CONTRACT NO.EG-77-C-03-1569
10 MWE INTEGRAL PLATFORM
CIRCULATING SEAWATER & COMPONENT COOLING WATER SYSTEM FLOW DIAGRAM
INFORMATION
ISSUED FOR
APPROVALS
SCALE: NONE
AA1-M-52

6-123/6-124

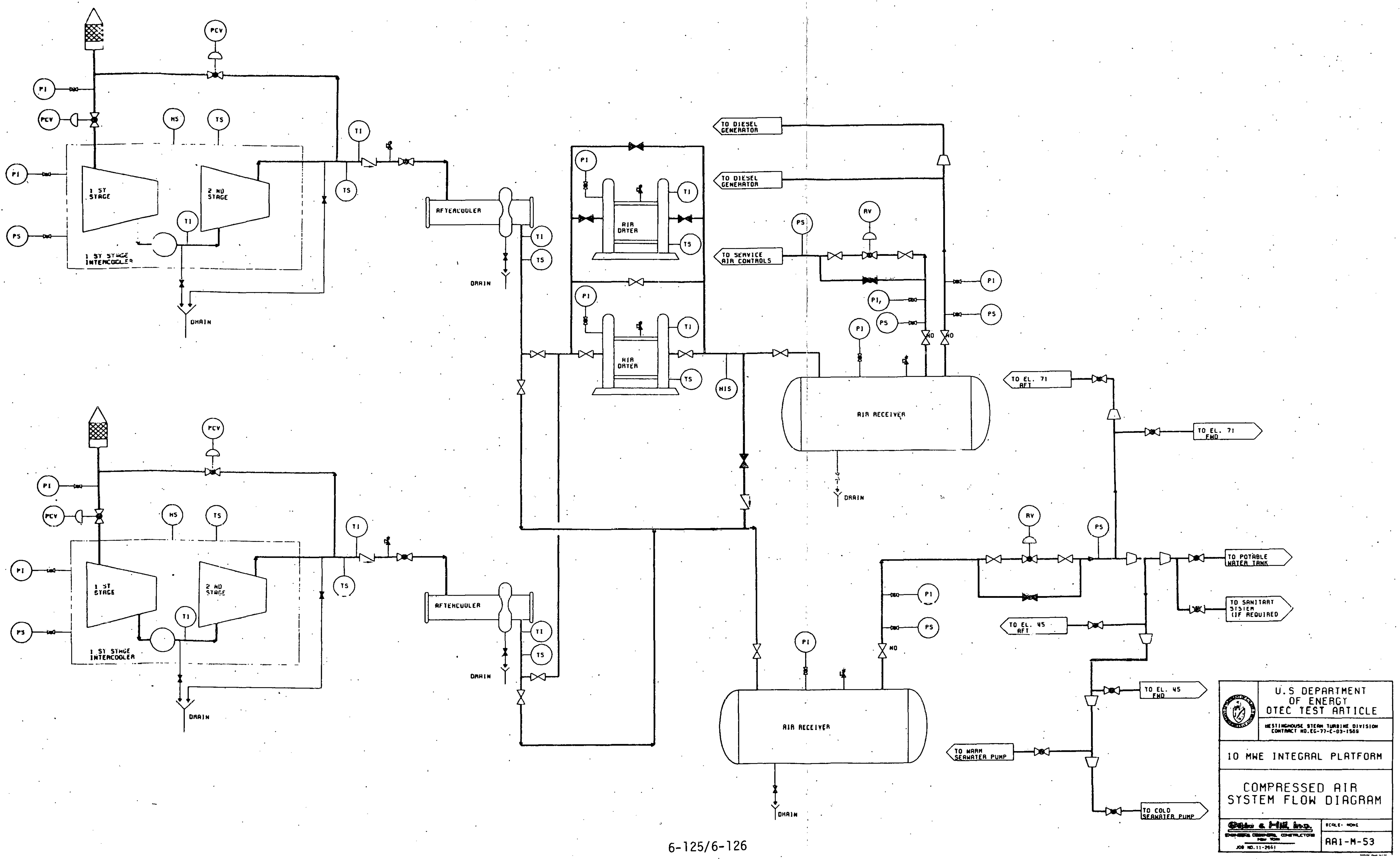

PCV
PI
HS
TS
TI
1 ST STAGE
2 ND STAGE
1 ST STAGE INTERCOOLER
DRAIN
AFTERCOOLER
AIR DRYER
TO DIESEL GENERATOR
TO DIESEL GENERATOR
TO SERVICE AIR CONTROLS
RV
PS
NO
HIS
AIR RECEIVER
TO EL. 71 AFT
TO EL. 71 FWD
TO POTABLE WATER TANK
TO SANITARY SYSTEM (IF REQUIRED
TO EL. 45 AFT
TO EL. 45 FWD
TO WARM SEAWATER PUMP
TO COLD SEAWATER PUMP
U.S DEPARTMENT OF ENERGY OTEC TEST ARTICLE
WESTINGHOUSE STEAM TURBINE DIVISION
CONTRACT NO.EG-77-C-03-1569
10 MWE INTEGRAL PLATFORM
COMPRESSED AIR SYSTEM FLOW DIAGRAM
SCALE: NONE
AA1-M-53
JOB NO.11-2661

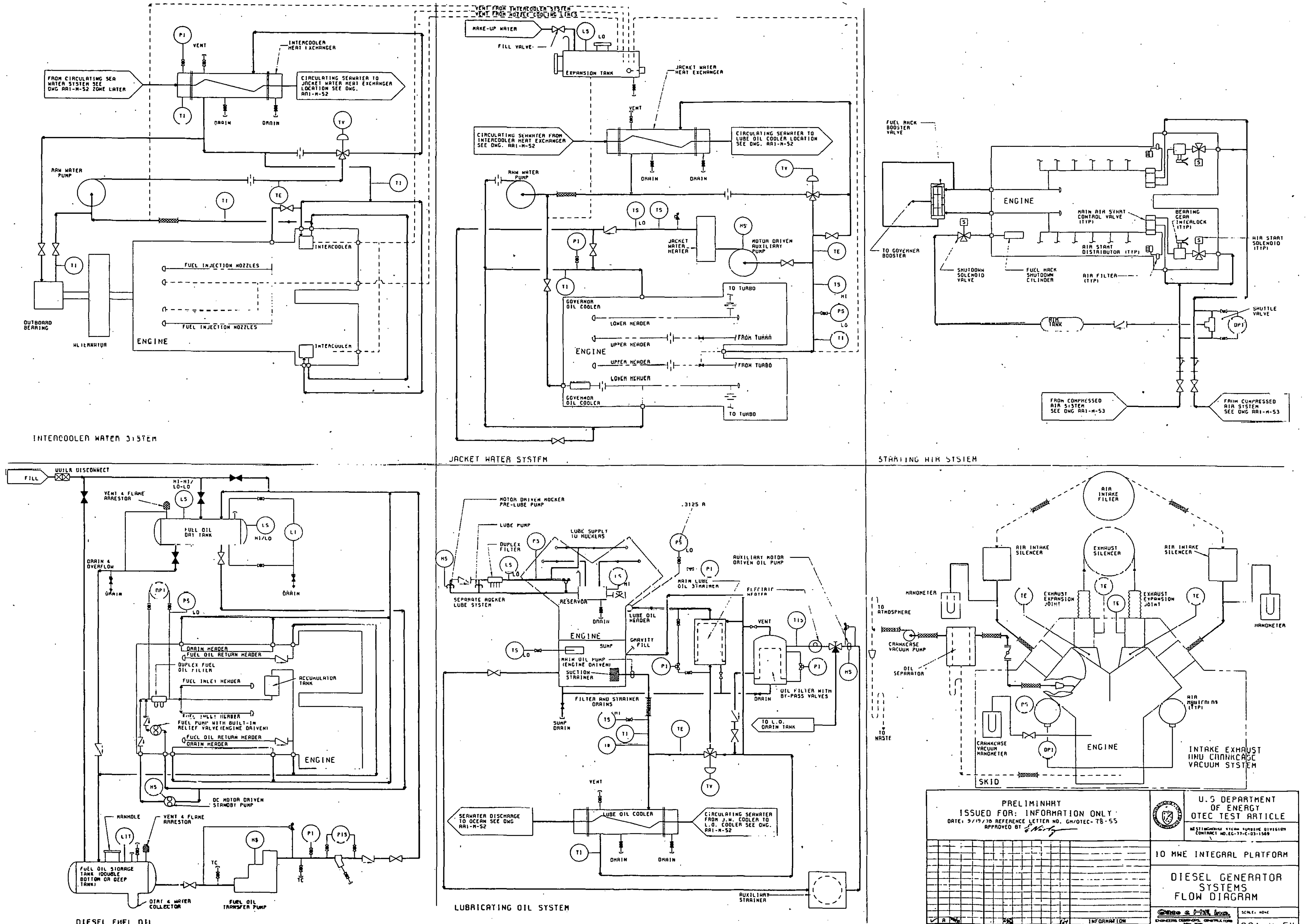
INTERCOOLER WATER SYSTEM
JACKET WATER SYSTEM
STARTING AIR SYSTEM
DIESEL FUEL OIL STORAGE & TRANSFER SYSTEM
LUBRICATING OIL SYSTEM
INTAKE EXHAUST AND CRANKCASE VACUUM SYSTEM
ENGINE
PRELIMINARY
ISSUED FOR: INFORMATION ONLY
U.S DEPARTMENT OF ENERGY
OTEC TEST ARTICLE
10 MWE INTEGRAL PLATFORM
DIESEL GENERATOR SYSTEMS FLOW DIAGRAM
AA1-M-54

generator support components are either integrally mounted on the engine, or grouped on common skid mountings. The major start-up loads supplied by the diesel-generator include the warm and cold seawater pumps, and the ammonia feed and recirculation pumps. It also supplies all platform hotel and auxiliary system loads during startup, scheduled and unscheduled maintenance, and storm survival conditions.

6.2.9.6 Electrical Distribution System

The electrical distribution system provides conditioning, distribution, monitoring, and control of power for operating OTEC plant auxiliaries and platform hotel loads supplied either by the auxiliary generator or by the OTEC plant turbo-generator. Figure 6-54 shows a preliminary one-line diagram of the electrical distribution system.

It commences at the terminals of the 6.9 kW turbo-generator with an 8-kW, 2000-ampere bus, connecting to metal clad switchgear and proceeding through intermediate to low voltage AC and DC systems using integrated transformation and switchgear arrangements. Start-up and emergency power from the 4500-kW diesel generator is taken into the system through a 6.9-kW, 2000-ampere bus. The total system includes 6900-volt and 460-volt AC and 125-volt DC power, low voltage control and instrumentation, grounding, and communication system distribution wiring and equipment.

6.3 System Design

6.3.1 Material Compatibility

6.3.1.1 Objectives

The purpose of the material compatibility study is to select materials which would enable the power module to function for 30 years in the seawater and ammonia environment. The components involved in this study included the tubes, tubesheets, shells, waterboxes, and structural members of the heat exchangers, rotor, disc, and blades of the ammonia turbine; seawater and ammonia pumps; and seawater and ammonia valves.

6.3.1.2 Material Alternatives

The materials considered in this study were

- Copper base alloys
- Nickel-containing alloys, including stainless steels
- Structural steels
- Aluminum alloys
- Titanium

6.3.1.3 Evaluation Criteria

The materials selected should endure the 30-year plant life in the seawater and/or ammonia environment without yielding to:

- Pitting corrosion
- Erosion, especially from seawater flow
- Galvanic corrosion, due to electrochemical dissimilarity of adjacent materials.
- Stress corrosion cracking

Information from systems where chlorine additions have been made for control of macrofouling suggests that chlorine has negligible, or only slight effects, on heat exchangers at levels less than 1 ppm. The expected OTEC chlorine dosage level is 0.25 ppm, maximum.

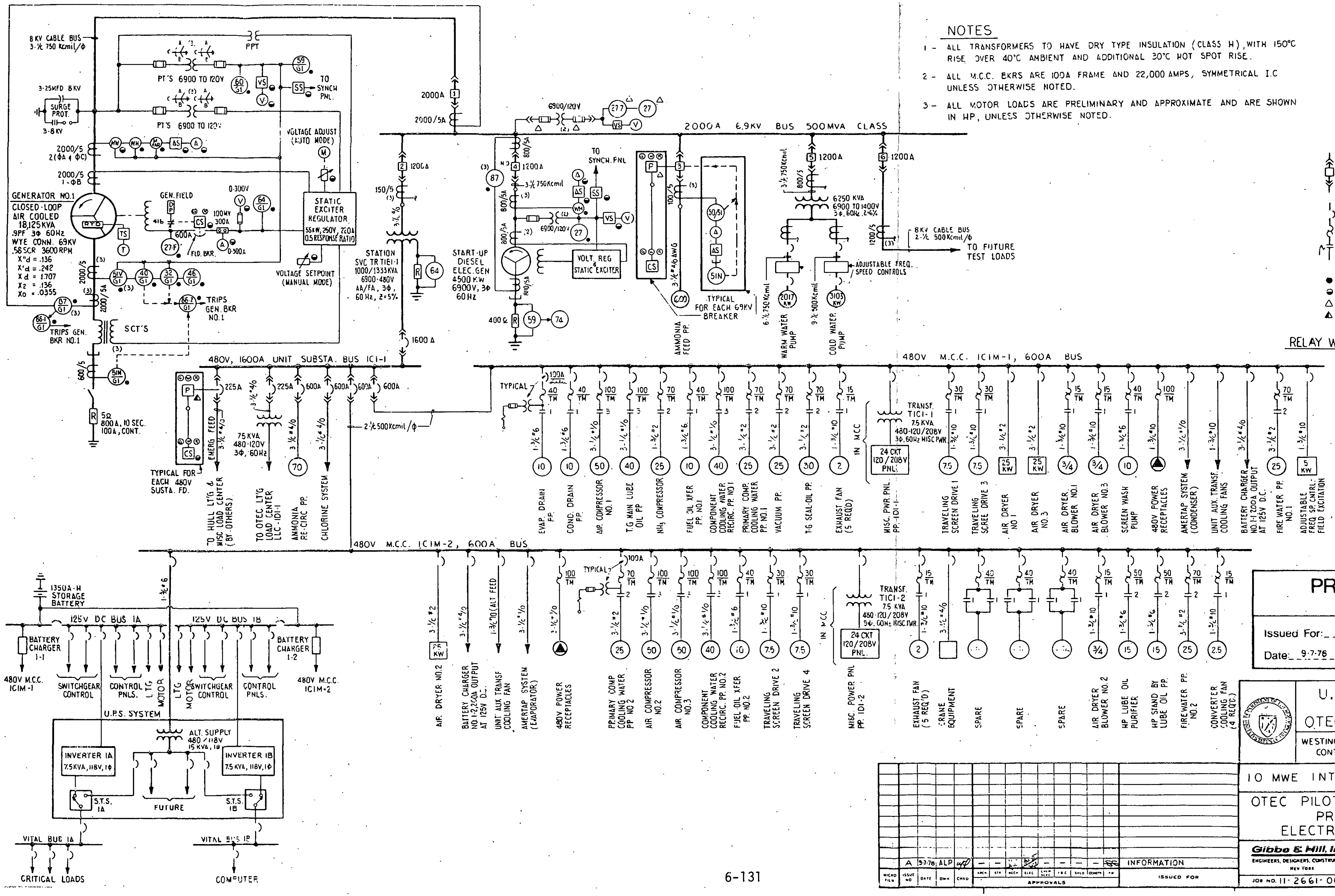

NOTES

1 - ALL TRANSFORMERS TO HAVE DRY TYPE INSULATION (CLASS H), WITH 150°C RISE OVER 40°C AMBIENT AND ADDITIONAL 30°C HOT SPOT RISE.

2 - ALL M.C.C. BKRS ARE 100A FRAME AND 22,000 AMPS, SYMMETRICAL I.C UNLESS OTHERWISE NOTED.

3 - ALL MOTOR LOADS ARE PRELIMINARY AND APPROXIMATE AND ARE SHOWN IN HP, UNLESS OTHERWISE NOTED.

LEGEND

OR	BREAKER (WITHDRAWABLE TYPE)
100 / 50 TM / 2	NEMA SIZE 2 MAGNETIC CONTACTOR WITH 100A FIXED FRAME BREAKER HAVING THERMAL MAGNETIC (TM) TRIP SET AT 50A AND CONTINUOUS SETTING TO BE ADDED LATER.
●	MAIN CONTROL PANEL (REAR)
◒	MAIN CONTROL PANEL (FRONT)
△	6.9KV SWITCHGEAR
▲	480V SWITCHGEAR

RELAY WITH DEVICE FUNCTION NUMBER

40	LOSS OF FIELD
60	VOLTAGE BALANCE
59	OVEREXCITATION
32	REVERSE POWER
87	DIFFERENTIAL CURRENT
51N	GROUND OVERCURRENT TIME DELAY
51V	PHASE OVERCURRENT TIME DELAY
50	PHASE OVERCURRENT-INSTANTANEOUS
64	GROUND VOLTAGE
27	UNDERVOLTAGE
86	TRIP & LOCKOUT
46	NEGATIVE SEQUENCE
74	ALARM RELAY

PRELIMINARY

Issued For: INFORMATION

Date: 9-7-76 Reference Letter No.

U. S. DEPARTMENT OF ENERGY
OTEC TEST ARTICLE

WESTINGHOUSE STEAM TURBINE DIVISION
CONTRACT NO. EG-77-C-03-1569

10 MWE INTEGRAL PLATFORM

OTEC PILOT PLANT MODULE
PRELIMINARY
ELECTRICAL ONE LINE

Gibbs & Hill, Inc.
ENGINEERS, DESIGNERS, CONSTRUCTORS
NEW YORK

SCALE: NONE

JOB NO. 11-2661-004

AAI-E-10

A	9-7-76	ALP									INFORMATION
ISSUE NO	DATE	DWN	CHKD	APPROVALS							ISSUED FOR

THIS PAGE
WAS INTENTIONALLY
LEFT BLANK

6.3.1.4 Materials Evaluation

6.3.1.4.1 Copper Base Alloys

Of the copper base alloys, Alloy 706 (90-10 CuNi) has a good record in seawater applications[15-26]. Copper alloys, however, have very poor resistance to ammonia and are not considered further.

6.3.1.4.2 Nickel-Containing Alloys

Many nickel-containing alloys have impressive records in seawater. Hastelloy C and Inconel 625 should both be acceptable, but are very expensive. Some austenitic stainless steels (300 series), usually 316L, have been used for seawater condenser tubing with poor results because of straight through cavernous pitting[27-29]. However, 316 S.S. pump impellers have been used successfully for seawater application[16]. Some of the new stainless steels, especially AL6X, show promise for OTEC tubing, after more experience is obtained.

The austenitic stainless steels appear to be completely compatible with ammonia and ammonium hydroxide environments. Instances of corrosion and intergranular attack have been reported in ammonia and urea synthesis plants, but these are probably associated with impurities and other components of the environments in these systems.

The ferritic and martensitic stainless steels appear to be satisfactory for use in ammonia systems. Instances of failure have been reported in ammonia plants, but these are not well documented and again were probably due to other contaminants.

There is relatively little data on other nickel alloys in ammonia. Available data indicates that intergranular cracking does not occur in nickel alloys at lower temperatures.

6.3.1.4.3 Structural Steels

Corrosion of carbon steel proceeds at a low surface recession rate of approximately 2 to 3 mils per year in seawater; however, pitting of 50-60 mils in the first 2 to 3 years is possible[30]. Coating of carbon steel in seawater with neoprene is recommended. Carbon steels and low alloy steels have been used for many years for agricultural ammonia storage and shipment tanks, and there have been several instances of failure, some with lethal effects. The alloys which were tested and found to fail in ammonia environments are listed in Table 6-13. In the case of the carbon steels, the stress corrosion cracking tendency in ammonia is effectively controlled by maintaining 0.2% water in the ammonia.

6.3.1.4.4 Aluminum

Aluminum alloys were investigated for tubing material because of their ready availability and low cost. The alloys studied were Al3003, Al3003 Al clad, Al5052, and Al 6061.

In the late 1950's and 1960's, a number of power plant condensers were manufactured with aluminum tubes[31-33]. Virtually all aluminum-tubed condensers (most on fresh water sources) had corrosion problems with the aluminum tubes (primarily erosion, impingement, and pitting) and have been retubed with alloys other than aluminum.

The Marston Excellsior process is a relatively new process for protecting aluminum in seawater, having a success record approaching 15 years in overseas applications; but, unfortunately this record is not fully documented.

Aluminum alloys are quite susceptible to erosion[34-38]. Although Israel has built a number of desalination plants using Al 5052 tubing with apparently good results[39, 40], aluminum was not used in rapidly flowing seawater because of the concern of erosion. Aluminum has been primarily restricted to film evaporation and steam condensing applications[40].

Table 6-13
STEELS SUSCEPTIBLE TO STRESS CORROSION CRACKING IN LIQUID AMMONIA*

Carbon Steel	API X-60
Mild Steel	ASTM A202 Grade B
T-1 Steel	ASME Case 1056
AISI 4130	ASTM A516 Grade 70
API X-42	ASTM A285
API X-46	ASTM A517 Grade F
API X-52	

Four general guidelines should be followed for the use of steels in liquid ammonia.

1. O_2, N_2, and CO_2, (air) should be avoided. These contaminants have been specifically identified as contributing to stress corrosion cracking of steels.

2. Inasmuch as very low impurity levels are sufficient to cause cracking, the attainment of ammonia of sufficiently high purity to preclude cracking will be practically impossible. Therefore, the use of water at a minimum concentration of 0.2%, by weight, as an inhibitor for stress corrosion cracking is recommended. This concentration should, however, be kept close to 0.2% to avoid impairing the overall heat transfer performance.

3. High strength steels should be avoided.

4. High residual stresses and cold worked materials should be avoided.

*Carbon steels have been successfully used in ammonia service when the ammonia contains 0.2% water.

The general corrosion rate of many aluminum alloys in seawater is relatively low[30, 41-47]. General corrosion/erosion is expected to be approximately 2 to 3 mils per year in seawater flowing at 5 to 7 feet per second inside the heat exchanger tubes.

Aluminum alloys are very susceptible to aggressive attack from mercury, copper, and to a lesser extent, iron. Eliminating contact of mercury and copper on or near aluminum alloys is critical to the success of using aluminum. For this reason, care should be taken in the use of antifouling paints around the ship, since these paints can contain mercury or copper.

One of the most critical forms of corrosion of aluminum alloys in seawater is pitting or crevice attack[48, 49]. Pitting depths as great as 122 mils in approximately 3 years on Al 3003, 15 mils in 197 days for Al 3003 Alclad, and 77 mils in 3 years for Al 6061 are reported. This data is primarily from specimen evaporation and does not represent a large statistical sample. If large sample areas on actual test units are evaluated, pitting may prove even more critical.

Flowing seawater decreases pitting tendencies in aluminum alloys, although increased tube velocities can also cause increased erosion damage to the aluminum tubes.

Some aluminum alloys are susceptible to stress corrosion cracking in seawater[50]; but, the alloys selected appear to be immune[51].

Aluminum alloys are anodic to most common structural metals in seawater, so that aluminum becomes the corroding member in contact with these metals, often requiring electrical isolation.

Aluminum alloys show no ductile-to-brittle transition, and remain tough to -425°F[52-54].

The welding of aluminum, in thicknesses up to approximately 2.75 inches of the large spherical liquid natural gas (LNG) tanks, is well understood.

Close corrosion matches can generally be made by the high deposition gas metal arc welding (GMAW) process or the gas tungsten arc welding (GTAW) process[55-59].

Explosive cladding of aluminum alloys on carbon steel has been well established by the Dupont Company, and used by the Navy for joining steel to aluminum in ship superstructures[60].

Aluminum alloys for anhydrous ammonia service appears acceptable. No instances of stress corrosion cracking have been reported, and provided certain precautions are taken, the general corrosion resistance is good. If aluminum alloys are coupled to steels or nickel alloys in an ammonia environment, galvanic coupling leads to slow preferential anodic dissolution of the aluminum. Air appears necessary for this type of corrosion.

After analysis of the tubing alloys, Al5052 was selected as the most promising seawater aluminum tubing alloy. Correspondingly, plate alloys Al5083 and Al5086 should be used in conjunction with the selected aluminum tubing alloy.

6.3.1.4.5 Titanium

Titanium and its alloys exhibit excellent corrosion resistance in seawater, in many cases nearly complete immunity[15, 61-76].

Westinghouse built its first titanium-tubed desalination plant in 1965, (with additional plants built since then) and put into service its first titanium-tubed power plant condenser in 1975, without any reported tube corrosion to date. A large number of American and Japanese power plant condensers have successfully used titanium tubing.

Further evidence of the availability of titanium may be found in a report of power plant condenser tube failures published in March 1977[15]. Fourteen units tubed with titanium were studied, having an average operating service of approximately 14,000 hours. In these units, 22 tube sets had no tube failures, and 10 tube sets had a total of 48 tube failures from steam impingement, vibration, ane mechanical damage; one tube failure has not yet been explained.

Pitting corrosion[15, 63-76], stress corrosion cracking[15, 64, 69, 71, 72, 76], galvanic corrosion (titanium is normally the cathode in seawater couples with any constructional alloys)[16, 69, 77], and erosion[16, 69, 78, 79] will not cause distress to unalloyed titanium in the OTEC environment. No embrittlement caused by atomic hydrogen forming on titanium in seawater exposures with potential differences of -0.7 volt[16, 69, 78, 79] or greater, at ambient temperatures has been noted in either Westinghouse plant condensers, desalination plants, or found in the literature. Titanium remains tough to temperatures far below the OTEC working temperatures[52].

Unalloyed titanium welding is usually accomplished by the GTAW process, with filler metals essentially matching wrought metal chemistry and, consequently, producing welds with the same good corrosion resistance as the base metal[55, 56].

Tube welding is considered critical to the reliability of the OTEC heat exchangers. Evaluation of tube weld types (Table 6-14) normally used by Westinghouse determined that the flush weld joint is the choice for low cost, coupled with good reliability.

Tube plugs will be round titanium Gr.2 var stock in the shape of a thimble welded to the cladding using titanium filler metal.

Explosively applied titanium cladding has been well established by DuPont[80] and has been used on a number of Westinghouse desalination plant tubesheets. Reference (81) shows also that titanium explosively clad on carbon steel is satisfactory for surface condensers.

Table 6-14
TITANIUM TUBE-TO-TUBESHEET JOINT SELECTION

Joint Type	Leak Tightness Reliability*	Inspection Reliability*	Repair Reliability*	Erosion/ Corrosion Resistance Reliability*	Total Reliability	Relative Cost	Reliability Divided By Cost
Rolled	1	1	2	2	6	0.6	10.0
Double Tubesheet	2	1	2	3	8	6.3	1.3
Integrally Grooved Tubesheet	2	1	2	3	8	1.3	6.2
Explosive Bonded	3	1	2	3	8	5.0	1.6
Fillet Weld	3	3	3	3	12	1.5	8.0
Fillet Weld With Trepan	3	3	3	3	12	1.9	6.3
Added Ring	2	2	3	3	10	2.5	4.0
Recessed	3	2	3	3	11	1.1	10.0
Recessed and Chamfered	3	2	3	3	11	1.3	8.5
Flush Weld	3	2	3	3	11	1.0	11.0

* 1 = Poor, 2 = Fair, 3 = Good

For ammonia service, little data is available on titanium and its alloys. The data available indicates that titanium is very good from the general corrosion point of view, but there is no information with respect to stress corrosion cracking.

6.3.1.5 Material Recommendations

Materials for the OTEC power modules were selected for high reliability, commercial availability, and to allow use of currently viable manufacturing techniques at reasonable cost. Material selections are:

- Tubing - Unalloyed Titanium, ASME SB338, Gr2.
- Tubesheets - Titanium, ASME SB265, Gr1, explosively clad on carbon steel, ASME SA516, Gr70 with 20 foot pounds average Charpy "V" notch toughness at +10°F to ASTM A370, clad to DuPont Specification Deta 600M.
- Tube Welds - Flush, autogenously (GTAW without filler metal) welded
- Shells, Waterboxes, Pipe - Carbon steel, ASME SA516, Gr70 with, the same toughness requirements as for tubesheets. For seawater exposure, the carbon steel will be coated with neoprene sheet, and cathodically protected by wasting plates on impressed current cathodic protection systems.
- Tube Supports - Carbon steel, ASME SA283, GrC
- Seawater Valves - Carbon steel coated with an elastomer
- Ammonia Valves - Carbon steel
- Seawater Pumps - 316L stainless steel impeller, austenitic cast iron body

- Ammonia Pumps - Cast iron impeller, carbon steel shaft

- Turbine Rotor - Ni-Cr-Mo-V steel, similar to ASTM A470, C15

- Turbine Disc - Ni-Cr-Mo-V steel, similar to ASTM A471, C11

- Turbine Blades - Type 403 stainless steel, similar to ASTM A276, Type 403 (80 ksi minimum yield strength)

- Turbine Bolting - Carbon steel, ASME SA193, Gr B7 or B16

6.3.1.6 Current Westinghouse Test Program

Although considerable data is available on materials for service in anhydrous ammonia, most of it has been generated on alloys used for agricultural or refrigeration equipment. Only recently has attention been given to alloys which could be used in an ammonia-cycle turbine system, such as that proposed for OTEC. A review of the available literature on the subject[82-127] revealed that a reasonable background of data existed on some materials for heat exchanger construction. Therefore, this test program was designed to obtain data on alloys for use in the turbine, and on those alloys for use in heat exchanger construction for which little or no data exists in the literature.

- Environmental Testing

  The effects of O_2 and N_2 in ammonia on corrosion were being tested in environments typical of uncontaminated and contaminated ammonia.

- Galvanic Coupling Test

  Galvanic coupling tests were conducted on some of the critical dissimilar metal joints in the OTEC system to evaluate galvanic corrosion between adjacent materials.

The test results in metallurgical grade ammonia produced the following expected corrosion rates after 300-hour tests:

Carbon steel coupled to 12% Cr SS ∿ 0.15 mpy
Carbon steel coupled to 304 SS ∿ 0.13 mpy
Carbon steel coupled to Titanium ∿ 0.12 mpy
Carbon steel coupled to Aluminum ∿ 0.09 mpy

There also was no measurable galvanic current measured between the Linde enhancement or the titanium tube after 100 hours exposure.

- Slow Strain Rate Test

The slow strain rate test currently in progress has been shown by several research establishments to be a good rapid screening test for stress corrosion susceptibility. Its suitability for testing in ammonia environments has been demonstrated[128].

Slow strain rate tests in air and in metallurgical grade anhydrous ammonia, both with and without oxygen additions (to simulate air contamination), show that no susceptibility to stress corrosion cracking exists in the tested materials.

- Stress Corrosion Crack Propagation Test

Fracture mechanics testing, to determine if stress corrosion cracks propagate from existing defects in gaseous anhydrous ammonia, was conducted on rotor and rotating blading steels.

Tests on Ni-Cr-Mo-V and 403 SS in metallurgical grade ammonia for 2300 hours show no evidence for stress corrosion cracking.

- Corrosion Fatigue Test

  In this investigation, constant stress amplitude fatigue testing was used to establish the stress-number of cycles to failure (S-N) curves in pure ammonia for 403 stainless steel in four surface conditions, smooth versus notched, shot peened versus relief annealed, while Ni-Cr-Mo-V was tested only in the notched as-machined condition to simulate fabrication practice.

  S-N curves were prepared for the 403 SS and Ni-Cr-Mo-V specimens exposed to metallurgical grade ammonia in pure ammonia form and in ammonia contaminated with oxygen, water, and sea salt deposits to simulate actual turbine conditions. No obvious degradation in fatigue characteristics was noted in 10^7 cycles.

6.3.1.7 Union Carbine Evaluation of the Linde-Enhanced Aluminum Surface on Titanium Turbine

Union Carbide conducted a test on the Linde-enhanced aluminum surface on titanium tubing for a 45-day exposure in anhydrous ammonia "as received", and contaminated with 0.2% and 2.0% seawater contamination. No catastrophic effects were noted on either the aluminum coating or titanium substrate. However, some minor deterioration of coating adhesion was observed as the result of flattening tests, especially at the 2% seawater contamination levels.

6.3.2 Arrangement

Study of the 10 MWe Modular Application power system commenced in the preliminary design phase. However, the requirements and constraints followed in the conceptual design phase arrangement studies also governed the 10 MWe Modular Application plant studies. These were platform producibility, power plant adaptibility to various platform configurations, operating efficiency, and maintainability while providing necessary spacial relationships between components. Significant effort also was exercised to reduce unit platform volume and displacement, as compared with those characteristics of the 100 MWe conceptual design. (Figures 6-55 and 6-56).

The critical spacial relationships and limits identified early in the study, continued to be observed during the preliminary design of the 10 MWe system; they were:

- Elevation of heat exchanger tops above sea level to be limited to no more than 20 feet.

- Minimum elevation of ammonia drain tank and hotwell to be 20 feet above ammonia circulation pump and feed pump suctions.

- Water and ammonia piping to be sized for lowest practical velocities, lengths to be kept short, and turns to be minimized.

- Turbines to be installed with adequate exhaust diffusers discharging directly into condenser shells.

- Warm water inlets to be a minimum of 15 feet below the operating waterline.

- Hot and cold water circulation pumps to be installed with adequate discharge diffusers.

- Hot and cold water discharge piping to be directed downward.

A series of tentative arrangements was developed using heat exchanger dimensions. Parametric turbine-generator and pump dimensions based upon power or capacity levels were determined by the total system computer program and special considerations noted above. These arrangement studies culminated in the configuration shown in Figure 1-6 and in Figures 6-57 through 6-60. The principal features of the selected preliminary arrangement for the 10 MWe Modular Application power system are:

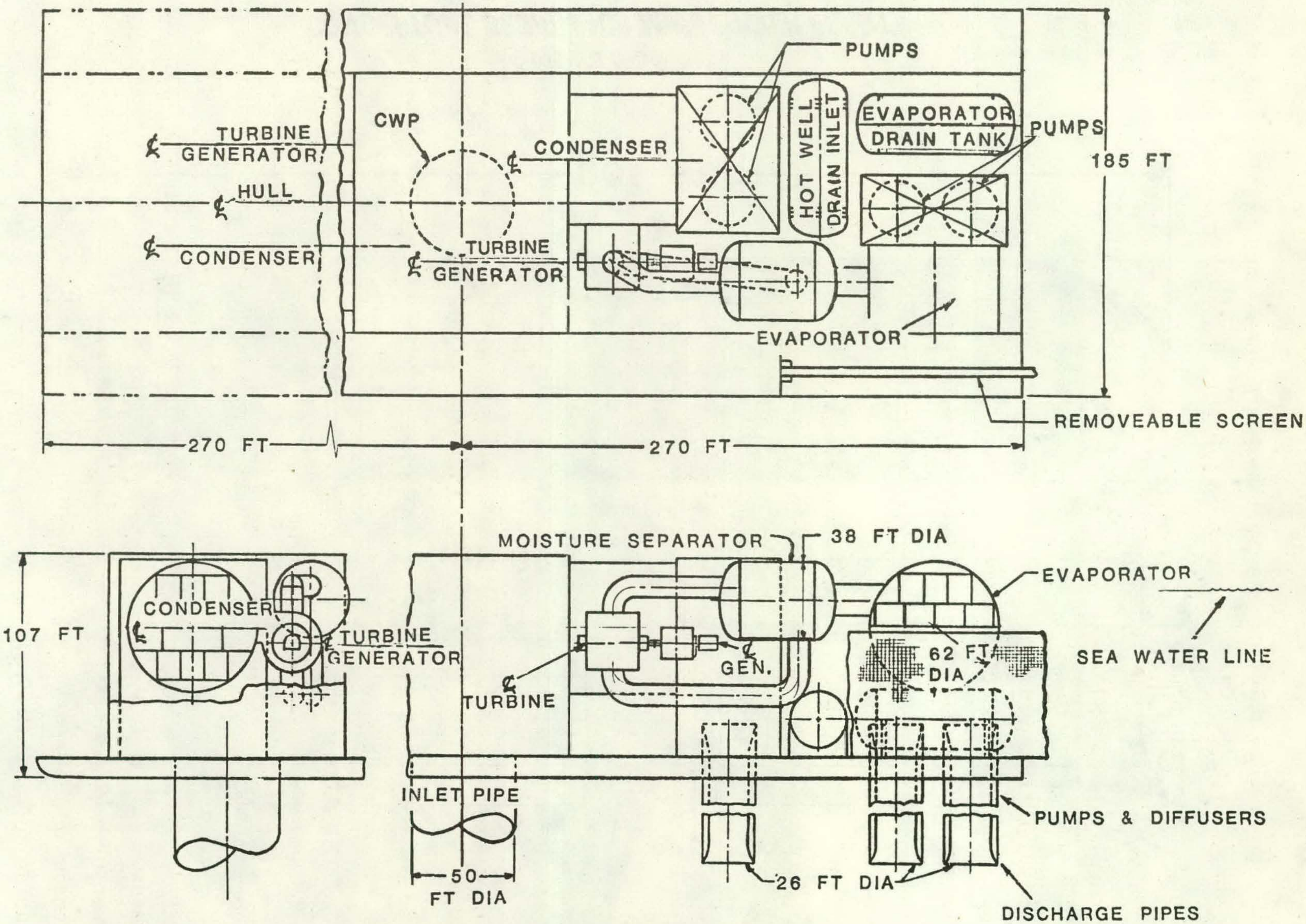

Figure 6-55
CONCEPTUAL DESIGN 50 MWe MODULE

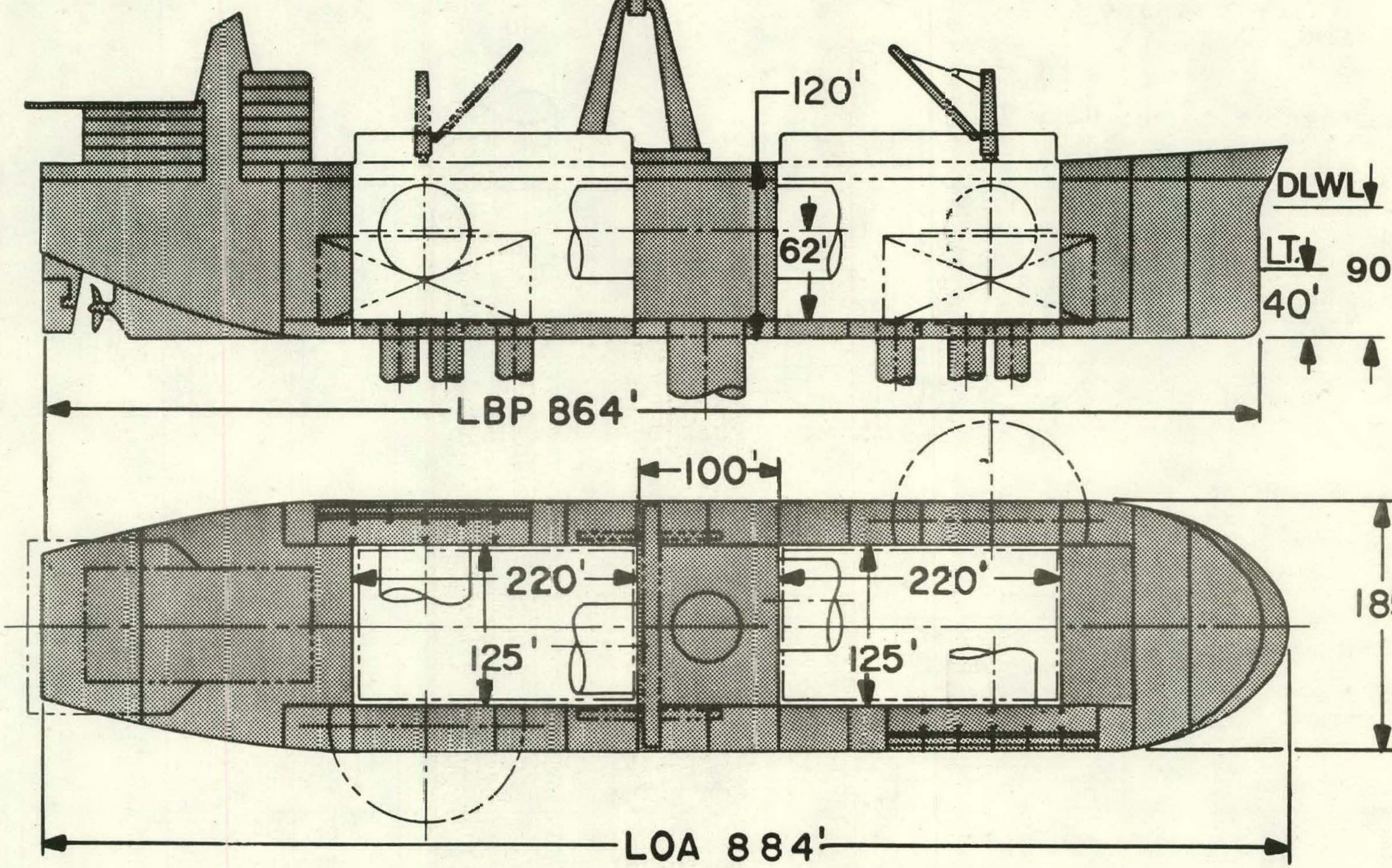

Figure 6-56
CONCEPTUAL DESIGN 100 MWe POWER PLANT

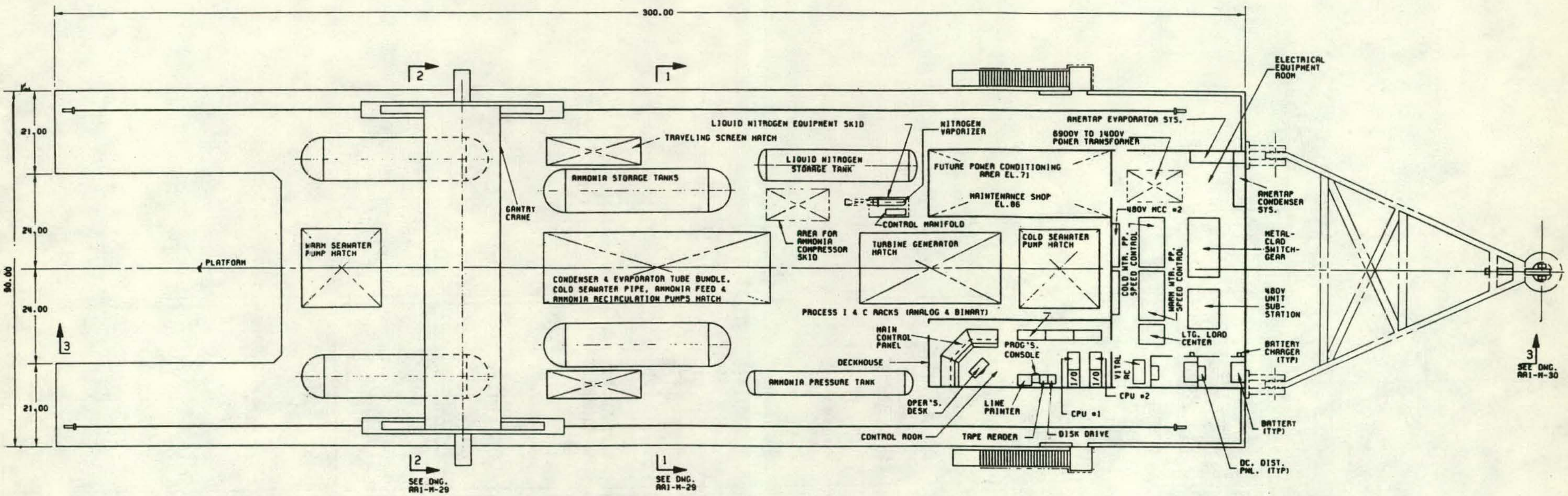

Figure 6-57

GENERAL ARRANGEMENT PLANT - ELEVATION 71

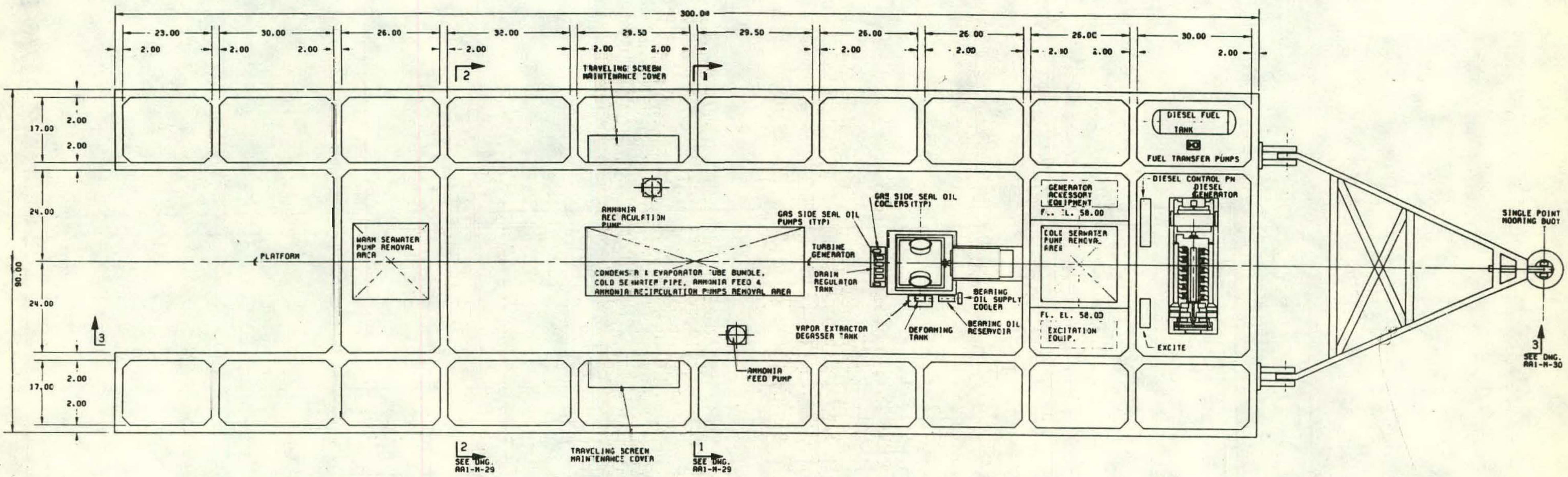

Figure 6-58

GENERAL ARRANGEMENT PLAN - ELEVATION 45

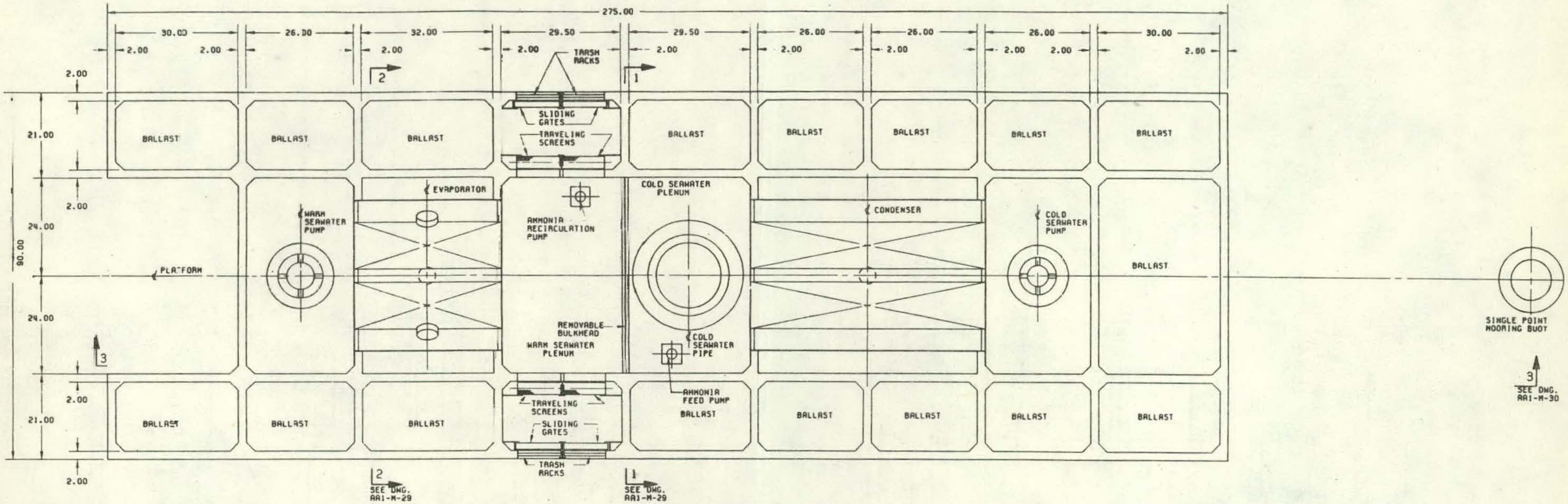

Figure 6-59

GENERAL ARRANGEMENT PLAN - ELEVATION 21

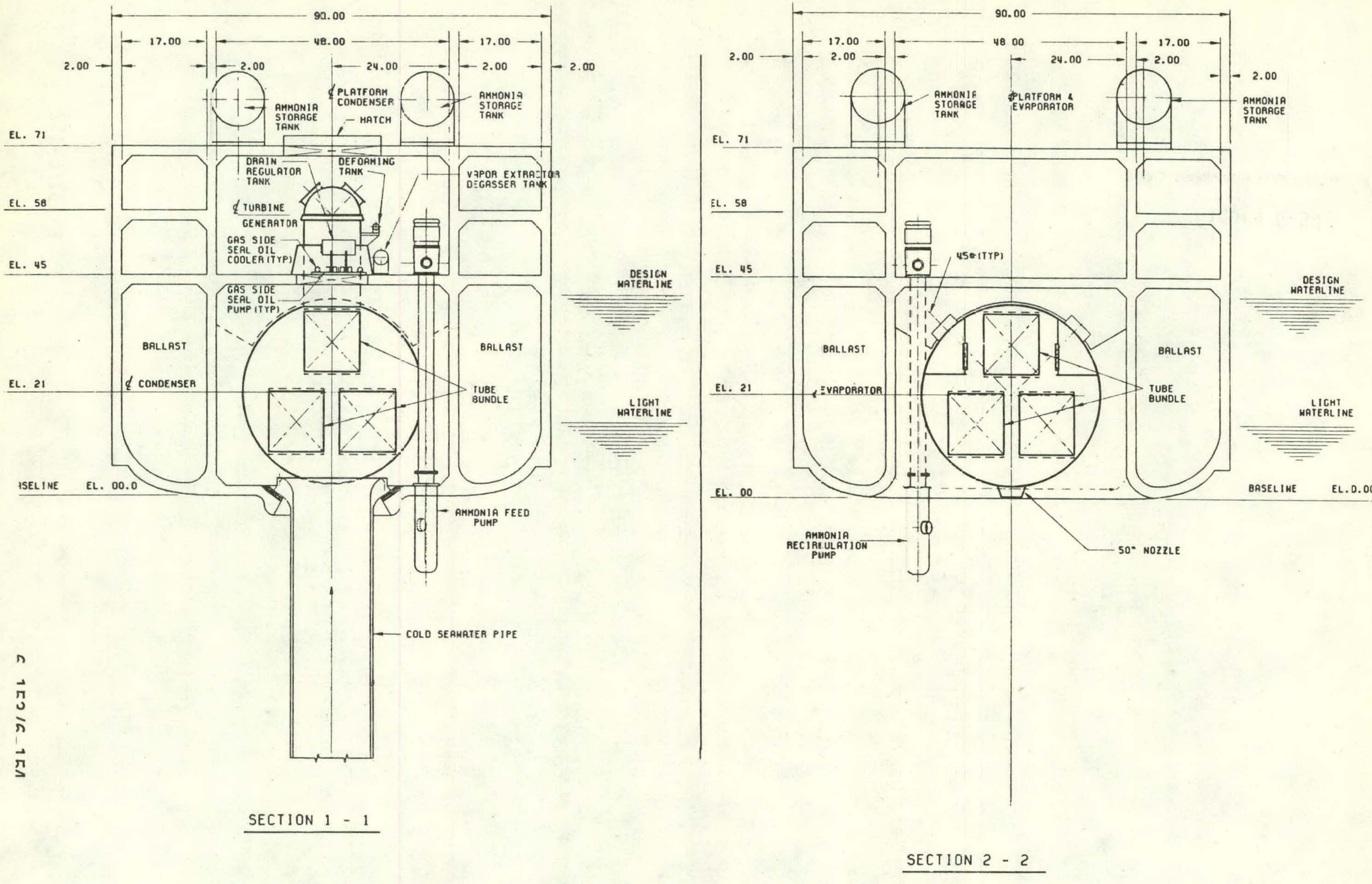

Figure 6-60

GENERAL ARRANGEMENT - SECTION 1-1 AND 2-2

- Linear arrangement of cold water discharge plenum, condenser, cold water inlet plenum, warm water inlet plenum, evaporator, and warm water discharge plenum

- Turbine generator mounted above the condenser with its exhaust diffuser discharging directly into the condenser shell

- Relatively short direct runs for all principal ammonia vapor and liquid piping

- Direct introduction of warm water into the evaporator and cold water into the condenser; and compact discharge plenums directly over the seawater pumps

- Incorporation of the hotwell within the condenser shell, and the moisture separators and excess evaporator liquid storage within the evaporator shell to minimize piping runs between components

- Arrangement of heat exchangers so that their shells contribute to platform buoyancy

- External location of seawater circulation pumps and their diffusers and ammonia feed and recirculation pumps

- Tube bundle pull-out space in the adjacent seawater inlet plenums without volumetric penalty to the design

- Unobstructed vertical access to all major components or component elements from a gantry crane

- Gates or temporary closures for all major hull penetrations

Using fluid flow rates generated by the system design program, and commonly accepted values for fluid velocities, all major ammonia piping and seawater ducting were sized and laid out on the arrangement plans. The seawater ducting is an integral part of the platform structure as indicated in the general arrangment plans. The configuration and dimensions of all major ammonia system piping runs are illustrated in Figures 6-61 through 6-65.

Weight and stability estimates were made for the 10 MWe power system. Although the power module itself can be housed in a platform only 52 feet wide, the stability estimates indicate that a minimum platform beam of approximately 90 feet is necessary to ensure adequate stability under all loading conditions. Hence the provision of "ballast" or wing tanks. Table 6-15 summarizes the estimated weights of the power plant and steel and concrete platforms. At just under 9500 tons light-ship displacement (e.g. the ship complete but without liquid loading, crew, stores, etc.), the steel platform draft of 19 feet leaves ample margin for negotiating normal channels with all machinery installed except the seawater pumps. At just over 21,300 tons light ship displacement, the concrete platform draft of 37.5 feet is a problem for all but the deepest channels. Close liaison is required between platform designers and power plant designers during future design efforts to ensure that all stability, buoyancy, and draft requirements or limitations are properly met in the final design.

To gauge the effectiveness with which space is utilized in the selected 10 MWe system arrangements, both the cubic feet of enclosed plant volume per kw and the tons of total system full load displacement per MWe were estimated. Volumetric and weight estimates are summarized along with estimates of cost in $ per kw in Table 6-16. The "Preliminary Design Platform" is the platform with wing tanks for stability. The "Minimum Platform" is the platform with just enough beam to house the power plant, and just sufficient length so that total displacement is no more than that required to lift the power plant and its platform at desired operating draft. Similar data also is shown for a 50 MWe module. The latter two sets of estimates are applicable to power plants made up of multiple modules (40 to 400 MWe).

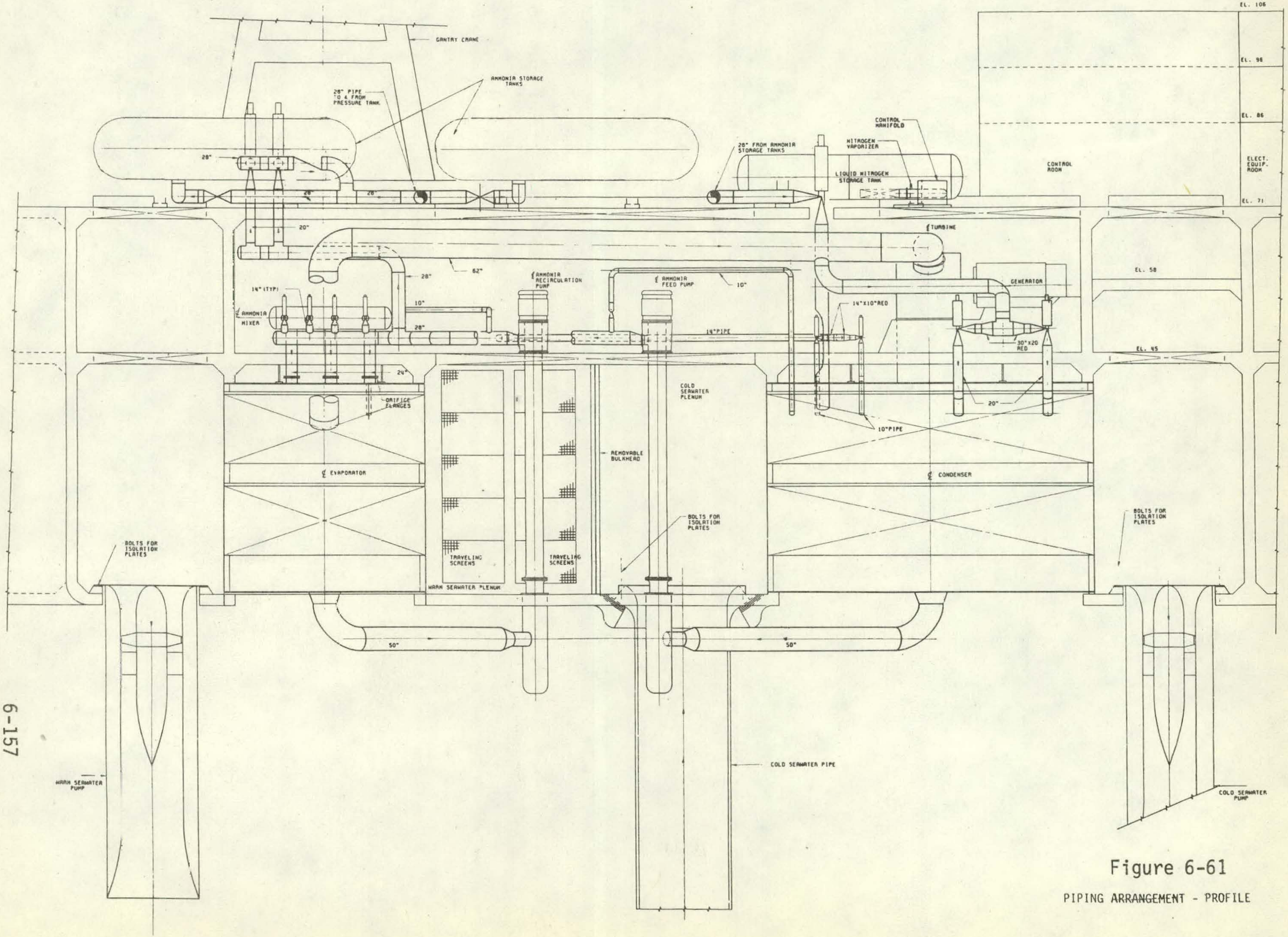

Figure 6-61

PIPING ARRANGEMENT - PROFILE

THIS PAGE

WAS INTENTIONALLY

LEFT BLANK

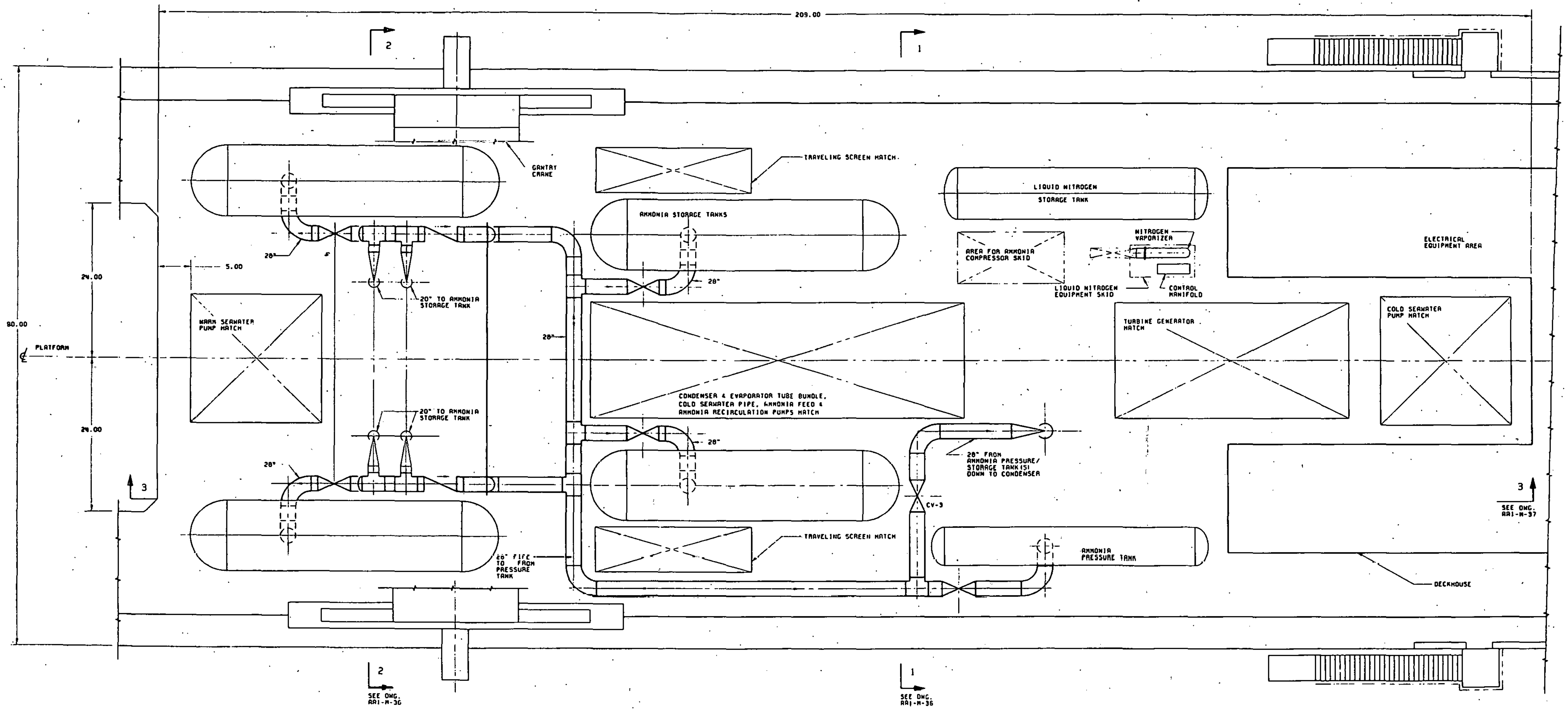

Figure 6-62

PIPING ARRANGEMENT - ELEVATION 71

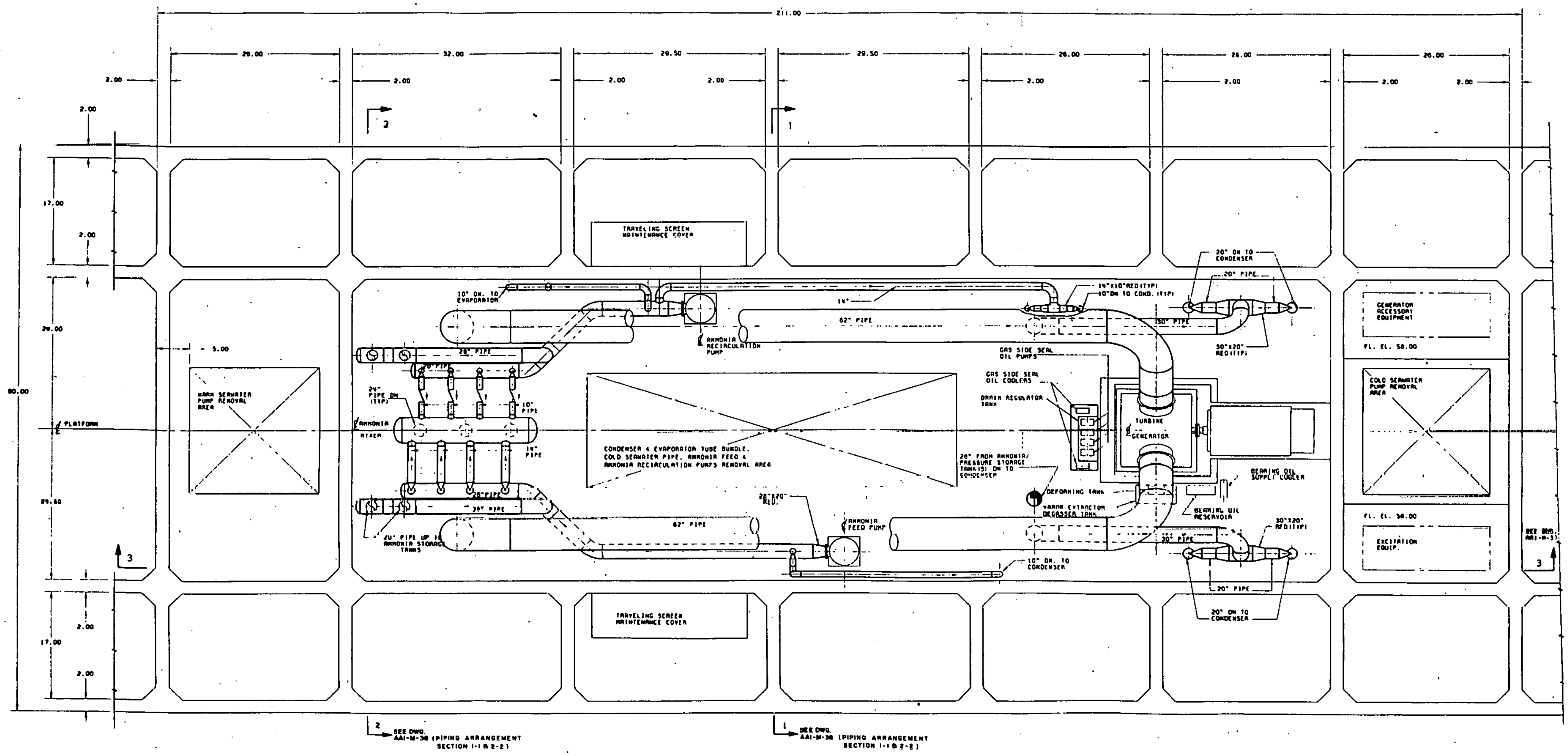

Figure 6-63

PIPING ARRANGEMENT - ELEVATION 45

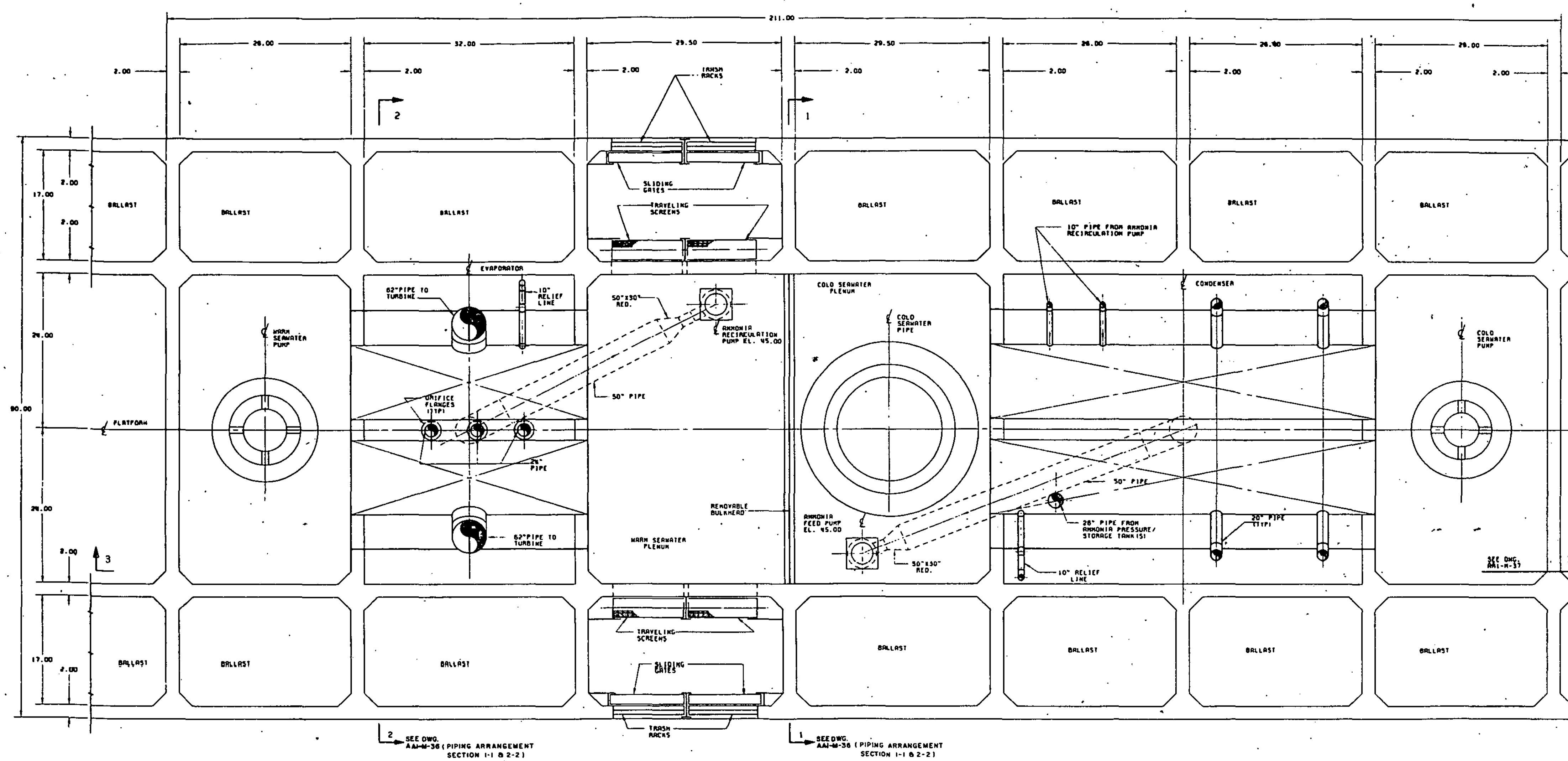

Figure 6-64

PIPING ARRANGEMENT - ELEVATION 21

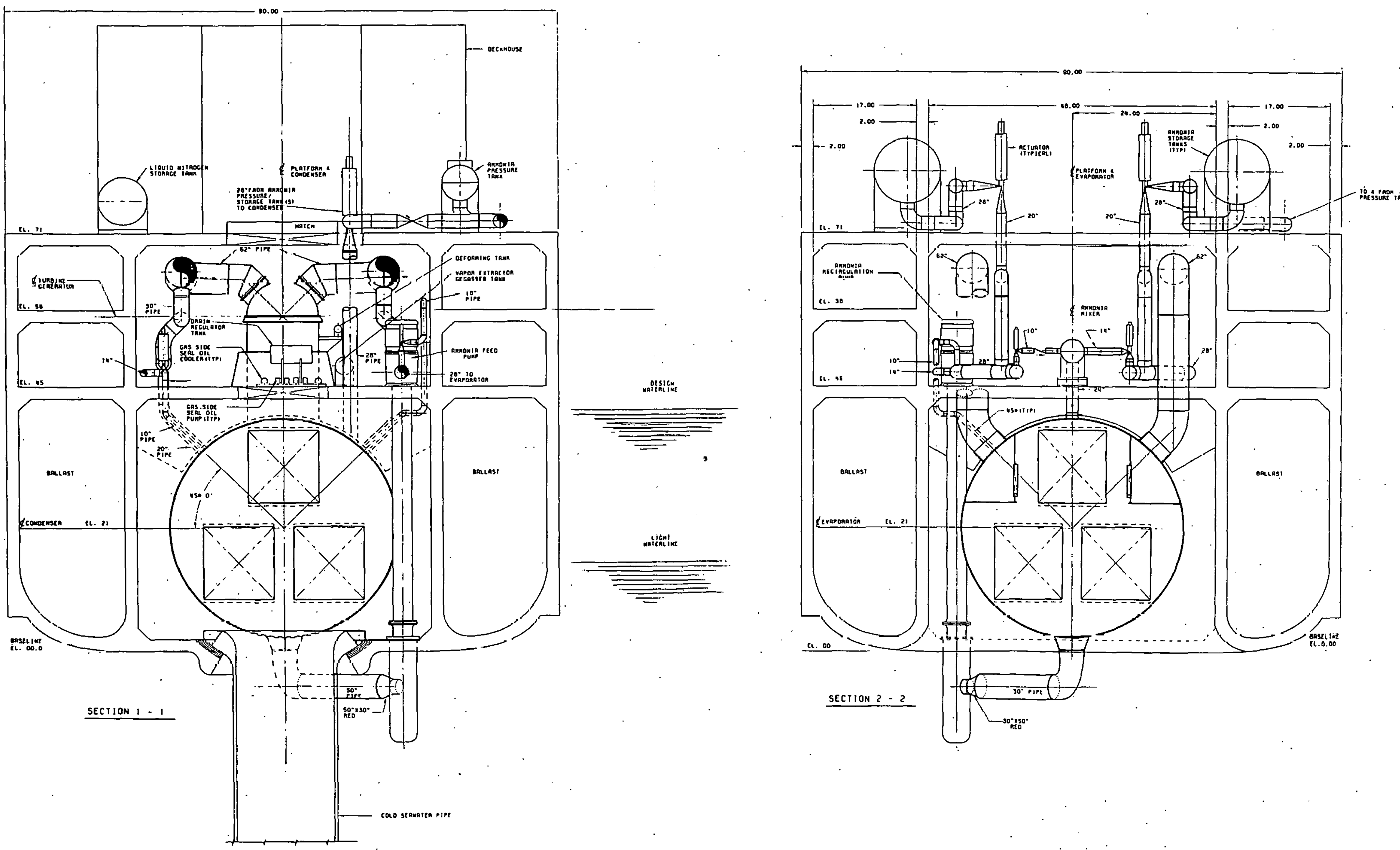

Figure 6-65

PIPING ARRANGEMENT - SECTION 1-1 AND 2-2

Table 6-15
10 MWe MODULAR APPLICATION POWER SYSTEM WEIGHT SUMMARIES

Power Plant	Steel Platform		Concrete Platform	
Heat Exchangers	817.8	tons		
Power Generation System	80.8			
Ammonia System Components	142.2			
Ammonia System Piping	97.7		Do	
Ammonia System Valves	106.4			
Seawater System	250.7			
Auxiliary and Sup. Systems	212.7			
Electric Distribution and Cond. System	130.8			
Sub-Total	1839.1	tons	1839.1	tons
Platform	5783.0		16563.0	
Deckhouse	257.0		257.0	
Outfit	735.0		735.0	
Margin (10%)	861.4		1939.4	
Total Light Ship	9475.5	tons	21333.5	tons
Seawater	8413.0		8413.0	
Ammonia	217.0		217.0	
Nitrogen	26.5		26.5	
Full Load	18132.0	tons	29990.0	tons
Displacement @ 44' WL	25500.0	tons	--	
Ballast Required	7368.0	tons	--	
Draft @ 30000 tons Displacement	--		51'	
Light Ship Draft	19'		37.5'	

Table 6-16
PACKING FACTOR AND COST DATA

Platform	Tons Δ / MW	Ft^3* / kw	Platform $ / kw
Conceptual Design 100 MWe Platform			
Steel Construction	3140	107	1109
Preliminary Design Platform			
Steel Construction	2550	89	1029
Concrete Construction	2999	89	602
Minimum Platform 10 MWe Module			
Steel Construction	1497	89	514.5
Concrete Construction	2714	89	546
Minimum Platform 50 MWe Module			
Steel Construction	1211	55	428
Concrete Construction	2257	55	466

*Platform volume required to provide bouyancy to lift total system, and/or to meet stability requirements.

6.3.3 System Control

6.3.3.1 Design Approach

Conceptual design studies of four proposed configurations for controlling an OTEC Power Cycle Module were made before a configuration was selected. Operating control requirements for the power system were first identified: from initial startup, to full load, and back down to system shutdown. Each configuration was evaluated as to its capability to meet these operating requirements and to satisfy safety, reliability, minimum flow loss, and cost considerations -- in that order of priority.

The design requirements for each of the control functions listed below were evaluated.

- Initial purging of air and N_2.
- On-line purging of non-condensible (air and N_2) gases.
- Start-up of system.
- Synchronization to electrical grid.
- Turbine speed and load control.
- Liquid level control of condenser and evaporator hotwells.
- On-line testing of valves.
- Emergency trip situations.
- Shut-down of system.
- Purging of NH_3 from power loop.
- "Fault Tree" analysis of system components.
- Scheduled and unscheduled maintenance.
- Environmental and safety considerations.

One of the objectives of the 10 MWe power module is to verify its control configuration before committing it to the larger 50 MWe power module. Therefore, the same control configuration was selected for both configurations. Similarity between the two power systems differs only in the size of the power loop components, scaled to accommodate the differences between design flow ratings at the same pressure and temperature levels.

This configuration features relatively stable system flow conditions during control transients at the expense of system efficiency (due to the losses across the turbine inlet valves at full rated flow). A total pressure drop across the inlet valves of 2.5% to 4.0% of the total available pressure drop across the turbine is estimated -- depending upon redundancy requirements.

A comparative analysis of all four configurations studied is presented in Section 6.3.3.3.

6.3.3.2 Control Requirements for Turbine Speed and Load

The control requirements for the turbine-generator are a function of the electrical load utilization. Modules are to be capable of providing AC power output. Turbine speed must be synchronized with the electrical frequency of either the station bus or the land-based grid before tie-in to minimize short circuit torque excursions. Synchronous speed regulation, under load, is required after tie-in to either system. If the AC power output is inverted and connected to the land-based grid by a DC cable, synchronous speed and base load regulation of modules could be very loose. In addition, a module should be capable of shedding load during valve testing operations and when removing load from the land-based grid.

To meet the above considerations, the turbine control system should be capable of: controlling speed, to synchronize when connecting to the A C bus; controlling load when operating at base load and at part load conditions; regulating synchronous speed when tied to a common grid; and shedding load when testing valves. For such requirements, conventional land-based turbine generator control systems must meet load frequency responses in the order of 2-5 Hz for phase angle lags of 90^0 and governor speed regulation of 2-5% of rated speed when controlling synchronous speed. It was necessary that these same control responses apply here -- except when connected to the land-based grid through a DC cable.

Because of temperature variations of the warm seawater passing through the evaporator and the gradual fouling of the heat exchanger tubes, heat transfer characteristics change with time. If the module is controlling at part-load demand, the control system should be capable of accommodating variations in energy input levels by adjusting to maintain constant electrical output load. If the module is controlling at base-load demand, the effect of fouling or reduction in warm seawater temperature would be to reduce base-load output; but, the control system must still be capable of adjusting power loop to the new steady-state flow conditions. If warm seawater temperature levels increase while operating at base-load conditions, maximum load output would be desired. Output could be increased by utilizing excess capacity in the NH_3 liquid pumps to increase vapor production in the evaporator, which in turn results in an increase in turbine flow. The control system should be capable of regulating the liquid ammonia pumps and other system components to exploit this situation.

Calculations of thermodynamic terminal speed indicate that if the electrical load was suddenly interrupted, the turbine would exceed 100% overspeed if turbine flow is not interrupted. Turbine overspeed protection is, therefore, required for this situation. One method to meet this requirement is to have the control system components quickly reduce the turbine inlet flow, thus limiting rotor overspeed to a value that can be handled in the turbine and generator design phases.

Some situations in which electrical load would be suddenly interrupted are:

- While connected to land-based grid, if partial grid load is lost and the proper switching of load to other generating units does not take place promptly, the OTEC system would be overloaded. This overload would disconnect the OTEC system from the land-based grid.

- Any short-circuit fault in OTEC network or in cable connecting to land-based grid would interrupt electrical load.

If certain system components fail, turbine flow should also be quickly interrupted to prevent system damage. Some system malfunctions which would require interruption of turbine flow are:

- Loss of turbine or generator bearing oil
- Excess turbine or generator bearing temperatures
- Excessive rotor vibration
- Loss of generator field excitation
- Loss of gland sealing systems
- Loss of electrical power to control system
- Malfunction of turbine flow control valves
- Malfunction of computer software in control system
- Loss of control oil
- Ammonia leakage

6.3.3.3 Candidate Control Configurations

A comparative design analysis of candidate control configurations was made to confirm the control configuration selected for the preliminary design of the 10 MWe power system.

The selection of the control configuration is significantly influenced by the sizes and operating requirements imposed upon its valving configurations. Therefore, this analysis was based upon the more stringent requirements of the larger 50 MWe size.

Figure 6-66 shows the four basic candidate configurations for controlling the ammonia flows in the power loop. The configuration selected for the preliminary design uses turbine bypass valves only to control the vapor flow through the turbine. The valving used to control the liquid NH_3 feed and recirculating flows into the evaporator is the same for all four configurations shown. The design considerations, advantages, and

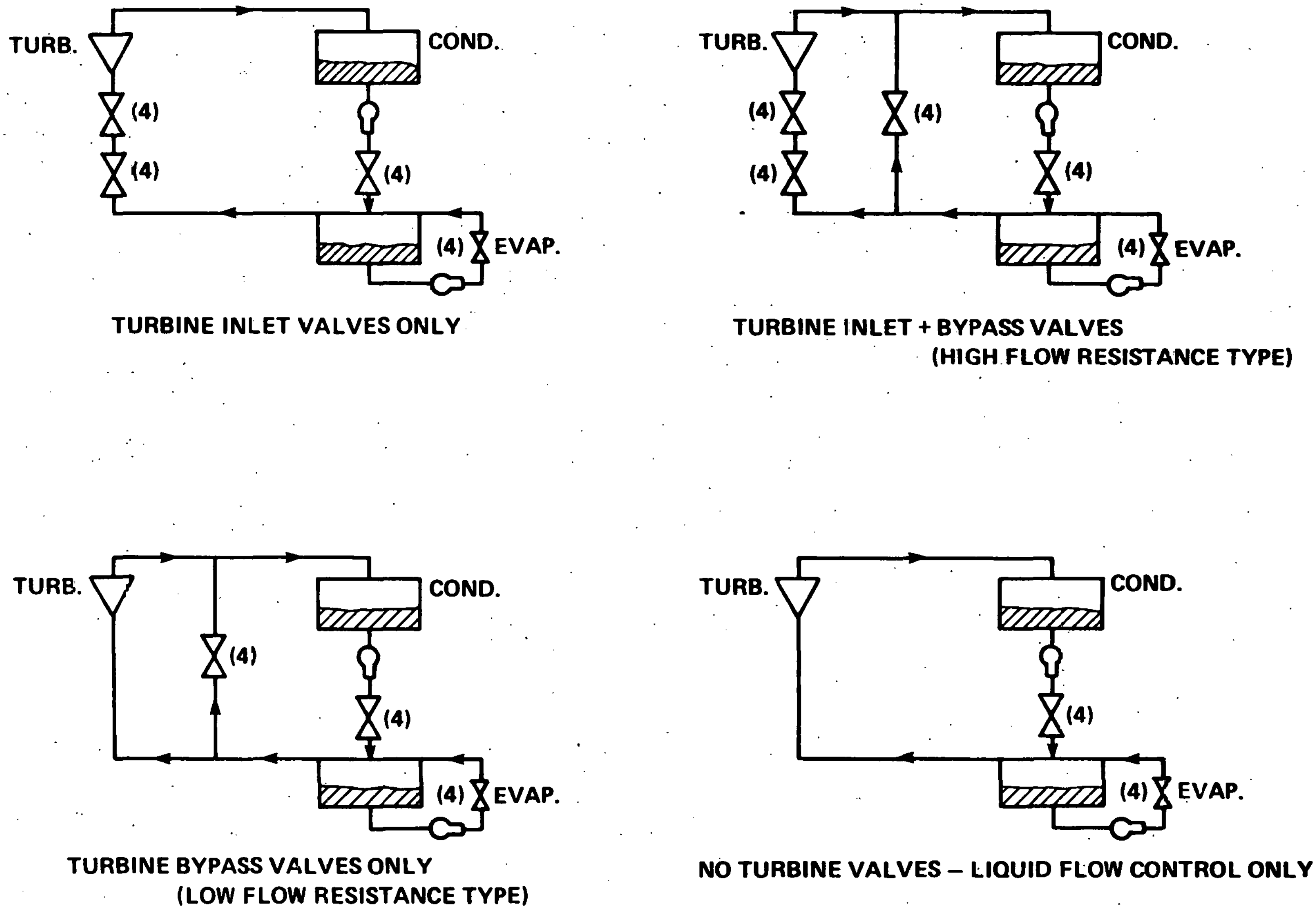

Figure 6-66
CANDIDATE CONTROL CONFIGURATIONS

disadvantages for each of the candidate configurations is summarized as follows:

Figure 6-67 shows a tabulation of the significant characteristics used to judge the adequacy of the proposed control configurations. Based on the previous design considerations, each of the configurations is rated as to its relative capability to meet each of these characteristics. The results indicate that the configuration in which only turbine bypass valves are used to control turbine vapor flow is the optimum configuration. This is the configuration selected for the preliminary design for both the 10 MWe and 50 MWe power modules.

Advantages

- Favorable space arrangement of turbine inlet piping.
- Elimination of inlet valves allows oversize turbine inlet piping diameters. Negligible vapor flow loss between evaporator and turbine.
- Control configuration meets utility standards for turbine speed and load control response.
- Control configuration provides adequate and redundant turbine overspeed protection.
- Valve configurations selected have good flow vibration resistance characteristics.
- Plug-type configurations can be fitted with a mechanical bellows seal arrangement, between the valve stem and guide bushing, to provide a zero stem leakage characteristic.

Disadvantages

- Requires a non-conventional 50% overspeed capability for the turbine and generator rotors.
- Requires tight control of the liquid NH_3 flow rates into the evaporator.

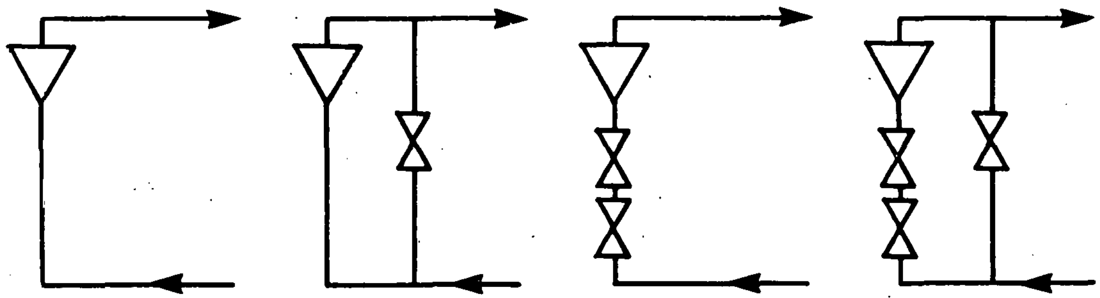

STARTUP/SHUTDOWN CONTROL STABILITY	POOR	GOOD	POOR	EXC.
FLOW CONTROL	UNACC.	GOOD	EXC.	EXC.
PRESSURE LOSS	EXC.	EXC.	POOR	POOR
RESPONSE TIME	POOR	GOOD	GOOD	GOOD
OVERSPEED PROTECTION	UNACC.	GOOD	EXC.	EXC.
REDUNDANCY	POOR	GOOD	GOOD	GOOD
VIBRATION	GOOD	GOOD	POOR	POOR
SEALS TO ATMOSPHERE	GOOD	GOOD	POOR	POOR
SPACING ARR'G'T	GOOD	GOOD	POOR	POOR

Figure 6-67
VALVE CONFIGURATION EVALUATION

6.3.3.4 Computer Simulations of Power System

Computer simulations of the power system shown in Figure 6-68 were made. Two computer programs were designed. One simulates the steady-state off-design system characteristics. The other simulates the static and dynamic response characteristics of the system: before and after sudden reduction of turbine flow, during emergency trip situations, and throughout transient flow conditions during the controlling operations. These computer system simulations were developed to provide a design tool to understand and verify the characteristic system responses to control operations of the proposed preliminary design configuration. The computer programs are described in Sections 6.5.2 and 6.5.3.

6.3.4 Availability

The objective of the availability assessment efforts was to consider supplier data, existing field history literature, and interviews with designers to arrive at a prediction for the 10 MWe system availability. To compute the system availability, an estimate of the unscheduled and scheduled outage times for all of the major components and subsystems were obtained.

In particular, the analysis began by estimating the amount of time required to shut down and start up the system, since this function is required for every outage. To do this, the control sequence was followed step by step through each of these operations with allowances made for operator and automatic actions. The shutdown/startup time estimates include time estimates for purging the system of ammonia and filling it with nitrogen or air because this step is required for access to internal parts of the system. Table 6-17 summarizes the findings of this phase of analysis.

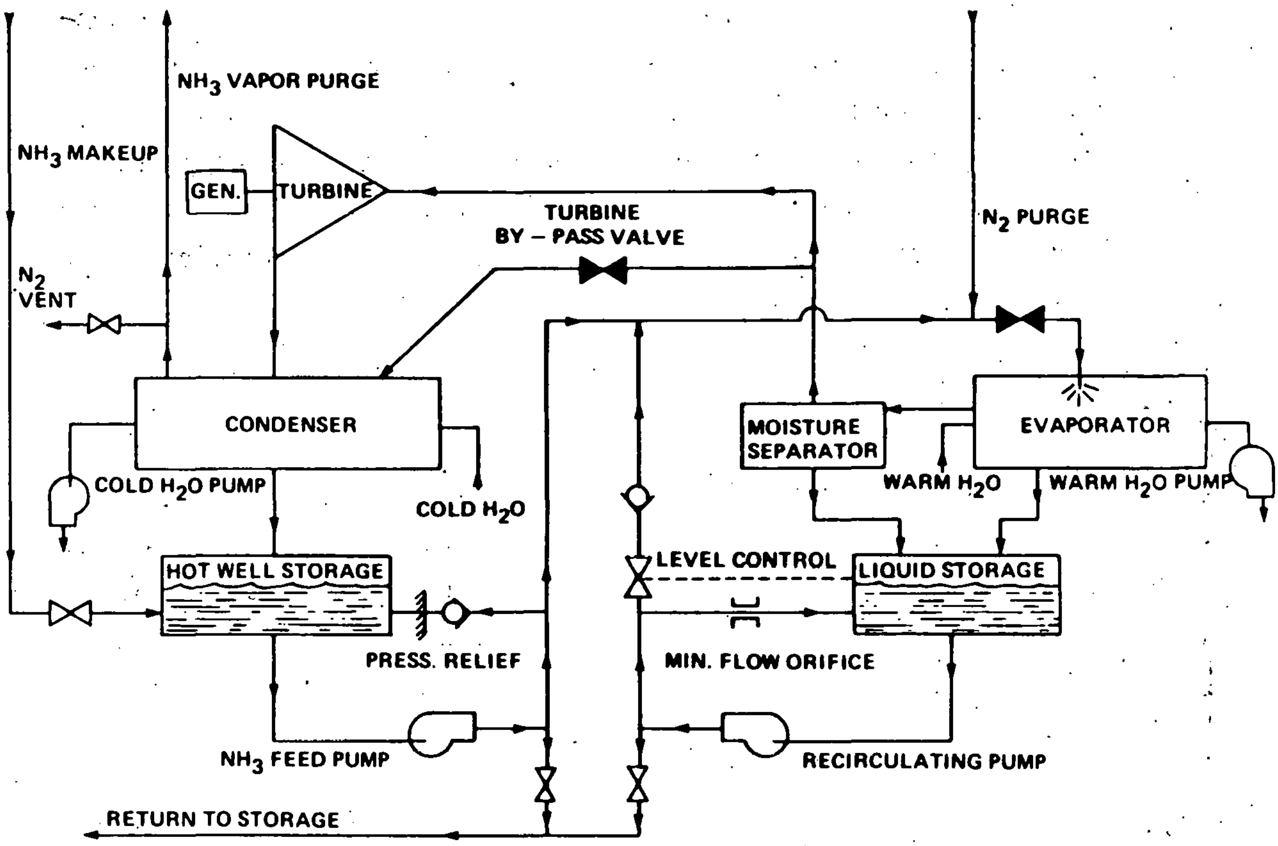

Figure 6-68
PRIMARY POWER SYSTEM

Table 6-17
SHUTDOWN/START-UP TIME ESTIMATE SUMMARY

Task	Time
Basic Shutdown	1.15 hours
NH_3 Vapor Purge	3.4 hours
Air-N_2 Purge	27.0 hours
Basic Startup	5.0 hours
TOTAL	36.55 hours

Equipment mean times between failures (MTBF) and mean times to repair (MTTR) were also estimated. These numbers apply to unscheduled outages. In addition, estimates were made for scheduled outage frequency and duration. The results of these investigations are presented in Table 6-18 and Figure 6-69. To make all of these estimates, task times and maintenance concepts were developed, field histories of similar equipment were examined, and design engineers were interviewed. The specifics of maintenance considerations and maintenance labor costs are dealt with in Sections 6.5.4 and 6.7.2, respectively.

One specific topic relating to the heat exchangers is tube leakage. This is an area of concern which is often thought of because of the large heat exchangers used in OTEC plants. The subject is dealt with in the demonstration plant availability Section 7.3.4 because there are approximately five times as many tubes in the heat exchangers for that system as for the 10 MWe system.

A summary of major availability parameters is given in Table 6-19.

Table 6-18
RAM SUMMARY FOR MAJOR COMPONENTS
10 MWe POWER MODULE

Major Component	Forced Outages		Scheduled Outages	
	MTBF	MTTR	Time Between Scheduled Outages	Scheduled Outage Time Each
1. Evaporator	15,554 hrs.	88 hrs.	8,678 hrs. (1)	88 hrs.
2. Condenser	15,554 hrs.	88 hrs.		
3. Turbine	7,077 hrs.	117 hrs.	42,953 hrs. (2)	877 hrs.
4. Generator	9,548 hrs.	67 hrs.		
5. Warm Sea Water Pump	25,320 hrs.	89 hrs.	8,683 hrs.	89 hrs.
6. Cold Sea Water Pump	25,320 hrs.	89 hrs.	8,683 hrs.	89 hrs.
7. Ammonia Feed Pump	26,280 hrs.	45 hrs.	8,721 hrs.	45 hrs.
8. Ammonia Circulate Pump	26,280 hrs.	45 hrs.	8,721 hrs.	45 hrs.
9. Power Loop Valves	70,128 hrs.	45 hrs.	None Required	0 hrs.
10. System Auxiliary and Control Components	669 hrs.	10 hrs.	8,721 hrs.	45 hrs.

(1) Scheduled maintenance performed on evaporator and condenser simultaneously.

(2) Scheduled maintenance performed on turbine and generator simultaneously.

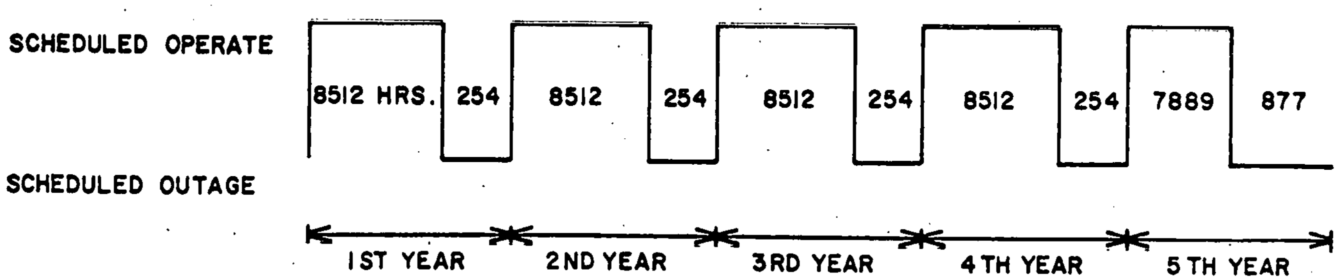

Figure 6-69
FIVE-YEAR SCHEDULED OUTAGE CYCLE

Table 6-19
RELIABILITY-AVAILABILITY-MAINTAINABILITY (RAM) CHARACTERISTICS OF 10 MWe MODULAR APPLICATION POWER MODULE

Item	Ram Parameters	Characteristics
1	Mean-time-between-failures (i.e. forced outages) of 10 MWe Module	491 Hrs.
2	Mean-time to repair forced outages	30 Hrs.
3	Maximum mean time to repair forced outages	117 Hrs.
4	Frequency of scheduled outages for maintenance	1 per Year
5	Average annual outage time per scheduled maintenance action	379 Hrs.
6	Maximum outage time for scheduled maintenance action (once every 5 years)	877 Hrs.
7	Availability of 10 MWe considering forced outages only	94.2%
8	Availability of 10 MWe considering scheduled outages only	95.7%
9	Availability of 10 MWe considering both scheduled and forced outages	90.1%
10	Startability of 10 MWe Power Module	95.5%

6.3.5 Safety

Floating platforms, electric power generation plants and ammonia plants are each, by themselves, not unique, and can be fabricated, tested, operated and maintained safely. It is the combination of these systems and subsystems, and the quantities and masses involved in a remote ocean environment that is unique and that is addressed in the system safety review.

The underlying feature in the OTEC concept which represents the greatest potential for a mishap is the anhydrous ammonia system. Thus, the main effort during this phase was directed to the NH_3 system, where the key safety issues are toxicity, corrosiveness and flammability.

With respect to toxicity, skin contacts with the liquid or high concentrations of vapor (approximately 500-1000 ppm) can produce burns and blisters similar to those received from much higher temperatures. Excessive inhalation of NH_3 vapors may cause severe damage to the lungs or even suffocation; however, expensive or sophisticated detection systems are not usually needed to warn of its presence because the pungent odor is readily detectible at low concentrations (50 ppm or less), which is far below hazardous levels for short-term exposures.

Corrosiveness in the presence of water is another key safety issue requiring special attention to design detail. Materials selection for this system is dealt with in component design and material compatibility sections of this report.

Flammability of ammonia does not present the same degree of risk as toxicity or corrosiveness. It is only flammable in the range of 16 to 25 percent in air and requires an ignition temperature of over 1200°F. The possibility of ignition by static electric discharge is remote because ammonia is a conductive gas, thus dissipating any build-up of charges. System bonding, to ensure good electrical conductivity, is called for in design to further reduce the risk. A review of accident reports filed on NH_3 does not contain any records of fires as the cause of a mishap.

Two codes researched for this report are:

- Safety Requirements for the Storage and Handling of Anhydrous Ammonia - American National Standard, ANSI K 61.1.
- Code of Federal Regulations, Title 46, Shipping.

Except for pressure vessel design, no modifications to the existing power system design are suggested by these codes. In the case of pressure vessel design, there will need to be a resolution of an apparent conflict between the application of ASME Boiler and Pressure Vessel Code Section VIII, Division 1 and subpart 5820 of title 46 in order to select the design pressure for tube and shell wall thickness calculations.

6.3.6 Plant Statistics Summary

Heat exchanger design data for the 10 MWe power module is given in Table 6-20. Rotating machinery design data is given in Table 6-21. A weight summary for the power module is shown in Table 6-22. Performance data for the Modular Application is given in Section 6.5.1.

6.4 Manufacturing and Installation

6.4.1 Heat Exchangers

Preliminary studies were made of the manufacturing processes and sequences required to fabricate and assemble both single bundle and modular-type heat exchangers. These studies were used to determine construction feasibility as a basis for preparing cost estimates. As indicated in the following discussion, the studies clearly illustrate the superior producibility and economy of the modular design for heat exchangers.

Shell plates for the two heat exchangers will be prepared for welding and shaped to the proper radius. Shell plates will be fitted using assembly fixtures (spiders) to establish and maintain circularity. The shells,

Table 6-20
HEAT EXCHANGES DESIGN DATA (10 MWe)

	Condenser	Evaporator
External Design Pressure (PSIG)	0	0
Internal Design Pressure (PSIG)	150	150
Tube Material	Titanium	Titanium
Tube O.D. (inches)	1.0	1.0
Tube Wall Thickness (inches)	0.028	0.028
Tube Length (ft)	56.5	34.7
Surface Area (ft^2)	623,007	382,786
Number of Tubes	42150	42107
Number of Modular Bundles	3	3
Shell Material	C-Steel	C-Steel
Shell Diameter (ft)	37	37
Shell Thickness (in)	2.0	2.0
Weight of Bundles (lb)	503,000	318,000
Weight of Shell (lb)	613,000	398,000
Dry Weight (lb)	1,116,000	716,000
Weight of Ammonia (lb)	142,000	211,000
Weight of Seawater (lb)	741,000	455,000
Operating Weight (lb)	1,999,000	1,382,000

Table 6-21
ROTATING MACHINERY
(per Baseline Module of 10 MWe (net))

ITEM	NUMBER	TYPE	RPM	HORSEPOWER	EFFICIENCY	COMMENTS
Turbine and Diffuser	1	Double Flow	3600	20142	0.827	All horespower values are shaft horsepower at Design Point.
Generator	1	Synchr.	3600	19437	9.967	
Warm Water Pump	2	Axial Flow	60.1	1238	0.757	
Warm Water Pump Motor	2	Snychr. (AC)	60.1	1238	0.912*	*Includes efficiency of power supply.
Cold Water Pump	2	Axial Flow	98.4	1857	9.757	
Cold Water Pump Motor	2	Synchr. (AC)	98.4	1857	0.912*	*Includes efficiency of power supply.
Ammonia Feed Pump	1	Turbine	900	332	0.85	
Ammonia Feed Pump Motor	1	Vertical AC Induction	900	400	0.88	
Ammonia Reflux Pump	1	Turbine	1200	61.3	0.82	
Ammonia Reflux Pump Motor	1	Vertical	1200	70	0.91	

Table 6-22
10 MWe MODULAR APPLICATION POWER SYSTEM WEIGHT SUMMARY

Heat Exchangers	817.8	tons
Turbine/Generator/Exciter	80.8	
Ammonia System Components	142.2	
Ammonia System Piping	97.7	
Ammonia System Valves	106.4	
Seawater System	250.7	
Auxiliary and Sup. Systems	212.7	
Electric Distribution and Cond. System	130.8	
Total	1839.1	tons

supported on powered positioning rolls, will be welded using automatic sub-arc equipment. When all shell and attachment welds are completed, the welds will be radiographed and repairs made as necessary (see Figure 6-70).

Materials, for the end assemblies and internal support structures, will be received as plates and shapes and fabricated as subassemblies then transported for final assembly of the shell.

The completed shell will receive post-weld heat treatment, blast and coat, and be prepared for shipment to the installation site.

Since the modular bundles are all identical and less than 12.5 feet wide, as described in Section 6.2.1, construction is greatly simplified. Obviously, there are a large number of standardized parts (tubesheets, tube support plates, boxes, rails, tubes, stiffeners, I-beams and pipe selections, etc.) so that large lot production can be used with attendant savings in manufacturing cost. The tubesheet will be much thinner (compared to one large plate required on the single unit design), so drilling cost also is minimized. The tubesheets and tube support plates are made of a single plate, avoiding the need for costly welding of many plates together (while maintaining flatness) required on large diameter single bundle units.

Tubesheets and support plates that have been gang-drilled and deburred on a numerically controlled multi-spindle Moline will be prepared for assembly. Tubes, enhanced and plain, will be purchased to length. Tube sheets and support plates will be set and aligned in the horizontal erection jig. Corner angles and bracing will be cut to length, fitted and welded to the support plates and tubesheets. The bundles with tubes installed will have the tubes expanded, welded with automatic gas tungsten arc welding (GTAW) tube welders, nondestructive examination performed, and weld repairs completed as necessary (see Figure 6-71).

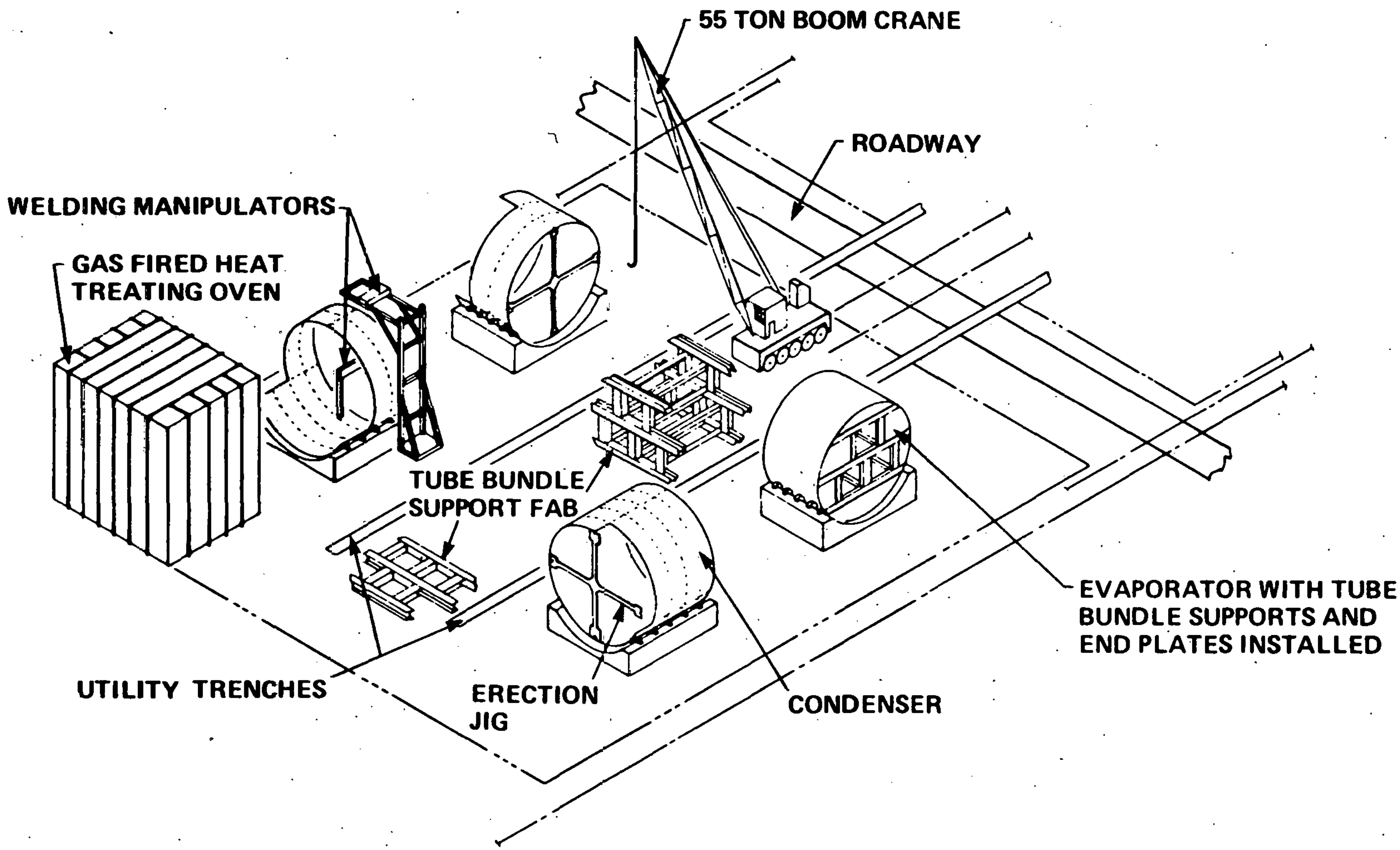

Figure 6-70
CONDENSER-EVAPORATOR ASSEMBLY

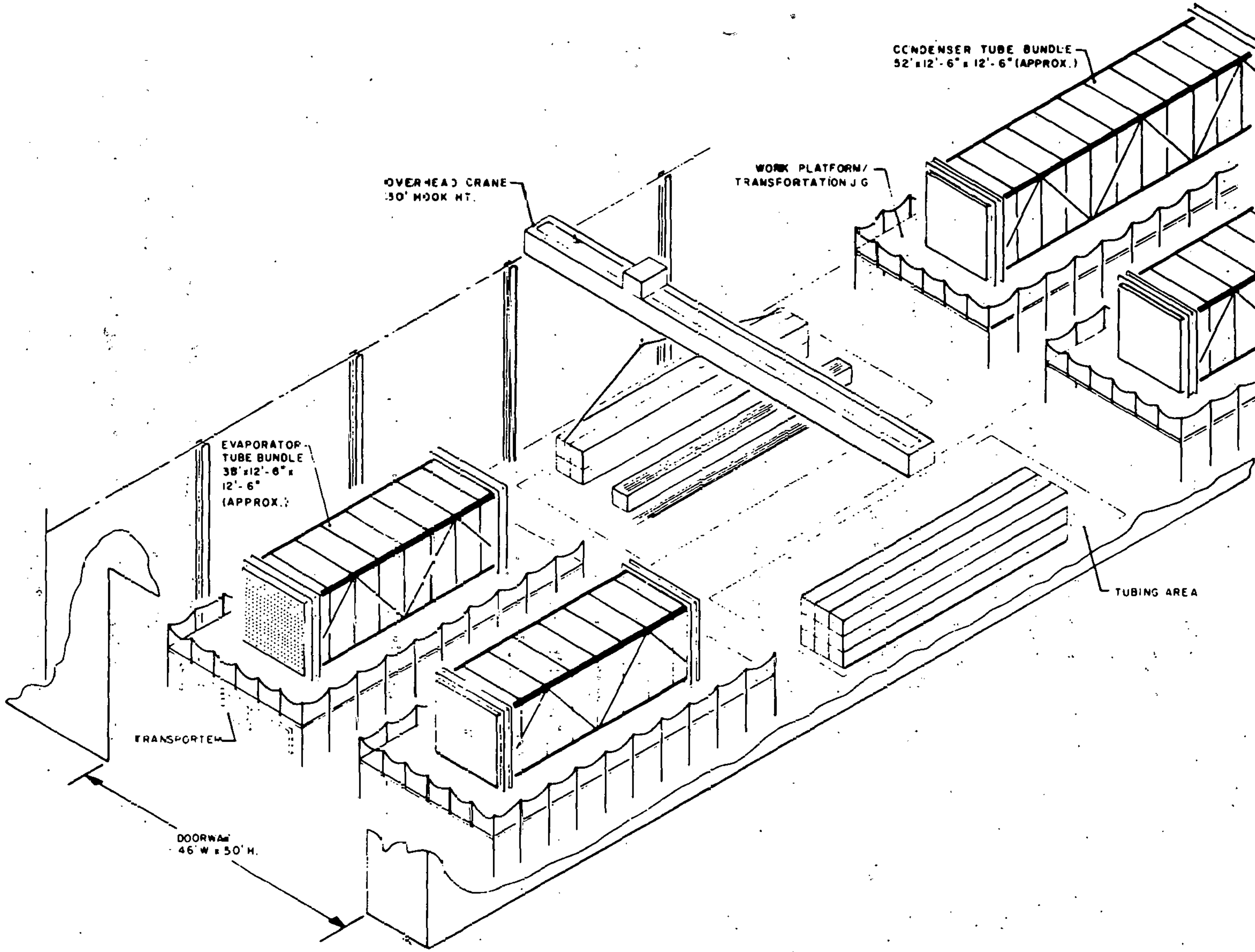

Figure 6-71
OTEC TUBE BUNDLE ASSEMBLY

Completed tube bundles will be placed in a test chamber and pressurized to test the tube-to-tubesheet welds. Repair welds will be made as required and the bundles will be given a final dimensional check and prepared for shipment to the installation site. No further testing of the completed bundles is required at the site.

The bundle design permits shipment of modular bundles by rail, and shipment of shell pieces by rail or barge, depending on the size of the shell subassemblies. The completed and inspected shell can be lifted onto the ship as a unit at several shipyards and at the Westinghouse offshore power systems plant -- for heat exchanger sizes up to larger than 50 MWe -- or the shell can be assembled on board the platform. Tube bundles are then lifted and placed into an opening at one end of the shell and pulled into it from the other end. A final carbon steel closure weld, full penetration through the box wall, is made at each end between the tubesheet and box.

A manufacturing chart is shown in Figure 6-72 for the modular heat exchanger design described in Section 6.2.1.2. A review of the key operations shows that the critical factors in the manufacture of heat exchangers have been simplified for lower cost and increased reliability. For example:

- Tubesheets can be produced from single mill size plates.

- Holes can be drilled with existing numerically controlled, ganged drilling machines.

- Economical jigs and fixtures can be used to facilitate alignment of tubesheets and support plates during tubing operations in normal heat exchanger manufacturing facilities.

- Completed modular tube bundles can be fully tested at the manufacturing facility prior to shipment.

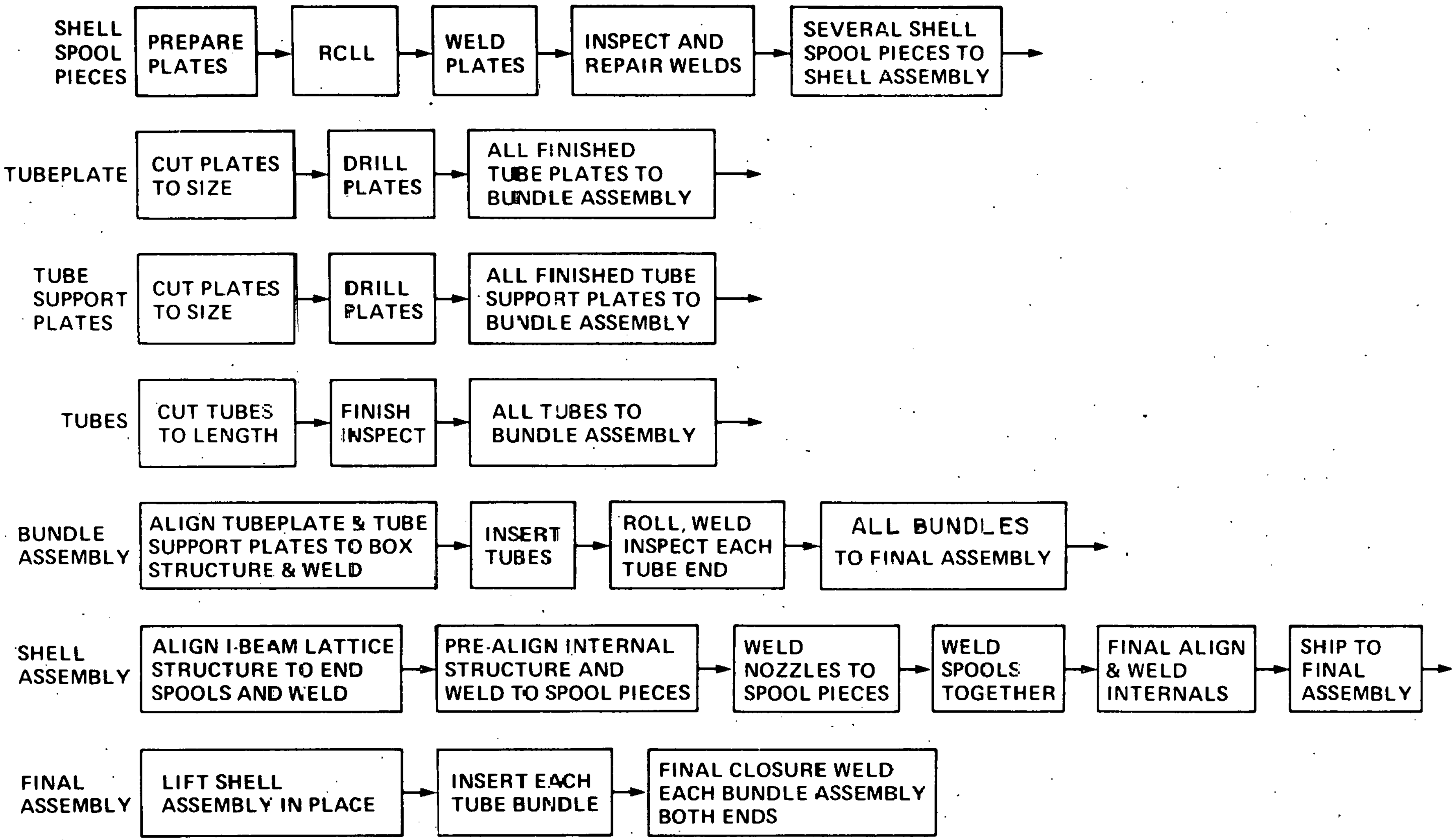

Figure 6-72

HEAT EXCHANGER MANUFACTURING FLOW DIAGRAM FOR MODULAR DESIGN

- Shipment to the OTEC plant assembly location can be accomplished by railroad.

- The heat exchanger shell and module cell structure can be assembled near the OTEC platform and lifted aboard as a subassembly.

A practical 10 MWe evaporator and condenser can be built to ASME requirements. The highlights of the manufacturing plan developed include:

- No new facilities required

- No advanced manufacturing development required

- Compact, completely shop-tested bundles prior to shipment for maximum reliability

- Automatic tube-to-tubesheet welding

- Explosively clad tubesheets (DuPont DETACLAD)

- Commercial techniques for inspection to ASME Code Section VIII, Div. I and/or U.S. Coast Guard requirements

- Additional inspection over code requirements

  a. Linde surface applied to tube outer surface, one sample per manufacturing lot will be subjected to:
     - Flatten and flare tests of bare tube to Section 8.1 and 9.1 of SB338GD.2.
     - Hydrostatic burst test
     - Heat transfer performance test

b. Tube-to-tubesheet welds will be subjected to:
   - Leak test with gas pressure on shell side
   - 100% dye-penetrant inspected to Westinghouse specification 600174.
   - All tube welds will be visually inspected at 5 to 10x magnification to Westinghouse specification 84353MA.

c. Tube sheet cladding bond will be subjected to:
   - 100% ultrasonic testing with maximum of 3/8-inch diameter unbond criteria to DuPont specification DETA 600M.

d. All shell welds not radiographed will be magnetic-particle tested to Westinghouse specification 600195 or dye-penetrant inspected to Westinghouse specification 600174.
e. A "Holiday" detector test of neoprene coating to locate voids to criteria of Gates Engineering Bulletin 142 using equipment by Tinker and Rasor.

6.4.2 Turbine

The turbine configuration is similar to typical low pressure steam turbines which Westinghouse has designed and manufactured for years, with the exception of the gland seal design which is a hydraulic "zero leakage" type.

From a manufacturing standpoint, the major components comprising the turbine design are:

- Blading (Rotating and Stationary)
- Rotor
- Cylinder
- Gland Ring

A description and comparison with similar type components previously manufactured by Westinghouse, follows. The projected lead time for ordering and manufacturing these components is shown in Figure 6-73.

6.4.2.1 Rotor

The rotor shaft forging is a long-lead time item will be ordered as early as possible in the manufacturing cycle. The rotor is relatively small, with an overall length of 135 inches and a weight of approximately 4,200 lbs. Consequently, there is no problem envisioned in machining or obtaining a quality forging.

6.4.2.2 Blading

The rotating blades, a twisted and tapered reaction type with a curved side entry root, will be manufactured by machining from bar stock or by forging, depending on which proves the more cost-effective in future analyses.

6.4.2.3 Cylinder Design

The cylinder will be fabricated and will be similar in construction to other Westinghouse turbines. Because of the relatively high pressure drop (75 PSI) across the walls in the exhaust end of the turbine, particular attention will be paid during the detail design to the reinforcement, welding and fabrication details of the cylinder. Additional non-destructive testing of the cylinder fabrication will be specified.

6.4.2.4 Gland Seal and Gland Ring Forging

The gland ring forging will be ordered at the same time as the rotor forging to ensure that no delay results in fitting the gland ring to the rotor. The ring will be fitted to the rotor with a light press fit and secured in place by means of the retaining ring. The machining accuracy and assembly required in this operation is similar to, but not as

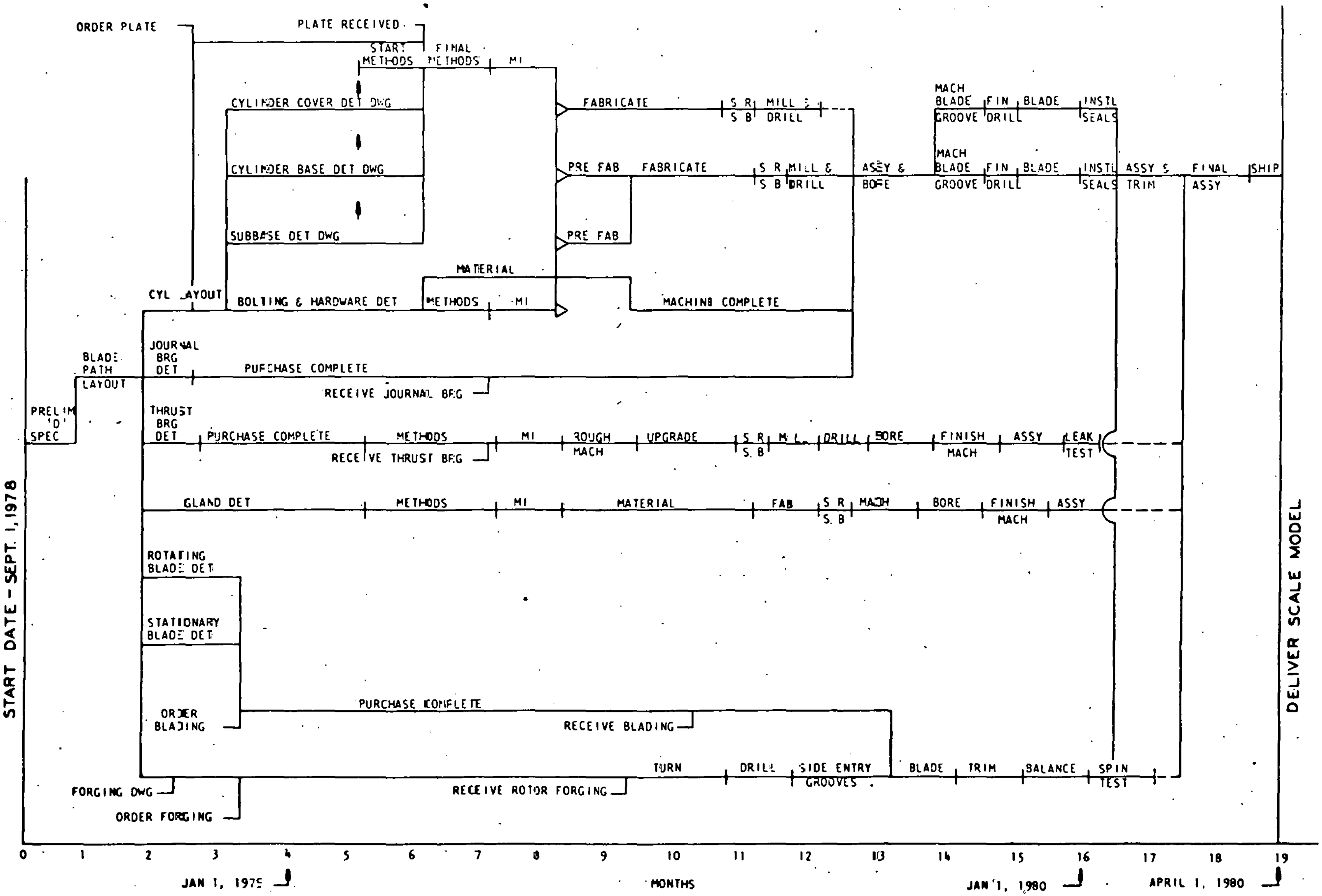

Figure 6–73
OTEC TURBINE 10 MWe SCALE MODEL LEAD TIME DIAGRAM

difficult as, a large number of operations performed in the manufacture of certain steam turbines and, consequently, should not be a problem.

As indicated previously, the turbine design is similar to turbines manufactured by Westinghouse for many years. Consequently, the facilities are readily available with adequate tooling and personnel having the skills to manufacture this component.

6.4.3 Generator

The major portion of the manufacture of the OTEC pilot plant generator will use well-established "state-of-the-art" procedures. However, in achieving the capability for 50% overspeed, a few areas exist in which the manufacturing engineers and the design engineers will develop design details consistent with design requirements, and such practical considerations as the availability and machinability of materials.

One of those areas involves the special size and shape of the non-magnetic metallic wedges which retain the insulated copper straps of the field coils in the specially shaped slots machined longitudinally in the rotor body.

Another area involves the redesign of the retaining rings surrounding the extensions of the field coils beyond the ends of the rotor body. The stress in the rings at 50% overspeed must be compatible with the yield strength of the forged steel retaining rings. This stress is reduced by increasing the radial thickness and hardness of the rings. The limit on material strength is set by the increased difficulty of machining the retaining rings due to the increased hardness of the material.

The most critical long-lead item to be purchased for the generator is the steel forging for the rotor body and its integral shaft ends. Accordingly, that item is indicated as the first one to be purchased in the chart of generator manufacturing events included in Figure 6-74. A material with a yield strength of 95,000 PSI is specified for this forging.

Although the purchase of other items requiring a long-lead time is not shown on the chart, the purchase of the generator air coolers is recognized as requiring early action.

The 50% overspeed requirement presented the problem of running the rotor at 5,400 rpm to demonstrate this overspeed capability by test. Fortun-

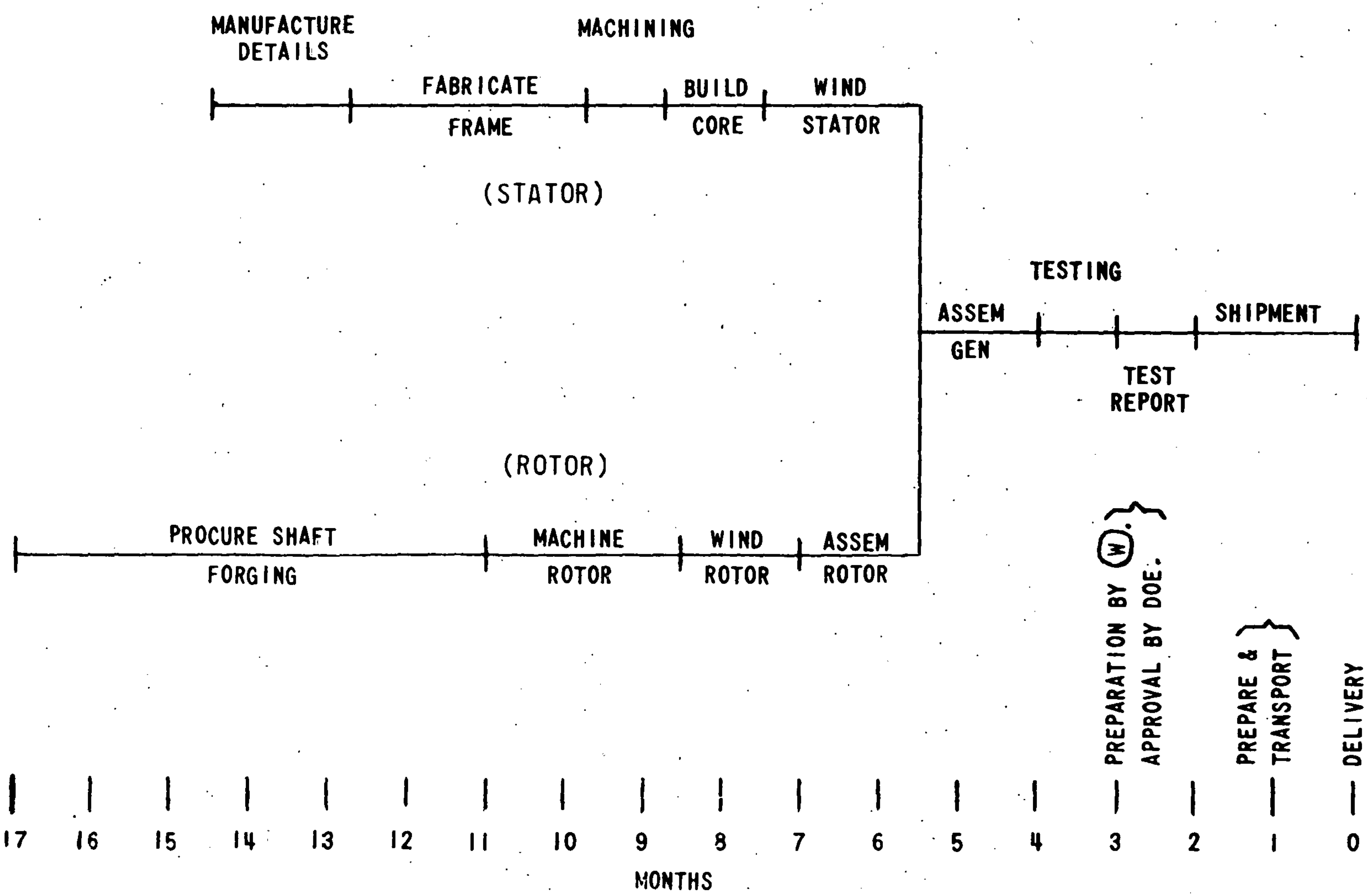

Figure 6-74
OTEC PILOT PLANT MANUFACTURING EVENTS

ately, it is not necessary to procure a special gear to obtain this overspeed. Instead, by electrically interconnecting two wound-rotor induction motors having a different number of poles in each and having their shafts solidly coupled together, it is possible to use this existing test equipment to produce power at a variable frequency up to 90 Hertz. This power can be applied to the 10 MWe generator to cause it to run as a synchronous motor at speeds up to 5,400 rpm.

6.4.4 Cold and Warm Water Pumps

6.4.4.1 Manufacturing

The seawater pumps will incorporate two major subassemblies; namely:

1) Rotor/upper bearing housing

2) Outer shell/pod/stator

The rotor/upper bearing housing subassembly schedule involves several long-lead items including rotor shaft forging, upper bearing housing casting, roller bearings and mechanical seals, propeller blade castings, nose fairing spinning, and motor rotor. Of these, the motor rotor delivery will pace the subassembly schedule. This subassembly requires a special assembly stand.

The outer shell/pod/stator subassembly long-lead items include lower bearing housing casting, stator vane castings, inlet spinning, roller bearings, mechanical seals, and motor stator. The motor stator will be the pacing item. Subassembly requires an overhead crane, but no special fixtures.

Final assembly of these subassemblies requires a special assembly stand. All major pod auxiliaries will be factory-installed. The tail cone will be fabricated as a separate component and shipped for field installation.

Existing techniques and facilities will be used for all components. Pilot castings will be included for bearing housing castings to assure a realistic schedule. The two assembly stands are the only new auxiliary equipment required. Seals will be factory-tested, and all running clearances will be set at the factory.

Table 6-23 is the manufacturing schedule for all major seawater pump system components, including final factory assembly. Note the dependence of overall schedule upon motor delivery. The controller, manufactured using existing techniques and facilities, represents an independent parallel manufacturing path.

6.4.4.2 Installation

The pump and pump pod tail cone will be assembled during installation. The completed assembly will be lowered into an access gallery in the plant platform, and the gallery/pump interface will be sealed and dewatered. The gallery provides dry access to pump wiring and plumbing connections, permitting final connections to be made in a shirt-sleeve environment.

The pump controllers will be installed in the plant control area, and pump auxiliary coolers and lube support equipment will be installed in conventional machine rooms.

6.4.5 Assembly and Checkout

The 10 MWe power module was designed so that an existing shipbuilding facility can build the platform and install the power plant components.

Individual components (Government-furnished equipment) will be received for installation in the hull. Because of a maximum use of large subassemblies and self-contained skid-mounted packages, integration of the equipment with the hull should present no major problem (see Figure 6-75). Major items to be handled:

Table 6-23
WARM AND COLD WATER PUMP SYSTEM, MANUFACTURING PLAN FABRICATION AND ASSEMBLY SCHEDULE

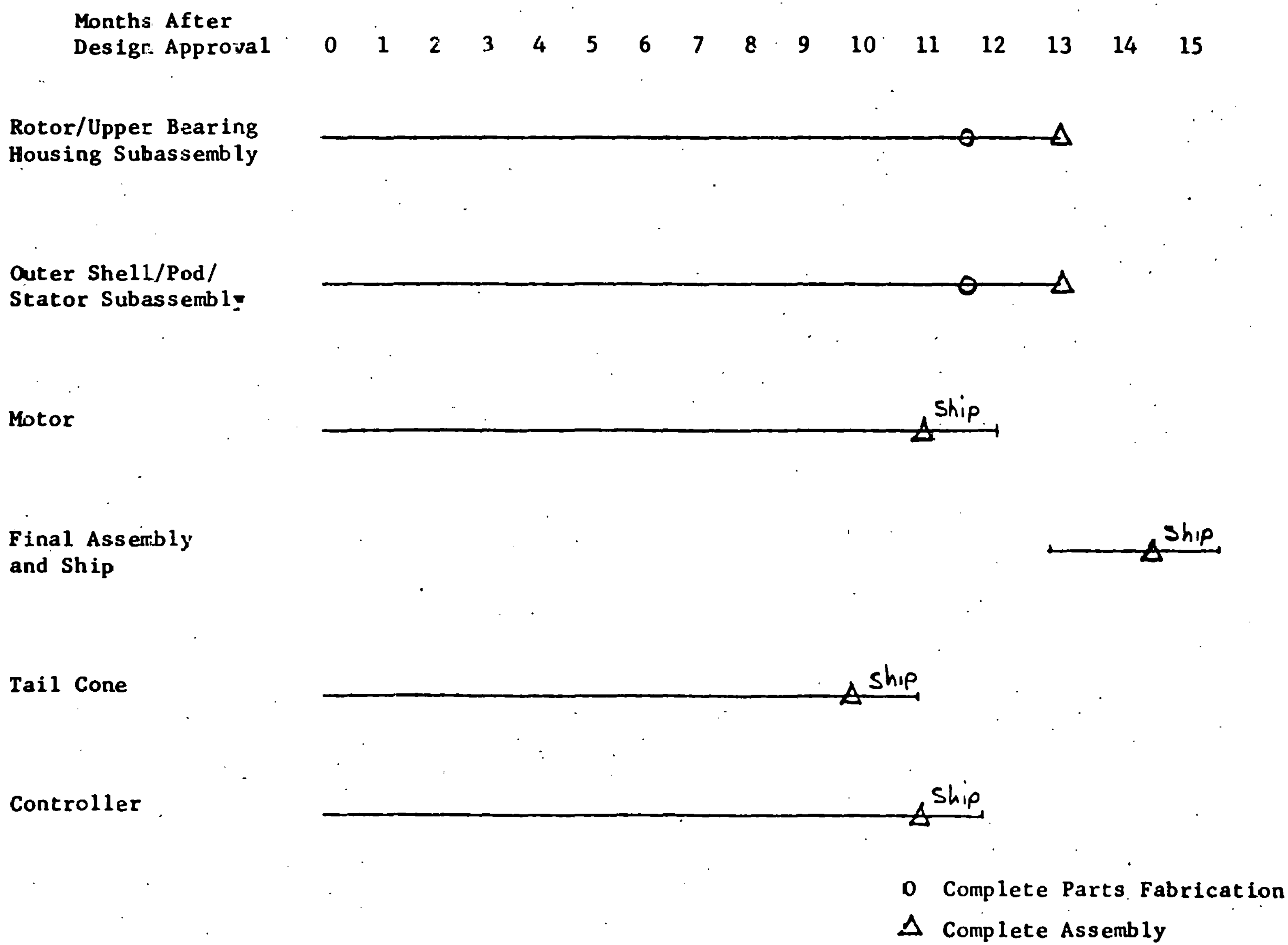

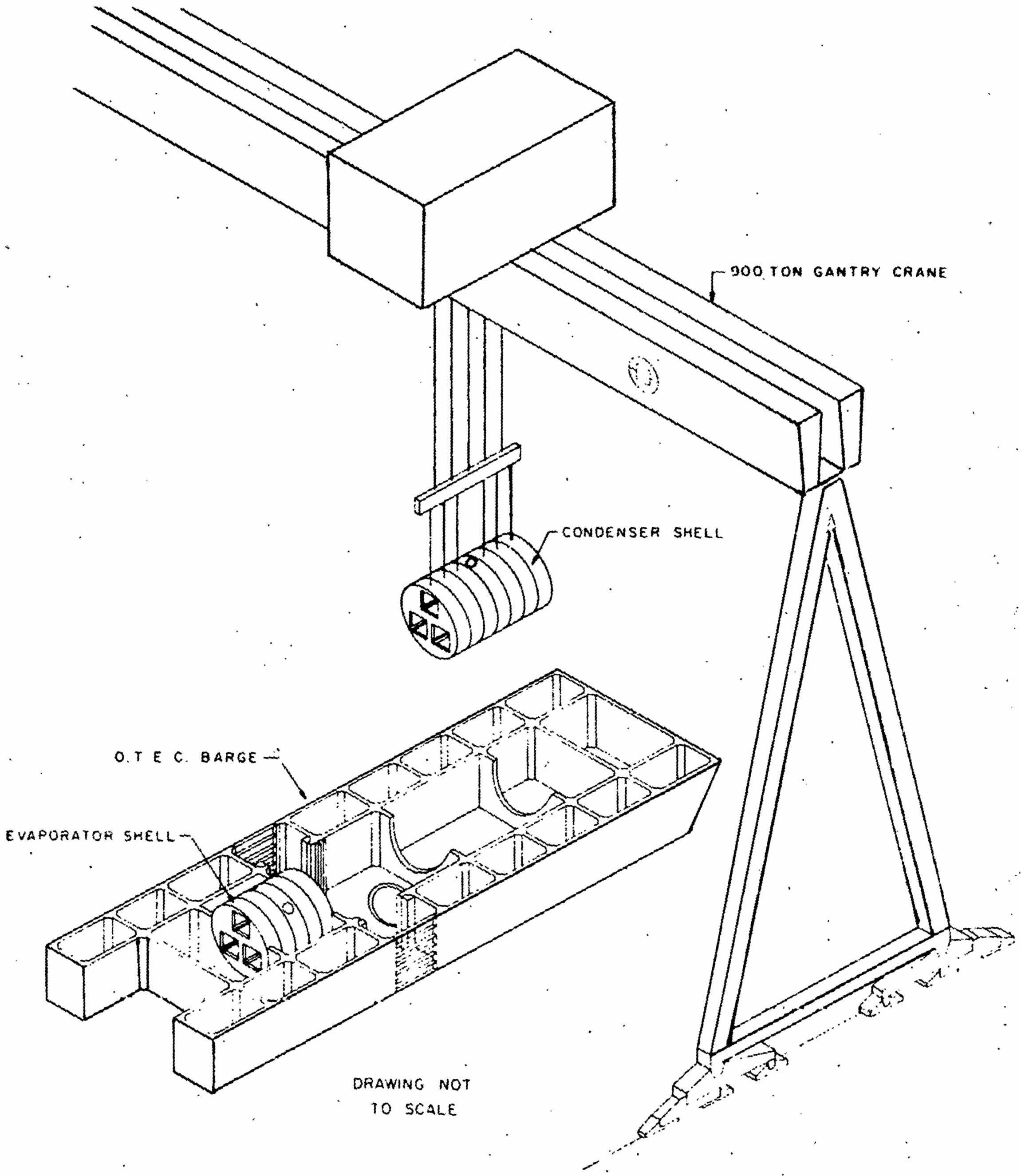

Figure 6-75
OTEC EQUIPMENT INSTALLATION SLIPWAY

- Condenser Shell (less tube bundles) approximately 300 short tons

- Evaporator Shell (less tube bundles) approximately 180 short tons

- Condenser Tube Bundles (3) approximately 84 short tons each

- Evaporator Tube Bundles (3) approximately 53 short tons each

- Turbine-Generator approximately 50 short tons

- Start-up Power Supply

- Ammonia Pumps (may be installed after platform leaves shipyard)

- Motor Control Center and Switchgear

- Ammonia Storage Tanks

- Nitrogen System

Piping subassemblies will be fabricated with some spool pieces cut to length and others with excess length to accommodate field fit up. All systems piping, with the exception of the feed and recirculation loops which project below the platform baseline, will be installed and completed simultaneously with the hull erection. Due to their configuration and location, the feed and recirculation loops may have to be installed after the hull is waterborne with sufficient channel depth to clear those projections.

To minimize handling and production costs, the process flow of OTEC parts through the facility will be carefully analyzed and maximized for smooth straight line movement of internally fabricated assemblies and finished assemblies. Close coordination with hull designers and constructors will facilitate movement of large pieces of equipment during installation. A preliminary manufacturing and assembly network is shown in Figure 6-76 and a manufacturing and assembly sequence in Figure 6-77.

Due to the modular design of the power plant, the building and outfitting of the platform presents no unique problems to the shipbuilder, with the exception of underwater installation of the ammonia feed and recirculation loops. These require templates of the as-built condition of hull relative to the heat exchanger and ammonia pump nozzles. Interfaces at each joint require diaphragms to preclude seawater entering previously cleaned components and piping. This type of installation is within the state-of-the-art for shipbuilders and offshore erectors.

Upon completion of the assembly of all parts, the main system and each subsystem, including the control room and electrical system will be thoroughly checked. Fluid systems will be leak-tested, and all systems will be tested to verify operational readiness. Only final startup need be accomplished at the ocean site.

6.5 System Operation

6.5.1 Normal Operation

The 10 MWe power module is designed to operate between a warm seawater temperature of 80°F and a cold seawater temperature of 40°F, with a biofouling thermal resistance of 0.00025 hr-ft^2-°F/BTU. Thermodynamic cycle data is given in Table 6-24.

The performance of the heat exchangers is shown in Table 6-25.

The performance of the rotating equipment and cleaning system is shown in Table 6-26.

The cycle flow diagram is shown schematically in Figure 6-78. Thermo dynamic state point data for this diagram is given in Table 6-27.

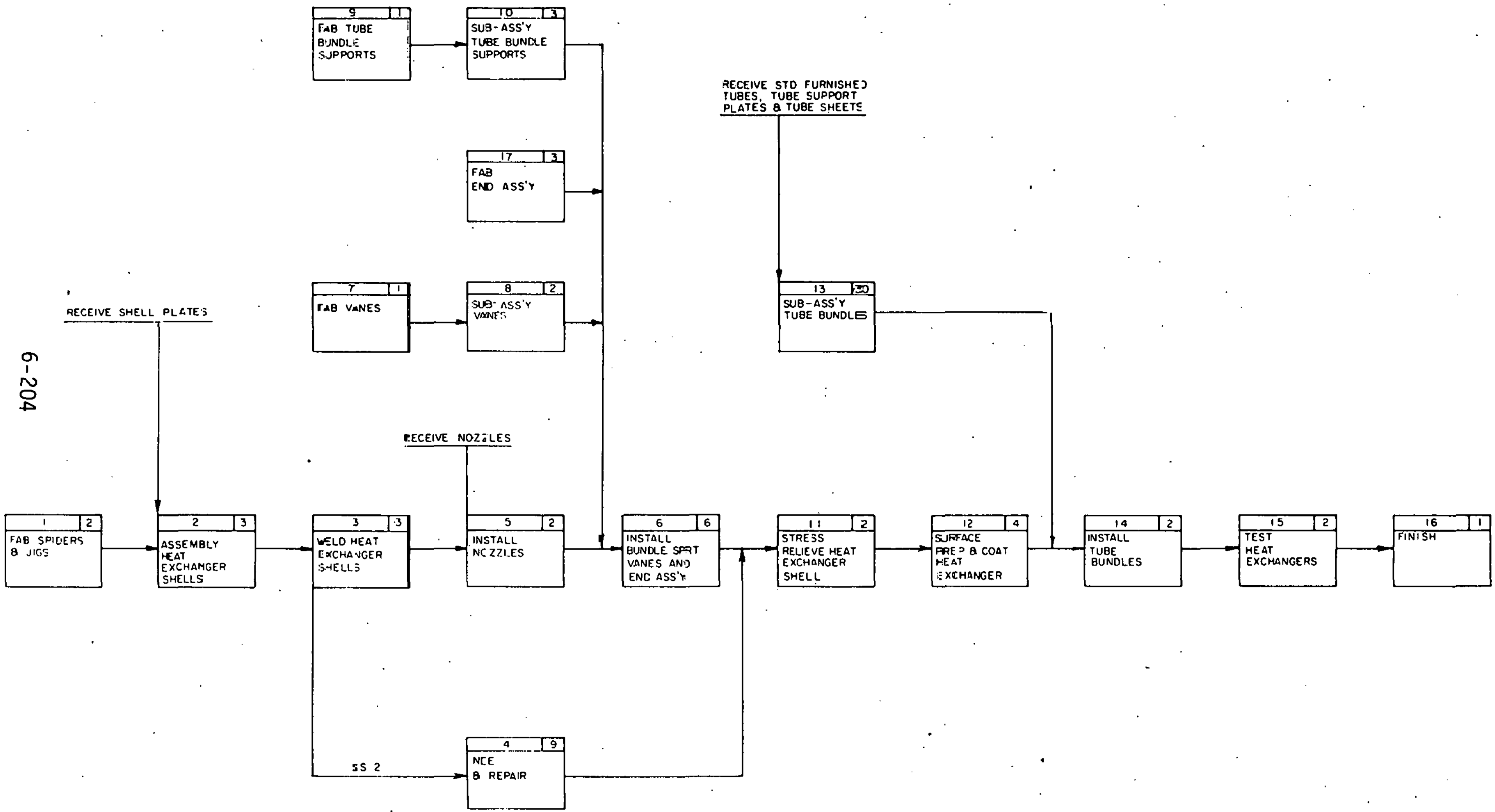

Figure 6-76
HEAT EXCHANGER MANUFACTURING AND ASSEMBLY NETWORK

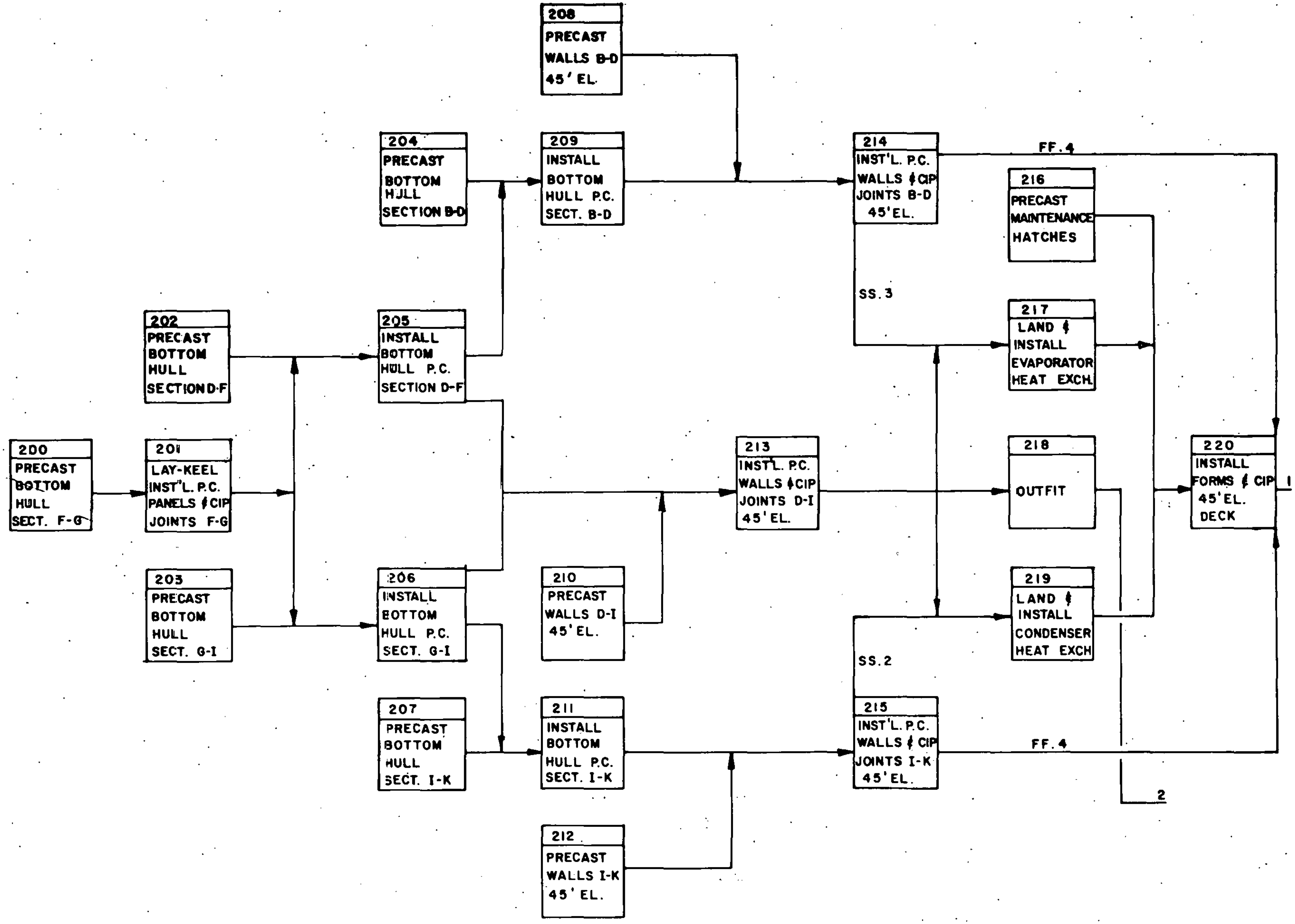

Figure 6-77 (Sheet 1 of 2)
SYSTEM MANUFACTURING AND ASSEMBLY SEQUENCE

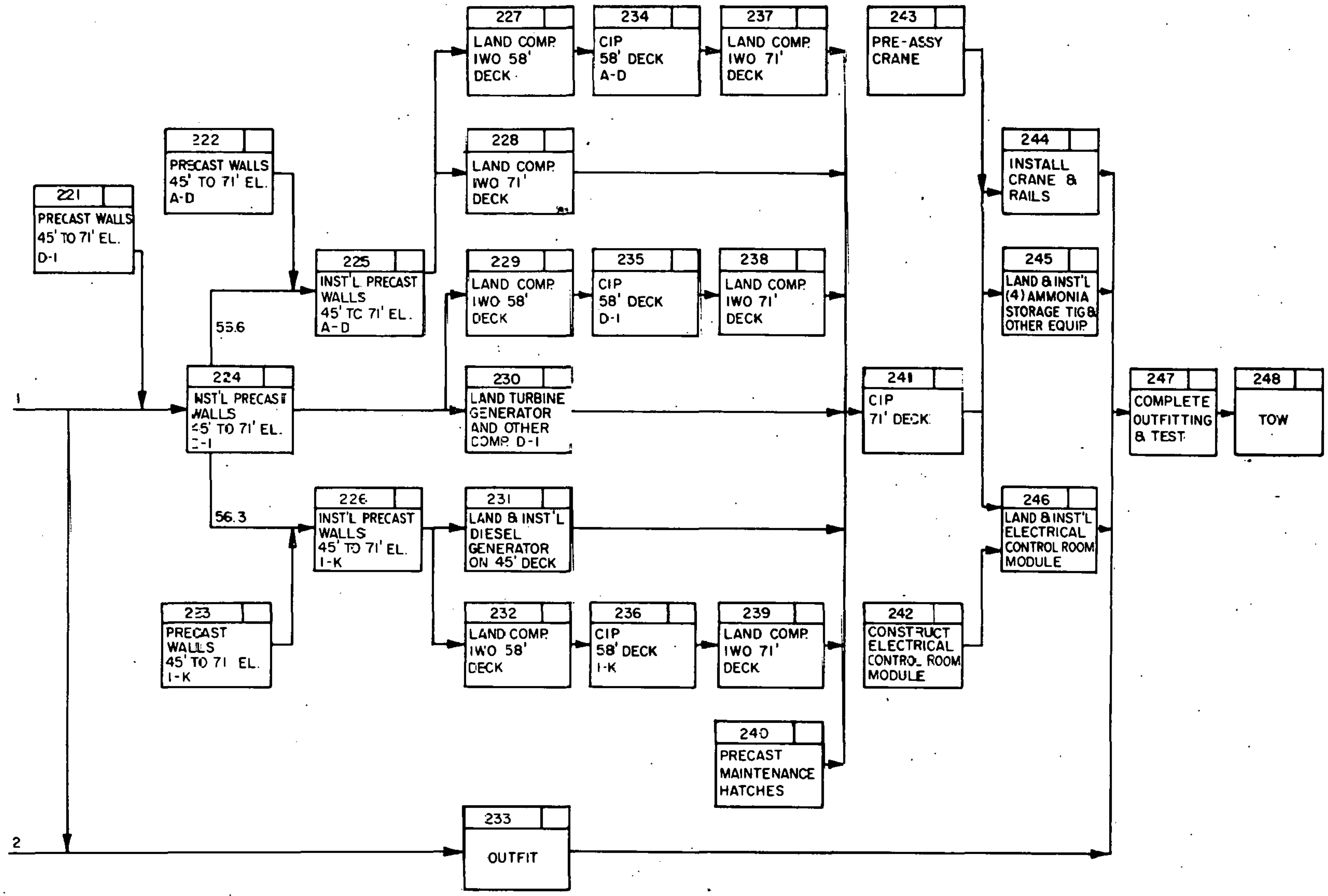

Figure 6-77 (Sheet 2 of 2)
SYSTEM MANUFACTURING AND ASSEMBLY SEQUENCE

Table 6-24
10 MWe THERMODYNAMIC CYCLE DATA

Heat Input	465.1 MW
Heat Rejection	449.9 MW
Rankine Cycle Efficiency	3.28%
Generator Gross Output	14.4 MW
Parasitic Losses	4.4 MW
Plant Net Output	10.0 MW
Overall Plant Efficiency	2.15%

Table 6-25
HEAT EXCHANGER DATA

	Condenser	Evaporator
Seawater Flow (10^6 lb/hr)	263	305
Seawater Inlet Temperature (°F)	40.0	80.0
Seawater Outlet Temperature (°F)	46.1	74.6
Ammonia Flow (10^6 lb/hr)	3	3
Ammonia Inlet Temperature (°F)	49.1	59.7
Ammonia Outlet Temperature (°F)	49.0	70.5
Log-Mean Temperature Difference (°F)	5.37	6.40
NTUs	1.14	0.85
Effectiveness	0.68	0.57
Heat Transfer Coefficient (BTU/hr-ft^2-°F)	459.3	648.2
Heat Transferred (10^6 BTU/hr)	1535	1587
Tubeside Velocity (ft/sec)	5.6	6.5
Tubeside Pressure Loss (psi)	3.72	2.90

Table 6-26
POWER SUMMARY DATA

Item	Efficiency	Power(MW)	% of Generator Power
Turbine/Generator	.790	14.42	100.0
Cold Water Pumping	.670	2.30	15.9
Warm Water Pumping	.670	1.52	10.6
Cycle Feed Pumping	.750	0.28	1.9
Recycle Pumping	.750	0.05	0.3
Chlorination	-	1.71	1.19
Estimated Hotel Load	-	0.10	0.7
Module Net Output	-	10.00	69.3

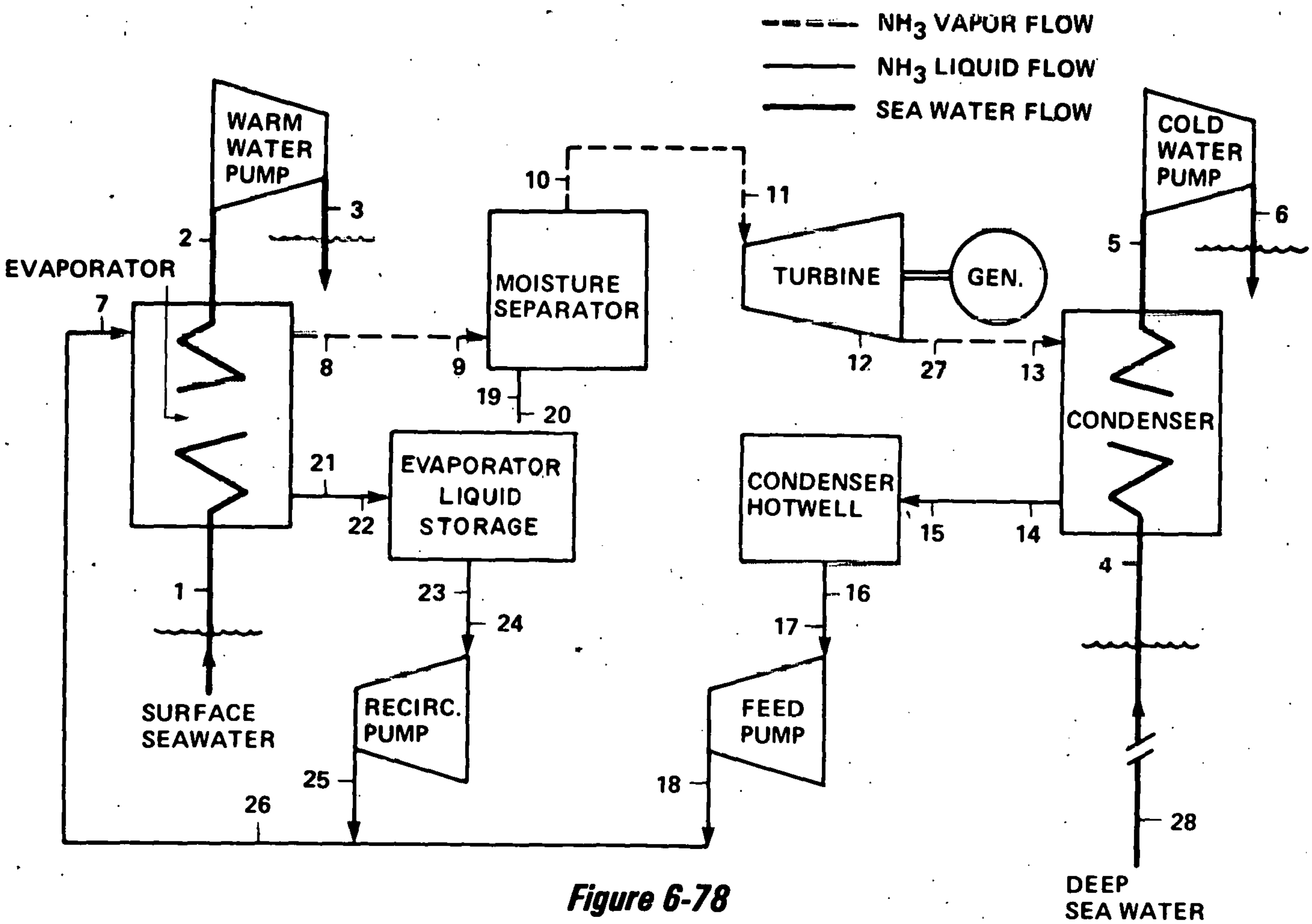

Figure 6-78
DETAILED OTEC POWER CYCLE SCHEMATIC

Table 6-27
10 MWe MODULAR APPLICATION AMMONIA FLOW DISTRIBUTION

KEY	LOCATION	WEIGHT FLOW (10^6 LB/HR)	ENTHALPY (BTU/HR)	TEMP. (°F)	PRESSURE (PSIA)	ENERGY FLOW (10^6 BTU/HR)
14	Condenser Discharge	2.987	97.481	49.000	87.646	291.17
15	Hotwell Inlet	2.987	97.481	49.000	87.622	
16	Hotwell Discharge	2.987	97.481	49.000	87.622	
17	Feed Pump Inlet	2.987	97.481	49.000	87.609	
18	Feed Pump Discharge	2.987	97.222	49.000	138.463	
19	Separator Drain Discharge	0.332	121.535	70.311	129.702	
20	Drain Tank Inlet from Separator	0.332	121.535	70.311	129.665	
21	Evaporator Drain Discharge	2.655	121.750	70.500	129.634	323.25
22	Drain Tank Inlet from Evaporator	2.655	121.750	70.500	129.611	
23	Drain Tank Discharge	2.987	121.726	70.479	129.611	
24	Recirculation Pump Inlet	2.987	121.726	70.479	129.611	
25	Recirculation Pump Discharge	2.987	121.769	70.479	138.365	
26	Combined Pump Flow	5.975	109.745	59.740	138.365	
7	Evaporator Inlet	5.975	109.745	59.740	138.365	655.73
8	Evaporator Discharge	3.319	578.486	70.500	129.634	1920.00
9	Separator Inlet	3.319	578.486	70.311	129.502	
10	Separator Discharge	2.987	629.253	70.232	129.321	
11	Turbine Inlet	2.987	629.253	70.199	129.058	
12	Turbine Exhaust	2.987	611.515	49.087	87.646	
13	Condenser Inlet	2.987	611.515	49.087	87.646	1826.60

As mentioned, fouling control is designed to maintain 0.00025 hr-°F-ft^2/BTU fouling resistance. Based on data available on the selected fouling control systems, fouling resistance may be maintained as low as 0.0001 hr-°F-ft^2/BTU. Dosage levels of chlorine have been selected to be 0.25 PPM and 0.1 PPM into the seawater inlets to the evaporator and condenser, respectively. This is a continuous dosage equivalent; thus, the instantaneous dosage and cycle time can be varied, depending on variations of fouling organisms, fouling rate, and environmental restrictions.

Amertap can be operated periodically or continuously. Present estimates, based on warm water oceanic fouling rates, are circulation for 1 hour per day to obtain essentially complete slime removal from the tubes.

Ammonia liquid cleanup should consist primarily of filtration of suspended solids. Removal of water and sea salts by distillation should be minimal due to the high pressures on the ammonia side of the heat exchangers.

6.5.2 Off-Design Performance

Significant impacts on performance are to be expected from variations in seawater temperature and fouling of heat exchangers. Lesser effects are expected from part-load and load-cycling operations and from water and non-condensible content in the ammonia.

6.5.2.1 Temperature Differences

Variations of the temperature difference between surface seawater and cold deep seawater impact heavily on performance. Figure 6-79 shows an approximate 4% variation of net power per 1°F variation near the design temperature difference of 40°F.

6.5.2.2 Fouling

The effect of fouling is expected to be less severe than temperature difference variations, since fouling control methods will be utilized.

At the initial or clean condition, incremental fouling has a larger percentage effect than at the design point of 0.00025 hr-°F-ft^2/BTU; there is a tendency for the effect of fouling to level off (Figure 6-80). This model considers only the increase in heat transfer resistance due to fouling (which is the major parameter in thin slime films of 2 mils or less), and it does not consider the effect of increased fluid frictional resistance or wall diameter decreases. When the latter parameters are considered, the slope of the curve will become more negative beyond the design point than the present model estimates.

6.5.2.3 Sea States

The sea-keeping parameters (e.g., pitch and roll) will vary with the type of platform. Pitch and roll estimates were used to design safe sizes of evaporator and condenser trays and hotwells. Slight maldistribution of liquid films on the evaporator tubes is possible at these conditions. The condenser tube liquid films should not be affected.

No anticipated problem is expected with liquid separator performance, since the chevrons are well above the height of the evaporator tube bundle.

Also, the ammonia feed and recirculating pumps should not be affected, since they are normally running full of liquid.

6.5.2.4 Effect of Water in Ammonia

Minute quantities of water are desirable in ammonia to lessen stress corrosion of high strength steels. The controlled water content will be 0.2 to 0.5% (by weight) in the bulk recycle liquid ammonia in the evaporator.

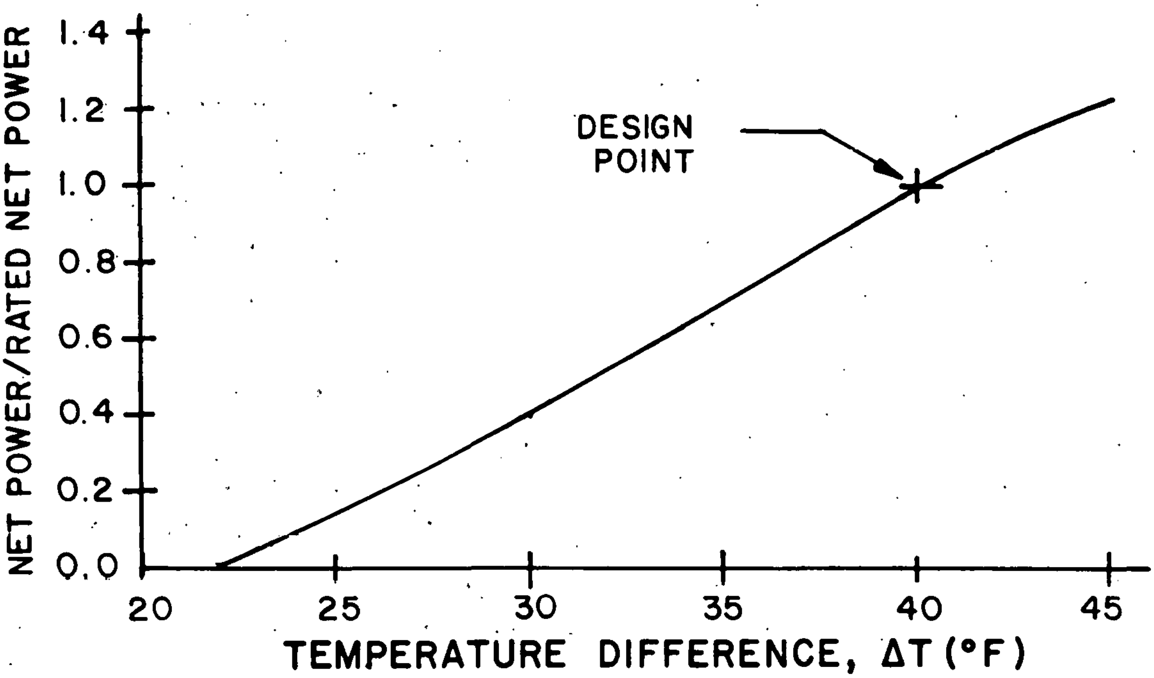

Figure 6-79
TEMPERATURE EFFECT ON PERFORMANCE

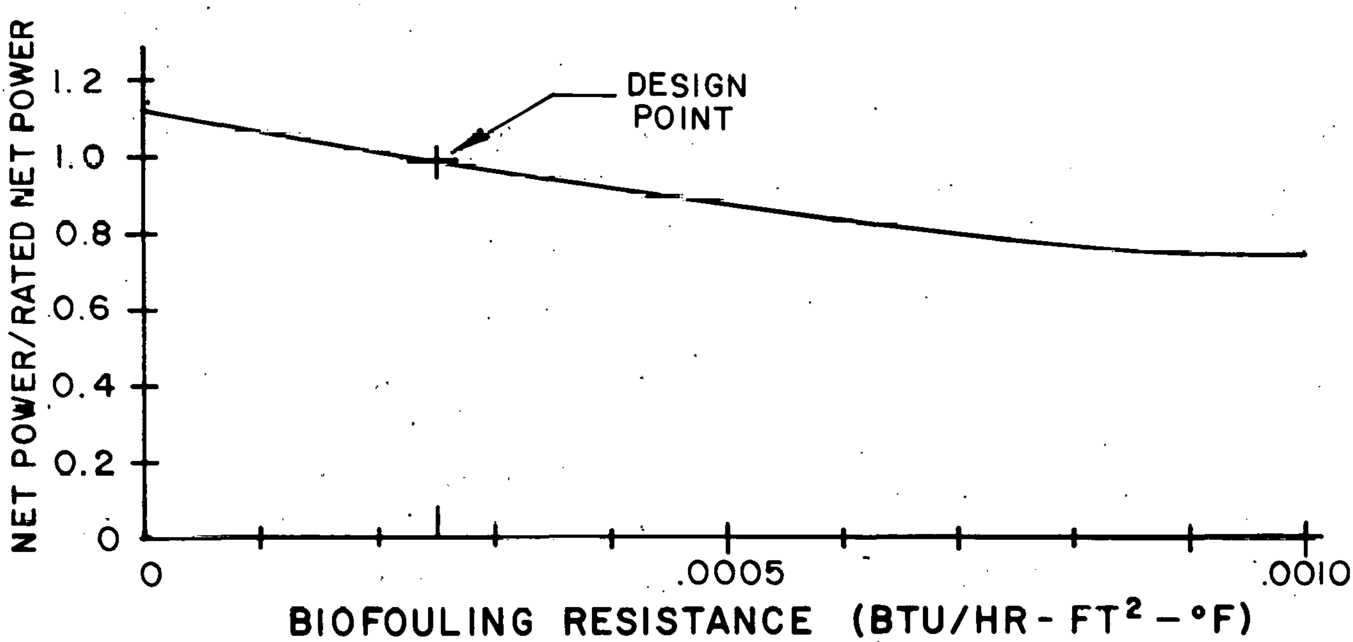

Figure 6-80
BIOFOULING EFFECT ON PERFORMANCE

The water content has a deleterious effect on heat exchanger performance, since it decreases the temperature differential driving force in the evaporator at constant pressure operation. Assuming no more than 50% of the ammonia/water mixture is evaporated from the liquid film on the evaporator tubes, it is estimated that the water content will not exceed about 0.4 to 1% by weight in the evaporating fluid. This water content can be translated into a decrease in heat exchanger temperature differential of 0.2 to 0.5°F. The net effect on performance will be the same as an equivalent loss of available temperature difference between warm and cold seawater (See Figure 6-79). However, larger effects on performance could occur if greater concentrations of water build up in a porous surface, such as the Linde-enhanced surface for the heat exchanger tubing.

6.5.2.5 Non-Condensible Effect on Ammonia

The condensing rate of ammonia in the condenser can be affected by residual non-condensibles (e.g., nitrogen) if they are not completely removed. The net effect on performance is similar to the fouling of the tubes.

Since the non-condensibles will be controlled by an ammonia-purging system, any performance effect will be minimal.

6.5.3 Dynamic Reponse

Preliminary analyses of dynamic responses of the 10 MWe OTEC power system to fast actions of the control valves were conducted. One dynamic response was the power-loop-to-valve motion for turbine-generator overspeed protection, following an electrical load dump at rated turbine flow and load conditions. Another dynamic response was the power loop to a small step in turbine bypass valve area from fully closed to slightly open at rated turbine flow conditions. These dynamic responses are discussed, respectively, in paragraphs 6.5.3.1 and 6.5.3.2.

6.5.3.1 Turbine Overspeed Characteristics

When a turbine is used to drive an electrical generator, turbine overspeed protection becomes an important design consideration. With an electrical load, most malfunctions of the electrical system will quickly disconnect the generator to protect the system. This sudden interruption of turbine load results in turbine overspeed. For the 10 MWe power system, the turbine and generator rotors are designed for a mechanical overspeed capability of 50%.

The following overspeed characteristics are based on preliminary computer system simulations of the 10 MWe system.

Figure 6-81 shows turbine speed versus elapsed time following an electrical load dump at maximum rated turbine flow conditions. Before the trip, the turbine bypass valves are closed and the liquid NH_3 feed and recirculating flow valves into the evaporator are open. Three responses to assumed actions taken following the loss of electrical load are shown as follows:

a. No Valves Act

Turbine speed quickly accelerates to a level just below 100% overspeed in approximately 30 seconds -- eventually stabilizing at 109% overspeed. The limiting 50% overspeed level is reached in approximately 5 seconds. Therefore, rapid signal response and fast-acting valves are required to provide turbine overspeed protection.

b. Only Turbine Bypass Valves Act

When the turbine reaches approximately 8-10% overspeed (0.5 second), only the bypass valves are tripped to their full-open positions. Turbine speed accelerates to approximately 90% overspeed before stabilizing.

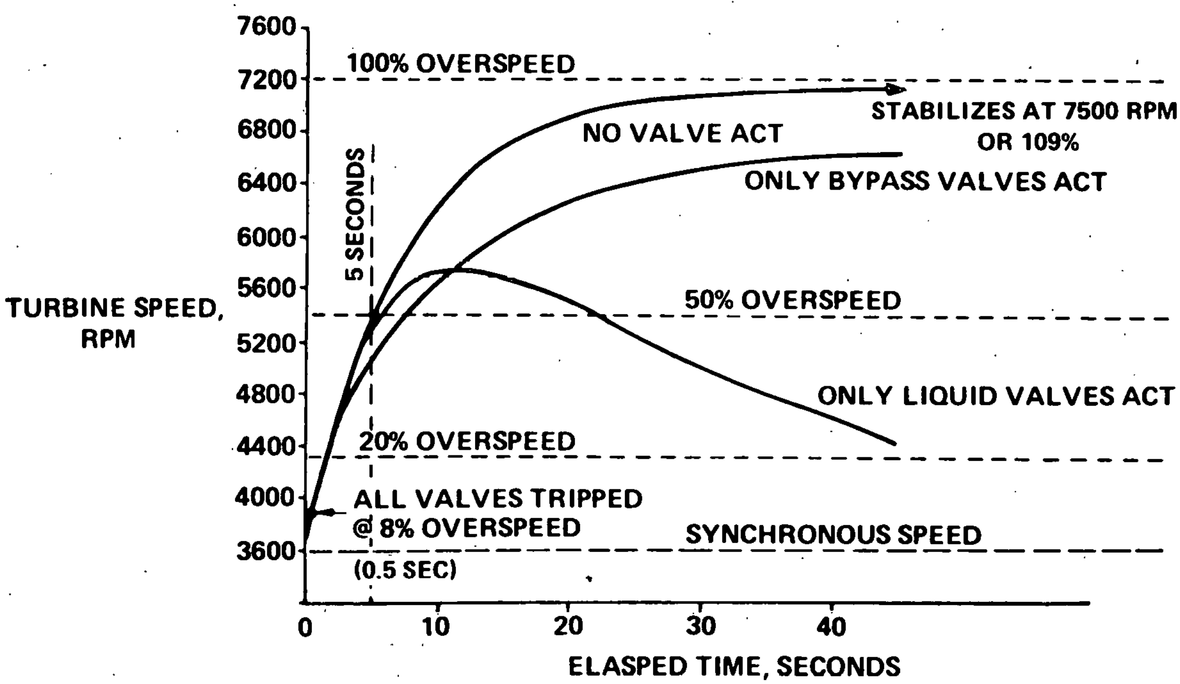

Figure 6-81
10 MWe TURBINE SPEED CHARACTERISTICS

c. Only Liquid Valves Act

When the turbine reaches approximately 8-10% overspeed (0.5 second), only the liquid feed and recirculating flow valves are tripped closed. Turbine speed accelerates to approximately 60% overspeed. With vapor production stopped, pressure differential between evaporator and condenser decays, reducing turbine speed.

6.5.3.2 Turbine Overspeed Protection

Figure 6-82 shows curves of turbine speed versus elapsed time for the normal trip operation and for the redundant trip operations.

From the previous overspeed characteristics, it was shown that neither the bypass valves acting alone nor the liquid valves acting alone were capable of preventing excess overspeed. However, by tripping all valves together, this design limitation can be met.

6.5.3.2.1 Normal Overspeed Trip

In the normal overspeed trip situation, the trip signal is simultaneously given to the four bypass valves to open, and to the liquid feed and recirculating valves to close. Redundancy in interrupting the liquid flow into the evaporator is provided by also electrically shutting off the evaporator liquid feed and recirculating pumps.

The bottom curve of Figure 6-82 shows this simulated operation. All valves are tripped when the turbine reaches 8 to 10% overspeed (0.5 sec. elapsed time). This trip operation limits turbine speed to approximately 40% overspeed, well below the design limitation of 50%.

6.5.3.2.2 Backup Overspeed Protection

The results of a fault tree analysis to determine the effect on overspeed margins, if combinations of bypass valves fail to respond to the trip signal, are also shown in Figure 6-82.

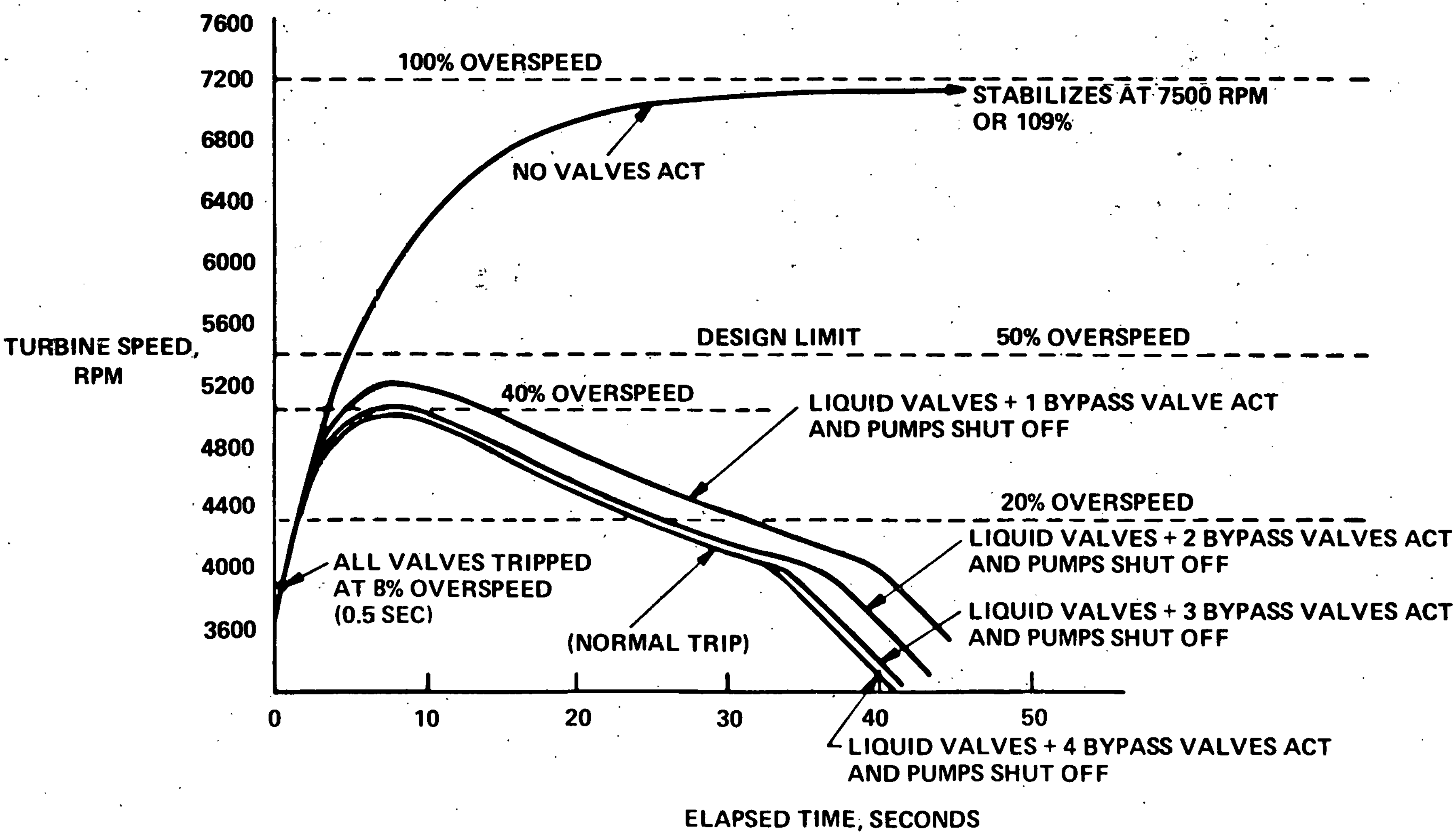

Figure 6-82
10 MWe TURBINE OVERSPEED PROTECTION

If three of the four bypass valves fail to act, turbine speed would reach a maximum value of 45% overspeed, still below the design limit of 50%. In Figure 6-81, it was shown that if all bypass valves fail to act (only liquid valves act), turbine speed would reach a maximum overspeed of 60%. This is above the design limitation of 50% overspeed, but still within the mechanical safety margins used to establish this design limitation.

This fault tree analysis shows that the maximum overspeed reached does not significantly change until three of the four bypass valves fail to act. This is a characteristic of the parallel flow paths formed by the turbine and bypass valves. As the total wide open flow area of the bypass valves is increased, the effect on total flow resistance approaches a constant minimum value. Further increase in flow area has negligible effect on turbine flow rate. For this configuration, the bypass valve sizes were selected to provide this additional overspeed protection characteristic.

6.5.3.3 Transient System Response Characteristics

Figure 6-83 illustrates the transient system response characteristics of the 10 MWe configuration to an opening step function of the bypass valves. With the vapor flow rate out of the evaporator just below the maximum vapor production capability of the evaporator, the closed bypass valves are stepped open from a total flow area of 0 to 88 square inches.

Results are based on preliminary analysis. The step function was arbitrarily chosen to illustrate system response. Actual time response is a function of both the magnitude and rate of change in valve position.

From Figure 6-83 it is apparent that the following significant effects occur when the system stabilizes following the transient step function:

- Turbine inlet pressure and temperature levels decrease
- Total mass flow rate of vapor out of the evaporator returns to its initial value, but the volumetric flow increases and energy flow rate (BTU/sec) decreases

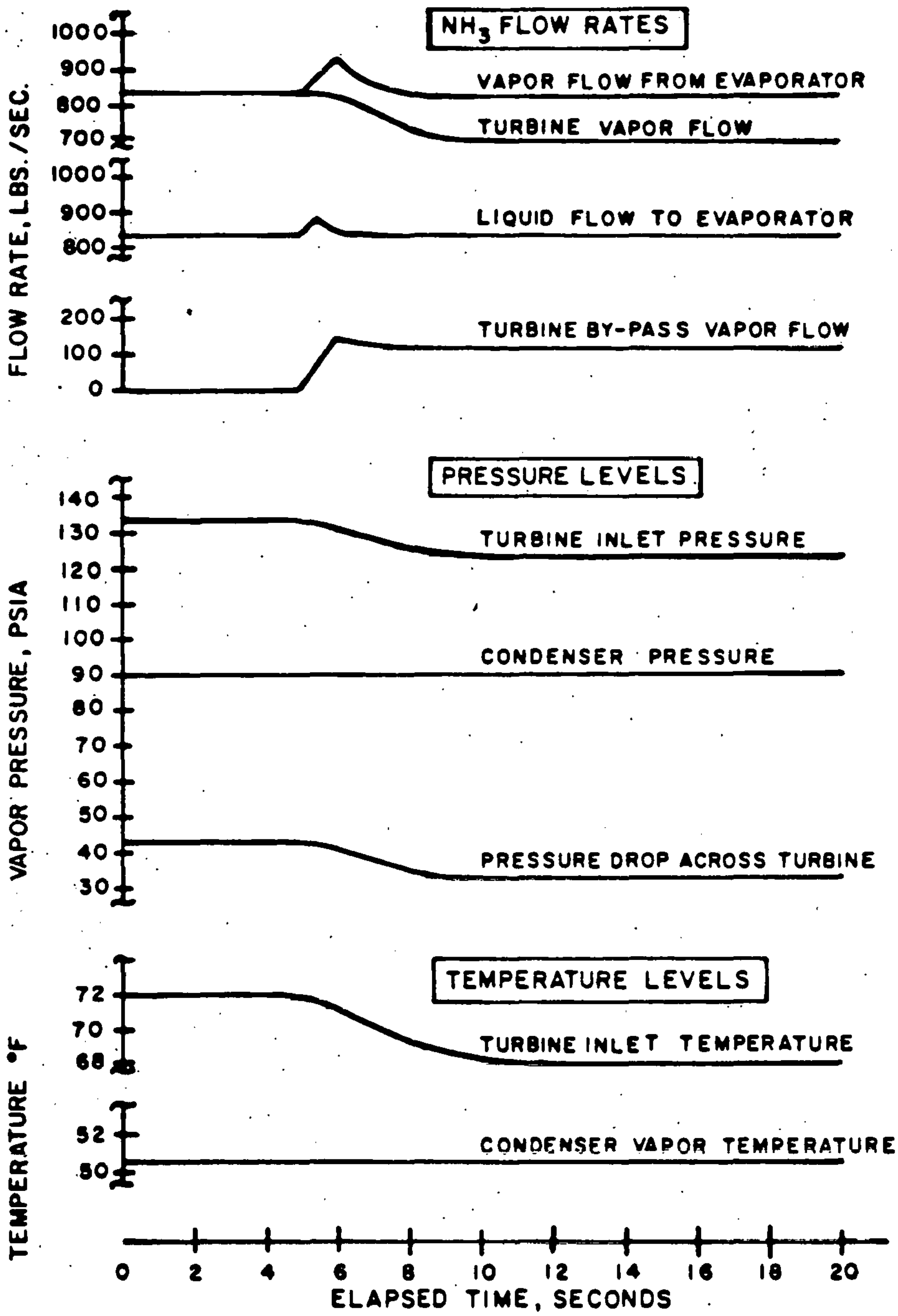

Figure 6-83

10 MWe TRANSIENT SYSTEM RESPONSE TO OPENING STEP FUNCTION OF BYPASS VALVES FLOW AREA FROM 0 TO 88.9 SQUARE INCHES

- Pressure drop across turbine decreases
- Mass flow rate through the turbine decreases

Turbine load, which is a function of both mass flow rate and inlet pressure and temperature conditions, decays.

6.5.4 Maintainability

The objective of the maintainability studies was to develop a practical maintenance program which will enable availability projections to be made and design work to proceed in light of the preliminary maintenance plans. Although station-keeping facilities, including radar, radio, hotel accommodations, transportation, etc., are not discussed, some of these facilities may impact maintenance effectiveness.

The maintenance concept assumes that the OTEC 10 MWe module platform will be positioned less than 5 miles off-shore. It will be operated and maintained by a selected crew either permanently assigned to the platform for indefinite periods or transported to and from shore per their watch/shift schedule. Infrequently needed special skills will be transported to the platform as required. It is assumed that personnel with specified skills are on duty 24 hours per day, and certain special skilled persons may be made available within 4 hours after notification. Barges will be used to support and resupply the platform for the larger/ heavier materials and equipment. Other than these barges, the platform itself will provide all necessary spares and maintenance support facilities.

More particularly, the maintenance facilities were assumed to be as follows:

a. Sheltered and environmentally controlled maintenance rooms available at elevation 82 on the OTEC platform.

b. With the exceptions included in c. below, the maintenance room is provided with sufficient quantities and types of the following items to effect all maintenance actions consistent with Section 6.3.4 of this report:

- Spare components and materials
- Consumables
- Test and inspection equipment
- Tools
- Machinery
- Fabrication facilities
- Jigs and handling equipment
- Diving gear
- Breathing apparatus

c. A space on the platform is provided with the necessary fixtures, handling equipment, and semi-permanent shelter to permit repair/replacement of the seawater pumps. Space is also provided for storing the larger/heavier spares and temporary storage of the larger platform access hatches when removed.

d. The platform is provided with a gantry crane to lift all major components, including the seawater pumps. The platform is also provided with dollies, jacks, and other handling fixtures as necessary for all maintenance requirements.

The costs associated with the specific maintenance tools and maintenance labor, as well as a breakdown of each, are given in Section 6.7.2.

6.6 Testing Considerations

The purpose of the test program is to demonstrate OTEC power system feasibility and operational performance in situ and to obtain data for future designs. This will be achieved by development of overall system and individual element research plans for operational data measurement, recording, playback and analysis.

The hardware includes an evaporator, condenser and an ammonia recycle pump, ammonia feed pump, seawater pumps, turbine, generator and all of the ancillaries of the 10 MWe Modular Application power system. Specific objectives achievable from testing include verification of:

- Thermodynamic performance
- System dynamic stability and operational controls
- Mechanical design
- Reliability/availability/maintainability and safety

6.6.1 Test Objectives

The scope of the testing program is to determine:

- Heat exchanger characteristics
- Overall system and individual element thermodynamic performance
- Fouling characteristics
- Effect of ammonia/seawater on materials
- Steady-state operating characteristics
- System transient dynamics
- Part-load and off-design conditions performance
- Reliability/availability/maintainability and safety performance

6.6.2 Program Development

By applying objectives to overall system and individual element operations, a series of test questions was developed by the individual component designers and systems designers. Next, research plans outlining an approach for the resolution of the questions were developed. They specify test procedures, data requirements, instrument locations, and data-sampling requirements. Finally, test hardware consisting of data acquisition, data playback, test instrumentation and data analysis equipment was developed to implement the research plans and fulfill test objectives to support design schedules.

This approach to program development is illustrated in Figure 6-84. A general overview of data requirements, obtained by an analysis of test objectives versus system elements, is presented in matrix form in Figure 6-85.

The instrumentation effort is a survey of hardware and technologies applicable to the test program, and considers parameters such as:

- Measurement range
- Measurement accuracy
- Compatibility with OTEC environment
- Cost
- Commercially availability versus development items

The data acquisition and analysis effort develops a design to meet the test requirements, but provides flexibility to adapt to changes in number of sensors, sample frequency rates, etc. The systems' real time analysis capability provides the operation with performance values, data tabulations and graphic displays. Another system feature is simplicity of installation, operation and maintenance. The system is designed for compatibility with the modular power system design concept. Satellite data modules are packaged within an envelope of a few cubic feet. The central processor, data storage, man-machine interfaces and system peripherals are designed to be installed in a mobile, 40-foot long trailer/laboratory.

The results of this effort are summarized in the sections that follow.

6.6.3 Research Plans

6.6.3.1 Measurement Frequency

Most temperatures, pressure and flows will be read every 10 minutes. Measurements required for the heat exchanger algorithm verification will be read every 5 minutes. These include seawater flow rates, inlet/outlet temperatures, ammonia flow rates, and saturation temperature.

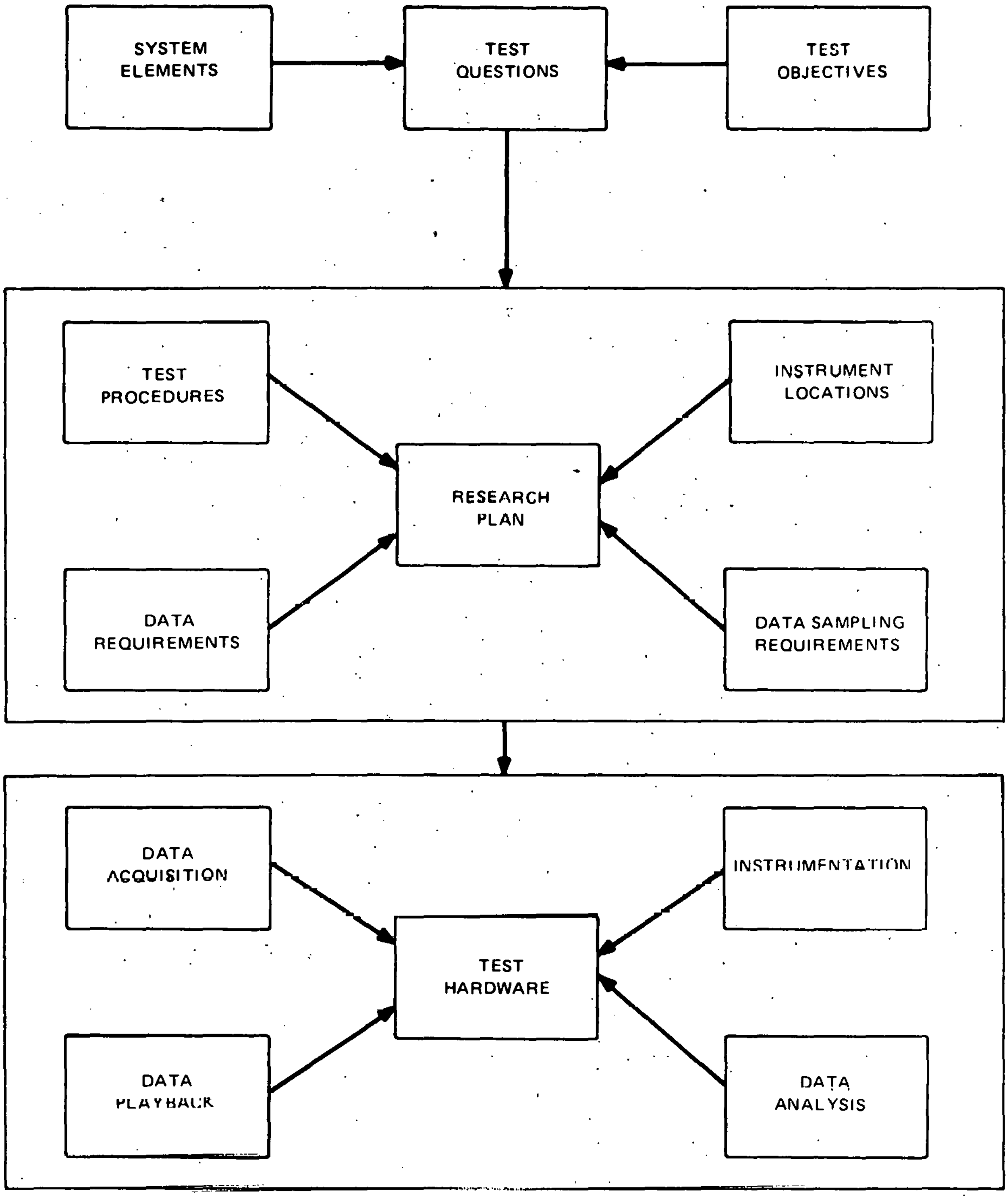

Figure 6-84
TEST PROGRAM DEVELOPMENT

KEY:

P – PRESSURE
T – TEMPERATURE
F – FLOW
A – ACCELERATION
C – CHEMICAL
B – BIOLOGICAL
E – POWER

TEST OBJECTIVES / SYSTEM ELEMENT	HX'S AND MOISTURE SEP.	TURBINE/GENERATOR	NH_3 FEED AND RECIRC PUMPS	WARM AND COLD SW PUMPS	CONTROL AND STORAGE SYSTEM	NH_3 AND SW PIPING
Overall System and Individual Element Themodynamic Performance	PTF	PTF E	PTF	PFE	PFE	PTF
Individual Element Vibration and Rotating Element Balancing	A	A	A	A		
Fouling Characteristics	BT	E		B		
Effect of Ammonia/Seawater on Materials	C	C	C	C	C	C
Steady State Operating Characteristics	PTF	PTF E	PTF E	PTF E	PFE	PTF
System Transient Dynamics	PTF	PTF E	PTF E	PTF E	PFE	PTF
Off-Design Conditions Performance	PTF	PTF E	PTF E	PTF E	PFE	PTF
Heat Exchanger Characteristics	PTF	E	F	F		
R/A/M and Safety Performance	All Measurements for all Elements					

Figure 6-85
TEST OBJECTIVES VS. SYSTEM ELEMENT DATA REQUIREMENTS MATRIX

The plant heat balance test will be 2 hours in duration. During this test interval, measurements used directly in the heat balance calculations will be ready every 5 minutes. Operational performance testing will require short duration, high frequency data measurements. Typically, during a loss of load test, measurements will be read 5 times a second for a period of 60 seconds.

These measurement frequencies represent typical values. Specific case sampling frequency and test duration should be determined by an accuracy analysis in a subsequent detail phase. The early segments of the test schedule will be concerned with special-purpose testing and will require relatively higher measurement frequency rates. Following this specified period of special purpose testing, the 10 MWe power system will be scheduled to run at steady-state design conditions for long periods with lower measurement rates.

6.6.3.2 Heat Exchanger Characteristics

The test and measurements for the Modular Application will be the same as those developed for the test articles, as described in section 5.5. In effect, the Modular Application will verify results obtained from test article testing. Testing will include verification of heat transfer algorithms, ammonia and seawater distribution, and steady-state and off-design performance as described for the test articles. However, the following will not be included in the Modular Application testing:

- There will not be a vapor recirculation loop; thus control of vapor velocity will be limited.
- Measurement of ammonia feed to individual distribution chambers.
- No heat exchanger sight ports are planned.

Of course, the reliability and materials testing described in section 5.5 will be expanded to reflect the need for data pertaining to a whole power system and not just heat exchangers.

6.6.3.3 Power System Thermodynamic Performance

Thermodynamic performance testing will consist of performing complete heat balance calculations of the power system while operating at an ocean site. Overall system and individual element performances will be analyzed. The test will be performed at designed steady-state conditions; but additional tests, measuring the same performance parameters, will be performed at off-design conditions. Tests will ascertain overall and individual element efficiencies and evaporator reflux rate.

The following plant/element performances will be calculated using test data:

- Gross power system efficiency
- Net power system efficiency
- Turbine cycle efficiency
- Turbine efficiency
- Generator efficiency
- Evaporator enthalpy
- Evaporator reflux rate

Heat balance calculations will be performed during steady-state plant operating conditions. During each test, the plant will be run at design load for a period of 2 hours. Additional time will be allowed to enable the power system to stabilize before testing begins. Data readings will be taken over the entire test period, and calculations will be performed using data averaged over the collection period.

A series of tests will be performed for off-design conditions. Off-design seawater temperature testing is achievable as such conditions become available on site, or by mixing the seawater in the plenums before the heat exchangers. A variation of $\pm 5\%$ in seawater pump flow capability provides additional potential off-design testing combinations.

6.6.3.4 Control System Performance

The control system is designed to maintain system stability during startup, during steady-state with design load, and during existence of normal and emergency transients. A dynamic computer model was designed to simulate control system response characteristics. One of the first test objectives will be the verification of the predictions of the control system dynamic models.

Tests are specifically concerned with the system operational performance characteristics during:

- System startup while coming up to full load
- Stabilized operation at full load
- Step load changes, or changes in operating parameters such as seawater temperature
- Loss of load conditions
- Emergency shutdown

Many of the measurements required for control system testing, including pressure and flow measurements in the ammonia loop, have already been identified in previous test descriptions. Others are unique to control system operation and include control valve position and control signals, and make-up and dump line flow rates.

Of special interest is the flow and pressure drop in the ammonia vapor lines. It is especially important that vapor flow be measured in the lines that split between the turbine and bypass valves. The flow and change in pressure across the ammonia pumps will be measured. All temperatures associated with ammonia flow will also be measured.

Recorded data will provide the material for performance curves that will be used to analyze system responses and evaluate computer predictions. These plots include:

- Turbine vapor flow vs lift/diameter of control and bypass valves
- Turbine vapor flow vs small changes in control valve position
- Ammonia vapor flow vs time
- Turbine speed vs time
- Ammonia vapor flow vs the sum of ammonia feed and recirculation flow
- Pump discharge flow vs pressure
- Valve position vs time
- Error signals vs time

The control system includes its own system operation simulation program. It will be used following the installation of the control system to verify control logic and valve responses to system operating conditions.

Following startup, turbine overspeed protection will be addressed during the first phase of the control system tests. The load will be dropped at a level of load or flow which is safe, with respect to overspeed, but yet high enough so that characteristics of overspeed protection can be verified. Analysis of the system characteristics plots will provide verification of system overspeed protection and verification of the computer dynamic model predictions.

The system will be operated with full rated load in a steady-state condition to test the ability to maintain stabilized operation. This ability will then be further tested with step load changes and off-design changes in available temperature differential and seawater flow rates. In addition to performing normal operating sequence shutdowns, a number of emergency shutdowns will be performed. During the emergency shutdowns, time requirements will be established for: (1) pumping out liquid ammonia and (2) drawing out vapor ammonia.

6.6.3.5 Rotating Elements

This section covers performance testing of the turbine/generator, seawater pumps and ammonia pumps.

The turbine and generator will be tested under actual operating conditions. As previously discussed, performance testing includes turbine, generator and turbine cycle efficiencies. The turbine and generator will be instrumented to measure vibration and rotor balance.

The Modular Application is the first opportunity to test the seawater pumps in operation with the total power system. Pump parameters, such as power requirements, flow rates, and speed will also be measured during all tests. Power requirements are a key measurement, since the seawater pumps are the system's greatest parasitic loss. These parameters will be used to develop pump performance curves for comparison with predicted pump characteristics. Other pump tests will address the following:

- Pressure profile across the pump
- Pump vibration and balance characteristics
- Pump seal leakage
- Pump characteristics at off-design flow rates
- Verification of actual pump start-up characteristics, as predicted

Pump flow rates, pressures, temperatures and power requirements are being measured for other system tests and will provide some of the pump data requirements. The pumps will be instrumented to measure vibration and rotor balance.

Ammonia pump test data will be collected during all the system and element testing. Pump power requirements, speed, ammonia flow rates, pressures and temperatures will be recorded during all tests. These parameters will be used to develop pump characteristic curves for comparison with predicted characteristics. The pumps will be instrumented to measure vibration and rotor balance.

6.6.3.6 Environmental Considerations

A certain correlation exists between the Modular Application performance and local environmental conditions. The following data will be recorded during testing, and data impact will be considered during performance analysis:

- Water column temperature distribution
- Water column currents
- Sea state
- Local biological data
- Weather conditions

In addition, the local chemical and biological baseline of the site will be determined before testing is started. Periodically the baseline will be updated to determine the effect of the OTEC plant on the local environment.

6.6.4 Test Setup

The test data requirements and instrumentation location for the Modular Application are shown in Figure 6-86. The Figure represents a summary of all the various data requirements identified by individual research plans. Individual sensors are numbered for purposes of identification.

6.6.4.1 Instrumentation

The instrumentation presented in the following paragraphs is the result of a survey of hardware and technologies applicable to the OTEC program. The results consider current practices in testing, availability, capabilities, and problems which can be encountered by using certain types of instrumentation.

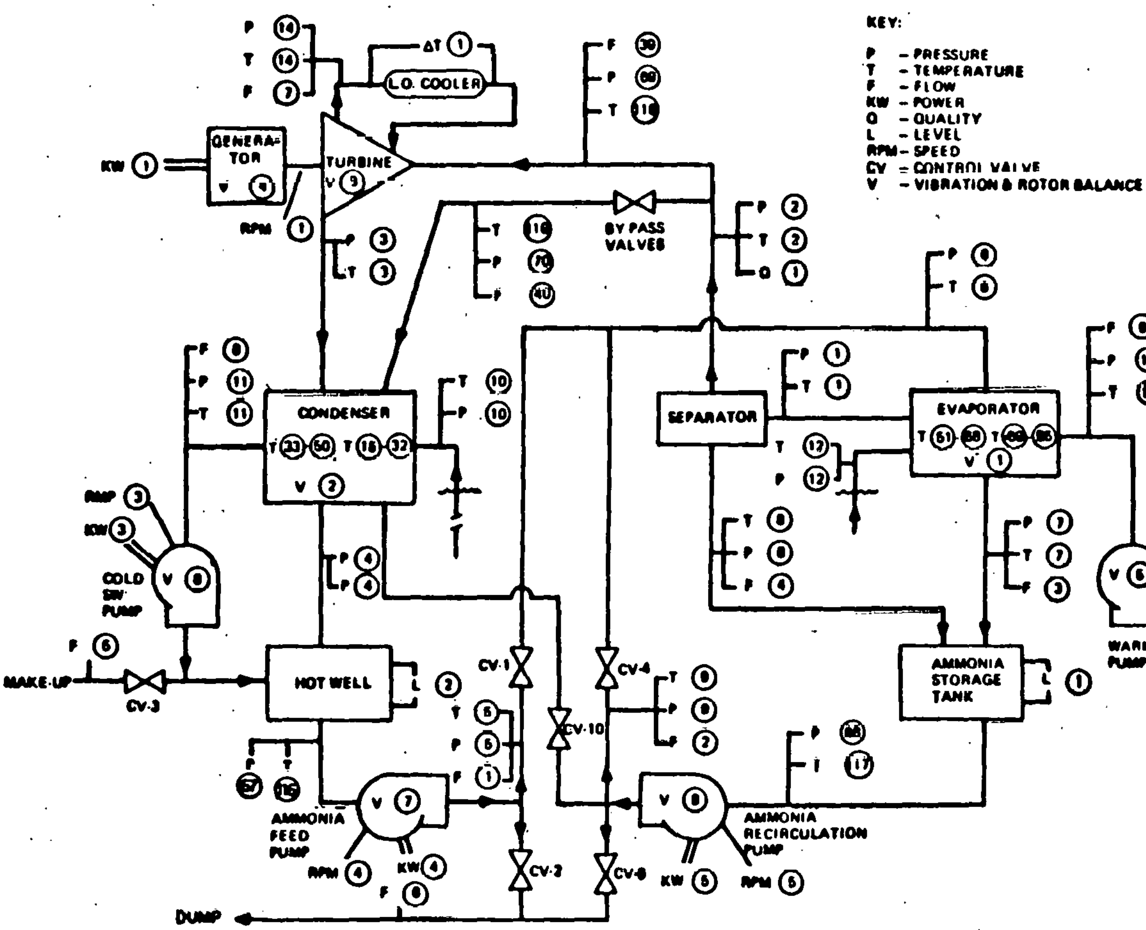

Figure 6-86
MODULAR EXPERIMENT - TEST DATA REQUIREMENTS

6.6.4.1.1 Temperature Measurement

Measurement of fluid temperature is required at a large number of locations. A fully automatic measurement system for continuous recording of temperature values is recommended.

Temperature measurements will be made by installing one or more thermocouples at all the required locations. Multiple sensors will be required to measure temperature in large diameter pipes. The thermocouples will be encased in metallic probes to measure temperatures at any point of the flow. The temperature will be monitored by attaching the thermocouple to an electronic ice point reference junction. The electronic ice point will compensate for the ambient temperature at the reference junction and then supply the correct EMF to the data acquisition system.

In certain locations, the measurement of temperature difference is probably more important than the value of the absolute temperature at the two locations. For these cases the use of thermopiles is recommended. Since the thermopile is basically a thermocouple with a measuring junction at each of the two locations, the problem of a reference junction is avoided and the thermopile measurement can be made with considerable accuracy. The EMF's generated at each location interact, and the result is a voltage proportional to the temperature difference between the two locations.

6.6.4.1.2 Static Pressure Measurement

The large number of static pressure measurement locations required suggest the use of electrical pressure transducers for automatic and continuous recording.

Static pressure measurement will be made by installing one or more passive pressure transducers (i.e., strain gage, capacitive or linear variable differential transformer) in each of the required locations. Pressure measurement in small piping (< 48 inches), around coupon rack locations, and the lube oil location will be made with one transducer. Measurement in larger components and large piping may require three to four transducers to obtain representative pressures if the flow is suspected to be non-uniform.

To monitor pressure, a known voltage is input and the change in electrical impedance is measured. The resulting millivolt signal, which is proportional to the pressure, is then amplified, conditioned, and converted into a form usable in the computer.

Fluid pressures will be sampled through wall taps and/or static pressure probes in the pipes or fluid chambers. The pressure transducers may be mounted directly onto the components using vibration isolation mounts or mounted in central locations with pneumatic lines between the components and the sensor. A Scanivalve may be used to decrease the number of transducers required in one location.

6.6.4.1.3 Velocity Measurement

Velocity measurement of ammonia vapor is required in the test article at the evaporator outlet, throttle inlet and vapor recirculation pump. The velocity at the throttle inlet and vapor recirculation pump may be deduced from the flow, temperature and pressure measurements at the same location.

To measure the velocity distribution across the evaporator bundle outlet, a series of pitot tubes or holes located at stagnation points on aerodynamic bodies may be used to traverse the length and breadth of the evaporator outlet. The number and spacing of pitot tubes would be determined by estimation of the velocity profile. The extent of pitot tube arrays should be determined in detailed design, and cost should be an important factor. Measurements may also be made individually if conditions permit.

6.6.4.1.4 Flow Measurement

Flow measurements are required for seawater and liquid and gaseous ammonia in the test article and 10 MWe Modular Application. Three methods of measuring flow will be described.

Flow metering devices such as nozzles and orifice plates are used in pipe diameters 16 inches or less and probably in pipes up to 24 inches in diameter. Further investigation and development for use in larger pipe sizes are necessary. The static pressures would be measured using the pressure transducers described in the pressure measurement section.

Flow measurement in pipe over 24 inches in diameter are made using acoustic flow meters. The acoustic flow meters used may be the Leading Edge Flow Meter (LEFM) system developed by Westinghouse Oceanic Division. Acoustic LEFM measurements for ammonia vapor may require further development due to anticipated OTEC pipe sizes. The LEFM system has a dedicated electronic console which can be patched into the main data acquisition computer for "real time" computation of heat balance, etc.

The use of chemical or radioactive tracers for flow measurement can be used if cost trade-offs for its research and development and practicality prove feasible with respect to the other methods.

6.6.4.1.5 Quality Measurement

The quality of ammonia vapor is required at two locations in the test article and one location in the 10 MWe Modular Application. Quality may be measured by either using current techniques or through the development of new innovative techniques.

Quality measurements may be made using available throttling or separating calorimeters which have an electrical output. The calorimeter system may be modified to provide on-demand sampling of ammonia vapor via a remote controlled valve. Low activity radioactive isotopes such as sodium-24, are used for quality determinations in steam power plants and cooling towers. A study of available tracers and their compatability with liquid ammonia is necessary to develop a safe and accurate system to handle, test and measure ammonia vapor quality.

The following innovative techniques using acoustic and laser light technologies are presently in developmental status. The first technique proposes using acoustic energy to disperse large droplets of water in wet steam to a uniform "fog". Then, using an acoustic flow meter, the acoustic velocity of the saturated vapor can be determined, from which the quality of the vapor can then be obtained. The second technique proposes using a laser light scattering probe to determine the quality of steam at the low pressure end of steam turbines. Vapor quality is a function of the attenuation of the emerging light beam.

There is no clear-cut approach to be taken. Many factors must be considered at the detailed design phase and trade-off studies should be made since the approaches presented here require some degree of development work for use in the OTEC 1 Program. The factors which enter into the consideration are as follows:

- Time necessary to develop and prove feasibility in saturated ammonia vapor
- Time necessary to procure the instrumentation for installation
- Cost of developmental work and production
- Automation of measurements and recording of data
- Accuracy, repeatability and sensitivity obtainable

6.6.4.1.6 Vibration Measurement

In the test article, measurement of heat exchanger tube vibration is required for each of six tubes in both the evaporator and condenser. In the Modular Application, these same measurements will be made for the evaporator and condenser. In addition, the vibration of the six major rotating components will be monitored. The purpose of the vibration measurements is to provide warning of excessive vibration levels in the heat exchanger tubes and rotating equipment. It will also be possible to monitor the state of balance in the rotating equipment and determine when overhaul and/or rebalancing is required. Pump balance will require a two-step process: (1) mechanical balance of machinery, and (2) thrust balance of the fluid moved.

Vibration measurements in the six tubes of each heat exchanger will be made by installing a two-axis piezoelectric accelerometer in each tube. Twelve sensors will be required for both the test article and Modular Application. The signals from the sensor will be routed to a signal conditioning box where they will be suitably amplified, filtered, level detached and then relayed to the computer for interpretation. The vibration measurements for the rotating equipment will be made by installing eddy current promixity devices at the journal bearings of the turbine, generator, ammonia and seawater pumps. A two-axis system at each bearing will be used to make journal orbit measurements and monitor the actual rotor vibration levels. Sixteen sensors will be required for the Modular Application. Considerations of cost and accessibility may make the technique of using accelerometers to measure pump vibration levels an attractive alternative. If this technique is used, measurement of pump vibration levels will be accomplished by installing piezoelectric accelerometers on the bearing housing of the pumps.

During routine plant operation an average value of the vibration level in the appropriate frequency band is determined at the signal conditioner to represent the vibration state at the measurement location. This average value is then sampled by the computer at the appropriate time intervals and compared with present levels stored in the computer's memory. This approach allows for an automatic monitoring of the vibrational condition of the heat exchanger tubes and the rotating equipment. Diagnostic investigation of the frequency response of the vibration at any of the sensors will be accomplished on an individual non-automatic basis by sampling the unfiltered amplifier output with a narrow band spectrum analyzer. This operation will be conducted by an OTEC plant technician on a much less frequent basis than the automatic computer sampling.

6.6.4.1.7 Speed Measurements

Speed measurements are required for the pumps and the turbine/generator in the 10 MWe Modular Application. These measurements will be used to monitor performance and efficiency of the power plant. To maintain commonality of sensors, the use of eddy current promixity probes may be desirable if they are used to monitor rotor balance. Speed measurements are also made by use of timing marks on the rotors.

6.6.4.1.8 Power Measurement

Power measurement is required at all pump inputs and the generator output is required for the 10 MWe Modular Application. The large power values expected will require the use of current and potential transformers to reduce power to measurable quantities. The power will be measured using watt transducers.

6.6.4.2 Data Acquisition System (DAS)

The data acquisition system should be a modularized system easily adaptable both physically and electrically to any ultimate system configuration. The basic subsystem should be made up of readily available commercial grade components. It is to be used as both a diagnostic and evaluation tool during the system tests of the power plant and as such should be configured to allow ease of operation and maintenance with a minimum of instructions. More specific design objectives are listed as follows:

- Provide a means of continuously monitoring and storing for permanent record up to 350 test parameters
- Provide on-line monitor, analysis and computation of all recorded parameters
- Provide graphic display of monitored, stored and analyzed data

- System accuracy must be at least 1% of dynamic range
- System bandwidth is to be sufficient to faithfully reproduce the various measurement response curves as predicted by the stem computer model for the transient test conditions
- Installation should be modular in concept with sensor signal conditioning configured for installation within the test article if that becomes necessary. Operation is to be controlled entirely from a keyboard or control panel with no access to remote locations. Maintainability should be minimal with replacement of failures done on a modular or component basis
- Flexibility should be incorporated to increase the measured parameters and change the analytical software
- Noise immunity to both electrically and magnetically coupled interference signals must be provided
- Operation must be possible from an uninterruptable power source regardless of demonstration power plant output fluctuations

A conceptual data acquisition system that meets the above objectives is presented in a functional diagram in Figure 6-87. The system utilizes a general purpose digital computer together with the necessary peripherals to provide the data storage and man-machine interfaces. Transducer outputs are signal conditioned, digitized and used as input to the computer for logging, monitoring and analysis by appropriate subsystems. A significant feature of the concept is the modular nature of the various elements of the system and the simplicity of interconnections derived from their relative independency.

The diagram illustrates that the various sensors are powered and monitored by a number of satellite stations. Each satellite is a self-contained data multiplexing module, powered by the uninterruptable source and providing all the hardware necessary to tend the sensors which it services. Signal conditioning will be fixed gain amplifiers with provisions for automatic calibration using precision voltage staircases. Bridge type sensors will be automatically calibrated with shunt

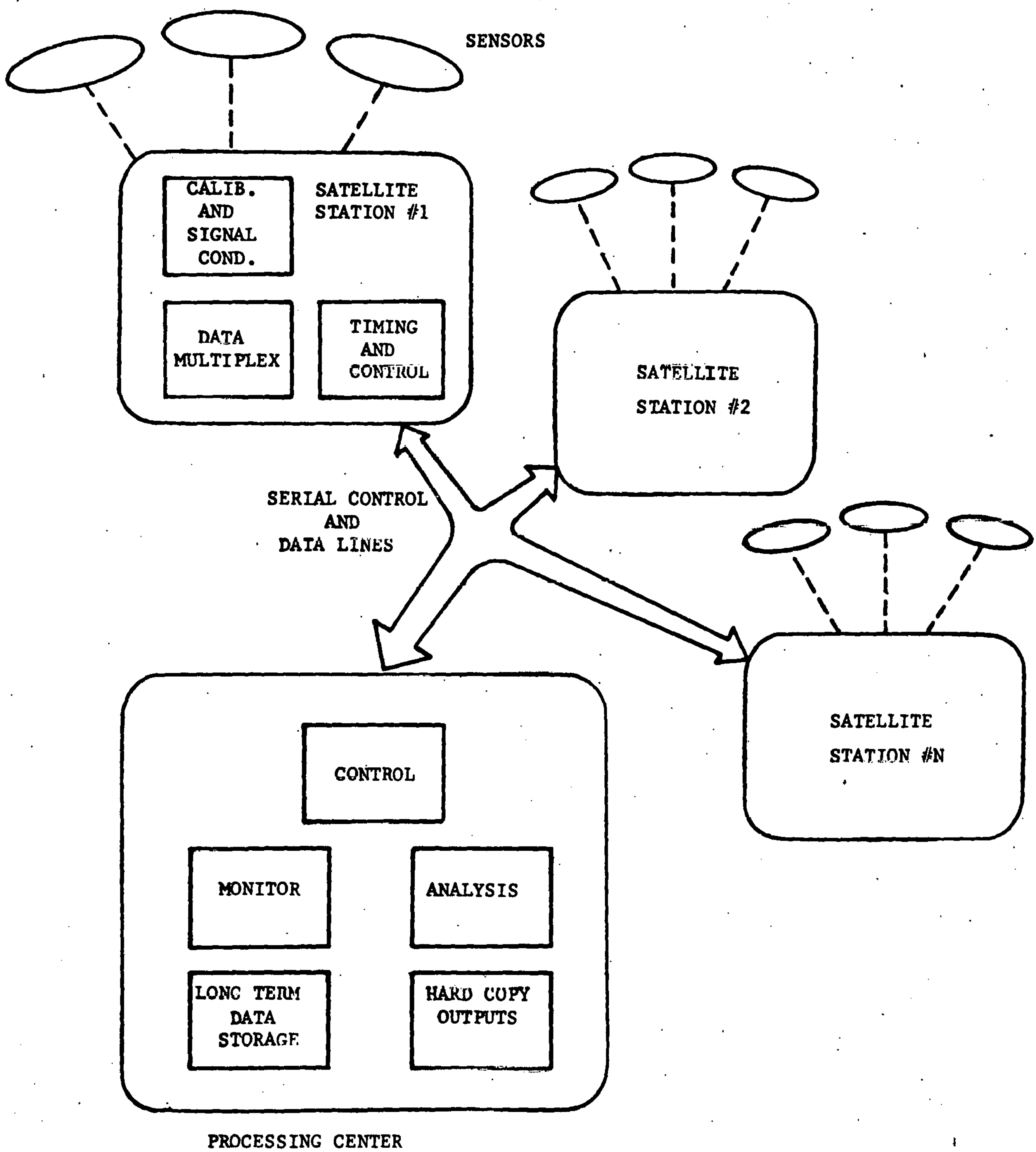

Figure 6-87
DATA ACQUISITION SYSTEM FUNCTIONAL BLOCK DIAGRAM

resistors. The calibration process will be under control of a single board processor commanded by the computer at the processing center. Multiple order low pass filters will be utilized for each channel prior to sampling in order to eliminate spurious input ("aliasing" errors). After low pass filtering, the data signals are routed to the multiplexer and digital converter.

Each of the satellite modules output data upon command to the central processor. The processor and peripherals are also modularized within a small trailer or van that may be located anywhere on the test platform. The data and calibration instructions are transferred between the processing center and each satellite in serial form. Since each module is an independent element, the information transfer is asynchronous. The relatively low sampling rates required of the data acquisition system allows the central processor to serially receive complete frames (all data channels) from all satellites between sample times. While satellites are not reporting they continue to update their output buffers with new data.

The data taken by the satellite stations is collected, analyzed and stored at the processing center. The operator controls the DAS from this center through the use of a general purpose digital computer. The computer will have a library of programs to perform various collection and analysis functions. Figure 6-88 shows a functional block diagram of the processing center.

Once the data from all satellite stations has been received, it is time tagged and recorded on both the data disk and the data tape recorder. In addition to being stored, the outputs of sensors selected by the operator can be directed to the data display for monitoring in either tabular or graphic form. A limited amount of on-line processing, depending on the system sampling rate, can also be accomplished with the results being displayed. A data printer will provide a permanent copy of any tables or graphs put on the data display. In the type of test where the sample rate is slow with minutes between samples, the computer can be used between samples to perform analysis on any of the data previously collected and

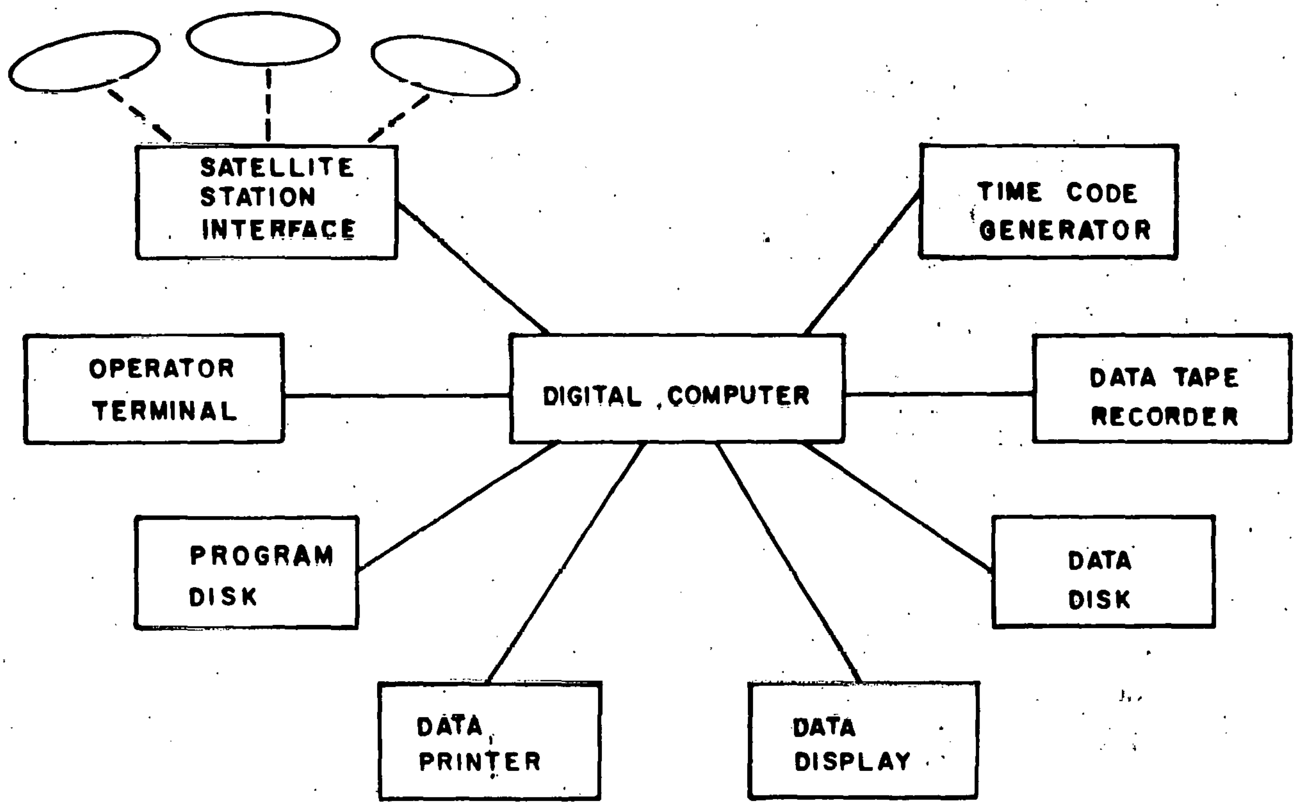

Figure 6-88
PROCESSING CENTER BLOCK DIAGRAM

stored on the data disk. After completion of the test, the computer can be dedicated to data analysis which is limited only by the software library. The digital tape provides a convenient medium for permanent storage of the data and for transferring the data to any other computer facility for further analysis. In addition to its data acquisition and analysis functions, the processing center computer can be used to develop and modify the software library.

6.6.5 Conclusions and Recommendations

This section provides a preliminary Test Program Plan for the 10 MWe power system. Its implementation will achieve OTEC Test Program objectives and goals. Future efforts should be directed to further develop the work as follows:

- Prepare a detailed test and evaluation plan
- Provide specifications for instrumentation and data acquisition system in detail sufficient for procurement
- Define in detail all interfaces between system testing hardware and platforms, system elements and control system

In addition to the above efforts, the tasks described below should also be initiated in support of the Test Program.

6.6.5.1 Accuracy Analysis

This analysis will define acceptable levels of performance calculation uncertainty for the system and individual elements. These accuracy requirements will be used to determine individual sensor accuracies. An accuracy versus cost and feasibility analysis of these requirements may, in some cases, require the employment of statistical techniques include increasing the number of sensors, varying sensor locations, increasing data sample frequency, and increasing test duration. In addition, system geometry and dynamics may also require statistical techniques to reduce data measurement uncertainty.

6.6.5.2 Design of Experiment

This technique determines the parameters of interest for a particular experiment and which parameters will be allowed to vary during the experiment. Predictions regarding parametric interactions known as multifactorial experiments are also developed.

6.6.5.3 Instrumentation Development

Certain measurement techniques discussed in this report require instrumentation development. If any of these techniques are selected as OTEC test instrumentation, a program will be started to develop the hardware required for testing.

6.7 Costs

6.7.1 Capital Costs

Since the 10 MWe power module was designed through the preliminary stage with currently available technology, the estimate of cost was obtained for the single chosen design configuration. This estimating approach is contrasted with the use of parametric cost algorithms in the conceptual design of the larger 50 MWe system.

The bases of the cost estimates of the components are listed below. The cost estimates based on actual costs of similar items of equipment are:

- Chlorination System
- Circulating Seawater System
- Compressed Air System

- Control System
- Diesel Oil System
- Generator
- Mechanical Tube Cleaning System
- Seawater Pumps

The component cost estimates based on vendor quotes and published price lists are:

- Ammonia Piping
- Ammonia Pumps
- Ammonia Support System
- Ammonia Valves
- Component Cooling Water System
- Electrical Equipment
- Nitrogen System
- Other Auxiliaries
- Startup/Standby Power System
- Turbine

Since the heat exchangers are large and of unique design, a detailed cost estimate was developed, rather than extrapolating existing cost data for conventional equipment based on dollars per pound or dollars per square foot of surface. Detailed cost estimates were made including labor and material needs. Concurrently, manufacturing feasibility of large heat exchangers of this type was established at three separate Westinghouse Divisions. The results of these studies were the cost estimates for the heat exchangers including separators and hotwells. Table 6-28 contains the form of the cost algorithm for each of the major cost areas.

The summation of these cost estimates, shown in Table 6-29 results in a cost of $2204/KWe for the Modular Application power system.

6.7.2 Operating Costs

Included in this section are the costs associated with operating and maintenance labor, as well as machinery tools and spare parts for maintenance of the 10 MWe power system.

The approach used to develop these costs is based on cost effectiveness. The level of maintenance equipment and spare parts is cost effective if their cost does not exceed the cost of the resulting system unavailability due to a lower level of spares. This trade-off requires detailed information concerning cost of spares, maintenance operations for various spares levels (i.e., repair versus replacement), spares storage, and cost of power plant downtime.

Four categories of maintenance activities are identified for the OTEC 10 MWe power module equipment as shown in Table 6-30.

Skill categories required to effect the defined maintenance activities include those given in Table 6-31.

Table 6-32 summarizes the average maintenance manhours per year estimated for the OTEC plant for the maintenance and skill categories as defined previously. It is estimated that two each of the category 1 and 2 skill levels, specifically trained for OTEC should be on call 24 hours per day

Table 6-28
HEAT EXCHANGER COST ALGORITHMS

	Material	Labor
Tube	$/Foot	$/Foot
Tubeplate	$/Square foot of Tubeplate	$/Hole + Constant
Tube Support Plate	$/Pound	$/Hole
Shell	$/Pound	$/Foot of Weld + Setup cost per plate per spool piece plus constants
Bundle Assemble		$/Tube support plate plus constant
Tubeplate Support Lattice Structure	$/Foot of Structure	$/Foot of Structure
Internal Lattice Structure	$/Foot of Structure	$/Foot of Structure

NOTES: 1) Material Cost is based on weight of material ordered not finished weight.

2) A miscellaneous material of 5% is added.

3) For actual tube material costs of various materials and enhancements, refer to Section 5.2.1.1.

4) Some representative material costs are:

C.S. Plate	.23/#
AL Plate	.95/#
C.S. Structural	.32/#
AL Structural	1.50/#

Table 6-29
10 MWe POWER SYSTEM COSTS ($/KWe)

Ammonia Piping	31
Ammonia Pumps	13
Ammonia Support System	36
Ammonia Valves	15
Chlorination System	30
Circulating Seawater System	16
Component Cooling Water System	18
Compressed Air System	2
Condenser	553
Control	150
Diesel Oil System	3
Electrical Equipment	48
Evaporator	626
Generator	124
Mechanical Tube Cleaning System	110
Nitrogen System	14
Other Auxiliaries	9
Seawater Pumps	208
Startup/Standby Power System	133
Turbine	65
Power System Total	2204

Table 6-30
MAINTENANCE ACTIVITY CATEGORIES

CATEGORY	ACTIVITY
1.	Scheduled maintenances activities not requiring system outage. ● Inspections ● Lubrication ● Cleaning ● Adjustments ● Calibration ● Data recording (levels, temperature, pressure, wear and vibration/noise changes).
2.	Repair of equipment failures/malfunctions not resulting in system outages.
3.	Repair of failures resulting in forced outages.
4.	Scheduled maintenance activities requiring system outage.

Table 6-31
SKILL LEVELS FOR MAINTENANCE

CATEGORY	SKILL
1.	General mechanics - specifically trained for OTEC
2.	Electronic technicians - specifically trained for OTEC
3.	Divers
4.	Welders (certified)
5.	Special mechanics (turbine-generator, seawater pumps)
6.	Special inspector (welding)
7.	Machinists

Table 6-32
MAINTENANCE PERSONNEL REQUIREMENTS SUMMARY

Maintenance Category	Maintenance Task	Skill Category	No. Required per Task	Man Hours per Year
1 & 2	General	1	2	17,532
1 & 2	General	2	2	17,532
1 & 2	Spare NH_3 Pump Bowl	7	1	16
1 & 2	Biofouling & Moving Screen Maintenance	3	3	196
3	Heat Exchanger Repair	1	2	131
3	Heat Exchanger Repair	3	3	196
3	Heat Exchanger Repair	4	1	65
3	Heat Exchanger Repair	6	1	65
3	Turbine Repair	5	1	154
3	Generator Repair	5	1	62
3	Seawater Pumps Repair	5	2	134
3	Seawater Pumps Repair	3	3	201
4	Heat Exchanger	1	2	116
4	Heat Exchanger	3	3	174
4	Heat Exchanger	4	1	58
4	Heat Exchanger	6	1	58
4	Seawater Pumps	5	2	194
4	Seawater Pumps	3	3	291
4	Turbine-Generator	5	2	354
				37,529 Hours

to properly perform the category 1 and 2 maintenance task and to readily effect most category 3 maintenance, if failures occur. The four maintenance persons on duty would be assisted for certain category 3 and 4 maintenance by other personnel as indicated in the Table. These additional persons would be transported to the OTEC platform within 4 hours after their need is determined. Additional manhours required for category 3 maintenance was determined as follows for each skill category.

Manhours (yearly average) = (number of persons required)
x (task time) x (hours per year divided by component MTBF)

Additional manhours required for the category 4 heat exchanger and seawater pumps maintenance task were determined as follows for each skill category.

Manhours (yearly) = (number of persons required) x (task time)

In the case of the turbine-generator category 4 maintenance, because their overhaul is made only once every 5 years, the additional manhours required are determined as follows:

Manhours (yearly average) = (number of persons required)
x (task time) divided by 5

Using this data, the average manhours per year for each skill category can be determined as shown in Table 6-33. Applying a labor costing rate of \$20 per manhour for categories 1 and 2, and \$35 per manhour for the other categories, an annual average maintenance labor cost of \$783,850 is realized.

The list of machinery, tools and parts for maintenance is given in Tables 6-34 and 6-35. This list is consistent with the above and with the availability predictions given in Section 6.3.4. Currently, expenditures of \$33,650 for machinery and tools and \$1,281,830 for spare parts are foreseen as prudent initial investments.

Table 6-33
ANNUAL MAINTENANCE MANHOUR REQUIREMENT BY SKILL CATEGORY

Category	Skill	Annual Manhours
1	OTEC Trained Mechanics	17,779 hours
2	OTEC Trained Electronic Technicians	17,532 hours
3	Divers	1,058 hours
4	Welders	181 hours
5	Special Equipment Mechanics	898 hours
6	Special Inspectors (Welding)	65 hours
7	Machinists	16 hours
	Total Per Year	37,529 hours

6.7.3 Economics of Multiple Plants

The Modular Application power system uses near-term technology based on extensive manufacturing and design experience. Some cost reductions are possible, however, by producing up to eight power modules.

Table 6-36 depicts the estimated costs of the prototype, first production, and eighth production power systems. Cost improvement ("learning") curves are expected to effect cost reductions in the fabrication of the heat exchangers and ammonia turbine. A reduction in titanium tube price is expected to result from the bulk ordering involved in the production of eight power modules. The control system software need only be written for the prototype unit, and the incentive of multiple orders are expected to precipitate an advanced, cost-reduced design of a mechanical cleaning system. All of these affects could result in an 18 percent overall cost reduction.

Table 6-34
LIST OF MACHINERY, TOOLS, AND PARTS FOR MAINTENANCE

Subsystem	Task	Machinery & Tools	Cost	Parts	Cost
Evaporator and Condenser	Leak Check	4 Floating platforms*	$10,000		
	Leak Repair	1 Lowerable platform*	1,000	Tube plugs	$ 100
		3 Plenum isolation plates	N.A.**		
		1 TIG welding equipment	6,000		
Turbine	Repair	Refer to Table 6-35	N.A.	Rotor*	700,000
				Refer to Table 6-35	N.A
Generator	Repair	1 Pulling tool for collector end	N.A.	Refer to Table 6-35	N.A.
		1 Curved steel shim	N.A.		
		1 Wooden support blocks	--		
Warm & Cold Seawater Pump	Repair Pumps	Lifting fixture	N.A.	2 Sets pneumatic seals	40,000
		Bearing installation and removal tools	1,500	2 Sets oil seals	400
		Seal ring installation tools	150	2 Sets bearings	5,000
		Motor tools	N.A.	2 Sets O-rings	300
				Stator coils Brushes Cooling fan motor	2,500
	Repair Power Supply			4 Thyristors 6 Deionizer cart. 40 PC Boards 12 Fuses 1 Surge Network	22,100

*Stored on shore
**Not Available

Table 6-34
LIST OF MACHINERY, TOOLS, AND PARTS FOR MAINTENANCE
(CONTINUED)

Subsystem	Task	Machinery & Tools	Cost	Parts	Cost
Ammonia Feed and Recirculate Pumps	Replace Bowl Assy	Cradles Refer to Table 6-35	N.A. N.A.	2 Bowl Assys 2 Sets Seals and bearings	$ 12,600 800
Power Loop Valves	Replace Bonnet Assy			5 Bonnet Assys	125,000
System Auxiliary & Control Components					
Control Room Equipment	Repair/Replace			List not avail.	100,000
Field Mtd. Sensors	Repair/Replace			List not avail.	100,000
Diesel-Gen	Repair	Supplied w/unit Refer to Table 6-35		Refer to Table 6-35	65,000
Travelling Screens	Repair			Refer to Table 6-35	50,000
Metal-Clad Switchgear	Replace Breaker	Transfer Truck furnished w/equip.		1 - 1200 amp breaker	20,000
480V Unit Substation	Replace Breaker	Furnished w/equip.		1 - 600 amp breaker	5,000

Table 6-34
LIST OF MACHINERY, TOOLS, AND PARTS FOR MAINTENANCE (CONTINUED)

Subsystem	Task	Machinery & Tools	Cost	Parts	Cost
480V Motor Control Center	Repair	Furnished w/equip.		5 - 100 amp molded case breakers 3 Size 1 full voltage starters 2 Size 2 full voltage starters 15 Trip coils Total	$ 7,000
Backup Battery	Replace Cell			1 Battery cell	30
Hydraulic Supply for Control Valves				N.A.	1,000
Cables	Replace faulty terminations			8 KV class cable 600 V power cable 600 V control cable Total	25,000
Ammonia Compressor	Repair				N.A.
N_2-Air				N.A.	
Air Compressors				N.A.	
Miscellaneous Tools for General Shipboard Use			$15,000		

Table 6-35
DETAIL LIST OF MACHINERY, TOOLS, AND PARTS FOR MAINTENANCE

Subsystem	Machinery & Tools	Parts
Turbine	4 Eye Bolts, 1-1/2" (Lifting Cyl. Cover) 2 Eye Bolts (Lifting Brg. Cover) 1 Extractor, Bushing 1 Gage, Micrometer Depth 4 Guide, Rotor 8 Dowel, Straight 2 Sling, Rotor 2 Jack, Rotor 4 Screw, Jack 1 Wrench, Nut Retaining 1 Wrench, RTD Plug 1 Wrench, RTD Thrust Brg.	1 Rotor* 1 Bearing, Thrust End 2 Temp. Detector, Resis. 2 Terminal Block Assy 1 Bearing Cplg. End 1 Bearing, Turb. Thrust Collar 12 Bearing, Turb. Thrust Shoes 2 Bushings 2 Retaining Nuts 4 Seals, Windback 2 Gland Seals, Static 2 Seal Ring, Gland 2 Seal Ring, Oil 4 Glass, Sight Flow 2 Bushings, Sight Flow 1 Set Bolting
Generator		1 Rotor* 1 Air Cooler, left side* 1 Air Cooler, right side* 1 Bearing 1 Set Oil Seals 1 Set Air Seals 1 Brushholder 1 Brushholder Spring 3 Set Brushes 1 Set Insul. for Brush Rigging 1 Space Heater 3 Sheets Gasket Mat'l, Seals 20 Tube Plugs, Air Coolers 16 Zinc Anode, Air Coolers 1 Set Gaskets, Air Coolers
Ammonia Feed & Recirculate Pumps	2 Sets Installing Clamps 2 Sets Chain Tongs 1 Hook Chain	

*Stored on Shore

Table 6-35
DETAIL LIST OF MACHINERY, TOOLS, AND PARTS FOR MAINTENANCE (CONTINUED)

Subsystem	Machinery & Tools	Parts
System Auxiliary & Control Components		
Diesel-Generator	Hyd. Tighteners, Main Brgs. & Cylinder Heads Extension Gauges Component Lifting Attach. Alignment Tools & Gauges Pullers Refacing & Grinding Tools Extractors Nozzle Tester Special Pliers Special Wrenches Cyl. Press Indicator Torque Wrench Turbocharger Tools Manual Lever, Engine Barring	1 Main Brg. 1 Big End Brg. 1 Cyl. Liner w/Joint Rings & Gaskets 1 Cyl. Head w/Valves, Joint Rings & Gaskets 1/2 Set Cyl. Head Bolts & Nuts for 1 Cyl. 2 Sets Cyl. Exh. Valves for 1 Cyl. 1 Set Cyl. Air Inlet Valves for 1 Cyl. 1 Cyl. Starting Air Valve 1 Cyl. Head Relief Valve 1 Set Cyl. Fuel Injectors 1 Set Connecting Rod Lower End Brg., Bolts, Nuts & Small End Bushing for 1 Cyl. 1 Piston w/Pin, Rings, & Connecting Rod 1 Set Piston Rings for 1 Cyl. 1 Set Gear Wheels 1 Fuel Injector Pump 1 Fuel Injector High Press. Tubing 1 Set Turbocharger Spares
Travelling Screens		1 Sprocket w/Keyseat and Set Screw 1 Sprocket 1 Set Bearing Halves 1 Set Tooth Inserts 1 Set Bolts w/Locknuts 10 Tray Frames 20 PCS Screen Cloth 40 Tray Bold w/Locknuts 1 Set Outside Drive Machinery Spares 1 Set Angle Guides 1 Set Wear Strips, Backup Beam

Table 6-36
10 MWe POWER SYSTEM COSTS ($/KWe)

	Prototype	First Production	Eighth Production
Ammonia Piping	31	31	31
Ammonia Pumps	13	13	13
Ammonia Support System	36	36	36
Ammonia Valves	15	15	15
Chlorination System	30	30	30
Circulating Seawater System	16	16	16
Component Cooling Water System	18	18	18
Compressed Air System	2	2	2
Condenser	553	546	491
Control System	150	140	140
Diesel Oil System	3	3	3
Electrical Equipment	48	48	48
Evaporator	626	546	350
Generator	124	124	124
Mechanical Tube Cleaning System	110	74	74
Nitrogen System	14	14	14
Other Auxiliaries	9	9	9
Seawater Pumps	208	208	208
Startup/Standby Power System	133	133	133
Turbine	65	58	47
Power System Total	2204	2064	1802

7. DEMONSTRATION PLANT (50 MWe)

7.1 Approach to Design Optimization

The objective of the optimization study was to minimize the cost of the power module, represented by the criterion function.

$$C = \text{Module Cost} = F(v_1, v_2, v_3, \ldots, v_n)$$

Where V_1, v_2, ..., v_n are the n independent system variables which define the module design. The actual system variables used are listed in Table 7-1.

Some of the system variables, such as tubeside velocity, are continuous, while others such as tube material, are discontinuous. A numerical optimization technique, pattern search, was used to determine the values of the continuous variables which result in the lowest cost power module for a given set of discontinuous variables. This optimization procedure was used for each combination of discontinuous variables to determine the final choice of a minimum cost power module.

Table 7-1
OTEC SYSTEM VARIABLES

Condenser Saturation Temperature	Continuous
Condenser Seawater Outlet Temperature	Continuous
Condenser Tubeside Velocity	Continuous
Condenser Tube Diameter	Discontinuous
Condenser Tube Material	Discontinuous
Condenser Tube Enhancement	Discontinuous
Number of Condenser Shells	Discontinuous

Table 7-1
OTEC SYSTEM VARIABLES (CONTINUED)

Evaporator Saturation Temperature	Continuous
Evaporator Seawater Outlet Temperature	Continuous
Evaporator Tubeside Velocity	Continuous
Evaporator Tube Diameter	Discontinuous
Evaporator Tube Material	Discontinuous
Number of Evaporator Shells	Discontinuous
Module Net Power Output	Discontinuous

7.1.1 Computer Model

To accurately model the power plant costs, a computer model was written to the following specifications:

- Power module cost and plant cost are functions of independent system variables.

- Heat exchangers and other components not commercially available are first designed to meet heat balance requirements, then lined up for manufacture, and finally cost estimated. Extrapolations of existing designs are not used.

- Commercially available components are evaluated based on suppliers' price data.

- Realistic cost penalties are assigned to unusual designs based on manufacturing difficulty. Multiple commercially available components are used when the capacity of a single component is exceeded. There are no arbitrary or prejudicial limits in the program.

- The optimization procedure is able to cope with non-linear discontinuous algorithms in the criterion function.

The computer model was designed such that a complete thermal and hydraulic balance was calculated for each plant design. Pumping requirements include fictional losses in the ammonia piping, the seawater piping, and the large cold seawater pipe, as well as loses due to the density variance between the warm and cold seawater.

Pattern search(129) was selected as the numerical optimization technique because of its ability to handle the realistic algorithms which generate the cost surface without having a general equation for that surface in a closed form.

In the pattern search method, each independent variable is perturbed in the search for a lower cost power module. After all the variables have been tested, the variable which caused the largest cost decrease is changed in the direction of the decrease, and the testing process is repeated. If any variable is at an apparent minimum (both positive and negative perturbations result in higher costs), the size of its perturbation increment is divided by two, and the search continues. An optimum is declared when the size of each increment is at its lower limit, and all perturbations result in higher costs. The lower incremental limits in the study were 0.125°F for the four temperatures and 0.125 ft/sec. for the two tubeside velocities.

The pattern search method works only if the criterion cost function is monotonic (i.e., has no false minima). The power module cost function used in the computer program was tested by starting the pattern search from different points and comparing the resulting optimum ending points. Results of these tests were consistent in all cases, indicating that the surface is monotonic, and the optimum is valid.

7.1.2 Results

The design optimization program was used to calculate the minimum cost power module of five module sizes: 6.25, 12.5, 25, 50, and 100 MWe.

The results of these runs are depicted in Figure 7-1. As shown, the cost per kilowatt of the power module decreases with increasing module size. The estimated cost of the hull shows a minimum at the 25 MWe size, above which the larger heat exchangers require more costly hulls with deeper drafts. The combined power module and hull cost decreases with increasing size, up to 50 MWe above which the cost slightly increases.

This combined cost criterion resulted in the choice of 50 MWe as the power module size.

Figure 7-2 shows that, although modules using aluminum tubes have a lower initial cost, the added cost of highly probable retubing makes aluminum less economically attractive than titanium, which should not require retubing. If an economical and effective tubeside coating, or a new aluminum alloy resistant to pitting and erosion can be developed, a reduction of up to $250/KWe in power module cost can be achieved. This cost saving would be reduced by the additional cost of the protected aluminum.

The baseline power module which was chosen differs slightly from the optimal power module. The comparison is presented in Table 7-2.

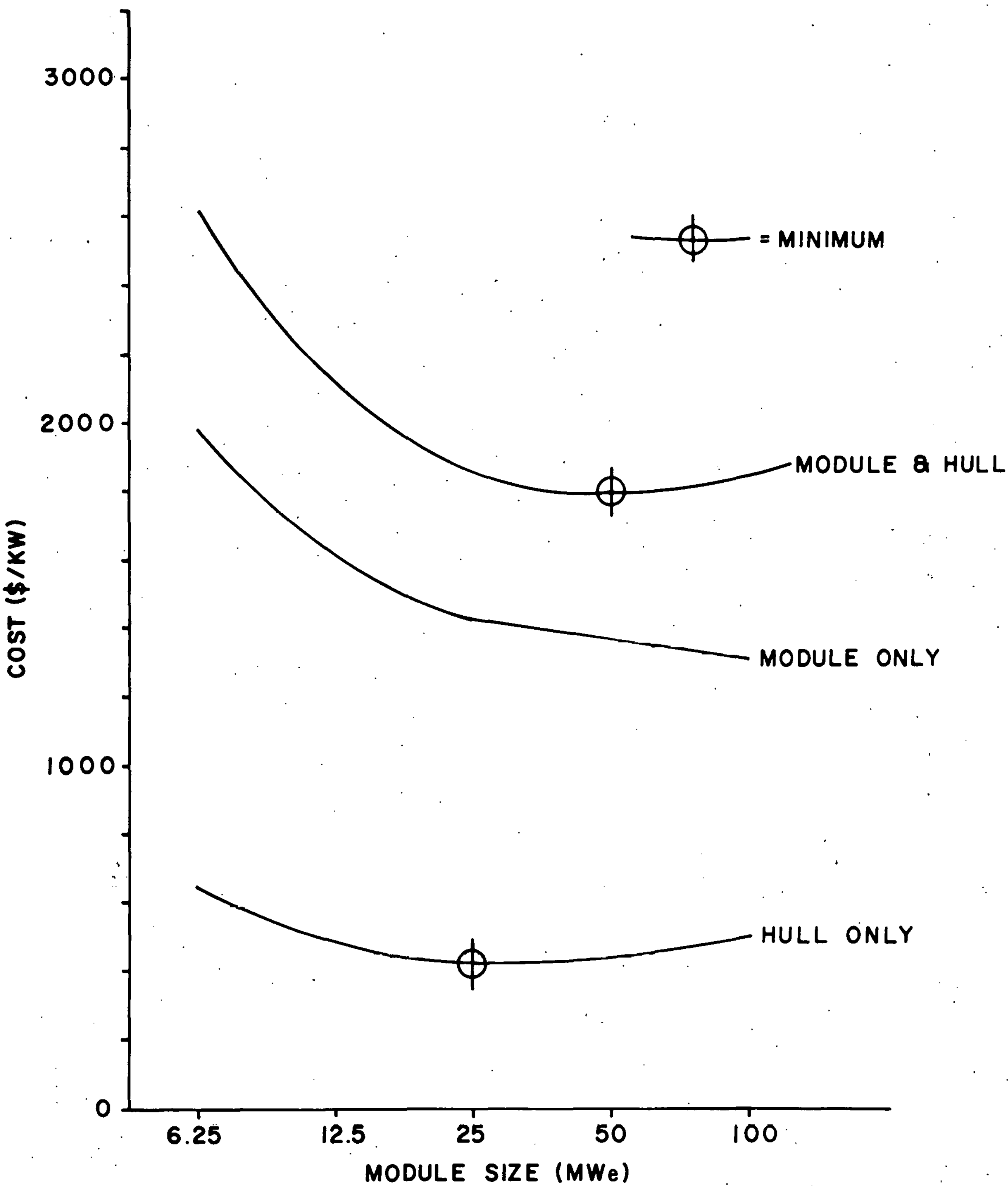

Figure 7-1
MODULE AND HULL COST

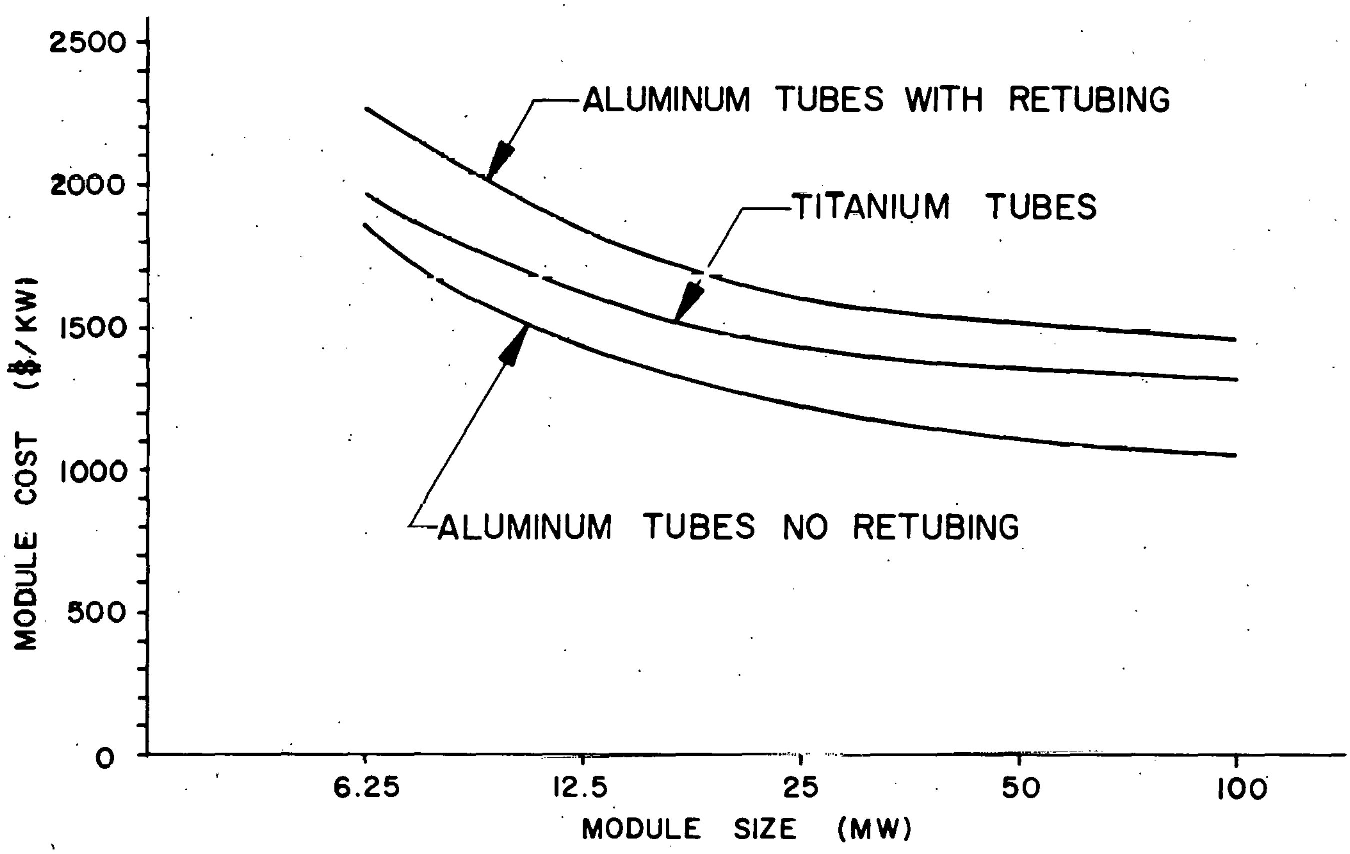

Figure 7-2
MODULE COST VS. MODULE SIZE

Table 7-2
50 MWe PRELIMINARY DESIGN

PARAMETER	BASELINE CONDENSER	BASELINE EVAPORATOR	OPTIMAL CONDENSER	OPTIMAL EVAPORATOR
Saturation Temp (°F)	49.500	70.250	49.500	70.250
Seawater Inlet Temp (°F)	40.000	80.000	40.000	80.000
Seawater Outlet Temp (°F)	46.151	74.505	46.125	74.500
Tubeside Velocity (ft/sec)	5.625	6.500	5.375	6.500
Tube Material	Titanium	Titanium	Titanium	Titanium
Tube Diameter (in.)	1.0	1.0	1.0	1.0
Tube Enhancement (ID/OD)	Plain/Plain	Plain/Linde	Plain/Plain	Plain/Linde
Number of Shells	1	1	1	1
Number of Tubes	206453	206649	214505	204126
Shell Diameter (ft.)	72	72	74	72
Shell Length (ft.)	52	34	50	34
Power Module Cost ($/KW)	1364		1362	

The baseline power module heat exchangers each have 14 tube bundles, while the optimized module has 15 and 14 bundles in the condenser and evaporator, respectively. The 14-bundle arrangement was chosen for ease of manufacture.

The cost impact of variations in each of the six continuous system variables is shown in Figure 7-3. For each of these curves, all system variables except the abscissa variable are held constant at the values for the optimum module. Therefore, each curve represents a two-dimensional slice through the cost function hypersurface. The data for these curves was generated by the design program OTOPT, with its optimization options suppressed.

7.1.3 Heat Transfer Enhancements

The objective of the study was to design the most cost effective power module, not merely the lowest cost heat exchangers. Of all of the enhancement types studied, the four most cost attractive enhancements were plain tubing, Korodense Low Pressure Drop tubing, Linde Condensation Promoter for the condenser, and Linde Porous Boiling Surface for the evaporator. Table 7-3 shows the total cost of optimized power modules made with each of the sixteen combinations of these enhancement types on one-inch titanium tubes. Plain condenser tubes and plain tubes with Linde outside enhancement in the evaporator resulted in the lowest cost power module, and this combination was selected for the preliminary design. The substitution of Korodense tubing in the condenser resulted in a 3% module cost increase, and other substitutions resulted in larger increases. In general, the superior heat transfer performance of the more exotic enhancements is offset by their higher pressure drops and higher tubing costs.

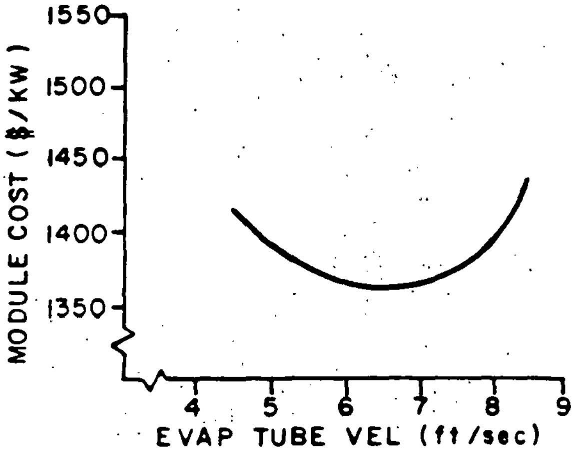

FIGURE A

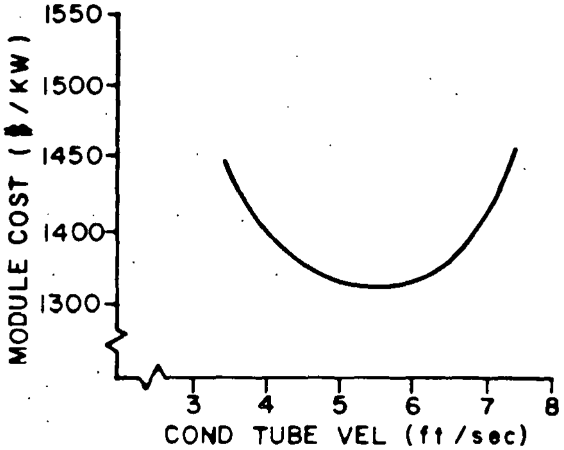

FIGURE B

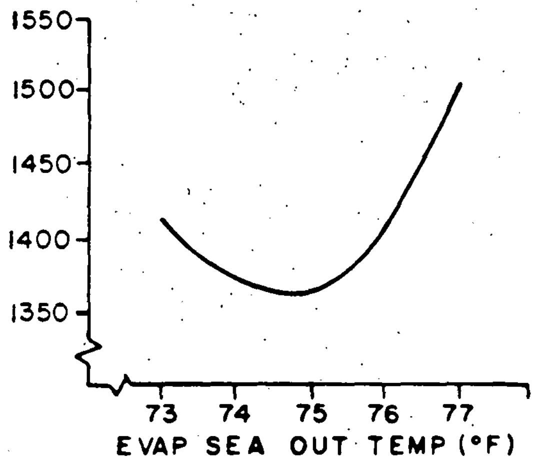

FIGURE C

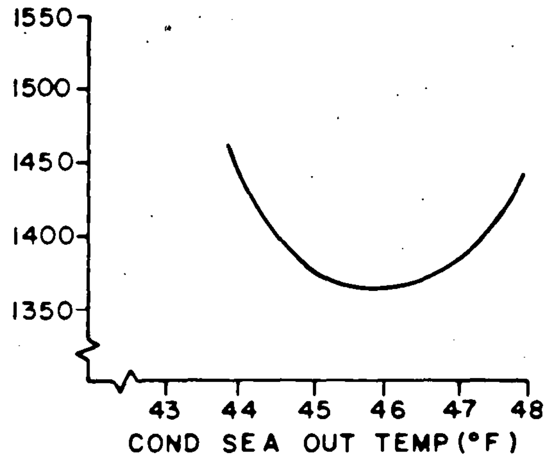

FIGURE D

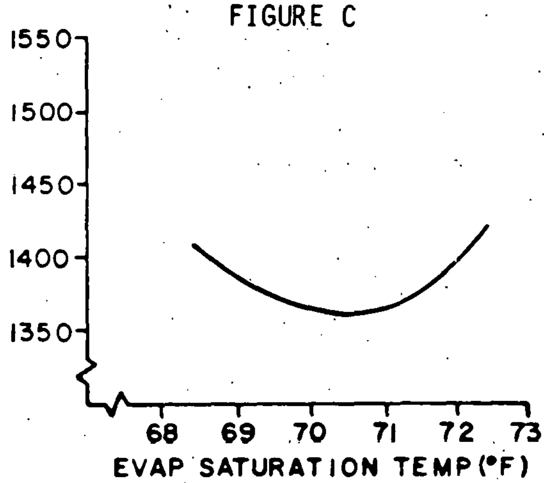

FIGURE E

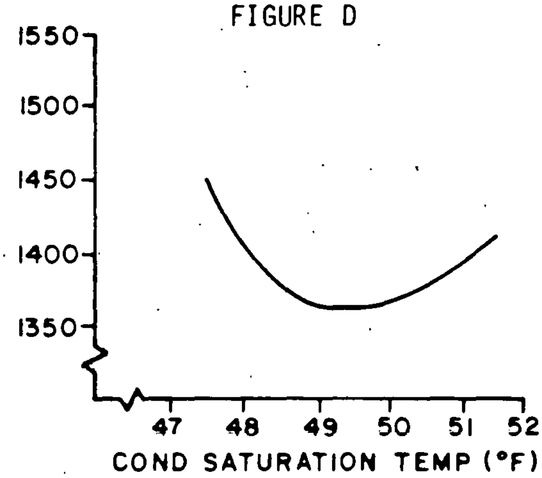

FIGURE F

Figure 7-3
MODULAR COST VS. SYSTEM VARIABLES

Table 7-3
MODULE COST OF ENHANCEMENT COMBINATIONS ($/KW)

Condenser Inside Enhancement -		Plain	Plain	Koro LPD	Koro LPD
Condenser Outside Enhancement -		Plain	Linde CP	Plain	Linde CP
Evap Inside Enhancement	Evap Outside Enhancement				
Plain	Plain	1441	1508	1473	1528
Plain	Linde PBS	1362	1429	1394	1451
Koro LPD	Plain	1562	1630	1593	1650
Koro LPD	Linde PBS	1426	1493	1459	1515

Legend: Plain = Unenhanced tubing
Koro LPD = Korodense Low Pressure Drop Tubing
Linde CP = Linde Condensation Promoter (for condenser)
Linde PBS = Linde Porous Boiling Surface (for evaporator)

Power modules using various tube diameters were designed with the most attractive enhancement (plain tubes in the condenser and Plain/Linde tubes in the evaporator). One inch is shown to be the tube diameter which results in the lowest cost power module, as shown in Figure 7-4.

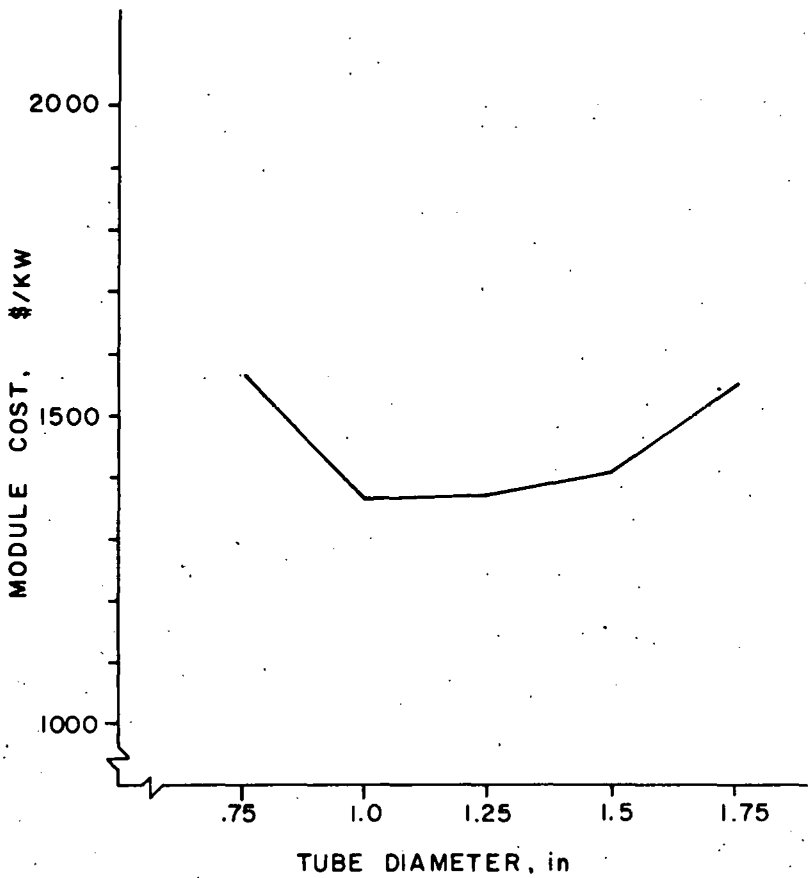

Figure 7-4
TUBE DIAMETER SELECTION

7.1.4 Single Heat Exchangers

The possible benefits of splitting the heat exchangers into multiple shells were investigated. Several factors combine to make this a costly alternative:

- The total cost of heat exchangers increases, as seen in Figure 7-5.
- The manifolding introduces added pressure losses.
- If the motivation for splitting heat exchangers into multiple shells is to allow maintenance of one shell while the module continues to operate at reduced power, leak tight isolation valves are required in each pipe to prevent leakage of toxic and potentially explosive ammonia vapor into the work space. These valves create additional pressure losses.

In conclusion, subdividing the heat exchangers into multiple shells is not desirable.

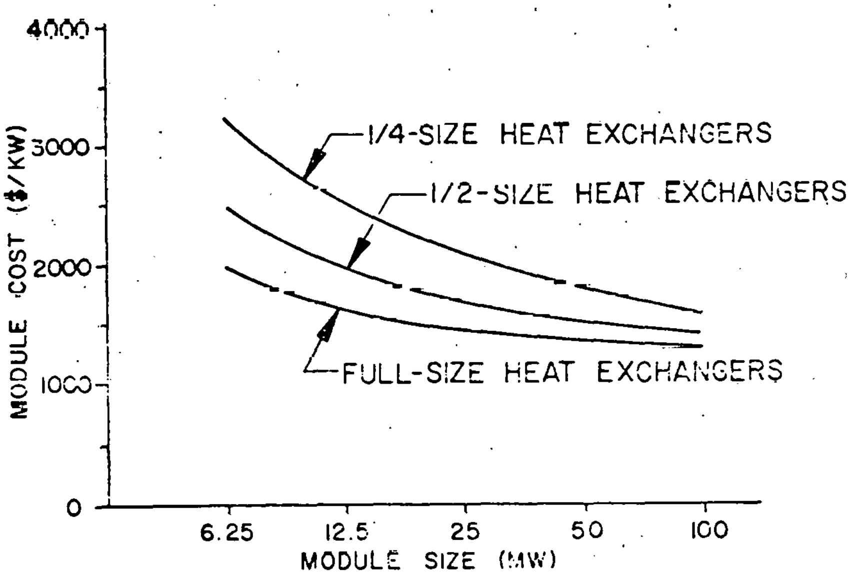

Figure 7-5
MULTIPLE HEAT EXCHANGERS PER POWER MODULE

7.2 Component Design

7.2.1 Heat Exchangers

7.2.1.1 Thermal Design

The major concerns in the conceptual thermal and hydraulic design of the 50 MWe heat exchangers are the determination of heat transfer rates and pressure losses.

7.2.1.1.1 Candidates and Their Correlations

Various types of enhanced heat transfer surfaces are commercially available, and these were evaluated in the context of the overall cost of the power module to arrive at a logical choice based on the cost of the enhancement, the amount of enhanced surface area, and the parasitic losses due to seawater flow resistance.

Seventeen different heat transfer surfaces were considered for use in the heat exchanger. Whenever possible, these were considered for both aluminum and titanium tubes. Of these, nine were appropriate for the condenser, four for the evaporator, and four for either heat exchanger. These surfaces included both plain and enhanced types. The enhanced surfaces fall into four general categories: applied coatings, fins, corrugations, and flutes. (Figure 7-6). The types investigated include only those for which heat transfer and pressure drop correlations or test data were available. In addition, only surfaces manufactured in sufficient quantity to establish realistic cost information were evaluated. The surface types considered are described below.

- Plain Tubes
  Common industrial practice uses the conservative Dittus-Boelter equation for the inside heat transfer coefficients in plain

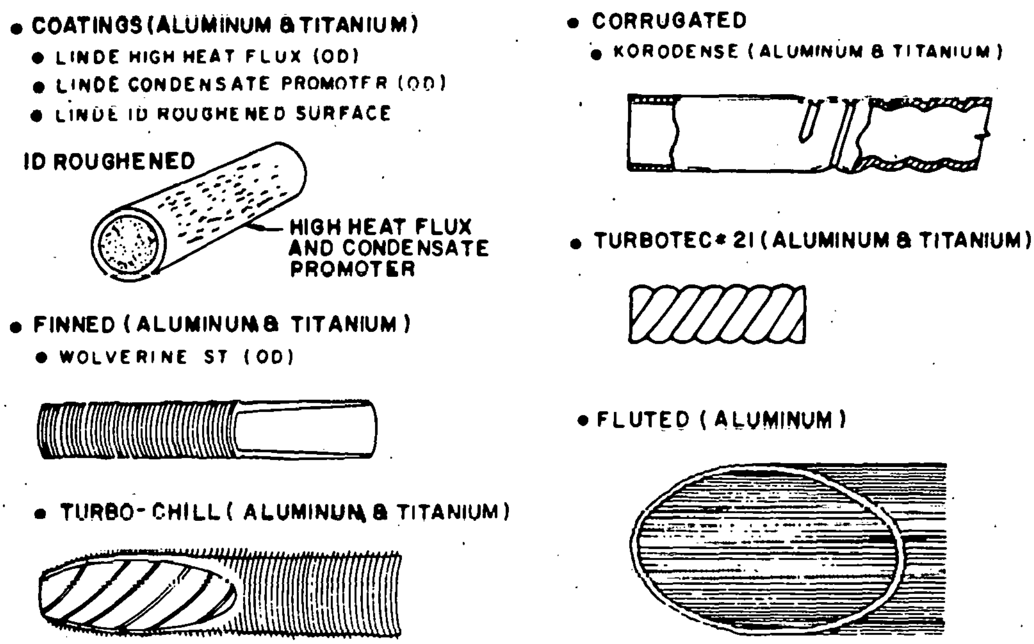

Figure 7-6
TUBE SURFACE ENHANCEMENTS

tubes to account for the flow characteristics peculiar to large cross-section heat exchangers.

$$Nu = .023\ Re^{0.8}\ Pr^{0.4}$$

The coefficients determined by this equation are up to 15% less than laboratory test results [130-132]. Since some of the enhancement effects were developed from such tests, their inside coefficients are reduced by 15% for consistency. Where the coefficient is a multiplier to the plain tube calculations, the reduction is inherent in the Dittus-Boelter equation. In addition, when seawater properties are used to calculate coefficients, the results are 3 to 5% lower than for fresh water[133].

The friction factor for plain tubes was determined from the Moody lot as a function of Reynolds number and roughness ratio.

The outside heat flux for plain tubing in the evaporator is included only for comparison purposes, since it is believed that some means of initiating and maintaining nucleate boiling is a necessity. This relationship is:

$$Q/A_o = 798\ (\Delta T_f)^{1.066}$$

In the condenser, a Nusselt-based rating method was used. This method does not consider mixed condensation, film rippling and turbulence, vapor velocity, presence of non-condensibles, vapor pressure drop, or condensing coefficients, although the latter three lead to lower values. No compensation or correction was applied for turbulence, mixed condensation, non-condensibles or vapor pressure drop. However, each of the modular bundles has its own vent and is surrounded by geneous vapor lanes to minimize the last two effects.

The single tube Nusselt condensing equation is:

$$h_o = 0.725 \left[\frac{3600g\ p^2 k^3\ \lambda}{\mu\ do\ \ \Delta\ T_f}\right]^{0.25}$$

The condensate loading effect was handled by a vertical row number correction, a practice consistent with the Nusselt-based condensing coefficient prediction method. This factor is:

$$h_{o_{bundle}} = h_{o_{single\ tube}} \left(\frac{1}{Nt}\right)^n$$

Where n is determined by test and Nt is the number of vertical tubes in the bundle. A value for n of .08 is used, based on tests conducted by Linde in a 10-row deep ammonia tube bundle.

- Applied Coatings

The coated tubes considered are the Linde "High Heat Flux" and "Condensate Promotor" outside coatings and the "Roughened" inside coatings. The inside coating was subsequently judged to be in the development stage without cost data, and was eliminated. Its correlations were included in the computer program for comparison, however, coatings can be applied to either aluminum or titanium tubes without length or diameter limitations. The Linde "High Heat Flux" surface is a porous aluminum matrix applied to approach a metallurgical bond to the prime tube surface. The coating is approximately 20 mils thick and is durable. If handled with normal shop care, the surface should not be excessively damaged.

The inside heat transfer correlation is:

$$h_i = [2.19 + 0.00001784\ (Re - 20000)]\ \ h_{i_{plain}}$$

The friction factor is:

$$f = [2.3 + 0.00002\ (Re - 20000)]\ \ f_{plain}$$

hi_{plain} is again obtained from the Dittus-Boelter equation, and f_{plain} is obtained from the Moody Plot described in the plain tube section. These correlations are curve-fits of data supplied by Linde.

The evaporator for this program is of the thin-film nucleate boiling type, only the plain and Korodense tubes were considered, since other types preclude a thin film. The high flux coating is porous, has good wetting properties, and is capable of initiating nucleate boiling at the very low temperature differential and over a wide range of liquid loading. The Linde equation below is based on single tube test data and is used directly. Multitube, bundle testing of this surface is continuing at Argonne National Laboratory.

$$Q/Ao = 5723 \quad (\Delta T_f)^{1.86}$$

In the condenser, the outside heat transfer coefficient for the Linde condensate promotor was obtained directly from Figure 7-7. Since Nusselt predictions were 15% lower than Linde plain tube test coefficients, this reduction was also applied to the Linde thin film promoter to incorporate the effects of non-condensibles and vapor pressure drop.

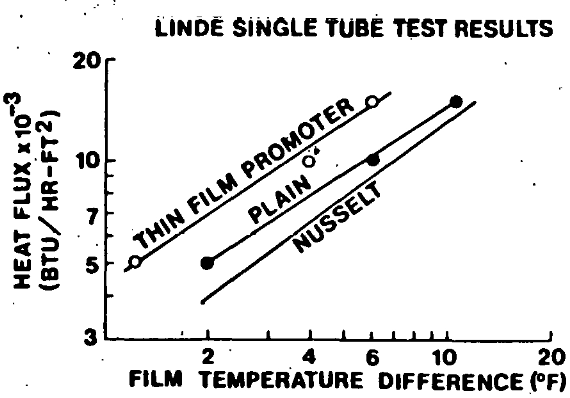

Figure 7-7
CONDENSER OUTSIDE HEAT FLUX

- Finned Tubes

The Wolverine and Turbochill surfaces fall into this finned tube category.

The inside heat transfer rate for finned tubes is:

$$h_i = \left(\frac{.052}{.023}\right) h_{i_{plain}}$$

The friction factor is:

$$f = 0.7364 \ Re^{-0.2696}$$

These correlations were supplied by Wolverine. $h_{i_{plain}}$ is the inside heat transfer coefficient from the Dittus-Boelter equation.

Finned tubes were not considered appropriate for the evaporator.

The Nusselt condensing analysis was modified and found adequate for predicting the outside heat transfer coefficients for finned tubes(134,135). An effective finned tube diameter was obtained by applying the horizontal tube Nusselt equation to the root surface of the fin, and the vertical tube Nusselt equation to the vertical finned portion of the finned tube. The resulting outside diameter used in the Nusselt equation is then:

$$\left(\frac{1}{do}\right)^{0.25} = \frac{Aroot}{Ao}\left(\frac{1}{dr}\right)^{0.25} + 1.3E \ \frac{A_{fin}}{Ao}\left(\frac{1}{\bar{H}m}\right)^{0.25}$$

Where E is the fin efficiency.

Heat Transfer Research Institute data show that if the fin-height-to-spacing ratio is such that surface tension forces overcome gravity forces, condensate is retained in the finned grooves and the fin effectiveness is lost. The correction for liquid retention is defined[136] as:

$$Fr = 1/(1 + r_c h_o)$$
$$r_c = .002 \left[1 + \tanh \left(\Lambda_r - 2.5\right)\right]^2$$
$$\Lambda_r = Cg \, \frac{\sigma \, g_c}{\rho \, g}$$
$$Cg = nf \left[\frac{4\, d_f - 2\, d_r + 2/nf}{\pi/4\, (d_f^2 - d_r^2)}\right]$$

This correlation was developed with experimental data which includes water, n-pentane, acetone and freon-113--but not ammonia. The value of σ/ρ for ammonia is between water and the other fluids tested, and therefore, the liquid retention must be considered. For ST 19 aluminum tubing, the retention factor was between 0.7 and 0.9. For the titanium-finned tubes with the smaller fin height, the calculated retention factors were very low, from 0.2 to 0.4. It is obvious that the retention should be reduced (higher retention factor) if the fin-height-to-spacing ratio is reduced. The above retention factor correlation was developed for St 19 tube geometry (aluminum finned tubes) only, and it appears that it cannot be used for other geometry (titanium finned tubes). Therefore, the assumption was made that the retention factor was always 0.9 for titanium. No correction was applied to the finned surfaces to account for bundle effects because the bulk Nusselt prediction method is used.

- Corrugated Tubes

Two types of Korodense (Wolverine) corrugated tubes were considered: the LPD (Low Pressure Drop) and the MHT (Maximum Heat Transfer). These were used with both plain and coated outside surface.

The Korodense inside heat transfer equation is:

$$h_i = \frac{Cp\ G \quad \sqrt{f/8}}{\beta\ \sqrt{Pr}\ \left[Re \quad \sqrt{f/8}\right]\ 0.127\ +_{\gamma}}$$

where the friction factor is defined as:

$$\sqrt{f/8} = \frac{-1}{2.46/n \left[r + \left(\frac{7}{Re}\right)^{m}\right]}$$

The operands are obtained from Table 7-4. A multiplier of 0.85 is applied to the heat transfer correlation.

Korodense was originally a joint development project of Wolverine and Linde; the outside was coated with the Linde high heat flux surface. Late tests by Wolverine on steam showed that some improvement in the outside condensing coefficient was obtained by the corrugations(137) alone. Corrugations lead to film thinning at the concave surfaces and condensate buildup at the grooves due to the action of surface tension (Gregorig effect).

For 1-inch tubes, Reference (137) recommended about a 40% improvement in the outside condensing coefficient due to the corrugations. An enhancement of 1.4 was used for all tube diameters even though this number was obtained with steam and not ammonia data. The accuracy of this assumption is unknown, and a test program to explore this point may be in order.

Table 7-4
OPERANDS

	Korodense Type MHT	Koredense Type LPD
m	0.77	0.61
r	.00595	.00088
γ	2.56	3.74

β VALUES FOR 1 IN. O.D. MINIMUM WALL

Wall Size In Inches	Korodense Type MHT	Korodense Type LPD
.020	7.12	6.70
.025	6.88	6.48
.032	6.62	6.24
.035	6.53	6.15
.042	6.31	5.94
.049	6.16	5.80
.065	5.84	5.50

- Fluted Tubes

The Turbotec #21 (Spiral Tubinq Corporation) had the only geometry with potential for this application. (Reference 138). The fluted tube considered was aluminum and for the condenser only.

The Turbotec #21 inside heat transfer correlation is:

$$Nu = .01707\ Re^{0.832}\ Pr^{0.4}$$

Its friction factor is:

$$f = 0.488\ Re^{-0.26}$$

The diameter used in the Nusselt and Reynolds numbers is the minimum, or inner, diameter of the corrugations. A 15% reduction is used for the heat transfer correlation.

The fluted correlations are proportional to those of plain tubes.

Inside heat transfer:

$$h_i = 1.57\ h_{i_{plain}}$$

Friction factor:

$$f = 1.57\ f_{plain}$$

Tests conducted by H.T.R.I. established that the groove valleys of the Turbotec #21 tube obviously contributed to the ease in condensate drainage, and thereby decrease the heat transfer resistance(138). The enhancement obtained for this surface type was mostly on the outside of the tube. The steamside heat transfer performance was more than double that of plain tubes. To our knowledge, no test data for condensing ammonia on this surface exists. An enhancement of 1.8 was therefore assumed for all tube diameters.

Fluted tubes were not considered for evaporators.

7.2.1.1.2 Evaluation of Enhancements

The studies of Dr. A.E. Bergles[139] were used as an aid in arriving at possible candidate tubes and in the preliminary screening.

After preliminary screening, thirteen surface combinations were selected as being promising. Seven of these were judged applicable to the condenser, three to the evaporator, and three to both. These are shown in Table 7-5.

Figure 7-6 illustrates the effect of various internal enhancements on the inside heat transfer coefficient and friction factor as compared to a smooth bore tube. The correlations used were developed during the study.

The selection of an internal enhancement requires an optimization considering both pumping power and heat exchanger cost. The inside heat transfer coefficient for both the evaporator and condenser can be approximately doubled with the Linde roughened or the Korodense MHT corrugated tube. This tends to balance the inside and outside coefficients; however, the friction factor and resulting pressure drop can be increased by as much as a factor of 5. To initiate the selection process, the relative effect of heat transfer enhancement to friction factor impairment was calculated fo various inside surfaces. Table 7-6 illustrates this effect and indicates that the fluted, Linde roughened, and Korodense LPD appear to have the most promise and are continued as candidates to the system optimization.

Table 7-5
ENHANCEMENT ARRANGEMENTS CONSIDERED

Code No.	Enhancement Type: Inside	Enhancement Type: Outside	Exchangers	Tube Material
1	Plain	Plain	Cond. & Evap.	Al & Ti
2	Plain	Wolverine ST/19	Cond.	Al & Ti
3	Korodense MHT	Plain	Cond. & Evap.	Al & Ti
4	Korodense LPD	Plain	Cond. & Evap.	Al & Ti
5	Plain	Linde Promoter	Cond.	Al & Ti
6	Plain	Linde High Heat Flux	Evap.	Al & Ti
7	Korodense MHT	Linde High Heat Flux	Evap.	Al & Ti
8	Korodense LPD	Linde High Heat Flux	Evap.	Al & Ti
9	Turbotec #21	Turbotec #21	Cond.	Al & Ti
10	Turbochill	Turbochill	Cond.	Al & Ti
11	Korodense MHT	Linde Promoter	Cond.	Al & Ti
12	Korodense LPD	Linde Promoter	Cond.	Al & Ti
13	Fluted	Linde Promoter	Cond.	Al

Table 7-6
RATIO OF HEAT TRANSFER IMPROVEMENT TO FRICTION FACTOR IMPAIRMENT

Heat Exchanger	Enhancement Types: Korodense MHT	Linde LPD	Linde Roughened	Fluted	Tubochill	Turbotec #21
Condenser	.52-.63	.82-.96	.95	1.0	.81-.84	.74
Evaporator	.48-.58	.74-.88	.95	Not Considered		

Since the evaporator is the thin-film nucleate boiling type, only the outside coated tubes hold promise. Uncoated tubes were included mainly for comparison purposes since some means of initiating and maintaining nucleate boiling at very low temperature differentials and over a wide range of liquid loadings is required.

Using the heat transfer and friction factor formulations developed in the previous section, computer programs were written to design and cost the heat exchangers. These programs were used first to select the most advantageous tube type, then incorporated in the overall plant system optimization program to obtain the most economical plant cost.

The selection procedure consisted of comparing each candidate surface to plain inside, plain outside tubes as designated in Table 7-5 by Code 1. The method of comparison is similar to that found in References 138, and 140 thru 142, except that the heat exchangers are completely designed, including all the heat transfer and pressure drop effects. Heat load, seawater inlet temperature, and ammonia saturation temperature were held constant. Seawater flow was fixed and a series of pressure drops were studied from 1 foot to 15 feet of seawater head such that the seawater pumping power, pump cost, and water side system could be considered constant for each of the fifteen power levels. The required number of tubes and the required heat transfer surface for each tube is compared to the bare tube for each power level by the ratios N/No and A/Ao. The results are plotted in Figure 7-8, identified by the tube enhancement identification code. Since the N/No ratio is a function of the shell size and the A/Ao ratio a function of both shell size and tube length, the figure shows that outside tube enhancement has a greater effect than inside tube enhancement on the required evaporator size. Figure 7-8 also shows that both inside and outside tube enhancement have a small effect on the required condenser size. To avoid confusion, only the effects of the best surface combinations have been plotted. Since the size and volume effect of the evaporator and condenser are assumed

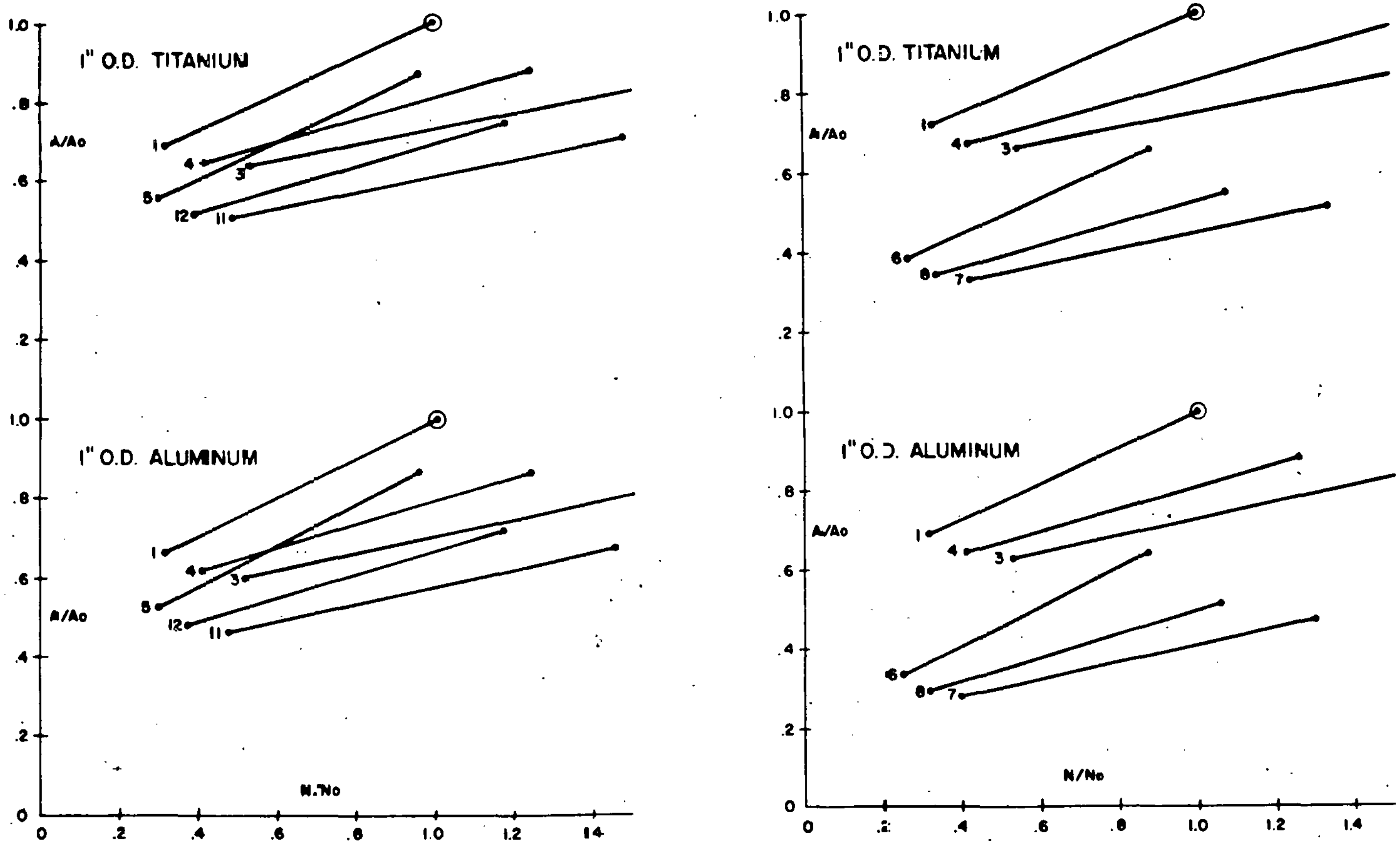

CONDENSER EVAPORATOR

Figure 7-8
HEAT TRANSFER SURFACE AREA RATIO VS. NUMBER OF TUBES RATIO

here to be secondary to the cost, each of the hardware items was cost evaluated and the relative values were plotted. The selection for the evaporator from Figure 7-9 is a plain inside, enhanced outside surface. In Figure 7-9, the unenhanced outside curve is almost coincident with the enhanced outside curve for each inside surface used in the condenser. The selection for the condenser is a plain inside, plain outside surface.

7.2.1.1.3 Optimized Thermal Design

The thermal and hydraulic calculation described previously were incorporated into the comprehensive cost optimization described in Section 7.1. The resulting module-optimum design of the heat exchangers is shown in Table 7-7.

7.2.1.2 Mechanical Design

A conceptual design of the 50 MWe heat exchanger has also been developed to include the same low cost, high reliability features described in section 6.2.1.2. These features include:

- Modular, compact, reliable, shippable bundles.
- Independent operation of each bundle for improved performance.
- Integral separator assembly in the evaporator.
- Integral hotwell for both heat exchangers.

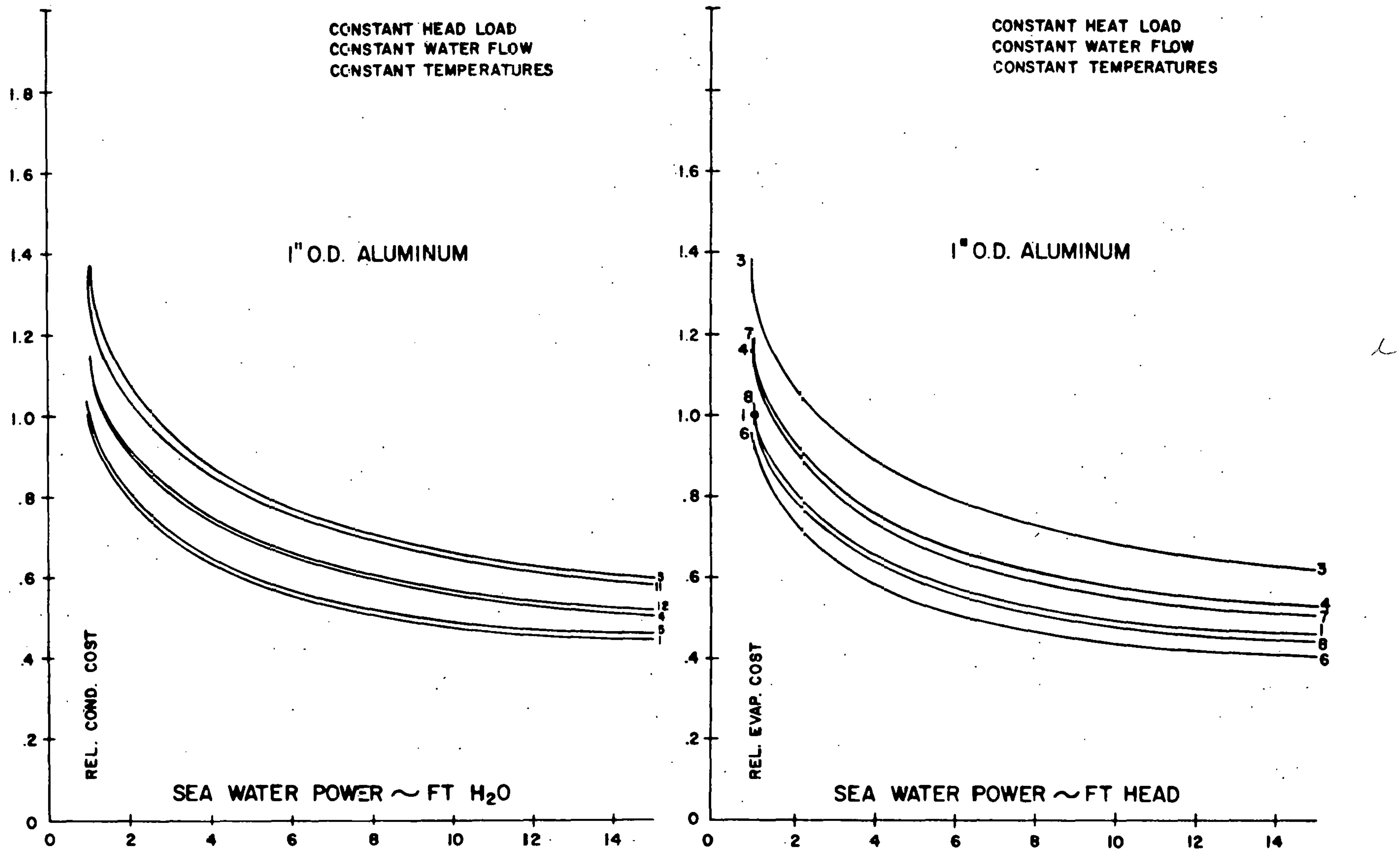

Figure 7-9

RELATIVE COST VS. POWER FOR THE CONDENSER AND EVAPORATOR

Table 7-7
THERMAL AND HYDRAULIC DESIGN PARAMETERS (50 MWe)

	Condenser	Evaporator
Ammonia Flow, lb/hr	14.8×10^6	19.3×10^6
Temp In, °F	49.59	54.27
Temp Out, °F	49.50	70.25
Seawater Flow, lb/hr	1300×10^6	1500×10^6
Temp In, °F	40.0	80.0
Temp Out, °F	46.17	74.51
Tube Metal	Titanium	Titanium
Tube O.D., in	1.0	1.0
Wall thickness, in.	0.028	0.028
LMTD, °F	5.90	6.63
Tube Velocity, ft/sec	5.6	6.5
HT Coefficient, BTU/hr-ft^2-°F	464.2	649.5
h(water)	862	1160
h(fouling)	3780	3780
h(metal)	4820	4770
h(ammonia)	1920	5010
No. Bundles	14	14
Total Tubes	206,453	206,646
Eff. Length, in.	620	417
Seawater Press. Drop, psi	3.5	2.8

For the 50 MWe size, a slight increase in evaporator shell diameter was necessary in order to include the separators and hotwells within the main shell. However, in spite of this increase there is a net savings of $23/KW in the evaporator design due to the elimination of two large vessels in the power system. For the condenser a larger hotwell volume is required and only one vessel is eliminated from the power system. For this situation, the increase in the main shell cost equaled the cost of the hotwell tank removed. Some further cost savings may be realized in reduced piping costs, but they were not considered in this study.

An early design of the 50 MWe units is shown in Figure 7-10. The updated conceptual 50 MWe evaporator, including the separator and hotwell, is shown in Figure 7-11. The 50 MWe condenser with integral hotwell is shown in Figure 7-12. Internal structural features for both heat exchangers are shown in Figure 7-13.

All materials and details of design and construction will be identical to those in the 10 MWe design described earlier. Of course, internal structural parts may be heavier due to the larger shell diameters. The bundle, bundle closure weld assembly, and separator valves are all identical. Some significant details of the 50 MWe conceptual design are:

- 80-foot diameter, 36-foot long evaporator.
- 82-foot diameter, 53-foot long condenser.
- Fourteen tube bundles per exchanger with about 14,000 1-inch diameter - 0.028 inch wall titanium tubes per bundle.
- Separator assembly consisting of four banks with three tiers per bank including 275 vanes per tier for a total of 3300 vanes (each 50 inches high)

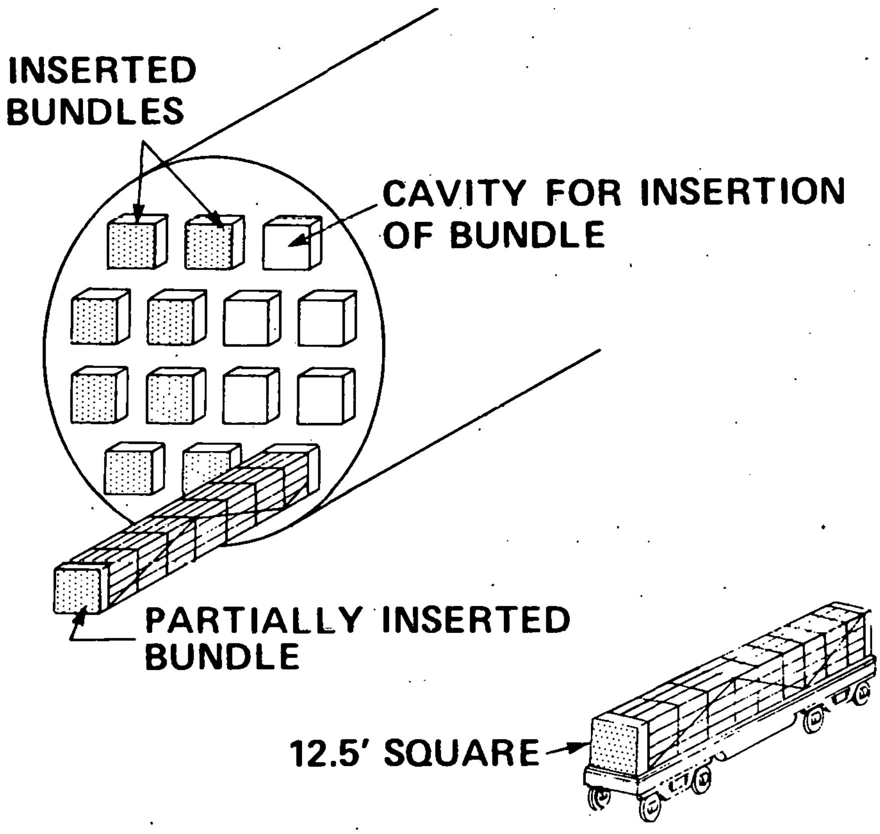

Figure 7-10
MODULAR HEAT EXCHANGER DESIGN

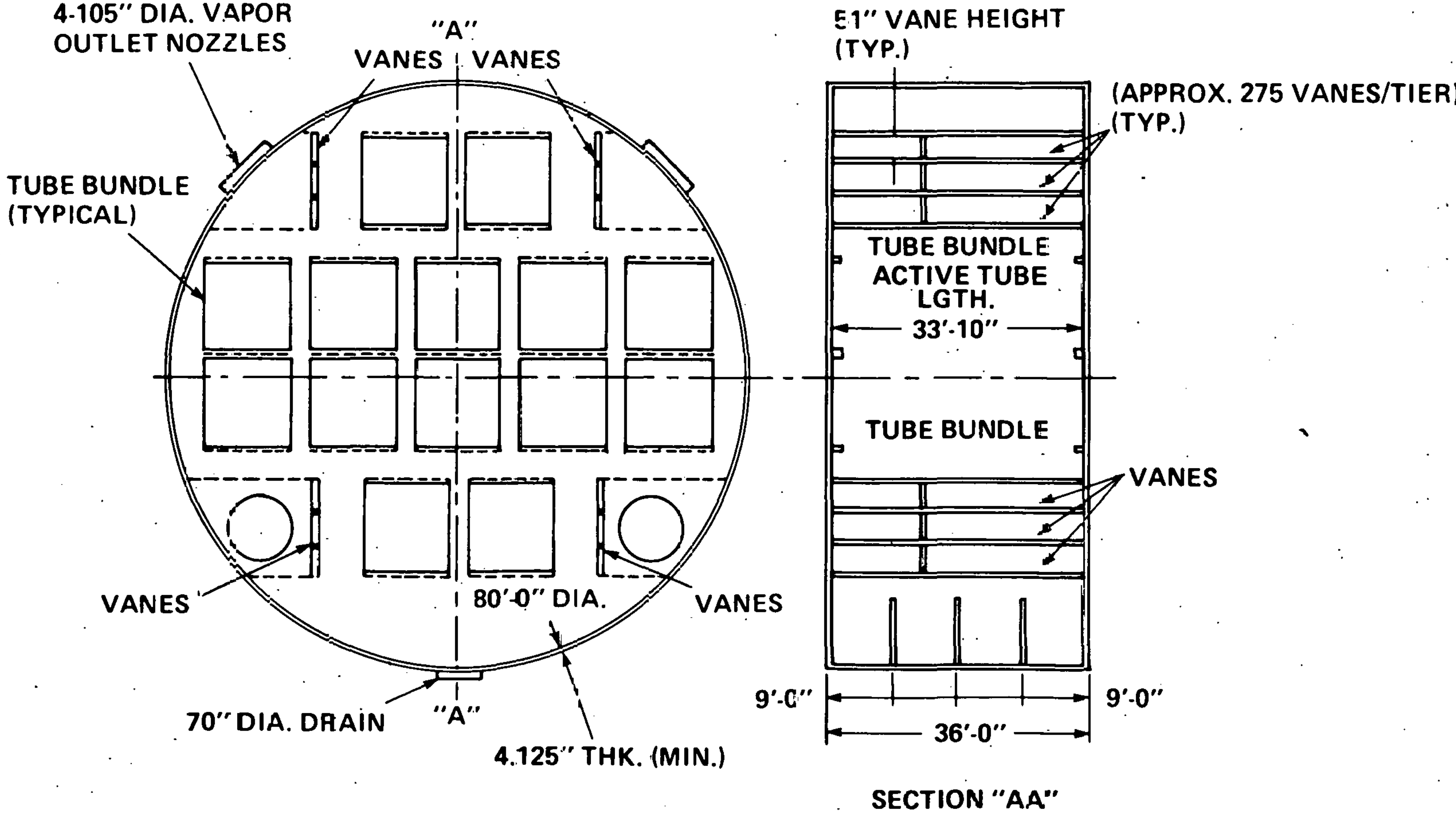

Figure 7-11
EVAPORATOR, 50 MWe

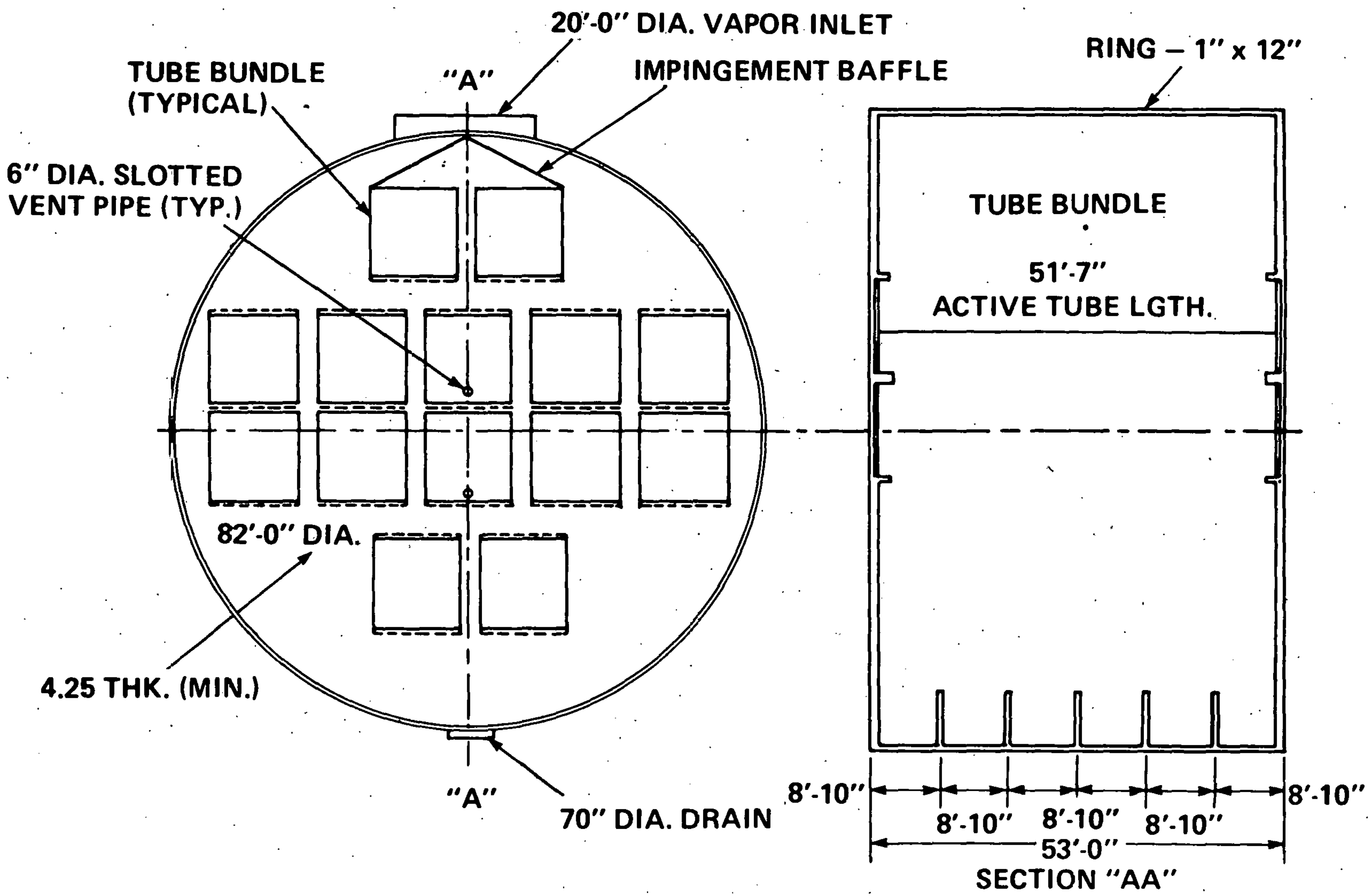

Figure 7-12
CONDENSER, 50 MWe

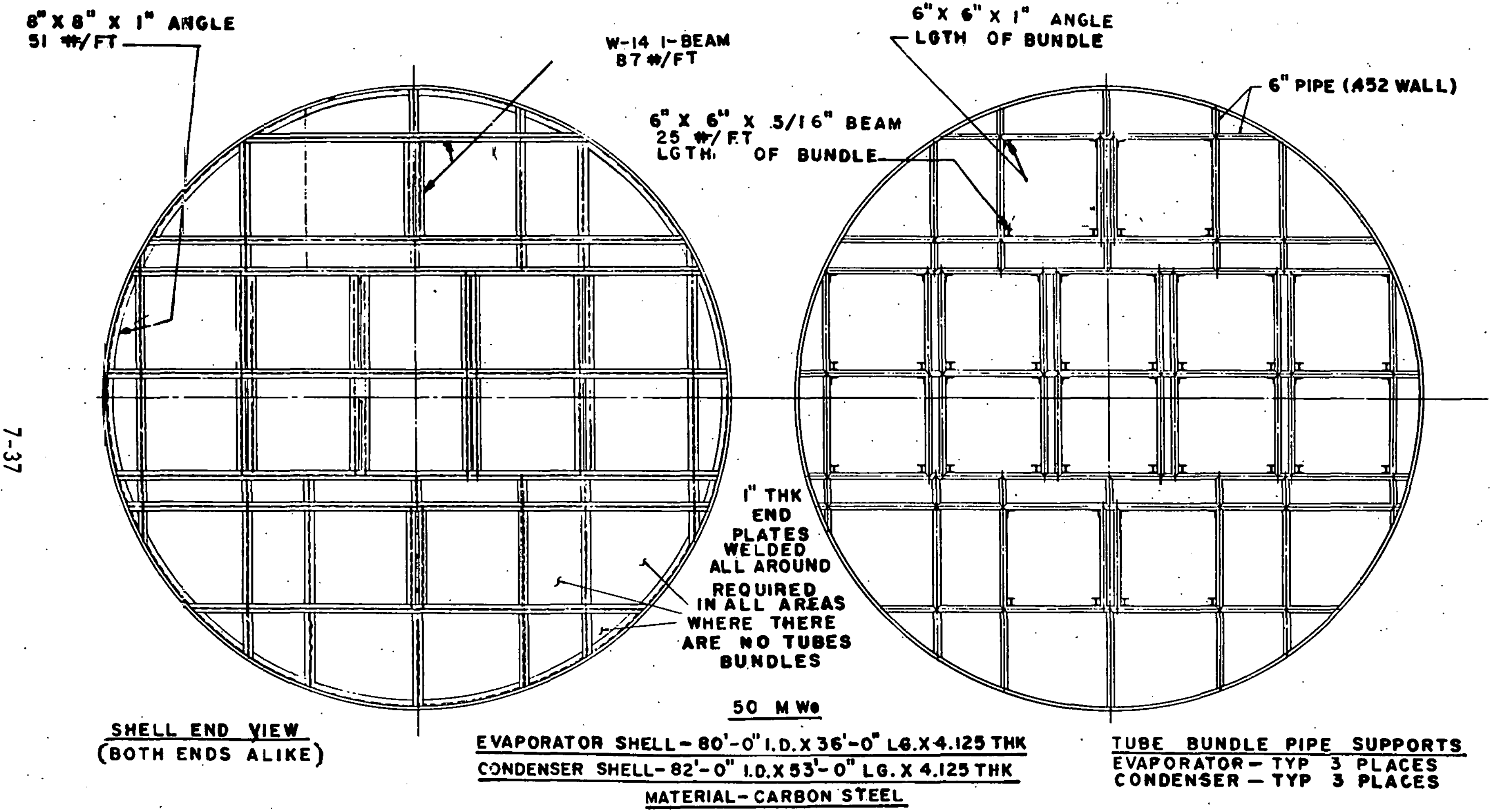

7-37

Figure 7-13
EVAPORATOR AND CONDENSER STRUCTURAL SUPPORTS AND INTERNAL BRACING, 50 MWe

All sizes of the 50 MWe heat exchangers were established through use of the cost optimization program. For flexibility in adapting to any subsequent platform arrangement, small variations in diameter and length in addition to nozzle location are permissible with little effect on overall cost.

A summary of pertinent data for the 50 MWe modular heat exchangers is given in Table 7-8.

Table 7-8
HEAT EXCHANGER MECHANICAL DESIGN DATA, MODULAR DESIGN - 50 MWe

Heat Exchanger Type		Evaporator	Condenser
Number of Bundles		14	14
Tubes			
Material		SB338GD2	SB228GD2
O.D.	Inches	1	1
Wall Thickness	Inches	.028	.028
Pitch	Inches	1.25	1.25
Layout	-	60° Tri.	60° Tri.
Active Length	Feet	33.8	51.6
Total Length	Feet	34	51.8
Number per Bundle	-	14761	14747
Total Number	-	206654	206458
Tube Sheet			
Size (Rectnagular)	Feet	12.33 x 11.46	12.33 x 11.46
Baseplate Material	-	SA516GD70	SA516GD70
Baseplate Thickness	Inches	2	2
Cladding Type	-	Explosive	Explosive
Cladding Material	-	SB265GD1	SB265GD1
Cladding Thickness	Inches	.25	.25
Tube Support Plate			
Size (Rectangular)	Feet	12.08 x 11.17	12.08 x 11.17
Material	-	SA283GD.C	SA283GD.C
Thickness	Inches	0.5	0.5
Number per Bundle	-	11	17
Spacing	Inches	33.8	34.4
Shell			
Material		SA516GD.70	SA516GD.70
I.D.	Feet	80	82
Thickness	Inches	4.125	4.25
Length (Overall)	Feet	36	53
Total Surface	Sq. Feet	1831138	2787795
Bundle Weight	Tons	55	81
Total H.X. Weight	Tons	1571	2430

7.2.2 Seawater Pumps

Method of Analysis

A design analysis computer program provided by Westinghouse Fluid System Laboratory provides a complete geometric description of an axial-flow turbomachine, based on requirements of head rise, volume flow rate, rotational speed and diameter. The solution or design procedure is based on three basic elements: an inviscid, incompressible flow field solution; a semi-empirical cascade life-prediction model; and an empirical loss and loading-limit calculation.

The methods used to analyze candidate configurations for the diffusers for the various pumps considered are based upon empirical results for axisymmetric annular diffusers, and for axisymmetric conical and exponential diffusers. Adequate diffuser design must include a determination of the stability of the flow in the diffusing element. If diffusion is too rapid, the flow will be characterized by very high losses, or by intermittent stall or pressure-flow oscillations of possibly disastrous magnitude. The diffusers used in this work have all been selected to lie in the stable flow range to achieve efficient and steady performance, to avoid pump and overall system problems, and to provide a degree of performance margin where various elementary diffusers are used in series in a single configuration.

The pump requirements for the 50 MWe module are:

- Evaporator Water Flow: 178 m^3/s
- Condenser Water Flow: 173 m^3/s

Pump Configuration and Performance

The seawater pump configuration selected combines an axial flow impeller direct coupled to a low speed synchronous motor in an integral pod design. This self-contained arrangement results in a high efficiency design which provides complete flexibility in plant arrangement and pump orientation. Pump speed control is provided by a remote frequency controller, further enhancing arrangement and operational flexibility. Modeling and efficiency considerations led to geometrically similar designs for both 50 MWe model and the 10 MWe Modelular Application.

Table 7-9 summarizes the 100 m^3/s pump characteristics selected for the 50 MWe module conceptual design. These configurations lead to a total pump/diffuser efficiency of 76% for a design point chosen to provide a reasonable surge margin at design point flow.

As discussed in Section 6.2.2, detailed pump optimization resulted in an increase in pump/diffuser efficiency to 80.6%. Multiple pumps of that design could be used for the 50 MWe module; however, pump similarity considerations indicate that the 80.6% efficiency should be achievable for a 100 m^3/s pump. This is the size recommended for the 50 MWe module with two warm and two cold water pumps required for each power module. The details of mechanical arrangement, materials selection, control, and installation would be similar to those detailed for the 10 MWe plant.

Table 7-9
PUMP/DIFFUSER DESIGN CONFIGURATION FOR 100 m^3/s FLOW CAPACITY AT 3.5 m HEAD

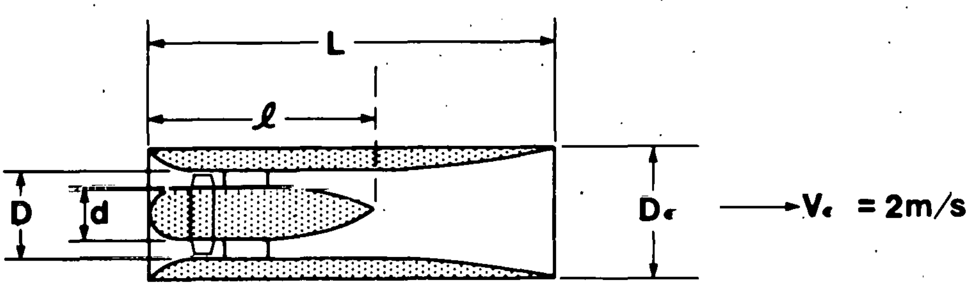

Number of Rotor Blades = 6
Number of Stator Blades = 11

Capacity, Q (m^3/s)	Head, H (m)	Speed, N (rpm)	Power, P (kW)	Efficiency, η' (%)	Casing Dia., D (m)	Hub Dia., d (m)	Length Overall, L (m)	Pod Length ℓ (m)	Exit Dia., D_ϵ (m)
100	3.5	55	4650	76	4.90	2.92	26.3	11.6	8

7.2.3 Turbine

7.2.3.1 Background

During the conceptual phase module power ratings of 12.5 MWe, 25 MWe and 50 MWe were evaluated from the standpoint of overall cost effectiveness including initial cost, performance reliability and maintainability.

To meet these different power levels, various turbine designs were evaluated and these included a vertical single flow design, one bearing single flow design (overhung) and a two bearing horizontal double flow design. Based on calculated blade stress levels, it was apparent that the single flow design was limited to a 25 MWe rating. In addition, and in order to insure a high degree of confidence in the operating performance and reliability it was agreed that wherever possible the turbine designs would be based on existing state-of-the-art concepts.

7.2.3.2 Configuration Selection

From the standpoint of platform arrangement and in consideration of the condenser and evaporator location, the vertical single flow design was considered to be most attractive. However, this feature was offset by the size of the thrust bearing and the attendant losses required with this design. From a maintenance aspect, it was further devalued because of the possibility of having to move or lift part of the generator to remove the turbine rotor. Inasmuch as the large majority of 12-25 MWe turbines are horizontal it was considered to be a departure from the state-of-the-art concept.

Initially, the horizontal, single flow design was developed on the basis of a single stage with two bearing and two gland arrangement. However, this was subsequently changed to a single stage one bearing, one gland design. A downward exhaust which was part of this design was subsequently changed to a straight diffusing exhaust when the turbine was arranged on the side of the condenser. From the standpoint of simplicity and diffuser performance, this design was considered favorable for a maximum rating of 25 MWe. However, the overall efficiency was partially offset by the loss in the relatively large thrust bearing required.

In consideration of all the various parameters, the most significant of which was initial cost of all of the components comprising the module, the horizontal, double flow 50 MWe design, as shown in Figure 7-14, was considered the most viable. In the performance evaluation, it was found that the reduced losses with the smaller size thrust bearing required with this design tended to compensate for the lower exhaust hood efficiency when compared to a single flow design. As a result, the overall efficiency of this design was approximately 1% less than the 25 MWe single flow design with diffusing exhaust.

The speed of 1800 RPM was selected as the best speed for the type of generator (AC synchronous speed), available energy from the ammonia, and required mean diameter of the turbine. In other words, the turbine efficiency is dependent on the ratio of the wheel speed to the gas velocity which in turn is a function of available energy. The efficiency for a reaction turbine is maximum for velocity ratios between .8 and 1.0 and decreases for values above or below that range.

7.2.3.3 Detail Design Considerations

Initial cost was a major consideration in the design and development of the various turbine arrangements. The design selected results in a reasonable size rotor forging, stationary and rotating blades, and a simple cylinder arrangement and support structure. The relatively simple and highly reliable spherical seated journal bearings coupled with a small diameter thrust bearing further enhances the design from a cost standpoint. The type of blade fastenings (side entry roots) contemplated for this design results in minimal manufacturing the assembly time.

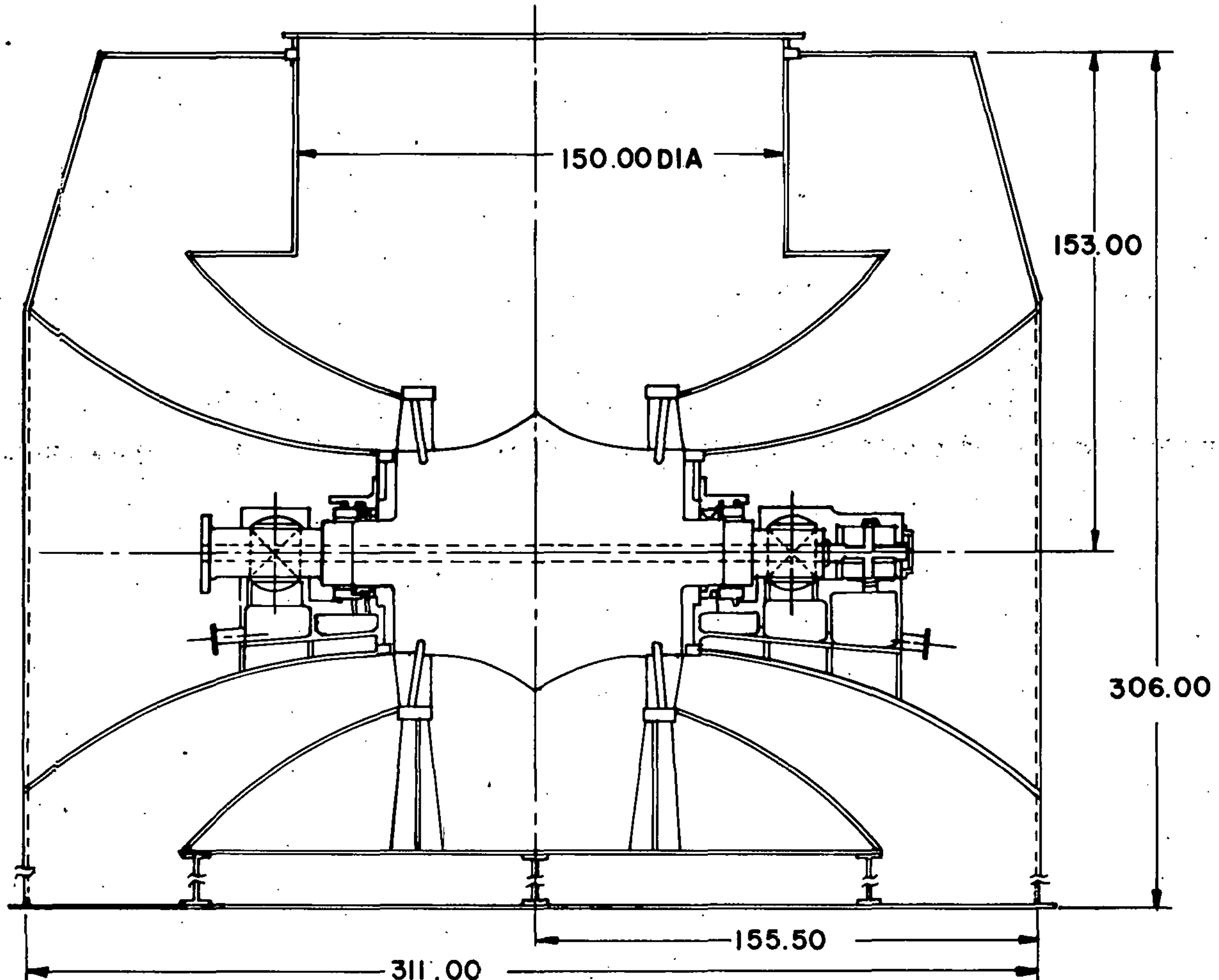

NOTE:

INLET & EXHAUST SIZE BASED ON GAS VELOCITY OF 90 FT/SEC.

ESTIMATED WTS	LBS
CLY COVER	73 500
CLY BASE	80 000
ROTOR WTS COMPLETE	85 300
GLAND & JOURNAL BRG COVER	450
COUPLING COVER	300
TOTAL WTS	239 550

Figure 7-14
LONGITUDINAL SECTION OTEC TURBINE 50 MWe NET

The design of the cylinder in conjunction with the location of the thrust and journal bearings and gland seal components, plus provision of a manholed cover in the cylinder, permit accessibility for inspection and/or maintenance of the bearing, seals and blading.

Consideration was given to designing the gland seal as a gas type, using nitrogen as the sealing gas. However, because of the additional complexity to the total system by the addition of a separate gas system, plus the difficulty in purging the nitrogen from the bearing oil and ammonia, the oil seal system was selected.

A preliminary study was conducted to assess the effect on the turbine and heat exchanger tubes in the event of oil leakage into the ammonia system. The study consisted essentially of discussion with manufacturers and operators of ammonia compressors, using the type of seal (oil) contemplated for the OTEC turbine. The concensus was that there have been very few problems in this area and, where leakage has occurred due to maloperation, the effect on the efficiency of the compressors or heat exchangers was unnoticeable. Subsequent examination of the system indicated no film or deposit in the compressors or heat exchanger tubes which they attributed to the low wax content in the oil used and, consequently, concluded that the oil had remained in suspension with the ammonia.

The area requirements of the rotating blade which are necessary for the imposed stresses result in a blade with a relatively large chord width. A blade performance test program should be part of the subsequent design of this turbine in order to establish the effect on calculated efficiency with the longer passage.

7.2.3.4 Performance

- Figure 7-15 is a plot of the parameter affecting the design of a tubine at various ratings. The curves shown for the 50 MWe rating are based on a single flow design for illustration purposes. The curves shown for 25 MWe rating are applicable to the selected 50 MWe double flow design.

- Figure 7-16 illustrates the relationship between efficiency and speed for a constant mean diameter of 80 inches. As noted, the efficiency is optimum for 1800 and decreases with changes of speed from that value.

- Figure 7-17 indicates the effect on efficiency of blade height, based on 35% gauging which results in reasonable blade bending stress at maximum power. Additional investigation, including a more detailed analysis, is recommended during the next phase toward lowering the gauging for additional improvement in efficiency.

- Figure 7-18 illustrates the relationship between wheel efficiency and wheel speed and blade gauging. At the present time, the design wheel speed for the 50 MWe turbine is 630 ft/sec.

- Figure 7-19 is based on the selected speed of 1800 RPM and blade gauging of 35%; this curve indicates that the design diameter of 80 inches is optimum.

- Figure 7-20 shows the effect on efficiency of the aspect ratio of blade HT divided by chord at mean diameter. As noted, a 1% improvement in efficiency is available with an aspect ratio of 4 versus the 1.96 design. However, the resulting increases in bending stress prohibit this change.

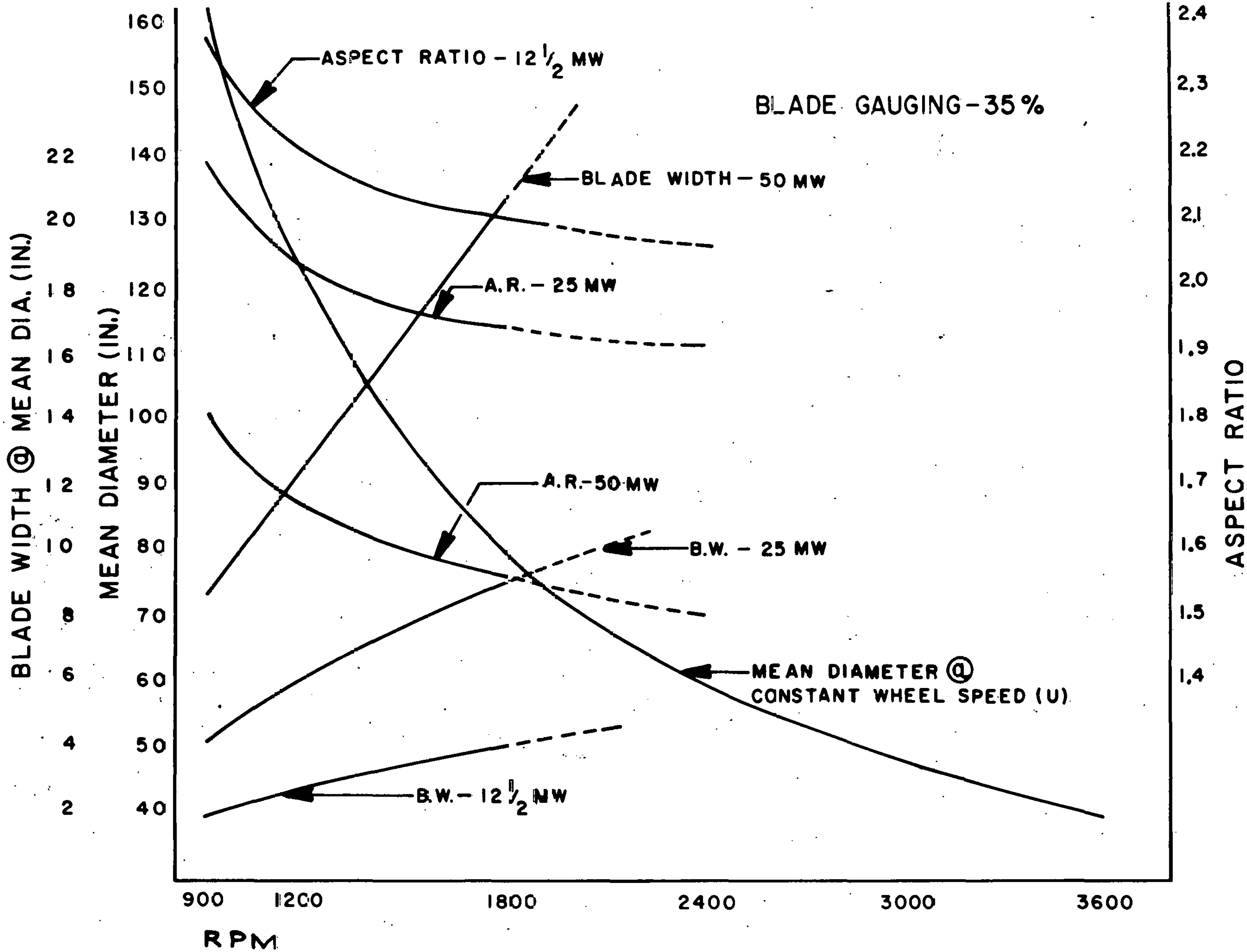

Figure 7-15

MEAN DIAMETER, BLADE WIDTH AND ASPECT RATIO AT VARIOUS LOADS VS. RPM

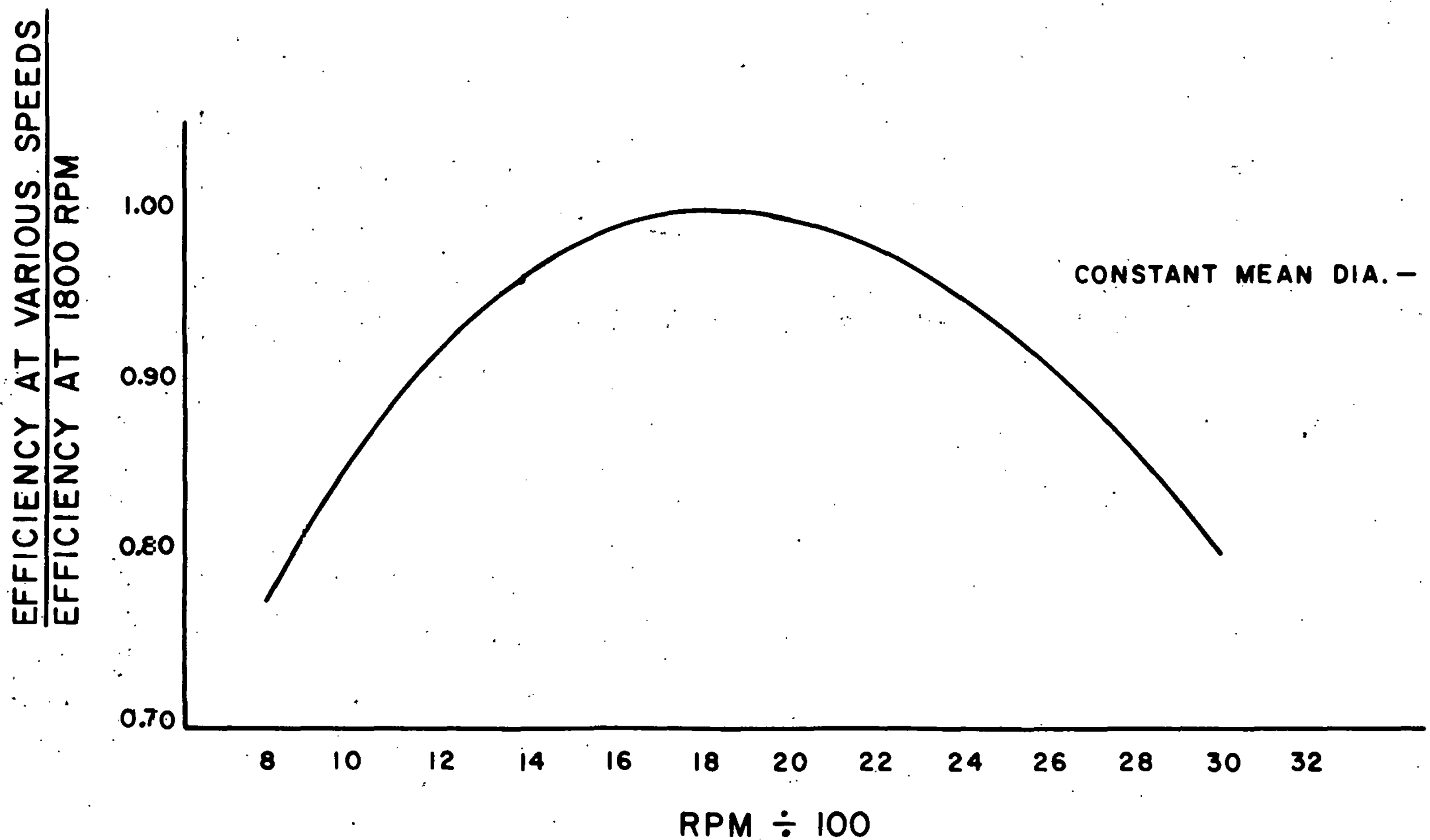

Figure 7-16
50 MWe RATING, OTEC TURBINE, EFFICIENCY VS. TURBINE RPM

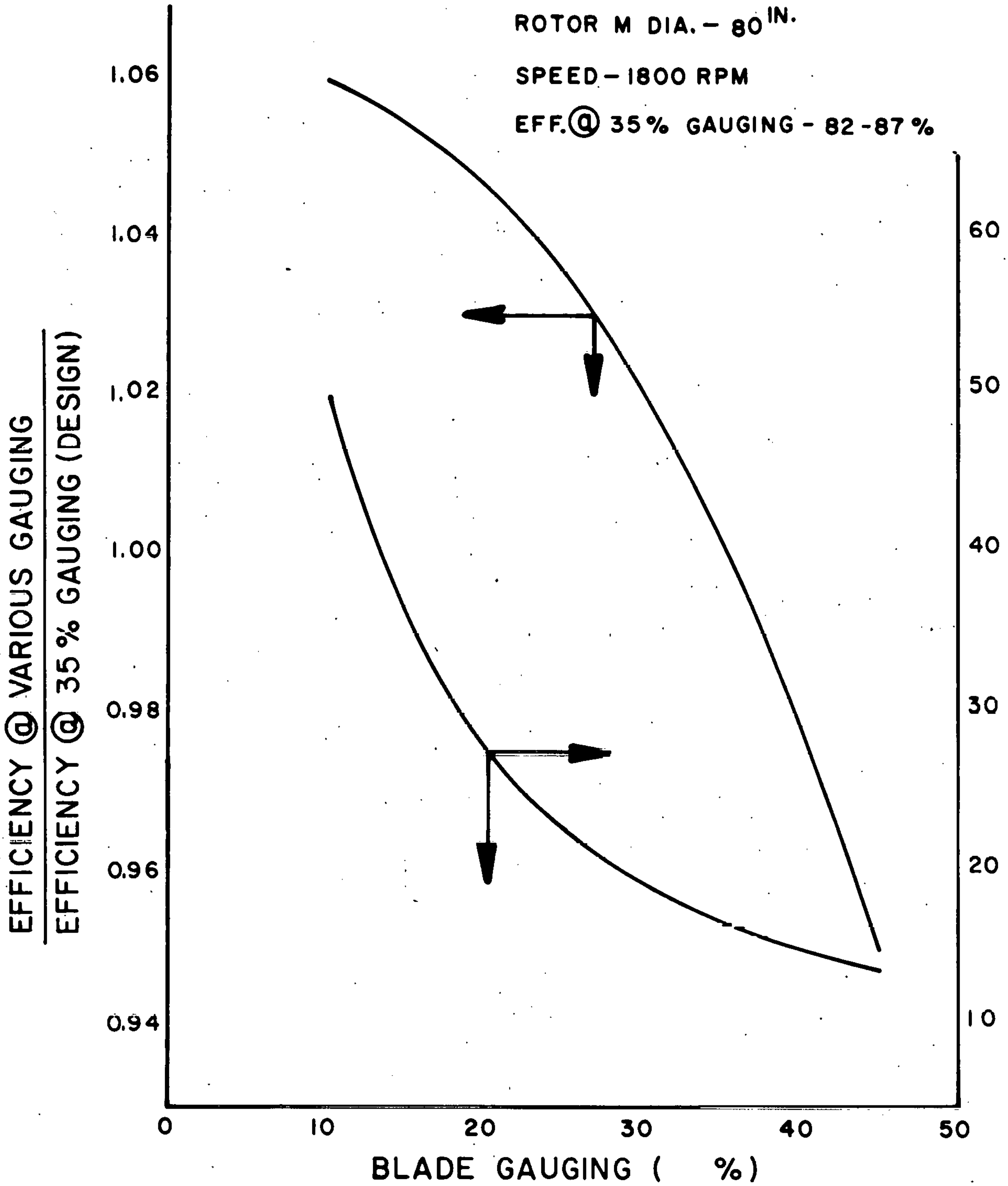

Figure 7-17
50 MWe OTEC TURBINE, EFFICIENCY AND BLADE HEIGHT VS. GAUGING

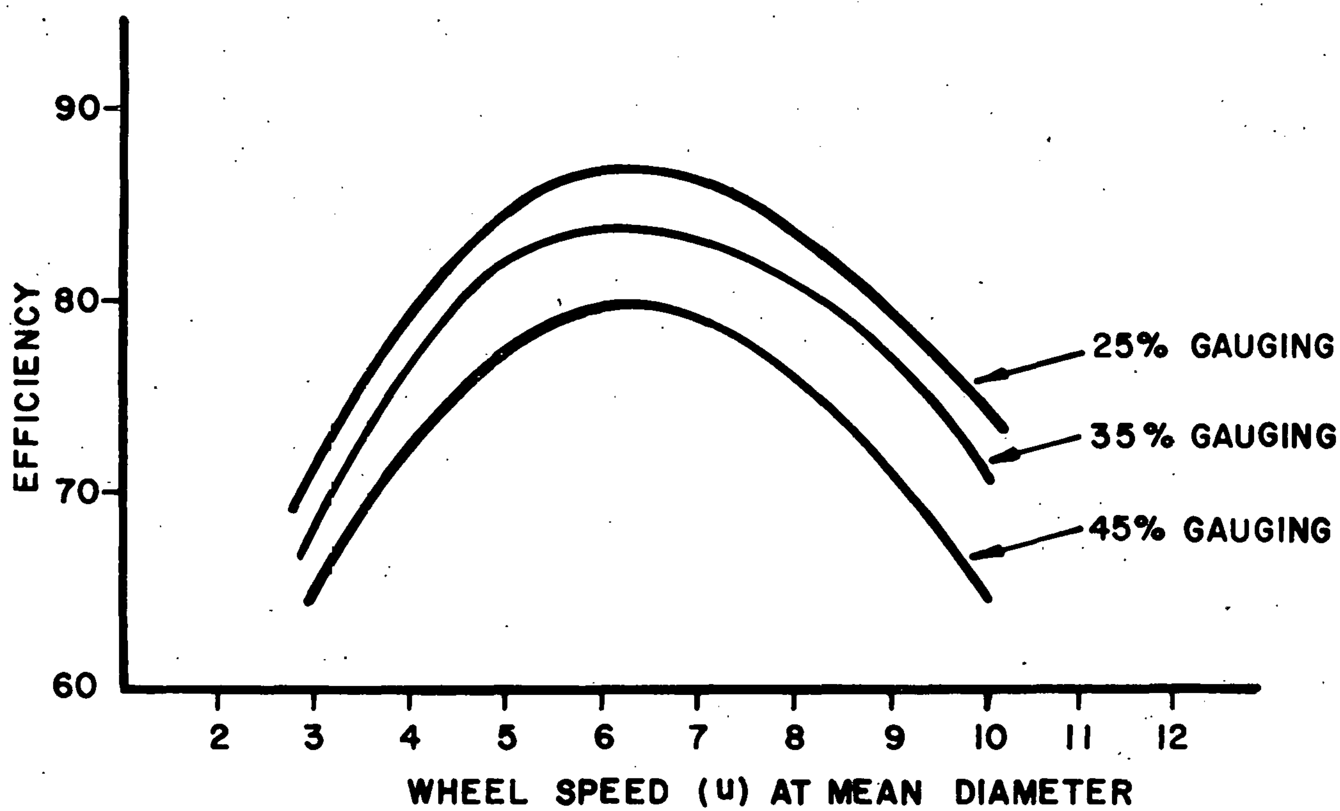

Figure 7-18
50 MWe OTEC TURBINE, EFFICIENCY VS. WHEEL SPEED AT VARIABLE GAUGING

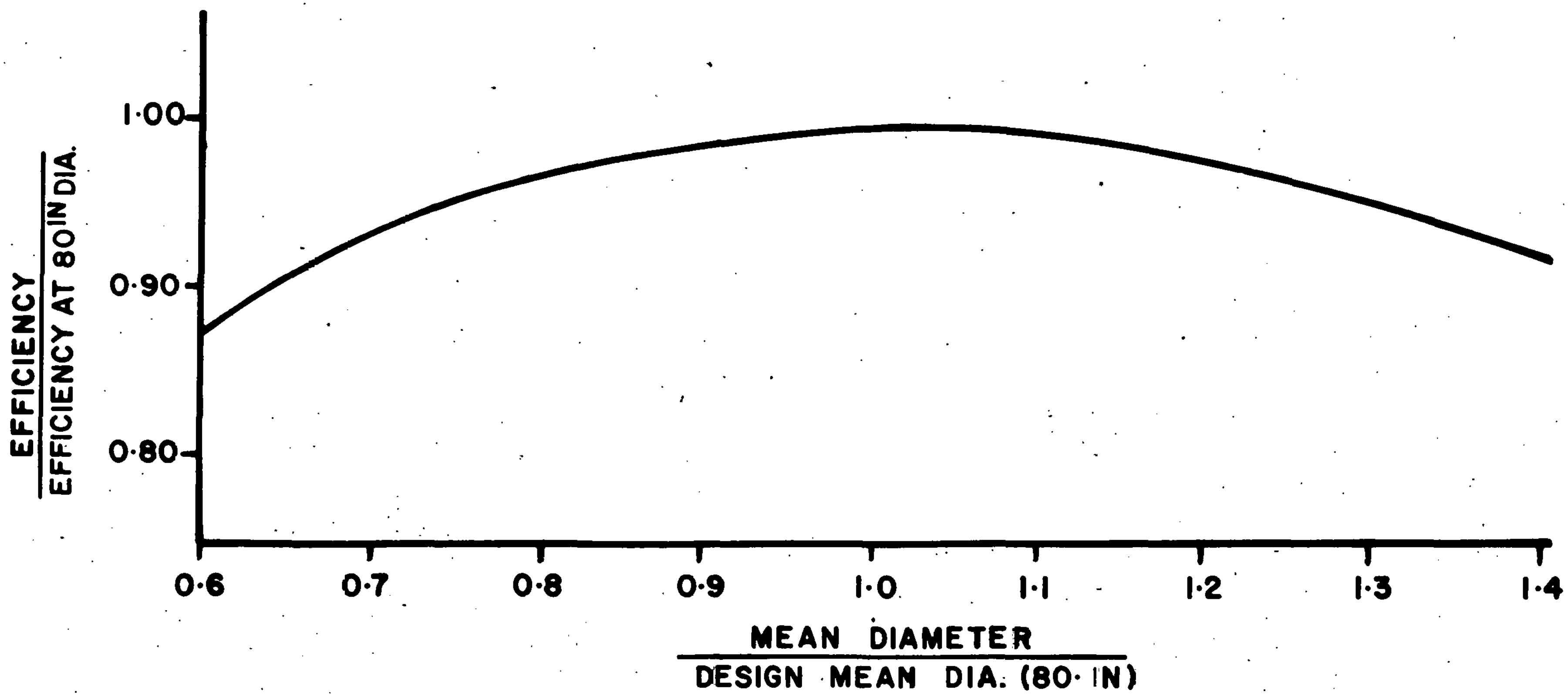

Figure 7-19
50 MWe OTEC TURBINE, EFFICIENCY VS. MEAN DIAMETER AT CONSTANT SPEED (1800 RPM)

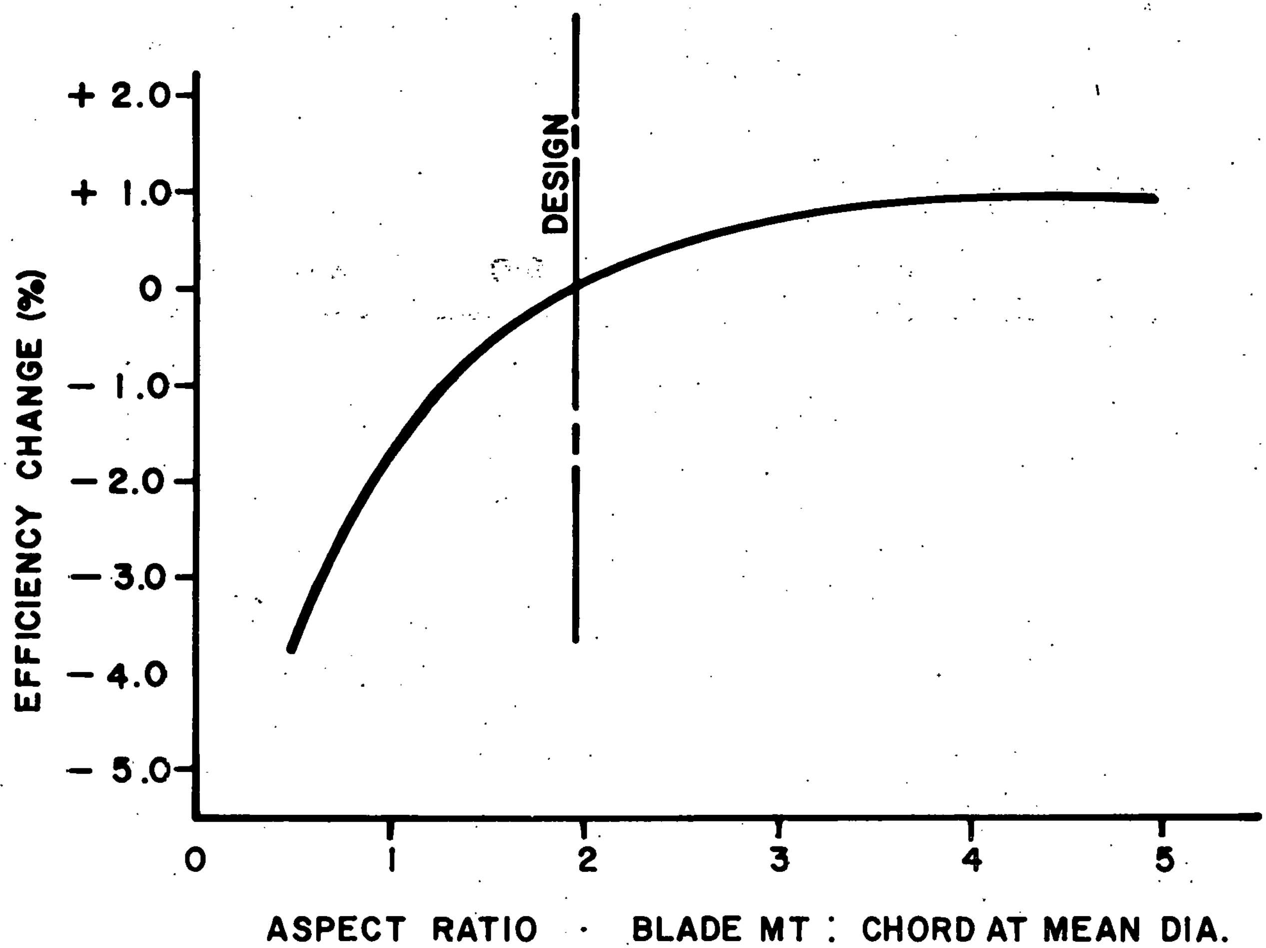

Figure 7-20
50 MWe OTEC TURBINE, CHANGE IN EFFICIENCY VS. ASPECT RATIO

- Figure 7-21 was developed for control purposes to determine the increase in speed with loss of load and failure of the by-pass valve.

7.2.4 Generator

The generator will be designed and constructed in accordance with conventional design technology developed for electric generators intended for electric utility central station and large industrial generator applications.

The generator will be totally enclosed, hydrogen cooled with integral coolers horizontal shaft arrangement, bracket-type main leads, and direct-coupled shaft-driven brushless exciter. It will operate at 1800 RPM.

A sketch of the internal construction is shown in Figure 7-22. A sketch of the corresponding outline dimensions is shown in Figure 7-23.

7.2.4.1 Generator Features

- The construction of the stator frame and bearing brackets will be designed to minimize the effects of shaft and core vibration and their transmission to the foundation parts.

- The rotor will be machined from a single solid-steel forging of high mechanical and metallurgical quality which will be assured by rigorous non-destructive testing including ultrasonic and magnetic particle inspection.

- Floating type retaining rings will be shrunk over the end turns of the rotor with sufficient shrink to assure tightness even at maximum overspeed.

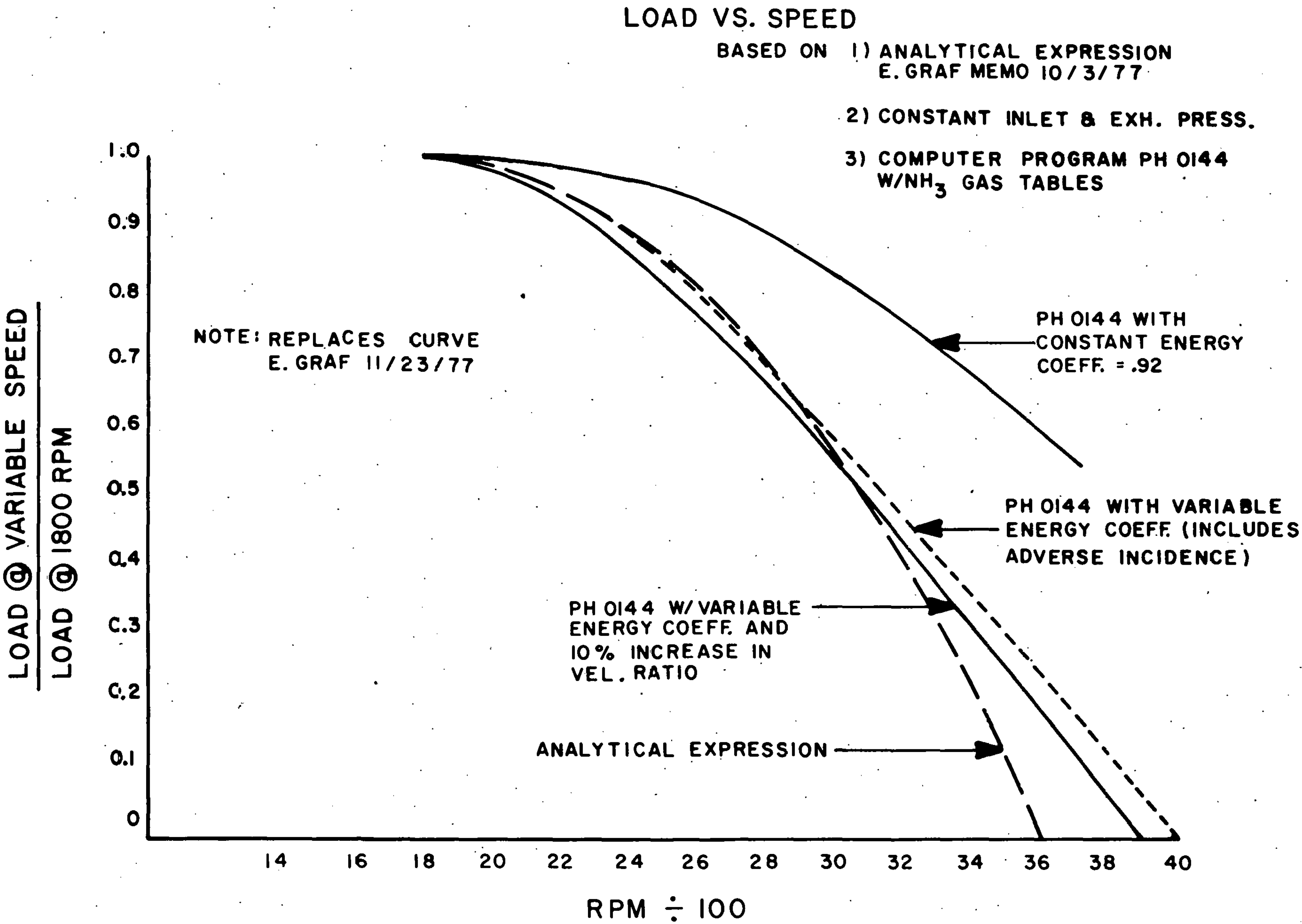

Figure 7-21
50 MWe OTEC TURBINE, LOAD VS. SPEED

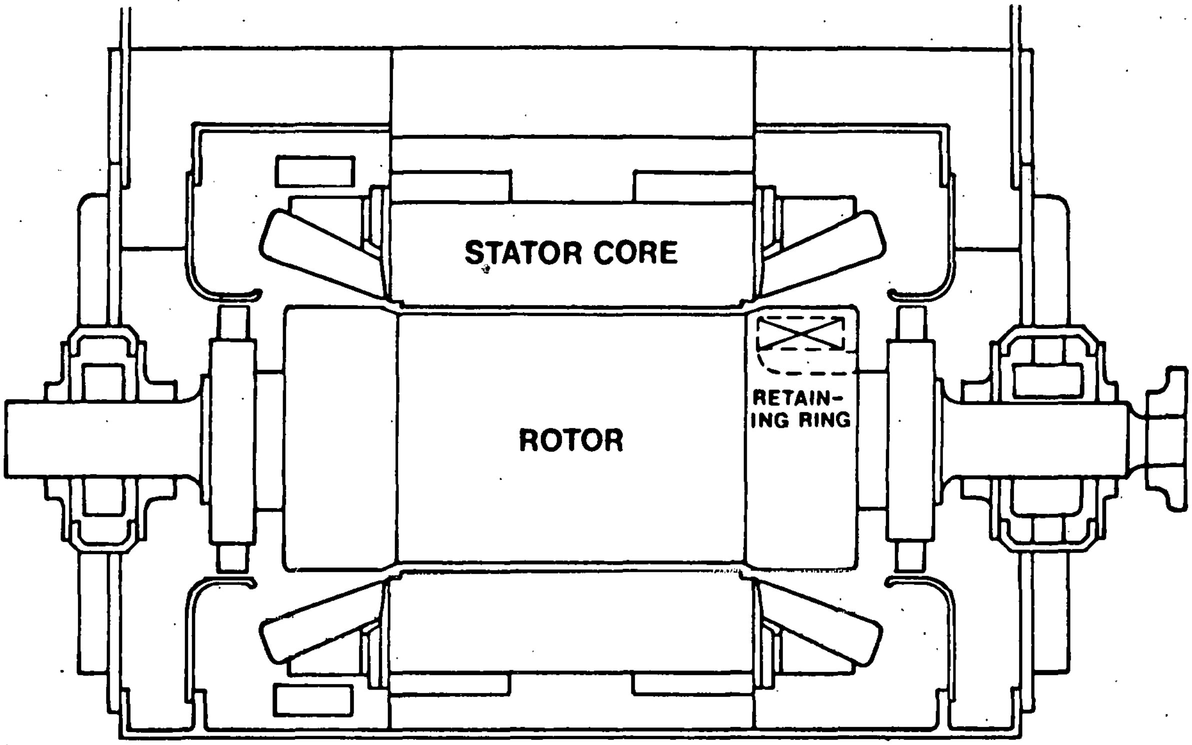

Figure 7-22
CROSS SECTION OF CONCEPTUAL DESIGN OF 50 MWe, 1800 RPM GENERATOR

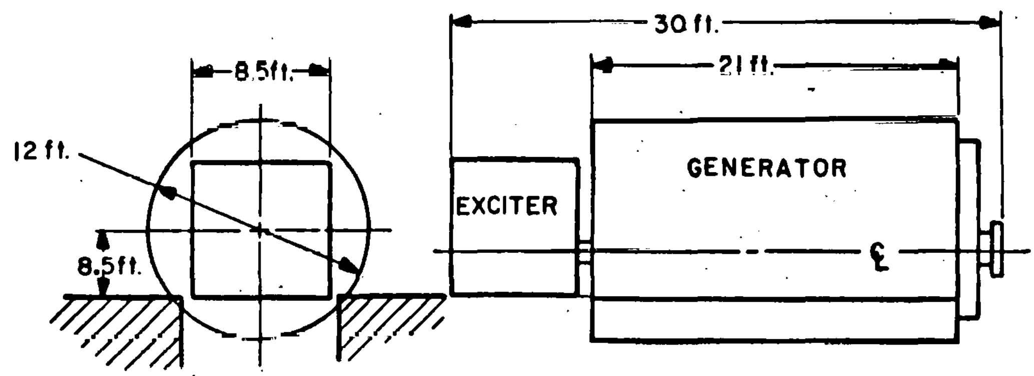

GENERATOR
MW
67.5

TOTAL GEN. & EXC.
WEIGHT- lbs.
365,000

NOTE:
(1) HYDROGEN COOLED - 1800 RPM
(2) SPECIAL OVERSPEED
REQUIREMENT - 3700 RPM

Figure 7-23
OTEC INITIAL GENERATOR ESTIMATES, BLOCK DIMENSIONS, AND WEIGHT

- Armature windings will be designed for reduction of internal losses and of localized heating, and their ventilation will be arranged to provide effective and uniform cooling. The insulation of the windings will have 155°C temperature capability, but will be rated at a hottest spot limit of 130°C to assure long life as well as an extra margin against possible abnormal operating conditions.

- Field windings will be made of creep-resistant silver-bearing copper. Winding insulation will be Class B and of high mechanical strength and abrasion resistance. The windings will be consolidated in the rotor, using thermosetting bonds.

- Shaft-mounted blowers will assure adequate ventilation at all times.

7.2.4.2 Cooling Arrangement

The generator will be hydrogen cooled. Hydrogen gas at a pressure of 30 PSIG will be continuously circulated through the stator and their windings by use of shaft-mounted and driven blowers. Cooler design will be suitable for use with seawater. The cooler design will permit the maximum (rated) output of the generator to be developed with a cooler water inlet temperature of 50°F.

The generator rotor winding will be directly cooled with a radial ventilation pattern. The generator stator winding will be indirectly cooled with a zoned multiple vent pattern.

7.2.4.3 Generator Relay Protection

The electric protection system surrounding the generator is designed to prevent damage to the generator from overheating during electrical or mechanical malfunctions. Protection is achieved by the interruption of circuits at the right time and in the proper sequence to eliminate dangerous electrical and thermal transients.

The following devices, shown in Figure 7-24, are provided to protect the generator against various types of faults or malfunctions. Among these various devices are

1) Reverse Current Relay (32) protects the generator from motorizing in the event of a current reversal from the system.

2) Loss of Field Relay (40) protects against loss of field and as a consequence a reactive load which results in loss of sychronism.

3) Negative Sequence Relay (46) protects against destruction of the rotor in the event a negative sequence occurs due to the opening of one phase of the three-phase system.

4) Ground (51G) - Detects a ground in the generator winding.

5) Lockout (86) - Prevents automatic resetting of the protective relays in the event of a trip.

6) Differential (87, 87G) detects various types of low level faults.

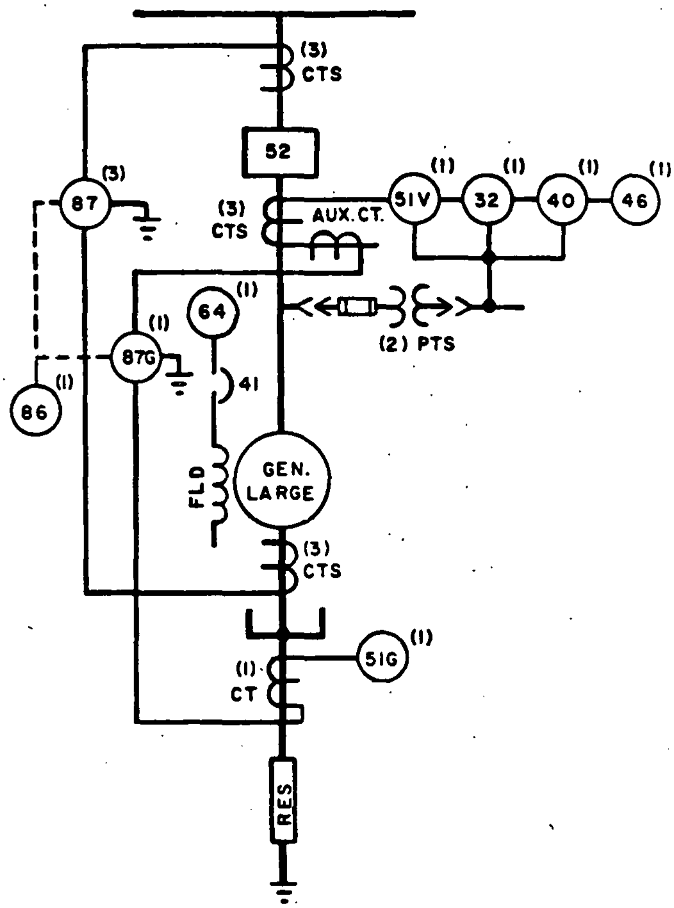

Figure 7-24
PROTECTIVE RELAY DIAGRAM

7.2.5 Fouling Control Systems

Fouling control for the 50 MWe plant will use the same primary fouling control method (chlorination) at the same rate as in the 10 MWe plant. No special size effects are seen other than the chlorination system must be proportionately larger.

One difference between the 10 MWe and 50 MWe designs is that no supplementary methods of fouling control (e.g. Amertap) are recommended at this time. Sufficient lead time is available to prove the adequacy of chlorination in earlier OTEC test programs. (Refer to section 6.2.5).

7.2.6 Instrumentation and Controls

The plant control system configuration discussed in Section 6.2.6 for the 10 MWe Modular Application will also apply for the 50 MWe Demonstration Plant. The system has sufficient flexibility to accommodate any differences in characteristics between the 10 MWe Power Module and the 50 MWe Demonstration Plant. Data for transmitters and gages shown in the Preliminary Instrument List (Table 7-10) will be a function of the parameters established for the 50 MWe module.

7.2.7 Valves

The valve type selection and design requirements as discussed in Section 6.2.7 for the 10 MWe Power Module apply also for the 50 MWe power module.

Valve sizes for 50 MWe Plant are as follows:

- Turbine Bypass Valve (TBV)
  Throat Diameter 45 inch
  Number of Valves 4
  (Parallel Flow Path)
  Active Stroke 13.5 inches

- NH_3 Feed Valve (CV-1)
  Throat Diameter 32 inch
  Number of Valves 4
  Active Stroke 9.6 inches

- NH_3 Recirculations Valve (CV-4)
  Throat Diameter 22 inch
  Number of Valves 4
  Active Stroke 6.6 inches

Table 7-10
PRELIMINARY INSTRUMENT LIST

CHANNEL NO.	MEASURED PARAMETER	INSTRUMENT DATA				OUTPUT SIGNAL			ALARM DATA			FUNCTION
		RANGE	SPAN	UNITS	PRIMARY ELEMENT	TYPE	RANGE	UNITS	LIMIT	SET PT.	UNITS	
FT-001	STBD NH_3 VAPOR HDR FLOW	0-40	10-40	FPS	NOTE-1 2%	E	4-20	MA				MCR INDICATION PRIMARY LOOP CONTROL
FT-002	PORT NH_3 VAPOR HDR FLOW	0-40	10-40	FPS	NOTE-1 2%	E	4-20	MA				MCR INDICATION PRIMARY LOOP CONTROL
PT-003	STBD NH_3 VAPOR HDR PRESS. (MEASURED AT FT-001)	0-200	0-200	PSIG	STRAIN GAUGE OR PIEZOELECTRIC 2%	E	4-20	MA				MCR INDICATION DENSITY COMPENSATION FOR FT-001
PT-004	PORT NH_3 VAPOR HDR PRESS.	0-200	0-200	PSIG	STRAIN GAUGE OR PIEZOELECTRIC 2%	E	4-20	MA				MCR INDICATION DENSITY COMPENSATION FOR FT-002
PT-005	TURBINE VAPOR INLET PLENUM PRESS.	0-200	0-200	PSIG	STRAIN GAUGE OR PIEZOELECTRIC 2%	E	4-20	MA				MCR INDICATION PRIMARY LOOP CONTROL
PT-006	TURBINE VAPOR INLET PLENUM PRESS.	0-200	0-200	PSIG	STRAIN GAUGE OR PIEZOELECTRIC 2%	E	4-20	MA				MCR INDICATION PRIMARY LOOP CONTROL
PT-007	CONDENSER SATURATION PRESS.	0-200	0-200	PSIG	STRAIN GAUGE OR PIEZOELECTRIC 2%	E	4-20	MA				MCR INDICATION PRIMARY LOOP CONTROL

NOTE-1: THE NH_3 VAPOR FLOW DETECTION WILL BE A MULTI-AXIS ANNUBAR DP ELEMENT MANUFACTURED BY AIR MONITOR CORPORATION.

Table 7-10 (CONTINUED)
PRELIMINARY INSTRUMENT LIST

CHANNEL NO.	MEASURED PARAMETER	INSTRUMENT DATA RANGE	SPAN	UNITS	PRIMARY ELEMENT	OUTPUT SIGNAL TYPE	RANGE	UNITS	ALARM DATA LIMIT	SET PT.	UNITS	FUNCTION
PT-008	CONDENSER SATURATION PRESSURE	0-200	0-200	PSIG	STRAIN GAUGE OR PIEZOELECTRIC 2%	E	4-20	MA				MCR INDICATION PRIMARY LOOP CONTROL
TT-009	CONDENSER SATURATION TEMPERATURE	0-100	0-100	°F	PLATINUM RTD 1/2%	E	4-20	MA				MCR INDICATION CONDENSATE DEPRESSION CALCULATION
TT-010	CONDENSER HOTWELL TEMPERATURE	0-100	0-100	°F	PLATINUM RTD 1/2%	E	4-20	MA				MCR INDICATION CONDENSATE DEPRESSION CALCULATION
LT-011	CONDENSER HOTWELL LEVEL	0-50	0-50	IN.	FLOAT/RESISTANCE (GEMS) 1%	E	4-20	MA	HI-HI HI LO LO-LO	48 43 20 15	IN. IN. IN. IN.	MCR INDICATION HOTWELL LEVEL CONTROL LOOP HH_3 INVENTORY CONTROL
LT-012	CONDENSER HOTWELL LEVEL	0-50	0-50	IN.	FLOAT/RESISTANCE (GEMS) 1%	E	4-20	MA	HI-HI HI LO LO-LO	48 43 20 15	IN. IN. IN. IN.	MCR INDICATION HOTWELL LEVEL CONTROL LOOP NH_3 INVENTORY CONTROL
PI-013	NH_3 FEED PUMP SUCTION PRESSURE	0-100	0-100	PSIG	BOURDON TUBE PRESSURE GAUGE 5%	N/A			N/A			LOCAL INDICATION (PUMP PERFORMANCE)
PI-014	NH_3 FEED PUMP DISCHARGE PRESSURE	0-300	0-300	PSIG	BOURDON TUBE PRESSURE GAUGE	N/A			N/A			LOCAL INDICATION (PUMP PERFORMANCE)

Table 7-10 (CONTINUED)
PRELIMINARY INSTRUMENT LIST

CHANNEL NO.	MEASURED PARAMETER	INSTRUMENT DATA RANGE	SPAN	UNITS	PRIMARY ELEMENT	OUTPUT SIGNAL TYPE	RANGE	UNITS	ALARM DATA LIMIT	SET PT.	UNITS	FUNCTION
FT-015	NH_3 FEED FLOW TO EVAPORATOR	$0\text{-}15\times10^3$	$0\text{-}15\times10^3$	GPM	4-AXIS ULTRA-SONIC (W LEF) 2%	E	4-20	MA				REMOTE INDICATION NH_3 FEED FLOW CONTROL
PT-016	NH_3 FEED HEADER PRESSURE	0-300	0-300	PSIG	STRAIN GAUGE OR PIEZOELECTRIC	E	4-20	MA				REMOTE INDICATION NH_3 FEED FLOW CONTROL
ZT-017	CV-1-1 POSITION				LVDT	E	0-10	VAC 1 KHZ				REMOTE INDICATION POSITIONER FEEDBACK
ZT-018	CV-1-2 POSITION				LVDT	E	0-10	VAC 1 KHZ				REMOTE INDICATION POSITIONER FEEDBACK
ZT-019	CV-1-3 POSITION				LVDT	E	0-10	VAC 1 KHZ				REMOTE INDICATION POSITIONER FEEDBACK
ZT-020	CV-1-4 POSITION				LVDT	E	0-10	VAC 1 KHZ				REMOTE INDICATION POSITIONER FEEDBACK
PT-021	EVAP. LIQUID NH_3 MANIFOLD PRESSURE	0-300	0-300	PSIG	STRAIN GAUGE OR PIEZOELECTRIC	E	4-20	MA				REMOTE INDICATION

Table 7-10 (CONTINUED)
PRELIMINARY INSTRUMENT LIST

CHANNEL NO.	MEASURED PARAMETER	INSTRUMENT DATA				OUTPUT SIGNAL			ALARM DATA			FUNCTION
		RANGE	SPAN	UNITS	PRIMARY ELEMENT	TYPE	RANGE	UNITS	LIMIT	SET PT.	UNITS	
TT-022	EVAPORATOR SATURATION TEMPERATURE	0-150	0-150	°F	PLATINUM RTD	E	4-20	MA				REMOTE INDICATION
PT-023	EVAPORATOR SATURATION PRESSURE	0-300	0-300	PSIA	STRAIN GAUGE OR PIEZOELECTRIC	E	4-20	MA				REMOTE INDICATION
PT-024	EVAPORATOR SATURATION PRESSURE	0-300	0-300	PSIA	STRAIN GAUGE OR PIEZOELECTRIC	E	4-20	MA				REMOTE INDICATION
LT-025	EVAP. STORAGE WELL LEVEL				FLOAT/RESISTANCE	E	4-20	MA	HI-HI HI LO LO-LO			REMOTE INDICATION LEVEL CONTROL
LT-026	EVAP. STORAGE WELL LEVEL				FLOAT/RESISTANCE	E	4-20	MA	HI-HI HI LO LO-LO			REMOTE INDICATION LEVEL CONTROL
FT-027	EVAP. RECIRCULATION FLOW	$0-1\times10^4$	$0-1\times10^4$	GPM	4-AXIS ULTRASONIC (W LEF)	E	4-20	MA				REMOTE INDICATION FLOW CONTROL
ZT-028	CV-4-1 POSITION				LVDT	E	0-10	VAC 1 KHZ				REMOTE INDICATION POSITIONER FEEDBACK

Table 7-10 (CONTINUED)
PRELIMINARY INSTRUMENT LIST

CHANNEL NO.	MEASURED PARAMETER	INSTRUMENT DATA				OUTPUT SIGNAL			ALARM DATA			FUNCTION
		RANGE	SPAN	UNITS	PRIMARY ELEMENT	TYPE	RANGE	UNITS	LIMIT	SET PT.	UNITS	
ZT-029	CV-4-2				LVDT	E	0-10	VAC 1 KHZ				REMOTE INDICATION POSITIONER FEEDBACK
ZT-030	CV-4-3				LVDT	E	0-10	VAC 1 KHZ				REMOTE INDICATION POSITIONER FEEDBACK
ZT-031	CV-4-4				LVDT	E	0-10	VAC 1 KHZ				REMOTE INDICATION POSITIONER FEEDBACK
ZT-032	BPV-1				LVDT	E	0-10	VAC 1 KHZ				REMOTE INDICATION POSITIONER FEEDBACK
ZT-033	BPV-2				LVDT	E	0-10	VAC 1 KHZ				REMOTE INDICATION POSITIONER FEEDBACK
ZT-034	BPV-3				LVDT	E	0-10	VAC 1 KHZ				REMOTE INDICATION POSITIONER FEEDBACK
ZT-035	BPV-4				LVDT	E	0-10	VAC 1 KHZ				REMOTE INDICATION POSITIONER FEEDBACK

Table 7-10 (CONTINUED)
PRELIMINARY INSTRUMENT LIST

CHANNEL NO.	MEASURED PARAMETER	INSTRUMENT DATA				OUTPUT SIGNAL			ALARM DATA			FUNCTION
		RANGE	SPAN	UNITS	PRIMARY ELEMENT	TYPE	RANGE	UNITS	LIMIT	SET PT.	UNITS	
PI-036	NH_3 RECIRCULATION PUMP DISCHARGE PRESSURE	0-500	0-300	PSIA	BOURDON TUBE							LOCAL INDICATION

7.2.8 Ammonia Pumps

7.2.8.1 Ammonia Feed Pump

The ammonia feed pumps transfer liquid ammonia from the condenser hotwell to the evaporator.

7.2.8.2 Ammonia Recirculation Pump

The pump selected for ammonia recirculation is similar to the feed pump. Flow rate, efficiency and other data are contained in Tables 7-11 and 7-12.

The ammonia feed pumps (two standard pumps in parallel are required) utilized in the OTEC power cycle are conventional horizontally oriented centrifugal-split casing pumps with nozzles integrally cast in the casing. They utilze mechanical shaft seals to prevent ammonia leakage. The pump and driver (electric motor) are mounted on a one-piece fabricated steel base plate.

Additional data pertaining to the ammonia feed pumps is contained in Tables 7-11 and 7-12.

7.2.9 Auxiliaries

7.2.9.1 Ammonia Storage, Handling and Purification System

This system is similar to the 10 MWe modular application. The storage requirement for the demonstration plant is approximately three and a half (3.5) times that of the 10 MWe module. The ammonia storage system will consist of fourteen (14) pressure vessels having sufficient capacity for storage of the total volume requirements of the 50 MWe ammonia Power Cycle. In addition to the storage vessels, this system will also be provided with a pressure tank and purification compressor, assorted piping, valves, instrumentation and controls.

Table 7-11
POWER SUMMARY DATA

ITEM	Efficiency	Power(MW)	% of Generator Power
Turbine/Generator	.800	70.01	100.0
Cold Water Pumping	.680	10.05	14.4
Warm Water Pumping	.680	6.65	9.5
Cycle Feed Pumping	.750	1.49	2.1
Recycle Pumping	.750	0.11	0.2
Chlorination	-	1.21	1.7
Estimated Hotel Load	-	0.50	0.7
Module Net Output	-	50.00	71.4

Table 7-12
50 MWe DEMONSTRATION PLANT AMMONIA FLOW DISTRIBUTION

LOCATION (KEY, FIGURE 6-78)	WEIGHT FLOW (10^6 LB/HR)	ENTHALPY (BTU/LB)	TEMP. (°F)	PRESSURE (PSIA)	ENERGY FLOW (10^6 BTU/HR)
Condenser Discharge(14)	14.840	98.040	49.500	88.492	1454.91
Hotwell Inlet(15)	14.840	98.040	49.500	88.467	
Hotwell Discharge(16)	14.840	98.040	49.500	88.647	
Feed Pump Inlet(17)	14.840	98.040	49.500	88.454	
Feed Pump Discharge(18)	14.840	98.297	49.500	142.745	
Separator Drain Discharge(19)	1.649	121.244	70.056	129.121	
Drain Tank Inlet from Separator(20)	1.649	121.244	70.056	129.082	
Evaporator Drain Discharge(21)	2.803	121.465	70.250	129.063	340.47
Drain Tank Inlet from Evaporator(22)	2.803	121.465	70.250	129.042	
Drain Tank Discharge(23)	4.452	121.383	70.178	129.042	
Recirculation Pump Inlet(24)	4.452	121.383	70.178	129.042	
Recirculation Pump Discharge(25)	4.452	121.449	70.178	142.524	
Combined Pump Flow(26)	19.292	103.640	54.272	142.524	
Evaporator Inlet(7)	19.292	103.640	54.272	142.524	1999.42
Evaporator Discharge(8)	16.489	578.419	70.250	129.063	9537.55
Separator Inlet(9)	16.489	578.419	70.056	128.922	
Separator Discharge(10)	14.840	629.211	69.976	128.741	
Turbine Inlet(11)	14.480	629.211	69.948	128.487	
Turbine Exhaust(12)	14.480	612.563	49.587	88.492	
Condenser Inlet(13)	14.480	612.563	49.587	88.492	9090.43

7.2.9.2 Nitrogen Storage and Supply System

During evacuation, prior to initial system startup, all 50 MWe components exposed to an anhydrous ammonia atmosphere will be filled with nitrogen gas to displace any air present in the system, thus avoiding direct contact between ammonia and air. Prior to performing maintenance on the ammonia power cycle, nitrogen gas will be used to displace residual ammonia gas present. The amount of nitrogen required to purge the 50 MWe system will occupy a large portion of the platform vessel. It is therefore recommended that in this case the nitrogen be stored on another vessel or transported as required via a support vessel.

7.2.9.3 Circulating Seawater and Component Cooling Water (CCW) System

The circulating seawater and component cooling water system for the 50 MWe system is similar to the one used on the 10 MWe system. It furnishes warm and cold water CCW to various OTEC power cycle components and also provides the hull support components with a source of cooling water.

7.2.9.4 Compressed Air System

During normal operation (including startup and shutdown) ship service, instrumentation, and diesel generator starting air will be supplied by a train of equipment consisting of a compressor, an aftercooler, air receivers and air dryers. This air is filtered and dried before it is delivered to the distribution network which will be similar in configuration to that illustrated for the 10 MWe power module. Compressed air may also be used to purge the system after the nitrogen has been evacuated, just prior to personnel access.

7.2.9.5 Auxiliary Power Supply System

The diesel generator system will be designed to furnish start-up and stand-by power for the OTEC 50 MWe power module under all operating and survival sea conditions. When multiple modules are used in a power plant, it may not be necessary to furnish start-up and stand-by power on a one-to-one basis with the power modules. The economical installation will be the greater of the two values, start-up power required for one 50 MWe module plus all concurrent platform auxiliary and hotel load, or the total platform auxiliary and hotel load imposed under emergency or survival operating conditions.

7.2.9.6 Electrical Distribution system

An electrical distribution system similar to that described for the 10 MWe power module, but sized to meet the auxiliary power requirements of a 50 MWe power module, will be provided.

7.3 System Design

7.3.1 Materials Compatibility

The material selections for the 50 MWe unit are identical to those described for the 10 MWe given in Section 6.3.1. However, the tubing material recommendation could be changed. A change would occur if data gathered before the 50 MWe tubing material is ordered indicates that titanium could be replaced with aluminum. (A principal purpose of the test articles is to qualify aluminum for OTEC service.) Pending the generation of additional materials data, the 50 MWe tubing material will be titanium.

7.3.2 Arrangement

Using the spatial relationships and limits discussed in Section 6.3.2 and component sizes determined by the total system optimization computer program, arrangement studies for three 50 MWe power module configurations were completed.

The back-to-back arrangement, Figure 7-25, is similar to the arrangement developed for the 10 MWe Modular Application power system. However, because multiple 50 MWe power modules are likely to draw from common cold water sources in commercial sized power plants, and may draw from common warm water sources, intake plenums were placed at the ends of the module, and discharge plenums were placed at the center. Heat exchanger bundles would be installed and removed by way of the adjacent seawater discharge plenums. At 55 cubic feet per kilowatt, it is the most compact of the arrangements.

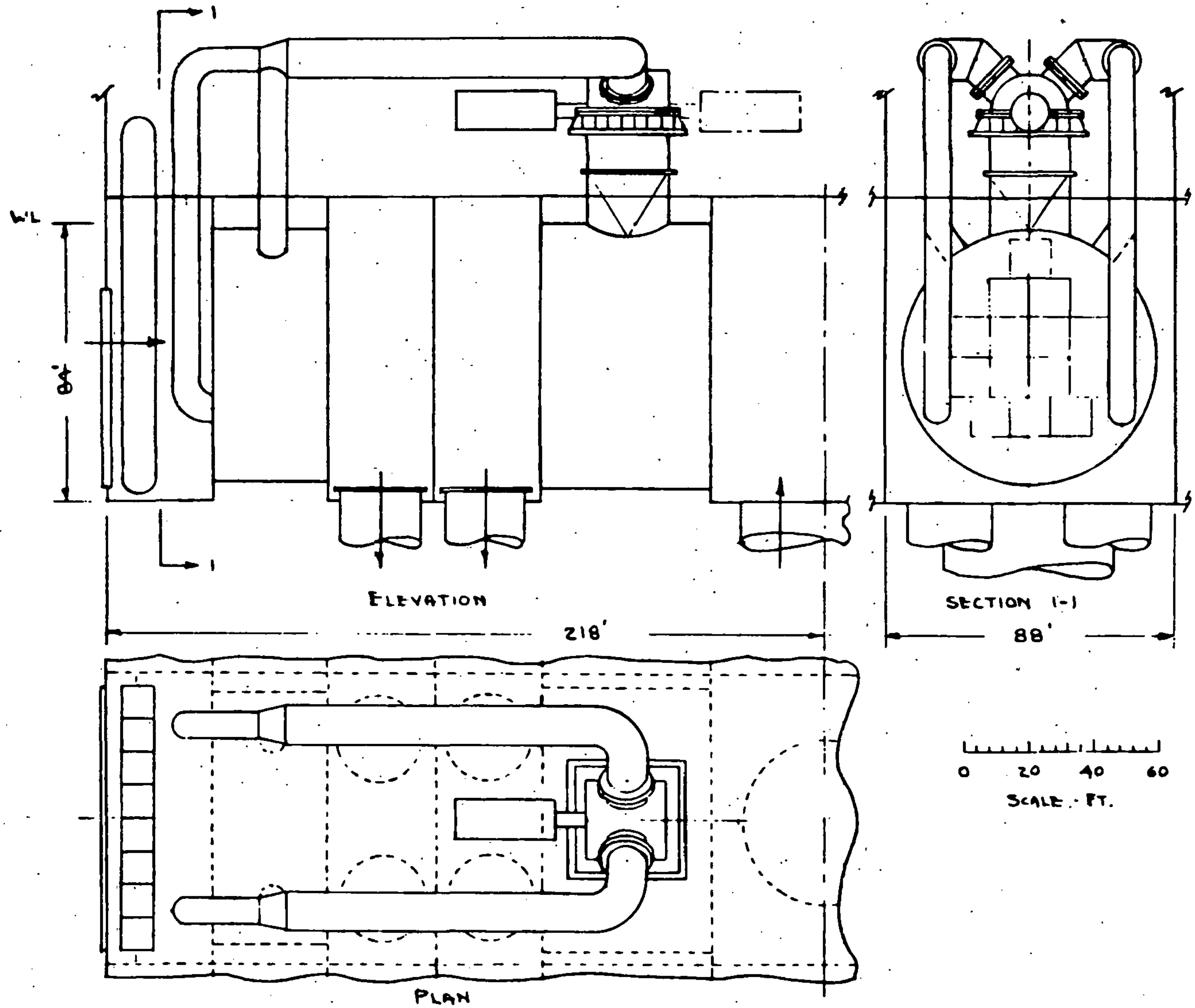

Figure 7-25
50 MWe OTEC MODULE
"BACK TO BACK" CONFIGURATION

A side by side arrangement, Figure 7-26, is particularly suitable to relatively long, narrow or ship-shape surface platforms. It has the shortest ammonia vapor piping runs of any of the arrangements. However, it requires approximately 61 cubic feet per kilowatt. In the most compact grouping of modules only four can be serviced by a single cold water pipe. To serve eight from a single pipe will require a significant increase in cold water ducting, with consequent enlargement of the platform. Evaporator tube bundles can be installed or removed by way of the warm water discharge plenum. Condenser tube bundles can be handled through the cold water intake plenum.

A stacked arrangement, Figure 7-27, was developed with spar-type platforms in mind. It also could be used in the legs of a column-stabilized semi-submersible, or in a tuned sphere. Although its actual enclosed volumes are less than those of the other two arrangements, its gross volume is approximately 66 cubic feet per kilowatt. In a spar installation the heat exchangers and their intake plenums could be immersed in seawater. The recommended vessel for the turbine-generator gallery is a sumberged pressure structure to permit a shirt sleeve atmosphere within. Seawater circulation pumps are on the intake sides of the heat exchangers rather than on the discharge side as in the other two arrangements.

It currently appears that tube bundles would have to be installed and removed with the module at a special facility, rather than on-board by way of seawater plenums as in the other two arrangements.

The three arrangements, back to back, side by side, or stacked give all of the flexibility required to adapt the 50 MWe power module design to any of the platform configurations which have been postulated for OTEC plants.

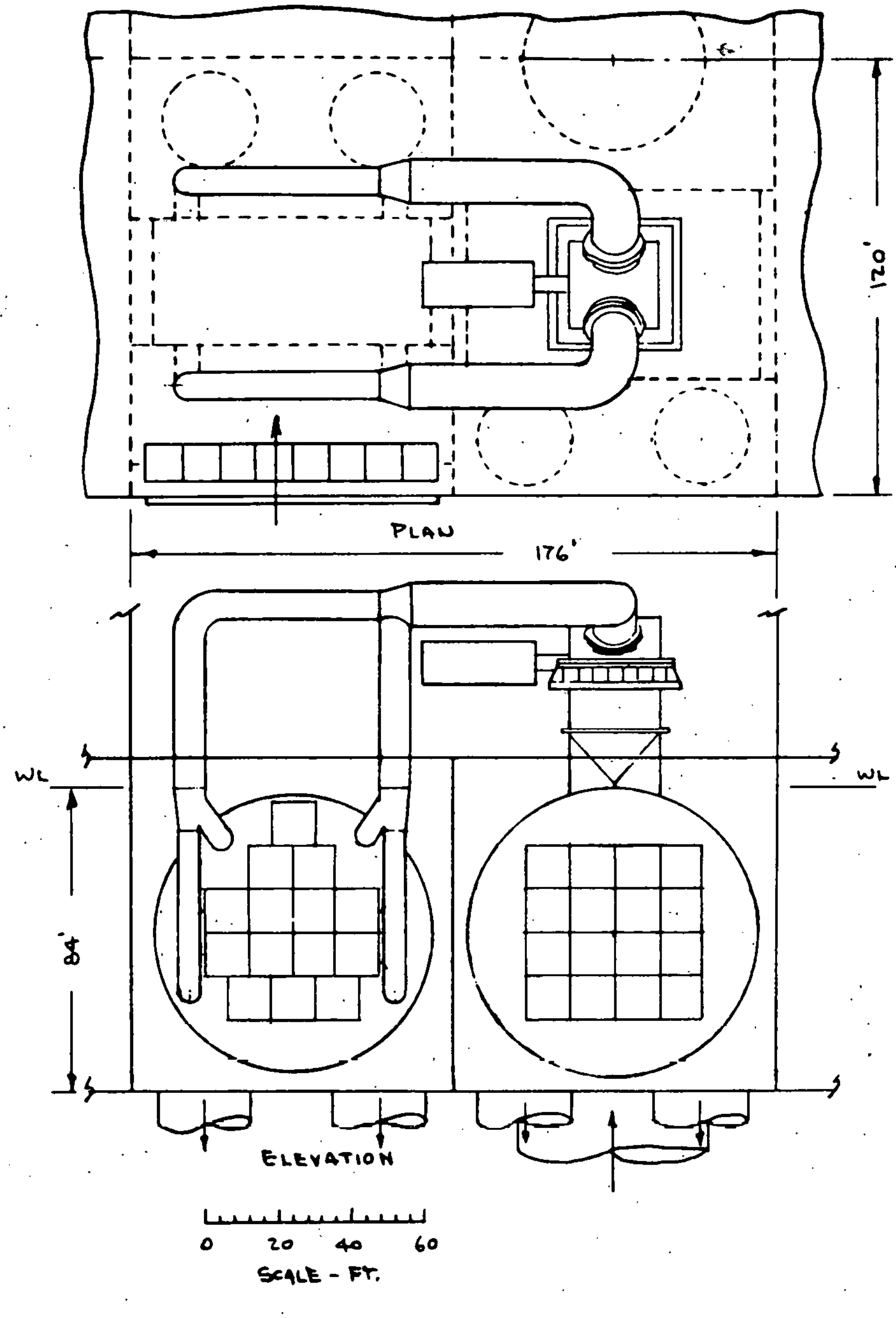

Figure 7-26
60 MWe OTEC MODULE
"SIDE BY SIDE" CONFIGURATION

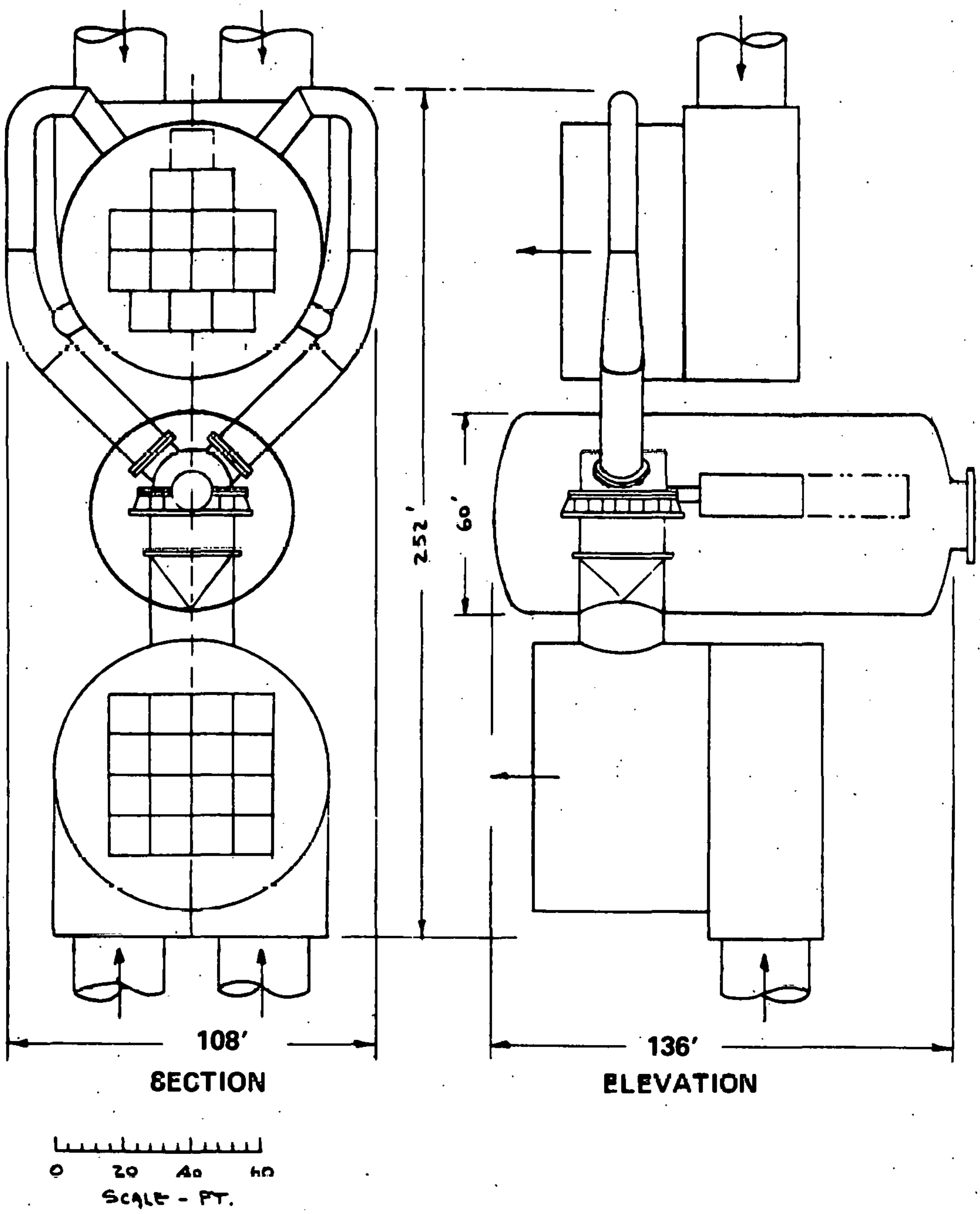

Figure 7-27
50 MWe OTEC MODULE
"STACKED" CONFIGURATION

7.3.3 System Control

The system control design approach discussed in Section 6.3.3 for the 10 MWe Modular Application will also apply for the 50 MWe Demonstration Plant. The selection of the control configuration, and particularly the valve selection was based upon the more stringent requirements of the larger 50 MWe size, as discussed in Section 6.3.3.3. Of the four proposed control configurations two basic configurations have emerged; the baseline design, and an alternate control configuration. The baseline design is the one with turbine bypass valves only; in the alternate design both turbine inlet valves and turbine bypass valves are used to provide overspeed protection and the controlling functions for the turbine. If tests verify that the baseline design meets the control requirements as the analysis has indicated, it will be adopted; otherwise the alternate design will be recommended as the back-up configuration.

7.3.4 Availability

As compared with the 10 MWe, there is little reason to believe that Demonstration Plant availability numbers will change sufficiently to prevent meeting the 90% availability goal. In fact, the conceptual level estimates of Table 7-13 show that little impact on availability is expected due to size increases. This is a reasonable expectation in light of the fact that there is intentional design similitude between the two units. Note also that compared to conventional units for which data exists, a 90% availability for the power system is realistic. Table 7-14 shows that fossil plants in the 60 to 80 MWe range have an availability of 90.1%. These fossil units have a great deal of their problems associated with high temperatures and pressures not found in OTEC plants. Hydroelectric plants show an availability of 95.4%. These plants are less complex than OTEC plants because they lack heat exchangers, therefore it is reasonable that their availability be higher.

Table 7-13
OUTAGE SUMMARY FOR MAJOR COMPONENTS OF 50 MWe POWER MODULE

Major Component	1 Unscheduled Outages: MTBF (Hrs.)	2 Unscheduled Outages: MTTR (Hrs.)	3 Scheduled Outages: Calendar time between maintenance actions (Hrs.)	4 Scheduled Outages: Mean Duration of Outage (Hrs.)
1 Evaporator	15554[1]	100	8499	267
2 Condenser	15554[1]	100	8499	267
3 Turbine	7077	103		
4 Generator	9548	63	34224	840
5 W.W. Pumps	40550	80	8499	32
6 C.W. Pumps	40550	80	8499	32
7 Condensate Pump	22077	80	8499	59
8 Recirculation Pump	22077	80	8499	59
9 Valves	70128	120	165	2.6
10 Other	9015	64	8499	70

[1]Zero downtime due to tube failures assumed.

Notes: A once per year scheduled maintenance cycle is effected during which, after 8,999 hours since the end of the last scheduled outage, the plant is down for 267.4 hours, and every fourth year, or more precisely after 34,244 hours since the last major shut down, 840 hours are taken for regular annual work plus a turbine/generator overhall and inspection. During the shut down periods, all maintenance is effected simultaneously.

Table 7-14
POWER INDUSTRY DATA

	Equivalent Availability*
Fossil Plants 60-89 MWe	90.10
Fossil Plants 90-129 MWe	86.30
Fossil Plants 600 MWe and Above	68.40
Nuclear Units	69.20
Diesel Units	94.50
Hydroelectric Units	95.40

*Reference 144 "Equivalent Availability" data.

The footnote on Table 7-13 refers to the fact that no tube failures have been included in the outage time estimates. Since the tubes in the heat exchangers are titanium and their reliability is .999973 (Reference 143), no tube failures are expected to cause an outage. It is expected that even if a tube failed by leaking slightly, it would not be necessary to shut the plant down. This is true because the normal mode of tube failure is to start with a small leak, often at the tube-to-tubesheet joint. Since the leaks do not grow rapidly, their presence would be detected during routine inspection of the heat exchangers. The methods of inspection and repair of the welded titanium tube-to-tubesheet joints have already been used in the power industry and therefore present no unexpected problems.

7.3.5 Safety

Because the 10 MWe is specifically designed to be similar to the demonstration plant size, little special considerations for the 50 MWe size are expected. It will be important only to take into account the larger equipment sizes in dealing with the hazards such as spillage and leakage.

7.3.6 Plant Statistics Summary

The design of the 50 MWe Demonstration Plant was kept at the conceptual level to focus the effort of preliminary design on the 10 MWe Modular Application. The heat exchangers, as the components of greatest interest, were specified to the extent shown in Table 7-15. Other components were specified only with respect to their performance and costs, which are discussed in Sections 7.5.1 and 7.7, respectively.

Table 7-15
HEAT EXCHANGER DESIGN DATA (50 MWe)

	Condenser	Evaporator
External Design Pressure (PSIG)	0	0
Internal Design Pressure (PSIG)	150	150
Tube Material	Titanium	Titanium
Tube O.D. (inches)	1.0	1.0
Tube wall thickness (inches)	0.028	0.028
Tube length (ft)	51.6	33.8
Surface Area (ft^2)	2,787,795	1,831,138
Number of Tubes	206,453	206,649
Number of Modular Bundles	14	14
Shell Material	C-Steel	C-Steel
Shell Diameter (ft)		
Shell Thickness (in)	3-750	3-875
Weight of Bundles (lb)	2,256,000	1,533,000
Weight of Shell (lb)	2,045,000	1,373,000
Dry Weight (lb)	4,301,000	2,906,000
Weight of Ammonia (lb)	665,000	999,000
Weight of Seawater (lb)	3,312,000	2,190,000
Operating Weight (lb)	8,278,000	6,095,000

7.4 Manufacturing and Installation

7.4.1 Heat Exchangers

The studies associated with manufacturing processes and sequences for the 10 MWe apply in all areas to the 50 MWe heat exchangers, with the exception of the shells. Shell diameters in the order of 82 feet dictate that the sections be assembled in the vertical plane rather than the horizontal. The tube bundles, on the other hand, being of the modular design, present no significant problems. Like the 10 MWe bundles they permit the use of normal manufacturing processes and techniques, thus reducing the labor, handling equiment and sophisticated tooling and fixtures required for manufacture and assembly.

With 14 tube bundles in each of the heat exchangers (condenser and evaporator), a total of 28 tube bundle assemblies are required. This allows use of manufacturing methods that will increase the effectiveness of both the tube installation and the tube welding processes. This, in turn, would significantly reduce the labor, and hence, the cost associated with tube bundle fabrication and assembly.

Shell plates for both the condenser and the evaporator will be purchased and received with all edges prepared for welding and shaped to the proper radius. Inspection at the supplier's facility will assure all dimensions are within the engineering tolerances. The shell plates will be fitted using assembly fixtures to establish and maintain alignment and circularity. The shells will then be welded using automatic sub-arc equipment, after which all welds will be radiographed and repairs made as necessary.

Materials for the end assemblies, and internal support structures will be received as plates and shapes and fabricated as subassemblies, in parallel with the shell fabrications. These subassemblies will then be delivered to the main assembly area where the I Beam lattice structures will be aligned to the shell end spool pieces and welded. The internal structure will then be pre-aligned and welded. All nozzles will be located, positioned and welded to the spool pieces. All spools will then be welded together, and final alignment of the internals and welding completed.

The completed shell will receive post-weld heat treatment, blast and coat, and hydrostatic test, and will be prepared for shipment to the installation site.

Tube sheets and support plates will be received having been drilled with existing numerically controlled, ganged Moline drilling machines, all holes deburred, and the plates ready for assembly. Tubes, coated and uncoated, will be received cut to the proper length.

The tube sheets and support plates will be set and aligned in the horizontal erection jig. Corner angles and bracing will be cut to length, fitted and welded to the support plates and tube sheets. It will be necessary for one tube sheet to be left off in the case of the evaporator, until the coated tubes have been placed in the support plates and one tube sheet. Finally, the second tube sheet is added and all the tubes inserted within it. The bundles with tubes installed will have the tubes expanded and welded with automatic GTAW tube welders. Nondestructive examination will be performed on all welds, and repairs will be made as necessary.

Completed test bundles will be placed in a test chamber and pressurized to test the tube-to-tube sheet welds. Repairs will be made as required. A final dimensional check will be made on the bundles which will then be prepared for shipment to the installation site.

Final installation of the tube bundles into the shell will be made on board the platform where the final closure weld for each bundle assembly will be made at both ends.

7.4.2 Turbine

The base diameter, blade height and rotor weight of the 50 MWe turbine are 63 inches, 17 inches, and 17000 lbs, respectively, as compared to 32 inches, 8 inches and 4200 lbs for the 10 MWe design. This increase in size will result in approximately a 25% increase in the manufacturing time listed in manufacturing events plan shown on Figure 6-73.

The manufacturing procedure listed for the 10 MWe scale model design will be applicable to the 50 MWe design. The larger size of the 50 MWe design makes it a medium size turbine; it is well within the manufacturing capability of existing Westinghouse turbine facilities.

It is envisioned that the design of the 50 MWe turbine(s) could be accomplished at one facility and manufactured at another plant located in closer proximity to the platform. This could permit the turbine(s) to be shipped assembled which would result in reduced shipping and reassembly cost.

7.4.3 Generator

The manufacturing procedure for the 10 MWe generator described in paragraph 6.4.3 is applicable to the 50 MWe design.

The following areas of design change of the 50 MWe compared to the 10 MWe will impact the manufacturing events plan to cause an additional 5 months construction time. The additional time will be required primarily in the machining and assembly areas.

- Size - the increased size will result in additional frame fabrication and rotor machining time.

- Cooling System - in order to improve the generator efficiency, the 50 MWe design will have hydrogen cooling versus the air cooling specified for the 10 MWe design. This will require fabrication and machining of additional components.

- Exciter - Westinghouse contemplates supplying a brushless type exciter which will meet the 50% overspeed requirement with the 1800 RPM generator versus the static exciter provided with the 10 MWe design. The series type machinery requirement necessitated by this design will result in additional machining time.

As noted in paragraph 7.4.2 the turbine is classified as a medium size turbine, so the generator design is well within the state-of-the-art in all respects.

7.4.4 Seawater Pumps

The demonstration plant seawater pumps are similar in design and manufacture to those for the Modular Application. Existing techniques and facilities are adequate for their manufacture. Details will be identical to those described in Section 6.4.4.

7.4.5 Assembly and Checkout

Studies completed during the conceptual design of Phase I, and confirmed during the preliminary design show the 50 MWe power module to be the optimum size for commercial OTEC power systems. The size and weight of the heat exchangers present unique problems both to their fabricator, as discussed in Section 7.4.1, and to the shipyard which will install them in the platform. At estimated weights of 1,297 tons for the evaporator and 1,920 tons for the condenser, they far exceed the capacity (900 tons) of the largest shipyard cranes currently available, and probably exceed the reasonable limit for crane lift capacity in a newly dedicated assembly facility. However, the unique modular design of the Westinghouse heat exchangers will limit their maximum lift requirement to no more than that of the next heaviest component, the generator at approximately 260 tons. Specific assembly procedures for a commercial plant can be developed only after the platform configuration has been selected and an integrated power plant and platform design completed, but some generalizations can be made which are applicable to the installation of any number of 50 MWe modules into a platform.

Installation of the heat exchangers will start with lifting of completed shells onto partial foundations incorporated into the plenum chamber bulkheads at their ends, essentially as described in Section 6.4.5 for the 10 MWe Modular Application plant. Supporting and bounding bulkheads and decks, and the balance of foundations or supporting saddles will then be completed. The nature of structural intersections between heat exchanger shells, bulkheads and supporting foundations, the manner of achieving watertight joints, and the need for and means of achieving flexibility at certain intersections will be dependent upon the configuration and choice of structural material for the platform. Assembly details will depend on the choices made. After installation of the shells, tube bundles can be installed at any time parallelling other plant assembly operations.

The balance of the power module components will be received at the assembly facility by rail, truck or barge. Where appropriate, major subassemblies will be shop erected prior to installation in the platform. This will maximize the amount of parallel work that can be achieved and optimize the working environment, thereby minimizing erection time and cost.

Early in the design stage, complete manufacturing process flow plans will be developed in close cooperation with the platform designers and potential builders. The plans will identify long-lead items, determine erection schedules, and identify problem areas. Problem areas will be resolved in such a manner as to minimize adverse effects on schedule and cost.

Upon completion of the assembly of all subsystems, each will be tested for electrical continuity, fluid or vapor tightness, and operational readiness as appropriate. Final start-up and test of the total power plant will be completed at the ocean site.

7.5 System Operation

7.5.1 Normal Operation

The 50 MWe power module is designed to operate between a warm seawater temperature of 80°F and a cold seawater temperature of 40°F, with a biofouling thermal resistance of 0.00025 (hr-ft^2-°F)/BTU. Thermodynamic cycle data is given in Table 7-16.

Table 7-16
50 MWe THERMODYNAMIC CYCLE DATA

Heat Input	2308.6 MW
Heat Rejection	2238.2 MW
Rankine Cycle Efficiency	3.05%
Generator Gross Output	70.0 MW
Parasitic Losses	20.0 MW
Plant Net Output	50.0 MW
Overall Plant Efficiency	2.17%

The performance of the heat exchangers is shown in Table 7-17.

Table 7-17
HEAT EXCHANGER DATA

	Condenser	Evaporator
Seawater Flow (10^6 lb/hr)	1302	1499
Seawater Inlet Temperature (°F)	40.0	80.0
Seawater Outlet Temperature (°F)	46.1	74.5
Ammonia Flow (10^6 lb/hr)	14.8	14.8
Ammonia Inlet Temperature (°F)	49.6	54.3
Ammonia Outlet Temperature (°F)	49.5	70.3
Log-Mean Temperature Difference (°F)	5.90	6.63
NTU's	1.04	0.83
Effectiveness	0.65	0.56
Heat Transfer Coefficient (BTU/hr-ft^2-°F)	464.2	649.5
Heat Transferred (10^6 BTU/hr)	7640	7880
Tubeside Velocity (ft/sec)	5.6	6.5
Tubeside Pressure Loss (psi)	3.47	2.81

The performance of the rotating equipment and cleaning system is tabulated in Table 7-11. Thermodynamic state point data is given in Table 7-12.

Fouling control is achieved by chlorination alone. Expected performance and chlorine dosage rate are the same as for the 10 MWe plant (refer to Section 6.5.1).

7.5.2 Off-Design Performance

Performance of the 50 MWe plant will be impacted by the same variables and to a similar degree as the 10 MWe plant. No special size effects appear evident in relation to off-design performance of the power module.

As with the 10 MWe system, major effects will be due to variations in seawater temperatures and fouling of heat exchangers. Lesser effects are expected from part load and load cycling operations, and water and noncondensibles in the ammonia. (Refer to Section 6.5.2 for discussion of effects).

7.5.3 Dynamic Response

The dynamic responses of the 50 MWe configuration to the control valve actions in the turbine overspeed protection system were obtained from a computer simulation during the conceptual design phase. The dynamic responses of the 10 MWe application to the turbine overspeed protection system (scaled version of 50 MWe) were obtained during the Preliminary Design Phase, using a revised dynamic computer model. The output of the 10 MWe computer study are presented herein. It is expected that the characteristics of the 50 MWe configuration during turbine overspeeds will be the same as those of the 10 MWe application.

7.5.4 Maintainability

During the conceptual design of the 50 MWe power system the maintainability analysis consisted of:

- Assuring accessibility for major equipment maintenance.
- Comparing the 10 MWe maintainability considerations with those of the 50 MWe.

The 50 MWe design does allow for accessibility of heat exchanger bundles and seawater pumps by design. The seawater plenums may be sealed off so that they may be pumped dry for "shirt-sleeve" environment access to tube bundles. This also enables on site repair of seawater pumps and removal capability for the seawater pumps and heat exchangers should major repair/replacement be necessary. The balance of the plant has an expected maintenance routine which does not differ in concept from that of the 10 MWe power system. This is, of course, a natural result of the fact that the 10 MWe design is a model of the larger system. Estimates for the 50 MWe scheduled outage frequency and duration are included in Table 7-13.

7.6 Net Energy Balance

7.6.1 Concept

The concept of net energy analysis is motivated by a growing concern that an energy supply system based on new energy technologies should be evaluated not only in terms of dollar economics but, also in terms of actual energy economics. Recent congressional action has mandated that net energy criteria be utilized as one of the criteria in evaluatiog proposed energy technologies. Specifically, the federal non-nuclear Energy Research and Development Act of 1974, PL 93-577 5(a)(5) stipulates that "Potential for production of net energy by the proposed technology at the state of commercial application shall be analyzed and considered in evaluating proposals."

The PL 93-577 does not define net energy, but the following definition is most commonly used by researchers in this field: "Net energy is the amount of energy that remains for consumer use after the energy costs of finding, producing, upgrading, and delivering the energy have been accounted for."

A net energy analysis was performed on a 50 MWe power module of the Westinghouse OTEC system. This system was segregated into the following major components.

1. A surface platform/ship designated as the basic hull (concrete or steel) and anchor system

2. A power module consisting of heat exchangers, turbine/generators, pumps, ammonia piping and other miscellaneous components

3. Cold water piping system

4. Other components

The energy required for towing the ship to the anchoring site, as well as the energy required in moving the parts to and from the shore both during construction and for maintenance over the service life of the plant are believed to be relatively small and hence not included in the computation of the input energy.

7.6.2 Methodology

The method employed for energy computations uses primary energy* coefficients (BTU/ton) and the masses of the OTEC power plant components. These energy intensity coefficients, obtained from published reports[145-148] were computed from the input-output analysis of U.S. economy consisting of 357 production sectors in 1967 and process analysis of specific materials or components.

The energy coefficient of nitrogen was estimated from the process and cost data supplied by Linde Air Products (Division of Union Carbide Corp.) and Research Corp.

*Primary energy is defined as the sum of coal, crude oil plus the fossil energy equivalent of the hydro and nuclear energy (used to produce electricity in 1967) for electrical energy used in the product.

Table 7-18 shows the mass in short tons for the above components. The mass of the platform/ship was prorated down from a 400 MWe plant ship while the masses of the other components were obtained from the corresponding masses of a 10 MWe module, by multiplying by 5 (except ammonia which was calculated separately).

7.6.3 Energy Input

The OTEC power system under study consists essentially of the following distinct materials and components:

1. Reinforced Concrete (optional)
2. Fabricated Steel Products
3. Stainless Steel Products
4. Fabricated Titanium Products
5. Manufactured Equipment
6. Ammonia
7. Nitrogen

Table 7-19 shows the energy coefficients, total energy, and annualized input energy from the components considered in the Westinghouse OTEC 50 MWe power plant system. Annualized energy inputs were obtained from the total input energy of each major component by dividing the latter by the expected service life of the individual components.

The economic analysis issued separately estimates the annual operating and maintenance (O&M) costs at $550,000 per year (1978 dollars). These costs include the personnel, fringes, material, supplies and contingency. These costs were deflated in 1967, and energy coefficients BTU per dollar from Bullard et. al.[148] were used to estimate the energy equivalents of O&M dollar costs. This was found to be 30,000 million BTU per year.

Table 7-18
50 MWe OTEC POWER PLANT - MASS OF MATERIALS
SHORT TONS

COMPONENT	FABRICATED STEEL	FABRICATED TITANIUM	TURBINE/ PUMP	MHE (1)	MOTOR/ GENERATOR	TRANSFORMER	SWITCHGEAR	OTHER
1. Platform/Ship								
a. Concrete, or								63,427 (2)
b. Steel	13,484							
c. Deck House and Anchor	3,087							
2. Power Module								
a. Condenser	1,363	787						
b. Evaporator	944	509						
c. Turbine/Generator			82		290			
d. Lube Oil System	35							
e. Ammonia Pumps			155					
f. Ammonia Pipes and Tanks	1,185							
g. Ammonia Valves	595							
h. Sea Pumps			675			50		
i. Sea Screens								460 (3)
j. Amertap								220 (3)
k. Diesel System	5				505			
l. Nitrogen Tank	75							
m. Gantry				600				
n. Cooling Water	5							
o. Power Conditions							665	
p. Wiring								65 (4)
3. Cold Water Pipe								
Pipe	2,845							
4. Other Components								
a. Ammonia								1,156
b. Nitrogen								148
5. TOTAL	23,623	1,296	912	600	795	50	665	65,476

(1) Mechanical heavy equipment

(2) Reinforced concrete

(3) Stainless steel

(4) Naval wiring material

Source: Westinghouse Electric Corporation
Power Generation Division

Table 7-19
WESTINGHOUSE OTEC POWER SYSTEM ENERGY ANALYSIS

A: INPUT ENERGY PLANT COMPONENTS	MASS SHORT TONS	PRIMARY ENERGY COEFFICIENT 10^6 Btu/ton	TOTAL PRIMARY ENERGY 10^6 Btu	SERVICE LIFE (YEARS)	ANNUALIZED ENERGY INPUTS ELECTRICAL 10^6 Btu	THERMAL 10^6 Btu	TOTAL PRIMARY 10^6 Btu
1. Platform							
a. Concrete Hull	63,437	2.74	173,790	100	360	1,378	1,738
or Steel Hull	13,484	111	1,496,724	50	7,880	22,055	29,935
b. Deck House and Anchor	3,087	111	342,657	50	1,804	5,049	6,853
c. Construction	(20% of subtotal)						
Concrete Hull			171,821	100	433	1,285	1,718
Steel Hull			367,876	50	1,937	5,421	7,358
Subtotal							
Concrete Hull			688,268		2,597	7,712	10,309
Steel Hull			2,207,257		11,621	32,525	44,146
2. Power System							
a. Steel Components	4,207	111	466,977	40	3,074	8,600	11,674
b. Titanium Components	1,296	626	811,296	40	16,915	3,367	20,282
c. Equipment							
Pumps/Compressors	912	110	100,320	40	842	1,666	2,508
Gantry	600	114	68,400	40	542	1,168	1,710
Transformers	50	85	4,250	40	38	68	106
Switchgear	665	252	167,580	40	1,660	2,530	4,190
Motor/Generators	795	131	104,145	40	944	1,660	2,604
Wiring Devices	65	113	7,345	40	85	99	184
Sea Screens and Amertap	680	111	75,480	40	497	1,390	1,887
d. Construction	(20% of steel & equipment)		198,900	40	1,094	3,879	4,973
Subtotal			2,004,693		25,691	24,427	50,118
3. Cold Water Pipe							
a. Steel	2,845	111	315,795	50	1,663	4,653	6,316
b. Fabrication	(20% of steel)		63,160	50	227	1,036	1,263
Subtotal			378,955		1,890	5,689	7,579
4. Other Components							
a. Ammonia	1,156	39	45,084	33	-	1,366	1,366
b. Nitrogen	148	12	1,776	0.17	7,319	3,335	10,654
Subtotal			46,860		7,319	4,701	12,020
5. Operation & Maintenance							
O&M Staff, Materials And Supplies					6,600	23,400	30,000
Total Input Energy							
a. Concrete Hull System					44,097	65,929	110,026
b. Steel Hull System					53,121	90,742	143,863
B: OUTPUT ENERGY							
1. Gross Output Power	70 MWe						
Less Auxiliaries	19.9 MWe						
Net Output Power	50.1 MWe						

2. Output energy per year (90%) availability = 395 x 10^6 kWh = 1,348,000 x 10^6 Btu

3. Output energy to input energy ratio

Concrete Hull System = 12.25

Steel Hull System = 9.37

7.6.4 Energy Output

The energy output of the 50 MWe power module is summarized in Table 7-20.

Table 7-20
POWER SUMMARY

Generator Gross Output	70.01 MWe
Cold Seawater Pump	10.05 MWe
Warm Seawater Pump	6.65 MWe
Cycle Feed Pump	1.49 MWe
Recycle Pump	0.11 MWe
Chlorination	1.21 MWe
Estimated Hotel Load	0.50 MWe
Parasitic Losses	20.01 MWe
Net Module Output	50.00 MWe

An availability of 90% is considered possible because of moderate temperature and pressure, and use of proven materials and design techniques.

A 90% availability would generate 395 million kWh per year. This is equivalent to 1,348,000 million BTUs per year.

7.6.5 Results

As shown in Table 7-19, the total inputs are thus 143,863 x 10^6 BTU. The bus bar output of electrical energy is estimated to be 1,348,000 x 10^6 BTU. Hence it is observed that the net annual electrical energy output of the OTEC power plant is 9.37 times (for steel hull) the annualized energy inputs during the construction and operation period (over the service life of the components).

If the total input energy is increased by 30 percent to allow for any estimating error, the net energy output to input ratio decreases to 7.20 for steel hull and 9.4 for concrete hull based system.

It is concluded that the OTEC system represents a highly favorable net energy balance. Even after allowing for a reasonably large error margin, the energy delivered is more than seven times the total direct and indirect input energy.

7.7 Costs

7.7.1 Capital Costs

The costs used in the optimization of the 50 MWe Demonstration Plant are those of the first production plant because these costs have the best-known interrelations, and because the optimization should not include the non-recurring costs of the prototype plant.

7.7.1.1 Power Module Cost

Cost estimates for major module components are based on procedures normally used on currently manufactured products. These costs are beyond the conceptual level, but not at the level of accuracy of the Preliminary Design. The cost algorithms used in the system computer model were developed through an iterative procedure by detailed cost estimating specific designs and adjusting the algorithms to eliminate discrepancies.

The power system analysis began at the seawater inlet and stopped downstream of the seawater pump. The inlet and outlet trunks are designed to be part of the ship structure. The hull, inlet screens, cold water pipe, and power conditioning system, were not evaluated for cost. The subsystems and their type of cost analysis are listed in Table 7-21. Three types of cost estimating procedures were used: a detailed engineering cost estimate; a cost estimate based on some performance parameter of the piece of equipment (parametric); and a cost estimate which is some factor of the overall module size (factored).

Table 7-21
SUBSYSTEM COST ANALYSIS TYPES

SUBSYSTEM	TYPE
Heat Exchangers	Detailed Engineering Cost Est.
Cleaning System	Parametric to Chlorination Rate
Turbine	Parametric to Gross Power
Generator	Parametric KVA, Speed
Seawater Pumps	Parametric Water Volume Flow
Ammonia Pumps	Parametric Ammonia Volume Flow
Controls	Factored
Ammonia Piping and Valves	Factored
Plant Auxiliaries	Factored

Cost algorithms were used as a general guide to forecast both prototype plant costs and subsequent production costs. Development of cost required the consideration of both new system uncertainty and potential cost improvements. The cost algorithms for the 50 MWe module used 1977 prices.

Cost estimates for the 50 MWe power module are summarized in Table 7-22, for both titanium and alumium modules.

Table 7-22
50 MWe POWER MODULE COST SUMMARY ($/KW)

	TITANIUM	ALUMINUM
Evaporator, incl. Hotwell	503	447
Separator	35	37
Condenser, incl. Hotwell	524	373
Turbine	37	37
Generator	37	37
Seawater Pumps	112	107
Ammonia		
Pumps	8	8
Piping and Controls	8	9
Auxiliaries	56	52
Chlorination	44	39
Subtotal	1364	1146
Installation	56	59
Module Total	1420	1205

7.7.1.2 Heat Exchanger Costs

Heat exchanger costs and the costs of related components are shown in Table 7-23, for both the proposed titanium module and the aluminum comparison module. The figures in Table 7-23 include indirect expenses, factory costs, and engineering expense associated with production. Overhead expenses are also included to deal with handling costs and general corporate costs.

The cost summaries in Table 7-23 are the results of cost-optimized titanium and aluminum power modules. The cost differences are due to the tube material, the additional shell preparation needed to attach aluminum bundles to steel shells, and minor size differences due to slightly different ammonia flow rates.

Table 7-23
HEAT EXCHANGER RELATED COSTS ($/KW)

	TITANIUM	ALUMINUM
Condenser		
Bundle Material	339.50	156.42
Bundle Labor	128.78	130.74
Shell Material	13.12	20.08
Shell Labor	32.38	54.61
Total Condenser	513.78	361.85
Evaporator		
Bundle Material	339.50	246.83
Bundle Labor	122.07	128.00
Shell Material	9.13	16.37
Shell Labor	29.25	51.78
Total Evaporator	499.05	442.98
Total Heat Exchangers	1,012.83	804.83
Provisions For Hotwells	14.82	15.08
Provisions For Separators	34.71	36.79
Total	1,062.36	856.70

The economic rationale for choosing titanium over aluminum as the tube material is discussed in Section 7.7.1.9.

7.7.1.3 Seawater Pump Costs

Cost data for both the warm and cold seawater pumps are based on the Westinghouse report "Deep Water Pipe, Pump and Mooring Study", ERDA No. COO-2642-3, prepared by Little, Marks, and Wellman. The cost data in this report was based on a survey of suppliers of large seawater pumps, and showed that the price of a seawater pump varies as the 0.384 power of its volumetric capacity. Multiple pumps were used when the total volumetric capacity exceeded 14,400,000 cubic feet/hour, which is the size of the largest supplier-offered pump.

7.7.1.4 Ammonia Pump Costs

The characteristics of the ammonia feed and recycle pumps are within the limits of commercially available off-the-shelf hardware.

Cost data for the ammonia feed and recycle pumps were based on the prices of representative pumps as quoted by Bingham Pump Division, Portland, Oregon.

7.7.1.5 Ammonia Turbine Cost

The ammonia turbine cost is based on a Westinghouse estimate of manufactured cost. The turbine used in the 50 MWe module is double flow.

7.7.1.6 Generator Cost

The generator cost is based on cost estimates from Westinghouse Large Rotating Apparatus Division.

7.7.1.7 Chlorination System Cost

The evaporator and condenser have different chlorination systems, and are priced separately. The cost of each chlorination system is proportioned to the chlorination rate raised to the 0.7 power.

7.7.1.8 Plant Auxiliaries Cost

Other plant auxiliaries are estimated to account for 0.0221 of the cost of the major plant power components. This factored estimate was obtained from "OTEC Power Plant Technical and Economic Feasibility", LMSC, April, 1976. The major power components are the heat exchangers, separator, turbine, generators, seawater pumps, ammonia pumps, piping, controls, and biocleaning systems.

7.7.1.9 Aluminum/Titanium Comparison

A power module with heat exchangers made of aluminum tubes is less expensive than a titanium-tubed module if the aluminum lasts for the 30-year life of the plant. The actual expected life of aluminum tubes is a matter of some debate, since there is very little data on aluminum in open (non-coastal) seawater, and the existing data on aluminum in seawater leads to a wide range of opinions by different metallurgists.

In order to provide a fair comparison of aluminum and titanium, a comparative study was made using 30-year discounted cash flow summaries and statistically distributed values for tube life duration.

The cash flow comparison involves the present value of the power module and bundle replacement as well as the income tax savings associated with depreciation of the power module and replacement bundles.

Many items normally present in a discounted cash flow statement have been omitted from this comparison because they are not affected by either the choice of tube material or the frequency of bundle replacement. These items are:

- Balance-of-plant financing (hull, cold water pipe, etc.)
- Routine operation and maintenance expense
- Insurance expense
- Taxes other than income tax
- Administrative and general expenses
- Revenue from sale of power

The cost of the power modules are taken from Table 7-22. The cost of replacing bundles is itemized in Table 7-24.

Table 7-24
50 MWe MODULAR BUNDLE COSTS ($/KW)

	TITANIUM		ALUMINUM	
Condenser Bundles				
Tube Material	314.51		138.06	
Tubesheet Material	20.90		15.76	
Baffle Material	4.08		3.60	
Tubing Labor	82.44		82.46	
Tubesheet Labor	25.51		25.58	
Baffle Labor	20.71		22.70	
Total Bundles (Cond)		468.27		288.16
Evaporator Bundles				
Tube Material	315.04		227.94	
Tubesheet Material	20.91		15.77	
Baffle Material	2.65		3.13	
Tubing Labor	82.52		82.53	
Tubesheet Labor	25.59		25.60	
Baffle Labor	13.97		19.87	
Total Bundles (Evap)		460.68		374.84
Total Bundles (=Retubing Cost)		928.95		663.08

The investment in the power system without tubes (Table 7-22 minus Table 7-24) is uniformly depreciated over 30 years, whereas the tube bundles are uniformly depreciated over the tube life. The tax saving is the present value of the annual depreciation expenses multiplied by a typical corporate tax rate of 48%.

Table 7-25 is the discounted cash flow summary for a 50 MWe power module with 30-year titanium tubing. Table 7-26 is the cash flow for a 50-MWe power module with 7-year aluminum tubes. Escalation in these exhibits is 6% and the interest rate is 10%.

Table 7-25
TITANIUM DISCOUNTED CASH FLOW SUMMARY

TUBE LIFE=30.0 YRS INFLATION RATE= .060 COST OF MONEY= .100

YEAR	/----INVESTMENT---- POWER SYSTEM W/O TUBES (PRES VAL)	----/ TUBES (PRES VAL)	/---DEPRECIATION--- POWER SYSTEM W/O TUBES (PRES VAL)	---/ TUBES (PRES VAL)	TAX SAVING DUE TO DEPR (PRES VAL)	TOTAL (PRES VAL)
1	435.00	929.00	-14.58	-30.97	-21.82	1342.18
2	0.00	0.00	-13.97	-29.84	-21.03	-21.03
3	0.00	0.00	-13.46	-28.76	-20.27	-20.27
4	0.00	0.00	-12.98	-27.71	-19.53	-19.53
5	0.00	0.00	-12.50	-26.70	-18.82	-18.82
6	0.00	0.00	-12.05	-25.73	-18.13	-18.13
7	0.00	0.00	-11.61	-24.80	-17.47	-17.47
8	0.00	0.00	-11.19	-23.89	-16.84	-16.84
9	0.00	0.00	-10.78	-23.03	-16.23	-16.23
10	0.00	0.00	-10.39	-22.19	-15.64	-15.64
11	0.00	0.00	-10.01	-21.38	-15.07	-15.07
12	0.00	0.00	-9.65	-20.60	-14.52	-14.52
13	0.00	0.00	-9.30	-19.85	-13.99	-13.99
14	0.00	0.00	-8.96	-19.13	-13.48	-13.48
15	0.00	0.00	-8.63	-18.44	-12.99	-12.99
16	0.00	0.00	-8.32	-17.77	-12.52	-12.52
17	0.00	0.00	-8.02	-17.12	-12.07	-12.07
18	0.00	0.00	-7.72	-16.50	-11.63	-11.63
19	0.00	0.00	-7.44	-15.90	-11.20	-11.20
20	0.00	0.00	-7.17	-15.32	-10.80	-10.80
21	0.00	0.00	-6.91	-14.76	-10.40	-10.40
22	0.00	0.00	-6.66	-14.23	-10.03	-10.03
23	0.00	0.00	-6.42	-13.71	-9.66	-9.66
24	0.00	0.00	-6.19	-13.21	-9.31	-9.31
25	0.00	0.00	-5.96	-12.73	-8.97	-8.97
26	0.00	0.00	-5.74	-12.27	-8.64	-8.64
27	0.00	0.00	-5.53	-11.82	-8.33	-8.33
28	0.00	0.00	-5.33	-11.39	-8.03	-8.03
29	0.00	0.00	-5.14	-10.98	-7.74	-7.74
30	0.00	317.32	-4.95	-10.58	-7.45	309.87
SUBTOT	435.00	1246.32			-402.62	1278.70
SALVAGE		-317.32				-317.32
TOTAL		929.00				961.38

Table 7-26
ALUMINUM DISCOUNTED CASH FLOW SUMMARY

TUBE LIFE= 7.0 YRS INFLATION RATE= .060 COST OF MONEY= .10

YEAR	/----INVESTMENT---- POWER SYSTEM W/O TUBES (PRES VAL)	TUBES (PRES VAL)----/	/---DEPRECIATION--- POWER SYSTEM W/O TUBES (PRES VAL)	TUBES (PRES VAL)---/	TAX SAVING DUE TO DEPR (PRES VAL)	TOTAL (PRES VAL)
1	482.00	663.00	-16.07	-94.71	-53.17	1091.83
2	0.00	0.00	-15.48	-91.27	-51.24	-51.24
3	0.00	0.00	-14.92	-87.95	-49.38	-49.38
4	0.00	0.00	-14.38	-84.75	-47.58	-47.58
5	0.00	0.00	-13.85	-81.67	-45.85	-45.85
6	0.00	0.00	-13.35	-78.70	-44.18	-44.18
7	0.00	530.88	-12.86	-75.84	-42.58	488.30
8	0.00	0.00	-12.40	-73.08	-41.03	-41.03
9	0.00	0.00	-11.95	-70.42	-39.54	-39.54
10	0.00	0.00	-11.51	-67.86	-38.10	-38.10
11	0.00	0.00	-11.09	-65.40	-36.71	-36.71
12	0.00	0.00	-10.69	-63.02	-35.38	-35.38
13	0.00	0.00	-10.30	-60.73	-34.09	-34.09
14	0.00	409.62	-9.93	-58.52	-32.85	376.77
15	0.00	0.00	-9.57	-56.39	-31.66	-31.66
16	0.00	0.00	-9.22	-54.34	-30.51	-30.51
17	0.00	0.00	-8.88	-52.36	-29.40	-29.40
18	0.00	0.00	-8.56	-50.46	-28.33	-28.33
19	0.00	0.00	-8.25	-48.62	-27.30	-27.30
20	0.00	0.00	-7.95	-46.86	-26.31	-26.31
21	0.00	316.07	-7.66	-45.15	-25.35	290.72
22	0.00	0.00	-7.38	-43.51	-24.43	-24.43
23	0.00	0.00	-7.11	-41.93	-23.54	-23.54
24	0.00	0.00	-6.85	-40.40	-22.68	-22.68
25	0.00	0.00	-6.60	-38.93	-21.86	-21.86
26	0.00	0.00	-6.36	-37.52	-21.06	-21.06
27	0.00	0.00	-6.13	-36.15	-20.30	-20.30
28	0.00	243.88	-5.91	-34.84	-19.56	224.32
29	0.00	0.00	-5.70	-33.57	-18.85	-18.85
30	0.00	0.00	-5.49	-32.35	-18.16	-18.16
SUBTOT	482.00	2163.44			-980.99	1664.45
SALVAGE		-161.76				-161.76
TOTAL		2001.68				1502.69

The probable distribution for tube life was generated by estimating values for the shortest probable, most probable, and longest probable tube life, such that there was a 97% confidence that the actual tube life would fall within that range. Metallurgical estimates are shown in Table 7-27, and in Figure 7-28.

Table 7-27
ESTIMATED TUBE LIFE (YEARS)

	TITANIUM	ALUMINUM
Shortest Probable Life	20	2
Most Probable Life	30	7
Longest Probable Life	40	20

A computer was used to randomly select values from the split-Gaussian aluminum life distribution and calculate many life-cycle costs in the manner of Table 7-25 to arrive at the distributed aluminum life-cycle module cost.

The same type of statistical calculations were performed for the titanium module for comparison, except that the tube life was longer, as shown in Figure 7-28. The two distributed life-cycle costs are compared in Figure 7-29, which is a cumulative frequency curve. Note that there is a 50% probability that the life-cycle cost of aluminum will be 1.56 times the cost of titanium, but only a 6.2% probability that the aluminum system will cost no more than the titanium system. There is an equal 6.2% probability that the aluminum cost will be at least 2.4 times the titanium cost. For this economic reason, titanium was chosen as the tube material.

The "break-even life" of aluminum tubing can be defined as that life distribution which results in a distributed module life cost identical to the distributed cost of titanium. The life costs of 20, 30, and 40-year titanium modules are 1108, 961, and 951 dollars per kilowatt, respectively. The aluminum module has identical costs with 12, 17, and 18-year aluminum. Therefore, the distributed "break-even life" is as tabulated in Table 7-28.

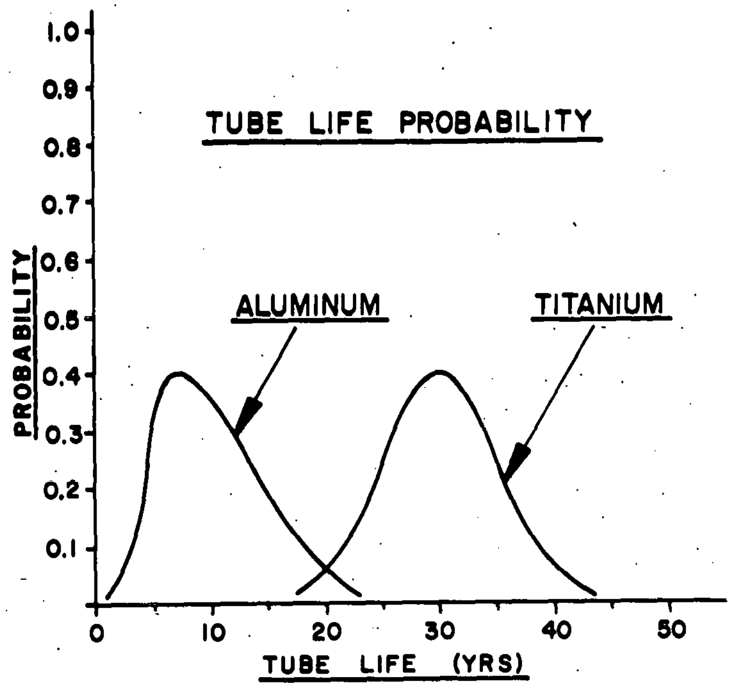

Figure 7-28
TUBE LIFE PROBABILITY

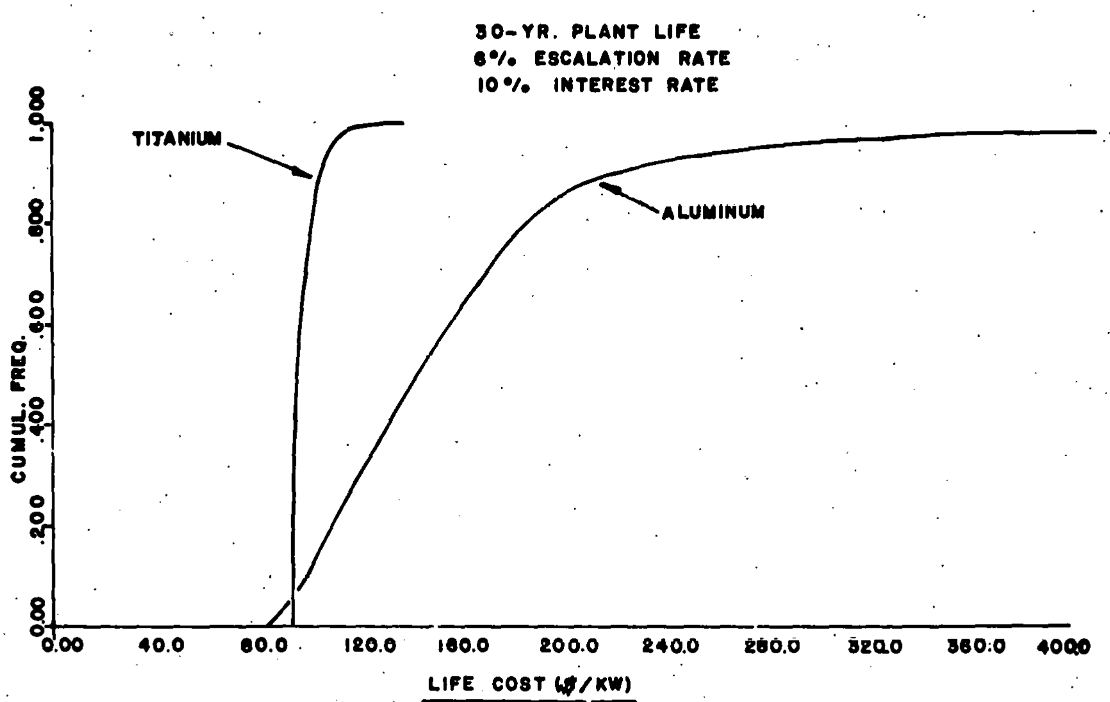

Figure 7-29
DISTRIBUTED LIFE-CYCLE COSTS

Table 7-28
BREAK-EVEN LIFE

	Titanium	Aluminum	Cost ($/KW)
Shortest Probable Life	20 Yr	12 Yr	1108
Most Probable Life	30 Yr	17 Yr	961
Longest Probable Life	40 Yr	18 Yr	951

7.7.2 Operating Costs

The operating costs for a single 50 MWe power module have not been specifically addressed because it is not part of the conceptual design. However, an estimate of the operating costs can be extracted from the information given in Section 8.4. In that section it is reported that for each of eight 50 MWe units the total operating costs are $183,000 for start-up plus $550,000 labor for operation and maintenance. The total of $723,000 is an estimate for a single 50 MWe power module but, would be somewhat low because the larger commercial units could take advantage of shifting a single team to several of the 50 MWe power modules as required. Detailed machinery, tools and spare parts cost estimates for a single 50 MWe unit have not been made. However, they could obviously be expected to be greater than the $1,315,480 reported for a single 10 MWe unit, not 5 times greater.

7.7.3 Economics of Multiple Plants

The effect of OTEC mass production on the cost of the 50 MW_e Demonstration Plant was investigated by assessing the cost of the eighth production plant. The eighth plant takes advantage of material discounts, improved fabrication techniques, and cost improvement curves. The projected costs of the prototype, first production, and eighth production plants are summarized in Table 7-29. These results do not include cost improvements discussed in Section 7.7.4.

Table 7-29
50 MWe POWER SYSTEM PROTOTYPE AND PRODUCTION COSTS, TITANIUM TUBING
(Figures Are $/KW)

Item	Prototype	First Production Plant	Eighth Production Plant
Evaporator, incl. Hotwell	503	503	404
Separator	35	35	35
Condenser, incl. Hotwell	524	524	422
Turbine	37	37	32
Generator	37	37	37
Seawater Pumps	112	112	90
Ammonia Pumps	8	8	8
Piping and Controls	8	8	8
Auxiliaries	56	56	56
Chlorination	44	44	38
Subtotal	1364	1364	1130
Installation	56	56	56
Subtotal	1420	1420	1186
Nonrecurring Cost	142	0	0
TOTAL	1562	1420	1186

Non-recurring costs in the prototype are defined as a one-time expenditure to provide special facilities, tooling, fixtures, and test equipment for the fabrication and factory testing of OTEC plant elements. This cost is only applied to the prototype plant in the cost summary. Best engineering judgement estimates this cost to be approximately 10% of total plant cost.

Costs developed during Preliminary Design were based on well-established industry practice. It is expected that discounts for large material purchases, improved fabrication techniques, and improvement curves for certain power system elements may yield significant future cost improvements.

Industry sources indicate the cost of titanium tubing could be reduced by more than 15% if sales were increased over their present values, as they would be in building titanium-tubed OTEC heat exchanger units. A 15% cost reduction would reduce the module cost by $94/KWe.

Low technology shop fabrication of tube bundles could reduce their assembly costs by 42%, and reduce the module cost by $107/KWe.

System elements, such as the seawater pumps, turbine, and chlorination system, are considered to be conceptual state-of-technology design. However, it is reasonable to expect that multiple unit fabrication of these elements will show improvement curves and yield cost improvements amounting to about $33/KWe.

7.7.4 Cost Improvements

This section addresses those areas which are seen as prime candidates for improvement. These areas are not ones which would be the natural result of building multiple OTEC plants. The economics of multiple plants were discussed in the previous section.

As can be seen from Table 7-22, the heat exchangers are by far the largest contributor to titanium-tubed power module cost. In Table 7-23 it is shown that the tube bundle material is the most significant part of the heat exchanger cost. The importance of trying to find material substitutions for titanium in OTEC plants is illustrated by the cost improvement scenarios in Table 7-30.

Table 7-30
COST OF ALL ALUMINUM TUBES VERSUS TITANIUM TUBES

Scenario	Result
Aluminum tubes with 17 year service life	Aluminum = Titanium
Aluminum tubes with 30 year service life	Aluminum $224/kWe < Titanium
Aluminum tubes at present prices/without corrosion allowance/30 year service life	Aluminum $378/kWe < Titanium
Aluminum without corrosion allowance/at aluminum strip (raw material for welded tubes) price/30 year service life	Aluminum $474/kWe < Titanium

Another important cost contributor to the heat exchangers is the fabrication labor. It is estimated that improved shell fabrication techniques and automated tube insertion into tube bundles could save as much as $39/KW.

8. COMMERCIAL PLANTS (100 MWe and 400 MWe)

8.1 Approach to Design

To date, some six different platform configurations have been suggested for commercial OTEC power plants. Four of these, surface barge or ship-type, spar, column-stabilized semi-submersible, and tuned sphere, have been studied in some detail. A 50 MWe module has been determined to be the optimum size for use in commercial plants. But no final selection has been made of a platform configuration. Therefore, the Westinghouse approach to make the arrangement of major components of a 50 MWe power module as flexible as possible. Section 7.3.2 discusses three feasible arrangements which meet the requirements of the four platform configurations. This Section discusses their incorporation into 400 MWe commercial power plants.

8.2 Systems Design

8.2.1 Arrangements

Commercial plants of 100 MWe to 400 MWe capacity would be made up of 50 MWe power modules. The power modules would have one of the three individual component arrangements discussed in Section 7.3.2.

Figure 8-1 illustrates a "square" configuration of eight 50 MWe "back to back" heat exchanger arrangement modules. The basic 400 MWe power plant measures 370 feet by 500 feet. The platform length required to lift the total system weight would increase from 370 feet to approximately 500 feet if built of steel, and to approximately 930 feet if built of concrete. Reductions in beam from 500 feet to approximately 470 feet could be achieved if two 70-foot diameter cold water pipes were installed; and to 450 feet if four 50-foot diameter pipes were used. This indicates a need for trade-off studies during Phase 2 to determine which combination of platform and piping size versus numbers of cold water pipes will result in a minimum system cost. Such a study was beyond the scope of this contract.

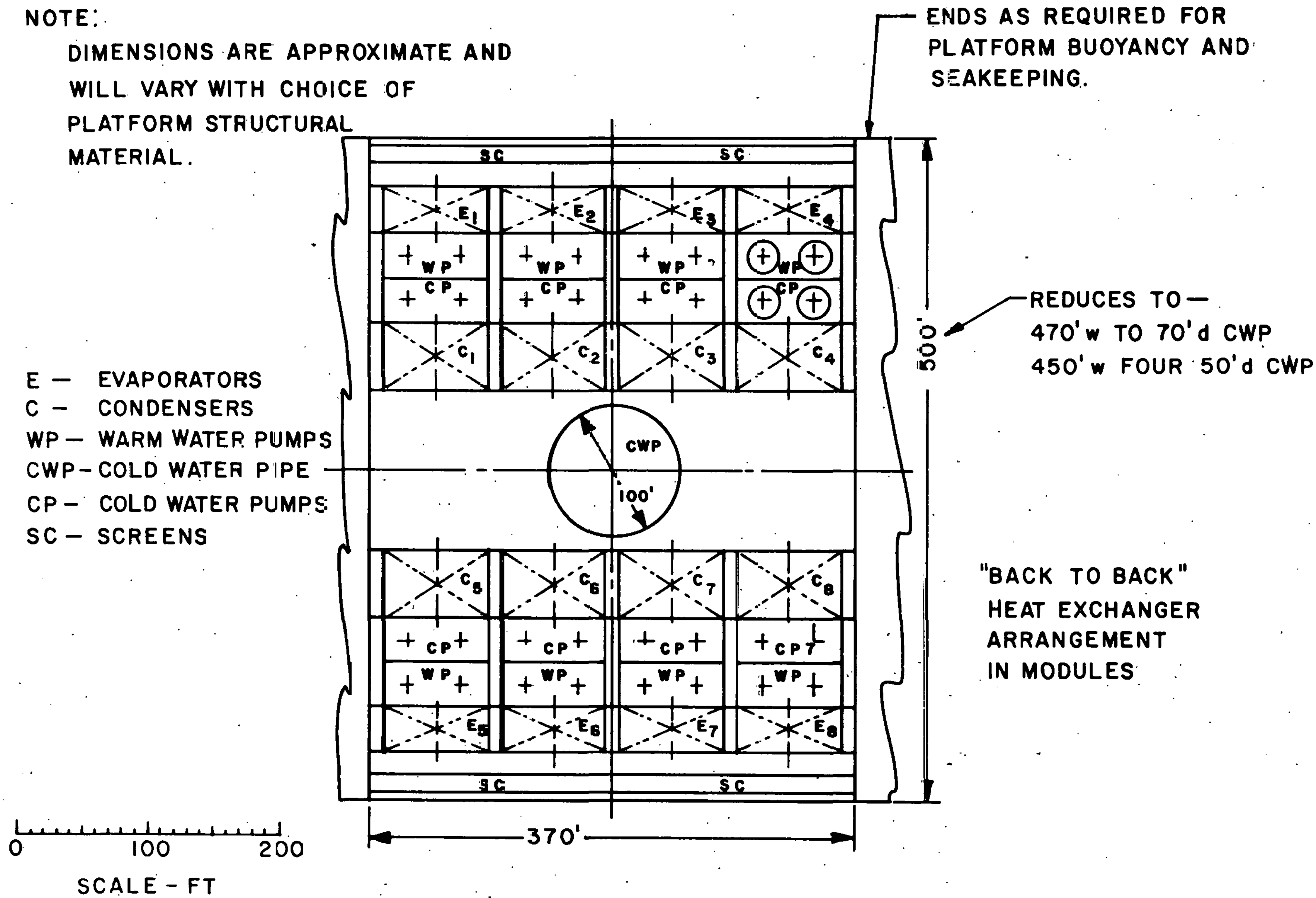

Figure 8-1
400 MWe OTEC PLANT SURFACE PLATFORM "SQUARE" CONFIGURATION

Figure 8-2 illustrates a "long" configuration of eight 50 MWe "side by side" heat exchanger arrangement modules. The basic 400 MWe power plant measures 720 feet by 240 feet. Additional lift capability to support total power plant and platform weight would be achieved by additional length alone as in the "square" configuration, or by a combination of additional length and beam depending upon the reasonableness of resulting length to beam ratios. It also should be noted that two, rather than the four, cold water pipes shown could be fitted with approximately a 20-foot increase in the minimum beam. A single 100-foot cold water pipe would require both an increase of 50 feet in minimum beam, and an increase of at least 110 feet in minimum length.

Figure 8-3 illustrates two potential "star" configurations of 50 MWe modules. The stacked modules are applicable to spar, semi-submersible, or tuned sphere platforms. The back-to-back modules are applicable to a circular raft surface platform.

8.2.2 Availability

The total power plant availability is equal to the availability of each of the constituent 50 MWe power modules, since the constituent modules are identical.

Power plant availability is defined as the ratio of actual generated power to rated power.

$$A_p = \frac{P'_p}{P_p}$$

where, A_p = Plant availability

P_p = Plant rated power

P'_p = Plant actual power

The rated and actual power outputs of the plant equal the sums of the power outputs of the n power modules.

$$P_p = n\,P_n$$

$$P'_p = n\,P'_n$$

where, n = Number of power modules

P_n = Module rated power

P'_n = Module actual power

Module availability (A_n) is defined in a similar manner as plant availability.

$$A_n = \frac{P'_n}{P_n}$$

Combining all of the above equations results in the equality of module and plant availabilities.

$$A_p = \frac{P'_p}{P_p} = \frac{nP'_n}{nP_n} = \frac{P'_n}{P_n} = A_n$$

8.3 Manufacturing

As previously noted, commercial OTEC power plants up to 400 MWe will be comprised of multiple 50 MWe modules. The assembly and preliminary testing of each module can proceed simultaneously following the procedures discussed in Section 7.4.5 for 50 MWe modules and in Section 6.4.5 for 10 MWe modules. The major problem is fabrication of the platform.

E — EVAPORATORS
C — CONDENSERS
WP — WARM WATER PUMPS
CWP — COLD WATEP PIPES
CP — COLD WATER PUMPS
SC — SCREENS

NOTE:
DIMENSIONS ARE APPROXIMATE AND WILL VARY WITH CHOICE OF PLATFORM STRUCTURAL MATERIAL.

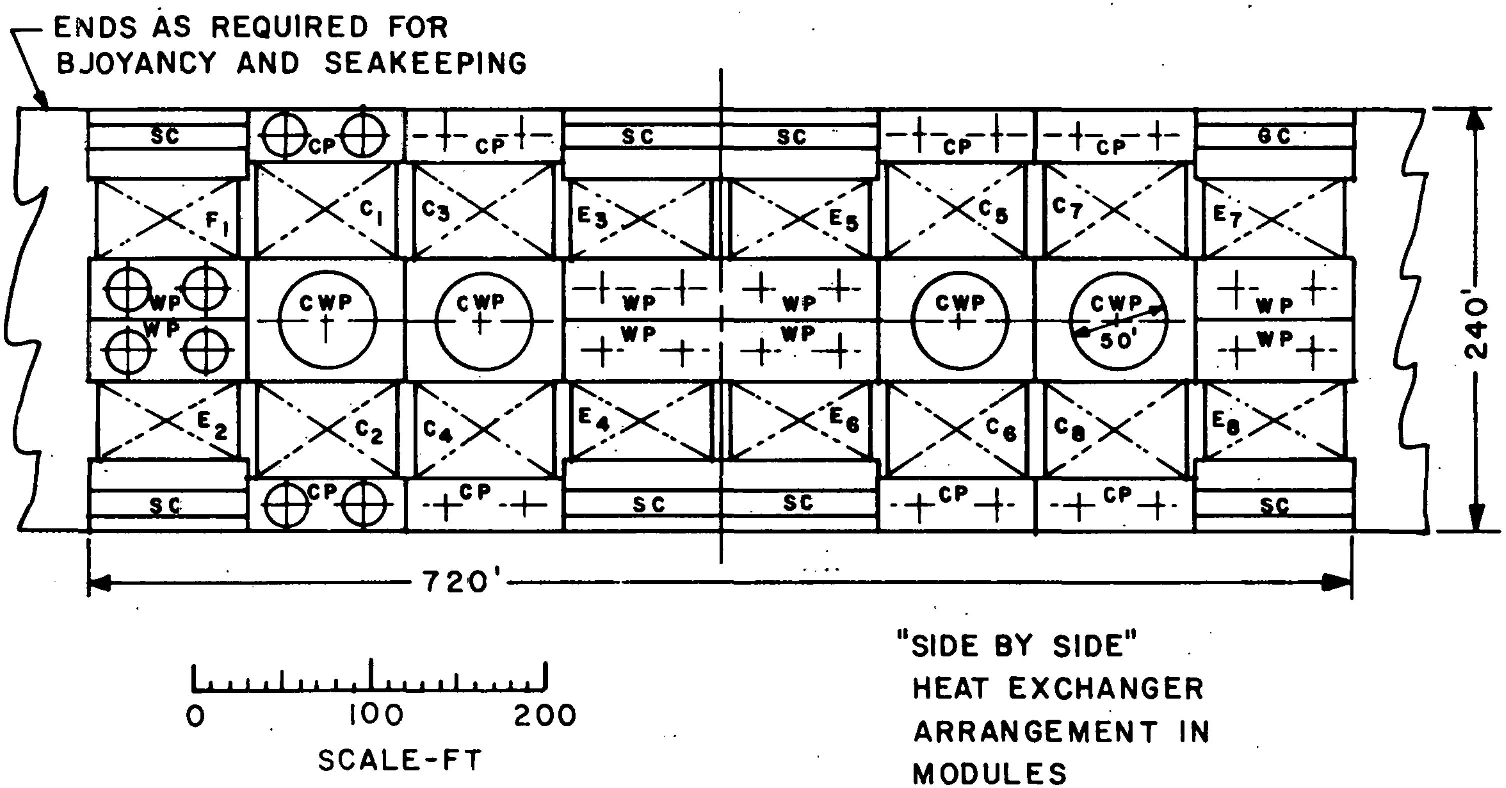

"SIDE BY SIDE"
HEAT EXCHANGER
ARRANGEMENT IN
MODULES

Figure 8-2
400 MWe OTEC PLANT SURFACE PLATFORM "LONG" CONFIGURATION

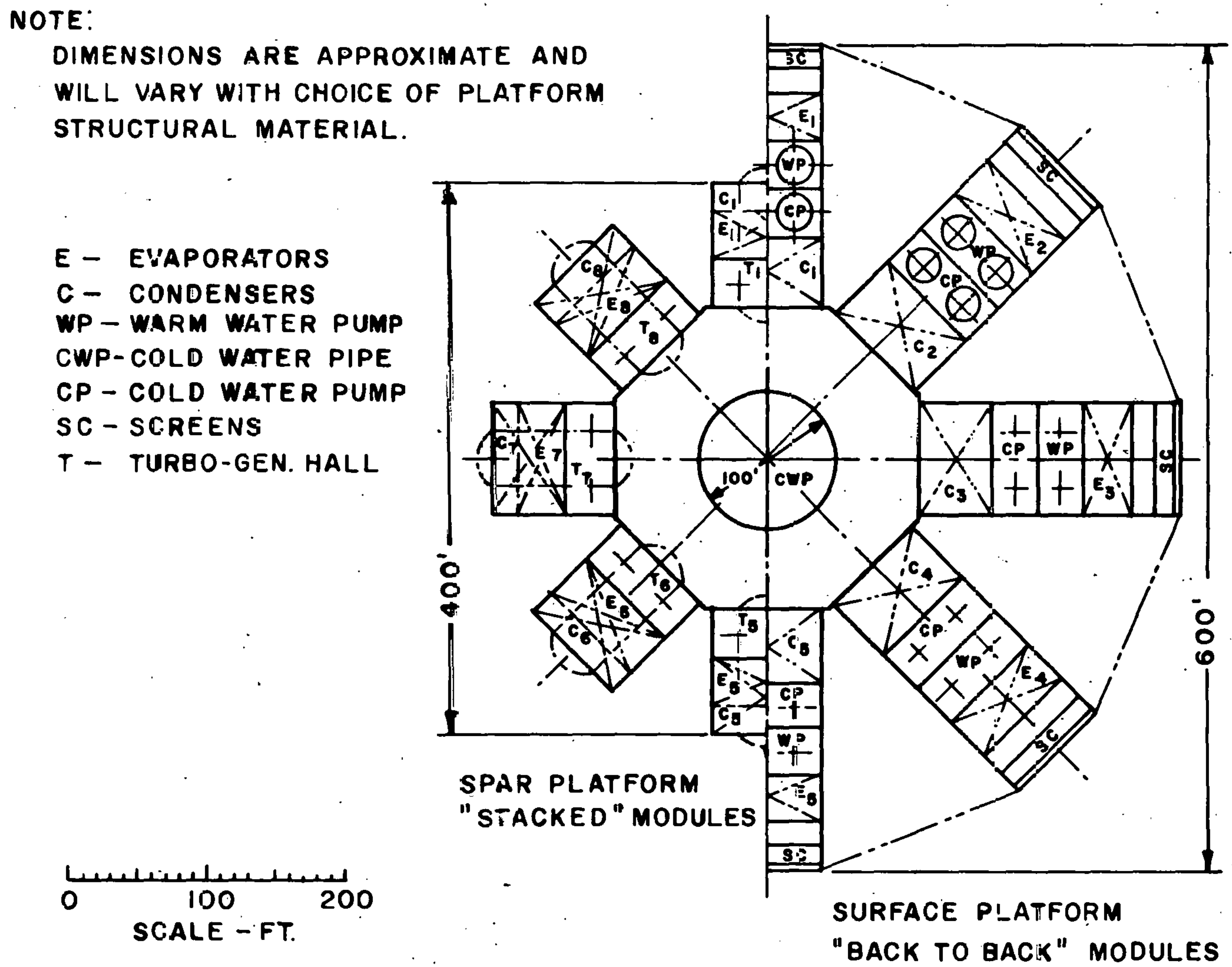

Figure 8-3
400 MWe OTEC PLANT "STAR" CONFIGURATION

Table 8-1 summarizes current shipbuilding capabilities in the U.S. It is evident that none of the 400 MWe arrangements discussed in Section 8.2.1 can be completed as a single unit at existing building facilities, either on ways or in docks. However, if constructed of steel, the square or long surface platforms could be built in sections at several of the facilities and assembled afloat. Techniques for mating and welding large subassemblies in this manner are well-developed in the shipbuilding industry.

If the platforms are of concrete construction, it is likely that new, dedicated facilities will be required for their fabrication. Such facilities may be as elaborate as existing building docks with crane capacities up to 900 tons, or they may be as simple as a large excavation on the shore with a removable dike giving access to the sea. Large offshore structures have been fabricated in such simple platform facilities. The major problem is adequate weight-handling capability.

8.4 Cost

Large commercial plants in excess of 100 MWe are expected to be constructed as aggregates of many optimized power modules generating 50 MWe each. With this approach, the cost per kilowatt for the commercial plant would equal the cost per kilowatt of the 50 MWe power module discussed in Section 7.7.

8.4.1 The Aluminum Scenario

It is reasonable to assume that, when OTEC becomes a commercially viable option, advances in research and development will have led to an aluminum capable of existing in seawater for the 30-year life of the plant.

The estimate of future power system module cost is shown in Figure 8-4. The upper bound cost is an aluminum tubed unit with expected replacement and current technology. The lower bound is an aluminum unit assuming tubing costs to be included at the simple strip cost without corrosion

Table 8-1
SHIPBUILDING CAPABILITIES

Name & Location	Maximum Ship Size (Feet)	Type*	Length (Feet)	Width (Clear Feet)	Depth (Sill Feet)	Water Depth /Channel (Feet)
Bath Iron Works	700 x 130	NA	NA	NA	NA	35/30
General Dyn. Quincy Division	936 x 143	BD	950	150	28	40/30
Sea Train (Brooklyn, N.Y.)	1094 x 143	GD	1092	143	41	--/42
Sun Ship (800 T. Crane)	1600 x 200	NA	NA	NA	NA	40/80
Beth Sparrows Point	1200 x 192	BD	1200	200	27	30/21
Newport News (900 T. Crane)	1600 x 222	GD	1600	230	NA	45/50
Ingalls	800 x 150	FD (38,000 T. Lift Capability)	640	177	41	38/40
Avondale	960 x 200	FD (81,000 T. Lift Capability)	960	220	35	37/40
Marathon Manufacturing	1400 x 200	NA	NA	NA	NA	NA
National Steel & SB	965 x 170	BD	1000	176	NA	28/30
Bethlehem Steel (San Francisco)	900 x 148	FD (65,000 T. Lift Capability)	900	148	37.6	39/30
Hunter's Point		GD	1092	143	47	39/30
Offshore Power (900 T. Crane)	495 x 400	BD	501	415	21	40/38

*BD = Building Dock
GD = Graving Dock
FD = Floating Dock

Source - Principal Shipbuilding and Repair Facilities of the United States, Department of Defense and Department of Commerce, Office of the Coordinator for Ship Repair and Conversion, June 1, 1975.

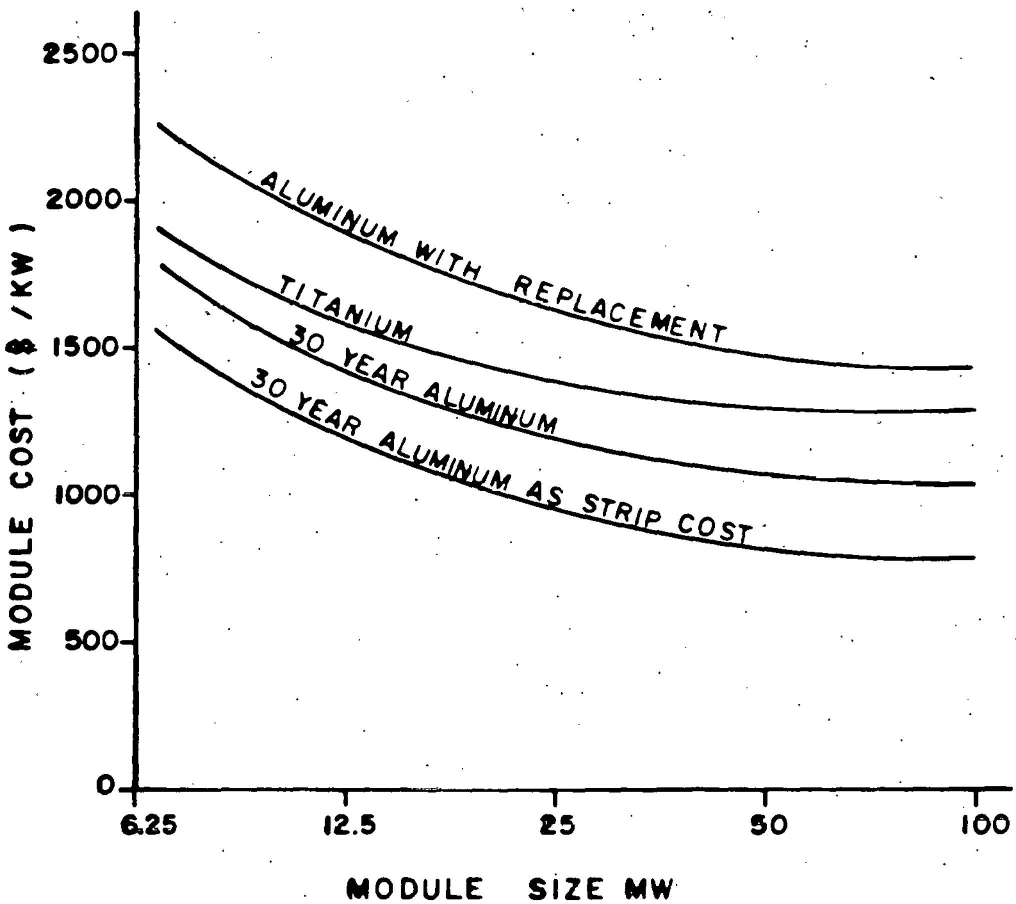

Figure 8-4
ULTIMATE POWER MODULE COST

allowance and assuming negligible manufacturing cost for producing the welded tubing.

In looking at long-term possibilities, if it is assumed that an aluminum tube can be made to last in seawater, and if this aluminum longevity can be obtained at no additional cost, and if the design criterion is to minimize the cost of the entire OTEC plant, not just the power module, then Korodense Low Pressure Drop tubing emerges as the most cost-effective shape, with Linde Porous Boiling Surface outside enhancement in the evaporator only.

Figure 8-5 illustrates the relative costs of the 16 enhancement combinations, coded with letters A through P. The codes are explained in Table 8-2. Each code letter is located above its cost to indicate the relative cost differences between enhancement combinations. The column on the left represents the cost of the power module only, the middle column represents the cost of the power module and the hull, and the right column represents the total plant cost. Separate optimization runs were made for each column, so the optimum system parameters for the right-hand column are not necessarily the same as the optimum system parameters for the left-hand or middle columns.

The steel hull cost was evaluated at $\$5.78/ft^3$, and is dependent on the sizes of the heat exchangers and their seawater plenums. The cost of the cold water pipe and startup systems was added to the cost of the module and hull to arrive at the cost of the entire plant.

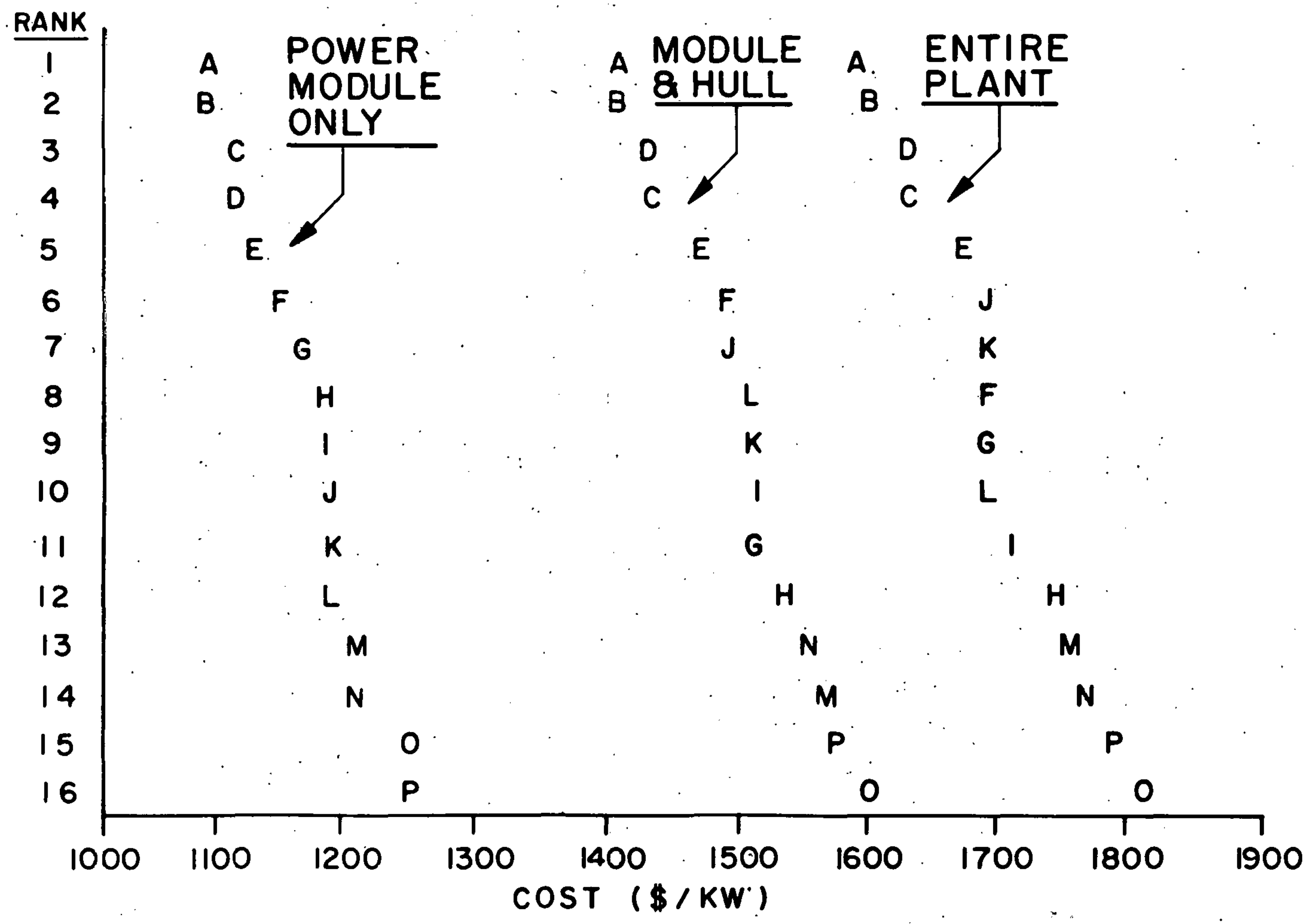

Figure 8-5
ALUMINUM MODULE COSTS

Table 8-2
ENHANCEMENT CODES FOR FIGURE 8-5

Code	Condenser Enhancement Inside/Outside	Evaporator Enhancement Inside/Outside
A	Koro/Plain	Koro/Linde
B	Koro/Plain	Plain/Linde
C	Plain/Plain	Koro/Linde
D	Plain/Plain	Plain/Linde
E	Koro/Plain	Plain/Plain
F	Plain/Plain	Plain/Plain
G	Koro/Plain	Koro/Plain
H	Plain/Plain	Koro/Plain
I	Plain/Linde	Koro/Linde
J	Koro/Linde	Koro/Linde
K	Koro/Linde	Plain/Linde
L	Plain/Linde	Plain/Linde
M	Koro/Linde	Plain/Plain
N	Plain/Linde	Plain/Plain
O	Plain/Linde	Koro/Plain
P	Koro/Linde	Koro/Plain

Koro = Korodense LPD Tubing
Linde = Linde Outside Coating
Plain = Plain Tubes

Enhancement combinations A through E are the five lowest cost combinations in all three systems, although C and D change places when the hull is evaluated. Combinations F through L remain in positions 6 through 12, although their order changes significantly when the hull cost is added, and changes again when the entire plant is evaluated. The remaining four combinations retain their expensiveness, changing positions slightly as the scope of the system increases. It should be noted that Linde enhancement is consistently effective on the evaporator tubes, and consistently ineffective on the condenser tubes.

8.4.2 Zoning of Heat Exchangers

A small increase in power output may be obtained from a given evaporator and condenser design by zoning the heat exchanger into two different ammonia pressure stages. Each completely isolated stage of the evaporator, turbine, and condenser operates as a separate parallel loop, but at the optimum ammonia pressure and temperature consistent with the associated seawater conditions. A comparison of the effect of a one-stage and two-stage design is illustrated by the simple temperature/area diagram, Figure 8-6.

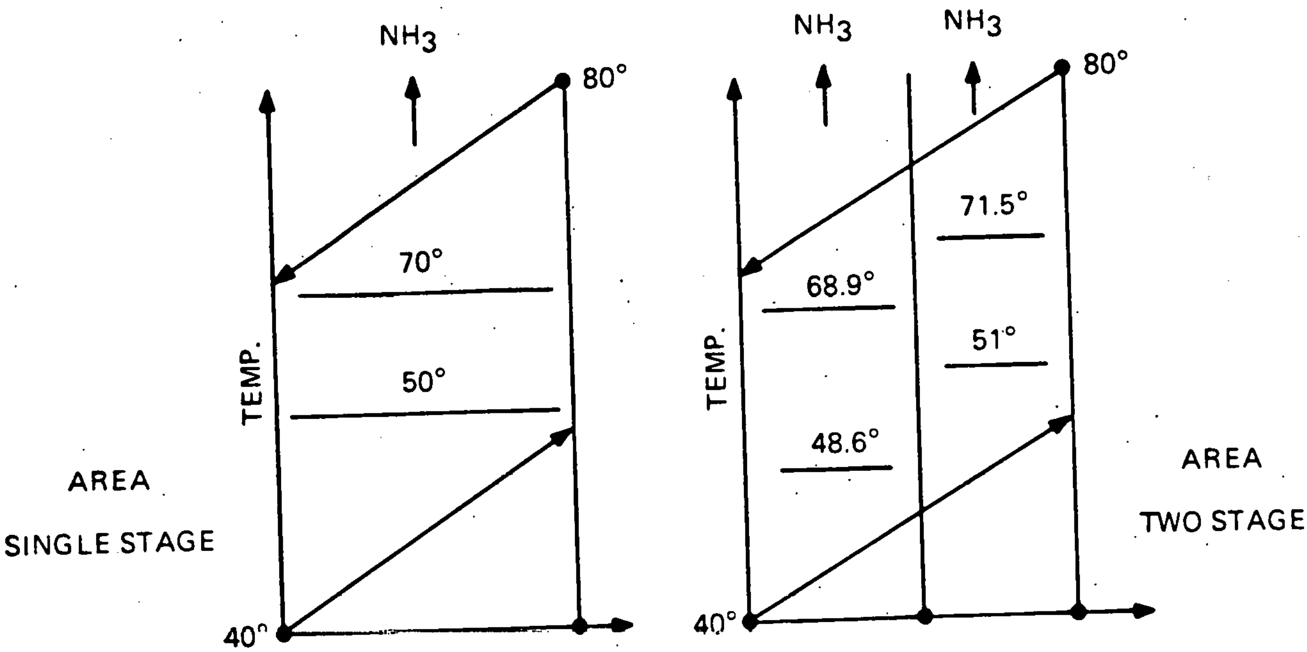

Figure 8-6
TEMPERATURE/AREA DIAGRAM

The evaporators and condensers are identical except for a sealed dividing plate in the two stage system. Each stage would supply half of a double entry turbine. No modification would be required except a heavier seal for the slight pressure differentials. The potential increase in power from the turbine is in the order of 3%. This zoning effect would be cost effective only in large scale plants and with multiple entry turbines so that the flow paths can be separated.

BIBLIOGRAPHY REFERENCES

The following publications are referenced throughout this report by numerical designation:

(1) "Calculation of the Performance of Surface Condensers by Digital Computer", E. J. Barsness, ASME Paper 63-PWR-2, Pages 4 and 5.

(2) "Investigations and Measurements on Church Window Condensers", H. Lang, Brown Boveri Review, Pages 342 and 343, July 8, 1973.

(3) American Society of Mechanical Engineers, Boiler and Pressure Vessel Code, Pressure Vessels, Section VIII, Division I.

(4) H.J. Connors, Jr., Westinghouse Research and Development Center, "Fluidelastic Vibration of Tube Arrays Excited by Crossflow", ASME Symposium Publication, Flow Induced Vibration in Heat Exchangers, December, 1970.

(5) Yung, Horenz, Gaic, "Vapor/Liquid Interaction and Entrainment in Shell and Tube Evaporators", ANL-OTEC-78-2, June 1978.

(6) Union Carbide Corp. Tubesheet Program No. 43100.

(7) K.A. Gardner, "Heat Exchanger Tube-Sheet Design," Journal of Applied Mechanics, December, 1948; K. A. Gardner, "Heat Exchanger Tube-Sheet Design-2, Fixed Tube-Sheets," Journal of Applied Mechanics, June, 1931.

(8) Yi Yuan Yu, "Rational Analysis of Heat-Exchanger Tube-Sheet Stresses," Journal of Applied Mechanics, September 1956.

(9) W.J. O'Donnell and B. F. Langer, "Design of Perforated Plates," Transactions of the ASME Journal of Engineering for Industry, November 1961.

(10) American Society of Mechanical Engineers, Boiler and Pressure Vessel Code, Pressure Vessels, Section VIII, Division 2.

(11) H.J. Connors, Jr., Westinghouse Research and Development Center, "Fluidelastic Vibration of Tube Arrays Excited by Crossflow", ASME Symposium Publication Flow Induced Vibration in Heat Exchangers, December 1970.

(12) "Performance Estimation of Axial Flow Turbines"; Craig and Cox; Proc. Instn. Mech. Engrs., 1970-1971.

(13) "A New Method of Calculating Natural Modes of Uncoupled Bending Vibrations of Airplane Wings and Other Types of Beams", Journal of Aeronautical Sciences, 1940; N. Myklestad.

(14) "A General Method of Calculating Critical Speeds of Flexible Rotors"; Journal of Applied Mechanics, 1945; M. Prohl.

(15) "Steam Plant Surface Condenser Leakage Study", Bechtel, San Francisco, Prepared for EPRI, EPRI NP 481, Project 624-1, Vol. 1, March 1977.

(16) Tuthill, A. H., and Schillmolley, C.M., Guidelines for Selection of Marine Materials, Inco Technical Literature, Presented to Ocean Science and Ocean Engineering Conference, Marine Technology Society, June 1965.

(17) Newton, E. H., et. al., Survey of Condenser Tube Life in Salt Water Service, U.S. Dept. of the Interior, R & D Progress Report No. 278, August 1967.

(18) Ross, R.W., Jr. and Anderson, D.B., "Hot Sea Water Corrosion of Copper Base Alloys", Materials Performance, Vol. 14, No. 9, September 1975, pp. 27-32.

(19) *The Design and Installation of 90-10 Copper-Nickel Seawater Piping Systems*, Inco Technical Literature, New York.

(20) LaQue, Frank, "Corrosion Resistance of Copper Nickel Alloys Containing 10 to 30% Nickel", *Corrosion*, Vol. 10, 1954, pp. 391-399.

(21) Butt, S. H., and Ford, J. A., *The Importance of Material Conductivity in Enhanced Tube*, U.S. Dept. of Interior Symposium on Enhanced Tubes for Desalinization Plants, Washington, D.C., March 1969.

(22) Tuthull, A. H. and Sudrabin, D. A., "Why Copper-Nickel Alloys for Desalinization"; *Metals Engineering Quarterly*, ASM, August 1967, pp. 10-26.

(23) Todd, B., et. al., *Desalinization - Lower Cost Water by Proper Materials Selection*, 3rd European Symposium on Fresh Water from the Sea, Dubrovnik, Yugoslavia, September 1970.

(24) *Corrosion Resistance of Wrought 90/10 Copper Nickel - Iron Alloy In Marine Environments*, INCO Technical Bulletin MCB-1, New York 1975.

(25) May, T. P., and Weldon, B. A., *Copper Nickel Alloys for Service In Seawater*, 24th International Congress on Fouling and Marine Corrosion, Cannes, France, June 1964.

(26) Cohen, A., and Rice, L., *Coppers and Copper Alloys in Desalting Environments*, Copper Development Association, Inc., New York.

(27) Walston, K. R., "Materials Problems in Salt Water Cooling Towers", *Materials Performance*, June 1975, pp. 22-26.

(28) Stille, M. M., "Tampa Electric Goes Stainless", Power Engineering, May 1971, pp. 44-45.

(29) Moller, G. E., "The Successful Use of Austenitic Stainless Steels in Seawater", Society of Petroleum Engineers Journal, April 1977, pp. 101-110.

(30) Boyd, W. K., and Fink, F. W., "Corrosion of Metals in Marine Environments", MCIC Report - 75-245R, Battelles Columbus Laboratories, Columbus, Ohio, May 1975.

(31) Pollock, W. A., "Aluminum Condenser Tubes", Proceedings of the American Power Conference, Volume XXI, 1959.

(32) Pollock, W. A., et al, "Results of Five Year Test on Aluminum Condenser Tubes", Proceeding of the American Power Conference, 1957.

(33) Verink, E. D., Jr., and Rucker, J. D., How About Aluminum Tubes; Eighteenth Annual Water Conference, Pittsburgh, Pa. 1957.

(34) Heymann, F. J., Toward Quantitative Prediction of Erosion Damage, Westinghouse STD Engineering Report E-1463, June 1969.

(35) Heymann, F.J., Erosion by Cavitation, Liquid Impingement, and Solid Impingement, A Review, Westinghouse STD Engineering Report, E-1460, March 1968.

(36) "Aluminum Condenser Tubes: A Status Report", Power, March 1963, pp. 49-50.

(37) Behrens, H.C., et al, Sea Water Corrosion Test Program - Second Report, U. S. Department of the Interior, R & D Progress Report No. 623, December 1970.

(38) W. H. Ailor, Flowing Sea Water Corrosion Potentials of Aluminum Alloys, Presented at NACE 26th National Conference, March 2-6 1970.

(39) Pachter, M., et. al., Reducing Costs by Using Aluminum Tubes in Multi-Effect Desalinization Plants, Israel Desalinization Engineering (Zarchin Process) LTD.

(40) Personal correspondence with Abraham Opiar, Israel Desalinization Engrg., 1977.

(41) Ailor, W. H., "Ten-Year Sea Water Tests on Aluminum", ASTM, Philadelphia, Pa. 1974.

(42) Lennox, T. J., Jr., et al, "Corrosion and Cathodic Protection of 5086-H32 Aluminum Coupled to Dissimilar Metals", Materials Performance, February 1974.

(43) Ailor, W. H., "Evaluation of Aluminum after One-Year Deep Sea Exposure", Hydronautics, Vol. 2, No. 1, January 1968.

(44) Reinhart, F. M., and Jenkins, J. F., "Corrosion of Alloys in Hydrospace 189 Days at 5900 Feet", Naval Civil Engineering Laboratory, Port Hueneme, California, Technical Note N-1224, April 1972.

(45) Boenwitz, R. A., Concurrent Studies of Enhanced Heat Transfer and Materials for Ocean Thermal Exchangers, Alcoa, ERDA Contract E(11-1)-2641, October 29, 1976.

(46) Schrieber, C.F., et al, "Behavior of Metals in Desalting Environments - Sixth Progress Report", Materials Performance, February 1975, pp. 9-14.

(47) Ailor, W. H., "A Review Paper - Aluminum in Desalinization", Naval Engineers Journal, October 1975, pp. 69-83.

(48) Lindberg, R. I., "Tests Indicate Aluminum has Future in Desalting", Materials Protection and Performance, Vol. 11, No. 2, February 1972, pp. 45-47.

(49) Ashbaugh, W. G., "Corrosion in Heat Exchangers Using Brackish Water", Chemical Engineering, July 5, 1965, pp. 146-152.

(50) Bogar, F. D., and Fujiii, C. T., NRL Memorandum Report 2721, January 1974.

(51) Neiderberger, R. B., et al, "Corrosion and Stress Corrosion of 5000 Series Al Alloys in Marine Environments", Corrosion, Vol, 22, March 1966, pp. 68-73.

(52) "Properties and Selection of Metals", Metals Handbook, American Society of Metals, Vol. 1, 8th Edition, 1961.

(53) Alco Aluminum - The Cryogenic Metal, Alcoa Technical Publication, Pittsburgh, Pa.

(54) Verinck, E. D., Jr. and Murphy, F. B., "Aluminum", Corrosion, December 1960, pp. 16-18.

(55) Hugh P. Godard, et al, The Corrosion of Light Metals, New York: John Wiley & Sons, Inc. 1967.

(56) "Welding and Brazing", American Society for Metals, 1971, 8th Edition, Volume 6.

(57) "Metals and Their Weldability", American Welding Society, 1972, 6th Edition, Section Four.

(58) Welding Aluminum, American Welding Society - The Aluminum Association, New York - 1966.

(59) Holt, Marshall, et. al, Aluminum and Aluminum Alloys for Pressure Vessels, Welding Research Council No. 75, New York, February 1972.

(60) Jefferson, T. B., "Welding Aluminum to Steel", Welding Design and Fabrication, May 1977.

(61) G. J. Danek, "The Effect of Sea Water Velocity on the Corrosion Behavior of Metals", Naval Engineers Journal, October 1966, pp. 763-769.

(62) Titanium for Industrial Brine and Sea Water Service, Titanium Metals Corporation of America, 1968.

(63) Orava, R. N., Stress Corrosion and Corrosion Behavior of Copper, Nickel and Titanium Under Simulated Desalinization Conditions, 25th NACE Conference, Houston, Texas, March 1969.

(64) Sato, et, al, Titanium Condenser Tubes - Problems and Their Solutions for Wider Application to Large Surface Condensers, Annual Meeting of Institute of Japan, Thermal and Nuclear Power Engineering, Tokyo, October 7, 1976.

(65) O'Keefe, W., "Better But Costlier Tube Metals Tackle Present and Future Condenser Problems", Power, August, 1973, pp. 43-44.

(66) Jacobs, R. L., and McMaster, J. A., "Titanium Tubing - Economical Solution to Heat Exchanger Corrosion", Materials Protection and Performance, Vol. 11, No. 7, July 1972, pp. 33-38.

(67) Feige, N. G., and Kane R. L., "Experience with Titanium Structures in Marine Service", Materials Protection and Performance, Vol. 9, No. 8, August 1970, pp. 13-16.

(68) Feige, N. G., and Kane, R. L., "The Application of Titanium for Desalinization Plants", Metals Engineering Quarterly ASM.

(69) Hanson, C. F., Some Technical Considerations on the Use of Titanium Condenser Tubing in Public Utility Power Generation Turbines, Meeting of the 2nd International Conference of AIME, ASM, Institute of Metals in Association with the Academy of Science of the U.S.S.R., and the Japan Institute of Metals at Massachusetts Institute of Technology, Plenum Press: New York, 1973.

(70) Millaway, E. E., "Titanium" Its Corrosion Behavior and Passivation", Materials Protection, January 1967, pp. 16-28.

(71) Titanium for Turbine Condensers and Power Station Auxiliary Heat Exchanger Equipment, Imperial Metals Industries Technical Bulletin, Birmingham, England.

(72) Franson, A. A., and Covrington, L. C., Titanium and the OTEC Environment, Biofouling and Corrosion in Ocean Thermal Energy Conversion Symposium, Seattle, Wa., October 1977.

(73) Boklmann, E. G., and Posey, F. A., Aluminum and Titanium Corrosion in Saline Waters at Elevated Temperatures, International Symposium on Water Desalinization, Washington, D.C., 1965.

(74) Muraoka, James S., Effect of Deep Ocean Organisms on Constructional Materials.

(75) Mifflin, R. C., and Bird, D. B., "Performance of Tube Alloys Cooled by Brackish Delaware River Water", Materials Protection, September 1967.

(76) Reinhart, F. M., "Corrosion of Materials in Hydrospace, Part III-Titanium and Titanium Alloys", Naval Civil Engineering Laboratory, Port Hueneme, Calif. Y-F015-01-05-002a, Technical Note N 291, September 1967.

(77) Hanson, C. F., Titanium Condenser Tube Application in Practice, Materials in Power Plant Conference, Institute of Met. Landon, 1975, pp. 98-103.

(78) Litvin, D. A., and Smith, D. E., "Titanium for Marine Applications", Naval Engineers Journal, October 1971, pp. 37-44.

(79) Danek, G. J., Jr., "The Effect of Sea Water Velocity on the Corrosion Behavior of Metals", Naval Engineering Journal, October 1966, pp. 763-769.

(80) Holtzman, A. H., and Cowan, G. R., "Bonding of Metals with Explosives", Welding Research Council Bulletin 104, April 1965.

(81) Engineering Data of Welded Titanium Tubes and Tube Plates for Large Surface Condensers, Sumtomo Light Metals Technical Data, April 1976.

(82) P. B. Ludwigsen and H. Arup, "Stress Cracking of Mild Steel in Ammonia Vapor Above Liquid Ammonia", Corrosion, Vol. 32, No. 11, November 1976.

(83) A. W. Loginow, and E. H. Phelps, "Stress-Corrosion Cracking of Steels in Agricultural Ammonia", Corrosion, Vol. 18, No. 8, August 1962, pp. 299t-309t.

(84) E. H. Phelps, "Causes of Stress-Corrosion Cracking of Steel in Ammonia", Ammonia Plant Safety, Vol. 16, pp. 32-38.

(85) D. C. Deegan and B. E. Wilde, "Stress Corrosion Cracking Behavior of ASTM A517 Grade F Steel in Liquid Ammonia Environments", Corrosion, Vol. 29, No. 8, August, 1973, pp. 310-315.

(86) C. D. Kim, B. E. Wilde, and E. H. Phelps, "Stress Corrosion Cracking of Line-Pipe Steels in Anhydrous Ammonia", Corrosion, Vol. 31, No. 7, July 1975, pp. 255-262.

(87) E. H. Phelps, Stress Corrosion Cracking in Ammonia.

(88) D. A. Jones, C. D. Kim, and B. E. Wilde, "The Electrochemistry and Mechanism of Stress Corrosion Cracking of Constructional Steels in Liquid Ammonia", NACE, Houston, Texas, March 1976. To be published, Corrosion.

(89) D. A. Jones and B. E. Wilde, "Corrosion Performance of Some Metals and Alloys in Liquid Ammonia", (to be published in Corrosion).

(90) Compatibility of Ammonia with Candidate Dry Cooling System Materials, Prepared for the Energy Research and Development Administration Under Contract B (45-1): 1830, by Battelle Pacific Northwest Laboratories.

(91) "Reactions Between Water, Ammonia, and Aluminum", Corrosion Group, Society Reports and Notices, Chemistry and Industry, December 19, 1964, pp. 2089-2090.

(92) I. D. Mechcheryakova, T. P. Kascheeva, and M. L. Rutkovskii, "Corrosion and Electrochemical Behavior of Carbon Steel in Ammonia Liquor", translated from Zaschita Metalloy, Vol. 11, No. 1, Jan.-Feb. 1975, pp. 42-44.

(93) E. R. Geib, "How Corrosion of the X-15 Was Solved", Materials Protection, March 1965, pp. 56-58.

(94) Prof. T. K. Ross and Dr. B. G. Callaghan, "Role of Ammonia in the Atmospheric Corrosion of Mild Steel", Nature, No. 5044, July 2, 1966, pp. 25-26.

(95) J. M. A. Van der Horst, "Grain Boudary Attack of the 316L Stainless Steel in Ammonia Rich Environments", Electrochem. Soc., Electrochemical Science and Technology, April 1973, pp. 512-515.

(96) Thomas J. Dawson, "Behavior of Welded Pressure Vessels in Agricultural Ammonia Service", The Welding Journal, June 1956, pp. 568-574.

(97) "Plumbing the Ocean Depths: A New Source of Power", Institute of Electrical and Electronics Engineers Spectrum, October 1973, pp. 22-27.

(89) L. A. Danielyan, A. I. Tsinman, V. S. Kuzub, V. G. Moisa, and N. N. Statsenko, "Anodic Protection of an Ammonia Liquor Storage Vessel", translated from Zaschita Metallov, Vol. 9, No. 4, July-August 1973.

(99) Kh. L. Tseitlin, Yu. I. Sorokin, A. A. Balashova, S. M. Babitskaya, Ya. S. Levin, A. T. Konyushenko, R. V. Golovkin, and B. S. Ladyzhinskii, "High Temperature Corrosion of Metals in Gaseous Ammonia", translated from Zaschita Metallov, Vol. 6, No. 4, July-August 1970, pp. 451-454.

(100) I. Tsinman and L. A. Danielyan, "Influence of Ammonia on the Passivation of Iron and the Formation of Pitting in Weakly Alkaline Solutions", translated from Zaschita Metallov, Vol. 10, No. 3, Jan.-June 1974, pp. 308-311.

(101) A. M. Hall, "Coal Gasification Poses Demanding Material Requirements", Materials Engineering, July 1974, pp. 16-18.

(102) A. I. Tsinman, L. A. Danielyan, and V. S. Kuzub, "Corrosion-Electrochemical Behavior and Anodic Protection of Carbon Steel in Aqueous Solutions of Ammonia", translated from Zashchita Metallov, Vol. 9, No. 2, March-April 1973, pp. 156-160.

(103) J. M. A. Van der Horst, "Corrosion of Stainless Steel by Aqua Ammonia", Corrosion Science, Vol. 12, 1972, pp. 7761-765.

(104) Yu. I. Sorokin, Kh. I. Tseitlin, A. A. Balashova, S. M. Rabitskaya, and Ya. S. Levin, "The Effect of Water Vapor and Its Mixture with Carbon Dioxide on the Corrosion of Metals in Ammonia at 500°C", translated from Zashchita Metallov, Vol. 8, No. 4, July-August 1972, pp. 430-434.

(105) H. H. Uhlig, The Corrosion Handbook, John Wiley and Sons, New York, 1948, p. 799.

(106) J. C. Hines, "Behavior of Aluminum in Ammonical Solutions", Allumino, Vol. 34, No. 5, 1965, pp. 231-234.

(107) D. C. Deegan, B. E. Wilde, and R. W. Staehle, "Some Electrochemical Aspects of the Stress Corrosion Cracking of Steels in Liquid Ammonia Environments", Corrosion, Vol. 32, No. 4, April 1976, pp. 139-142.

(108) Olen L. Riggs, Jr., "A Potentiostatic and Galvanostatic Study of Carbon Steel Surfaces in NH_3-NH_4HO_3-H_2O Solutions", Corrosion, Vol. 26, No. 6, June 1970, pp. 155-157.

(109) B. E. Wilde, "The Influence of Hydrogen, Oxygen, and Ammonia on the Corrosion Behavior of Plain Carbon Steel in High Temperature Water", Corrosion, Vol. 24, No. 10, Oct. 1968, pp. 338-343.

(110) A. W. Loginow, "Detection and Diagnosis of Stress Corrosion Cracking in Ammonia Tanks", Materials Performance, June 1976, pp. 33-38.

(111) A. Ya. Yalova, A. Yu Bulavko, and V. Kuz'micheva,"Improving the Water Chemistry Conditions in Supercritical Units", Teploenergetika, Vol. 18, No. 12, 1971, pp. 69-71.

(112) E. F. Ehmke, "Corrosion Correlations with Ammonia and Hydrogen Sulfide in Air Coolers", Materials Performance, July 1975, pp. 20-28.

(113) "Solving the Corrosion Problem in Sugar Refineries", Materials Protection and Performance, September, 1972, pp. 52-53.

(114) J. A. Manning and S. V. Carleton, "A Study of Corrosion Rates in an Operating Desalting Plant", Materials Performance, Aug. 1975, pp. 9-14.

(115) O. I. Martynova, B. S. Rogatskin, "The Behavior of Corrosion Products in the Feedwater Circuit of Supercritical Units", Teplenergetika, Vol. 18, No. 12, 1971, pp. 65-69.

(116) V. P. Razygraev, E. N. Mirolyubov, and T. A. Pisarenko, "Mechanism of Corrosion of Nickel in Nitric Acid Solutions", Zashchita Metallov, Vol. 9, No. 1, Jan.-Feb., pp. 48-50.

(117) H. W. Wilten, "Failure of High Strength 410 Bolts in Ammonia Contaminated Water", Corrosion, Vol. 17, August 1961, pp. 10-11.

(118) Robert C. Axtmann and Lawrence B. Peck, "Geothermal Chemical Engineering", AICHE Journal, Vol. 22, No. 5, September 1976, pp. 817-825.

(119) L. D. Martin and W. P. Banks, "Electrochemical Investigation of Passivating Mild Steel Surfaces", Materials Performance, September 1975, pp. 33-37.

(120) S. Kh. Shvydkii, I. A. Tevin, I. K. Burtseva, and A. V. Kazarin, "Effect of Carbon Dioxide Concentration on Corrosion of Steels in Monoethanolamine Solutions", Zashchita Metallov, Vol. 10, No. 7, July-August 1974, pp. 410-413.

(121) T. W. Schoene, E. O. Winkler, P. Fortescue, "The Gas Turbine HTGR Plant-Economical Dry Cooling or a Wet-Cooled High-Efficiency Binary Configuration", Proceedings of the American Power Conference, Vol. 37, 1975, pp. 363-378.

(122) L. E. Tesurf, P. E. C. Bryant and M. G. Tanner, "Use of Ammonia to Supress Oxygen Production and Corrosion in Boiling-Water Reactors", Corrosion, 23, 3, March 1967, p. 57.

(123) L. M. Dvoracek, and L. L. Neff, "Effect of pH on Anodic Behavior of Carbon Steel in Sodium Chloride Solutions Containing Ammonia", Corrosion 20, 1964, pp. 303t-306t.

(124) L. M. Dvoracek and L. L. Neff, "Use of the Polarization Technique to Study Corrosion in Aqueous Ammonia Systems", Corrosion, Vol. 18, No. 3, March 1962, pp. 85t-90t.

(125) O. L. Riggs, Jr., "Technical Note: Effect of Bulk Oxides on Anodic Polarization of Steel in NH_3-$NH_4NO_3H_2O$ Solutions", Corrosion, Vol. 25, No. 4, April 1969, pp. 170-172.

(126) V. A. Fishman, V. V. Dobrolyuboy, and V. A. Rogova, "Andoic Behavior of Stainless Steels in NH_3-NH_4PO_3-H_2O Solutions with Added Urea", Translated from Zashchita Metallov, Vol. 12, March-April 1976, pp. 180-182.

(127) J. R. Willard and R. B. Mears, "Aluminum in Refrigerating Equipment", Journal of the American Society of Refrigeration Engineering, December 1940, pp. 381-387.

(128) C. D. Kim, B. E. Wilde, E. H. Phelps, "Stress Corrosion Cracking of Line Pipe Steels in Anhydrous Ammonia", Corrosion pp. 255-262, 1975.

(129) Hooke, R., and Jeeves, "Direct Search Solution of Numerical and Statistical Problems", J. Assoc. Computing Machinery, Volume 8, No. 119, 1961.

(130) A. E. Bergles and W. M. Rohsenow, "The Influence of Temperature Difference on the Turbulent Forced Convection Heating of Water", Journal of Heat Transfer, Transactions ASME, August 1962.

(131) I. T. Aladyer, NASA, TM 1356, 1954.

(132) D. L. Katz, et al, "Condensation of Freon-12 with Finned Tubes", Journal of ASRE, March 1947.

(133) A. E. Dukler, Distillation Plant Data Book, Office of Saline Water, January 1971.

(134) Beatty, K. O. Jr. and Katz, D. L.: "Condensation of Vapors on Outside of Finned Tubes", Chem. Eng. Progress 44, No. 1, 1948.

(135) Young, E. Hand Word, D. J.: "How to Design Finned Tube Shell and Tube Heat Exchangers, Part 2 Design of Finned Tube Condensers", The Refining Engineer, 7-10, Nov. 1957.

(136) Katz, D. L. Hope, R. C. and Datsko, S. C. "Liquid Retention of Finned Tubes", Dept. of Engineering Research, University of Michigan, 1947.

(137) Withers, J. G. and Young, E. M., "Steam Condensing on Vertical Rows of Horizontal Corrugated and Plain Tubes", I & EC Progress Vols., January 1971.

(138) A. Blumenkranz and J. Taborek, "Heat Transfer and Pressure Drop Characteristics of Turbotec Spirally Deep Grooved Tubes in the Turbulent Regime", H.T.R.I. Report 2439-300/7 Proprietary Tests for Turbotec Corp., December 1970.

(139) A. E. Bergles and M. K. Jensen, Enhanced Single-Phase Heat Transfer for Ocean Thermal Energy Conversion Systems, Final Report, Engineering Research Institute Iowa State University, AMES, April 1977.

(140) Bergles, Bunn, Junkhan, "Extended Performance Evaluation Criteria for Enhanced Heat Transfer Surfaces", Heat and Mass Transfer, Volume 1, 1974.

(141) Bergles, Bynn, Junkhan, "Performance Criteria for Cooling Systems in Agricultural and Industrial Machines", HTL-6, ISU-ERI-Ames 74267, December 1974.

(142) Bergles, A. E., Jensen, M. L., "Enhances Single Phase Heat Transfer for OTEC Systems", HLL-13, Ames 773.4, April 1977.

(143) "Steam Plant Surface Condenser Leakage Study", W. B. Lawrence, et al, Electric Power Research Institute Report, Number NP-481, March 1977.

(144) "Equipment Availability for the Ten Year Period 1966-1975", Equipment Availability Task Force of the Prime Movers Committee of the Edison Electric Institute, New York, EEI Publication Number 76-85, December 1976.

(145) Perry A. M., et al, Net Energy Analysis of Five Energy Systems, Institute for Energy Analysis, Oak Ridge Associated University, September 1977.

(146) Battelle Columbus Laboratories, "Energy Use Patterns in Metallurgical and Nonmetallic Mineral Processing (Phase 4 - Energy Data and Flowsheets, High-Priority Commodities)", prepared for the U.S. Bureau of Mines, Report OFR 80-75, Columbus, Ohio, July 1975. (Available from the National Technical Information Service, PB-245-759).

(147) Battelle Columbus Laboratories, "Energy Use Patterns in Metallurgical and Nonmetallic Mineral Processing (Phase 5 - Energy Data and Flowsheets, Intermediate-Priority Commodities)", prepared for the U.S. Bureau of Mines, Report OFR 96-75, Columbus, Ohio, September 1975. (Available from the National Technical Information Service, PB-246-357).

(148) Bullard, C. W., P. S. Penner, and D. A. Pilati "Energy Analysis Handbook", 1976 CAC Document 214, Center for Advanced Computation, University of Illinois, Urbana, Ill.

OTHER BIBLIOGRAPHY

The following publications are included to provide further insight into methods and techniques described throughout this report:

1. Measurements of Biofouling in OTEC Heat Exchangers, J. G. Fetkovich, G. N. Grannemann, L. H. Mahalingam and D. L. Meier, Carnegie-Mellon University, Pittsburgh, PA.

2. Personal Communication, W. Adamson and A. Fritson, the David W. Taylor Center N.S.R.&D., Annapolis, MD.

3. Personal Communication, C. Sengupta, Public Service Electric and Gas, Newark, NJ.

4. Thermal Fouling Rates of 90-10 Copper Nickel, and Titanium in Seawater Service, R. B. Ritter and J. W. Suitor, Heat Transfer Research, Inc., Alhambra, CA., and George Cypher, International Copper Research Association, New York, NY.

5. Nature of Primary Organic Films in the Marine Environment and Their Significance for OTEC Heat Exchange Surfaces, E. C. Haderlie, Department of Oceanography, February 1977 (revised May 1977) Naval Post-Graduate School, Monterey, California.

6. "How Bacteria Stick", J. W. Costerton, G. G. Geesey, and K. J. Cheng, Scientific American, January 1978.

7. Primary Biofouling Films: Formation and Destruction, W. G. Characklis and B. F. Picologlow, Rice University, Houston, Texas.

8. Biological Fouling, Velocity and Temperature Effects, T. R. Bott and M.M.P.S. Pinheiro, University of Birmingham, Birmingham, U.K.

9. EPRI Journal, July/August 1978.

10. Fluid Mechanics, V. L. Streeter.

11. Hydrodynamic Control of Biofouling in OTEC Heat Exchangers, J. S. Tennant and M. A. Wood, Department of Ocean Engineering, Florida Atlantic University, Boca Raton, Florida.

12. "Scaling of Enhanced Heat Exchanger Tubes", A. P. Watkinson, L. Louis and R. Brent, Department of Chemical Engineering, University of British Columbia, Vancouver, B.C., Canadian Journal of Chemical Engineering, Volume 52, October 1974.

13. Marine Fouling of Titanium Heat Exchangers, Wayne S. Adamson, David W. Taylor Naval Ship Research and Development Center, Betheseda, Maryland.

14. Tests of a Seeding Process to Prevent Scale Formation in Evaporators, C. J. Bowden, May 1973, Westinghouse Electric Corporation, Lester, PA.

15. Personal Communication, John Gary, Marine Research, East Wareham, Mass.

16. Conceptualizations for Cleaning OTEC Heat Exchangers, February 1978, M. S. Rice, D. Hagel and A. Conn.

17. "Water Chlorination, Environmental Impact and Health Effects, Volume 2", Ann Arbor Science, P.O. Box 1425, Ann Arbor, MI.

18. Mitsubishi Marine Growth Preventing System, Mistsubishi Heavy Industries, Ltd.

19. EPRI Study RP902, Rice University.

20. Handbook of Chlorination, G. C. White.

21. "Amertap at English Station", C. K. Kuester, C. E. Lynch, American Society of Mechanical Engineers, Paper 66-WA/CT-1, November 1966.

22. Personal Communication, Al Gould, Florida Power and Light, Miami, Florida.

23. 2nd International Symposium on Ozone Technology, May 1975.

24. "Steam Electric Power Generating Point Source Category Effluent Guidelines and Standards", U.S. EPA, Federal Register 39 (Part III): 36199-36201 (1974).

25. "Corrosion Resistance of Wrought 90/10 Copper-Nickel-Iron Alloy in Marine Environment", Marine Corrosion Bulletin, MCB-1, International Nickel Company, New York.

26. B. F. Goodrich "No-Foul" Elastomeric Sheet Product Bulletin, B. F. Goodrich Engineering System Company, Akron, Ohio.

27. A. Blumenkrang and J. Taborek, Heat Transfer and Pressure Drop Characteristics of Turbotec Spirally Deep Grooved Tubes in the Turbulent Regime, H.T.R.I. Report 2439-300/7 Proprietary Tests for Turbotec Corp., December 1970.

28. A. E. Bergles and M. K. Jensen, Enhanced Single-Phase Heat Transfer for Ocean Thermal Energy Conversion Systems, Final Report, Engineering Research Institute Iowa State University, AMES, April 1977.

29. "High-Flux Heat Transfer Surface-Thermoexcel", Hitachi Review, Volume 24 (1975) No. 8.

30. Sabin, Poppendiek, et al, "Nucleating Vaporization and Extended Surface Heat Transfer at Low Temperature Difference", U.S. ERDA, Contract AT 04-3-1094, Annual Report, May 1976.

31. Bergles, Blunenkrastz, Taborek, "Performance Evaluation Criteria for Enhanced Heat Transfer Surfaces", Heat Transfer, 1974, Volume II, 1974.

32. Bergles, Bunn, Junkhan, "Extended Performance Evaluation Criteria for Enhanced Heat Transfer Surfaces", Heat and Mass Transfer, Volume 1, 1974.

33. Bergles, Bunn, Junkhan, "Performance Criteria for Cooling Systems in Agricultural and Industrial Machines", HTL-6, ISU-ERI-AMES 74267, December 1974.

34. Bergles, A. E., Jensen, M. K., "Enhanced Single Phase Heat Transfer for OTEC Systems", HLL-13, ISU-ERI, AMES 773.4, April 1977.

35. Personal correspondence with Charles Schrieber, Dow Chemical Company, December 1977; and Bill Grimes, Dow Chemical Company, January 1978.

36. Bonewitz, R. A., Concurrent Studies of Enhanced Heat Transfer and Materials for Ocean Thermal Exchangers - Final Report, Energy Research and Development Administration, Contract No. E(11-1), Carnegie Mellon/Alcoa Subcontract No. 1-53500, October 29, 1976.

37. Ivins, V. S., "Flash Evaporator Uses Titanium to Minimize Corrosion and Erosion", Power Engineering, July 1965, pp. 52-53.

38. Aoyama, H., et all, The Behavior of Ammonia in the Air Cooling Zone of Large Site Utility Condensers and Methods of Preventing Ammonia Attack, 33rd American Power Conference, 1971.

39. E. H. Haynie, and W. K. Boyd, "Stress Corrosion Cracking of Aluminum Alloys", DMIC Report 288, July 1, 1966, pp. 3-7 (Batelle Memorial Institute).

40. W. H. Caruthers, Jr., Aluminum and Its Alloys, Reynolds Aluminum Technical Publication, Richmond, Virginia.

41. Horst, R. L., Jr., "Selecting Aluminum Alloys for Process Equipment", Materials in Design Engineering, May 1960, pp. 130-135.

42. H. P. Godard, et al, "The Corrosion of Light Metals", Wiley & Sons, 1967.

43. Wanderer, E. T., and Wei, M. E., "Applicability of Aluminum for Desalinization Plants", Metals Engineering Quarterly - ASM, August 1967, pp. 30-36.

44. First U.S. Built LNG Ship Nearing Completion at Quincy Yard, Marine Engineering Log, September 1976, pp. 52-53.

45. Holtzman, A. H., and Cowan, G. R., Bonding of Metals with Explosives, Welding Research Council Bulletin 104, April 1965.

46. T. J. Lennox and M. H. Peterson, NRL Memorandum Report 8016, August 4, 1976.

47. Maurer, J. R., A Review of New Austenitic and Ferritic Stainless Steels for Corrosion Service, Allegheny Ludlum Technical Literature.

48. Personal correspondence with Jack Mauver, Allegheny Ludlum, and Claude Lynch, United Illuminating Co., November 1977.

49. H. R. Capson, "Effects of Velocity on Corrosion", Corrosion, February 1960, pp. 86-92.

50. "Report on Galvanic, Pitting Corrosion", Metal Progress, February 1975, pp. 48-49.

51. "Military Standard - Dissimilar Metals", MIL-STD-889A, 5/5/72.

52. M. G. Fontana and N. D. Greene, Corrosion Engineering, McGraw-Hill, 1967, pp. 31-37.

53. E. L. Littauer, Corrosion Protection, Geo-Marine Technology, June 1966, pp. 17-23.

54. M. H. Peterson, T. J. Lennox and R. E. Groover, "A Study of Crevice Corrosion in Type 304 Stainless Steel", Proc. 25th NACE Conference, March 1969, pp. 314-317.

55. E. Snape, "Sulfide Stress Corrosion of Some Medium and Low Strength Steels", Corrosion, June 1967, pp. 154-172.

56. I. L.W. Wilson, A. B. Dunlap, Materials for Service on Ammonia Side, Westinghouse R&D Document No. 77-9D2-OTECS-R1, November 11, 1977.

57. W. H. Ailor, "Aluminum in Seawater", Geo-Marine Technology, March 1965, pp. 130-134.

58. J. Symonds, Effect of Velocity on the Seawater Corrosion Resistance of Two Aluminum Alloys, Paper Presented At Fifth OTEC Conference, February 1978.

59. F. M. Reinhart, "Corrosion of Materials in Hydrospace, Part V - Aluminum Alloys", U.S. Naval Civil Engineering, Technical Note N-1008, January 1969.

60. H. H. Uhlig, "Distinguishing Characteristics of Pitting and Crevice Corrosion", Materials Protection and Performance, February 1973, pp. 42-44.

61. F. D. Bogar and C. T. Fujii, NRL Memorandum Report 2726, January 1976.

62. Banning, L. H., and Oden, L. L., Corrosion Resistance of Metals in Hot Brines: A Literature Review, U.S. Department of Interior, Bureau of Mines, BuMines IC8601, PB223715, August 1973.

63. Jenkins, G., F., Analysis of Hydroplane Support Structure After 52-1/2 Months Exposure at a Depth of 5270 Feet in the Barking Sands Test Range, Kauai, Hawaii, Naval Civil Engineering Laboratory, Port Hueneme, CA., AD 759-674.

64. Crack Growth Properties of Welds in HY80, HY100, and HY130/150 High Strength Steels in a Seawater Environment, U.S. Naval Applied Science Laboratory, Brooklyn, N.Y., SF020-01-01, Project 9300-1, Technical Memorandum #39, Task 0722, September 1965.

65. Porte, H. A., The Effect of Environment on the Corrosion of Metals in Seawater, U.S. Naval Civil Engineering Laboratory, Port Hueneme, CA., Y=F020-03-01-003, Technical Note N-907, July 1967.

66. Reinhart, F. M., Corrosion of Materials in Hydrospace - Part I, Irons, Steels, Cast Irons, and Steel Products, U.S. Naval Civil Engineering Laboratory, Port Hueneme, CA., Y-F-015-01-05-002A, Technical Note N-900, July 1967.

67. George, P. F., Maning, Jr., J. A., Schrieber, C. F., Desalination Materials Manual, Office of Water Research and Technology prepared by Dow Chemical Company, P.B. 252-043.

68. Henrikson, S. and Knutsson, L., "Corrosion Tests in Baltic Seawater on Heat Exchanger Tubes of Various Metallic Materials", British Corrosion Journal, Vol. 10 No. 3, 1975, pp. 128-135.

69. Reinhart, F. M., Effect of Deep Ocean Environments on the Corrosion of Selected Alloys, U.S. Naval Civil Engineering Laboratory, Port Hueneme, Ca., Y-F015-01-05-002a, TN781, October 1965.

70. Reinhart, F. M., et al, Corrosion of Alloys in Hydrospace - 189 Days at 5,900 Feet, U.S. Naval Civil Engineering Laboratory, Port Hueneme, Ca., Y-F38.535.005.01.004, TN1224, April 1972.

71. Hack, H. P., Seawater Corrosion of Fasteners in Various Structural Materials, U.S. Naval Ship Research and Development Center, Bethesda, MD., AD-A022 885, Report 76-0034, April 1976.

72. McMann, J.H.S., Corrosion and Fouling Study, U.S. Naval Surface Weapons Center, Silver Springs, MD., AD-A020 071, TR75-113, July 1975.

73. Reinhart, F. M., et al, Corrosion of Materials in Surface Seawater After 12 and 18 Months of Exposure, U.S. Naval Civil Engineering Laboratory, Port Hueneme, CA, AD-743-872, Technical Note N-1213, January 1972.

74. Boyd, W. K., and Fink, F. W., Corrosion of Metals in Marine Environments, Metals and Ceramic Information Center, Battello, Columbus, Ohio, MCIC-75-245R, May 1975.

75. Lula, R. A., New Austenitic and Ferritic Stainless Steels for Seawater Applications, Offshore Technology Conference, Houston, Texas, May 1974.

76. Pryor, M. J., Materials Evaluation for Desalination, Olin Report, New Haven, CT., MRL-65-PR-42, November 1965.

77. Cotton, J. B., "Pitting Corrosion of Titanium", British Corrosion Journal, Vol. 7, March 1972.

78. Cohen, A., and Lyman, W. S., Material Selection for Desalting Plant Heat Exchangers, 6th Annual Liberty Bell Corrosion Course, Drexel Institute of Technology, September 1968.

79. Gutzeit, Joerg, "Corrosion and Fouling of Admiralty, Aluminum, and Steel Tubes in Open Recirculating Cooling Water Systems", Materials Protection, July 1965, pp. 28-34.

80. Feige, N. G., and Kamp, R. L., "The Application of Titanium for Desalination Plants", Metals Engineering Quarterly, August 1967.

81. Hildebrand, R. L., "Aluminum Exchanger and Condenser Tubes in Petroleum Service", Division of Refining, Vol. 40 (III) 1960, pp. 118-130.

82. Griess, Jr., J. C., "Crevice Corrosion of Titanium in Aqueous Salt Solutions", Corrosion - NACE, Vol. 24, No. 4, April 1968, pp. 96-109.

83. Ailor, W. H., Jr., and Reinhart, F. M., "Three Year Tidewater Corrosion of Aluminum Alloys", Naval Engineers Journal, June 1964, pp. 443-449.

84. Wanderer, F. T., and Maurice, W. W., "Applicability of Aluminum for Desalination Plants", Metals Engineering Quarterly, ASM, August 1967, pp. 30-36.

85. Manning, J. A. and Carleton, S. V., "A Study of Corrosion Rates in an Operating Desalination Plant", Materials Performance, August 1975, pp. 9-14.

86. Jones, R. T., Application of Steels for Desalination Plants, ASM National Conference, Chicago, Ill., 1966.

87. Baker, D.W.C., et al, "The Evaluation of Stainless Steels for Condenser Tube Nest Construction", Corrosion Science - British, Vol. 12, 1972, pp. 247-264.

88. Boneuitz, R. A., "An Electrochemical Evaluation of 3003, 3004, and 5050 Aluminum Alloys for Desalination", Corrosion - NACE, Vol. 30, No. 2, February 1974, pp. 53-59.

89. Gainey, R. J., "Use of Aluminum for Portable Seawater Distillation Equipment", Corrosion - NACE, Vol. 17, November 1961, pp. 98-100.

90. Jenkins, J. F., Analysis of Hydrophase Support Structure After 52-1/2 Months Exposure at a Depth of 5270 Feet in the Barking Sands Test Range, Kauai, Hawaii, U.S. Naval Civil Engineering Laboratory, Port Hueneme, CA., YF38.534.007.01.011, Technical Note N-1267, March 1973.

91. Jenkins, J. F., Analysis of the Condition of the SNAP 7-E Acoustic Beacon Installation After 64 Months at 2,650 Fathoms, U.S. Naval Civil Engineering Laboratory, Port Hueneme, CA., YF38.534.006.01.001, Technical Note N-1192, February 1972.

92. Jenkins, J. F., Analysis of Conditions of Echo Tower, Azores Fixed Acoustic Range, After One Year at 1500 Feet of Depth, U.S. Naval Civil Engineering Laboratory, Port Hueneme, Ca., 52-921, Technical Note N-1284, May 1973.

93. Equipment Availability Component Cause Code Summary Report, Equipment Availability Task Force of the Prime Movers Committee of the Edison Electric Institute, New York.

94. "Steam Plant Surface Condenser Leakage Study", W. B. Lawrence, et al, Electric Power Research Institute Report Number NP-481, March 1977.

95. "The Rance Tidal Power Station", C. H. Lebarbier, Naval Engineers Journal, April 1975, pp. 57-71.

96. Revision of RADC Nonelectronic Reliability Notebook, Index and Revision to Section 2, prepared by Martin Marietta Aerospace for RADAC, October 1974.

97. Qualification of Aluminum for OTEC Heat Exchanger Tubes, Dr. F. L. LaQue; Paper received from J. S. Horowitz of Argonne National Laboratory, August 21, 1970.

98. Oregon Office of Energy Research and Planning, Office of the Governor, Transition, 1975.

99. Lockheed Missiles and Space Company, Inc., "Ocean Thermal Energy Conversion (OTEC) Power Plant Technical and Economic Feasibility", 2 Volumes, LMSC-D056566, April 1975.

100. Westinghouse Electric Corporation, Ocean Thermal Energy Conversion Power System Development - Conceptual Design, Phase I, January 30, 1978.

101. Bullard, C. W. and R. A. Herendeen, "The Energy Cost of Goods and Services", Energy Policy, December 1975.

U.S. GOVERNMENT PRINTING OFFICE: 1979—640-258/ 1393